Building up molecular complexity through transition-metal catalyzed functionalization of inert C-H bonds

Pierre M.N.J.D. Querard

Thesis submitted to McGill University in partial fulfillment of the requirements for the degree of

Doctor of Philosophy

Department of Chemistry
McGill University, Montreal
March 2018

Abstract

This thesis is an investigation on the widespread C-H bond functionalization field, towards the synthesis of complex molecules catalyzed by transition metal.

In Chapter 1 of this thesis, a brief introduction of molecular complexity is given, followed by a broad overview of the C-H bond functionalization field. History, characterizations, mechanisms and applications are presented.

Chapter 2 describes the development of a gold-catalyzed *sp* C-H functionalization reaction for the synthesis of oxazoles. The multicomponent coupling reaction between terminal alkynes, aldehydes and amines occurs very efficiently and produces water as the only side product.

Chapter 3 explores the discovery of a rhodium catalyzed functionalization of aryl sp^2 C-H bond. The development of a multicomponent reaction between internal alkynes, aldehydes and amines is presented, along with detailed investigations of the mechanism using DFT calculation. Diverse indene structures can be synthesized by this method with very high regioselectivity control.

Chapter 4 describes the development of an enantioselective visible light mediated arylation reaction of sp^3 C-H bond. Via this chemistry, arylation of N-arylated tetrahydroisoquinolines is efficiently prepared using iridium photocatalyst, in combination with copper transition metal catalyst and chiral pybox ligand. This enantioselective arylation reaction occurs efficiently at 4°C.

Chapters 5 and 6 summarize the contribution to fundamental knowledge for the whole thesis, and examine future works.

Résumé

Cette thèse examine le concept répandu de la fonctionnalisation de la liaison C-H, vers la synthèse de molécules complexes catalysées grâce aux métaux de transition.

Dans le chapitre 1 de cette thèse, une introduction brève est faite sur la complexité de molécules, suivi d'un aperçu sur la fonctionnalisation de la liaison C-H. Les antécédents, les caractéristiques, les mécanismes et les applications seront présentés.

Le chapitre 2 décrit la création d'une réaction de fonctionnalisation Csp-H avec l'or catalysé pour la synthèse d'oxazole. La réaction multicomposants à partir d'alcynes terminaux, d'aldéhydes et d'amines est efficace et forme uniquement de l'eau comme produit secondaire.

Le chapitre 3 explique la découverte d'une réaction de fonctionnalisation, de liaison aryl Csp^2-H, catalysée par du rhodium. Le développement d'une réaction multicomposantes entre alcynes internes, aldéhydes et amines est présenté, ainsi qu'une étude détaillée du mécanisme en utilisant le calcul DFT. Plusieurs structures d'indènes peuvent être synthétisées avec cette méthode en contrôlant de près la régioselectivité.

Le Chapitre 4 décrit le développement d'une réaction énantiosélective d'arylation de liaison Csp^3-H, catalysée par lumière visible. À travers cette chimie, l'arylation de N-aryle tetrahydroisoquinolines est préparée efficacement en utilisant la photocatalyse grâce à un complexe d'iridium avec un métal de transition comme le cuivre, ainsi qu'un ligand chiral pybox. Cette réaction d'arylation énantiosélective se produit efficacement à 4^{o}C.

Chapitre 5 et 6 démontrent la contribution de connaissances fondamentales pour écrire cette thèse, ainsi que les plans futurs.

Acknowledgments

The successful completion of this thesis would not have been possible without the support and assistance of many people.

Firstly, I would like to thank my supervisor, Professor Chao-Jun Li for his wisdom, support, and guidance through my PhD studies. I feel that I was granted an enormous privilege to be part of this research group, and I am truly and eternally grateful. Thank you, Professor Li, for accepting me as a PhD student.

I have also been lucky to learn from brilliant professors who have enlightened me and challenged me. To my professors at McGill, Dr. Bruce Arndtsen, Dr. James Gleason, and Dr. Chao-Jun Li, who taught me some of the most interesting and fulfilling courses I have ever had during my graduate studies. To my professors at the University of Rennes, Dr. Olivier Basle and Dr. Christophe Darcel. A special and sincere thank you goes to Olivier, without whom I would not have been able to do my PhD here, in the Li group. I am truly and eternally grateful.

I worked with some remarkable people and friends, during my time in the Li group. Thank you to Dr. Feng Zhou, Dr. Soumen Kundu, Dr. Thomas Knauber, Dr. Shingo Ishikawa, Dr. Haining Wang, Dr. Nick Uhlig, Dr. Simon Girard, Dr. Wenbo Liu, Dr. Lu Li, Dr. Mingxin Liu, Jason Struyk, Zoe Hearne, Zihang Qiu, Chen Chen. A very special thank for Dr. Inna Perepichka for being a superb lab mate, and being my second mum. Thank you to Dr. Xijie Dai and the nice philosophical discussions we had. Big thank you, to Alain Li who started his PhD the same day as me and for being an OSS 117 fan. To Allie Dominguez who organized the “Best Wife” event, that I won. To Sosthene Ung and his famous Ricard. Finally, I would like to thank everyone who came through our group.

I would like to thank the McGill departmental and administrative staff, with special thanks to Chantal Marotte who is always smiling and helping. Thank you to Dr. Nadim Saade and Dr. Alexander Wahba for their work with HRMS spectra. Thank you to Dr. Fred Morin and Robin Stein for the NMR facility.

Thank you to my friends from the chemistry department and from outside the university. Alice Baslé, Aurélie Lacroix and Marc-Antoine Lambert for being funny roommates. It had to be done once for all, the unicorn legend is in black and white in this manuscript. To my friends from France who visited me here in Montreal: Chochotte, Mathéo, Marion, Florian L, Théo, Jérémie, Anne-Laure. To the Deportivo soccer team, Capitaine Cousteau, Heppais, Adri, Momo, PFK, Aulas (and his good drolets). Thank you to my neighbors Adri, Max and P-J. Thank you to Robin Summer, Corentin Monfort, Franck Feral-Basin, Charlotte Matiere, and my friends from Montreal. Thank you to Lisa and Laura Demeester, aka “La Belgique une fois” and to Victor Sarkissian and his awesome barbecue skills.

My final thanks goes to my family. My parents, who helped me succeed, offered me the chance to pursue these long studies and who kept remembering me what is truly important in life. To both my sisters Pauline and Adele (aka Paulinoramix and Adeloramix the druids) thank you for the confidence, the laughs and reminding me of all the funny memories that we shared younger. Please, keep making sure I never take myself too seriously. To my grandparents for encouraging me.

Lastly, I would like to thank my irresistible girlfriend Laurie, for believing in me, sharing wonderful moments and laughing at my exceptionally funny jokes.

For my parents

Contributions and publications

During my doctoral research, the following publications (consisting of literature research and original research) have resulted from my dissertation, and are therefore the basis of, or are discussed within this thesis:

1) “Gold-catalyzed tandem reactions of amide–aldehyde–alkyne coupling and cyclization-synthesis of 2,4,5-trisubstituted oxazoles” **Querard, P.**; Girard, S. A.; Uhlig, N.; Li, C. J., *Chem. Sci*., **2015**, *6*, 7332-7335.

2) “Direct synthesis of indenes via a rhodium-catalyzed multicomponent Csp^2–H annulation reaction” **Querard, P.**; Li, C.-J., *Org. Biomol. Chem*., **2018**, *16*, 8042-8047.

3) “Copper-catalyzed asymmetric Csp^3–H arylation of tetrahydroisoquinoline mediated by a visible light photo redox catalyst” **Querard, P.**; Perepichka, I.; Zysman-Colman, E.; Li, C.-J., *Beilstein J. Org. Chem*., **2016**, *12*, 2636-2643.

4) “Exploration of New Reaction Tools for Late-Stage Functionalization of Complex Chemicals” Dominguez-Huerta, A.; Dai, X.-J.; Zhou, F.; **Querard, P.**; Qiu, Z.; Ung, S.; Liu, W.; Li, J.; Li, C.-J., *Can. J. Chem*., **2019**, *97*, 67-85.

Table of contents

Table of schemes

Table of tables

Table of equations

List of abbreviations

Ac	acetyl ($C(O)CH_3$)
Ar	aryl
Bn	benzyl ($C_6H_5CH_2$)
Boc	*tert*-Butoxycarbonyl
*n*Boc	*n*-butoxycarbonyl
Bz	benzoyl ($C_6H_5CO_2$)
CDC	cross-dehydrogenative coupling
CMD	concerted metalation-deprotonation
Cp*	pentamethylcyclopentadienyl ($C_5(CH_3)_5^-$)
d	doublet (^{1}H NMR)
DCE	1,2-dichloroethane
DDQ	2,3-Dichloro-5,6-dicyano-1,4-benzoquinone
Ee	enantiomeric excess
equiv.	equivalents
HRMS	high resolution mass spectrometry
Hz	hertz (s^{-1})
J	coupling constant (^{1}H and ^{13}C NMR)
KIE	kinetic isotope effect
LC-MS	liquid chromatography-mass spectroscopy
[M]	metal
m	*meta*

m	multiplet (^{1}H and ^{13}C NMR)
m.p.	melting point
NMR	nuclear magnetic resonance spectroscopy
Nu	nucleophile
[O]	oxidant; or oxidizing conditions
o	*ortho*
p	*para*
ppm	parts per million
QLF	que la famille
q	quartet (^{1}H and ^{13}C NMR)
rds	rate-determining step
r.t.	room temperature
s	singlet (^{1}H NMR)
SEAr	electrophilic aromatic substitution
SET	single electron transfer
t	triplet (^{1}H NMR)
TBAF	tetra-*n*-butylammonium fluoride
TFA	trifluoroacetic acid (CF_3CO_2H)
THF	tetrahydrofuran
TLC	thin-layer chromatography
TMS	trimethylsilyl ($Si(CH_3)_3$)
Ts	tosyl, *para*-toluenesulfonyl (H_3C-C_6H_4-SO_2)
X	halides

Chapter 1 – Introduction

1.1. Molecular complexity

Recently, the concept of molecular complexity has received a lot of attention by the chemistry community. “Complexity” is an ambiguous word and highly reliant on context. Just as there is no absolute definition of "intelligence", there is no absolute definition of "complexity"; the only consensus among researchers is that molecular complexity refers to structural and molecular properties of a molecule. In chemistry, almost everything of interest is complex by any definitions. Steven H. Bertz said in 1980: *“Synthetic chemists have been defining a complex molecule in the way that many people define art: they know it when they see it”*.[1] However, molecular complexity is becoming a crucial aspect in drug discovery. This notion has been associated with target selectivity success in progressing into clinical development and other factors.

In addition to simply observe and analyze, chemistry is a branch of science that tries to predict and control. Faced with the difficulty of defining any such real molecular system, chemistry has evolved a series of approaches to characterize complex systems. Originally, Bertz was pioneering the term of molecular complexity by explicitly describing a measure of a complexity index C of a molecule.[1] His formula is derived from information theory and is based on the sum of bond connectivities on non-hydrogen atoms as well as on the variety of kinds of these atoms (Equation 1). The first and major term, C_n, measures skeletal complexity as a function of bond connectivities (n) and the second term, C_e, is a function of the diversity of elements, or kinds of atoms.

$$\mathbf{C} = \boldsymbol{Cn} + \boldsymbol{Ce}$$

$$Cn = 2n\lg(n) - \sum_i ni\lg(ni)$$

$$Ce = E\lg(E) - \sum_j Ej\lg(Ej)$$

Equation 1. Bertz’s measure of complexity C

Following this exciting and new concept, many chemists and theorists have developed more and more detailed equation-graph relation to calculate and measure information in molecules.[2-5] Later, Morgan introduced the notion of extended connectivity, which gives a value to each atoms in a molecule relative to its connection to other atoms.[6] This notion has shown limitations producing oscillating values of extended connectivity for selected atoms. To overcome these limitations, Hendrickson, Huang, and Toczko, amongst others, developed many more complex or simplified forms of Bertz's formula and applied them to computational calculations.[7] Most of these developed complexity indices are based on graph theory, in which chemical structures are transformed into skeletal molecular graphs. However, graph-theory-based indices essentially address skeletal complexity and have been criticized for having certain limitations.[8-9] The most important one is its failure to address chirality in graph-theoretical approaches and the missing sensitivity to skeletal structure, branching, and symmetry.

Despite the fact that Bertz's complexity index C is still probably the most popular measure of molecular complexity today, people tried to develop a more precise model to describe molecular complexity. Inspired by Bertz's work, Böttcher recently proposed a novel approach for molecular complexity relying on both mathematical rigor and chemical logic.[10] The complexity is calculated by using the chemical microenvironment of each individual atom of a molecule (Equation 2). This new model consists of adding an index, to avoid the biases resulting from graph-theoretical approaches, while considering symmetry and stereochemistry.

$$\mathrm{Cm} = \sum_i di \times ei \times si \times \log_2(Vi \times bi) - \frac{1}{2} \sum_j dj \times ej \times sj \times \log_2(Vj \times bj)$$

Vi defines the number of valence electrons (i.e. Vi = 1 (H), 3 (B)…).
bi defines the number total of bonds to any other atom
di defines the number of chemically nonequivalent bonds to atoms
ei defines the number of different non-hydrogen elements in the bonding situation
si defines the number of isomeric possibilities si at the i position

Equation 2. Böttcher's calculation of molecular complexity Cm

This approach is to date one of the most accurate model that addresses the major deficiencies of other indices, including stereochemistry, unsaturated bonds, branching, and symmetry, and can be simply calculated manually. Intuitively, organic chemists agreed that certain features that bring variety into the molecules (e.g., chiral centers, sp^3 carbons, fused rings, bridged rings, and hetero atoms) also increase molecular complexity, but only if these features are not repetitive. On the other hand, repetition of identical or very similar molecular features lowers the complexity of a molecule.

In order to simplify this fundamental and unusual metric, an example of molecular complexity calculation for methane will be described. As mentioned above in Equation 1, the first term C_n is a function of bond connectivities (n) and C_e is a function of the diversity of elements. The molecular complexity of methane is calculated as following in Equation 3:

$$Term\ 1 : Cn = 2n\lg(n) - \sum_i ni\lg(ni) \qquad n = \frac{1}{2} \times \sum_i (4 - h_i)(3 - h_i) - D - 3T$$

$$n_{CH_4} = \frac{1}{2} \times \sum_i (4-4)(3-4) - 0 - 0 = 0 \qquad Cn_{CH_4} = 2 \times 0 \times \lg(0) - \sum_i 0 \times \lg(0) = 0$$

n defines the bond connectivities
h_i defines the number of hydrogen atoms connected to this atom
D defines the number double bond
T defines the number triple bond

$$Term\ 2 : Ce = E\lg(E) - \sum_j Ej\lg(Ej) \qquad Ce = 0 \times \lg(0) - \sum_j 0 \times \lg(0) = 0$$

E defines the total number of non-hydrogen atoms
E_j defines the number of type j

Thus, it results from these calculations that:

$$C_{CH_4} = Cn + Ce = 0 + 0 = 0$$

Equation 3. Calculation of molecular complexity of methane

Below, in Scheme 1, it represented the calculated complexity of known structures. Comparing the molecular complexity of benzene and phenol (respectively 15.5 and 46.1) clearly shows the impact of symmetry on this metric.

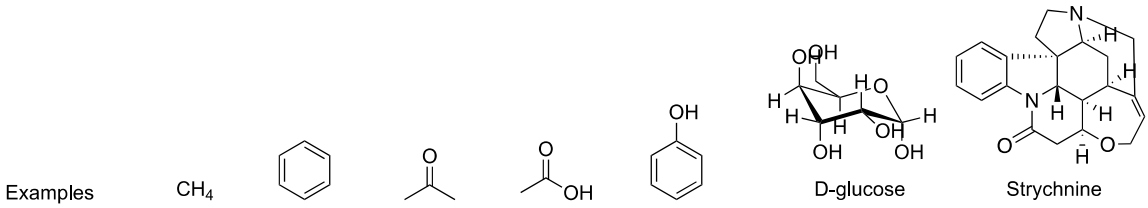

Examples	CH_4					D-glucose	Strychnine
Molecular Complexity	0	15.5	26.3	31	46.1	151	689

Scheme 1. Molecular complexity calculated for common and complex structures

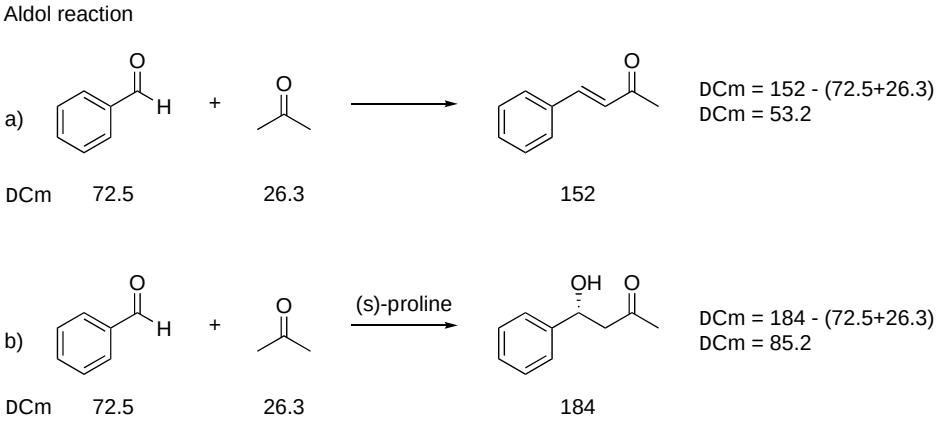

Scheme 2. Changes in molecular complexity for selected aldol reactions

The molecular complexity of chemical transformations, ΔCm, is calculated as the complexity of products minus the complexity of educts. Thus, different chemical reactions can be directly compared thanks to their corresponding ΔCm even for reactions with substrates that differ significantly in molecular complexity. As an example, a stereoselective aldol reaction with benzaldehyde and acetone results in ΔCm=85.2 (Scheme 2). The aldol reaction generates stereochemical information, yielding a higher ΔCm, in contrast to aldol condensation reactions, where a significant part of the functionality and complexity is subsequently lost during dehydration.

The index Cm developed by Böttcher represents a valuable tool for medicinal chemistry to investigate drug candidates. Molecular complexity has been associated with a number of properties related to drug discovery and development.[11-15] Quantification of molecular complexity and its use in drug discovery is not a fully solved problem and it is still under development. Advances in the field are closely related to the study of large libraries of existing structures, which can be produced from classical chemistry methods. Developing new reactions allowing to build molecular complexity in an efficient way is attractive and rewarding. In Böttcher's equation, atom efficiency is very important. The second term of his equation describes the stereochemistry, unsaturated bonds, and symmetry of the generated side product or by products. To maximize the benefits of building molecular complexity, this study investigates C-H functionalization reactions. These reactions shorten classical organic synthetic routes to produce direct benefits both in energy costs and atom-economy, and are presented in the following section.

1.2. C-H bond functionalization

The activation of different chemical bonds is one of the most important and most rapidly evolving field of modern chemistry. Chemical bond activation is a key step in organic chemistry and it is used to functionalize simple to complex molecules towards more diversified useful structures. Organic chemistry has been revolutionized by the tremendous efforts towards reducing pre-activation of substrates over the last decades, diminishing the waste production and shortening the synthetic steps. The use of abundant and very inexpensive potential sources, which are usually unreactive species, is of huge interest to achieve such an objective. Traditionally, the activation of relatively inert bonds, such as the C-Cl, C-F, C-O bonds, has found its importance in the modification of toxins and non-easily degradable materials. Activating less reactive chemical bonds, such as C-C and C-H bonds, is becoming remarkably attractive economically. The activation of the carbon-carbon bond is challenging because of its inherent stability. The synthetic utility of functionalization of C-H bonds has been distinguished in modern chemistry mainly owing to its ability to provide a platform for a rapid generation of waste-free, and atom-economic transformations of valuable functionalized organic compounds

(Scheme 3). Bypassing unnecessary traditional steps, such as protection, activation and de-protection reactions, C-H activation represents a higher-level methodology in the organic synthesis field. One of the most common examples is the modification of methane to methanol, for various industrial applications. Advantages of processing for large-scale production are attractive for applications as an automobile alternative fuel, a cheaper synthesis of methanol solvent and an easily processed chemical feedstock.

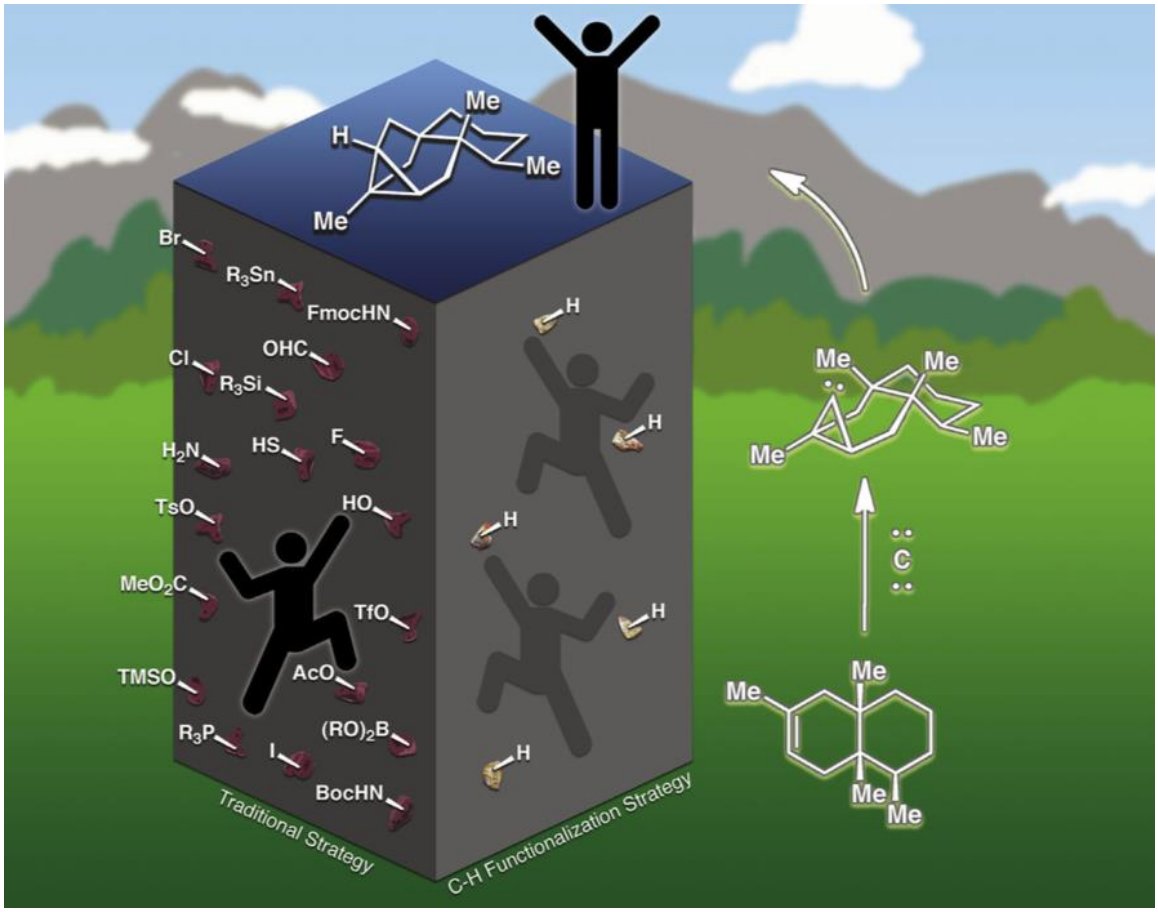

Scheme 3. Potential efficiency of C-H functionalization strategy[16]

C-H bond functionalization represents a paradox from our logic and knowledge of traditional organic chemistry. Given that chemistry essentially occurs at the most reactive

functional group in a molecule, it is counter-intuitive that a reaction proceeds at another position. This paradox represents the overall logic of the C-H activation field.

1.2.1. History

1.2.1.1. Free radical transformation

The first pioneering developments in the field of C-H activation were established in the mid-19th century. Free-radical halogenation and electrophilic aromatic substitution are early developments of C-H bond functionalization reactions.

In 1840, Jean-Baptiste Dumas, discovered the chlorination of unreactive alkane.[17] The chlorination of relatively simple alkanes is one of the oldest organic reactions but is still currently used industrially for methane conversion (Scheme 4).[18]

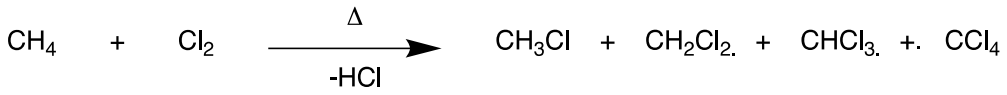

Scheme 4. Industrial oxychlorination of methane

This industrial application, generally occurring under high temperature, has been modified many times due to the strong exothermic properties of radicals formed during the reaction. The thermal initiation of the homolytic splitting of chlorine forms chloride free radicals. The propagation step is driven by the abstraction of one hydrogen atom from methane leaving a primary methyl radical. The methyl radical can abstract a chlorine radical from chlorine gas. Different degrees of chlorinated alkanes are produced. Numerous methodologies and applications used free radicals to activate C-H bonds have emanated by Dumas' seminal work. The total synthesis of nicotine was published by Löffler in 1909. The reaction operates through nitrogen radical intermediate which can then abstract a hydrogen atom regioselectively via a 6-membered ring transition state (Scheme 5).[19]

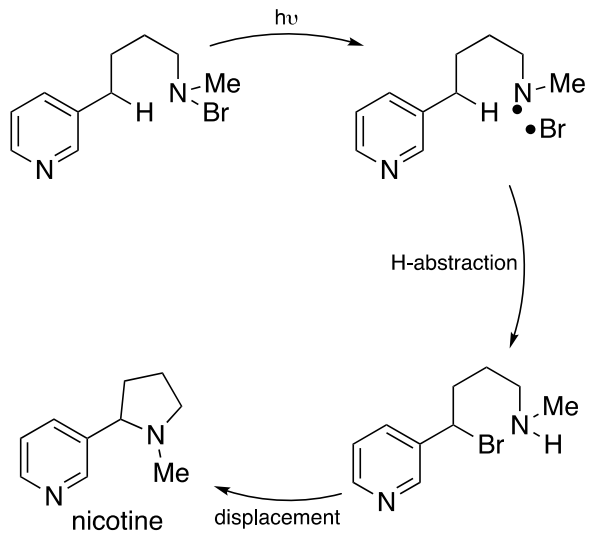

Scheme 5. Löffler's total synthesis of nicotine

Further numerous bioactive molecules and natural products total synthesis were achieved following the same strategy over the course of the 20th century.[16] For instance, Woodward published the synthesis of cephalosporin C through an unprecedented C-H amination reaction.[20] Later, in 1960, Barton and co-workers reported the total synthesis of aldosterone acetate (Scheme 6).[21-22] The mechanism involved in this reaction, analogous to the Löffler's mechanism mentioned above, goes through an alkyl radical that reacts with a persistent nitrosyl radical to finally and quickly tautomerizes to an oxime species.

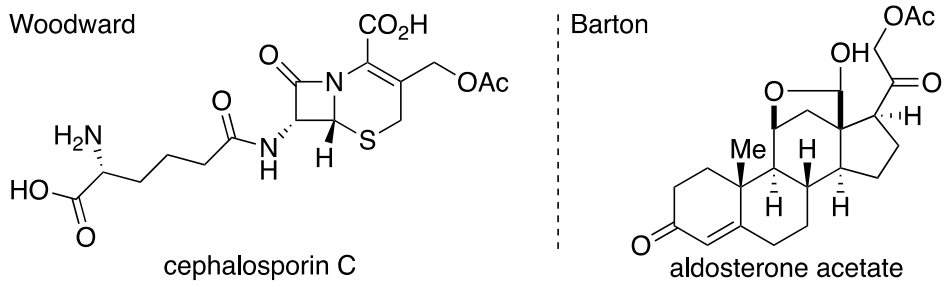

Scheme 6. Example natural product's total synthesis (via radical C-H activation mechanism)

1.2.1.2. Use of transition metal catalyst

Processes like electrophilic aromatic substitution (EAS) reactions or Friedel-Crafts reactions cleave a C-H bond by initial electrophilic attack on aromatic π-system. The mechanism described for these types of EAS does not involve a direct activation of the C-H bond as the corresponding C-H bond is cleaved by a base. "C-H activation" usually refers to reactions involving the cleavage of an unreactive C-H bond, which could be favored by the help of transition metal complexes.

The earliest report about C-H activation reaction dates to Fenton's 1894 paper on the matter, where a transition metal C-H bond oxidation reaction was described for the first time.[23] The study observed the oxidation of tartaric acid to dihydroxymaleic acid in presence of iron and external oxidants. Later, the well-known Gif process was developed, establishing the transformation of aliphatic C-H bonds into C-O bonds (Scheme 7).[24-25] The Gif process, named after the city Gif-sur-Ivette in France, received remarkable attention because of Fenton's reaction limitations. The generation of very reactive hydroxyl radicals makes the oxidation reaction unselective. The role of oxygen in Gif process mechanism and the role of carbon radicals has been the source of debate.[26-28]

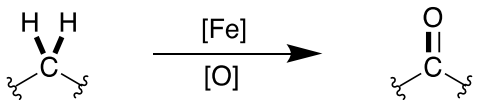

Scheme 7. The Gif process

The first application of C-H bond functionalization mediated by transition metal catalyst in total synthesis was reported by B. Trost in 1978.[29] He achieved the total synthesis of ibogamine using $PdCl_2(MeCN)_2$ and $AgBF_4$ in presence of $NaBH_4$ (Scheme 8). Under these conditions, the C-H bond was activated via the palladium to form a C-2 indolyl palladium species. Through a carbo-palladation to the unsaturated double bond followed by β-hydride elimination and reduction via $NaBH_4$, the ibogamine product was formed and the catalyst regenerated consequently.

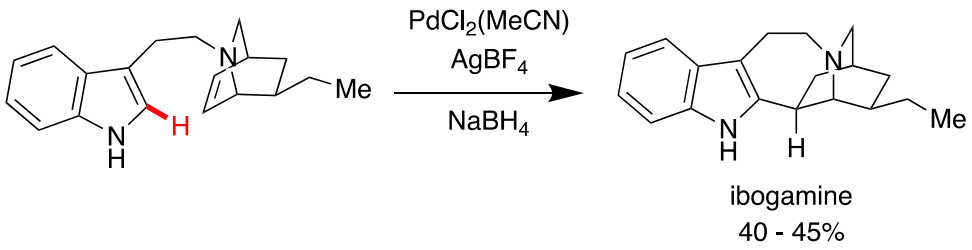

Scheme 8. C-H functionalization step in total synthesis of ibogamine

The activation of C–H bonds remains the matter of current investigative research. The C–H bond strength is a factor that does not determine its reactivity on its own.

1.2.2. Goals and challenges of C-H activation

1.2.2.1. Reactivity of sp, sp2 and sp3 C-H bonds

The C-H bond is the most fundamental and ubiquitous linkage in organic chemistry. It is relatively resistant to chemical transformations because of its intrinsically low reactivity. C-H bonds do not possess suitable lone pairs to coordinate to a catalyst, which makes C-H bond activation also kinetically challenging in comparison to other C-X bond cleaving reactions. For instance, the bond dissociation energy of the sp^3 C-H bond in methane and the sp^2 C-H bond in benzene are respectively 105 kcal.mol^{-1} and 110 kcal.mol^{-1} (Scheme 9).[30] In comparison, the BDEs for Me-Cl and Me-Br, which are easily functionalized, are 83.7 and 72.1 kcal.mol^{-1}, respectively. Thus, to undergo C-H activation reaction, a large kinetic barrier must be typically overcome by using harsh-condition reactions. The synthetic use of C-H bond activation reaction is therefore severely impinged by these negative aspects.

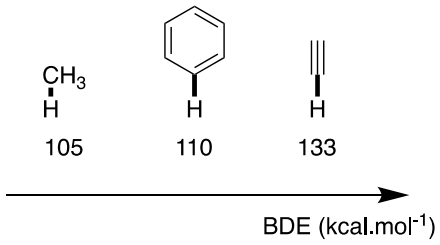

Scheme 9. BDE of C-H bonds

Furthermore, due to the high pK_a values of sp, sp^2 and sp^3 C-H bonds (≈ 40), their heterolytical cleavage is difficult. The high cost of cleaving such stable bonds must be compensated by forming a new stronger organometallic bond to make this process feasible. C-M bonds with weak bonds have usually been created using different approaches: intramolecular reaction by pre-metallation or directing group.

1.2.2.2. Selectivity and compatibility of C-H activation

One of the biggest limitations of C-H activation reaction is the regiocontrol control of the C-H functionalization, despite the ubiquitous nature of C-H bonds in organic molecules and its potential to become a highly general process. Numerous efforts have been made to achieve a C-H activation reaction in a chemoselective manner in the last decades. The predominant strategy developed to control chemoselectivity is the use of a coordinating neighboring heteroatom to the metal catalyst. The metal-coordinating functionality helps the interaction and proximity with the proximal C-H bond (Scheme 10), allowing the addition of a functional group (FG). However, the synthetic practicality of the directing groups (DGs) strategy is compromised if the synthetic target does not hold such functionality. A detailed investigation on the development of DGs and their uses in the C-H activation reaction will be discussed in the directing group strategy section (see 1.2.1.1 DG).

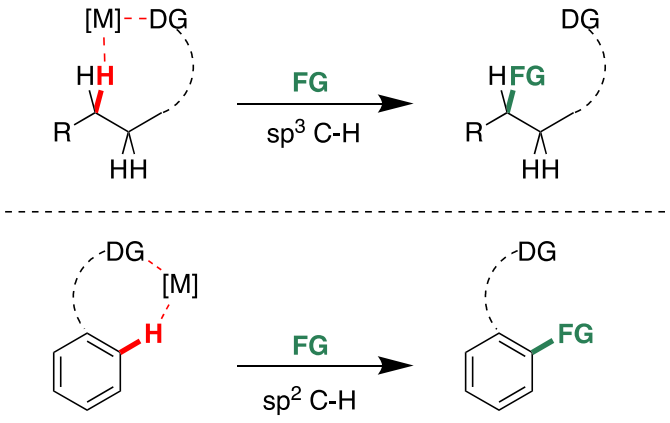

Scheme 10. Directing group strategy

1.3. Classification of C-H activation reactions

Nature remains the greatest performer and most efficient user of C-H bond functionalization reactions amongst all the research carried out in the C-H activation field.[31-32] Nature processes enzymatic C-H functionalization reactions without limitations. Both early and late-stage modifications at any site, a biosynthetic process, can be accomplished by Nature regardless of other reactive moieties. The biosynthesis of biotin, which through the cleavage of two C-H bonds forms a cyclic thioether, represents a typical example (Scheme 11).

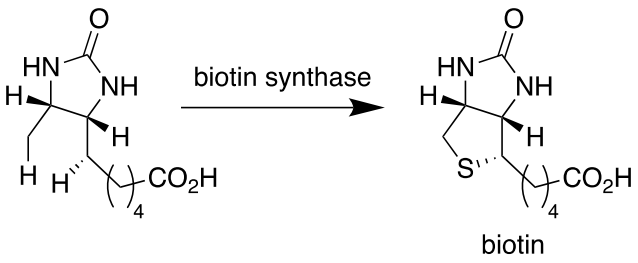

Scheme 11. Biotin synthesis

As shown in Scheme 11, the activation and cleavage of two C-H bonds occurs with concomitant sulfur insertion between carbons 6 and 9, results in the formation of the thiophane ring.[33-34]

The study of C-H activation reactions by organic chemists has a long history. It has been the subject of considerable interests and has even been considered as a “Holy Grail” of chemistry due to its numerous advantages: step efficiency, atom economy and high selectivity.[35] Direct C–H functionalization methods are also reported as *greener* than conventional methods.[36] This strategy is expected to continue to significantly contribute to the mission of green chemistry: low transition metal catalytic loading, low-energy, waste-free, and atom-economic transformations for the synthesis of organic materials and biologically active molecules, conversion of cheap and abundant alkanes into valuable functionalized organic compounds.

1.3.1. **Functionalization of activated C-H bonds**

The formation of carbon-carbon (C-C) bonds by transition metal catalyst has been recognized as amongst the most important recent discoveries.[37] The development of efficient synthesis is key and requires flexibility by controlling selectivity and the atom economy. The ability of transition metal complexes to process a functionalization reaction constitutes one of the most powerful strategies to control those features. Metal mediated reactions can be efficiently accomplished through designed combination of transition metal catalyst with a properly chosen ligand environment. The cross-coupling processes are probably among the most useful tools to achieve C-C bond formation and they can be described by four different approaches (Scheme 12).

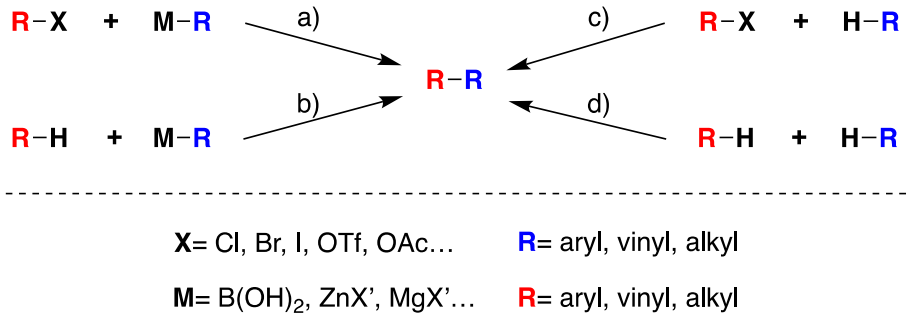

Scheme 12. Different approaches to cross-coupling reactions

Recent Chemistry Nobel Laureates Heck, Negishi and Suzuki have significantly contributed to the development of palladium catalyzed cross-coupling reactions (Scheme 12, path a).[38-39] The use of expensive and pre-elaborated molecules is generally mandatory as part of these studies The pre-functionalization and isolation of two independent substrates used to perform the reaction, represent stoichiometric amounts of waste materials added to the reaction's waste. Due to these reasons, the atom economy suffers tragically. Thus, the chemistry community aimed to develop similar reactions with greener and more sustainable processes.

C-H bonds are ubiquitous in most organic molecules. Consequently, the consideration of C-H bonds as reactive sites in molecules implies that the pre-functionalization of

substrates becomes irrelevant. Additionally, the waste material from the cross-coupling reaction will be drastically diminished. To achieve this goal, researchers have developed different approaches. In Scheme 12, path b), the C-H activation is performed at the electrophilic coupling partner, avoiding the use of halogenated and R-X derivatives.[40-46] On the other way around, changing the nucleophilic partner from an organometallic reactive coupling substrate to a C-H containing molecule is of great interest.[47-50] The reduction of waste in this example is considerable, since no stoichiometric amount of metal waste is created from any of the coupling partners. Lastly, by far the most interesting option theoretically, the Cross-Dehydrogenative Coupling reaction is a combination of both pathway b) and c). This process enables the formation of C-C bonds directly from the coupling of two distinct C-H bonds and will be described in depth in chapter 4.[51-55] However, two principal concerns remain unsolved from these two approaches: a large amount of energy is necessary for the activation of inert C-H bonds (Scheme 9) and the selectivity control between a large range of C-H bonds is difficult.

The use of transition metal catalysts to lower the activation energy of C-H bonds was discovered during the last decades to solve these issues. Over the years, two different features characterizing two distinct forms of C-H functionalization appeared: “innate” and “guided”.[56] Established in 2011 by Baran, those terms correspond respectively to the presence or absence of an outer directing group influencing the regiocontrol of the reaction (Scheme 13).

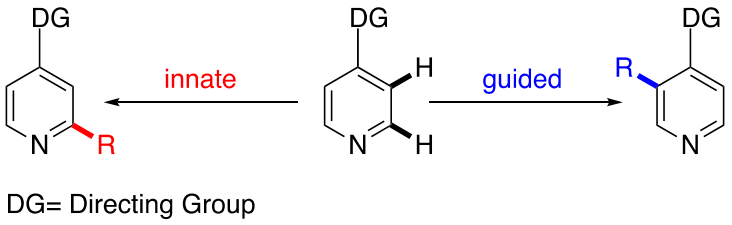

Scheme 13. Innate & guided C-H functionalization

To date, most practical functionalizations of C-H bonds have occurred to add new groups at naturally unreactive C-H bonds in molecules containing existing functionality or directing group.

1.3.1.1. Undirected or innate C-H functionalization

Undirected C-H functionalization reactions are underdeveloped compared to the directed functionalization of C-H bonds. However, a lot of research efforts have been undertaken. Such reactions would have an enormous impact by proposing new synthetic capabilities: no directing group, step-economy, and direct conversion of raw material to synthetically useful compounds. Without assistance from the DG, the control of regioselectivity remains the biggest challenge. Moreover, the thermodynamic of the reaction is decreased when the chelation of the substrate to the DG is absent because the intramolecular C-H bond cleavage is favored due to the higher stability of the organometallic intermediate formed. The reactivity of comparable C-H bonds should be similar by this argument. However, C-H bonds react with different rates as a function of the setting's inductive effects, conjugation, hyperconjugation, steric hindrance, and strain release.[56] The effect of these is as follows.

First, the inductive effect plays an important role for the rate of C-H bond oxidation in the presence of electron-withdrawing groups (EWGs) nearby. The selectivity of an oxidation reaction is dominated by the nature and the distance of the EWGs to the C-H bond. Numerous examples showing reactivity trends between different C-H bonds[57-60] or radical chlorination of C-H bonds have been reported.[61-62] Conjugation and hyperconjugation also drive the selectivity of C-H bond functionalization. These effects represent another type of electronic activation of C-H bonds but are weaker compared to inductive effects. This activating effect requires orbital overlap between electron pair and the σ C-H anti-bonding orbital, lowering the energy of the C-H bond. Various examples showing selective C-H activation in cyclopropane have been described.[63-67] Beyond cyclopropane chemistry, heteroatoms donate electron density to the neighboring C-H bond through hyperconjugation. For instance, in tetrahydrofuran or tetrahydropyran, the functionalization of the alpha C-H bond to the heteroatom is exceptionally selective.[68-75]

Third, the steric hindrance of the substrate governs significantly the selectivity of non-directed C-H bond functionalization. For instance, in the rhodium catalyzed C-H bond functionalization for the synthesis of β^2-amino acids, reported by Davies, the C-H oxidation occurs selectively at the methyl group instead of the benzylic position.[76] He reported that the selectivity observed is essentially the result of a less hindered environment at the methyl group. Analogously, the iron-catalyzed selective C-H oxidation of menthol derivatives is governed by steric (Scheme 14).[77-78]

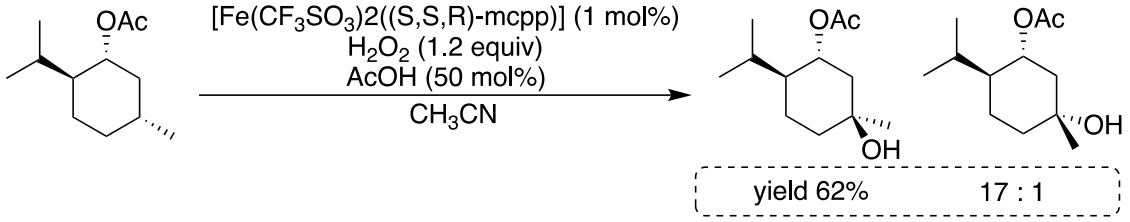

Scheme 14. Iron catalyzed selective C-H oxidation of menthol derivatives.

To rationalize the selective oxidation at the tertiary position on the cyclohexyl ring, White and Miquel stipulate that the isopropyl group is more hindered and that the rigidity of the ring may contribute in this example. Eventually, the strain release comes from the factors governing selectivity of non-directed C-H bonds functionalization reactions. C-H bonds with faster reactions the equatorial position than its equivalent oriented axially have also been observed.[79-84]

With a panel of properties associated to the "innate" reactivity, the functionalization of inaccessible C-H bonds by "innate" reactivity must be performed through a directed process to achieve a high degree of selectivity.

1.3.1.2. Transition metal catalyst free C-H activation: C-C, C-O, C-N, C-S bond formation.

The sustainable chemistry movement have further driven scientists to explore novel coupling strategies separate from tradition metal catalyzed cross-coupling reactions. Research and industrial interest in radical C−H activation/radical cross-coupling chemistry has continued to grow over the past few decades. These reactions offer fascinating and

unconventional approaches toward connecting molecular fragments with high atom- and step-economy that are often complementary to traditional methods. Particularly, the oxidative cross-coupling reaction has become the most useful method to construct C-C and C-X (X = O, N, S) bonds.[85]

Radical cations, usually generated from a single electron transfer reaction (Scheme 23) can take part in cyclo-addition, nucleophilic addition and radical cascade reactions.[86] Li and co-workers have made the premise that C-C bond formation can be obtain from the oxidation of two different C-H bonds.[51, 87] They reported the first example of 2,3-Dichloro-5,6-dicyano-1,4-benzoquinone (DDQ) mediated direct cross-dehydrogenative-coupling (CDC) reaction between isochroman and ketones.[88-89] A radical mechanism was proposed with a single electron transfer (SET) reaction from the ether to DDQ, generating a radical cation and DDQ radical anion (Scheme 15). The authors then proposed a hydrogen abstraction from the benzylic position by DDQ radical anion, forming a benzoxy cation. Finally, the product was obtained by nucleophilic addition of the enolate form of the coupling partner. Successively, this seminal work created a large novel area to explore in the radical oxidative coupling of ethers and their analogues. In 2013, Liu and co-workers developed a simple and efficient oxidation system promoting identical alkylation of isochroman.[90] The use of MnO_2 and excess CH_3SO_3H was ideal to perform this transformation in good to moderate yield. To compete against traditional metal-based oxidative cross-coupling reaction, this methodology had to lower the typical high temperature needed and the excessive amount of oxidant.

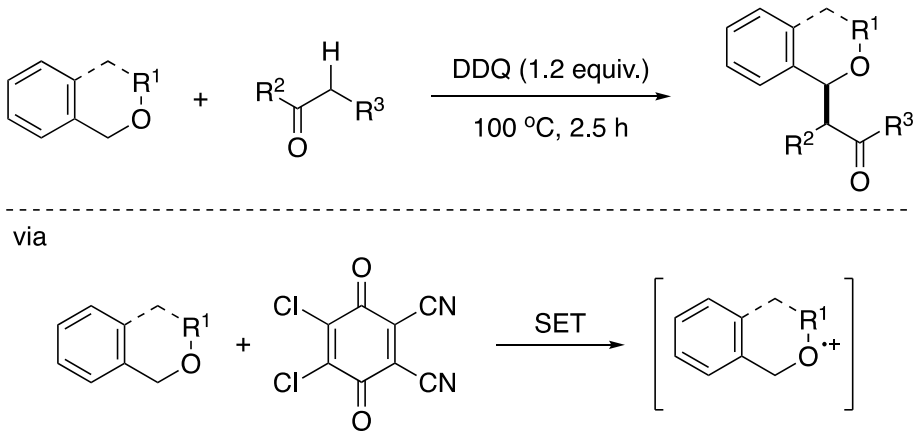

Scheme 15. DDQ-mediated direct cross-dehydrogenative-coupling between benzyl ethers and ketones

Visible light photo-redox catalysis has attracted significant interest for the transformation of C-H bonds under mild and environmentally friendly conditions.[91-93] In 2014, MacMillan and co-workers designed a visible light mediated photo redox approach for the arylation of ethers using iridium photo redox complex (Scheme 16).[94] The author believed that the oxyalkyl radical was generated through a hydrogen atom transfer (HAT) pathway. The electron deficient heteroarenes coupled with the oxyalkyl radicals and formed a reaction similar to the Minisci reaction.[95] It was remarkable that the efficient C-H bond functionalization of both coupling partners proceeded at room temperature.

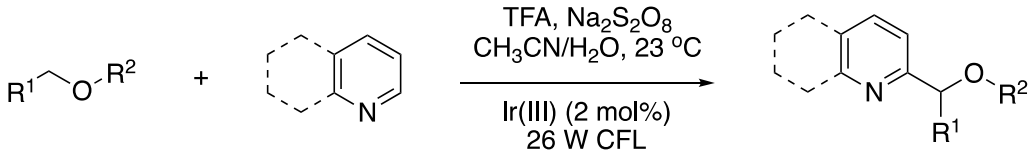

Scheme 16. Visible-light photo redox cross coupling reaction

Besides radical cations, the carbon centered radicals are versatile chemical species. Oxidative carbon center radical intermediates have been the subject of a considerable number of recent studies. The pioneering work of Zhang and co-workers established a

transition metal catalyzed radical oxidative addition reaction.[96] Later, in 2014, Ji and co-workers achieved a transition metal-free synthetic route for the direct Csp^3-H bond functionalization of ethers (Scheme 17).[97] Better understanding of the mechanism was obtained when TEMPO reacted with the alkoxy radical to form TEMPO -1,4-dioxane. The authors proposed a thermal homolysis of TBPB forming tert-butoxyl radical. This reactive species undergoes hydrogen abstraction at the alpha position to the ether **I** which then adds to the allylic alcohol forming an alkyl radical intermediate **II**. Subsequently, intramolecular radical addition at the ipso-carbon of the benzene ring to generates the spiro[2,5]octadienyl radical **III**. This intermediate is subjected to a migration of the electron deficient aryl group to release **IV**. Finally, the product is obtained after further oxidation and deprotonation (Scheme 18). In 2015, Han and co-workers reported a similar metal-free oxidative functionalization of Csp^3-H bond adjacent to oxygen and radical addition to olefins.[98] Promoted by DTBP, the carbon centered radical underwent addition reaction to the alkene, under metal-free and without light initiation reaction condition.

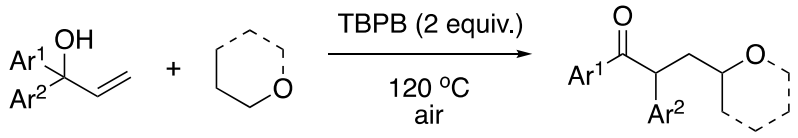

Scheme 17. Metal-free oxidative direct Csp^3-H bond functionalization of ethers with diaryl allylic alcohols

Similar to alkenes, alkyne derivatives can also react with ethers to afford alkenyl or alkynyl products via intermolecular addition. Widely used as radical acceptor, the alkyne functionality was evaluated in metal-free radical cross coupling in the seminal work of Liu and co-workers.[99]

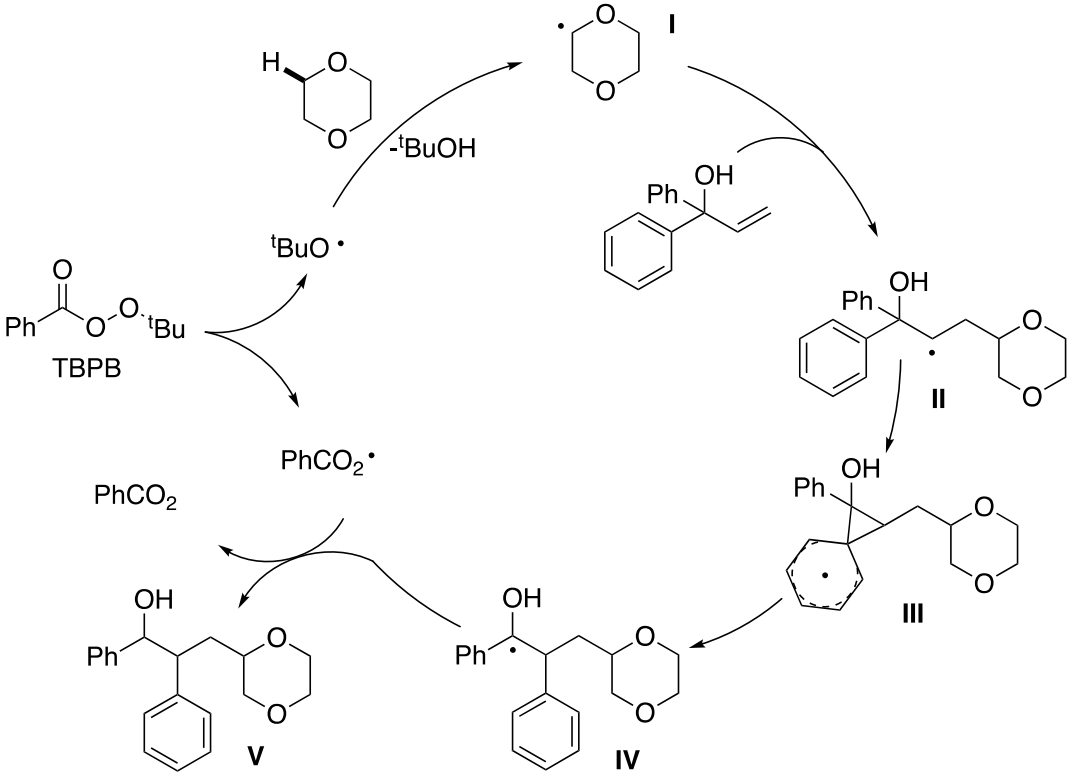

Scheme 18. Mechanism of C*sp*^{3}-H alkylation of ethers with diaryl allylic alcohols

In this example, they disclosed an efficient radical-mediated addition reaction of alcohols with alkynes. The mechanism is supposed to go through a peroxide initiated C–H bond activation, giving the allylic alcohol product in moderate to high yields.

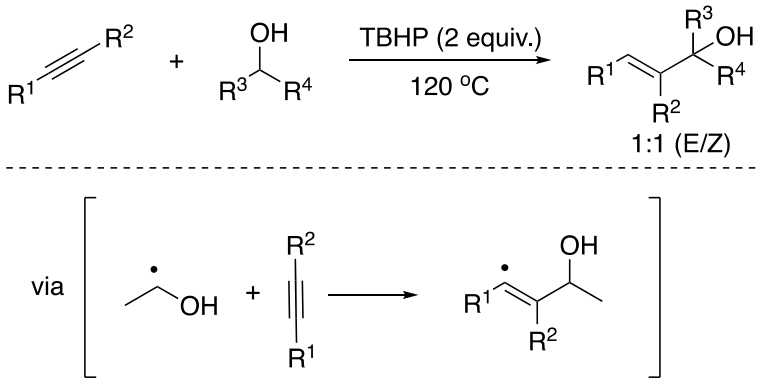

Scheme 19. Allylic alcohols formation via radical addition of aliphatic alcohols and electron-rich alkynes

This reaction is suitable for a large range of aliphatic alcohols and a radical addition chain process was proposed as shown in Scheme 19. In parallel, other research group have described a series of direct α-alkenylation reactions of ethers with alkynes using TBHP as an external oxidant.[100-101] Arylation and heteroarylation reactions are attractive methodologies for the construction of C-C bonds. For instance, in 2011, Wang and co-workers established a new protocol for the oxidative coupling of azoles with ethers (Scheme 20).[102] The use of TBHP was found to be essential under metal-free condition for the arylation of ethers. The authors proposed a free-radical process[99] initiated by the homolytic cleavage of TBHP, followed by hydrogen abstraction. They suggested that the carbon-carbon bond is formed by the cross-termination of two radicals generated from starting materials. We proposed that the sp^3 C-H bond is homolytically cleaved, forming the corresponding alkyl radical which would then be reactive towards the heteroaromatic benzoxazole or analogues, and prone to addition at electron deficient locations. More importantly, this procedure is a very simple and powerful green process for alkylation of heteroarenes.

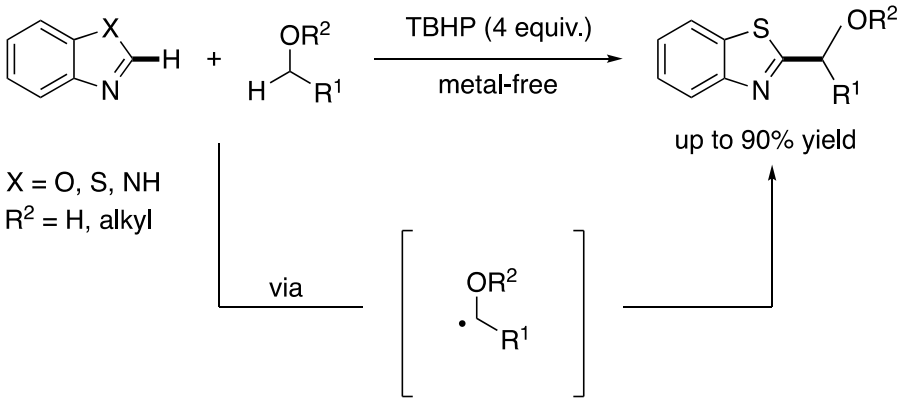

Scheme 20. Alkylation of azoles with alcohols and ethers through dehydrogenative cross-coupling

As previously mentioned, the oxidative cross-coupling reaction became a very useful method to construct C-X (X = O, N, S) bonds. In fact, the construction of the C–O bond via a α-C–H bond functionalization of a heteroatom is one of the hot topics in the area of C-

H bond activation.[103-106] In 2011, Wan and co-workers reported a radical coupling of carboxylic acids with ethers using TBHP as oxidant under metal-free conditions.[107] A series of α-acyloxy ethers was synthesized with a large functional groups tolerance. The authors described the reaction mechanism as a SET process as shown in Scheme 21.

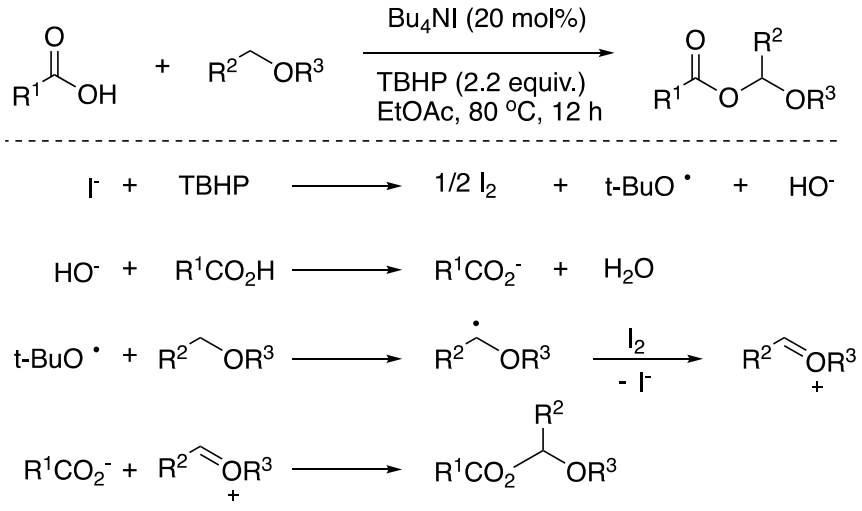

Scheme 21. Bu_4NI catalyzed C-O bond formation via CDC reaction

The peroxy radical abstracts a hydrogen atom from the ether substrate to form an alkoxyl radical, then this alkoxyl radical is converted into an oxonium ion via a SET process. Finally, the nucleophilic attack of the oxonium ion with the carboxylic anion provided the desired product. Later, in 2013, Duan and co-workers expanded this protocol to the synthesis of α-acyloxy ethers under metal-free conditions using TBAI and TBHP as oxidizing system.[108]

The formation of C-N bond under metal-free conditions has also spiked interest in the C-H bond functionalization field since the construction of nitrogen containing organic compounds remains a top research topic.[109-111] Further work by Du and co-workers developed alternative methods for C-N bond formation by a TBAI/TBHP mediated direct amination of ethers with a large variety of amines (Scheme 22).[112] The authors proposed the oxidation of ether to the corresponding oxonium ion, by hydrogen abstraction and single electron transfer pathway. Similarly, the group of Hu developed hypervalent iodine

mediated mild and versatile amination reaction, in presence of NaH.[113] This amination reaction occurs at room temperature without transition metal catalyst and the authors showed the significance of this strategy in synthesizing anti-cancer pro-drug and analogues.

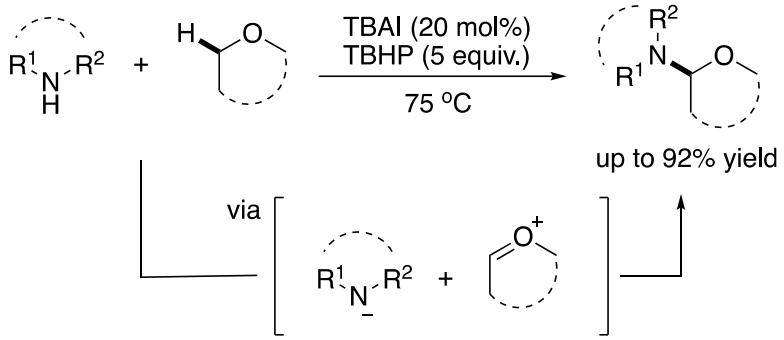

Scheme 22. Organocatalytic amination of alkyl ethers via TBAI/TBHP catalytic system

Less common but as attractive as the building of C-N bonds, C-S bond formation is of interest for the generation of pharmaceutical, biological and natural useful compounds.[114] The C-S bond can be generated with an oxidative system under metal-free condition through a transition metal catalyzed procedures with Pd, Cu, Rh, Ru and Fe,. In 2011, Li and co-workers developed a TBHP mediated oxidative thiolation of a Csp^3-H bond adjacent to a nitrogen atom under metal-free condition.[115]

1.3.2. **Functionalization of unreactive C-H bonds**

While recent reports of C-H bonds functionalization using late transition metal catalyst continue to emerge, significant concerns arise from their toxicity and their cost efficiency. During the development of new catalyst system, it has been found that first-row transition metals generally undergo single electron transfer processes. Direct C–H bond functionalization via a radical pathway has emerged as a promising approach toward molecular construction with high atom- and step-economy.

As mentioned previously, the transition metal C-H activation occurs under specific conditions and forms correspondingly C-M bonds. Another type of C-H bond activation occurs via the loss of one proton. By SET, the corresponding radical is formed (Scheme 23) and can get further oxidized towards the formation of the corresponding cation. Radicals and radical cations are very reactive intermediates and possess relatively specific range of properties and reactivities.[116] Indeed, they have nucleophilicity and electrophilicity, and can undergo hydrogen abstraction and self-coupling reactions.

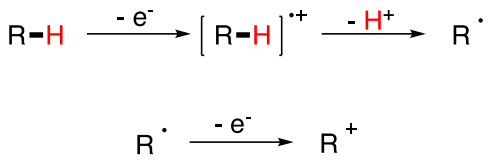

Scheme 23. C-H activation via SET pathway

1.3.2.1. Directed C-H bond functionalization

The directed or guided methodology features the coordination of a metal center to a proximal organic group, guiding the metal towards a specific position. Commonly called "coordination-directed metalation", this strategy has to be seen as complementary to the innate strategy.

The directed strategy was for the first time revealed by two independent discoveries in 1939 and 1938 by Gilman and Wittig, while they were developing a method to metalate an organic molecule with an organolithium reagent.[117-118] Gilman observed the formation of carboxylic acid at the C_1 and C_3 position of 2-methoxydibenzofuran with 60% yield, after reaction with n-butyl lithium followed by subsequent carbonation (Scheme 24). The coordination of the lithium cation to the Lewis-basic oxygen heteroatom, enhanced its basic properties and guided its proximity towards the proton at the C_1 and/or C_3 positions. The aryllithium intermediate formed by deprotonation is highly reactive and rapidly generates the corresponding carboxylic acid derivative by carbonation reaction.[119] During the same period, Wittig demonstrated that anisole derivatives undergo the same ortho-deprotonation in the presence of n-BuLi and react with carbon dioxide to yield the

corresponding carboxylic acids. Although initial yields were relatively low, the high regioselectivity attracted interest. These results were evaluated and developed to a general synthetic strategy: the so-called direct ortho-metalation.

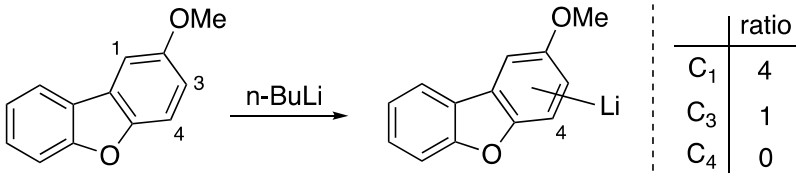

Scheme 24. First example of proximity effect deprotonation

Since the pioneering development of DoM, many different heteroatom-based directing groups have been evaluated.[120] Despite their efficiency to selectively functionalize the ortho-positions of the directing groups, this method relies on the stoichiometric use of organolithium reagents or their equivalents, such as organozinc reagents.

During the development of DoM, numerous researchers found out that other transition-metals had abilities to perform metalation reaction under similar conditions. Thanks to the weak coordination with the directing groups, transition metals are positioned in the vicinity of only certain C-H bonds and, therefore, only selected C-H bonds can be activated. This strategy was then termed “coordination-mediated metalation”. According to the definitions, the metallic systems generated after C-H activation and C-M bond formation, are labelled as cyclometalated complex species (see Scheme 25). Chronologically, the first example of guided C-H functionalization of organic molecules was established by Kleiman and Dubeck in 1963.[121] They discovered the formation of nickelacycles from a stoichiometric amount of zinc complex and azobenzene. Later in 1965, Cope and Siekman developed the analogous reaction of azobenzene with platinum and palladium transition metal complexes.[122] Using nitrogen heteroatom as coordinating group to transition metals, a few examples of C-H activation reactions were achieved with different azobenzene derivatives.[123-126]

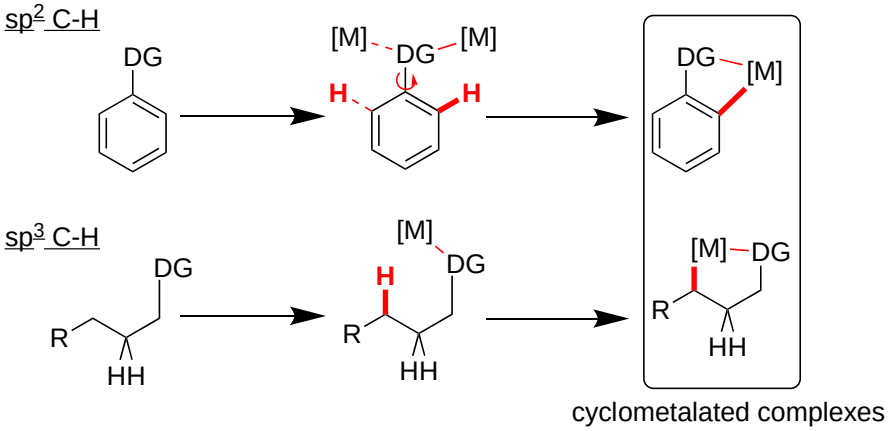

Scheme 25. Cyclometalated complexes

To generalize this strategy, numerous Lewis base ligands can position the transition metals close to an adjacent C-H bonds. Directed metalation groups are formally categorized in two classes: carbon and heteroatom based, referring to the atom which directly connects the DMG to the aromatic ring (Scheme 26).[127-134]

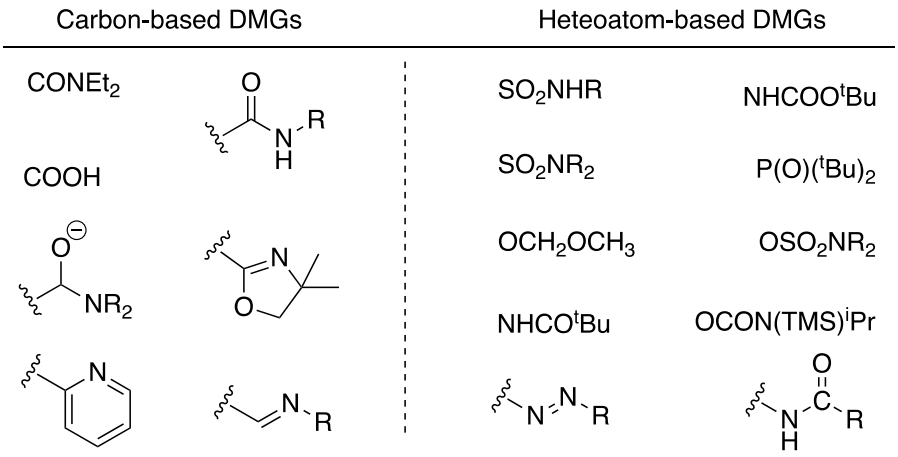

Scheme 26. Selected carbon and heteroatoms-based DMGs

Over the years, the number of functional groups amenable to be used as directing groups have seen a tremendous enhancement. These heteroatoms are generally N, O, P, S (as shown in Scheme 26) but some examples encompassing other heteroatoms are also known. Even if a wide diversity of DGs are available, limitations appeared since the metals

used for these stoichiometric transformations were expensive and the applications were not significant enough, albeit some examples.[135] Over the past thirty years, the development of directed C-H functionalization reactions has resulted in the general usage of numerous transition metals such as palladium,[48, 50] ruthenium,[136-139] rhodium,[140-141] copper,[106, 142] nickel,[143] iron,[36] cobalt,[144] etc.

1.3.2.2. Variety of functional directing groups for C-H functionalization reactions

After the emergence of the C-H bond activation chemistry in the 1970s, Murai and co-workers reported in 1993 the first synthetically useful directed catalytic C-H bond functionalization reaction (Scheme 27).[145] This work involved ruthenium catalyzed selective ortho-alkylation reaction of aromatic ketone with an olefin. The process displays the carbonyl group as a potential directing group to succeed selective metal mediated ortho functionalization of aryl ketone. Analysis of this process shows that the use of olefin is limited to terminal alkene and vinylsilanes derivatives, which do not possess allylic hydrogens. Thanks to this discovery, the ketone directing group was used in many reactions by Murai and others during the following years.[146-148]

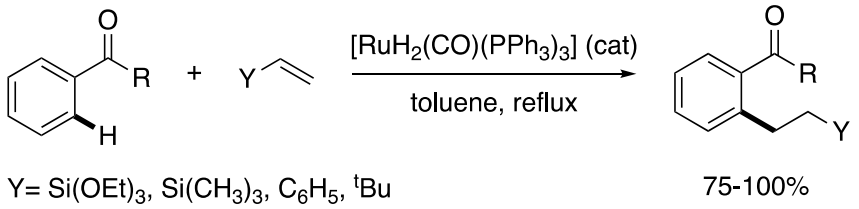

Scheme 27. First example of directed C-H functionalization

Pyridine chelating fragment has also been widely employed to perform selective ortho C-H functionalization. Specifically, 2-phenylpyridines derivatives were employed as substrate subject, or as a proof-of-concept for novel C-H bond functionalization reactions. Classified as a "typical" directing group in modern organic chemistry, the pyridine moiety was an efficient chelating guiding group for arylation,[149-150] alkylation[151-153] and acylation[154-156] reactions of sp^2 C-H bonds (Scheme 28).

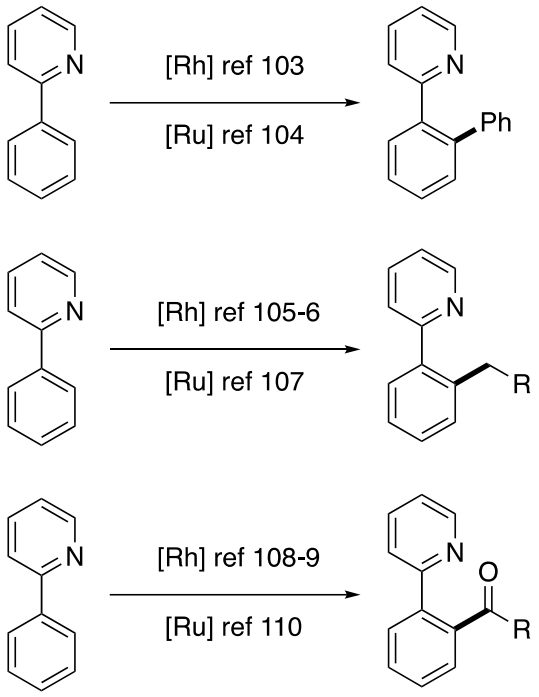

Scheme 28. Examples of pyridine guided C-H functionalization reactions

Despite the excitement of developing more efficient directing group such as pyridines, oxazoles, pyrimidines, oxazolines, pyrazoles etc;[157-160] it is possible that DGs are no longer needed after the C-H activation reaction. Sometimes, these highly efficient DGs are very difficult to remove or cannot undergo further modification or functionalization. Moreover, with the growing field of green chemistry,[161-162] the need of greener reactants and reaction conditions does not match the use of dificult and or non-removable DGs. The extensive research has led to the development of guiding groups that can perform multiple tasks such as oxidizing DGs, incorporated DGs, modifiable DGs or even traceless DGs.

Oxidizing DGs[163-166] represents a viable opportunity to remove any oxidant additives from a reaction condition. The DG contains a covalent bond which is the responsible for the oxidation of the transition metal, allowing to reduce waste generated by external oxidants. Generally, these types of guiding moiety are N-based ligands and possess N-O bond to play the role of oxidants (Scheme 29).

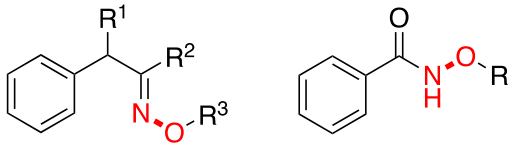

Scheme 29. Directing groups with internal oxidant

According to the principles of green chemistry, and particularly its atom-economic aspect, an optimized DG must remain on the synthesized molecules. With this in mind, scientists have demonstrated the achievability of this challenge using, for instance, alcohol as a DG.[167] This concept, although extremely interesting and useful in total synthesis, is scarcely developed. In Yu's work, the hydroxyl-directing group strategy was employed to guide the palladium catalyst. After the insertion of carbon monoxide into the C-Pd bond, a reductive elimination of the palladium(II) occurred and consequently, the substrate formed an ester from the hydroxyl-DG and the carbon monoxide (Scheme 30). Similarly, in 2011 Lautens and co-workers showed the potential activity of ketimine DG to conduct C-H activation reactions and incorporated the DG to the final product.[168] They combined aryl triflates and aryl ketimines to produce phenanthidinine derivatives (precursors of Nitidine and NK109), using palladium as a catalyst.

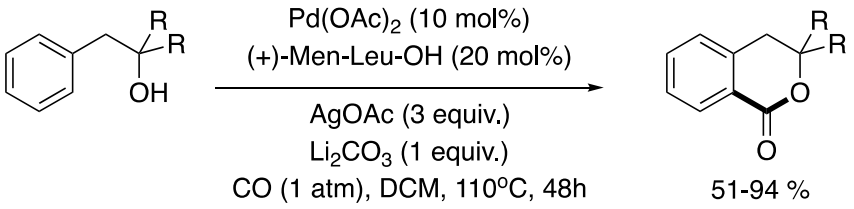

Scheme 30. Hydroxyl-directed C-H carbonylation

Modifiable and traceless DGs belong to a type of DG that, after proper orientation of the reaction, the guiding group is either transformed or removed by reaction with an external reagent. Cutting edge advances in terms of traceless DGs were made using silyl-based DGs,[169-172] carboxylic acids[173-174] and imines.[175-178] Regarding the multi-tasking ability of DGs, the carboxylic acid functional group is a paradigm of this aspect. In fact, the

weak coordination to the metal center allows the regioselective reaction to occur, and its simple and wide potential transformation or incorporation to the target molecule makes carboxylic acid important DGs. In addition, the carboxylate functional group can act as traceless DG, orienting the reaction followed by decarboxylation reaction (Scheme 31).

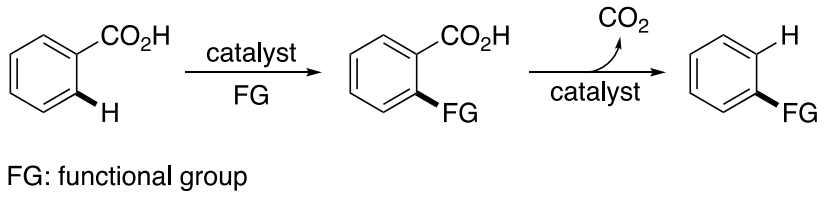

Scheme 31. CO_2H as a traceless promoter in C-H bond functionalization

The pioneer work of Daugulis and co-workers from 2007 features the use of carboxylic acid as DG for the regioselective functionalization of an aryl C-H bond followed by decarboxylation, through a bi-metallic and two steps process (

Scheme 32).[179] The investigators disclose in this work that the carboxylic acid moiety is removable by using copper oxide in presence of nitrogen donor ligand and NMP/quinolone solvent mixture. In the original publication from Gooßen, he observed that electron poor benzoic acid were more reactive towards decarboxylation reaction.[180]

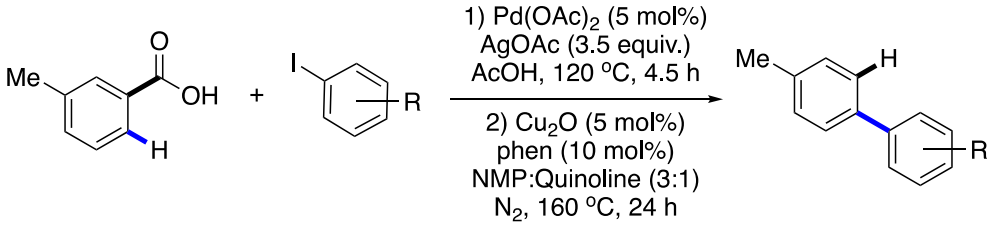

Scheme 32. First C-H bond arylation reaction via a CO_2H traceless DG

Keeping the same philosophy, people aimed to develop more efficient methodologies using carboxylic acid DGs. The contribution of realizing the same reactions through a one-pot process was a considerable improvement,[173, 181-183] but the optimal process remains

the use of a single catalyst for both reactions and decarboxylation in a one-step process.[184-189]

The metal mediated C-H functionalization reaction has become an efficient method for the site-selective derivatization of C-H bonds and is now broadly used in synthesis. The regioselectivity is controlled by two different strategies based on the electronic properties of the substrate and/or the help of an external guiding functionality. However, the use of cheaper and greener methods remains challenging due to the increasing practicality of the chemistry, the reaction cost and the sustainability of synthesis. Radical chemistry has led to many new advances in the C-H functionalization field since the last decades and represents a potentially environmentally-friendlier alternative.

1.3.2.3. Coupling of radicals and metal-carbon bonds

With the advances made on C-H functionalization reactions and the development of DGs, the combination of radical chemistry with a guiding methodology is of huge interest. Extremely reactive species, radicals are generally neglected for the design of a regioselective synthesis. However, with the help of a DG, the regioselectivity can be controlled. As mentioned above, the pyridine motif has strong abilities to orientate and position transition metal catalysts towards the vicinal C-H bonds, thus activating it. For instance, Li and co-workers achieved a palladium catalyzed directed ortho acylation of arenes with radicals issued from aldehydes (Scheme 33).[190] It is worth mentioning that this reaction is carried under solvent free conditions and yields the desired aryl ketones. According to the mechanistic studies undertaken, a Pd(II)/Pd(IV) catalytic cycle governs the reaction. The oxidation of the palladium(II) complex by peroxide in presence of aldehydes generates the formation of a palladium(IV) intermediate (Scheme 34).

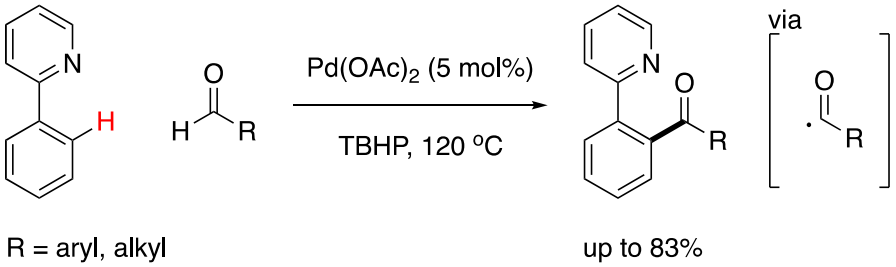

Scheme 33. Palladium catalyzed directed ortho acylation of arenes

Similar to 2-arylpyridine, a large variety of N-based directing groups were used for ortho Csp^2-H acylation reactions. Benzoxazole,[191] benzothiazole,[192] 3,5-diarylsoloxazoles[193] and 2,3 diarylquinoxalines[194] belong to the DG diversity, developed for acylation reactions of arenes with aldehydes, catalyzed by a $Pd(OAc)_2$/TBHP system.

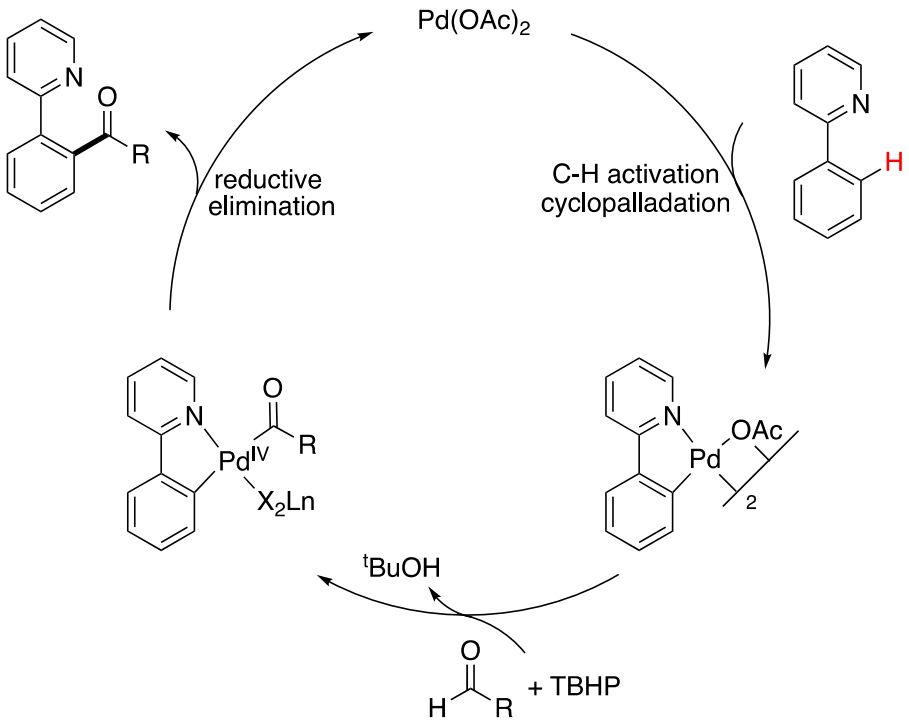

Scheme 34. Palladium catalyzed acylation of arenes – mechanism

Acylation of arenes were extended to many other substrates. For instance, the acylation of indoles was achieved by C-H bond functionalization. Using N-based DGs, the

regioselective introduction of acyl group at the C2 and C3 positions were accomplished using a $Pd(OAc)_2$/TBHP catalytic system (Scheme 35).[195-197]

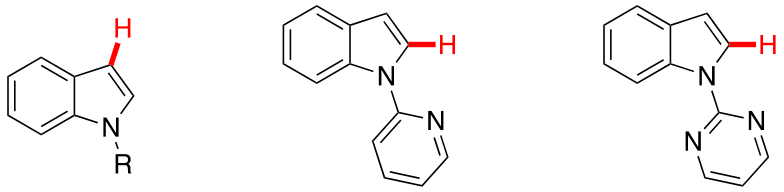

Scheme 35. Regioselective C-H acylation of indole with aldehydes catalyzed by $Pd(OAc)_2$/TBHP system.

A number of different DGs were found to be very efficient for acylation reaction of arenes. Some of them were developed to undergo C-H functionalization, followed by annulation reaction. In this aspect, a few examples shown by Zhao and co-workers, described a Pd-catalyzed C-H activation/annulation reaction with amides as DGs, for the synthesis of hydroxyl isoindolones.[198] Wang and Zhao reported a Pd-catalyzed intermolecular [4+1] annulation of 1,2-benzoisoxazoles from the coupling of N-phenoxyacetamides and aldehydes (Scheme 36).[199] It is notable that the method has been successfully applied to the synthesis of active pharmaceutical intermediates, such as risperidone. The authors proposed a Pd(II)/Pd(IV) catalytic cycle on the basis of DFT calculations.

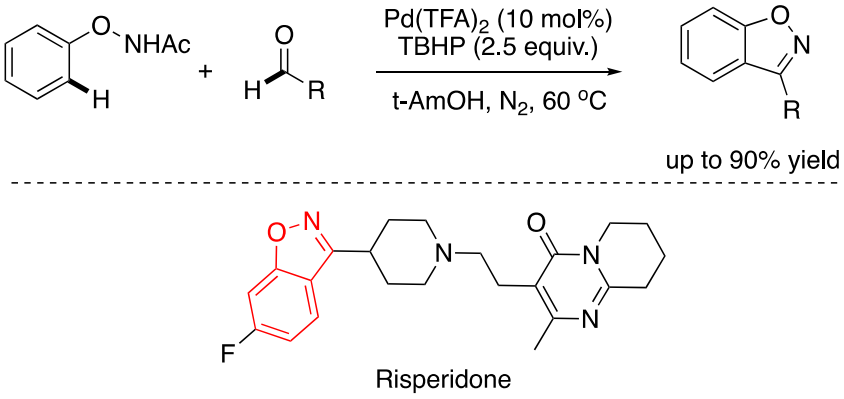

Scheme 36. Pd-catalyzed intermolecular [4+1] annulation of 1,2-benzoisoxazoles

As mentioned earlier, the functionalization of sp^3 C–H bonds is a unique and powerful transformation in modern organic synthesis. To convert C–H bonds into other functional groups towards the synthesis of a wide range of more complicated materials, such as polymers and bioactive molecules, remains a central challenge in catalysis and represents an area of invaluable and practical chemistry.[200-203] One of the most efficient and widely used strategies, is the use of weak coordinating auxiliary groups, coordinating with the transition metal catalyst. These methods were developed either by 1) intramolecular oxidative addition of the catalyst, positioning the metal close to the corresponding C-H bond or 2) by the traditional coordination of the catalyst to the functional auxiliary (Scheme 37).[175, 204-207]

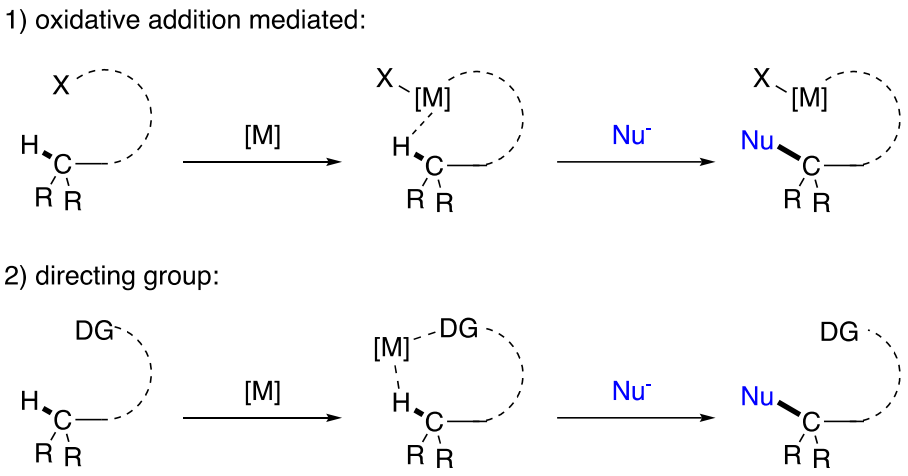

Scheme 37. Strategies for sp^3 C-H functionalization

The discovery of novel transformations that improve the step and atom economy of existing processes is the long-standing goal of synthetic chemists. In this regard, the role of a DG is arguable because of its limitations. In most cases, additional synthetic steps are often required to both install the DG into the starting material and to manipulate it after C–H functionalization.[208] Towards a greener alternative, the direct oxidative sp^3 C-H functionalization methodology was developed, allowing the cross-coupling of large variety of substrate without DG (Scheme 38).

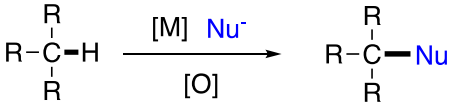

Scheme 38. Direct oxidative *sp*^{3} C-H functionalization

The radical strategy is not just efficient for the C-C bond formation but also for C-X bond formation.[104-106, 209] Numerous of research groups have contributed to advances in C-N and C-O bond formations. Among them, Hartwig and co-workers reported a copper catalyzed intermolecular amidation and imidation of unactivated alkanes, yielding the corresponding N-alkyl target products (Scheme 39).[210] The authors have observed that the amidation reaction occurs more favourably at secondary C-H bonds sites than tertiary sites. With CuI as catalyst and DTBP as external oxidant, the C-H cleavage of cyclohexane by tert-butoxy radical seems to be the rate determining step, on the basis of KIE and radical trapping experiments. By using CuBr as catalyst and TBHP as oxidant, Bolm and co-workers accomplished a dual C-H/N-H functionalization reaction.[211] Under these conditions, the coupling of sulfoximines and aldehydes provides a diverse series of N-acylsufoximines. This process was described by the authors as a radical mechanism pathway with a Cu(I)/Cu(II) catalytic cycle.

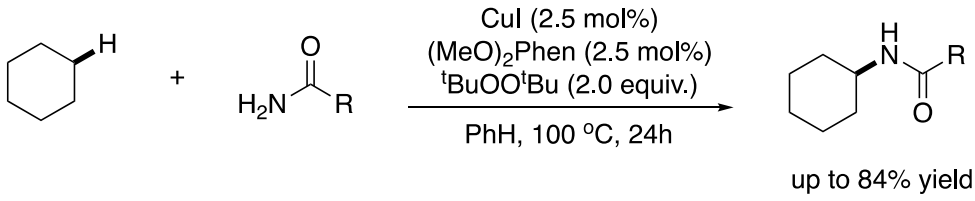

Scheme 39. Copper catalyzed intermolecular amidation of unactivated alkanes

Copper-catalyzed protocols for C–O bond formation have also attracted much investigation. Recently, in 2015, Li and co-workers described a new copper catalyzed oxidative coupling of acids with alkanes for the selective synthesis of allylic ester and alkylalkenes.[212] This method characterizes a novel strategy for unactivated C*sp*^{3}-H oxidative esterification of acids and alkanes. Some experiments were investigated to

better understanding of the mechanism and the author concluded that the coupling proceeded through a radical pathway with a Kharasch-Sosnovsky mechanism.[213-215]

Alongside the coupling methodology between radical and C-H bonds, a large range of transition metal catalysts have been used. As shown above, palladium and copper were the most popular in this type of chemistry, but examples with Ni, Mn or Fe were also described. For instance, You and co-workers developed a coordinating activation strategy to illustrate a nickel-catalyzed radical oxidative coupling of α-Csp^3–H bonds of amines with (hetero)arylmethyl free radicals.[216] Groves, in 2013, used manganese porphyrins as catalyst for C-H benzylic fluorination via easily handled nucleophilic fluoride reagents (TREAT.HF) without any DGs.[217] Later Han and Pan developed an iron catalyzed cross-dehydrogenative coupling esterification of inactive Csp^3-H bonds with carboxylic acids for the synthesis of α-acyloxy ethers.[214]

Most of such strategies that perform C-H bond functionalization reactions have prerequisites including at least one metal catalyst and, most often, prefunctionalization of both coupling partners. Transition metal catalysts are associated with high costs as well as toxicity, whereas prefunctionalization of coupling partners adds extra steps to the whole synthetic scheme.

1.4. Mechanisms

The focus of this section is to describe the different C-H activation reaction mechanisms that operates via organometallic routes, i.e., those in which a bond is formed between the metal centre and the carbon undergoing the reaction. An overview of classical mechanisms is presented amongst a very large and highly active field.[218] There are three accepted mechanisms of C-H bond cleavage – namely, electrophilic activation, oxidative addition and the σ-bond metathesis - which will be detailed in the following paragraphs.[219-221]

1.4.1. Electrophilic activation

In 1972, Shilov published a dramatic advance on his earlier report of C-H activation with Pt(II) (Scheme 40). The addition of Pt(IV) to the aqueous reaction lead to the

production of oxidized species methanol and methyl chloride, but this reaction is stoichiometric in Pt(IV).[222]

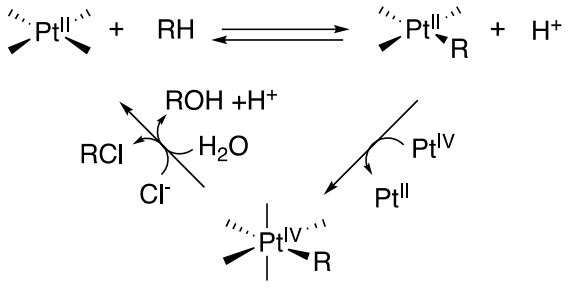

Scheme 40. Proposed mechanism for Shilov's platinium catalyzed alkane oxidation

The final step of the Shilov cycle, occurs via nucleophilic attack at the carbon center. The mechanism of the C-H activation step which forms the Pt(II)-methyl intermediate was evaluated using computational methods and it was found that an electrophilic mechanism for C-H activation was favored over other type of C-H activation pathways.[223] Others have pursued investigation following from Shilov's original observations and numerous systems involving oxidation of alkanes by metal cations in acidic solution have been reported. For instance, Sen reported an interesting bimetallic electrophilic system for the selective oxidation of methane and alkanes using Pd(II).[224] Reactions classified as going through an electrophilic activation mechanism can be categorized to reactions catalyzed by late or post-transition metals [M^{x+2}] (Pd^{2+}, Pt^{2+}/Pt^{4+}, Hg^{2+}, Tl^{3+}), usually in a strongly polar medium such as water or anhydrous strong acid.[225-227] Reactions categorized as such, result in functionalized alkanes without any observance of organometallic species, as illustrated in Scheme 41.

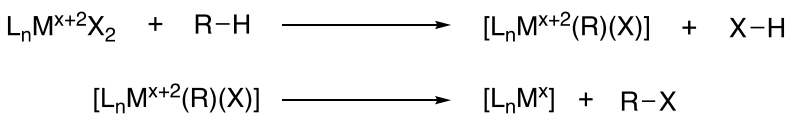

Scheme 41. Representative scheme for electrophilic activation of C-H bond

While these methods are very efficient, especially for methane oxidation, the yield and selectivity need improvement. As an opposite direction, observations from other research groups tend to describe mechanisms going through oxidative addition route.

1.4.2. **Oxidative addition**

The oxidative addition is a traditional term used to describe a type of reaction in which transition metal catalyst inserts into a C-H bond. This reaction oxidizes the metal center from its original oxidation state M^x to M^{x+2} (Scheme 42).

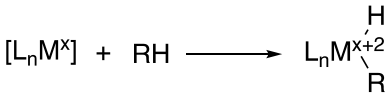

Scheme 42. Representative oxidative addition of C-H bond to a metal

Oxidative addition reactions generally occur with electron-rich, low-valent complexes of the late transition metals such as Re, Fe, Ru, Os, Rh, Ir, Pt, etc. The reactive species L_nM^x is usually generated in situ by thermal or photochemical decomposition from a stable precursor.[228]

1.4.3. **σ-bond metathesis**

The existence of stable agostic complexes (Scheme 43, path b) with C-H bonds coordinated to metal centres suggested that C-H bond activation might involve the initial formation of a so-called sigma (σ-)complex.[229] No stable σ-complexes have yet been isolated, but a substantial body of evidence suggests that they do exist. The σ-complex can form a metala-cyclic transition state, activating the C-H bond and functionalizing it. However, the bond cleavage step may not be straightforward because ligand dissociation often precedes ligand interconversion.[230] After numerous studies, σ-bond metathesis mechanism is generally described by the reaction of a reactive complex with an empty σ-type molecular orbital and a high energy molecular orbital containing an electron lone pair which will be transferred into the σ* orbital of the C-H bond during the oxidative addition reaction.[231] As an example, transition metal complexes with d0 configuration (ex:

Cp_2ZrRCl, WMe_6…) often undergo a concerted process (Scheme 43, path b) as oxidative addition reaction (Scheme 43, path a) is forbidden.

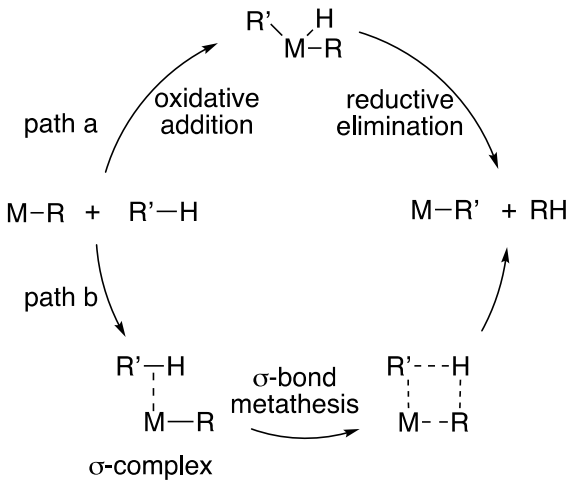

Scheme 43. Representative scheme for σ-bond metathesis of C-H bond

To conclude this part, the exact pathway of C-H bond activation is generally difficult to predict and typically depends on the identity of the metal, its oxidation state, and the ancillary ligands.

1.5. Application of C-H functionalization methodology

Amongst the recent methodological advances, the transition-metal mediated C-H activation processes has revolutionized the field of organic synthesis in a unique manner. The advances and the effectiveness of C-H functionalization logic offers great potential economic value.[232] In this regard, the field of total synthesis research field would be a natural extension and will strengthen the utility of C-H activation processes beyond academic curiosities.[233] Moreover, many other fields in needs of improvement to achieve higher levels of recognition in industry and, or currently hot research fields would benefit from this C-H functionalization area.

1.5.1. **Application in total synthesis**

C−H functionalization is revolutionizing the way that organic chemists approach the synthesis of target molecules. Several reviews have been published discussing the potential of this new way of thinking for complex target synthesis.[234-236] Early in the 20th century, Löffler and Freytag discovered the first total synthesis of nicotine via a regioselective C-H abstraction from N-radical, generated under photochemical conditions (Scheme 5).[19] One of the most influential chemists who illuminated this application is Phil. S. Baran. He contributed to the strategic analysis of C-H bond disconnections and illustrated it in various reviews and publications.[16, 56, 83] He achieved the total synthesis of cortistatin A, an unusual *abeo*-androstane steroid isolated from a marine sponge that selectively inhibits proliferation of HUVEC cells, by using C-H bond functionalization (Scheme 44). Designing the retro-synthesis of cortistatin A from a readily and available homologous steroid, they opted for the use of prednisone.

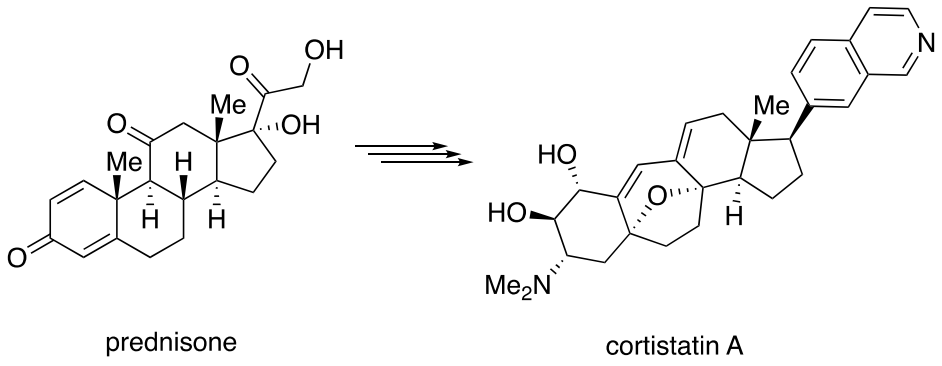

prednisone cortistatin A

Scheme 44. From prednisone to cortistatin A using C-H bond functionalization

The strategy was via the dibromination of the C-19 methyl group shown in Scheme 45. In presence of Br_2 and $PhI(OAc)_2$, acetyl hypobromite is generated. Subjected to light and acetyl hypobromite, the C-19 methyl group could be directly brominated. The reaction was kept under low temperature to favor the dibromination and supressed the etherification from the axial alcohol group. This C–H activation strategy allowed for the preparation of cortistatin A in only 13 steps from prednisone, and was extended to a gram-scale production.[237]

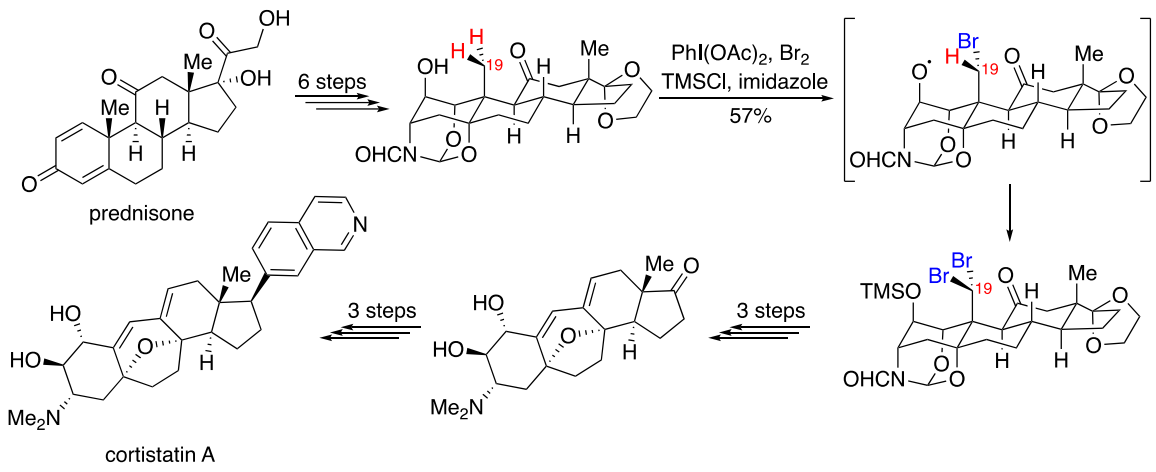

Scheme 45. Selective dibromination enable synthesis of cortistatin A from prednisone

Another quite recent and famous example of total synthesis using C-H functionalization was developed by Ellman and Bergman.[238] In 2005, they achieved the total synthesis of (+)-lithospermic acid by asymmetric intramolecular alkylation via C-H bond activation. In Scheme 46, they proposed the rhodium catalyzed annulation reaction to produce the corresponding dihydrobenzofuran ring.

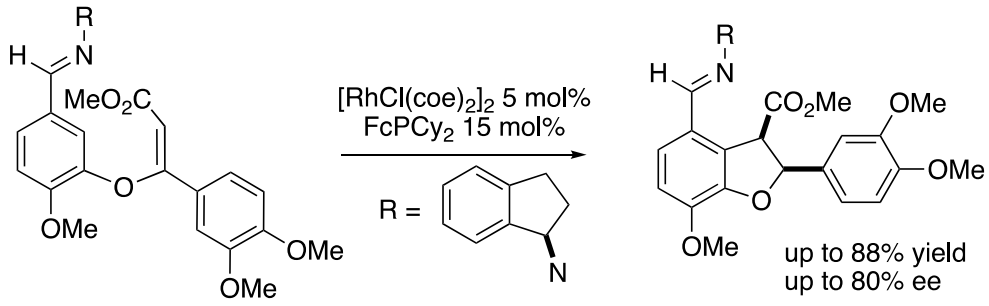

Scheme 46. Asymmetric cyclization using chiral imines

It is notable that this system represents a very challenging process for C-H activation since it is densely functionalized. The overall total synthesis of (+)-lithospermic acid was achieved in only 10 steps with an overall yield of 5.9% (Scheme 47).

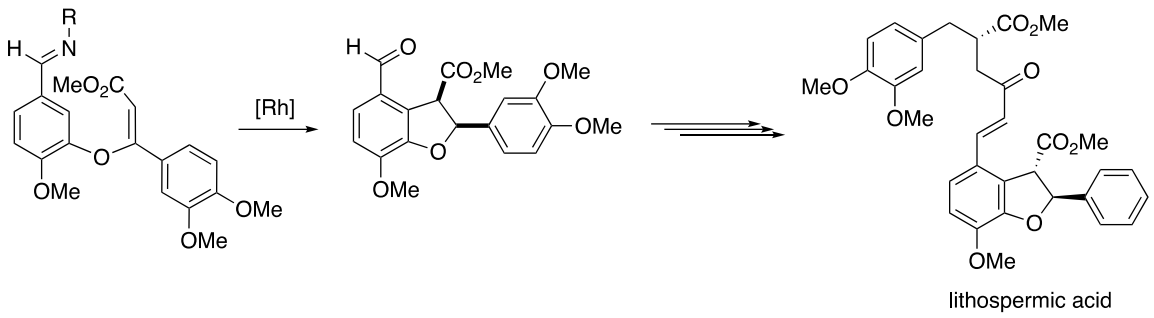

Scheme 47. Selected C-H activation step from lithospermic acid total synthesis

More recently, the total synthesis of natural (-)-quinine and analogues was described by Maulide and co-workers.[239] The quinine analogues exhibit enhanced antimalarial activity compared to the natural (-)-quinine when evaluated in vitro and in infected mice. To achieve the total synthesis of (-)-quinine, the authors proposed the novel C-8/C-9 and C-3/C-10 disconnections (Scheme 48). Based on the pioneering work of Daugulis and co-workers,[240-242] the authors used similar picolinamide directing group for the *sp*^{3} C-H activation.

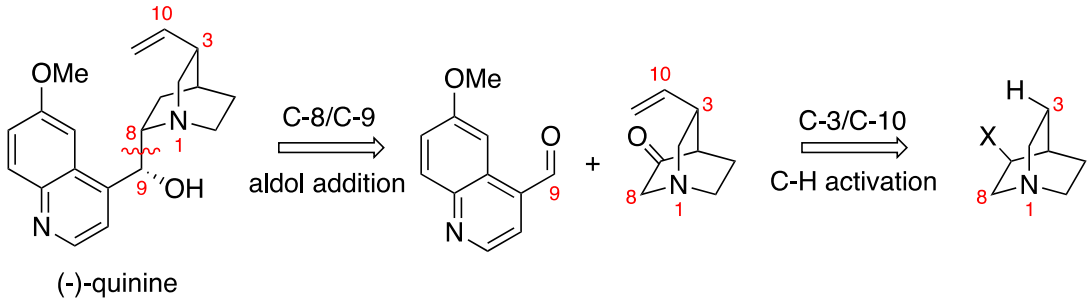

Scheme 48. Overview of novel retrosynthetic approach to (-)-quinine

Starting from 3-aminoquinuclidine, the directing group was easily introduced from the picolinic acid. Once the directing group installed, the evaluation of conditions concluded that Pd(OAc)2 with aryl iodide was the best conditions to perform the cross coupling reaction as shown in Scheme 49.

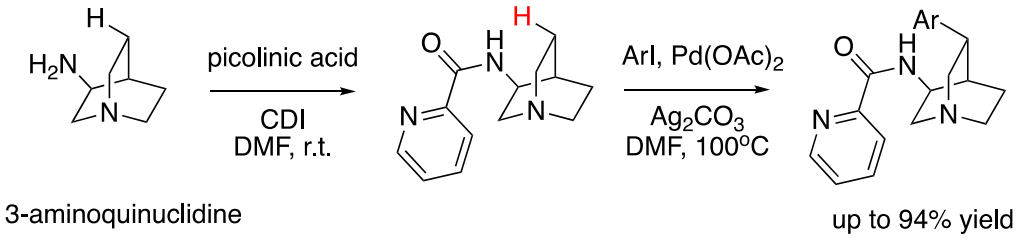

Scheme 49. *Sp*^{3} C-H arylation of quinuclidine

The synthetic examples highlighted above represent only a minor fraction of the total synthesis processes which were developed using the C-H functionalization strategy. This approach is considered extremely effective for generating various types of complex natural products, including steroids, alkaloids and so on. Selective C–H functionalization remains an immature field and sometimes still requires harsh conditions. However, organic chemists already believe in the full potential of C-H activation processes and their applications in multicomponent synthesis.

1.5.2. **Application in multicomponent synthesis**

The combination of chemical transformations in the manner of multicomponent reactions with C-H bond functionalization represents a beneficial tool in the synthesis of small organic molecules. Such reactions provide a platform for the rapid generation of high molecular diversity and complexity by making use of the advantages of both multicomponent reaction and the selective C-H functionalization. In recent years, with the worldwide and overwhelming interest in the concept of sustainability, the chemistry field progressed very rapidly towards more sustainable synthesis, such as developing multicomponent reactions among many others. A classical example is the A^3 coupling reactions developed in the laboratory supporting the investigation presented in this work, involving an alkynyl *sp* C-H activation.[243] Since this topic has been described in reviews,[244] this section illustrates only a few MCR examples related to *sp*, *sp*^{2} and *sp*^{3} C-H functionalization.

In 2013, Rueping and co-workers developed a visible light mediated heterogeneous C-H functionalization using recyclable TiO_2 catalyst.[245] The application of TiO_2 in

photocatalytic transformation is highly sustainable and is well documented for the oxidation of alcohols to carbonyl compounds[246-248] and amines to imines.[249] They designed α-functionalization of N,N-dimethylaniline in the oxidative Ugi-type reaction (Scheme 50).

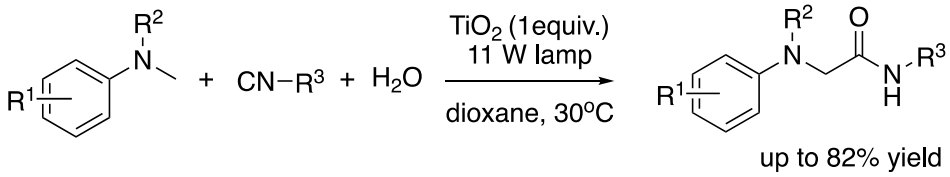

Scheme 50. Photoredox multi-component Ugi-type reaction catalyzed by TiO_2 metal oxides

A large variety of N,N-dimethylanilines and different isocyanides were tolerated under these conditions affording the corresponding α-amino amides in moderate to good yield. The author conducted catalyst recycling evaluation by centrifugal separation and the TiO_2 catalyst was reused without loss of activity. They proposed a reaction mechanism as shown in Scheme 51. The first step is suggested to be the oxidation of the amine center into iminium ion from light and TiO_2. The nucleophilic attack of isocyanide follows to form the nitrilium ion. This species is trapped by water and then tautomerizes to the corresponding α-amino amides.

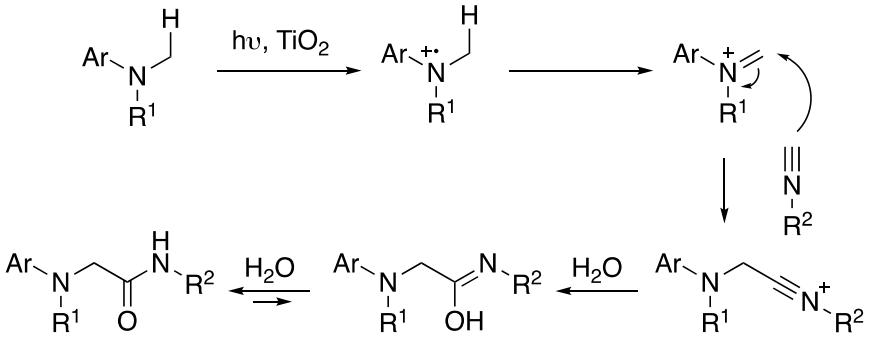

Scheme 51. Mechanism of photoredox Ugi-type reaction

Another very beautiful and efficient multicomponent example which involves *sp*^{3} C-H functionalization was described by Meshram and co-workers.[250] They developed the reactions of methyl ketones, o-tosylhydroxylamines and pyridine-2(1H)-one catalyzed by copper for the synthesis of imidazole fused heterocycles. This reaction shown in Scheme 52, occurs very rapidly and goes through a C-H activation step under microwave irradiation.

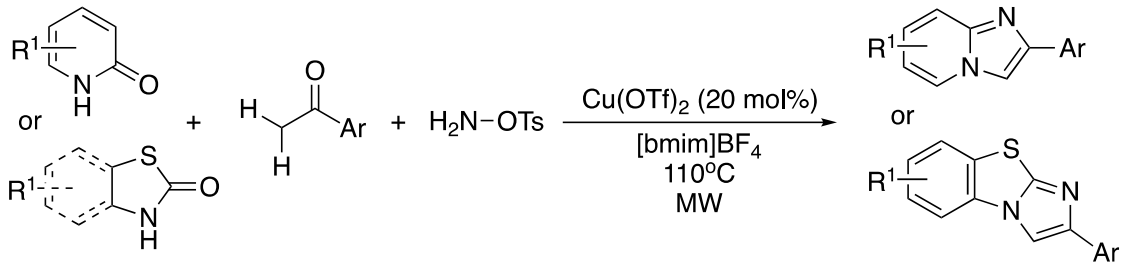

Scheme 52. Copper catalyzed MCR for the synthesis of imidazo-heterocycles

In recent years, the research on C-H activation reactions was essentially focused on *sp*^{2} C-H bonds compared to their corresponding analogues *sp* and *sp*^{3} C-H bonds. Thus the MCRs involving *sp*^{2} C-H bond functionalization are much more diverse. A good illustration of this topic was described by Zhu and co-workers in 2007.[251] They reported a three component process for the synthesis of 3-(diarylmethylene)oxindoles from N-aryl-N-alkyl propiolamides and two different aryl iodides. In presence of $Pd(PPh_3)_4$ and CuI, the mechanism follows a Sonogashira type coupling and a carbopalladation by *sp*^{2} C-H aryl bond activation. However, this example is a sequential multicomponent reaction, since the aryl iodides were added stepwise because of their similarity in reactivity. The corresponding 3-(diarylmethylene)oxindoles were obtained with a maximum of 82% yield, as shown in Scheme 53.

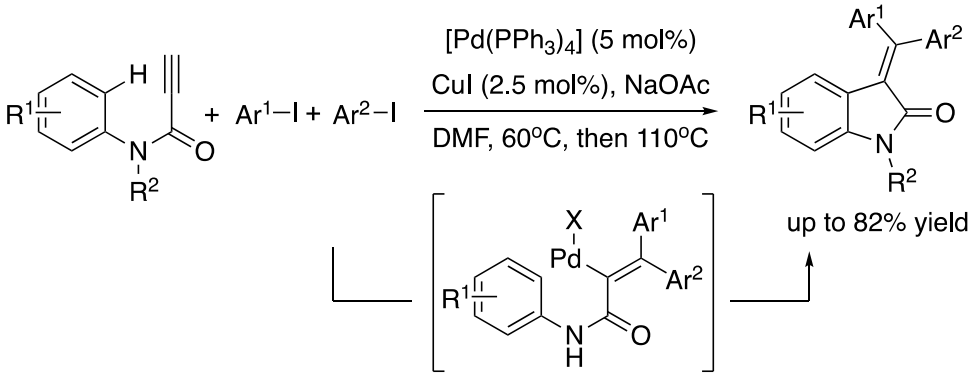

Scheme 53. Three-component synthesis of 3-(diarylmethylene)oxindoles via C-H bond activation

With the endeavour in developing more efficient and easily available directing group for C-H activation reactions, Wan and Liu discovered the multicomponent synthesis of *o*-arylated benzamides using *o*-aminophenol as directing group for C-H activation.[252] In presence of $Pd(OAc)_2$, the assemblies of benzoyl chlorides, aryl iodides and *o*-aminophenols provided the arylated products with broad substrate tolerance (Scheme 54).

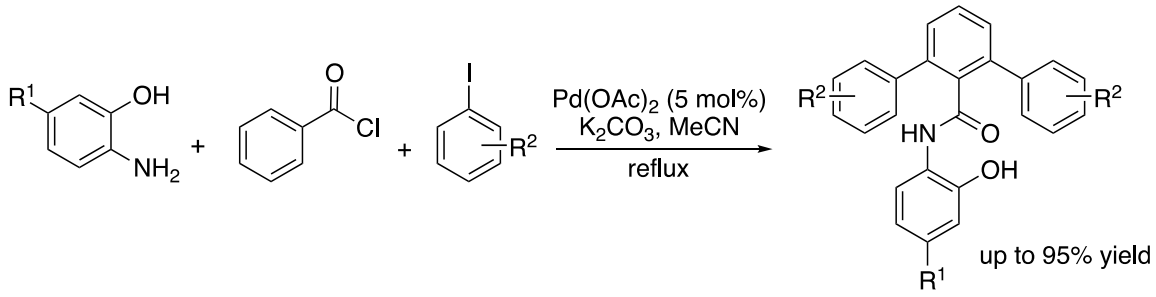

Scheme 54. Multicomponent *o*-aminophenol directed Ar-H arylation

The multicomponent coupling of arynes with Csp^2–H substrates and other suitable components constituted another type of useful method. Greaney and co-workers reported the palladium-catalyzed reactions of benzyne precursors with alkyl halides and alkyl acrylates for the synthesis of *o*-difunctionalized benzenes (Scheme 55).[253] Compared with traditional methods using organometallic reagents, Greaney and co-workers

illustrated the power of developing sustainable reaction alternatives by functionalizing C-H bonds.

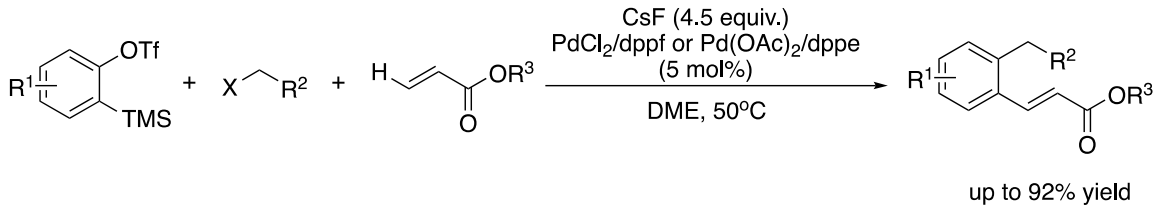

Scheme 55. Three-component coupling of benzynes

The *sp* C-H bond featured in terminal alkynes has been known to undergo transformation in a large variety of different organic reactions. Related to MCR, the use of terminal alkynes witnessed important advances in the past decades in the synthesis of diverse organic products via the transition metal-catalyzed transformation of this *sp* C-H bond. Closely related to the previous example, Cheng and co-workers reported in 2008 a three-component reaction of benzyne precursors with terminal alkynes and allyl halides (Scheme 57).[254] The authors suggested that the reaction proceeded through the formation of a π-allyl palladium intermediate and a copper acetylide, being involved in a transmetalation step.

Later, in 2011, Ogata and co-workers reported a highly chemoselective nickel catalyzed three component process between two distinct terminal alkynes and an internal alkyne (Scheme 56).[255]

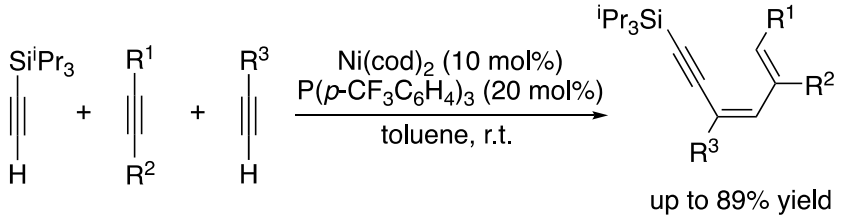

Scheme 56. Chemoselective nickel catalyzed three-component process between two distinct terminal alkynes and an internal alkyne

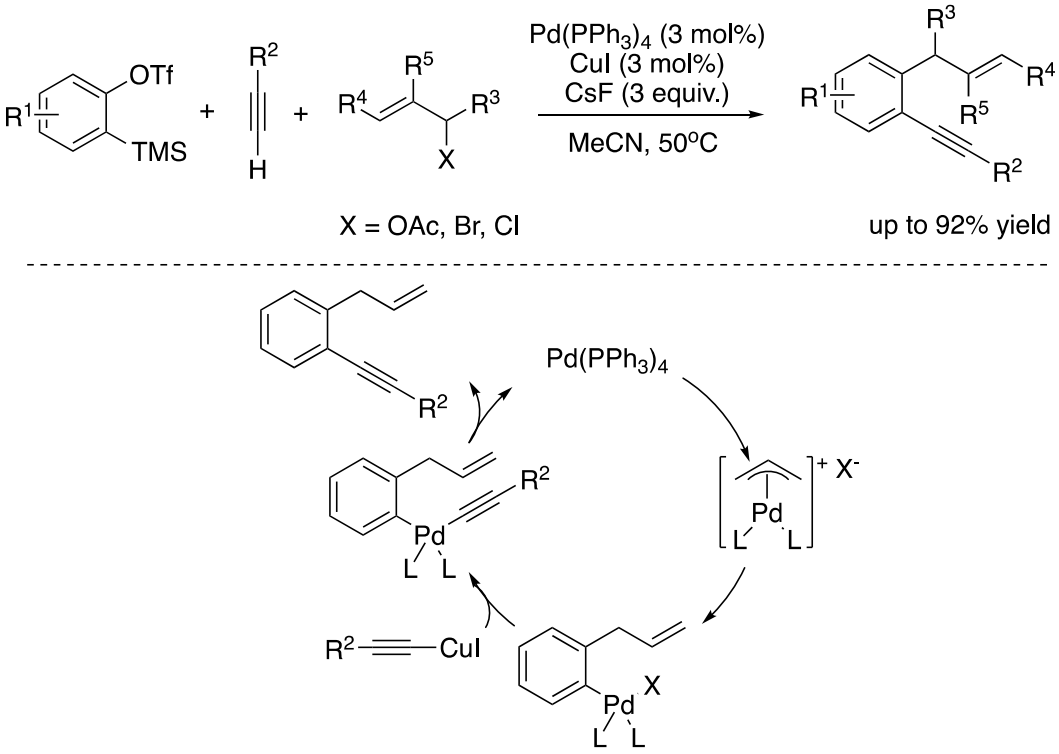

Scheme 57. Palladium-catalyzed three-component coupling of arynes with allylic acetates or halides and terminal alkynes

This method allows the rapid construction of conjugated enynes in presence of $Ni(cod)_2$. The authors suggested a mechanism with a series of nickel insertion into *sp* C-H bonds and insertion of the internal alkyne into the Ni-H bond. Related to this mechanism and briefly described above in introduction, the MCR A^3 coupling developed in Li's laboratory involves a terminal alkyne *sp* C-H activation (Scheme 58).

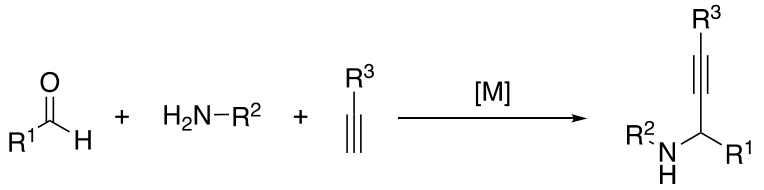

Scheme 58. MCR A^3 coupling catalyzed by transition metal

Typically, this reaction requires copper, silver or gold transition metal catalyst and produces propargyl amine derivatives from the coupling of aldehyde, amine and alkynes. Asymmetric reactions, heterogeneous catalysts and so on belong to the numerous variations that have been developed since its discovery.[256-258]

In conclusion, the use of C-H bond functionalization methodology has been extended to many different chemistry areas. The field is rapidly expanding to embrace the advantages offered by already known chemistry areas such as MCR and total synthesis among many others, driving the development of increasingly selective and efficient transformations.

1.6. Summary & outlook

A paradigm shift in the design of new reactions has been observed alongside growing environmental concerns. In the past few decades, methods have shifted from accessing target molecules at all cost to the design of more efficient reactions. The shift has allowed the use of simpler and readily available starting materials, permitting the exploitation of highly functionalized and complex structures. With the benefit of decades of development, C–H bonds functionalization is now seeing diverse applications such as in total synthesis and multicomponent reactions. Its tunability and ease of incorporation into tandem- and one-pot reactions make it a powerful transformation. Moreover, the late-stage functionalization of complex molecules and high-value compounds by C-H activation methods is strongly beneficial. In the future, the expansion of this portfolio is highly desirable, to allow more direct modification of wider varieties of compounds and structures. C–H activation is well positioned to become a useful synthetic technique in industry as well as in academia, in particular for applications where the classical coupling reactions is less advantageous technically, financially, and environmentally. Finally, the use of C-H activation will drastically increase the rate of creating molecular complexity.

1.7. References

[1] Bertz, S. H., *J. Am. Chem. Soc.,* **1981,** *103*, 3599-3601.
[2] Bonchev, D.; Trinajstić, N., *J. Chem. Phys.,* **1977,** *67*, 4517-4533.
[3] Shannon, C. E., *Bell Sys. Tech.l J.,* **1948,** *27*, 379-423.
[4] Rashevsky, N., Bull. Math. Biophys., **1955,** 17, 229-235.
[5] Mowshowitz, A., Bull. Math. Biophys., **1968,** 30, 175-204.
[6] Morgan, H. L., J. Chem. Doc., **1965,** 5, 107-113.
[7] Hendrickson, J. B.; Huang, P.; Toczko, A. G., *J. Chem. Inf. Comput. Sci.,* **1987,** *27*, 63-67.
[8] Chanon, M.; Barone, R.; Baralotto, C.; Julliard, M.; Hendrickson, J. B., *Synthesis,* **1998,** *11*, 1559-1583.
[9] Randić, M.; Plavšić, D., *Int. J. Quantum Chem.,* **2002,** *91*, 20-31.
[10] Böttcher, T., *J. Chem. Inf. Model.,* **2016,** *56*, 462-470.
[11] Hann, M. M.; Leach, A. R.; Harper, G., *J. Chem. Inf. Comput. Sci.,* **2001,** *41*, 856-864.
[12] Schuffenhauer, A.; Brown, N.; Selzer, P.; Ertl, P.; Jacoby, E., *J. Chem. Inf. Model.,* **2006,** *46*, 525-535.
[13] Ruijter, E.; Scheffelaar, R.; Orru, R. V., *Angew. Chem. Int. Ed.,* **2011,** *50*, 6234-46.
[14] Nicolaou, K. C.; Hale, C. R. H.; Nilewski, C.; Ioannidou, H. A., *Chem. Soc. Rev.,* **2012,** *41*, 5185-5238.
[15] Méndez-Lucio, O.; Medina-Franco, J. L., *Drug Discovery Today,* **2017,** *22*, 120-126.
[16] Gutekunst, W. R.; Baran, P. S., *Chem. Soc. Rev.,* **2011,** *40*, 1976-1991.
[17] Dumas, J. B., *Liebigs Ann. ,* **1840,** *33*, 187-191.
[18] Weissermel, K. A., Hans-Jürgen, *Industrial Organic Chemistry 4e*. Weinheim, **1978**.
[19] Kober, K. L. S., *Ber.,* **1909,** *42*, 3431–3438.
[20] Woodward, R. B.; Heusler, K.; Gosteli, J.; Naegeli, P.; Oppolzer, W.; Ramage, R.; Ranganathan, S.; Vorbrüggen, H., *J. Am. Chem. Soc.,* **1966,** *88*, 852-853.
[21] Barton, D. H. R.; Beaton, J. M., *J. Am. Chem. Soc.,* **1960,** *82*, 2641-2641.
[22] Barton, D. H. R.; Beaton, J. M.; Geller, L. E.; Pechet, M. M., *J. Am. Chem. Soc.,* **1960,** *82*, 2640-2641.
[23] Fenton, H. J. H., *J. Chem. Soc.,* **1894,** *65*, 899-910.
[24] Doller, D. H. R. B. a. D., *Pure Appl. Chem.,* **1991,** *63*, 1567-1576.
[25] Barton, D. H. R.; Doller, D., *Acc. Chem. Res.,* **1992,** *25*, 504-512.
[26] Stavropoulos, P.; Çelenligil-Çetin, R.; Tapper, A. E., *Acc. Chem. Res.,* **2001,** *34*, 745-752.
[27] Barton, D. H.; Csuhai, E.; Doller, D.; Ozbalik, N.; Balavoine, G., *Proc. Natl. Acad. Sci. U.S.A.,* **1990,** *87*, 3401-3404.
[28] Smythe, C. V., *J. Biol. Chem.,* **1931,** *90*, 251-265.
[29] Trost, B. M.; Godleski, S. A.; Genet, J. P., *J. Am. Chem. Soc.,* **1978,** *100*, 3930-3931.
[30] Blanksby, S. J.; Ellison, G. B., *Acc. Chem. Res.,* **2003,** *36*, 255-263.
[31] Bollinger, J. M.; Broderick, J. B., *Curr. Opin. Chem. Biol.,* **2009,** *13*, 51-57.
[32] Booker, S. J., *Curr. Opin. Chem. Biol.,* **2009,** *13*, 58-73.
[33] Sanyal, I.; Cohen, G.; Flint, D. H., *Biochemistry,* **1994,** *33*, 3625-3631.

[34] Escalettes, F.; Florentin, D.; Tse Sum Bui, B.; Lesage, D.; Marquet, A., *J. Am. Chem. Soc.,* **1999,** *121*, 3571-3578.
[35] Arndtsen, B. A.; Bergman, R. G.; Mobley, T. A.; Peterson, T. H., *Acc. Chem. Res.,* **1995,** *28*, 154-162.
[36] Shang, R.; Ilies, L.; Nakamura, E., *Chem. Rev.,* **2017,** *117*, 9086-9139.
[37] Meijere, A. d., Diederich, F., *Metal Catalyzed Cross-Coupling Reactions*. Wiley-VCH Verlag GmbH: **2004**.
[38] Negishi, E.-i., *Angew. Chem. Int. Ed.,* **2011,** *50*, 6738-6764.
[39] Suzuki, A., *Angew. Chem. Int. Ed.,* **2011,** *50*, 6722-6737.
[40] Ackermann, L.; Vicente, R.; Kapdi, A. R., *Angew. Chem. Int. Ed.,* **2009,** *48*, 9792-9826.
[41] Wencel-Delord, J.; Droge, T.; Liu, F.; Glorius, F., *Chem. Soc. Rev.,* **2011,** *40*, 4740-4761.
[42] Sun, C.-L.; Li, B.-J.; Shi, Z.-J., *Chem. Commun.,* **2010,** *46*, 677-685.
[43] Chen, X.; Engle, K. M.; Wang, D.-H.; Yu, J.-Q., *Angew. Chem. Int. Ed.,* **2009,** *48*, 5094-5115.
[44] Jazzar, R.; Hitce, J.; Renaudat, A.; Sofack-Kreutzer, J.; Baudoin, O., *Chem. Eur. J.,* **2010,** *16*, 2654-2672.
[45] Shi, W.; Liu, C.; Lei, A., *Chem. Soc. Rev.,* **2011,** *40*, 2761-2776.
[46] Liu, C.; Zhang, H.; Shi, W.; Lei, A., *Chem. Rev.,* **2011,** *111*, 1780-1824.
[47] Liégault, B.; Petrov, I.; Gorelsky, S. I.; Fagnou, K., *J. Org. Chem.,* **2010,** *75*, 1047-1060.
[48] Daugulis, O.; Do, H.-Q.; Shabashov, D., *Acc. Chem. Res.,* **2009,** *42*, 1074-1086.
[49] Liégault, B.; Lapointe, D.; Caron, L.; Vlassova, A.; Fagnou, K., *J. Org. Chem.,* **2009,** *74*, 1826-1834.
[50] Lyons, T. W.; Sanford, M. S., *Chem. Rev.,* **2010,** *110*, 1147-1169.
[51] Girard, S. A.; Knauber, T.; Li, C.-J., *Angew. Chem. Int. Ed.,* **2014,** *53*, 74-100.
[52] Girard, S. A.; Knauber, T.; Li, C.-J., CHAPTER 1 The Evolution of the Concept of Cross-Dehydrogenative-Coupling Reactions. In *From C-H to C-C Bonds: Cross-Dehydrogenative-Coupling*, The Royal Society of Chemistry: 2015; pp 1-32.
[53] Yeung, C. S.; Dong, V. M., *Chem. Rev.,* **2011,** *111*, 1215-1292.
[54] Li, Z.; Bohle, D. S.; Li, C.-J., *Proc. Natl. Acad. Sci. U. S. A.,* **2006,** *103*, 8928-8933.
[55] Le Bras, J.; Muzart, J., *Chem. Rev.,* **2011,** *111*, 1170-1214.
[56] Newhouse, T.; Baran, P. S., *Angew. Chem. Int. Ed.,* **2011,** *50*, 3362-3374.
[57] Tedder, J. M.; Walton, J. C., *Tetrahedron,* **1980,** *36*, 701-707.
[58] Tedder, J. M., *Angew. Chem. Int. Ed.,* **1982,** *21*, 401-410.
[59] Fokin, A. A.; Schreiner, P. R., *Chem. Rev.,* **2002,** *102*, 1551-1594.
[60] Hass, H. B.; McBee, E. T.; Weber, P., *Ind. Eng. Chem.,* **1936,** *28*, 333-339.
[61] Eck, C. R.; Hunter, D. J.; Money, T., *J. Chem. Soc., Chem. Commun.,* **1974**, 865-866.
[62] Eigendorf, G. K.; Ma, C.-L.; Money, T., *J. Chem. Soc., Perkin Trans. 1,* **1979**, 896-904.
[63] Hehre, W. J., *Acc. Chem. Res.,* **1975,** *8*, 369-376.
[64] de Meijere, A., *Angew. Chem. Int. Ed.,* **1979,** *18*, 809-826.
[65] Olah, G. A.; Reddy, V. P.; Prakash, G. K. S., *Chem. Rev.,* **1992,** *92*, 69-95.
[66] Proksch, E.; de Meijere, A., *Angew. Chem. Int. Ed.,* **1976,** *15*, 761-762.

[67] D'Accolti, L.; Dinoi, A.; Fusco, C.; Russo, A.; Curci, R., *J. Org. Chem.,* **2003,** *68*, 7806-7810.
[68] Barton, D. H. R.; Boivin, J.; Gaudin, D.; Jankowski, K., *Tetrahedron Lett.,* **1989,** *30*, 1381-1382.
[69] Reutrakul, V.; Poolsanong, C.; Pohmakotr, M., *Tetrahedron Lett.,* **1989,** *30*, 6913-6916.
[70] Davies, H. M. L.; Hansen, T., *J. Am. Chem. Soc.,* **1997,** *119*, 9075-9076.
[71] Davies, H. M. L.; Hansen, T.; Churchill, M. R., *J. Am. Chem. Soc.,* **2000,** *122*, 3063-3070.
[72] Díaz-Requejo, M. M.; Belderraín, T. R.; Nicasio, M. C.; Trofimenko, S.; Pérez, P. J., *J. Am. Chem. Soc.,* **2002,** *124*, 896-897.
[73] Davies, H. M. L.; Jin, Q., *Org. Lett.,* **2004,** *6*, 1769-1772.
[74] Davies, H. M. L.; Ni, A., *Chem. Commun.,* **2006**, 3110-3112.
[75] Chen, M. S.; White, M. C., *Science,* **2010,** *327*, 566.
[76] Davies, H. M. L.; Venkataramani, C., *Angew. Chem. Int. Ed.,* **2002,** *41*, 2197-2199.
[77] Gómez, L.; Garcia-Bosch, I.; Company, A.; Benet-Buchholz, J.; Polo, A.; Sala, X.; Ribas, X.; Costas, M., *Angew. Chem. Int. Ed.,* **2009,** *48*, 5720-5723.
[78] Vermeulen, N. A.; Chen, M. S.; Christina White, M., *Tetrahedron,* **2009,** *65*, 3078-3084.
[79] Varkony, H.; Pass, S.; Mazur, Y., *J. Chem. Soc., Chem. Commun.,* **1974**, 437-438.
[80] Schneider, H. J.; Mueller, W., *J. Org. Chem.,* **1985,** *50*, 4609-4615.
[81] Mello, R.; Fiorentino, M.; Fusco, C.; Curci, R., *J. Am. Chem. Soc.,* **1989,** *111*, 6749-6757.
[82] Likhotvorik, I. R.; Yuan, K.; Brown, D. W.; Krasutsky, P. A.; Smyth, N.; Jones, M., *Tetrahedron Lett.,* **1992,** *33*, 911-914.
[83] Chen, K.; Baran, P. S., *Nature,* **2009,** *459*, 824.
[84] Chen, K.; Eschenmoser, A.; Baran, P. S., *Angew. Chem. Int. Ed.,* **2009,** *48*, 9705-9708.
[85] Qin, Y.; Zhu, L.; Luo, S., *Chem. Rev.,* **2017,** *117*, 9433-9520.
[86] Forbes, M. D., Carbon-centered free radicals and radical cations: structure, reactivity, and dynamics. John Wiley & Sons: **2010**; Vol. 2.
[87] Li, C.-J., *Acc. Chem. Res.,* **2009,** *42*, 335-344.
[88] Zhang, Y.; Li, C.-J., *J. Am. Chem. Soc.,* **2006,** *128*, 4242-4243.
[89] Zhang, Y.; Li, C.-J., *Angew. Chem.,* **2006,** *118*, 1983-1986.
[90] Liu, X.; Sun, B.; Xie, Z.; Qin, X.; Liu, L.; Lou, H., *J. Org. Chem.,* **2013,** *78*, 3104-3112.
[91] Narayanam, J. M. R.; Stephenson, C. R. J., *Chem. Soc. Rev.,* **2011,** *40*, 102-113.
[92] Prier, C. K.; Rankic, D. A.; MacMillan, D. W. C., *Chem. Rev.,* **2013,** *113*, 5322-5363.
[93] Ravelli, D.; Protti, S.; Fagnoni, M., *Chem. Rev.,* **2016,** *116*, 9850-9913.
[94] Jin, J.; MacMillan, D. W. C., *Angew. Chem. Int. Ed.,* **2015,** *54*, 1565-1569.
[95] Minisci, F.; Bernardi, R.; Bertini, F.; Galli, R.; Perchinummo, M., *Tetrahedron,* **1971,** *27*, 3575-3579.
[96] Cheng, K.; Huang, L.; Zhang, Y., *Org. Lett.,* **2009,** *11*, 2908-2911.
[97] Chu, X.-Q.; Meng, H.; Zi, Y.; Xu, X.-P.; Ji, S.-J., *Chem. Commun.,* **2014,** *50*, 9718-9721.

[98] Zhou, W.; Qian, P.; Zhao, J.; Fang, H.; Han, J.; Pan, Y., *Org. Lett.,* **2015,** *17*, 1160-1163.
[99] Liu, Z.-Q.; Sun, L.; Wang, J.-G.; Han, J.; Zhao, Y.-K.; Zhou, B., *Org. Lett.,* **2009,** *11*, 1437-1439.
[100] Tusun, X.; Lu, C.-D., *Synlett,* **2013,** *24*, 1693-1696.
[101] Guo, S.-r.; Kumar, P. S.; Yang, M., *Adv. Synth. Catal.,* **2017,** *359*, 2-25.
[102] He, T.; Yu, L.; Zhang, L.; Wang, L.; Wang, M., *Org. Lett.,* **2011,** *13*, 5016-5019.
[103] Majji, G.; Guin, S.; Rout, S. K.; Behera, A.; Patel, B. K., *Chem. Commun.,* **2014,** *50*, 12193-12196.
[104] Beccalli, E. M.; Broggini, G.; Martinelli, M.; Sottocornola, S., *Chem. Rev.,* **2007,** *107*, 5318-5365.
[105] Song, G.; Wang, F.; Li, X., *Chem. Soc. Rev.,* **2012,** *41*, 3651-3678.
[106] Zhang, C.; Tang, C.; Jiao, N., *Chem. Soc. Rev.,* **2012,** *41*, 3464-3484.
[107] Chen, L.; Shi, E.; Liu, Z.; Chen, S.; Wei, W.; Li, H.; Xu, K.; Wan, X., *Chem. Eur. J.,* **2011,** *17*, 4085-4089.
[108] Zhang, S.; Guo, L.-N.; Wang, H.; Duan, X.-H., *Org. Biomol. Chem.,* **2013,** *11*, 4308-4311.
[109] Shin, K.; Kim, H.; Chang, S., *Acc. Chem. Res.,* **2015,** *48*, 1040-1052.
[110] Wan, J.-P.; Jing, Y., *Beilstein J. Org. Chem.,* **2015,** *11*, 2209-2222.
[111] Subramanian, P.; Rudolf, G. C.; Kaliappan, K. P., *Chem. Asian J.,* **2016,** *11*, 168-192.
[112] Dian, L.; Wang, S.; Zhang-Negrerie, D.; Du, Y.; Zhao, K., *Chem. Commun.,* **2014,** *50*, 11738-11741.
[113] Buslov, I.; Hu, X., *Adv. Synth. Catal.,* **2014,** *356*, 3325-3330.
[114] Shen, C.; Zhang, P.; Sun, Q.; Bai, S.; Hor, T. S. A.; Liu, X., *Chem. Soc. Rev.,* **2015,** *44*, 291-314.
[115] Tang, R.-Y.; Xie, Y.-X.; Xie, Y.-L.; Xiang, J.-N.; Li, J.-H., *Chem. Commun.,* **2011,** *47*, 12867-12869.
[116] Togo, H., Advanced Free Radical Reactions for Organic Synthesis. Elsevier: Amsterdam, Boston, **2004**, 5.
[117] Gilman, H.; Bebb, R. L., *J. Am. Chem. Soc.,* **1939,** *61*, 109-112.
[118] Wittig, G.; Pockels, U.; Dröge, H., *Ber. Bunsen-Ges.,* **1938,** *71*, 1903-1912.
[119] Snieckus, V., *Chem. Rev.,* **1990,** *90*, 879-933.
[120] Whisler, M. C.; MacNeil, S.; Snieckus, V.; Beak, P., *Angew. Chem. Int. Ed.,* **2004,** *43*, 2206-2225.
[121] Kleiman, J. P.; Dubeck, M., *J. Am. Chem. Soc.,* **1963,** *85*, 1544-1545.
[122] Cope, A. C.; Siekman, R. W., *J. Am. Chem. Soc.,* **1965,** *87*, 3272-3273.
[123] Parshall, G. W., *Acc. Chem. Res.,* **1970,** *3*, 139-&.
[124] Hata, G.; Kondo, H.; Miyake, A., *J. Am. Chem. Soc.,* **1968,** *90*, 2278-2281.
[125] Kasahara, A., *Bull. Chem. Soc. Jpn.,* **1968,** *41*, 1272-1272.
[126] Nonoyama, M.; Yamasaki, K., *Inorg. Nucl. Chem. Lett.,* **1971,** *7*, 943-946.
[127] Puterbaugh, W. H.; Hauser, C. R., *J. Org. Chem.,* **1964,** *29*, 853-856.
[128] Gschwend, H. W.; Hamdan, A., *J. Org. Chem.,* **1975,** *40*, 2008-2009.
[129] Beak, P.; Brown, R. A., *J. Org. Chem.,* **1977,** *42*, 1823-1824.
[130] Comins, D. L.; Brown, J. D.; Mantlo, N. B., *Tetrahedron Lett.,* **1982,** *23*, 3979-3982.

[131] Sibi, M. P.; Snieckus, V., *J. Org. Chem.,* **1983,** *48*, 1935-1937.
[132] Gray, M.; Chapell, B. J.; Felding, J.; Taylor, N. J.; Snieckus, V., *Synlett,* **1998,** *1998*, 422-424.
[133] Thery, N.; Szymoniak, J.; Moïse, C., *Tetrahedron Lett.,* **1999,** *40*, 3155-3158.
[134] Macklin, T. K.; Snieckus, V., *Org. Lett.,* **2005,** *7*, 2519-2522.
[135] Ryabov, A. D., *Synthesis,* **1985,** *1985*, 233-252.
[136] Ackermann, L., *Chem. Rev.,* **2011,** *111*, 1315-1345.
[137] Arockiam, P. B.; Bruneau, C.; Dixneuf, P. H., *Chem. Rev.,* **2012,** *112*, 5879-5918.
[138] Leitch, J. A.; Frost, C. G., *Chem. Soc. Rev.,* **2017**.
[139] Arockiam, P. B.; Bruneau, C.; Dixneuf, P. H., *Chem. Rev.,* **2012,** *112*, 5879-5918.
[140] Colby, D. A.; Bergman, R. G.; Ellman, J. A., *Chem. Rev.,* **2010,** *110*, 624-655.
[141] Qi, X.; Li, Y.; Bai, R.; Lan, Y., *Acc. Chem. Res.,* **2017,** *50*, 2799-2808.
[142] Wendlandt, A. E.; Suess, A. M.; Stahl, S. S., *Angew. Chem. Int. Ed.,* **2011,** *50*, 11062-11087.
[143] Tasker, S. Z.; Standley, E. A.; Jamison, T. F., *Nature,* **2014,** *509*, 299.
[144] Ackermann, L., *J. Org. Chem.,* **2014,** *79*, 8948-8954.
[145] Murai, S.; Kakiuchi, F.; Sekine, S.; Tanaka, Y.; Kamatani, A.; Sonoda, M.; Chatani, N., *Nature,* **1993,** *366*, 529.
[146] Trost, B. M.; Imi, K.; Davies, I. W., *J. Am. Chem. Soc.,* **1995,** *117*, 5371-5372.
[147] Kakiuchi, F.; Tanaka, Y.; Sato, T.; Chatani, N.; Murai, S., *Chem. Lett.,* **1995,** *24*, 679-680.
[148] Kakiuchi, F.; Yamamoto, Y.; Chatani, N.; Murai, S., *Chem. Lett.,* **1995,** *24*, 681-682.
[149] Oi, S.; Fukita, S.; Inoue, Y., *Chem. Commun.,* **1998**, 2439-2440.
[150] Oi, S.; Fukita, S.; Hirata, N.; Watanuki, N.; Miyano, S.; Inoue, Y., *Org. Lett.,* **2001,** *3*, 2579-2581.
[151] Lim, Y.-G.; Kang, J.-B.; Kim, Y. H., *J. Chem. Soc., Perkin Trans. 1,* **1996**, 2201-2206.
[152] Lim, Y.-G.; Kang, J.-B.; Hae Kim, Y., *J. Chem. Soc., Perkin Trans. 1,* **1998**, 699-708.
[153] Jun, C.-H., *Chem. Commun.,* **1998**, 1405-1406.
[154] Chatani, N.; Asaumi, T.; Ikeda, T.; Yorimitsu, S.; Ishii, Y.; Kakiuchi, F.; Murai, S., *J. Am. Chem. Soc.,* **2000,** *122*, 12882-12883.
[155] Chatani, N.; Ishii, Y.; Ie, Y.; Kakiuchi, F.; Murai, S., *J. Org. Chem.,* **1998,** *63*, 5129-5136.
[156] Chatani, N.; Ie, Y.; Kakiuchi, F.; Murai, S., *J. Org. Chem.,* **1997,** *62*, 2604-2610.
[157] Hashimoto, Y.; Hirano, K.; Satoh, T.; Kakiuchi, F.; Miura, M., *J. Org. Chem.,* **2013,** *78*, 638-646.
[158] Dick, A. R.; Hull, K. L.; Sanford, M. S., *J. Am. Chem. Soc.,* **2004,** *126*, 2300-2301.
[159] Oi, S.; Sasamoto, H.; Funayama, R.; Inoue, Y., *Chem. Lett.,* **2008,** *37*, 994-995.
[160] Ackermann, L.; Althammer, A.; Born, R., *Tetrahedron,* **2008,** *64*, 6115-6124.
[161] Anastas, P. T. W., J. C. , *Green Chemistry: Theory and Practice*. Oxford University Press: Oxford: **1998**.
[162] Anastas, P.; Eghbali, N., *Chem. Soc. Rev.,* **2010,** *39*, 301-312.
[163] Patureau, F. W.; Glorius, F., *Angew. Chem. Int. Ed.,* **2011,** *50*, 1977-1979.
[164] Tan, Y.; Hartwig, J. F., *J. Am. Chem. Soc.,* **2010,** *132*, 3676-3677.
[165] Guimond, N.; Gouliaras, C.; Fagnou, K., *J. Am. Chem. Soc.,* **2010,** *132*, 6908-6909.

[166] Hyster, T. K.; Rovis, T., *Chem. Commun.,* **2011,** *47*, 11846-11848.
[167] Lu, Y.; Leow, D.; Wang, X.; Engle, K. M.; Yu, J.-Q., *Chem. Sci.,* **2011,** *2*, 967-971.
[168] Blanchot, M.; Candito, D. A.; Larnaud, F.; Lautens, M., *Org. Lett.,* **2011,** *13*, 1486-1489.
[169] Huang, C.; Chattopadhyay, B.; Gevorgyan, V., *J. Am. Chem. Soc.,* **2011,** *133*, 12406-12409.
[170] Chernyak, N.; Dudnik, A. S.; Huang, C.; Gevorgyan, V., *J. Am. Chem. Soc.,* **2010,** *132*, 8270-8272.
[171] Dudnik, A. S.; Chernyak, N.; Huang, C.; Gevorgyan, V., *Angew. Chem. Int. Ed.,* **2010,** *49*, 8729-8732.
[172] Huang, C.; Chernyak, N.; Dudnik, A. S.; Gevorgyan, V., *Adv. Synth. Catal.,* **2011,** *353*, 1285-1305.
[173] Cornella, J.; Righi, M.; Larrosa, I., *Angew. Chem. Int. Ed.,* **2011,** *50*, 9429-9432.
[174] Zhang, Y.; Zhao, H.; Zhang, M.; Su, W., *Angew. Chem. Int. Ed.,* **2015,** *54*, 3817-3821.
[175] Liu, Y.; Ge, H., *Nat.* Chem., **2016,** advance online publication.
[176] Wu, Y.; Chen, Y.-Q.; Liu, T.; Eastgate, M. D.; Yu, J.-Q., *J. Am. Chem. Soc.,* **2016**.
[177] Yang, K.; Li, Q.; Liu, Y.; Li, G.; Ge, H., *J. Am. Chem. Soc.,* **2016,** *138*, 12775-12778.
[178] Liu, X. H.; Park, H.; Hu, J. H.; Hu, Y.; Zhang, Q. L.; Wang, B. L.; Sun, B.; Yeung, K. S.; Zhang, F. L.; Yu, J. Q., *J. Am. Chem. Soc.,* **2017,** *139*, 888-896.
[179] Chiong, H. A.; Pham, Q.-N.; Daugulis, O., *J. Am. Chem. Soc.,* **2007,** *129*, 9879-9884.
[180] Gooßen, L. J.; Thiel, W. R.; Rodríguez, N.; Linder, C.; Melzer, B., *Adv. Synth. Catal.,* **2007,** *349*, 2241-2246.
[181] Luo, J.; Preciado, S.; Larrosa, I., *Chem. Commun.,* **2015,** *51*, 3127-3130.
[182] Arroniz, C.; Denis, J. G.; Ironmonger, A.; Rassias, G.; Larrosa, I., *Chem. Sci.,* **2014,** *5*, 3509-3514.
[183] Luo, J.; Preciado, S.; Larrosa, I., *J. Am. Chem. Soc.,* **2014,** *136*, 4109-4112.
[184] Kumar, N. Y. P.; Bechtoldt, A.; Raghuvanshi, K.; Ackermann, L., *Angew. Chem. Int. Ed.,* **2016,** *55*, 6929-6932.
[185] Huang, L.; Biafora, A.; Zhang, G.; Bragoni, V.; Gooßen, L. J., *Angew. Chem. Int. Ed.,* **2016,** *55*, 6933-6937.
[186] Shi, X.-Y.; Liu, K.-Y.; Fan, J.; Dong, X.-F.; Wei, J.-F.; Li, C.-J., *Chem. Eur. J.,* **2015,** *21*, 1900-1903.
[187] Biafora, A.; Khan, B. A.; Bahri, J.; Hewer, J. M.; Goossen, L. J., *Org. Lett.,* **2017,** *19*, 1232-1235.
[188] Zhang, J.; Shrestha, R.; Hartwig, J. F.; Zhao, P., *Nat. Chem.,* **2016,** *8*, 1144.
[189] Simonetti, M.; Larrosa, I., *Nat. Chem.,* **2016,** *8*, 1086.
[190] Baslé, O.; Bidange, J.; Shuai, Q.; Li, C.-J., *Adv. Synth. Catal.,* **2010,** *352*, 1145-1149.
[191] Zhang, Q.; Li, C.; Yang, F.; Li, J.; Wu, Y., *Tetrahedron,* **2013,** *69*, 320-326.
[192] Banerjee, A.; Santra, S. K.; Guin, S.; Rout, S. K.; Patel, B. K., *Eur. J. Org. Chem.,* **2013,** *2013*, 1367-1376.
[193] Banerjee, A.; Bera, A.; Santra, S. K.; Guin, S.; Patel, B. K., *RSC Adv.,* **2014,** *4*, 8558-8566.
[194] Santra, S. K.; Banerjee, A.; Patel, B. K., *Tetrahedron,* **2014,** *70*, 2422-2430.
[195] Kianmehr, E.; Kazemi, S.; Foroumadi, A., *Tetrahedron,* **2014,** *70*, 349-354.

[196] Kumar, G.; Sekar, G., *RSC Adv.,* **2015,** *5*, 28292-28298.
[197] Yan, X.-B.; Shen, Y.-W.; Chen, D.-Q.; Gao, P.; Li, Y.-X.; Song, X.-R.; Liu, X.-Y.; Liang, Y.-M., *Tetrahedron,* **2014,** *70*, 7490-7495.
[198] Yu, Q.; Zhang, N.; Huang, J.; Lu, S.; Zhu, Y.; Yu, X.; Zhao, K., *Chem. Eur. J.,* **2013,** *19*, 11184-11188.
[199] Duan, P.; Yang, Y.; Ben, R.; Yan, Y.; Dai, L.; Hong, M.; Wu, Y.-D.; Wang, D.; Zhang, X.; Zhao, J., *Chem. Sci.,* **2014,** *5*, 1574-1578.
[200] Pitts, C. R.; Bloom, S.; Woltornist, R.; Auvenshine, D. J.; Ryzhkov, L. R.; Siegler, M. A.; Lectka, T., *J. Am. Chem. Soc.,* **2014,** *136*, 9780-9791.
[201] Hartwig, J. F.; Larsen, M. A., *ACS Cent. Sci.,* **2016,** *2*, 281-292.
[202] Labinger, J. A.; Bercaw, J. E., *Nature,* **2002,** *417*, 507.
[203] He, J.; Li, S.; Deng, Y.; Fu, H.; Laforteza, B. N.; Spangler, J. E.; Homs, A.; Yu, J.-Q., *Science,* **2014,** *343*, 1216-1220.
[204] Dyker, G., *Angew. Chem. Int. Ed.,* **2003,** *31*, 1023-1025.
[205] Dangel, B. D.; Godula, K.; Youn, S. W.; Sezen, B.; Sames, D., *J. Am. Chem. Soc.,* **2002,** *124*, 11856-11857.
[206] Ryabov, A. D., *Chem. Rev.,* **1990,** *90*, 403-424.
[207] Zhang, F.; Spring, D. R., *Chem. Soc. Rev.,* **2014,** *43*, 6906-6919.
[208] Kuhl, N.; Hopkinson Matthew, N.; Wencel-Delord, J.; Glorius, F., *Angew. Chem. Int. Ed.,* **2012,** *51*, 10236-10254.
[209] Krylov, I. B.; Vil', V. A.; Terent'ev, A. O., *Beilstein J. Org. Chem.,* **2015,** *11*, 92-146.
[210] Tran, B. L.; Li, B.; Driess, M.; Hartwig, J. F., *J. Am. Chem. Soc.,* **2014,** *136*, 2555-2563.
[211] Wang, L.; Priebbenow, D. L.; Zou, L.-H.; Bolm, C., *Adv. Synth. Catal.,* **2013,** *355*, 1490-1494.
[212] Wang, C.-Y.; Song, R.-J.; Wei, W.-T.; Fan, J.-H.; Li, J.-H., *Chem. Commun.,* **2015,** *51*, 2361-2363.
[213] Kharasch, M. S.; Sosnovsky, G.; Yang, N. C., *J. Am. Chem. Soc.,* **1959,** *81*, 5819-5824.
[214] Zhao, J.; Fang, H.; Zhou, W.; Han, J.; Pan, Y., *J. Org. Chem.,* **2014,** *79*, 3847-3855.
[215] Conde, A.; Vilella, L.; Balcells, D.; Díaz-Requejo, M. M.; Lledós, A.; Pérez, P. J., *J. Am. Chem. Soc.,* **2013,** *135*, 3887-3896.
[216] Li, K.; Wu, Q.; Lan, J.; You, J., *Nat. Commun.,* **2015,** *6*, 8404.
[217] Liu, W.; Groves, J. T., *Angew. Chem. Int. Ed.,* **2013,** *52*, 6024-6027.
[218] Guo, S.; Cong, F.; Guo, R.; Wang, L.; Tang, P., *Nat. Chem.,* **2017,** *advance online publication*.
[219] Crabtree, R. H., *Chem. Rev.,* **1985,** *85*, 245-269.
[220] Halpern, J., *Inorg. Chim. Acta,* **1985,** *100*, 41-48.
[221] Deem, M. L., *Coord. Chem. Rev.,* **1986,** *74*, 101-125.
[222] Lin, M.; Shen, C.; Garcia-Zayas, E. A.; Sen, A., *J. Am. Chem. Soc.,* **2001,** *123*, 1000-1001.
[223] Kua, J.; Xu, X.; Periana, R. A.; Goddard, W. A., *Organometallics,* **2002,** *21*, 511-525.
[224] Lin, M.; Hogan, T.; Sen, A., *J. Am. Chem. Soc.,* **1997,** *119*, 6048-6053.
[225] Lin, M.; Hogan, T. E.; Sen, A., *J. Am. Chem. Soc.,* **1996,** *118*, 4574-4580.
[226] Muehlhofer, M.; Strassner, T.; Herrmann, W. A., *Angew. Chem. Int. Ed.,* **2002,** *41*, 1745-1747.

[227] Periana, R. A.; Mironov, O.; Taube, D.; Bhalla, G.; Jones, C. J., *Science,* **2003,** *301*, 814.
[228] Janowicz, A. H.; Bergman, R. G., *J. Am. Chem. Soc.,* **1982,** *104*, 352-354.
[229] Thompson, M. E.; Baxter, S. M.; Bulls, A. R.; Burger, B. J.; Nolan, M. C.; Santarsiero, B. D.; Schaefer, W. P.; Bercaw, J. E., *J. Am. Chem. Soc.,* **1987,** *109*, 203-219.
[230] Bromberg, S. E.; Yang, H.; Asplund, M. C.; Lian, T.; McNamara, B. K.; Kotz, K. T.; Yeston, J. S.; Wilkens, M.; Frei, H.; Bergman, R. G.; Harris, C. B., *Science,* **1997,** *278*, 260.
[231] Rabaa, H.; Saillard, J. Y.; Hoffmann, R., *J. Am. Chem. Soc.,* **1986,** *108*, 4327-4333.
[232] Newhouse, T.; Baran, P. S.; Hoffmann, R. W., *Chem. Soc. Rev.,* **2009,** *38*, 3010-3021.
[233] Davies, H. M.; Morton, D., *J. Org. Chem.,* **2016,** *81*, 343-50.
[234] Chen, D. Y. K.; Youn, S. W., *Chem. Eur. J.,* **2012,** *18*, 9452-9474.
[235] Qiu, Y.; Gao, S., *Nat. Prod. Rep.,* **2016,** *33*, 562-581.
[236] Chen, D. Y. K.; Youn, S. W., *Chem. Eur. J.,* **2012,** *18*, 9452-9474.
[237] Shenvi, R. A.; Guerrero, C. A.; Shi, J.; Li, C.-C.; Baran, P. S., *J. Am. Chem. Soc.,* **2008,** *130*, 7241-7243.
[238] O'Malley, S. J.; Tan, K. L.; Watzke, A.; Bergman, R. G.; Ellman, J. A., *J. Am. Chem. Soc.,* **2005,** *127*, 13496-13497.
[239] O' Donovan, D. H.; Aillard, P.; Berger, M.; de la Torre, A.; Petkova, D.; Knittl-Frank, C.; Geerdink, D.; Kaiser, M.; Maulide, N., *Angew. Chem. Int. Ed.,* **2018,** *57*, 10737-10741.
[240] Zaitsev, V. G.; Shabashov, D.; Daugulis, O., *J. Am. Chem. Soc.,* **2005,** *127*, 13154-13155.
[241] Nadres, E. T.; Santos, G. I. F.; Shabashov, D.; Daugulis, O., *J. Org. Chem.,* **2013,** *78*, 9689-9714.
[242] He, G.; Chen, G., *Angew. Chem. Int. Ed.,* **2011,** *50*, 5192-5196.
[243] Li, C.-J.; Wei, C.; Li, Z., *Synlett,* **2004,** *2004*, 1472-1483.
[244] Wan, J. P.; Gan, L.; Liu, Y., *Org. Biomol. Chem.,* **2017,** *15*, 9031-9043.
[245] Vila, C.; Rueping, M., *Green Chem.,* **2013,** *15*, 2056-2059.
[246] Tsukamoto, D.; Ikeda, M.; Shiraishi, Y.; Hara, T.; Ichikuni, N.; Tanaka, S.; Hirai, T., *Chem. Eur. J.,* **2011,** *17*, 9816-9824.
[247] Augugliaro, V.; Palmisano, L., *ChemSusChem,* **2010,** *3*, 1135-1138.
[248] Wang, Q.; Zhang, M.; Chen, C.; Ma, W.; Zhao, J., *Angew. Chem. Int. Ed.,* **2010,** *49*, 7976-7979.
[249] Palmisano, G.; García-López, E.; Marcì, G.; Loddo, V.; Yurdakal, S.; Augugliaro, V.; Palmisano, L., *Chem. Commun.,* **2010,** *46*, 7074-7089.
[250] Kumar, G. S.; Ragini, S. P.; Kumar, A. S.; Meshram, H. M., *RSC Adv.,* **2015,** *5*, 51576-51580.
[251] Pinto, A.; Neuville, L.; Zhu, J., *Angew. Chem. Int. Ed.,* **2007,** *46*, 3291-3295.
[252] Liu, Y.; Zhang, Y.; Wan, J.-P., *J. Org. Chem.,* **2017,** *82*, 8950-8957.
[253] Henderson, J. L.; Edwards, A. S.; Greaney, M. F., *J. Am. Chem. Soc.,* **2006,** *128*, 7426-7427.
[254] Bhuvaneswari, S.; Jeganmohan, M.; Yang, M.-C.; Cheng, C.-H., *Chem. Commun.,* **2008**, 2158-2160.

[255] Ogata, K.; Atsuumi, Y.; Fukuzawa, S.-i., *Org. Lett.,* **2011,** *13*, 122-125.
[256] Yoo, W. J.; Zhao, L.; Li, C. J., *Aldrichim. Acta,* **2011,** *44*, 43-51.
[257] Liu, Y., *Arkivoc,* **2013,** *2014*.
[258] Peshkov, V. A.; Pereshivko, O. P.; Van der Eycken, E. V., *Chem. Soc. Rev.,* **2012,** *41*, 3790-3807.

Chapter 2 – Gold Catalyzed Tandem Reactions of Amide-Aldehyde-Alkyne Coupling and Cyclization - Synthesis of 2,4,5 -Trisubstituted Oxazoles.

2.1 Background

Since its first recorded synthesis in 1840 by Zinin[1], oxazole heterocyclic compound has played an increasingly important role in heterocycle chemistry research. Its first synthesis was observed by obtaining azobenzil, or benzilam product from the reaction of benzil with alcoholic ammonia. During the World War II, Cornforth and others carried out penicillin synthesis, which was thought to contain an oxazole core, and greatly advanced our knowledge of the chemistry of oxazoles.[2] The parent oxazole was for the first time synthesized by Cornforth and Cornforth in 1946 by utilizing a complex series of reactions.[3] Although the parent oxazole does not exist naturally, a large number of substituted oxazole-containing natural products have been isolated, mostly from marine invertebrates and microorganisms. Because of their structural complexity, many of these isolated oxazole containing molecules drove a large interest in pursuing their total synthesis and thus resulted in many of the recent discoveries of novel oxazole chemistry.

Generally known as the classical method to synthesized oxazole compound, the Fischer synthesis discovered in 1896, is a reaction between a cyanohydrin and an aldehyde under acidic conditions (Scheme 59).[4]

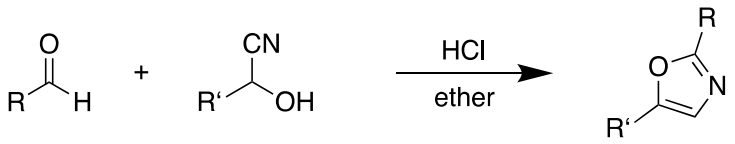

Scheme 59. Emil Fischer oxazole synthesis

Many different aromatic aldehydes and cyanohydrins were evaluated and converted to the corresponding 2,5-diaryloxazoles following this procedure, with yields obtained up to 80%. Regarding the synthesis of oxazoles, numerous methodologies were developed

during the last century. This motif can be achieved from many different starting molecules, such as: α -amino acids[5], benzalaminoacetals,[6-7] amides and α-halo ketones,[8-10] via 1.3-dipolar addition of carbonylcarbenes to nitriles[11-12] and many others reported in published reviews.[5, 13-17] Another classical and widely used reaction, is the Robinson-Gabriel oxazole synthesis (Scheme 60).[18-19] This method, named after S. R. Robinson and S. Gabriel who discovered the reaction in 1909 and 1910, respectively, describes a cyclization and dehydration of a α-acylamino ketones when treated with PCl_5 or a strong dehydrating agent.[20] Various modifications of this synthesis were developed following its discovery, ranging from the use of one-pot strategy[21] to the use of readily available α-amino acid derivatives.[22]

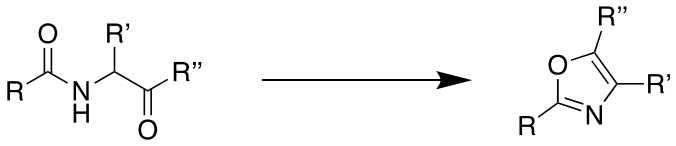

Scheme 60. Robinson-Gabriel oxazole synthesis

Moreover, the Van Leusen synthesis also belongs to the well-known methods to access oxazoles and imidazoles.[23] The reaction consists of the coupling of a carbonyl compound with toluenesulfonylmethyl isocyanide (TOSMIC) producing the corresponding heterocycle under basic conditions. Discovered in the 1970's, the reaction is driven by the peculiar reactivity of TOSMIC, which possesses acidic protons, sulfinic acid as a leaving group and an isocyano group that contains an oxidizable carbon atom. After deprotonation of TOSMIC, the addition to the carbonyl moiety occurs, followed by cycloaddition and based-promoted elimination reaction leading to the oxazole product (Scheme 61). This strategy found considerable use in the preparation of Dupont's benzamidine, a Factor Xa inhibitor (anticoagulant drugs - Scheme 62).[24] Moreover, the robustness of this methodology found applications in methionine aminopeptidase inhibitor[25] and prostacyclin receptor antagonist programs.[26]

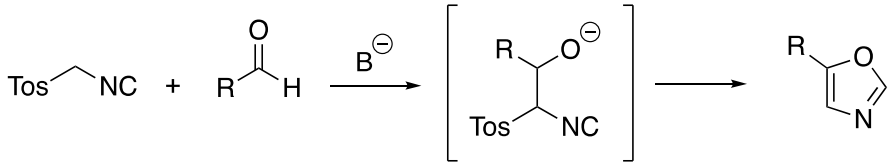

Scheme 61. Van Leusen oxazole synthesis

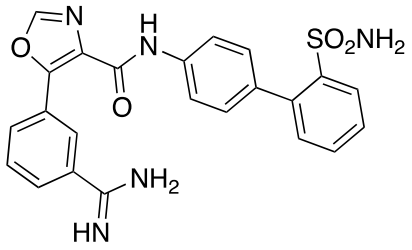

Scheme 62. Dupont's benzamidine

Besides organic named reactions, the syntheses of oxazole core have been developed by many research groups, generally using intramolecular cycloaddition strategies. Cycloaddition reactions are among the synthetic tools that best fit the criteria of methods and strategies that allow the transformation of readily available precursors into complex products in an efficient, rapid and economical manner. Regrettably, the realm of classical cycloaddition reactions is quite small and limited to precursors presenting specific and suitable electronic properties.[27-29] In this regard, transition metal complexes offer great opportunities for the discovery of new cycloaddition alternatives, and in many cases they can be used in a catalytic manner. While transition metal-catalyzed cycloadditions were discovered in the mid-20th century and more recently developed and established as important strategy to access heterocycles, most of the examples were described with the use of rhodium, ruthenium, or palladium catalysts.[30] Propargyl alcohols and esters react with amides or nitriles in the presence of certain catalysts and cyclodehydrating agents to afford alkyl- or aryl-oxazoles. For instance, 2-phenyl-4-methyloxazole was obtained from the reaction of propargyl alcohol and benzonitrile in concentrated sulfuric acid.[31-32] More recently, thanks to the properties of transition metal catalysts, intramolecular cyclization of propargyl amide has been achieved.[33] The first transition-metal-catalyzed

cycloisomerization of propargyl amides delivering the corresponding oxazole, was described by Eloy and Deryckere in 1973 by employing $Hg(OAc)_2$ as catalyst.[34] This method was then adopted in the synthesis of oxazole-containing bioactive molecules by Beer and co-workers.[35] Later, in 1995, Costa and co-workers reported a Pd/C or Pd(II) catalyzed oxidative cyclization-alkoxylation of propargylic amides into the corresponding oxazolines with great yields.[36] Cacchi and Broggini demonstrated later that palladium transition metal catalysts were efficient to catalyze 5-exo-dig cyclization reaction of porpargyl amides under different conditions (Scheme 63).[37-38]

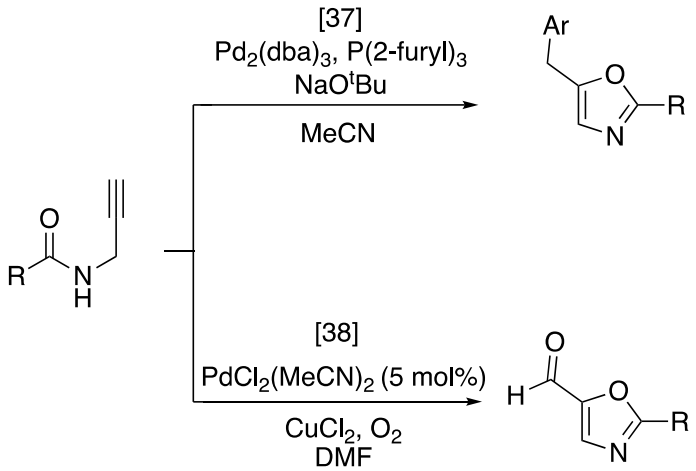

Scheme 63. Palladium catalyzed cyclization of propargyl amides

More recently, gold complexes, due to their excellent ability to coordinate to C-C multiple bonds, have been widely employed to catalyze the cyclization of propargyl amides. In 2004, Hashmi and Nishibayashi along with their co-workers independently described a 5-*exo-dig* cycloisomerization of propargyl amides into oxazoles, catalyzed by gold (III) complexes (Scheme 64).[39-40]

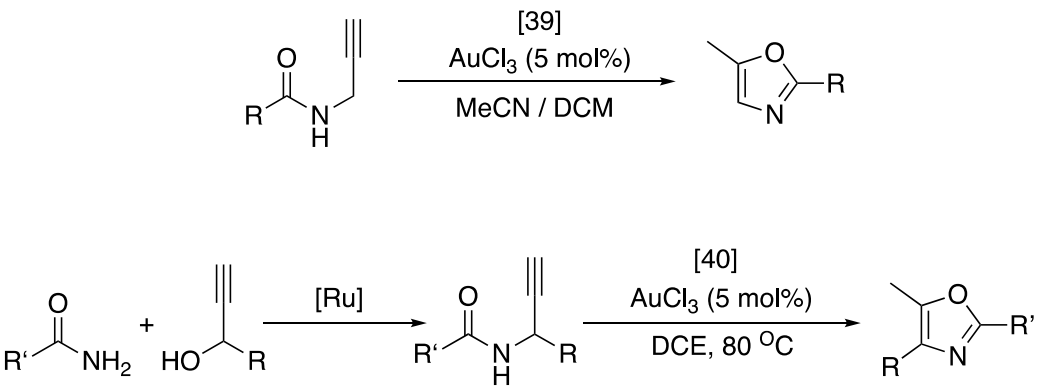

Scheme 64. Gold catalyzed cyclization of propargyl amides

As mentioned above, oxazole containing compounds exhibit highly variable and bioactive properties and their structures are extremely diverse. As such, some efficient synthetic methods accessing highly functionalized oxazoles have been developed, yet overall remain challenging. Regarding the aspect of building up molecular complexity, introduced earlier in Chapter 1, these methods disclose various advantages. However, limitations in scope diversity and or potential stability of functional groups under these reaction conditions were exposed. For instance, in Fisher's oxazole synthesis, the use of already complex cyanohydrin starting molecule reduces the potential gain of molecular complexity through the reaction. Moreover, under strongly acidic conditions, many different functional groups are not tolerated. Similarly, Robinson-Gabriel oxazole synthesis occurs with a pre-synthesized starting material under very strong and concentrated acidic conditions, diminishing the potential scope of oxazole compounds; thus weakening the overall gain of molecular complexity. The Van Leusen oxazole synthesis proceeds under basic condition with generally elevated temperature. The pre-synthesis of TOSMIC is prerequisite to the reaction to occur, which consequently renders this reaction as being non-efficient regarding ΔCm gain after the reaction. Analogously, the cycloisomerization of reactive intermediates into oxazoles involves one or more pre-synthesis steps to generate the corresponding reactive intermediates. We summarize the molecular complexity gain or loss using these methods, in Scheme 65. Surprisingly, the complexity calculated resulting from these four different syntheses of oxazoles is

dramatically low. In fact, only the Fischer oxazole synthesis has an overall molecular complexity being positive of ΔC_m= 34.6. The organic reactions such as the Robinson-Gabriel and the Van Leusen oxazole syntheses show negative values of molecular complexity with ΔC_m= -63 and ΔC_m= -232.4, respectively. Regarding the cycloisomerization of propargyl reactive intermediate, the molecular complexity calculated is negative with a value of ΔC_m= -52.

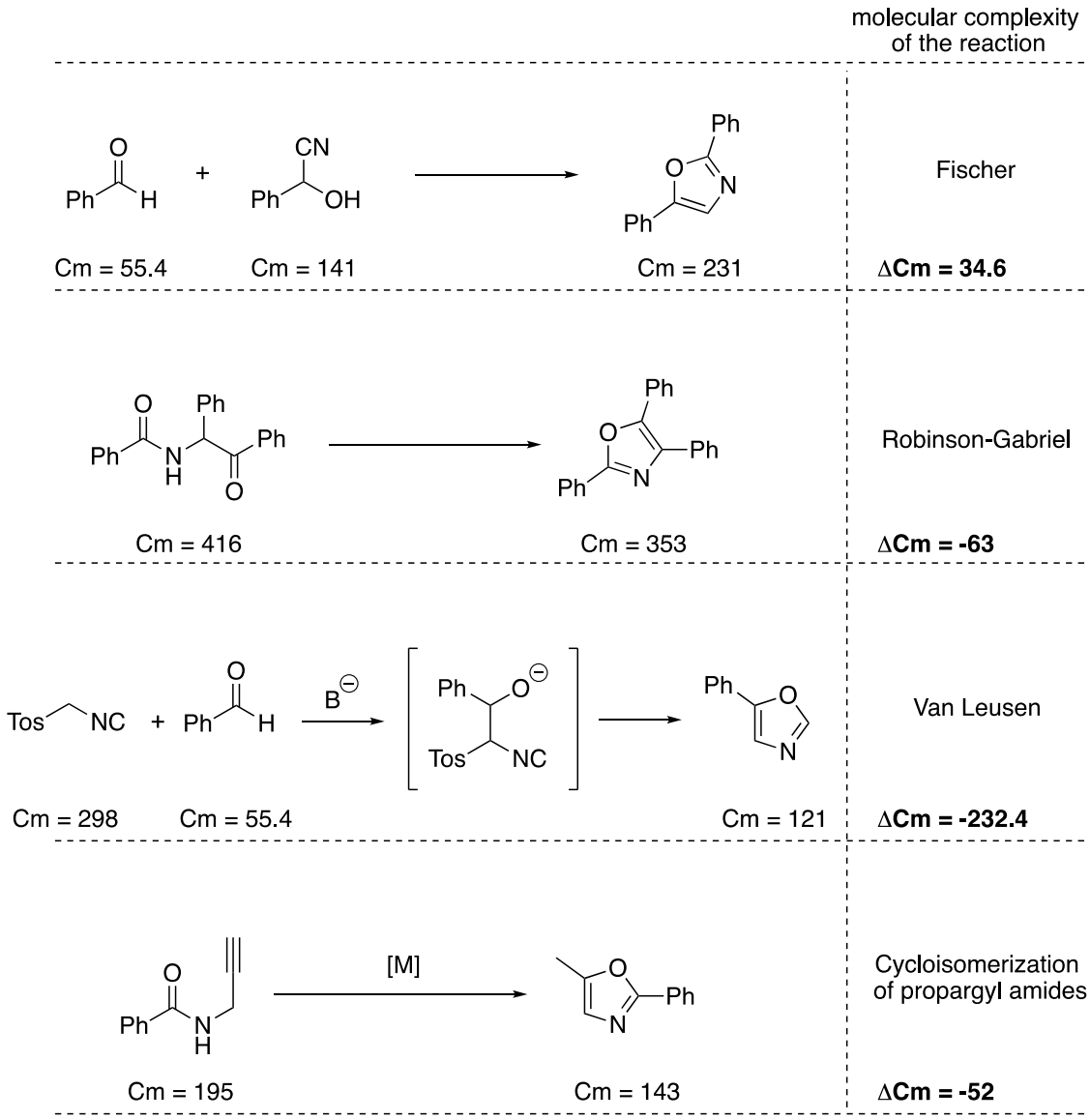

Scheme 65. Comparison of molecular complexity gain from classical oxazole synthesis

From these observations, the development of a new and efficient method to build up oxazole heterocycles with a high gain of molecular complexity, is of huge interest.

2.2 Research objectives & plan

Oxazoles are important heterocyclic motifs present in a wide range of bioactive molecules,[41-42] natural products,[43-47] advanced materials,[48] and ligand frameworks[49-50] (Scheme 66).

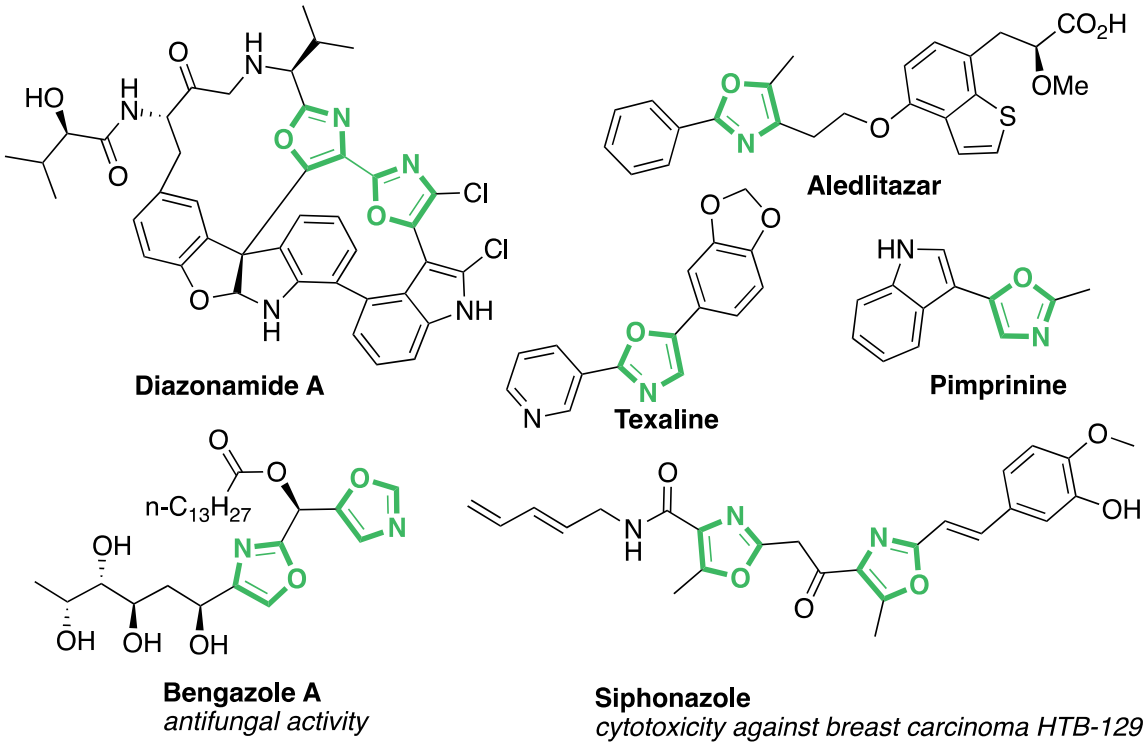

Scheme 66. Examples of bioactive molecules and natural products containing oxazole moiety

Functionalization of pre-existing oxazole skeletons is one important strategy used to access highly functionalized derivatives, but some regioselectivity issues can limit such methods.[51-57] Moreover, the potential gain of molecular complexity through direct functionalization of pre-existing oxazole skeletons is diminished since the heterocycle needs pre-synthesis step. As such, efficient synthetic methods accessing highly functionalized oxazoles are of great interest, yet remain challenging. From an atom

economic perspective, the intramolecular cyclization from acyclic precursors represents an attractive strategy for the preparation of substituted oxazoles.[58-70] In the past decades, various transition metals have been reported to catalyze the cyclization of acetylenic precursors. Among these different methods, some use strong Brönsted acids or Lewis acid reagents, which restrict the functional group tolerance.[71] Thus, it is desirable to develop a simple approach with high enhancement of molecular complexity to synthesize a broad variety of oxazoles derivatives.

By furnishing complex products from simple building blocks in a minimum number of steps, multicomponent reactions represent efficient and rapid alternatives to traditional stepwise syntheses.[72-78] One such reaction that has proven highly versatile and useful is the aldehyde-alkyne-amine coupling (A^3-coupling) for the formation of propargylamines.[79-82] Since its discovery,[83-84] the multicomponent A^3-coupling has been extensively developed by numerous authors, showing great promise as a tool for the synthesis of complex molecules. In particular, its amenability to tandem transformations, especially cyclization, makes it an attractive technique for the synthesis of drug-like molecules. We envisioned that oxazoles might be accessed through such a tandem A^3-coupling-cyclization, making use of amides instead of amines (Scheme 67). However, to the best of our knowledge, the formation of propargyl amides via the coupling of amides, aldehydes and alkynes has never been reported before.[85-87] Coinage transition-metal catalysts, such as gold, have shown excellent activity for the A^3-coupling[88-90] as well as, have been highly effective for the cyclization of acetylenic compounds.[39, 91-114] Thus, we envisioned that a judicious gold catalyst might effectively catalyze both A^3-coupling and the tandem cyclization steps, gaining access to highly functionalized oxazoles in a single pot.[115-123] We aimed to develop a novel strategy for the multicomponent, one-pot synthesis of highly substituted oxazoles from simple amides, aldehydes and alkynes.

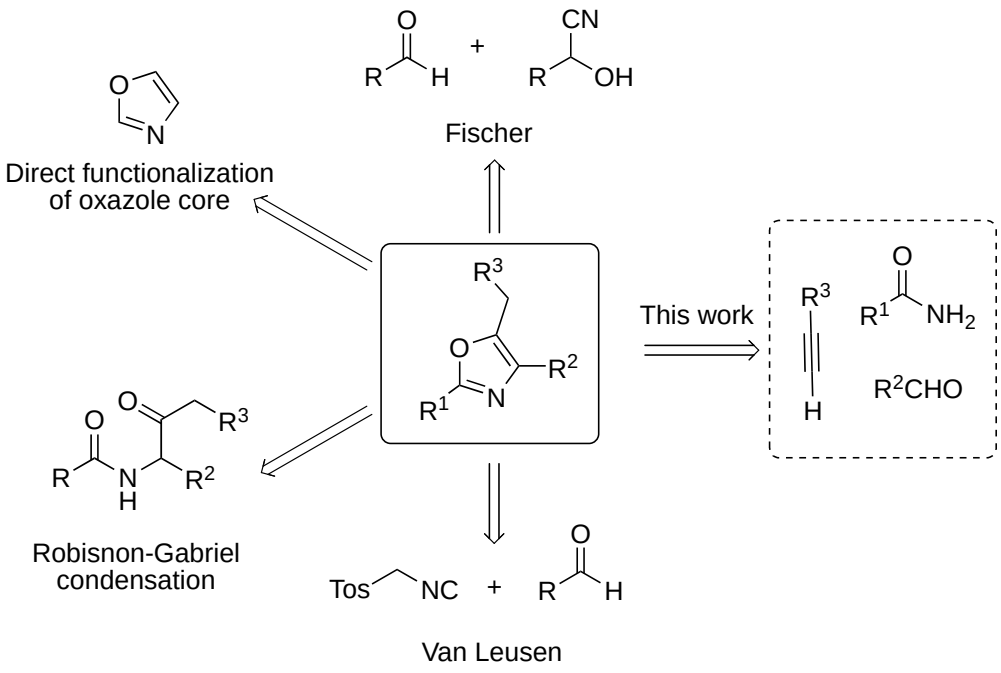

Scheme 67. Designed strategy of one-pot gold-catalyzed A^3 / cyclization reaction

Our first attempt to achieve the coupling of amides, aldehydes and alkynes was undertaken with simple substrates to develop an exemplary reaction. Towards this goal, we selected gold catalyst to conduct both multicomponent coupling and the corresponding cyclization reaction. Lastly, with numerous different, functionalized and readily available substrates, we envisioned the rapid construction of molecular complexity for the construction of oxazole heterocycles.

2.3 Results and discussion

2.3.1 Condition screening

Inspired by our previous work on gold-catalyzed A^3 reactions, we began our investigation using benzamide (**1a**), and cyclohexanecarboxaldehyde (**2a**) and phenyl acetylene (**3a**) as substrates. While gold(I) chloride and gold(III) chloride complexes, on their own, did not yield any desired product, the use of NHC-gold(I) cationic complex furnished the corresponding product (**4a**) in 1% yield (entry 6). Triphenylphosphine ligand was found to be beneficial to the reaction (entry 8) compared with triethylphoshine and the corresponding N-heterocycle carbene ligand reported (entries 6 and 7). The counter-

anion of silver salt dramatically influenced the yield of the reaction, with triflate yielding the best result (entries 8-11). When Ph_3PAuCl/AgOTf was used in toluene at 100 °C, a significant amount of 3-acylamidoketone (**5a**) was detected, together with its regioisomer (**5b**) in a minor yield (< 10%, Scheme 69). To investigate the influence of water on the formation of this side-product, 4Å molecular sieves were added (entry 12), which resulted in the complete inhibition of the desired reaction possibly due to gold poisoning from the molecular sieves.[124] Whereas it has been reported that a suitable acid activator (i.e. AgOTf) prevents the degradation of the gold catalyst,[124] the addition of 50 mol% AgOTf was not beneficial to the reaction (entry 13). Tuning the reaction conditions for better solubility and stability of reactive intermediate, a series of reaction times and solvents were evaluated (entries 14-21). A reaction time of 6 hours in combination with toluene as solvent were found to be the best conditions. Although, considering the weak nucleophilicity of the amide, the increase of reaction temperature was evaluated. Increasing from 100 ˚C to 130 ˚C slightly improved the yield. A drastic acceleration of the reaction was observed at 150 ˚C, showing complete conversion and excellent yield of the desired product (entries 23-24). In the absence of metal catalyst or additive, no desired product was observed (entry 25-27). The silver chloride formed during the catalyst preformation likewise showed no activity in the reaction (entry 27).

Table 1. Optimization of reaction conditions

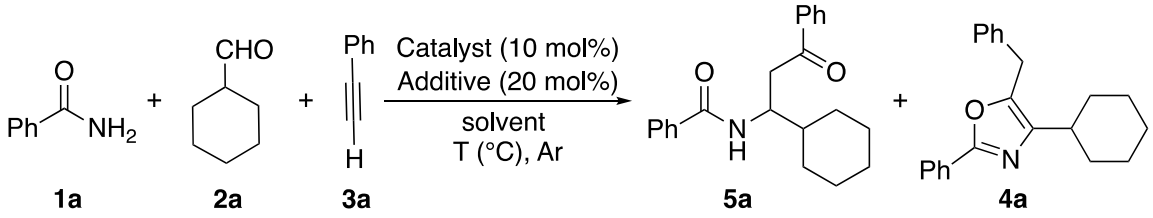

Entry	Catalyst	Additive	Solvent/time/T (°C)	Yield %	
				5a	**4a**
1	AuCl(SMe)	-	PhMe/18h/10	10	0
2	$AuBr_3$	-	PhMe/18h/10	15	0
3	Ph_3PAuCl	-	PhMe/18h/10	5	0
4	AuCl	iPr.Cl	PhMe/18h/10	5	0
5	$AuCl_3$	AgOTf	PhMe/18h/10	46	0
6	iMesAuCl	AgOTf	PhMe/18h/10	38	1
7	Et_3PAuCl	AgOTf	PhMe/18h/10	44	14
8	Ph_3PAuCl	AgOTf	PhMe/18h/10	45	30
9	Ph_3PAuCl	$AgBF_4$	PhMe/18h/10	10	6
10	Ph_3PAuCl	$AgSbF_6$	PhMe/18h/10	10	7
11	Ph_3PAuCl	$AgNTf_2$	PhMe/18h/10	7	5
12	Ph_3PAuCl	AgOTf + 4Å MS	PhMe/18h/10	0	0
13	Ph_3PAuCl	AgOTf (50 mol%)	PhMe/18h/10	30	8
14	Ph_3PAuCl	AgOTf	PhMe/3h/100	18	7
15	Ph_3PAuCl	AgOTf	PhMe/6h/100	45	30
16	Ph_3PAuCl	AgOTf	PhMe/18h/10	43	26
17	Ph_3PAuCl	AgOTf	PhMe/64h/10	50	25
18	Ph_3PAuCl	AgOTf	DCE/6h/100	44	0
19	Ph_3PAuCl	AgOTf	MeCN/6h/100	nd	0
20	Ph_3PAuCl	AgOTf	THF/6h/100	8	0
21	Ph_3PAuCl	AgOTf	H_20/6h/100	0	0
23	Ph_3PAuCl	AgOTf	PhMe/6h/130	5	45
24	Ph_3PAuCl	AgOTf	PhMe/6h/150	0	99
25	-	-	PhMe/6h/150	0	0
26	-	AgOTf	PhMe/6h/150	10	0
27	-	AgCl	PhMe/6h/150	0	0

Reaction conditions: benzamide (0.1 mmol), cyclohexylcarboxaldehyde (0.15 mmol), phenyl acetylene (0.15 mmol), solvent (0.5 mL), under Argon atmosphere. All reported yields were determined by ^1H NMR spectroscopy using dibromomethane as internal standard. Reported yield in brackets are isolated yield.

2.3.2 Mechanistic considerations

The efficiency of triphenylphosphine gold(I) cationic complex to catalyze the multicomponent reaction, led us to the mechanistic hypothesis shown below (Scheme 68). The gold(I) cationic complex **I** is form by abstraction of chlorine anion from triphenylphosphine gold chloride complex, catalyzed by silver triflate salt. Under its cationic form, gold(I) complex **I** reacts with phenyl acetylene, generating the gold acetylide species **II**.[125-126] In the meantime, the condensation reaction between amide (**1**) and aldehyde (**2**) results in the formation of the corresponding imide **III**, and generates the only by-product of the reaction: water. The following addition of gold acetylide **II** to the imide **III** affords the propargyl-amide **IV**, identically as the traditional A^3 reaction developed by our group. Thanks to the remarkable coordination ability of cationic gold species to alkyne,[127-129] the catalyst can facilitate the intramolecular 5-*exo*-*dig* cyclization reaction to generate a cyclic organogold complex **V**. Succeeding the formation of **V**, the oxazoline intermediate **VI** is obtained via protodeauration, which further tautomerize into the desired tri-substituted oxazole product (**4**).

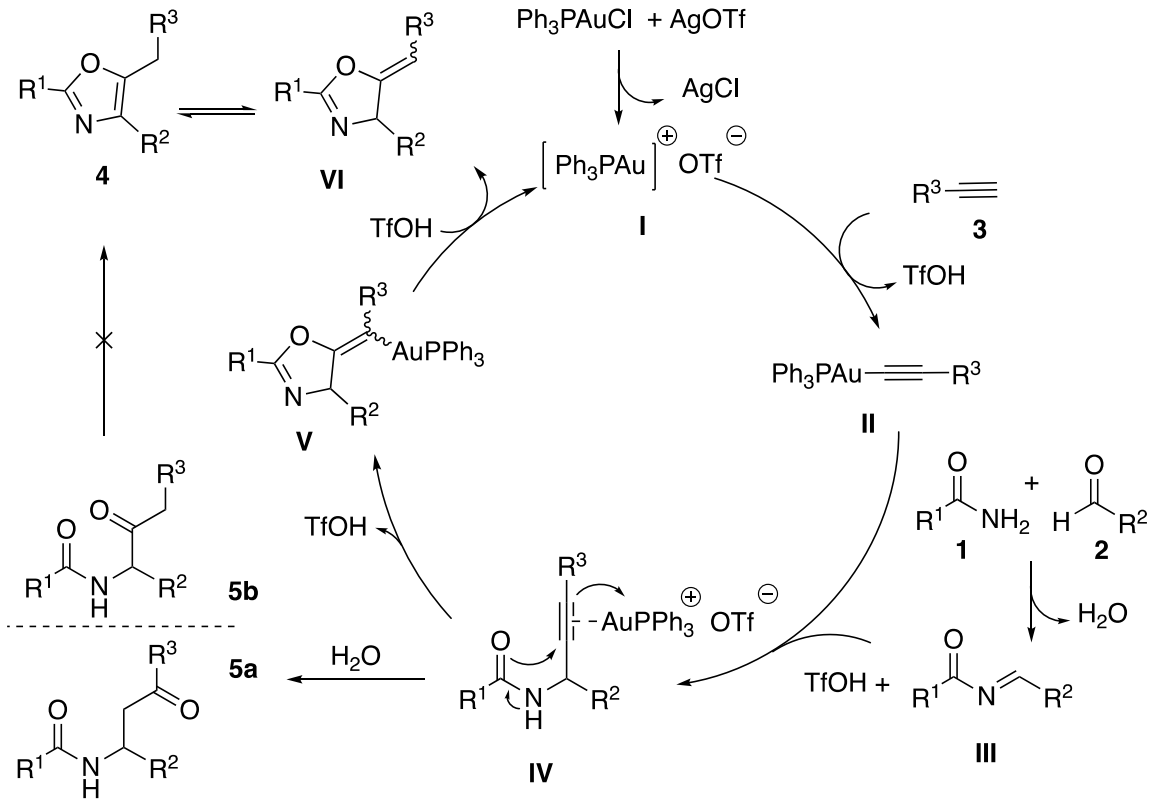

Scheme 68. Proposed mechanism for the gold catalyzed A^3 coupling / cycloisomerization reaction

2.3.3 Substrate scope for the gold catalyzed A^3 coupling / cycloisomerization reaction

With the optimized conditions in hand and a better understanding of the catalytic system, our system was applied to a variety of amides, aldehydes and alkynes. Firstly, we focused our evaluation on the influence of different aldehydes (Table 2).

Table 2. Scope of aldehydes

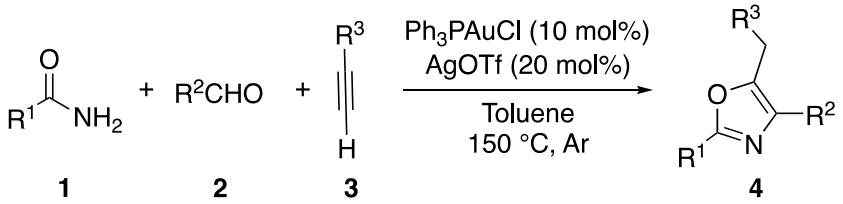

1 **2** **3** **4**

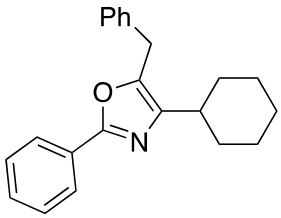

4a, 95%

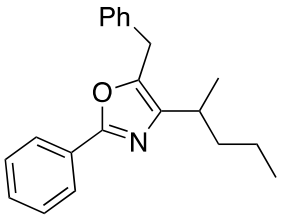

4b, 50%

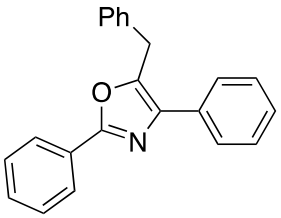

4c, 80%

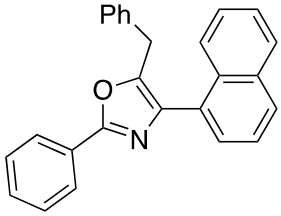

4d, 65%

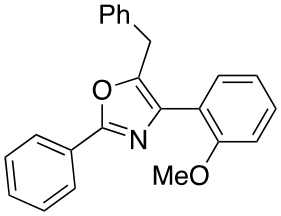

4e, 61%

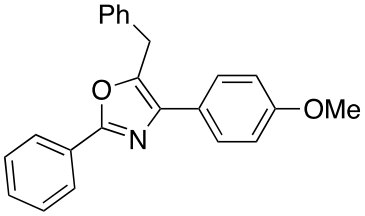

4f, 47%

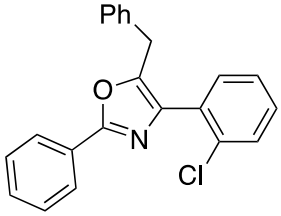

4g, 95%

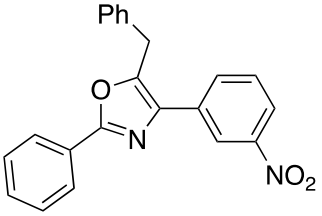

4h, 55%

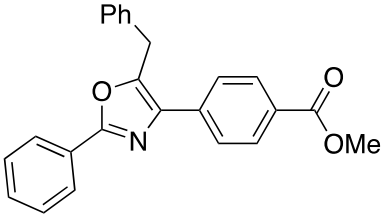

4i, 75%

Conditions: Amides (0.2 mmol), Aldehydes (0.3 mmol), Alkynes (0.3 mmol), Ph_3PAuCl (10 mol%), AgOTf (20 mol%), 0.5 mL of toluene, 6 h, under argon. Isolated yields reported.

Both aliphatic and aromatic aldehydes efficiently delivered the corresponding oxazoles in moderate to excellent yields. The cyclic cyclohexanecarboxaldehyde and the acyclic 2-methylpentanal afforded the corresponding oxazole (**4a**) and (**4b**) in 95% and 50% yield, respectively. Aromatic aldehydes with various functional groups were well tolerated and the corresponding products were isolated in good to excellent yields. The

reaction of benzaldehyde with other coupling partner afforded the oxazole (**4c**) in 80% yield. While aromatic aldehydes with both electron-withdrawing groups (EWG) and -donating groups (EDG) were well tolerated under the reaction conditions, aldehydes bearing EWGs such as *ortho*-Cl, *para*-NO_2 and ester substituents generally provided the desired product (**4g**, **4h** and **4i**, respectively) in higher yields compared to the ones bearing EDGs such as -OMe (**4e**, **4f**).

Secondly, the effect of both amide and alkyne partners were investigated in Table 3. In general, substituted benzamides possessing different EWGs and EDGs showed excellent reactivity resulting in good reaction yields (**4j**, **4k**, **4l**, **4m**, **4n**). Interestingly, the yield decreased slightly (87% to 70%) upon changing the *para*-MeO EDG to a *para*-Cl EWG. This decrease in the product yield can possibly be attributed to the lower nucleophilicity property of the *para*-Cl benzamide; the reactive intermediate **III** was arduously formed. Besides, alkyl amide exposed to our reaction system produced **4r** in a moderate yield.

Table 3. Scope of amides and alkynes

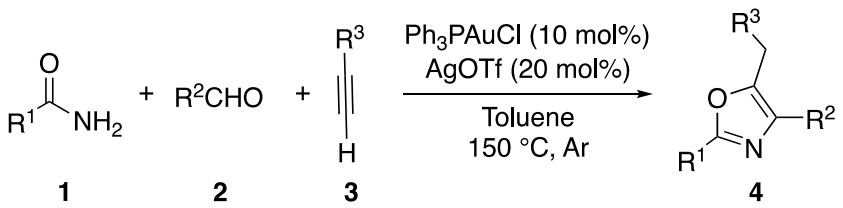

1 **2** **3** **4**

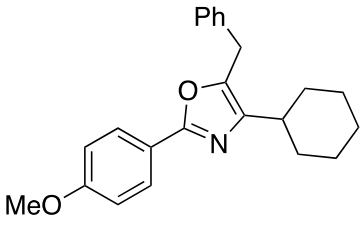

4j, 87%

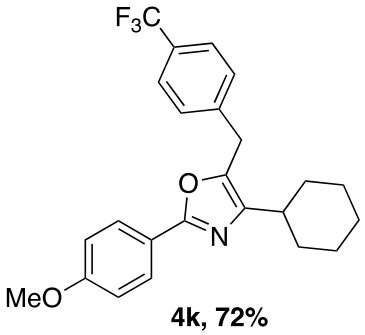

4k, 72%

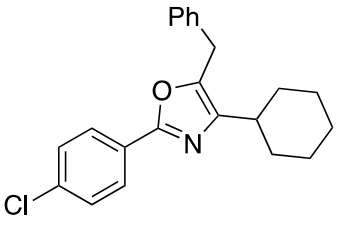

4l, 70%

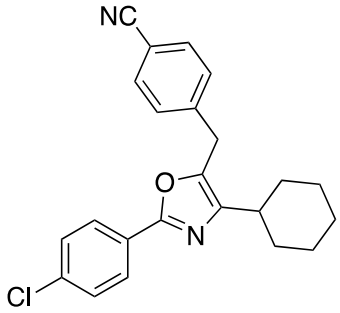

4m, 78%

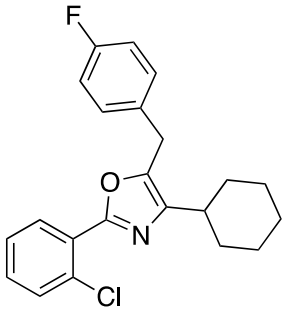

4n, 72%

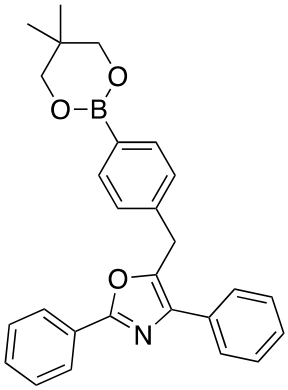

4o, 50%

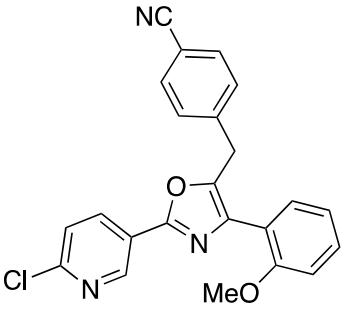

4p, 62%

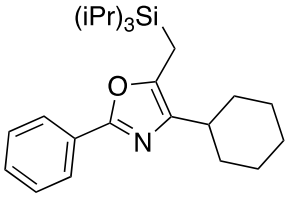

4q, 42%

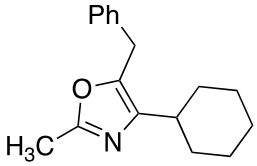

4r, 52%

Conditions: Amides (0.2 mmol), Aldehydes (0.3 mmol), Alkynes (0.3 mmol), Ph_3PAuCl (10 mol%), AgOTf (20 mol%), 0.5 mL of toluene, 6 h, under argon. Isolated yields reported.

Next, it is noteworthy that terminal alkynes bearing boronic ester were tolerated under the reaction conditions, providing the oxazole **4o** and a handle for further functionalization via the Suzuki coupling. To our delight, our method can be further extended to the substrates bearing heterocycle. The reaction of *para*-chloronicotinamide afforded the oxazole product **4p** in 62% yield**.** Fortunately, subjecting the substrate triisopropylsilyl acetylene to the standard reaction conditions could successfully afford the corresponding oxazole heterocyclic compound **4q**, albeit in a slightly lower yield.

2.3.4 Control experiments

Due to the elevated yield of side products during our investigation for the best reaction conditions, we envisioned the compound **5a** to be a potential reaction intermediate since it presents a similar structure as the starting material used in Robinson Gabriel reaction (Scheme 60). Along with the reaction time studies we have found that two hydrated isomers were generated during the reaction at 100 °C, **5a** and **5b** (Table 4).

Table 4. Time study

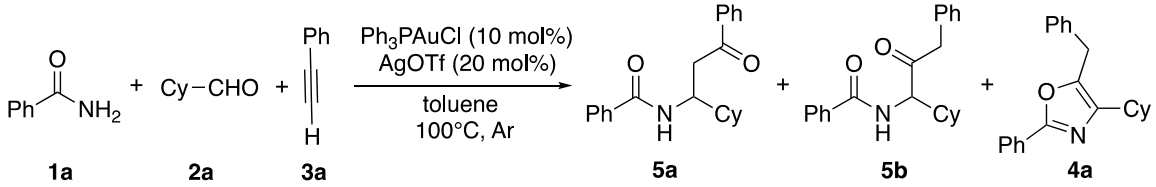

Entry	Time	Yield %		
		5a	5b	4a
1	3	18	11	7
2	6	45	10	30
3	18	43	12	26
4	64	50	10	25

Reaction conditions: benzamide (0.1 mmol), cyclohexylcarboxaldehyde (0.15 mmol), phenyl acetylene (0.15 mmol), solvent (0.5 mL), under Argon atmosphere. All reported yields were determined by ^{1}H NMR spectroscopy using dibromomethane as internal standard.

It is noteworthy that those hydrated products were produced at lower temperature exclusively. Control experiments with and without gold catalyst were conducted under

our optimized reaction conditions. We observed that compounds $\mathbf{5_a}$ and $\mathbf{5_b}$ did not lead to the formation of the corresponding oxazoles, and thus they do not represent a reactive intermediate.

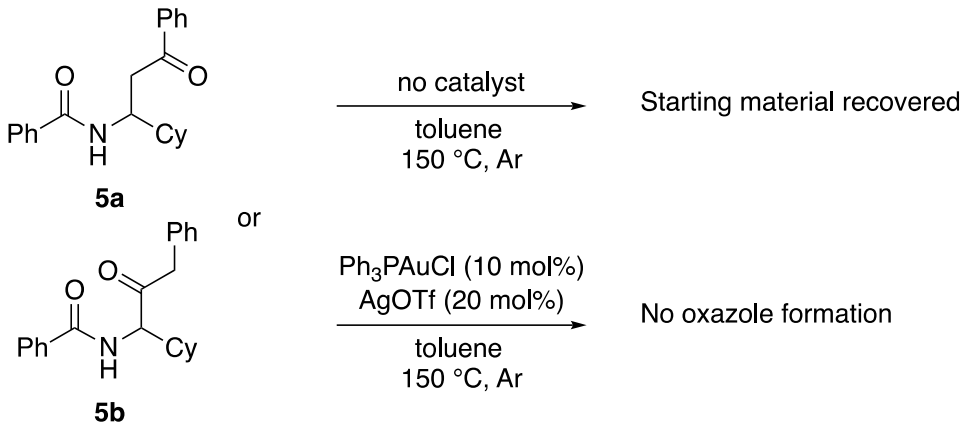

Scheme 69. Control experiments related to the side-products observed

Novel synthetic strategies have rarely been flawless with respect to the reaction scope, and this chemistry is certainly no exception. Apart from the low conversion found in a few substrates listed in Scheme 70, we observed a few problematic substrates that either remain unreactive or contain incompatible functional groups under standard conditions. Substrates bearing proximal chelating heteroatoms, in particular 2-ethynylpyridine **3s**, cyclohex-1-ene-1-carbaldehyde **2v** and picolinamide **1y** have respectively very low or no reactivity towards the formation of the corresponding oxazoles. Linear long chain aldehyde **2u** was found to be a limitation of this reaction. Modification from an unprotected amide to a –Bn and –Me protected amide, or thiobenzamide resulted in the absence of reaction with recovering of the starting material.

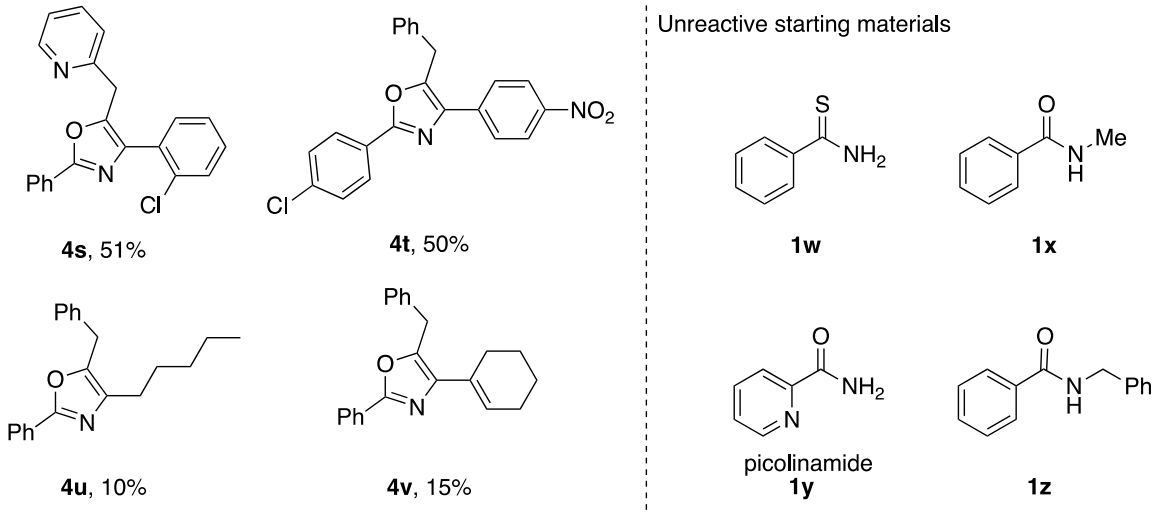

Scheme 70. Substrates with low or no activity under our reaction condition

2.4 Conclusions

To summarize chapter 2, we have successfully discovered and developed a highly efficient one-pot coupling method for the direct synthesis of tri-substituted oxazoles via an unprecedented amide, aldehyde and alkyne coupling (A^3). Using a single cationic gold(I) catalyst in one-pot, to accomplish both the A^3 and the cycloaddition reactions, this method provides a novel atom economical and practical way and a convenient alternative to construct important heterocyclic compounds, as water is the only side product. Concerning the rapid increase of molecular complexity along the reaction, we were satisfied to calculate a high and positive value of ΔC_m= 164.7, when all substituents are aromatic groups (Scheme 71).

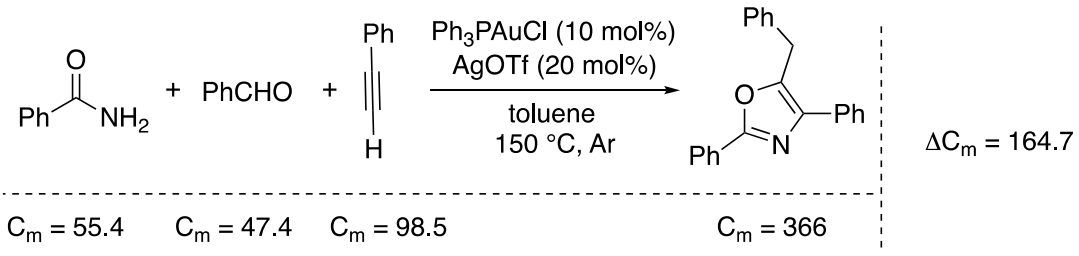

Scheme 71. Calculated molecular complexity for our model reaction

We further envisioned that this tandem reaction could be extended towards the synthesis of many other synthetically useful motifs, but also for the modification and use of amino acid and peptide structures. Moreover, a polymerization reaction approach by this method can be projected to access highly functionalized and complex oxazole based polymers.

2.5 Contributions

The reaction and conditions for the multicomponent A^3-cycloisomerization were developed by me (Pierre Querard), with supervision by Prof. Dr. Chao-Jun Li. All reactions, isolations, and characterizations (with the exception of high-resolution mass spectrometry) were performed by me. High-resolution mass spectrometry was performed by Dr. Nadim Saadeh at the McGill University Department of Chemistry Mass Spectrometry Laboratory. The manuscript upon which this chapter is based was prepared by me, with revision by Dr. Nicholas Uhlig, Dr. Simon Girard and Prof. Dr. Chao-Jun Li.

2.6 Experimental section

2.6.1 General information

Reaction setup: All reactions were carried out in flamed-dried V-shaped microwave reaction vials, covered by aluminum seals with PTFE-faced silicone septa, under an atmosphere of argon. All reported reaction temperatures correspond to oil bath temperatures.

Purifications: All work-up and purification procedures were carried out with reagent-grade solvents. Analytical thin-layer chromatography (TLC) was performed using E. Merck silica gel 60 F254 pre-coated plates (0.25 mm). Flash column chromatography was performed with E. Merck silica gel P60 (40–63 μm particle size, 230–400 mesh) (SiO2). Visualization was accomplished with UV light and/or iodine (I_2) or potassium permanganate (KMnO4) solution. Retention factor (Rf) values reported were measured using a 6 × 2 cm TLC plate in a developing chamber containing the solvent system (10 mL) described. Automated flash column chromatography was performed on Biotage Isolera™ Spektra Systems with ACI™.

Solvents: Dimethyl sulfoxide (DMSO), tetrahydrofuran (THF) and toluene were taken directly from the Pure Solvent MD-7 purification system (Innovative Technology). Solvents for filtration, transfers, chromatography, and recrystallization were dichloromethane (CH_2Cl_2) (ACS grade, amylene stabilized), ether (Et_2O) (Fisher, BHT stabilized ACS grade), acetone (ACS grade), ethyl acetate (EtOAc) (Fisher, ACS grade), hexane (Fisher, ACS grade), pentane (ACS grade), methanol (ACS grade).

NMR spectroscopy: Nuclear magnetic resonance (^1H, ^{13}C and ^{31}P $\{^1H\}$ NMR) spectra were recorded on a Bruker AV500 equipped with a 60-position SampleXpress sample changer (^1H, 500 MHz; ^{13}C, 125 MHz; ^{31}P, 202 MHz), a Varian MERCURY plus-500 spectrometer (^1H, 500 MHz; ^{13}C, 125 MHz) or Bruker AV400 spectrometer (^1H, 400 MHz; ^{13}C, 100 MHz). Chemical shifts for both ^1H NMR and ^{13}C NMR spectra were expressed in parts per million (ppm) units downfield from TMS, with the solvent residue peak as the chemical shift standard ($CDCl_3$: δ 7.28 ppm in ^1H NMR; δ 77.0 ppm in ^{13}C NMR; DMSO-d6: δ 2.50 ppm in ^1H NMR; δ 39.5 ppm in ^{13}C NMR). Data were reported as following: chemical shift, multiplicity (s = singlet, d = doublet, dd = doublet of doublets, t = triplet, td = triplet of doublets, q = quartet, quin = quintet, sep = septet, m = multiplet, br = broad singlet), coupling constants J (Hz), and integration.

Mass spectrometry: Mass spectrometry (MS) was performed by the McGill Chemistry Department Mass Spectrometry Facility. High Resolution Mass spectra were recorded using electrospray ionization (ESI+) and/or atmospheric pressure chemical ionization APCI (+/-), performed either on "Exactive Plus Orbitrap" a ThermoScientific high resolution accurate mass (HR/AM) FT mass spectrometer, or a Bruker Daltonics Maxis Impact quadrupole-time of flight (QTOF) mass spectrometer.

2.6.2 General procedure

A V-shaped 10 mL Biotage reaction vial was charged with Ph_3PAuCl (10 mol%), AgOTf (20 mol%), and the corresponding amide (0.2 mmol), evacuated and refilled with argon three times. Freshly distilled toluene (0.5 mL) was added followed by subsequent addition of aldehyde (0.3 mmol) and the terminal alkyne (0.3 mmol). The reaction vessel was

sealed, placed in an oil bath pre-heated at 150 °C under vigorous stirring (approx. 1400 rpm) and hold for 6 hours. The mixture was cooled to room temperature, diluted with ethyl acetate, filtered through a pad of silica, and rinsed with additional ethyl acetate. The combined rinsings were concentrated and purified by column chromatography or preparative thin layer chromatography to yield the corresponding oxazoles (**4**). Dibromomethane was used as internal standard for ^{1}H-NMR analysis.

2.6.3 Characterization of newly synthesized compounds

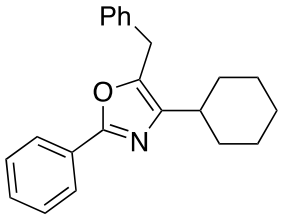

5-benzyl-4-cyclohexyl-2-phenyloxazole, (**4a**)

Use the general procedure described above, compound **4a** was obtained from benzamide (0.2 mmol, 24.2 mg), cyclohexane carboxaldehyde (0.3 mmol, 36.3 uL) and phenylacetylene (0.3 mmol, 34 uL) as a white solid (62.7 mg) in 95% yield.

^{1}H NMR ($CDCl_3$, 500 MHz): δ = 8.00-7.98 (m, 2H), 7.43-7.39 (m, 3H), 7.33-7.32 (m, 2H), 7.27-7.25 (m, 3H), 4.08 (s, 2H), 2.61-2.55 (tt, J = 11.7, 3.5 Hz, 1H), 1.87−1.80 (m, 4H), 1.74−1.69 (m, 3H), 1.38−1.34 (m, 3H).

^{13}C NMR ($CDCl_3$, 126 MHz): δ = 159.7, 143.9, 142.1, 138.0, 129.6, 128.6, 128.5, 128.3, 128.0, 126.6, 126.1, 35.7, 32.4, 31.1, 26.5, 25.8.

HRMS (ESI) m/z: [M + H]+ calculated for $C_{22}H_{24}NO$ 318.1858, found 318.1858.

Rf (hexane/EtOAc 4:1): 0.5.

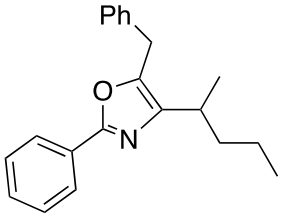

5-benzyl-4-(pentan-2-yl)-2-phenyloxazole, (**4b**)

Use the general procedure described above, compound **4b** was obtained from benzamide (0.2 mmol, 24.2 mg), 2-methylpentanal (0.3 mmol, 37 uL) and phenylacetylene (0.3 mmol, 34 uL) as a white solid (30.5 mg) in 50% yield.

^{1}H NMR ($CDCl_3$, 500 MHz): δ = 8.01-7.99 (m, 2H), 7.42-7.39 (m, 3H), 7.35-7.32 (m, 2H), 7.27-7.25 (m, 3H), 4.05 (s, 2H), 2.73-2.80 (sext, J = 6.8 Hz, 1H), 1.76−1.70 (m, 1H), 1.61−1.54 (m, 1H), 1.29-1.28 (d, J = 6.9 Hz, 3H), 1.28−1.24 (m, 1H), 0.99-0.92 (m, 1H), 0.87-0.90 (t, J = 7.4 Hz, 3H).

^{13}C NMR ($CDCl_3$, 126 MHz): δ = 159.8, 144.4, 141.6, 137.9, 129.6, 128.5, 128.4, 128.36, 128.0, 126.6, 126.1, 38.4, 31.0, 30.6, 20.8, 20.5, 14.7.

HRMS (ESI) m/z: [M + H]+ calculated for $C_{21}H_{24}NO$ 306.1858, found 306.1854.

Rf (hexane/EtOAc 4:1): 0.5.

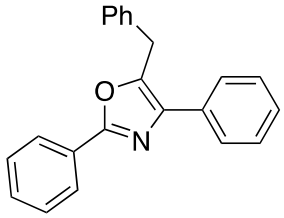

5-benzyl-2,4-diphenyloxazole, (**4c**)

Use the general procedure described above, compound **4c** was obtained from benzamide (0.2 mmol, 24.2 mg), benzaldehyde (0.3 mmol, 32 uL) and phenylacetylene (0.3 mmol, 34 uL) as a white solid (49.7 mg) in 80% yield.

^{1}H NMR ($CDCl_3$, 500 MHz): δ = 8.11-8.10 (m, 2H), 7.78-7.76 (m, 2H), 7.49-7.44 (m, 5H), 7.38-7.32 (m, 5H), 7.30-7.28 (m, 1H), 4.34 (s, 2H).

^{13}C NMR ($CDCl_3$, 126 MHz): δ = 160.2, 145.6, 137.3, 137.2, 132.0, 130.1, 128.8, 128.7, 128.2, 127.7, 127.5, 127.0, 126.8, 126.3, 31.9.

HRMS (ESI) m/z: [M + H]+ calculated for $C_{22}H_{18}NO$ 312.1388, found 312.1387.

Rf (hexane/EtOAc 4:1): 0.4.

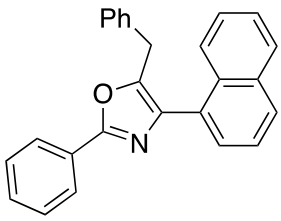

5-benzyl-4-(naphthalen-1-yl)-2-phenyloxazole, (**4d**)

Use the general procedure described above, compound **4d** was obtained from benzamide (0.2 mmol, 24.2 mg), 1-naphthaldehyde (0.3 mmol, 40.8 uL) and phenylacetylene (0.3 mmol, 34 uL) as a white solid (46.9 mg) in 65% yield.

^{1}H NMR ($CDCl_3$, 500 MHz): δ = 8.16-8.12 (m, 3H), 7.94-7.92 (m, 2H), 7.57-7.51 (m, 5H), 7.50-7.46 (m, 3H), 7.33-7.30 (m, 2H), 7.26-7.24 (m, 3H), 4.11 (s, 2H).

^{13}C NMR ($CDCl_3$, 126 MHz): δ = 160.3, 147.5, 137.3, 136.6, 133.9, 132.2, 130.1, 129.1, 129.0, 128.6, 128.5, 128.3, 128.1, 127.8, 127.6, 126.6, 126.4, 126.3, 126.07, 126.03, 125.2, 31.4.

HRMS (ESI) m/z: [M + H]+ calculated for $C_{26}H_{20}NO$ 362.1545, found 362.1543.

Rf (hexane/EtOAc 4:1): 0.6.

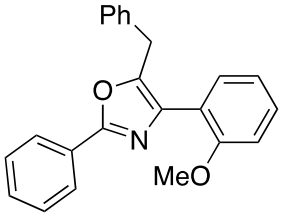

5-benzyl-4-(2-methoxyphenyl)-2-phenyloxazole, (**4e**)

Use the general procedure described above, compound **4e** was obtained from benzamide (0.2 mmol, 24.2 mg), 2-methoxybenzaldehyde (0.3 mmol, 36.3 uL) and phenylacetylene (0.3 mmol, 34 uL) as a white solid (41.5 mg) in 61% yield.

^{1}H NMR ($CDCl_3$, 500 MHz): δ = 8.09-8.07 (m, 2H), 7.63-7.61 (m, 1H), 7.46-7.43 (m, 3H), 7.39-7.36 (m, 1H), 7.33-7.27 (m, 4H), 7.27-7.24 (m, 1H), 4.15 (s, 2H), 3.75 (s, 3H).

^{13}C NMR ($CDCl_3$, 126 MHz): δ = 160.2, 156.7, 147.3, 137.8, 133.9, 131.3, 129.7, 129.5, 128.6, 128.5, 128.41, 127.6, 126.4, 126.3, 121.0, 120.8, 111.0, 55.3, 32.1.

HRMS (ESI) m/z: [M + H]+ calculated for $C_{23}H_{20}NO_2$ 342.1494, found 342.1494.

Rf (hexane/EtOAc 4:1): 0.6.

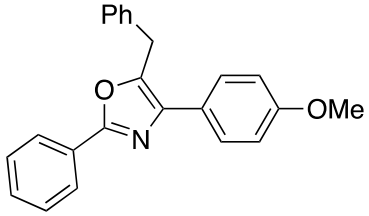

5-benzyl-4-(4-methoxyphenyl)-2-phenyloxazole, (**4f**)

Use the general procedure described above, compound **4f** was obtained from benzamide (0.2 mmol, 24.2 mg), 4-methoxybenzaldehyde (0.3 mmol, 36.6 uL) and phenylacetylene (0.3 mmol, 34 uL) as a white solid (32.0 mg) in 47% yield.

^{1}H NMR ($CDCl_3$, 500 MHz): δ = 8.10-8.08 (m, 2H), 7.70-7.67 (m, 2H), 7.48-7.43 (m, 3H), 7.37-7.28 (m, 4H), 7.00-6.97 (m, 2H), 4.31 (s, 2H), 3.86 (s, 3H).

^{13}C NMR ($CDCl_3$, 126 MHz): δ = 160.0, 159.2, 144.7, 137.4, 137.0, 130.0, 128.7, 128.6, 128.3, 128.2, 127.6, 126.7, 126.2, 124.6, 114.1, 55.3, 31.9.

HRMS (ESI) m/z: [M + H]+ calculated for $C_{23}H_{20}NO_2$ 342.1494, found 342.1494.

Rf (hexane/EtOAc 4:1): 0.6.

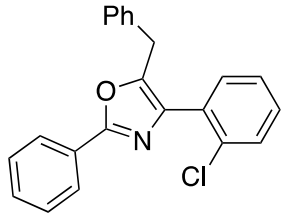

5-benzyl-4-(2-chlorophenyl)-2-phenyloxazole, (**4g**)

Use the general procedure described above, compound **4g** was obtained from benzamide (0.2 mmol, 24.2 mg), 2-chlorobenzaldehyde (0.3 mmol, 33.6 uL) and phenylacetylene (0.3 mmol, 34 uL) as a white solid (65.7 mg) in 95% yield.

^{1}H NMR ($CDCl_3$, 500 MHz): δ = 8.08-8.06 (m, 2H), 7.52-7.49 (m, 2H), 7.46-7.45 (m, 3H), 7.36-7.34 (m, 2H), 7.32-7.29 (m, 2H), 7.25-7.24 (m, 3H), 4.11 (s, 2H).

^{13}C NMR ($CDCl_3$, 126 MHz): δ = 160.3, 147.5, 136.9, 135.1, 133.9, 132.0, 131.0, 130.21, 129.9, 129.7, 128.6, 128.5, 128.5, 127.4, 126.8, 126.7, 126.3, 55.3, 31.9.

HRMS (ESI) m/z: [M + H]+ calculated for $C_{22}H_{17}ClNO$ 346.0999, found 346.0996.

Rf (hexane/EtOAc 4:1): 0.6.

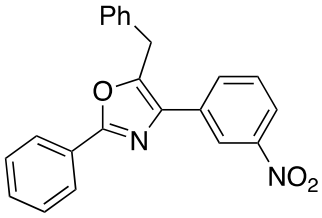

5-benzyl-4-(3-nitrophenyl)-2-phenyloxazole, (**4h**)

Use the general procedure described above, compound **4h** was obtained from benzamide (0.2 mmol, 24.2 mg), 3-nitrobenzaldehyde (0.3 mmol, 45.3 mg), and phenylacetylene (0.3 mmol, 34 uL) as a white solid (65.7 mg) in 55% yield.

^{1}H NMR ($CDCl_3$, 500 MHz): δ = 8.64 (s, 1H), 8.18-8.19 (m, 1H), 8.12-8.08 (m, 3H), 7.62-7.58 (m, 1H), 7.50-7.49 (m, 3H), 7.39-7.33 (m, 4H), 7.31-7.29 (m, 1H), 4.38 (s, 2H).

^{13}C NMR ($CDCl_3$, 126 MHz): δ = 160.5, 148.5, 147.1, 136.2, 135.0, 133.8, 132.5, 130.5, 129.6, 128.9, 128.8, 128.6, 128.3, 127.1, 126.4, 122.2, 121,7, 32.1.

HRMS (ESI) m/z: [M + H]+ calculated for $C_{22}H_{17}N_2O_3$ 357.1239, found 357.1234.

Rf (hexane/EtOAc 4:1): 0.6.

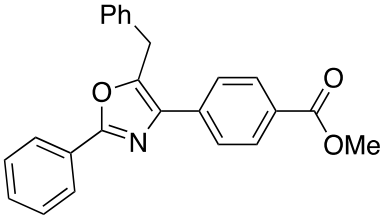

methyl 4-(5-benzyl-2-phenyloxazol-4-yl)benzoate, (**4i**)

Use the general procedure described above, compound **4i** was obtained from benzamide (0.2 mmol, 24.2 mg), methyl 4-formylbenzoate (0.3 mmol, 49.2 mg) and phenylacetylene (0.3 mmol, 34 uL) as a white solid (83.1 mg) in 75% yield.

^{1}H NMR ($CDCl_3$, 500 MHz): δ = 8.13-8.09 (m, 4H), 7.86-7.84 (m, 2H), 7.49-7.47 (m, 3H), 7.36-7.35 (m, 2H), 7.32-7.29 (m, 3H), 4.37 (s, 2H), 3.95 (s, 3H).

^{13}C NMR ($CDCl_3$, 126 MHz): δ = 166.8, 160.4, 146.9, 136.7, 136.5, 136.3, 130.3, 130.0, 129.1, 128.8, 128.7, 128.2, 127.2, 126.9, 126.7, 126.3, 52.1, 32.1.

HRMS (ESI) m/z: [M + H]+ calculated for $C_{24}H_{20}NO_3$ 370.1443, found 370.1446.

Rf (hexane/EtOAc 4:1): 0.5.

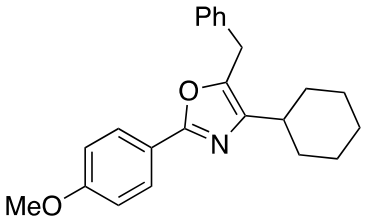

5-benzyl-4-cyclohexyl-2-(4-methoxyphenyl)oxazole, (**4j**)

Use the general procedure described above, compound **4j** was obtained from 4-methoxybenzamide (0.2 mmol, 30.24 mg), cyclohexane carboxaldehyde (0.3 mmol, 36.3 uL) and phenylacetylene (0.3 mmol, 34 uL) as a white solid (90.6 mg) in 87% yield.

^{1}H NMR ($CDCl_3$, 500 MHz): δ = 7.93-7.91 (m, 2H), 7.35-7.32 (m, 2H), 7.28-7.25 (m, 3H), 6.94-6.92 (m, 2H), 4.06 (s, 2H), 3.85 (s, 3H), 2.59-2.54 (tt, J = 11.7, 3.5 Hz, 1H), 1.86−1.80 (m, 4H), 1.73−1.67 (m, 3H), 1.38−1.28 (m, 3H).

^{13}C NMR ($CDCl_3$, 126 MHz): δ = 160.8, 159.8, 143.2, 141.8, 138.1, 128.5, 128.3, 127.7, 126.5, 120.9, 113.9, 55.3, 35.7, 32.4, 31.1, 26.5, 25.8.

HRMS (ESI) m/z: [M + H]+ calculated for $C_{23}H_{26}NO_2$ 348.1964, found 348.1957.

Rf (hexane/EtOAc 4:1): 0.5.

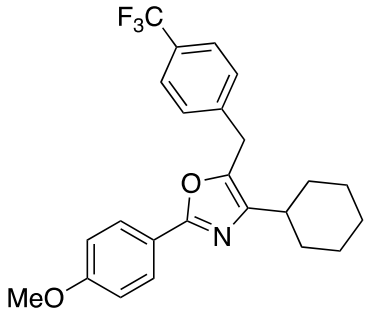

4-cyclohexyl-2-(4-methoxyphenyl)-5-(4-(trifluoromethyl) benzyl)oxazole, (**4k**)

Use the general procedure described above, compound **4k** was obtained from 4-methoxybenzamide (0.2 mmol, 30.24 mg), cyclohexane carboxaldehyde (0.3 mmol, 36.3 uL) and 1-ethynyl-4-(trifluoromethyl) benzene (0.3 mmol, 32.6 uL) as a white solid (59.8 mg) in 72% yield.

^{1}H NMR ($CDCl_3$, 500 MHz): δ = 7.92-7.90 (m, 2H), 7.59-7.58 (m, 2H), 7.37-7.35 (m, 2H), 6.94-6.92 (m, 2H), 4.11 (s, 2H), 3.85 (s, 3H), 2.58-2.53 (tt, J = 11.7, 3.5 Hz, 1H), 1.87−1.79 (m, 4H), 1.73−1.66 (m, 3H), 1.38−1.31 (m, 3H).

^{13}C NMR ($CDCl_3$, 126 MHz): δ = 160.9, 160.1, 142.3, 142.2, 142.2, 142.1, 128.6, 127.7, 125.5 (q, J = 3 Hz), 120.6, 113.9, 55.3, 35.74, 32.4, 30.9, 26.5, 25.8.

HRMS (ESI) m/z: [M + H]+ calculated for $C_{24}H_{25}F_3NO_2$ 416.1837, found 416.1830.

Rf (hexane/EtOAc 4:1): 0.5.

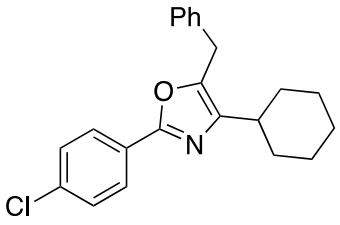

5-benzyl-2-(4-chlorophenyl)-4-cyclohexyloxazole, (**4l**)

Use the general procedure described above, compound **4l** was obtained from 4-chlorobenzamide (0.2 mmol, 31.10 mg), cyclohexane carboxaldehyde (0.3 mmol, 36.3 uL) and phenylacetylene (0.3 mmol, 34 uL) as a white solid (49.2 mg) in 70% yield.

^{1}H NMR ($CDCl_3$, 500 MHz): δ = 7.93-7.91 (m, 2H), 7.40-7.37 (m, 2H), 7.35-7.30 (m, 2H), 7.28-7.24 (m, 3H), 4.07 (s, 2H), 2.60-2.54 (tt, J = 11.9, 3.6 Hz, 1H), 1.87−1.79 (m, 4H), 1.75−1.66 (m, 3H), 1.41−1.31 (m, 3H).

^{13}C NMR ($CDCl_3$, 126 MHz): δ = 158.8, 144.3, 142.3, 137.8, 135.6, 128.8, 128.6, 128.3, 127.4, 126.6, 126.4, 35.5, 32.4, 31.1, 26.5, 25.8.

HRMS (ESI) m/z: [M + H]+ calculated for $C_{22}H_{23}ClNO$ 352.1468, found 352.1463.

Rf (hexane/EtOAc 4:1): 0.5.

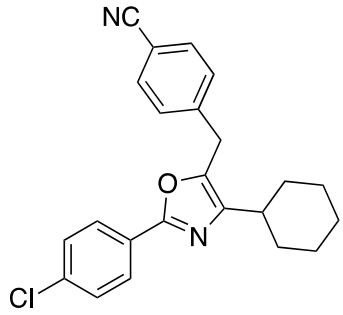

4-((2-(4-chlorophenyl)-4-cyclohexyloxazol-5-yl)methyl) benzonitrile, (**4m**)

Use the general procedure described above, compound **4m** was obtained from 4-chlorobenzamide (0.2 mmol, 31.10 mg), 4-ethynylbenzonitrile (0.3 mmol, 38.2 mg) and cyclohexane carboxaldehyde (0.3 mmol, 36.3 uL) as a white solid (58.7 mg) in 78% yield.

^{1}H NMR ($CDCl_3$, 500 MHz): δ = 7.91-7.89 (m, 2H), 7.64-7.62 (m, 2H), 7.40-7.38 (m, 2H), 7.35-7.33 (m, 2H), 4.12 (s, 2H), 2.57-2.52 (tt, J = 11.8, 3.6 Hz, 1H), 1.87−1.74 (m, 4H), 1.71−1.67 (m, 3H), 1.38−1.33 (m, 3H).

^{13}C NMR ($CDCl_3$, 126 MHz): δ = 159.2, 143.3, 143.0, 142.5, 135.9, 132.5, 129.0, 128.9, 127.4, 126.1, 118.7, 110.7, 35.6, 32.3, 31.2, 26.4, 25.7.

HRMS (ESI) m/z: [M + H]+ calculated for $C_{23}H_{22}ClN_2O$ 377.1421, found 377.1417.

Rf (hexane/EtOAc 4:1): 0.3.

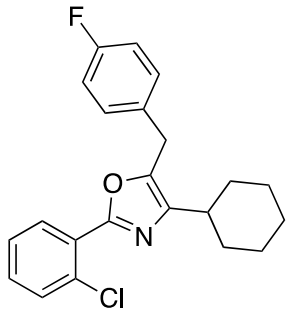

2-(2-chlorophenyl)-4-cyclohexyl-5-(4-fluorobenzyl)oxazole, (**4n**)

Use the general procedure described above, compound **4n** was obtained from 2-chlorobenzamide (0.2 mmol, 31.10 mg), cyclohexane carboxaldehyde (0.3 mmol, 36.3 uL) and 1-ethynyl-4-fluorobenzene (0.3 mmol, 34.4 uL) as a white solid (53.2 mg) in 72% yield.

^{1}H NMR ($CDCl_3$, 500 MHz): δ = 7.94-7.91 (m, 1H), 7.47-7.44 (m, 1H), 7.33-7.29 (m, 2H), 7.25-7.21 (m, 2H), 7.04-6.99 (m, 2H), 4.05 (s, 2H), 2.61-2.55 (tt, J = 11.7, 3.5 Hz, 1H), 1.85−1.80 (m, 4H), 1.76−1.66 (m, 3H), 1.42−1.30 (m, 3H).

^{13}C NMR ($CDCl_3$, 126 MHz): δ = 162.6, 160.7, 157.8, 144.5 141.7, 133.49, 133.46, 132.3, 130.9, 130.5, 129.88, 129.81, 126.9, 126.6, 115.4, 115.3, 35.5, 32.4, 30.4, 26.5, 25.8.

HRMS (ESI) m/z: [M + H]+ calculated for $C_{22}H_{22}ClFNO$ 370.1374, found 370.1372.

Rf (hexane/EtOAc 4:1): 0.8.

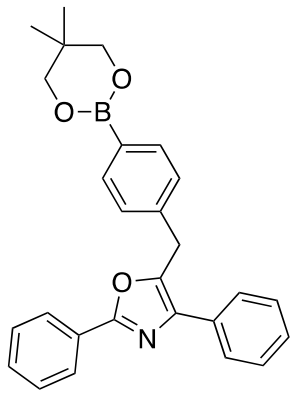

5-(4-(5,5-dimethyl-1,3,2-dioxaborinan-2-yl)benzyl)-2,4-diphenyloxazole, (**4o**)

Use the general procedure described above, compound **4o** was obtained from benzamide (0.2 mmol, 24.2 mg), 2-(4-ethynylphenyl)-5,5-dimethyl-1,3,2- dioxaborinane (0.3 mmol, 32 mg) and benzaldehyde (0.3 mmol, 32 uL) as a white solid (42.3 mg) in 50% yield.

^{1}H NMR ($CDCl_3$, 500 MHz): δ = 8.10-8.08 (m, 2H), 7.80-7.78 (m, 2H), 7.76-7.74 (m, 2H), 7.47-7.43 (m, 5H), 7.37-7.36 (m, 1H), 7.32-7.30 (m, 2H), 4.34 (s, 2H), 3.78 (s, 4H), 1.03 (s, 6H).

^{13}C NMR ($CDCl_3$, 126 MHz): δ = 160.1, 145.5, 143.9, 139.7, 137.7, 134.3, 132.0, 130.1, 128.6, 127.5, 127.0, 126.3, 72.3, 32.1, 31.8, 21.9.

HRMS (ESI) m/z: [M + H]+ calculated for $C_{27}H_{27}BNO_3$ 423.2084, found 423.2074.

Rf (hexane/EtOAc 4:1): 0.5.

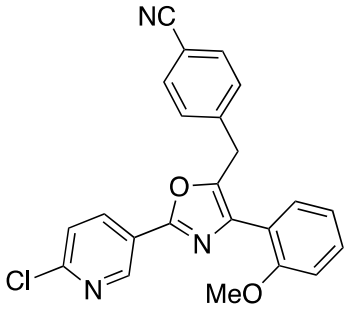

4-((2-(6-chloropyridin-3-yl)-4-(2-methoxyphenyl)oxazol-5-yl)methyl)benzonitrile, (**4p**)

Use the general procedure described above, compound **4p** was obtained from 6-chloronicotinamide (0.2 mmol, 31.31 mg), 4-ethynylbenzonitrile (0.3 mmol, 38.2 mg) and 2-methoxybenzaldehyde (0.3 mmol, 36.3 uL) as a white solid (49.8 mg) in 62% yield.

^{1}H NMR ($CDCl_3$, 500 MHz): δ = 9.04-9.03 (m, 1H), 8.28-8.25 (m, 1H), 7.62-7.59 (m, 3H), 7.43-7.39 (m, 2H), 7.37-7.35 (m, 1H), 7.11-7.08 (m, 1H), 6.99-6.97 (m, 1H), 4.22 (s, 2H), 3.71 (s, 3H).

^{13}C NMR ($CDCl_3$, 126 MHz): δ = 157.3, 156.4, 152.7, 147.4, 146.7, 142.9, 135.9, 135.2, 132.3, 131.1, 130.1, 129.2, 124.3, 122.6, 121.1, 120.0, 118.7, 111.1, 110.6, 55.3, 32.3.

HRMS (ESI) m/z: [M + H]+ calculated for $C_{23}H_{17}ClN_3O_2$ 402.1009, found 402.1007.

Rf (hexane/EtOAc 4:1): 0.5.

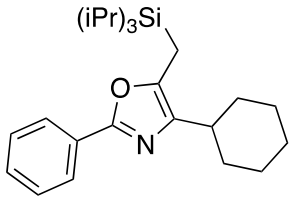

4-cyclohexyl-2-phenyl-5-((triisopropylsilyl)methyl)oxazole, (**4q**)

Use the general procedure described above, compound **4q** was obtained from benzamide (0.2 mmol, 24.2 mg), cyclohexane carboxaldehyde (0.3 mmol, 36.3 uL) and triisopropylsilyl acetylene (0.3 mmol, 67.3 uL) as a white solid (33.4 mg) in 42% yield.

^{1}H NMR ($CDCl_3$, 500 MHz): δ = 7.97-7.95 (m, 2H), 7.44-7.41 (m, 2H), 7.39-7.38 (m, 1H), 2.51-2.46 (tt, J = 11.7, 3.5 Hz, 1H), 2.13 (s, 2H), 1.87−1.85 (m, 2H), 1.78−1.69 (m, 5H), 1.37−1.35 (m, 3H), 1.19-1.16 (m, 3H), 1.10-1.08 (d, J = 5.4 Hz, 18H).

^{13}C NMR ($CDCl_3$, 126 MHz): δ = 158.2, 144.8, 129.1, 128.6, 128.5, 125.7, 125.7, 35.5, 32.2, 26.6, 25.9, 18.5, 11.3, 6.7.

HRMS (ESI) m/z: [M + H]+ calculated for $C_{25}H_{40}NOSi$ 398.2879, found 398.2875.

Rf (hexane/EtOAc 4:1): 0.8.

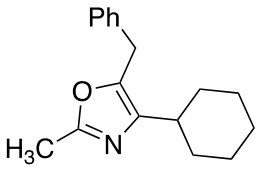

5-benzyl-4-cyclohexyl-2-methyloxazole, (**4r**)

Use the general procedure described above, compound **4r** was obtained from acetamide (0.2 mmol, 17.4 mg), cyclohexane carboxaldehyde (0.3 mmol, 36.3 uL) and phenylacetylene (0.3 mmol, 34 uL) as a yellowish solid (26.5 mg) in 52% yield.

^{1}H NMR ($CDCl_3$, 500 MHz): δ = 7.33-7.30 (m, 2H), 7.26-7.23 (m, 1H), 7.20-7.19 (m, 2H), 3.94 (s, 2H), 2.50-2.44 (tt, J = 11.9, 3.5 Hz, 1H), 2.37 (s, 3H), 1.84−1.82 (m, 2H), 1.75−1.71 (m, 3H), 1.65−1.58 (m, 2H), 1.37-1.27 (m, 3H).

^{13}C NMR ($CDCl_3$, 126 MHz): δ = 159.5, 143.3, 140.2, 138.0, 128.5, 128.2, 126.5, 35.2, 30.8, 26.5, 25.8, 14.0.

HRMS (ESI) m/z: [M + H]+ calculated for $C_{17}H_{22}NO$ 255.1623, found 255.1624.

Rf (hexane/EtOAc 4:1): 0.7.

2.7 References

[1] Zinin, N., *Ann.,* **1840,** *34*, 186-192.
[2] Cornforth, J. W., *The Chemistry of Penicillin*. Princeton University Press, Princeton, N.J.: **1949**.
[3] Cornforth, J. W.; Cornforth, R. H., *J. Chem. Soc.,* **1947**, 96-102.
[4] Fischer, E., *Ber.,* **1896,** *29*, 205.
[5] Wiley, R. H., *Chem. Rev.,* **1945,** *37*, 401-442.
[6] Cass, W. E., *J. Am. Chem. Soc.,* **1942,** *64*, 785-787.
[7] Rosenbaum, J. J.; Cass, W. E., *J. Am. Chem. Soc.,* **1942,** *64*, 2444-2445.
[8] Hantzsch, A., *Justus Liebigs Ann. Chem.,* **1889,** *250*, 257-273.
[9] Hantzsch, A., *Ber.,* **1888,** *21*, 942-946.
[10] Lewy, M., *Ber.,* **1888,** *21*, 924-931.
[11] Huisgen, R., *Angew. Chem.,* **1963,** *75*, 604-637.
[12] Buu, N. T.; Edward, J. T., *Can. J. Chem.,* **1972,** *50*, 3730-3737.
[13] Lakhan, R.; Ternai, B., Advances in Oxazole Chemistry. In *Adv. Heterocycl. Chem.*, Katritzky, A. R.; Boulton, A. J., Eds. Academic Press: 1974; Vol. 17, pp 99-211.
[14] Turchi, I. J.; Dewar, M. J. S., *Chem. Rev.,* **1975,** *75*, 389-437.
[15] Turchi, I. J., *Ind. Eng. Chem. Prod. Res. Dev.,* **1981,** *20*, 32-76.
[16] Charles Dylan, T.; Huan Steven, L., *Curr. Org. Chem.,* **2011,** *15*, 2846-2870.
[17] Zhang, H.; Zhou, C.; Geng, R.; Ji, Q., *Recent Advances in Syntheses of Oxazole Compounds*. **2011**; Vol. 31, p 1963-1976.
[18] Robinson, R., *J. Chem. Soc.,* **1909,** *95*, 2167-2174.
[19] Wasserman, H. H.; Vinick, F. J., *J. Org. Chem.,* **1973,** *38*, 2407-2408.
[20] Gabriel, S., *Ber.,* **1910,** *48*, 1283.
[21] Keni, M.; Tepe, J. J., *J. Org. Chem.,* **2005,** *70*, 4211-4213.
[22] Wipf, P.; Miller, C. P., *J. Org. Chem.,* **1993,** *58*, 3604-3606.
[23] Van Leusen, A. M.; Hoogenboom, B. E.; Siderius, H., *Tetrahedron Lett.,* **1972,** *13*, 2369-2372.

[24] Quan, M. L.; Pruitt, J. R.; Ellis, C. D.; Liauw, A. Y.; Galemmo, R. A.; Stouten, P. F. W.; Wityak, J.; Knabb, R. M.; Thoolen, M. J.; Wong, P. C.; Wexler, R. R., *Bioorg. Med. Chem. Lett.,* **1997,** *7*, 2813-2818.
[25] Wang, W.-L.; Chai, S. C.; Huang, M.; He, H.-Z.; Hurley, T. D.; Ye, Q.-Z., *J. Med. Chem.,* **2008,** *51*, 6110-6120.
[26] Brescia, M.-R.; Rokosz, L. L.; Cole, A. G.; Stauffer, T. M.; Lehrach, J. M.; Auld, D. S.; Henderson, I.; Webb, M. L., *Bioorg. Med. Chem. Lett.,* **2007,** *17*, 1211-1215.
[27] Wipf, P.; Rahman, L. T.; Rector, S. R., *J. Org. Chem.,* **1998,** *63*, 7132-7133.
[28] Yura, Y., *Chem. Pharm. Bull.,* **1962,** *10*, 1087-1093.
[29] Nilsson, B. M.; Hacksell, U., *J. Heterocycl. Chem.,* **1989,** *26*, 269-275.
[30] Lautens, M.; Klute, W.; Tam, W., *Chem. Rev.,* **1996,** *96*, 49-92.
[31] Y. Yasuo Japanese Patent. 29,849, **1964**.
[32] Y. Yasuo, *Chem. Abstr.,* **1965,** *62*, 11818.
[33] Hu, Y.; Xin, X.; Wan, B., *Tetrahedron Lett.,* **2015,** *56*, 32-52.
[34] Eloy, F. D., A., *Chim. Ther.,* **1973,** *8*, 437.
[35] Street, L. J.; Baker, R.; Castro, J. L.; Chambers, M. S.; Guiblin, A. R.; Hobbs, S. C.; Matassa, V. G.; Reeve, A. J.; Beer, M. S., *J. Med. Chem.,* **1993,** *36*, 1529-1538.
[36] Bonardi, A.; Costa, M.; Gabriele, B.; Salerno, G.; Chiusoli, G. P., *Tetrahedron Lett.,* **1995,** *36*, 7495-7498.
[37] Arcadi, A.; Cacchi, S.; Cascia, L.; Fabrizi, G.; Marinelli, F., *Org. Lett.,* **2001,** *3*, 2501-2504.
[38] Beccalli, E. M.; Borsini, E.; Broggini, G.; Palmisano, G.; Sottocornola, S., *J. Org. Chem.,* **2008,** *73*, 4746-4749.
[39] Hashmi, A. S. K.; Weyrauch, J. P.; Frey, W.; Bats, J. W., *Org. Lett.,* **2004,** *6*, 4391-4394.
[40] Milton, M. D.; Inada, Y.; Nishibayashi, Y.; Uemura, S., *Chem. Commun.,* **2004**, 2712-2713.
[41] Desroy, N.; Moreau, F.; Briet, S.; Fralliec, G. L.; Floquet, S.; Durant, L.; Vongsouthi, V.; Gerusz, V.; Denis, A.; Escaich, S., *Biorg. Med. Chem.,* **2009,** *17*, 1276-1289.
[42] Wang, W.-L.; Yao, D.-Y.; Gu, M.; Fan, M.-Z.; Li, J.-Y.; Xing, Y.-C.; Nan, F.-J., *Bioorg. Med. Chem. Lett.,* **2005,** *15*, 5284-5287.
[43] Yeh, V. S. C., *Tetrahedron,* **2004,** *60*, 11995-12042.
[44] Wipf, P., *Chem. Rev.,* **1995,** *95*, 2115-2134.
[45] Jin, Z., *Nat. Prod. Rep.,* **2006,** *23*, 464-496.
[46] Jin, Z., *Nat. Prod. Rep.,* **2009,** *26*, 382-445.
[47] Jin, Z., *Nat. Prod. Rep.,* **2011,** *28*, 1143-1191.
[48] Iddon, B., *Heterocycles,* **1994,** *37*, 1321-1346.
[49] Jones, R. C.; Chojnacka, M. W.; Quail, J. W.; Gardiner, M. G.; Decken, A.; Yates, B. F.; Gossage, R. A., *Dalton Trans.,* **2011,** *40*, 1594-1600.
[50] Decken, A.; Gossage, R. A., *J. Inorg. Biochem.,* **2005,** *99*, 664-667.
[51] Piguel, S.; Besselièvre, F.; Lebrequier, S.; Mahuteau-Betzer, F., *Synthesis,* **2009,** *20*, 3511-3518.
[52] Lassalas, P.; Marsais, F.; Hoarau, C., *Synlett,* **2013,** *24*, 2233-2240.

[53] Strotman, N. A.; Chobanian, H. R.; Guo, Y.; He, J.; Wilson, J. E., *Org. Lett.,* **2010,** *12*, 3578-3581.
[54] Shen, X.-B.; Zhang, Y.; Chen, W.-X.; Xiao, Z.-K.; Hu, T.-T.; Shao, L.-X., *Org. Lett.,* **2014,** *16*, 1984-1987.
[55] Ackermann, L.; Kornhaass, C.; Zhu, Y., *Org. Lett.,* **2012,** *14*, 1824-1826.
[56] Huang, J.; Chan, J.; Chen, Y.; Borths, C. J.; Baucom, K. D.; Larsen, R. D.; Faul, M. M., *J. Am. Chem. Soc.,* **2010,** *132*, 3674-3675.
[57] Verrier, C.; Martin, T.; Hoarau, C.; Marsais, F., *J. Org. Chem.,* **2008,** *73*, 7383-7386.
[58] Shin, C.-g.; Sato, Y.; Sugiyama, H.; Nanjo, K.; Yoshimura, J., *Bull. Chem. Soc. Jpn.,* **1977,** *50*, 1788-1792.
[59] Das, J.; Reid, J. A.; Kronenthal, D. R.; Singh, J.; Pansegrau, P. D.; Mueller, R. H., *Tetrahedron Lett.,* **1992,** *33*, 7835-7838.
[60] Chattopadhyay, S. K.; Kempson, J.; McNeil, A.; Pattenden, G.; Reader, M.; Rippon, D. E.; Waite, D., *J. Chem. Soc., Perkin Trans. 1,* **2000,** *1*, 2415-2428.
[61] Glorius, F.; Schuh, K., *Synthesis,* **2007,** *15*, 2297-2306.
[62] Martín, R.; Cuenca, A.; Buchwald, S. L., *Org. Lett.,* **2007,** *9*, 5521-5524.
[63] Lechel, T.; Gerhard, M.; Trawny, D.; Brusilowskij, B.; Schefzig, L.; Zimmer, R.; Rabe, J. P.; Lentz, D.; Schalley, C. A.; Reissig, H.-U., *Chem. Eur. J.,* **2011,** *17*, 7480-7491.
[64] Ferreira, P. M. T.; Monteiro, L. S.; Pereira, G., *Eur. J. Org. Chem.,* **2008,** *27*, 4676-4683.
[65] Ferreira, P. M. T.; Castanheira, E. M. S.; Monteiro, L. S.; Pereira, G.; Vilaca, H., *Tetrahedron,* **2010,** *66*, 8672-8680.
[66] Wendlandt, A. E.; Stahl, S. S., *Org. Biomol. Chem.,* **2012,** *10*, 3866-3870.
[67] Zheng, Y.; Li, X.; Ren, C.; Zhang-Negrerie, D.; Du, Y.; Zhao, K., *J. Org. Chem.,* **2012,** *77*, 10353-10361.
[68] Misra, N. C.; Ila, H., *J. Org. Chem.,* **2010,** *75*, 5195-5202.
[69] Bathula, S. R.; Reddy, M. P.; Viswanadham, K. K. D. R.; Sathyanarayana, P.; Reddy, M. S., *Eur. J. Org. Chem.,* **2013,** *21*, 4552-4557.
[70] Panda, N.; Mothkuri, R., *New J. Chem.,* **2014,** *38*, 5727-5735.
[71] Cheung, C. W.; Buchwald, S. L., *J. Org. Chem.,* **2012,** *77*, 7526-7537.
[72] Xu, H.; Ma, S.; Xu, Y.; Bian, L.; Ding, T.; Fang, X.; Zhang, W.; Ren, Y., *J. Org. Chem.,* **2015,** *80*, 1789-1794.
[73] Balme, G.; Bouyssi, D.; Monteiro, N., Metal-Catalyzed Multicomponent Reactions. In *Multicomponent Reactions*, Wiley-VCH Verlag GmbH & Co. KGaA: 2005; p 224.
[74] Toure, B. B.; Hall, D. G., *Chem. Rev.,* **2009,** *109*, 4439-86.
[75] Estevez, V.; Villacampa, M.; Menendez, J. C., *Chem. Soc. Rev.,* **2010,** *39*, 4402-21.
[76] Muller, T. J., *Beilstein J. Org. Chem.,* **2011,** *7*, 960-1.
[77] Huang, Y.; Yazbak, A.; Dömling, A., Multicomponent Reactions. In *Green Techniques for Organic Synthesis and Medicinal Chemistry*, John Wiley & Sons, Ltd: 2012; p 497.
[78] Brauch, S.; van Berkel, S. S.; Westermann, B., *Chem. Soc. Rev.,* **2013,** *42*, 4948-62.
[79] Peshkov, V. A.; Pereshivko, O. P.; Van der Eycken, E. V., *Chem. Soc. Rev.,* **2012,** *41*, 3790-3807.
[80] Li, C.-J.; Wei, C.; Li, Z., *Synlett,* **2004,** *9*, 1472-1483.

[81] Li, C.-J., *Acc. Chem. Res.,* **2010,** *43*, 581-590.
[82] Yoo, W. J.; Zhao, L.; Li, C. J., *Aldrichim. Acta,* **2011,** *44*, 43-51.
[83] Li, C.-J.; Wei, C., *Chem. Commun.,* **2002,** *3*, 268-269.
[84] Dyatkin, A. B.; Rivero, R. A., *Tetrahedron Lett.,* **1998,** *39*, 3647-3650.
[85] Feng, H.; Ermolat'ev, D. S.; Song, G.; Van der Eycken, E. V., *Adv. Synth. Catal.,* **2012,** *354*, 505-509.
[86] Dou, X.-Y.; Shuai, Q.; He, L.-N.; Li, C.-J., *Adv. Synth. Catal.,* **2010,** *352*, 2437-2440.
[87] Black, D. A.; Arndtsen, B. A., *Org. Lett.,* **2004,** *6*, 1107-1110.
[88] Wei, C.; Li, C.-J., *J. Am. Chem. Soc.,* **2003,** *125*, 9584-9585.
[89] Cheng, M.; Zhang, Q.; Hu, X.-Y.; Li, B.-G.; Ji, J.-X.; Chan, A. S. C., *Adv. Synth. Catal.,* **2011,** *353*, 1274-1278.
[90] Wong, K.-F.; Deng, J.-R.; Wei, X.-Q.; Shao, S.-P.; Xiang, D.-P.; Wong, M.-K., *Org. Biomol. Chem.,* **2015,** *13*, 7408-7411.
[91] Wang, Y.-M.; Lackner, A. D.; Toste, F. D., *Acc. Chem. Res.,* **2013,** *47*, 889-901.
[92] Davies, P. W.; Cremonesi, A.; Dumitrescu, L., *Angew. Chem. Int. Ed.,* **2011,** *50*, 8931-8935.
[93] Ferrer, C.; Echavarren, A. M., *Angew. Chem. Int. Ed.,* **2006,** *45*, 1105-1109.
[94] Hashmi, A. S. K.; Hutchings, G. J., *Angew. Chem. Int. Ed.,* **2006,** *45*, 7896-7936.
[95] Hashmi, A. S. K.; Schuster, A. M.; Rominger, F., *Angew. Chem. Int. Ed.,* **2009,** *48*, 8247-8249.
[96] Ma, Y.; Zhang, S.; Yang, S.; Song, F.; You, J., *Angew. Chem. Int. Ed.,* **2014,** *53*, 7870–7874.
[97] Hoffmann, M.; Miaskiewicz, S.; Weibel, J.-M.; Pale, P.; Blanc, A., *Beilstein J. Org. Chem.,* **2013,** *9*, 1774-1780.
[98] Campbell, M. J.; Toste, F. D., *Chem. Sci.,* **2011,** *2*, 1369-1378.
[99] Patil, N.; Inamdar, S. M.; Konala, A., *Chem. Commun.,* **2014,** *50*, 15124-15135.
[100] Dorel, R.; Echavarren, A. M., *Chem. Rev.,* **2015**.
[101] Adcock, H. V.; Langer, T.; Davies, P. W., *Chem. Eur. J.,* **2014,** *20*, 7262–7266.
[102] Wachenfeldt, H. v.; Röse, P.; Paulsen, F.; Loganathan, N.; Strand, D., *Chem. Eur. J.,* **2013,** *19*, 7982-7988.
[103] Wang, T.; Huang, L.; Shi, S.; Rudolph, M.; Hashmi, A. S. K., *Chem. Eur. J.,* **2014,** *20*, 14868–14871.
[104] Weyrauch, J. P.; Hashmi, A. S. K.; Schuster, A.; Hengst, T.; Schetter, S.; Littmann, A.; Rudolph, M.; Hamzic, M.; Visus, J.; Rominger, F.; Frey, W.; Bats, J. W., *Chem. Eur. J.,* **2010,** *16*, 956-963.
[105] Xin, Z.; Kramer, S.; Overgaard, J.; Skrydstrup, T., *Chem. Eur. J.,* **2014,** *20*, 7926–7930.
[106] Hashmi, A. S. K.; Rudolph, M.; Schymura, S.; Visus, J.; Frey, W., *Eur. J. Org. Chem.,* **2006,** *21*, 4905-4909.
[107] Ghosh, N.; Nayak, S.; Prabagar, B.; Sahoo, A. K., *J. Org. Chem.,* **2014,** *79*, 2453–2462.
[108] Jeong, Y.; Kim, B.-I.; Lee, J. K.; Ryu, J.-S., *J. Org. Chem.,* **2014,** *79*, 6444-6455.
[109] Tang, J.-M.; Liu, T.-A.; Liu, R.-S., *J. Org. Chem.,* **2008,** *73*, 8479-8483.
[110] Zhu, S.; Huang, H.; Zhang, Z.; Ma, T.; Jiang, H., *J. Org. Chem.,* **2014,** *79*, 6113–6122.

[111] He, W.; Li, C.; Zhang, L., *J. Am. Chem. Soc.,* **2011,** *133*, 8482-8485.
[112] Yao, X.; Li, C.-J., *Org. Lett.,* **2006,** *8*, 1953-1955.
[113] Zhang, Y.; Donahue, J. P.; Li, C.-J., *Org. Lett.,* **2007,** *9*, 627-630.
[114] Hashmi, A. S. K.; Salathe, R.; Frey, W. G., *Synlett,* **2007,** *11*, 1763-1766.
[115] Asao, N.; Yudha S, S.; Nogami, T.; Yamamoto, Y., *Angew. Chem. Int. Ed.,* **2005,** *44*, 5526-5528.
[116] Chernyak, N.; Gevorgyan, V., *Angew. Chem. Int. Ed.,* **2010,** *49*, 2743-2746.
[117] Ohno, H.; Ohta, Y.; Oishi, S.; Fujii, N., *Angew. Chem. Int. Ed.,* **2007,** *46*, 2295-2298.
[118] Cao, K.; Zhang, F.-M.; Tu, Y.-Q.; Zhuo, X.-T.; Fan, C.-A., *Chem. Eur. J.,* **2009,** *15*, 6332-6334.
[119] Zhang, Y.; Li, P.; Wang, L., *J. Heterocycl. Chem.,* **2011,** *48*, 153-157.
[120] Saifuddin, M.; Agarwal, P. K.; Kundu, B., *J. Org. Chem.,* **2011,** *76*, 10122-10128.
[121] Zhang, Q.; Cheng, M.; Hu, X.; Li, B.-G.; Ji, J.-X., *J. Am. Chem. Soc.,* **2010,** *132*, 7256-7257.
[122] Xiao, F. P.; Chen, Y. L.; Liu, Y.; Wang, J. B., *Tetrahedron,* **2008,** *64*, 2755-2761.
[123] Syeda Huma, H. Z.; Halder, R.; Singh Kalra, S.; Das, J.; Iqbal, J., *Tetrahedron Lett.,* **2002,** *43*, 6485-6488.
[124] Kumar, M.; Hammond, G. B.; Xu, B., *Org. Lett.,* **2014,** *16*, 3452-3455.
[125] Bucher, J.; Wurm, T.; Nalivela, K. S.; Rudolph, M.; Rominger, F.; Hashmi, A. S. K., *Angew. Chem. Int. Ed.,* **2014,** *53*, 3854-3858.
[126] Gorin, D. J.; Toste, F. D., *Nature,* **2007,** *446*, 395-403.
[127] Stephen, A.; Hashmi, K., *Gold Bull.,* **2004,** *37*, 51-65.
[128] Gorin, D. J.; Toste, F. D., *Nature,* **2007,** *446*, 395.
[129] Hashmi, A. S. K., *Gold Bull.,* **2003,** *36*, 3-9.

Chapter 3 – Direct Synthesis of Indenes via a Rhodium-Catalyzed Multicomponent Csp^2–H Annulation Reaction

3.1 Background

Aromatic C–H bond activation has been extensively exploited for its potential use in various synthetic applications over the past decades.[1-3] Facilitated by transition-metal catalysts, Csp^2–H functionalization has become a prospering field offering highly efficient access to a wild range of important building blocks. When combined with the use of directing groups, these C–H activation methods now present a viable alternative to methods such as the Heck coupling, and have seen considerable use in total syntheses (see Chapter 1). Directing group (DG) strategy is a traditional method used to control the regioselectivity of the Csp^2–H activation, in which coordination of a neighboring heteroatom to the transition–metal catalyst creates a cyclometalated reactive intermediate.[4-5] The utilization of such directing group in the development of sustainable transformations, albeit highly effective, is considered as a downside since it generally needs to be installed and removed, which adds extra synthetic steps. Recently, progress has been made at simplifying those unnecessary steps by developing alternative strategies, such as the use of traceless removal DG.[6-8] Yu and Ge developed another strategy named as transient directing group.[9-10] It allows the *in–situ* formation and total recovery of the directing group.

C–H activation/functionalization and multicomponent reactions (MCRs) are obviously two of the most representative organic reactions which have exerted a huge influence on the advances in the field of organic synthesis. Individually, C–H functionalization is extraordinarily efficient in the construction of new C–C and C–heteroatom bonds[11-17] by converting latent C–H bonds, which allows the direct synthesis of numerous organic products from raw chemicals. On the other hand, MCRs are well recognized for their unique features in forging structurally diverse and complex products via the reactions of more than two different organic substrates wherein multiple new chemical bonds are formed in one-pot. Access to elegant organic structures through one-pot multicomponent

reactions is of huge economical interest for pharmaceutical and agrochemical industries.[18-30]

In recent years, the concept of sustainable synthesis has received worldwide attention.[31] Deliberately, both C–H functionalization, which skips the pre-elaboration of specific functional group or latent chemical bond, and the MCRs, which enable multiple chemical bond formation by one-step operation, are ideal tools for such sustainable synthesis.[32-35] Rationally, developing MCRs in conjunction with C–H functionalization transformations, which simultaneously possesses the advantages of synthetic sustainability and the power in the rapid generation of molecular libraries, has become highly attractive.

Within the many directed C–H functionalization reactions developed to date, olefination and hydro-olefination reactions possess unique characteristics. These reactions are achievable with the use of alkenes, having terminal or internal alkynes as reactive partner. Specifically, the ability of these reactions to produce single to multiple cyclic products in a single step, represent a colossal benefit in drug discovery. This introduction will be concentrated on the use of imine DGs since this functionality can be easily installed and modified subsequently during the same process (Scheme 72).

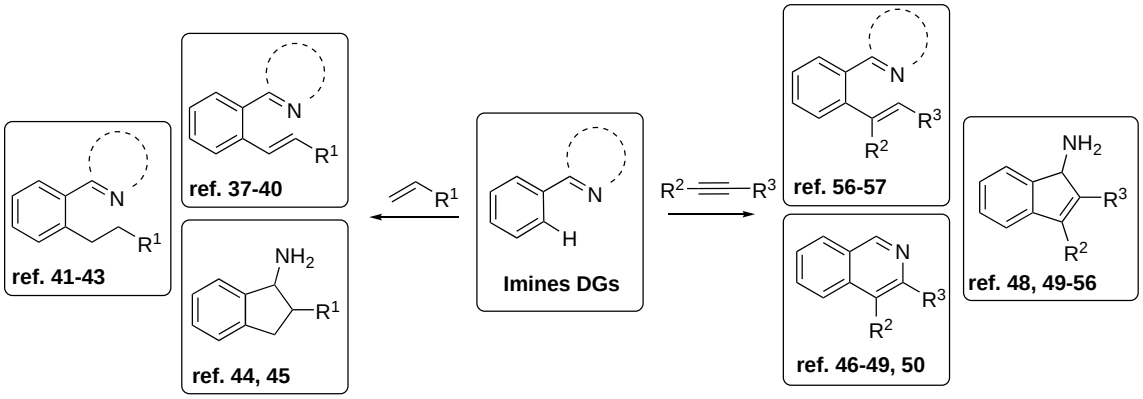

Scheme 72. Diverse alkene and heterocyclic products can be synthesized from simple aryl bearing aldimines DGs (or related compounds) via olefination and hydro-olefination reactions

The Heck-type arene olefination is arguably one of the most important reactions in the field of C-H activations, owing to its excellent compatibility with the conditions for transition-metal-catalyzed C−H activation.[36] Simple olefination reactions were some of the first examples reported for the directed C-H olefination of aryl compounds. In 2007, Shi and co-workers developed a palladium catalyzed ortho olefination of N,N-dimethylbenzylamines under slightly acidic conditions.[37] Later, Li and Wu reported the synthesis of ortho-olefinated benzaldehydes.[38] They reported efficient diolefination using acrylates using rhodium catalyst. A slightly modified imines directing groups were described by different authors to produce similar olefinated products.[39-40] Using rhodium as catalyst and 2 equivalents of copper, Huang and co-workers reported the C-H functionalization of arenes with removable triazene DGs. Alkylations of aryl substrates using alkenes have also been explored by numerous authors using various transition metal catalyst such as Co,[41] Mn[42] and Rh[43] among others. Such processes were extended to a cyclization/annulation reaction using alkenes, allowing the production of fused ring compounds. For instance, Bergman and Ellman described in 2005, an intramolecular annulation reaction with a protected aldimine DG.[44] They postulated that the mechanism proceeds through a C-H activation followed by insertion of the olefin, and then reductive elimination. Ten years later, Ackermann and co-workers proposed a manganese catalyzed C-H functionalization/annulation reaction to produce cyclic β-amino acid esters.[45] Detailed mechanistic studies showed a kinetic isotope effect (KIE) of k_H/k_D = 2.4 for the manganese-catalyzed C-H functionalization, indicating a relevant C-H metalation step.

These olefination and annulation processes were extended to other systems, activating C≡C triple bonds leading to isoquinolines or indenes. Jiao and co-workers described a Pd(II) catalyzed iminoannulation reaction using internal alkynes and dioxygen as oxidant to produce isoquinolines.[46] Following these discoveries, a few research groups described the use of Co,[47] Rh,[48-49] or Mn[50] transition metal catalyst to achieve annulation reactions. In 2014, Wang reported a manganese catalyzed dehydrogenative annulation reaction to access isoquinoline derivatives (Scheme 73).[50] In this publication, the authors proposed a mechanism pathways based on KIE experiments and control reactions in

which they isolated the reactive intermediate **A**, a five-membered manganacycle (Scheme 74).

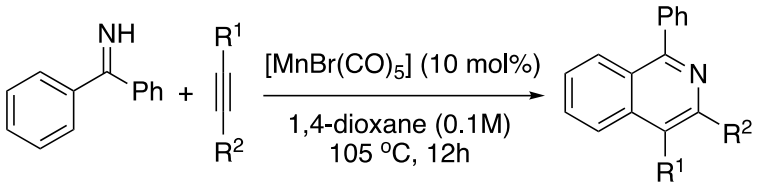

Scheme 73. Manganese catalyzed dehydrogenative annulation of N-H imines and alkynes by C–H/N–H activation

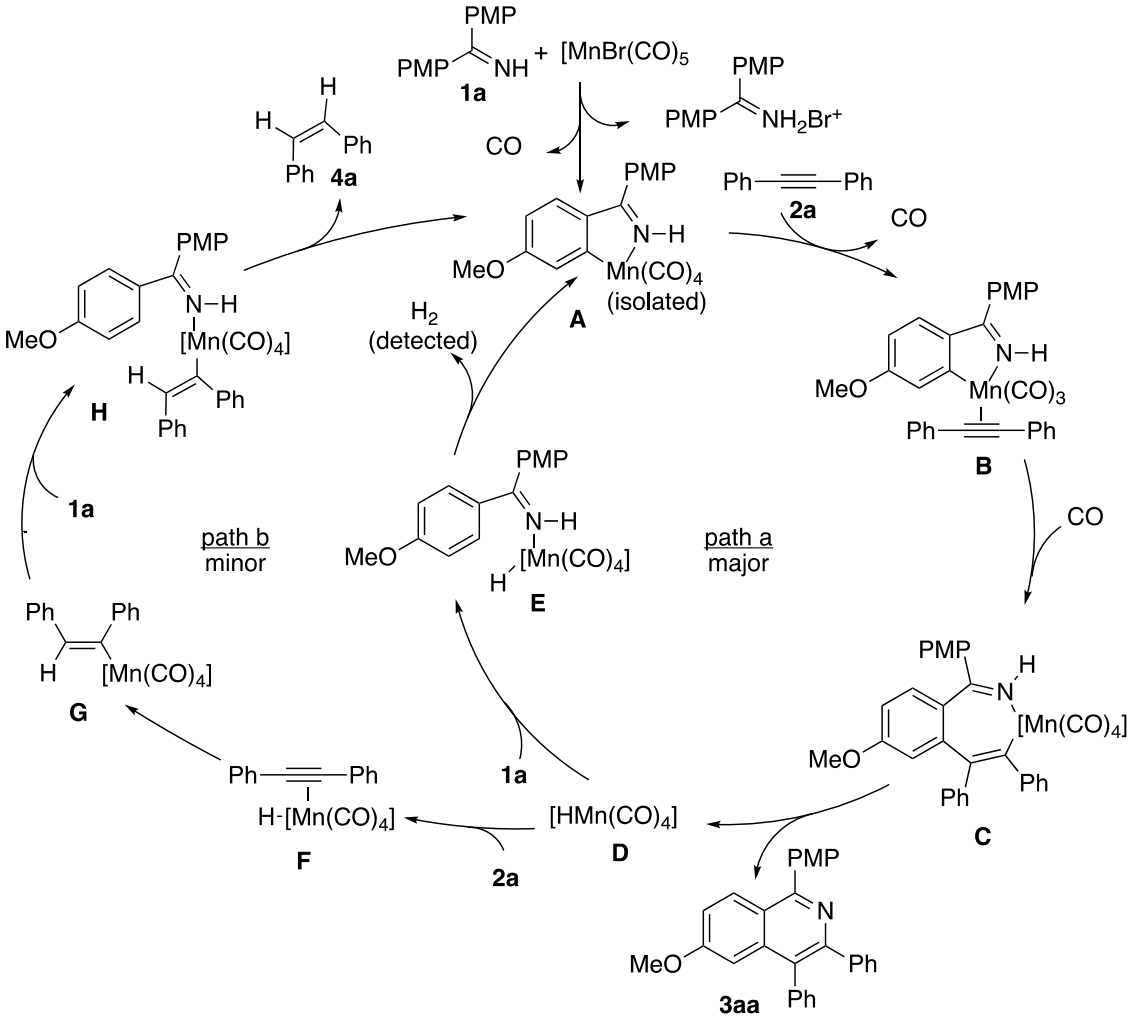

Scheme 74. Proposed catalytic cycle for manganese catalyzed synthesis of isoquinoline

In the major path a, the insertion of **2a** into the Mn-C bond generated to the formation of the intermediate **C**, a seven membered manganacycle. By C-N reductive elimination, the formation of the corresponding isoquinoline **3aa** occurs, leading to the complex **D**. In presence of substrate **1a**, the manganese complex **D** coordinates with the nitrogen atom from the imine directing group. The path a cycle is closed by C-H activation and elimination of dihydrogen, producing the intermediate **A**. In the minor path b, a different reactivity is shown. The internal alkyne **2a** coordinates to the manganese center and inserts into the hydride manganese bond in complex **D**, to form intermediate **G**. Coordination of **G** to substrate **1a** results in the formation of **H**, which then undergoes C-H activation and reductive elimination to produce compound **4a** and the reactive species **A**, to complete other catalytic cycles.

While manganese was found to be very efficient for the synthesis of isoquinolines, Satoh and Miura reported that rhodium catalyst (Cp^*RhCl_2) was very efficient for this process and for the formation of five membered ring indene compounds.[48] The formation of isoquinoline derivatives is govern essentially by C-H activation and C-N reductive elimination step. Considering that no C-N bond is formed during the synthesis of indenes, the C-N reductive elimination step involved in isoquinoline formation must be avoided. Miura showed that the use of two equivalents of oxidant (copper salt) drove the formation of isoquinoline products. However, in presence of lower amount of oxidant, the major products formed were 5-membered ring indene derivatives. Later in 2010, Zhao and co-workers reported similar indenes synthesis from aromatic ketimines, catalyzed by a different rhodium catalyst $[[(COD)Rh(OH)]_2]$ and a ruthenium catalyst $[(p\text{-cymene})RuCl_2)_2]$.[49, 51] This very efficient reaction was then extended to many different transition metals such as Pd,[52-53] Re,[54] Ru,[55] and to enantioselective version (Scheme 75). Cramer described a highly enantioselective [3+2] additions of aryl ketimines with internal alkynes using a similar rhodium catalyst system to Zhao's. Unfortunately, the

regioselectivity of their process was not extremely efficient and appeared to be a strong limitation.[56]

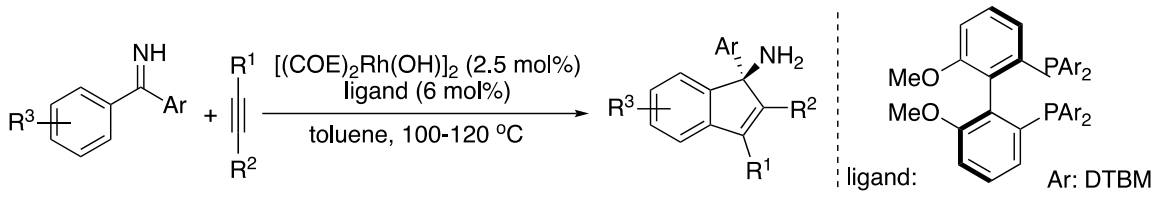

Scheme 75. Enantioselective rhodium(I)-catalyzed annulations of aromatic ketimines

On the other hand, classic alkenylation reactions were also reported using aldimines via chelation. A recent example was described by Yoshikai in 2013. He established an ortho-alkenylation reaction of aromatic aldimines with internal alkynes promoted by a cobalt catalyst generated from $CoBr_2$, phosphine ligand and a Grignard reagent.[57] Concurrently, a similar C-H alkenylation reaction using terminal alkynes was described by Wang. He reported a dehydrogenative annulation reaction for the formation of isoquinolines derivatives, using manganese catalyst.[58]

3.2 Research objectives & plan

Inspired by these advantageous features described above, we aimed at developing an atom-[59-61] and step-economical[62-63] route to synthesize indenes. Molecules containing the indene scaffold are of important interest since they are frequently found in natural products[64-65] and exhibit important biological activities (Scheme 76).[66-69] To access this class of compounds, to the best of our knowledge, only a few methodologies employing transition metal catalyzed multicomponent reaction (MCR), have been developed.[69-71] However, these reactions catalyzed by transition metal complexes under high temperature, require either stoichiometric amount of zinc, complex and specific starting materials or show good to moderate regioselectivity. Considering non-MCRs and previous approaches shown in Scheme 72, many different transition metal catalysts were evaluated towards the synthesis of indenes.

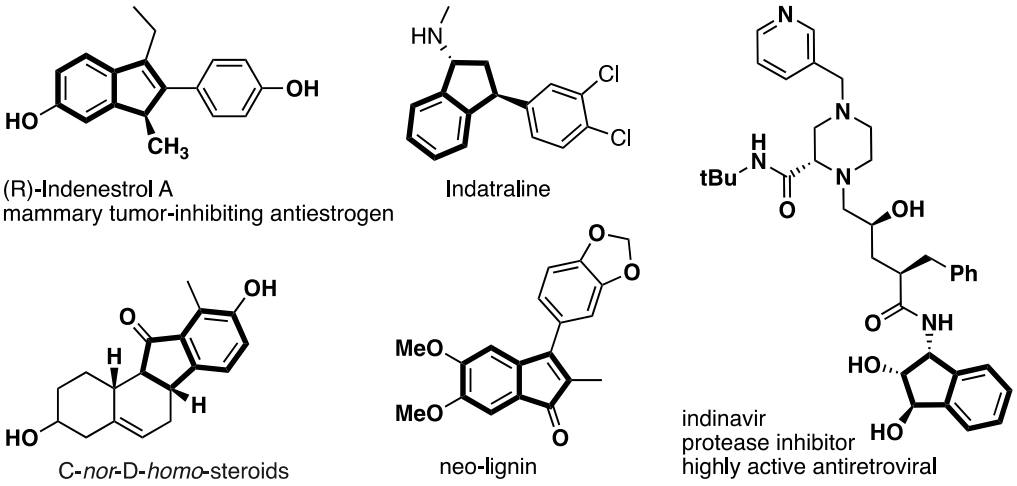

Scheme 76. Examples of natural products and bioactive molecules containing indene scaffold

In recent works, Wang[54] and Cheng[55] have developed a metal-catalyzed C–H activation/annulation reaction system between an imine and internal alkynes. In both cases, the imine substrate requires pre-synthesis, which is considered as downside since it adds extra organic synthetic steps. Prior to these C–H functionalization methods, the functionalization of aryl halides or aryl boronic acids have been reported in the synthesis of indenes (Scheme 77).[69, 71] Regardless of the efficiency of these reactions, the selectivity towards the desired indene products is mediocre. Cheng reported that high selectivity was obtained, when electron-withdrawing esters or keto groups were present on the unsymmetrical alkynes, however with a double bond migration adjacent to the nitrogen atom of the desired products. In Scheme 77-b, the author described that these arylimine substrates were susceptible to decomposition and the yields were sharply diminished with the generation of alcohol by-products which were formed by the reaction of 2-formylarylbonic acids and the alkynes.

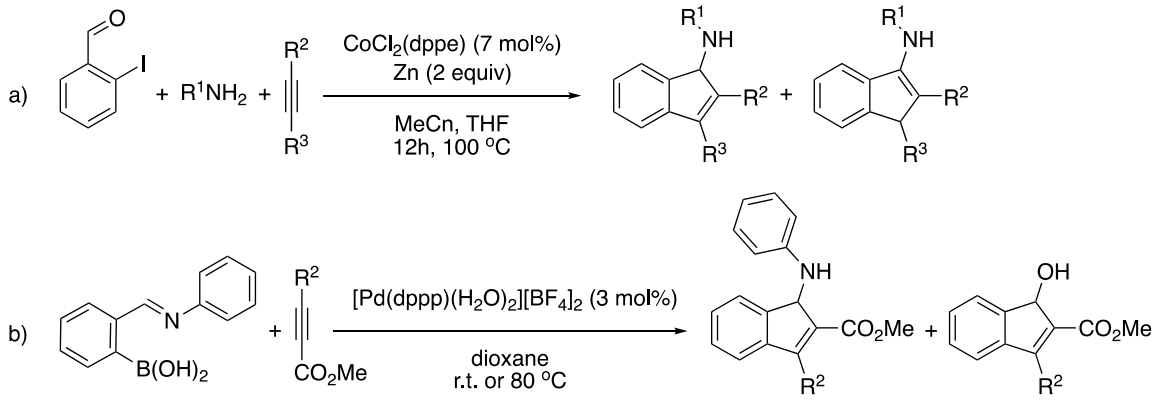

Scheme 77. Indene formation from a) C-I and b) C-B bond functionalization reactions

It is notable that from an atom-economy perspective, the consideration of a C–H bond functionalization approach represents a sagacious choice. Thus, to overcome any of these disadvantages, the development of an atom and step-economical multicomponent alternative, using very simple substrates, is of great interest. Hence, we designed a rhodium catalyzed redox-neutral three component coupling, via a mild and successive C–H activation/annulation reactions sequence (Scheme 78).

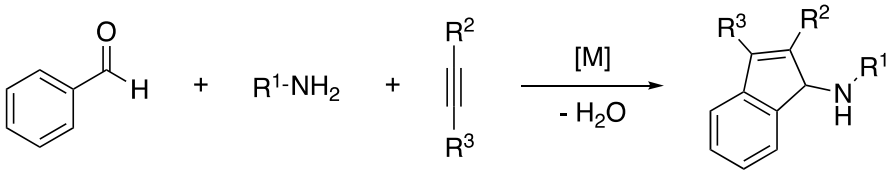

Scheme 78. Designed multicomponent reaction for the synthesis of indenes

The multicomponent aldehyde-amine-alkyne (A^3) reaction, previously reported by our group, generates imine as intermediate by condensation reaction.[72-74] We envisioned exploiting this imine source as directing group to activate the aryl Csp^2–H bonds. Imine-directed C–H activation has been used in numerous tandem catalytic reactions and cyclization reactions involving alkyne reagents (Scheme 72).[75] The combination of imine

directing group and alkyne represents a highly judicious approach to provide a cyclic indene library, with potential regioselective control.[54-55, 71, 76-82]

3.3 Results and discussion

Following our postulation described in Scheme 78, we started to evaluate the reaction of 4-methoxybenzaldehyde (**1f**), benzylamine (**2**) and 1-propynylbenzene (**3**) as the model reaction (Scheme 79). We specifically choose 4-methoxybenzaldehyde (**1f**) as starting material since the aromatic ring bears an electron donating group, diminishing the electrophilicity of the aldehyde and making the condensation more difficult. Moreover, since the designed C-H activation step is thought to go through a concerted metalation and deprotonation mechanism, the deprotonation of an electron rich C-H bond is more difficult. Our goal is to investigate the reaction conditions with difficult substrate to discover a robust catalytic system.

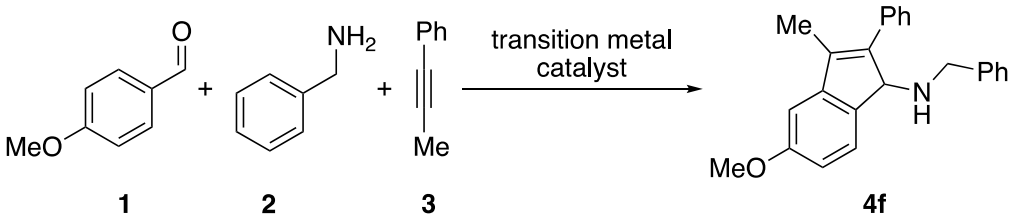

Scheme 79. Evaluation of designed reaction

3.3.1 Condition screening

To explore the C–H functionalization key step, a non-exhaustive list of rhodium catalysts was examined in the presence of copper(II) acetate (Table 1). The use of copper(II) acetate in the ruthenium(II) catalyzed synthesis of indenamines was described by Gandeepan and Cheng as an acetate source assisting the deprotonation mechanism.[83] Supported by several reviews, the copper(II) acetate source is very powerful and, thus we considered the use of this acetate source at first to evaluate the reaction conditions.[84-85]

The oxidation state of the catalyst involved seemed of vital importance for the reaction to occur. As shown in Table 1 (entries 1–3), no desired product was obtained

when Rh(0), Rh(I) or Rh(II) were used as catalyst. Gratifyingly, the corresponding indene product (**4f**) was obtained in presence of a catalytic amount of Rh(III). We then recognized that Cp*Rh(III) complex was an active catalyst under its cationic form; since while the use of $[Cp^*RhCl_2]_2$ (Table 1, entry 4) gave no desired product, its cationic analogue $Cp^*Rh(SbF_6)_2(MeCN)_3$ gave the indene (**4f**) in 25% yield, with toluene as solvent (Table 1, entry 5). We were extremely surprised to observe that the reaction was highly regioselective as the regioisomeric ratio detected was 99:1, when $Cp^*Rh(SbF_6)_2(MeCN)_3$ was used as catalyst. Further investigations about solvent effect on our reaction system were conducted and toluene was found to be the most effective, since solvents such as DCE, EtOAc or THF weakly impeded the reaction (Table 1, entries 6–8). Subsequent optimization indicated that the increase of reaction temperature was not beneficial to our reaction system. A rise in temperature from r.t. to 60^{o}C did not result in any change in yield (Table 1, entries 9–10). Shortening the reaction time from 18h to 6h and 12h was not beneficial to our reaction system and resulted in lower yield (Table 1, entries 11–12). No drastic enhancement of yield was observed by extension of reaction time either (Table 1, entry 13). Stuck at 25% yield, the reaction conditions were not optimal yet. Later, we undertook the evaluation of a series of additional acetate sourcess hoping to accelerate the C-H activation step. Acid additives are well-known to play an important role in the proposed key metalation-deprotonation step. The evaluation of acid additives showed that soft acids with intermediate pKa (4.5-5) were less advantageous than strong acid such as TFA (Table 1, entries 14-16). The use of 10 mol% of TFA showed an increase formation of the indene derivatives (**4f**), with up to 70% yield. We ascribed this behavior by the fact that a strong acid has a weak conjugated base, which coordinates weaker to the rhodium center compared to a strong base. The weak coordination is important to allow the ligand exchange with the alkyne substrate. Finally, with our optimized conditions, compound (**4f**) was isolated in 60% yield with exceptionally high selectivity ratio, as confirmed by ^{1}H NMR.

Table 5. Optimization of reaction conditions

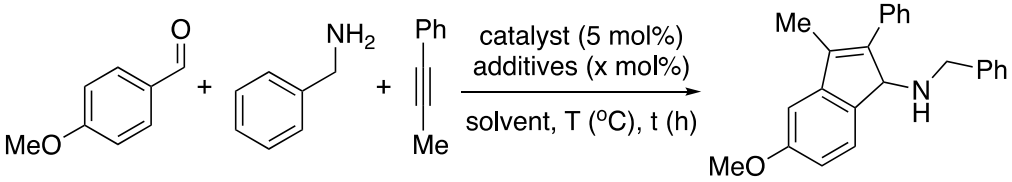

1f **2** **3** **4f**

entry	catalyst	additives	solvents	T (°C)	t (h)	**4f** (%)[b]
1	$Rh_6(CO)_{16}$	-	toluene	r.t	18	0
2	$Rh(COD)_2BF_4$	-	toluene	r.t	18	0
3	$[Rh(OAc)_2]_2$	-	toluene	r.t	18	0
4	$[Cp^*RhCl_2]_2$	-	toluene	r.t	18	0
5	$Cp^*Rh(SbF_6)_2(MeCN)_3$	-	toluene	r.t	18	25
6	$Cp^*Rh(SbF_6)_2(MeCN)_3$	-	DCE	r.t	18	16
7	$Cp^*Rh(SbF_6)_2(MeCN)_3$	-	EtOAc	r.t	18	20
8	$Cp^*Rh(SbF_6)_2(MeCN)_3$	-	THF	r.t	18	17
9	$Cp^*Rh(SbF_6)_2(MeCN)_3$	-	toluene	40	18	25
10	$Cp^*Rh(SbF_6)_2(MeCN)_3$	-	toluene	60	18	25
11	$Cp^*Rh(SbF_6)_2(MeCN)_3$	-	toluene	r.t	6	20
12	$Cp^*Rh(SbF_6)_2(MeCN)_3$	-	toluene	r.t	12	22
13	$Cp^*Rh(SbF_6)_2(MeCN)_3$	-	toluene	r.t	24	25
14	$Cp^*Rh(SbF_6)_2(MeCN)_3$	PivOH (10 mol%)	toluene	r.t	18	37
15	$Cp^*Rh(SbF_6)_2(MeCN)_3$	AcOH (10 mol%)	toluene	r.t	18	62
16	$Cp^*Rh(SbF_6)_2(MeCN)_3$	TFA (10 mol%)	toluene	r.t	18	70 (**60**)

[a]Reactions were performed on a 0.1 mmol scale using 5 mol% of catalyst, 5 mol% $Cu(OAc)_2{\cdot}H_2O$, **1** (0.1 mmol), **2** (1.2 equiv), **3** (1.2 equiv), in 0.25 mL of solvent and open air. [b]Average NMR yields from two runs are reported and isolated yields are reported in parentheses.

With our optimized conditions in hand, we investigated the influence of a number of acetate sources as well as the acid on the reaction between benzaldehyde (**1a**), benzylamine (**2**) and 1-propynylbenzene (**3**). As shown in Table 6, the amount of TFA as acid source does not influence the yield of the reaction since both 1 equivalent and a catalytic amount of (10 mol%) led to quantitative yield (entries 1-4). When the acid was changed to weaker acetic acid or pivalic acid, the reaction produced compound (**4a**) in

lower yield (entries 5-7). With a stronger acid such as tosylic acid, the reaction proceeded more efficiently with a yield of 94% (entry 8). As mentioned above, we believe that the strength of the coordination of the conjugate base is highly important, allowing a fast acetate de-coordination after the deprotonation step. Substituting copper(II)acetate with another source of acetate such as NaOAc, KOAc or NH_4OAc decreased the yield of indene (**4a**) by 30%, 10% and 40%, respectively (entries 9, 10, 13). An increase in loading of KOAc acetate source from 5 mol% to 10 and 20 mol%, significantly decreased the yield from 90% to 68% and 69% yield (entries 11 & 12). Since all these acetate sources are Brönsted bases, and their higher catalytic loading is detrimental to the reaction, we concluded that our system requires an acidic pH to perform efficiently. In absence of acid and in presence of acetate (5 mol% of KOAc, entry 14), the reaction was still performing but in lower yield. Besides, while only TFA was used in presence of rhodium catalyst (entry 15), our reaction system was not as efficient as the best conditions with $CuOAc_2$, shown in entry 1. The yield obtained was 80% in presence of TFA only. To conclude, copper(II)acetate is a Lewis acid that does not influence the pH of the reaction media and a potential acetate source. In our system, it represents the perfect match between adjusting pH of our media and accelerating the C-H activation step via the concerted metalation and deprotonation mechanism.

Table 6. Adjustment of reaction condition/additives.

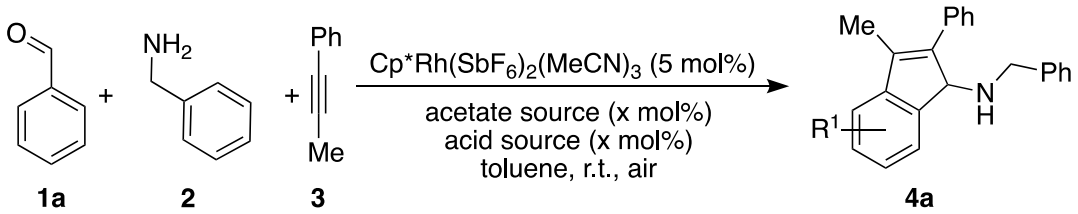

entry	acetate source	acid source	**4a** (%)[b]
1	$Cu(OAc)_2.H_2O$ (5 mol%)	TFA (10 mol%)	**>99**
2	$Cu(OAc)_2.H_2O$ (5 mol%)	TFA (20 mol%)	**>99**
3	$Cu(OAc)_2.H_2O$ (5 mol%)	TFA (50 mol%)	**>99**
4	$Cu(OAc)_2.H_2O$ (5 mol%)	TFA (100 mol%)	**>99**
5	$Cu(OAc)_2.H_2O$ (5 mol%)	AcOH (10 mol%)	56
6	$Cu(OAc)_2.H_2O$ (5 mol%)	AcOH (50 mol%)	88
7	$Cu(OAc)_2.H_2O$ (5 mol%)	PivOH (50 mol%)	53
8	$Cu(OAc)_2.H_2O$ (5 mol%)	TosOH (50 mol%)	94
9	NaOAc (5 mol%)	TFA (10 mol%)	77
10	KOAc (5 mol%)	TFA (10 mol%)	90
11	KOAc (10 mol%)	TFA (10 mol%)	68
12	KOAc (20 mol%)	TFA (10 mol%)	69
13	NH_4OAc (5 mol%)	TFA (10 mol%)	60
14	KOAc (5 mol%)	-	75
15	-	TFA (10 mol%)	80

[a]Reactions were performed on a 0.1 mmol scale using 5 mol% of catalyst, 5 mol% $Cu(OAc)_2{\cdot}H_2O$, **1** (0.1 mmol), **2** (1.2 equiv), **3** (1.2 equiv), in 0.25 mL of solvent and open air. [b]Average NMR yields from two runs are reported.

3.3.2 Mechanistic considerations

Based on the experiments, a mechanism is proposed for this transformation (Scheme 80). The $Cp^*Rh(SbF_6)_2(MeCN)_3$ catalyst first undergoes ligand exchange with TFA to generate the active rhodium(III) **I** catalyst.[86] In parallel, the condensation reaction between amine (**1**) and aldehyde (**2**) results in the formation of imide **II**, releasing water as the only by-product.

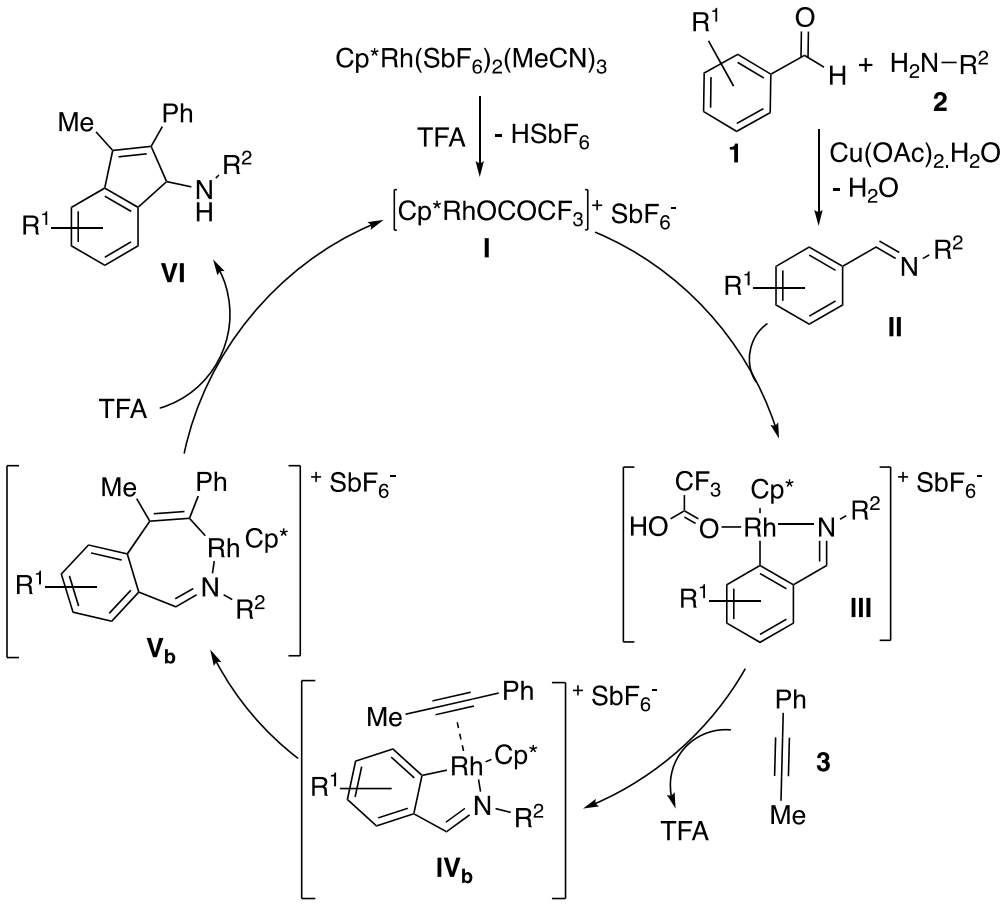

Scheme 80. Proposed mechanism

Coordinating to the imine DG, the Rh(III) complex undergoes *ortho* C–H bond activation assisted by TFA through the six membered–ring metalacycle. We calculated the energy of intermediates and transition states using density functional theory to have more insights concerning the reaction mechanism. We computed the C-H activation transition state **TS1,** shown in Scheme 81.

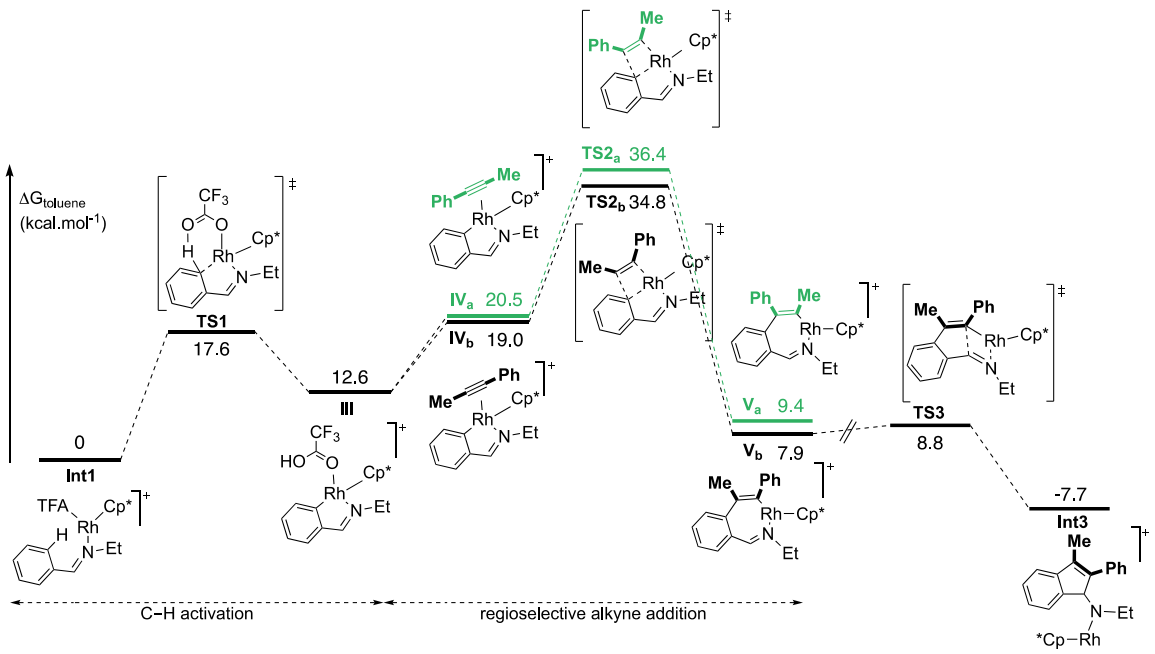

Scheme 81. Calculated mechanism

This step seems to be rate determining due to its high Gibbs energy of activation (ΔG_a = 17.6 kcalmol^{-1}). Intermediate **III** is formed after this Csp^2–H bond activation.[87] The subsequent coordination of the asymmetric alkyne (**3**) occurs regioselectively and is followed by the alkyne addition into the Csp^2–Rh bond, resulting in the seven-membered-ring organorhodium(III) complex $\mathbf{V_b}$. The formation of the indene **VI** derived from the intramolecular carbocyclization of **V** through the transition structure **TS3** and the succeeding protonation of the secondary amine, **Int3**. The active rhodium catalyst is regenerated during the protonation step for further catalytic cycles.

The carbometallation occurs regioselectively in favor of the intermediate $\mathbf{IV_b}$ compared to $\mathbf{IV_a}$, which presents a slightly lower Gibbs energy of activation ($\Delta G_{\mathbf{IVb}}$ = 6.4 kcal.mol^{-1} versus $\Delta G_{\mathbf{IVa}}$ = 7.9 kcal.mol^{-1}). The activation free energy of $\mathbf{TS2_a}$ was found to be 0.1 kcal.mol^{-1} higher than that of $\mathbf{TS2_b}$. Interestingly, these results were very similar to those from Hook and Lan.[88] It is known that the alkynyl triple bond insertion is controlled by electronic, as well as steric factors.[89-90] In their study of regioselectivity in the rhodium-catalyzed cyclization of N-arylnitrones with asymmetric alkyne, a very small difference

was calculated from the same corresponding transition states **TS2$_a$** and **TS2$_b$**. They described the regioselectivity by calculating distortion-interaction energy.[91] The total activation energy ($\Delta E^{‡}$) is decomposed into the sum of distortion energy (ΔE_{dis}) and interaction energy (ΔE_{int}) between distorted reactants (Scheme 82). Distortion energy (ΔE_{dis}) is controlled by the rigidity of reacting molecules and the flexibility of molecular orbitals, and interaction energy (ΔE_{int}) is determined by the orbital interactions between reacting molecules, closed shell repulsion, steric repulsion and dispersion interactions. The calculation revealed that in their example, the interaction energy of both transition states differ from 2.8 kcal/mol, while the distortion energies are both the same. The authors concluded that the activation free energy was mainly attributed to its interaction energy, and thus the regioselectivity was governed by electronic effects.[86]

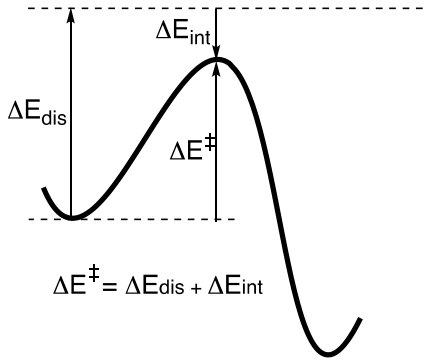

Scheme 82. Relationship between activation, distortion and interaction energies

Consequently, having a very similar catalytic system, we proposed that the regioselective alkyne insertion was essentially controlled by electronic effects.

3.3.3 Substrate scope reaction

We then examined the reaction of various amine derivatives (**2a**–**2e**) under our optimized system. As shown in Table 7, primary benzylic amine (**2a**), α-branched primary amine (**2b**) and primary aniline (**2c**) afforded the desired products in moderate to good yields (35–99% yields) with tremendously good regioselectivity (up to 99:1). Notably, the nucleophilicity of the amines was of high importance. Indeed, when fewer nucleophilic

amine substrates such as aniline were used, the yield of the reaction decreased (**4a**–**4c**), without affecting the high regioselectivity of the desire product. Following this trend, we were pleased to see that long alkyl chain amines were suitable under our reaction system and led to the corresponding indene (**4d**) in excellent yield and as a major regioisomer (99%, rs 99:1). Impressively, our process can be extended to amines bearing heterocycles, such as a furan ring (**4e**). The corresponding moderate yield obtained was attributed to the coordination of the rhodium catalyst to the furan moiety.

Table 7. Scope of amines[a]

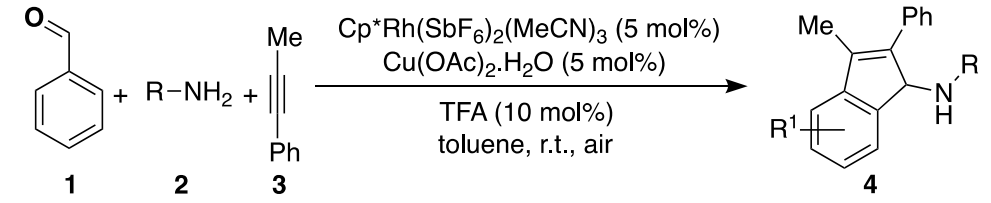

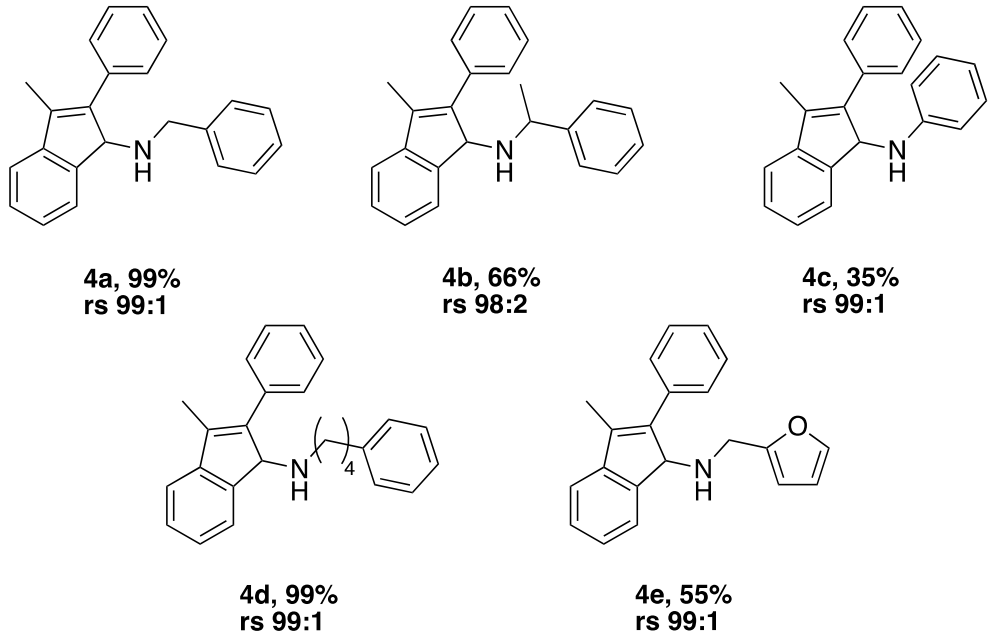

[a]All reactions were performed on a 0.1 mmol scale using 5 mol% $Cp^*Rh(SbF_6)_2(MeCN)_3$, 5 mol% $Cu(OAc)_2{\cdot}H_2O$, **1** (0.1 mmol), **2** (1.2 equiv), **3** (1.2 equiv), in 0.25 mL of a stock solution of toluene/TFA at room temperature and open air. Average isolated yields of two runs are reported in this table. The regioselectivity (rs) was determined by 500 MHz ^1H NMR analysis.

In Table 8, electron-rich benzaldehyde substrates bearing electron-donating group such as –OMe, –OH or –Me (**2f**–**2h**) yielded the corresponding indene products (**4f**–**4h**) in moderate to good yields (40–85% yields) with high regioselectivity (rs up to 97:3). Diminution of yield was observed when phenols were used as substrate. A potential coordination of the hydroxy group to the metal center might with compete the coordination of the acetate group, resulting in the inhibition of the C-H activation step via a CMD mechanism. In case of electron-deficient benzaldehydes possessing withdrawing substituents such as $–CF_3$ and –Br, the yields and selectivity obtained were generally superior (**4j**–**4k**) (84% yield, rs 99:1). Interestingly, ortho-chloro substituted benzaldehyde (**2i**) gave significantly lower yield of the desired product (**4i**) (56% yield), which can be rationalized by the removal of one active C-H bond site. We efficiently obtained the X-Ray structure of this compound (**4i**), verifying the regioselectivity of our major isomer (Scheme 83.).

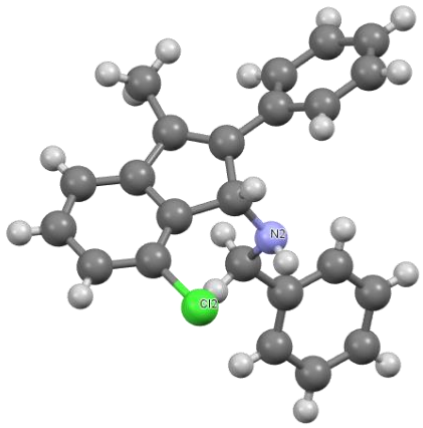

Scheme 83. X-Ray structure of compound (4i)

The efficient alkyne regioselectivity obtained during our designed process was examined in presence of an asymmetrical internal di-alkyl alkyne, 2-hexyne (**3l**). As previously reported by Cramer and Fagnou, the differentiation in regioselectivity between two different alkyl groups is challenging.[92-93] We were extremely pleased to observe the

formation of compound (**4l**) in 70% yield, however with moderate regioselectivity (rs 1:2). When a symmetrical di-aryl alkyne substrate was used, the corresponding product was obtained in moderate yield, probably due to the high steric hindrance of (**3m**). We were delighted to obtain excellent yields when alkynes bearing long alkyl chains were engaged in our reaction system. Indeed, simple alkyl chain afforded the desired product (**4n**) in 82% yield.

Table 8. Scope of aldehydes[a]

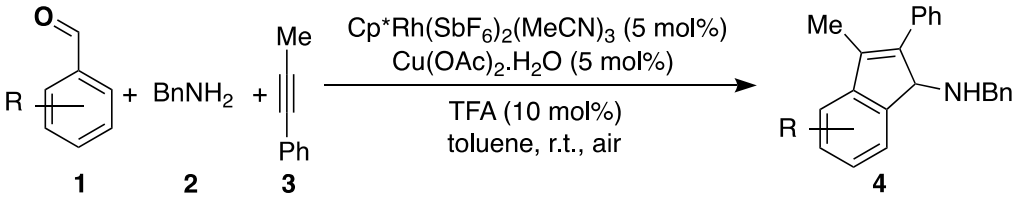

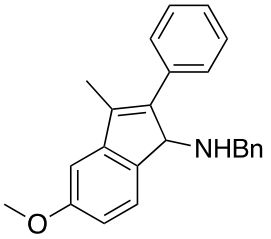

4f, 60%
rs 98:2

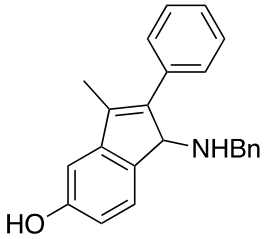

4g, 40%
rs 97:3

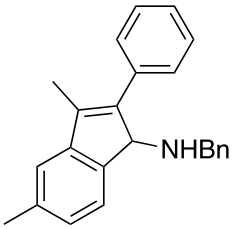

4h, 85%
rs 97:3

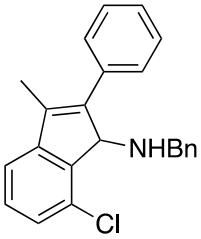

4i, 56%
rs 92:8

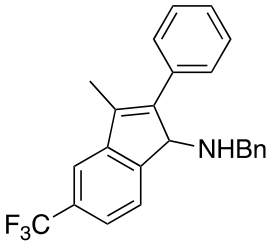

4j, 84%
rs 99:1

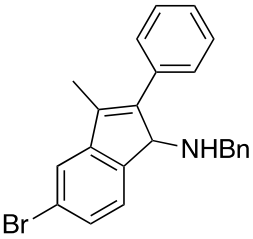

4k, 84%
rs 99:1

[a]All reactions were performed on a 0.1 mmol scale using 5 mol% $Cp^*Rh(SbF_6)_2(MeCN)_3$, 5 mol% $Cu(OAc)_2{\cdot}H_2O$, **1** (0.1 mmol), **2** (1.2 equiv), **3** (1.2 equiv), in 0.25 mL of a stock solution of toluene/TFA at room temperature and open air. Average isolated yields of two runs are reported in this table. The regioselectivity (rs) was determined by 500 MHz ^1H NMR analysis.

Many other distinctive substituents such as aliphatic ketones (**3o**), primary alcohol (**3q**), ester (**3r**) and bromide group (**3p**) were then subjected to the standard reaction conditions, successfully affording the corresponding desired indene products (**4o**-**4r**) in very high yield (60-85% yields) and with particularly high regioselectivity (rs up to 99:1).

Table 9. Scope of internal alkynes

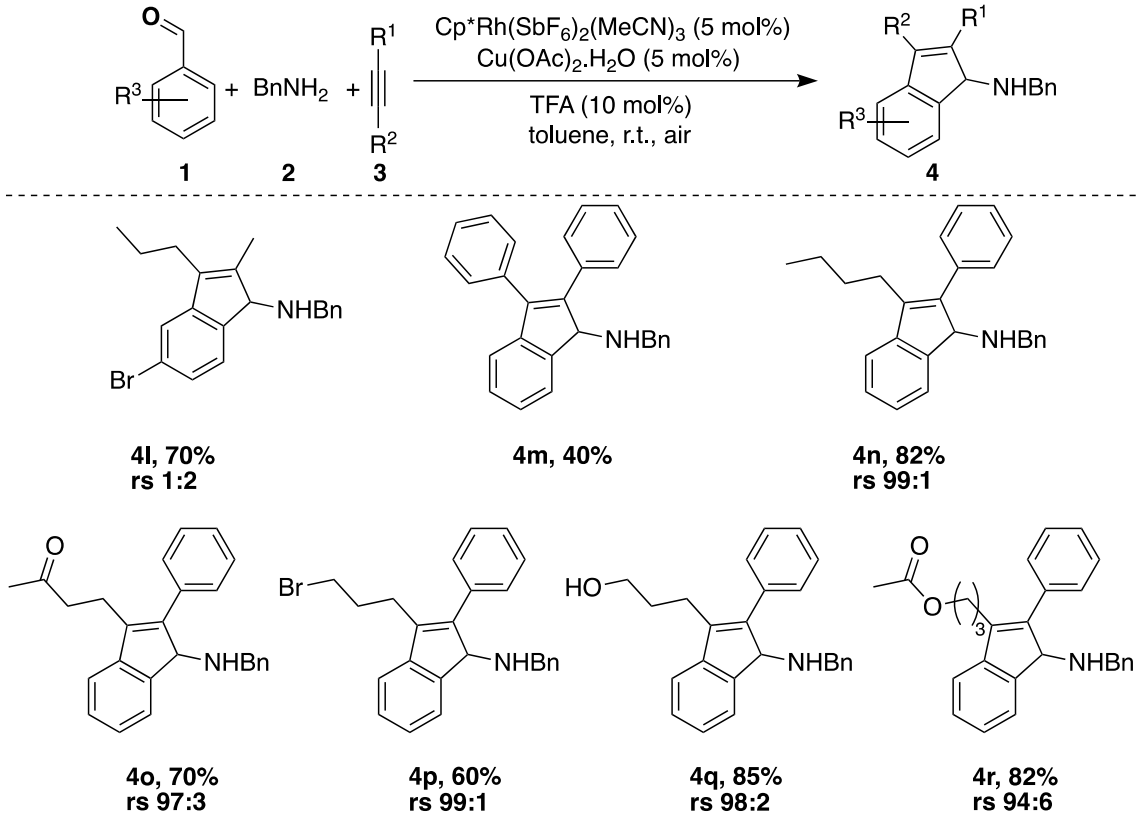

[a]All reactions were performed on a 0.1 mmol scale using 5 mol% $Cp^*Rh(SbF_6)_2(MeCN)_3$, 5 mol% $Cu(OAc)_2{\cdot}H_2O$, **1** (0.1 mmol), **2** (1.2 equiv), **3** (1.2 equiv), in 0.25 mL of a stock solution of toluene/TFA at room temperature and open air. Average isolated yields of two runs are reported in this table. The regioselectivity (rs) was determined by 500 MHz ^1H NMR analysis.

3.3.4 Additional experiments

Several control experiments were conducted to obtain more insights about the reaction mechanism previously shown in section 3.3.2. In absence of rhodium catalyst,

the reaction was inhibited and no product was observed. When copper(II) acetate was removed from the standard conditions, a very low yield was observed. This result suggested that copper(II) acetate was important for the turn-over of the reaction. We evaluated the potential formation of side products that would come from the addition of the alkyne directly to the starting materials, either aldehyde or amine. In Scheme 84-A) and Scheme 84-B), both possibilities were tested, which resulted in the total recovery of the starting materials under our optimized conditions. This suggests that the rhodium catalyst coordinates preferentially to the imine DG to perform C-H activation. In Scheme 84-C), we suggested ammonium acetate into our reaction system. We thought that this substrate may release acetate in order to help the CMD mechanism and generate ammonia *in-situ*.

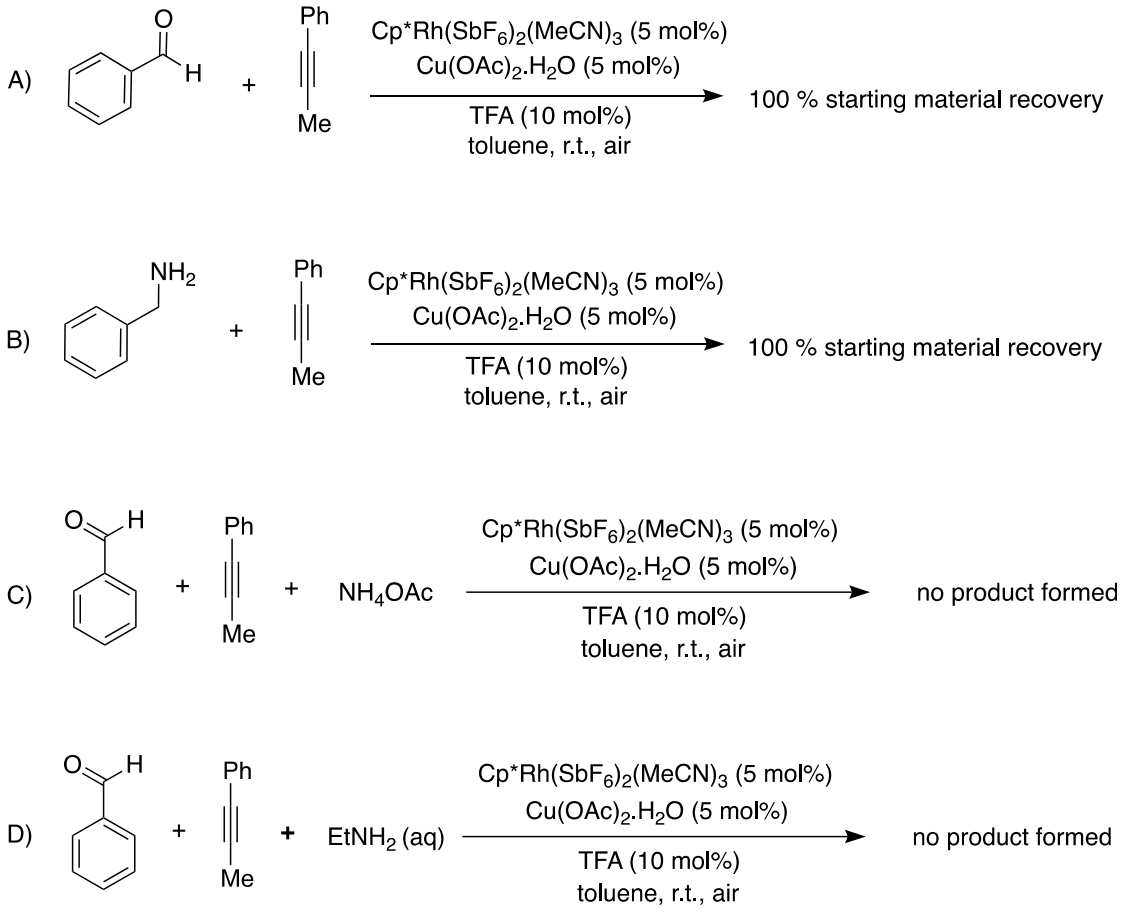

Scheme 84. Control experiments

However, no reaction was observed, probably due to the hygroscopic properties of this compound. In fact, a large amount of water in the reaction seems detrimental. We conducted an experiment with a primary amine solution in water and no product was produced. We proposed that the equilibrium of the condensation reaction is clearly shifted to the amine and aldehyde side, since no indene was observed. The rate of the hydrolysis of imines is considered faster than the C-H activation step.

3.4 Conclusion and outlook

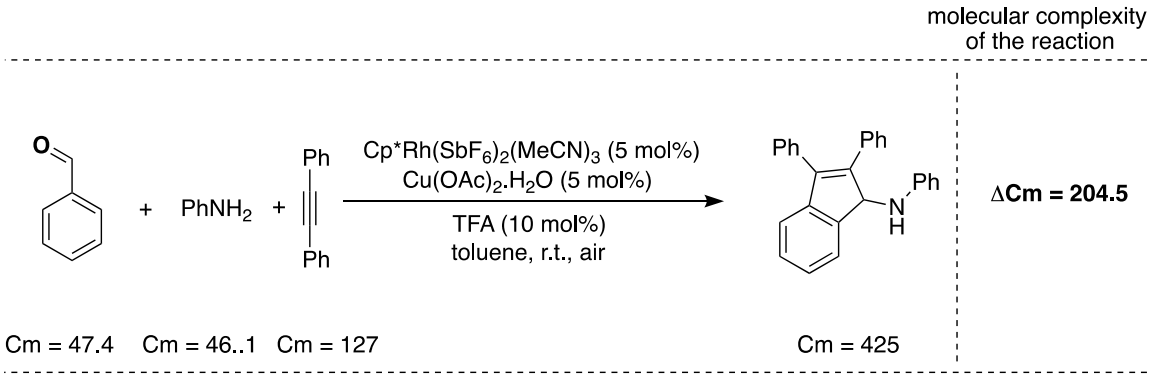

Scheme 85. Calculated molecular complexity for our model reaction

In summary, we have developed a direct and highly efficient multicomponent one-pot tandem C-H activation and annulation protocol towards the generation of indenes. The developed methodology is catalyzed by rhodium and features a great atom-economy and high regioselectivity. This process occurs at room-temperature with water being the only stoichiometric side-product. Moreover, the synthetic viability and efficiency of this process towards a large range of functional groups has been presented. Moreover, this method shows a very satisfying gain of molecular complexity with a value of ΔC_m= 204.5, with simple substrates (Scheme 85).

Thanks to the results obtained with the DFT, we envisioned that the reverse regioselectivity can be controlled by modifying the interaction energy (ΔE_{int}). Being determined by different factors such as steric repulsion, ΔE_{int} might be tuned using very large ligand.

3.5 Contribution

The reaction and conditions for the multicomponent sp^2 C-H activation annulation reaction were developed by me (Pierre Querard), with the supervision of Prof. Dr. Chao-Jun Li. All reactions, isolations, and characterizations (with the exception of high-resolution mass spectrometry) were performed by me. High-resolution mass spectrometry was performed by Dr. Nadim Saadeh at the McGill University Department of Chemistry Mass Spectrometry Laboratory. The manuscript upon which this chapter is based was prepared by me with revision by Prof. Dr. Chao-Jun Li.

3.6 Experimental section

3.6.1 General information

Reaction setup: All reactions were carried out in flamed-dried V-shaped microwave reaction vials, in open air conditions and at room temperature.

Purifications: All work-up and purification procedures were carried out with reagent-grade solvents. Analytical thin-layer chromatography (TLC) was performed using E. Merck silica gel 60 F254 pre-coated plates (0.25 mm). Flash column chromatography was performed with E. Merck silica gel P60 (40–63 μm particle size, 230–400 mesh) (SiO_2). Visualization was accomplished with UV light and/or iodine (I_2) or potassium permanganate ($KMnO_4$) solution. Retention factor (Rf) values reported were measured using a 6 × 2 cm TLC plate in a developing chamber containing the solvent system (10 mL) described. Automated flash column chromatography was performed on Biotage Isolera™ Spektra Systems with ACI™.

Solvents: Tetrahydrofuran (THF), methanol and toluene were taken directly from the Pure Solvent MD-7 purification system (Innovative Technology). Solvents for reaction, filtration, transfers, chromatography, and recrystallization were dichloromethane (CH_2Cl_2) (ACS grade, amylene stabilized), ether (Et_2O) (Fisher, BHT stabilized ACS grade), dichloroethane (ACS grade), acetonitrile (ACS grade), acetone (ACS grade) and ethyl acetate (EtOAc) (Fisher, ACS grade).

NMR spectroscopy: Nuclear magnetic resonance (^{1}H and ^{13}C $\{^{1}H\}$) spectra were recorded on a Bruker AV500 equipped with a 60-position SampleXpress sample changer (^{1}H, 500 MHz; ^{13}C, 125 MHz), a Varian MERCURY plus-500 spectrometer (^{1}H, 500 MHz; ^{13}C, 125 MHz) or Bruker AV400 spectrometer (^{1}H, 400 MHz; ^{13}C, 100 MHz). Chemical shifts for both ^{1}H NMR and ^{13}C NMR spectra were expressed in parts per million (ppm) units downfield from TMS, with the solvent residue peak as the chemical shift standard ($CDCl_3$: δ 7.28 ppm in ^{1}H NMR; δ 77.0 ppm in ^{13}C NMR; DMSO-d6: δ 2.50 ppm in ^{1}H NMR; δ 39.5 ppm in ^{13}C NMR). Data were reported as following: chemical shift, multiplicity (s = singlet, d = doublet, dd = doublet of doublets, t = triplet, td = triplet of doublets, q = quartet, quin = quintet, sep = septet, m = multiplet, br = broad singlet), coupling constants J (Hz), and integration.

Mass spectrometry: Mass spectrometry (MS) was performed by the McGill Chemistry Department Mass Spectrometry Facility. High Resolution Mass spectra were recorded using electrospray ionization (ESI+) and/or atmospheric pressure chemical ionization APCI (+/-), performed either on "Exactive Plus Orbitrap" a ThermoScientific high resolution accurate mass (HR/AM) FT mass spectrometer, or a Bruker Daltonics Maxis Impact quadrupole-time of flight (QTOF) mass spectrometer.

3.6.2 General procedure

A V-shaped 10 mL Biotage reaction vial was charged with $Cp^*Rh(SbF_6)_2(MeCN)_3$ (5 mol%, 4.2 mg), $Cu(OAc)_2$ (5 mol%, 2.0 mg), followed by solid reagents if present. Toluene-TFA (0.25 mL, 10%) stock solution was added followed by subsequent slow addition of the corresponding benzaldehyde (0.1 mmol), followed by the amine derivatives (0.12 mmol) and the internal alkyne (0.12 mmol). The reaction vessel was, placed on vigorous stirring (approx. 1200 rpm) and hold for 18 hours while open to air. The mixture was diluted with ethyl acetate (2 mL), washed with saturated solution of $NaHCO_3$ (2 mL), filtered through a pad of silica, and rinsed with additional ethyl acetate. The combined rinsings were concentrated and purified by column chromatography or preparative thin layer chromatography to yield the corresponding indene compound (**4**).

Nitromethane was used as internal standard for ^{1}H-NMR analysis.

3.6.2.1 Synthesis of $Cp^*Rh(SbF_6)_2(MeCN)_3$

$Cp^*Rh(SbF_6)_2(MeCN)_3$ was synthesized following the procedure reported by Shi (*Angew. Chem. Int. Ed.* **2011***, 50,* 2115) and originally described by Maitlis (*J. C. S. Dalton*, **1977**, 1654-1661).

To the suspension of $[Cp^*RhCl_2]_2$ (2.27 mmol) in dried CH_3CN (18 mL), the solution of $AgSbF_6$ (9.96 mmol) in dried CH_3CN (20 mL) was added in 2 min. Then the white solid precipitated immediately. The reaction was stirred at rt for another 3 h. Then the solid was removed by filtration on celite and washed with CH_3CN (20 mL x 3). The filtrate was evaporated in vacuo to 20 mL, and Et_2O (30 mL) was added dropwise to generate the pale yellow solid precipitate. The pale yellow solid was collected by filtration, washed with EtOAc (20 mL x 3) and Et_2O (20 mL), and dried in vacuo to afford the corresponding $[Cp^*Rh(MeCN)_3][SbF_6]_2$ (94% yield).

^{1}H NMR (300 MHz, DMSO-d_6) δ = 2.07 (9H), 1.54 (15H).

3.6.3 Computational Studies

3.6.3.1 Computational details

The theoretical calculations were carried out by using Gaussian 09 program. Geometry optimizations were performed using the B3LYP functional with a standard 6-31G(d) basis set (lanl2DZ basis set for Rh) using CPCM solvation model (solvent = toluene). Throughout the paper, the energies presented are the calculated Gibbs free energies in toluene as solvent with B3LYP-calculated thermodynamic corrections.

3.6.3.2 Summary of calculation results

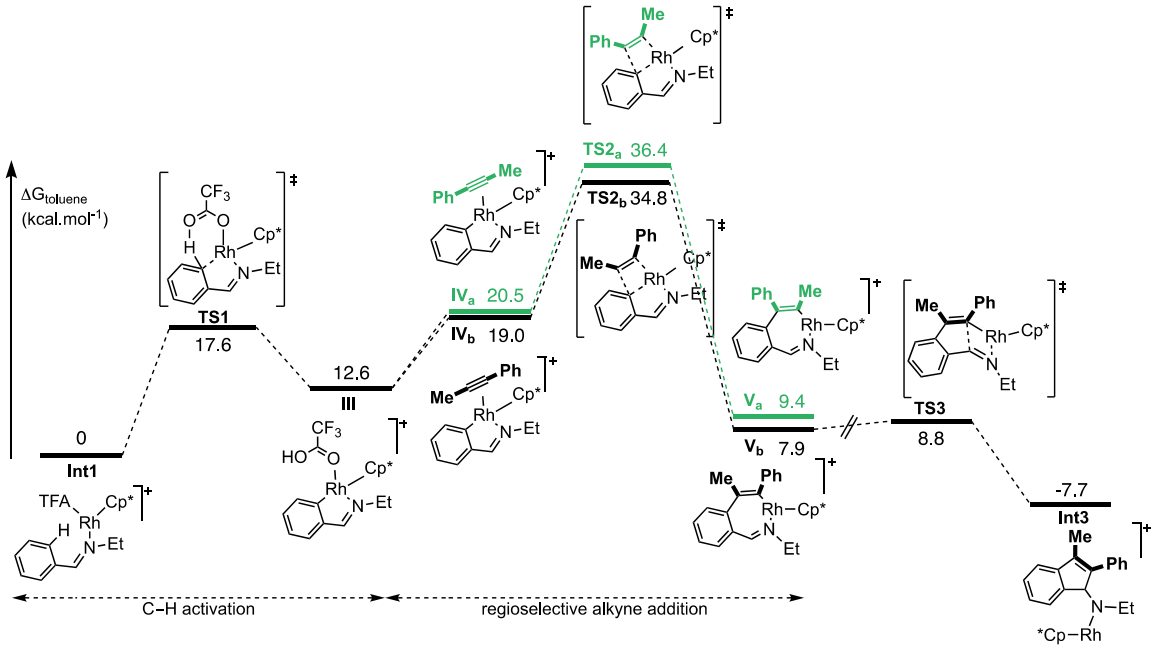

Scheme 86. DFT computed mechanism pathway

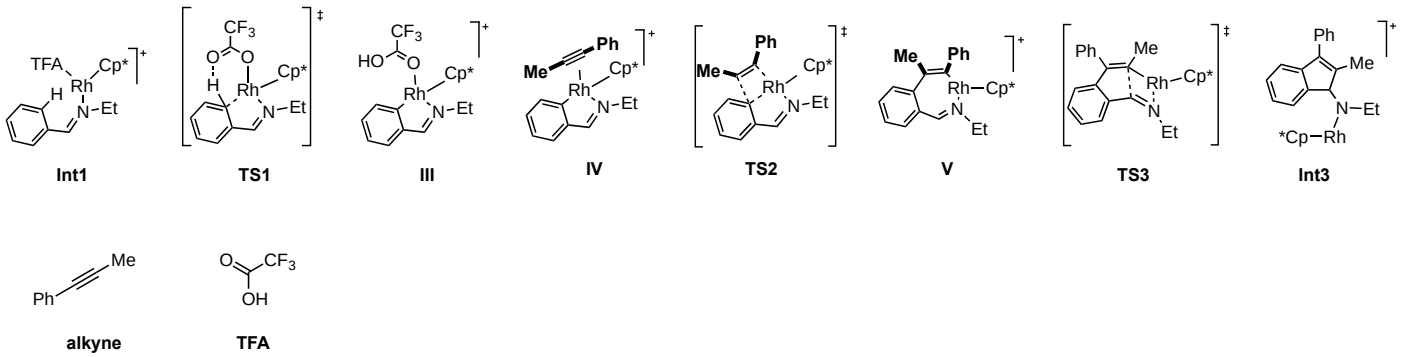

Scheme 87. List of intermediates and transition states

3.6.3.3 Various energy values for all the relevant intermediates and transition states

Int1

Zero-point correction= 0.435668 (Hartree/Particle)
Thermal correction to Energy= 0.467175
Thermal correction to Enthalpy= 0.468119
Thermal correction to Gibbs Free Energy= 0.370065
Sum of electronic and zero-point Energies= -1429.250365

Sum of electronic and thermal Energies= -1429.218858
Sum of electronic and thermal Enthalpies= -1429.217914
Sum of electronic and thermal Free Energies= -1429.315967

TS1

Zero-point correction= 0.430904 (Hartree/Particle)
Thermal correction to Energy= 0.461238
Thermal correction to Enthalpy= 0.462182
Thermal correction to Gibbs Free Energy= 0.369462
Sum of electronic and zero-point Energies= -1429.226534
Sum of electronic and thermal Energies= -1429.196200
Sum of electronic and thermal Enthalpies= -1429.195256
Sum of electronic and thermal Free Energies= -1429.287976

TFA

Zero-point correction= 0.037675 (Hartree/Particle)
Thermal correction to Energy= 0.044018
Thermal correction to Enthalpy= 0.044963
Thermal correction to Gibbs Free Energy= 0.006301
Sum of electronic and zero-point Energies= -526.597762
Sum of electronic and thermal Energies= -526.591419
Sum of electronic and thermal Enthalpies= -526.590475
Sum of electronic and thermal Free Energies= -526.629136

III

Zero-point correction= 0.435116 (Hartree/Particle)
Thermal correction to Energy= 0.465566
Thermal correction to Enthalpy= 0.466510
Thermal correction to Gibbs Free Energy= 0.372004
Sum of electronic and zero-point Energies= -1429.232856
Sum of electronic and thermal Energies= -1429.202406
Sum of electronic and thermal Enthalpies= -1429.201462
Sum of electronic and thermal Free Energies= -1429.295967

Alkyne

Zero-point correction= 0.139600 (Hartree/Particle)
Thermal correction to Energy= 0.147816
Thermal correction to Enthalpy= 0.148760
Thermal correction to Gibbs Free Energy= 0.105145

Sum of electronic and zero-point Energies= -347.506531
Sum of electronic and thermal Energies= -347.498316
Sum of electronic and thermal Enthalpies= -347.497371
Sum of electronic and thermal Free Energies= -347.540986

IV

Zero-point correction= 0.538434 (Hartree/Particle)
Thermal correction to Energy= 0.570848
Thermal correction to Enthalpy= 0.571792
Thermal correction to Gibbs Free Energy= 0.476249
Sum of electronic and zero-point Energies= -1250.132982
Sum of electronic and thermal Energies= -1250.100568
Sum of electronic and thermal Enthalpies= -1250.099624
Sum of electronic and thermal Free Energies= -1250.195167

TS2

Zero-point correction= 0.537599 (Hartree/Particle)
Thermal correction to Energy= 0.569138
Thermal correction to Enthalpy= 0.570082
Thermal correction to Gibbs Free Energy= 0.476347
Sum of electronic and zero-point Energies= -1250.108614
Sum of electronic and thermal Energies= -1250.077076
Sum of electronic and thermal Enthalpies= -1250.076132
Sum of electronic and thermal Free Energies= -1250.169866

V

Zero-point correction= 0.539640 (Hartree/Particle)
Thermal correction to Energy= 0.571385
Thermal correction to Enthalpy= 0.572329
Thermal correction to Gibbs Free Energy= 0.476691
Sum of electronic and zero-point Energies= -1250.149867
Sum of electronic and thermal Energies= -1250.118122
Sum of electronic and thermal Enthalpies= -1250.117177
Sum of electronic and thermal Free Energies= -1250.212816

TS3

Zero-point correction= 0.537375 (Hartree/Particle)
Thermal correction to Energy= 0.568696
Thermal correction to Enthalpy= 0.569641

Thermal correction to Gibbs Free Energy= 0.475319
Sum of electronic and zero-point Energies= -1250.131803
Sum of electronic and thermal Energies= -1250.100482
Sum of electronic and thermal Enthalpies= -1250.099537
Sum of electronic and thermal Free Energies= -1250.193859

Int3

Zero-point correction= 0.541150 (Hartree/Particle)
Thermal correction to Energy= 0.571260
Thermal correction to Enthalpy= 0.572204
Thermal correction to Gibbs Free Energy= 0.481260
Sum of electronic and zero-point Energies= -1250.160252
Sum of electronic and thermal Energies= -1250.130142
Sum of electronic and thermal Enthalpies= -1250.129198
Sum of electronic and thermal Free Energies= -1250.220142

3.6.3.4 Cartesian coordinates for all the relevant intermediates and transition states

Int1

Symbolic Z-matrix:
Charge = 1 Multiplicity = 1

C	-4.32514	2.82062	-0.44076
C	-3.43721	3.11292	0.60345
C	-2.33626	2.27897	0.84117
C	-2.12363	1.15253	0.03499
C	-3.01159	0.86017	-1.00904
C	-4.11226	1.69428	-1.24702
H	-5.16561	3.45743	-0.62243
H	-3.59984	3.97281	1.21914
H	-2.84917	0.00008	-1.62449
H	-4.79009	1.47114	-2.04432
C	-1.35981	2.60009	1.9881
H	-1.52163	3.46005	2.60383
N	-0.34383	1.82972	2.20663
Rh	0.72634	-0.58011	0.55091
C	2.00666	-3.19184	0.31246
C	1.01184	-3.26149	1.64589
C	-0.42956	-3.40205	1.15045

C	1.09246	-3.05945	-0.95379
C	-0.49041	-3.05987	-0.4502
H	-1.28322	0.51566	0.21659
C	2.90527	1.79812	-0.06954
O	2.8035	1.21371	-1.17932
C	3.98523	2.87656	0.1366
F	5.11704	2.29864	0.59219
F	3.54952	3.78369	1.03646
F	4.23596	3.49263	-1.03816
O	2.09803	1.49106	0.90386
C	3.38693	-3.87312	0.26539
H	3.9226	-3.65622	1.16588
H	3.25939	-4.9314	0.17235
H	3.93785	-3.50504	-0.5748
C	1.51724	-3.59512	-2.33369
H	0.86438	-3.20255	-3.08509
H	2.52219	-3.29133	-2.54024
H	1.46028	-4.66358	-2.33452
C	-1.69053	-3.50198	-1.308
H	-1.62858	-3.04188	-2.27205
H	-1.67682	-4.5661	-1.41911
H	-2.60006	-3.20509	-0.82888
C	-1.6267	-3.16654	2.0901
H	-1.95411	-2.15159	2.00305
H	-2.42672	-3.8238	1.82019
H	-1.331	-3.36055	3.09998
C	1.39375	-3.91628	2.98641
H	2.36853	-3.58646	3.27953
H	0.68247	-3.63678	3.7353
H	1.39562	-4.98056	2.87579
C	0.58967	2.13558	3.30009
H	0.06568	2.63761	4.08638
C	1.19416	0.82624	3.84038
H	0.41067	0.1959	4.20602
H	1.71821	0.3242	3.05411
H	1.87361	1.04889	4.63642
H	1.37313	2.76584	2.93436

TS1

Symbolic Z-matrix:
Charge = 1 Multiplicity = 1

C	-2.41903	4.03271	-0.30654
C	-1.965	3.48808	0.90443

C	-1.15148	2.35035	0.8799
C	-0.73458	1.74301	-0.36418
C	-1.22424	2.32361	-1.55115
C	-2.05824	3.44965	-1.52816
H	-3.0429	4.91871	-0.28879
H	-2.24845	3.94119	1.84879
H	-0.90156	1.90824	-2.49908
H	-2.40997	3.88603	-2.45685
C	-0.66768	1.70776	2.09342
H	-0.69752	2.22707	3.0556
N	-0.16964	0.51104	1.99374
C	0.45469	-0.14675	3.16427
H	0.10248	-1.1794	3.21006
Rh	-0.4159	-0.39635	0.06764
C	-2.46796	-1.19345	-0.04917
C	-1.99499	-1.15773	-1.42887
C	-0.83217	-1.98614	-1.51993
C	-1.67887	-2.20833	0.65451
C	-0.64987	-2.66097	-0.22867
H	0.6409	1.74638	-0.48178
C	2.39406	0.58078	-0.4674
O	1.9026	1.74947	-0.58965
C	3.91008	0.43822	-0.61514
F	4.46159	1.46239	-1.35617
F	4.23392	-0.75908	-1.22046
F	4.4987	0.46119	0.64645
O	1.74927	-0.48009	-0.16444
C	-2.69039	-0.47987	-2.5662
H	-3.20611	0.4374	-2.27384
H	-2.02098	-0.25846	-3.40008
H	-3.44998	-1.17549	-2.95143
C	-3.74017	-0.57302	0.43636
H	-3.91848	0.40154	-0.02867
H	-4.60373	-1.21304	0.19145
H	-3.73151	-0.43895	1.51909
C	-1.96423	-2.70287	2.03591
H	-2.33265	-1.90919	2.69246
H	-2.75643	-3.46621	1.98582
H	-1.09247	-3.17114	2.50305
C	0.42493	-3.65941	0.05417
H	0.35133	-4.06261	1.06479
H	0.37399	-4.49751	-0.65536
H	1.42076	-3.20723	-0.07339
C	-0.00315	-2.25547	-2.73467

H	1.05156	-2.38499	-2.47252
H	-0.34306	-3.1794	-3.22709
H	-0.07402	-1.4447	-3.46438
C	1.9884	-0.1293	3.04551
H	2.4278	-0.50667	3.97667
H	2.33188	-0.76764	2.22406
H	2.36658	0.88816	2.87772
H	0.12184	0.36561	4.07784

TFA

Symbolic Z-matrix:
Charge = 0 Multiplicity = 1

H	1.17953	1.6448	-0.8628
C	2.27594	0.06499	-0.43411
O	2.02334	1.28174	-1.14166
C	3.72378	-0.36214	-0.12929
F	3.79628	-1.70956	-0.08826
F	4.10102	0.14534	1.06346
F	4.54325	0.10338	-1.09586
O	1.31513	-0.65672	-0.06054

III

Symbolic Z-matrix:
Charge = 1 Multiplicity = 1

C	0.30694	4.66498	-0.12233
C	0.06624	3.98107	1.07408
C	-0.19978	2.60209	1.04533
C	-0.25098	1.87591	-0.18116
C	0.02271	2.58014	-1.36631
C	0.29418	3.96507	-1.33381
H	0.5121	5.72923	-0.10963
H	0.09384	4.50969	2.02239
H	0.00559	2.07564	-2.32692
H	0.49178	4.48927	-2.2634
C	-0.39851	1.8067	2.23706
H	-0.34648	2.25372	3.23049
N	-0.61741	0.5334	2.09035
C	-0.77976	-0.34158	3.27043
H	-1.76369	-0.81587	3.19965
Rh	-0.67706	-0.11913	0.05304
C	-2.79846	-0.56772	-0.30138
C	-2.22144	-0.22165	-1.59448

C	-1.20221	-1.18685	-1.8724
C	-2.29269	-1.90679	0.07388
C	-1.29852	-2.25904	-0.85312
H	1.89791	1.60653	-0.70287
C	2.56403	-0.17073	-0.2119
O	2.73814	1.06964	-0.64866
C	3.87807	-0.95022	-0.17277
F	3.635	-2.28184	0.07298
F	4.69148	-0.45687	0.83068
F	4.54968	-0.83887	-1.37261
O	1.49933	-0.69677	0.15233
C	-3.96851	0.11222	0.33939
H	-3.97538	1.18503	0.13076
H	-4.90843	-0.30721	-0.04604
H	-3.96969	-0.02184	1.42459
C	-2.68774	0.88553	-2.48594
H	-3.57926	0.55409	-3.03548
H	-2.96017	1.78222	-1.92405
H	-1.93469	1.16373	-3.22655
C	-0.36471	-1.28374	-3.11124
H	-0.86346	-1.91291	-3.86135
H	-0.19247	-0.30535	-3.56768
H	0.60885	-1.73734	-2.9034
C	-0.44647	-3.48911	-0.85444
H	-0.59638	-4.0635	-1.77714
H	0.61915	-3.23551	-0.79981
H	-0.67682	-4.13972	-0.008
C	-2.81049	-2.74363	1.20851
H	-2.73579	-3.80786	0.96622
H	-2.26556	-2.58944	2.14544
H	-3.86412	-2.52202	1.40271
H	-0.78101	0.27946	4.17578
C	0.32109	-1.40448	3.35713
H	0.33525	-2.04013	2.46655
H	1.30563	-0.93713	3.4599
H	0.14986	-2.03934	4.23252

Alkyne

Symbolic Z-matrix:
Charge = 0 Multiplicity = 1

C	-0.91877	-0.07236	2.6331
C	-0.10189	-0.94958	2.55504
C	0.94535	-2.07424	2.45495

H	0.98721	-2.43404	1.44813
H	1.90475	-1.69447	2.73817
H	0.67171	-2.87563	3.10901
C	-1.96604	1.05227	2.73317
C	-3.32603	0.74098	2.73308
C	-1.55502	2.38207	2.824
C	-4.27472	1.75936	2.82313
H	-3.64977	-0.30745	2.66068
C	-2.50385	3.40081	2.91507
H	-0.48317	2.62758	2.82426
C	-3.86354	3.0897	2.91452
H	-5.3467	1.51412	2.82244
H	-2.17947	4.44917	2.98709
H	-4.61172	3.89248	2.98557

IV

Symbolic Z-matrix:
Charge = 1 Multiplicity = 1

C	3.08512	-2.11612	-1.89687
C	3.08052	-0.71819	-1.95789
C	1.98532	0.01332	-1.47718
C	0.84764	-0.69564	-0.90867
C	0.88583	-2.09774	-0.86476
C	1.99364	-2.8018	-1.35371
H	3.92709	-2.66285	-2.26739
H	3.92024	-0.20293	-2.37537
H	0.0581	-2.63588	-0.45232
H	2.00499	-3.87083	-1.31136
C	2.04757	1.56702	-1.58144
Rh	-0.84057	0.21013	-0.15435
C	-3.65155	1.00273	-0.24303
C	-3.18498	0.62096	-1.81918
C	-2.9146	-0.91614	-1.86723
C	-3.77177	-0.32137	0.48025
C	-3.32129	-1.512	-0.52383
C	0.7575	1.06453	2.28481
C	1.55657	0.03137	1.70494
C	0.72559	2.04972	3.46823
H	1.20228	2.96447	3.18355
H	-0.29013	2.24679	3.74122
H	1.24251	1.62254	4.30203
C	2.87766	-0.73369	1.90816
C	3.70159	-0.42959	3.00029

C	3.25618	-1.73351	1.00197
C	4.90379	-1.12528	3.18646
H	3.4127	0.33385	3.69213
C	4.45859	-2.42919	1.18816
H	2.62729	-1.96579	0.16804
C	5.28236	-2.12506	2.2804
H	5.53267	-0.89305	4.02044
H	4.7477	-3.1926	0.49636
H	6.20038	-2.65622	2.42259
C	-3.86273	-0.45899	2.01139
H	-4.88154	-0.62167	2.2951
H	-3.26678	-1.28825	2.33088
H	-3.50296	0.43728	2.47204
C	-2.93613	-2.92681	-0.05358
H	-2.66769	-2.89768	0.98183
H	-3.768	-3.5862	-0.18796
H	-2.10504	-3.27954	-0.62779
C	-3.02869	-1.76198	-3.14923
H	-2.58157	-2.72019	-2.9853
H	-4.06059	-1.88848	-3.40231
H	-2.52324	-1.26502	-3.95075
C	-4.54159	2.18915	0.17124
H	-5.55259	1.99595	-0.12107
H	-4.49525	2.31605	1.23264
H	-4.19521	3.07987	-0.30996
C	-3.67159	1.40874	-3.04967
H	-4.69729	1.17241	-3.24176
H	-3.57634	2.45782	-2.86192
H	-3.07914	1.14341	-3.90027
N	1.03652	2.1599	-1.13047
C	0.84329	3.6169	-1.10398
H	1.79355	4.10126	-1.01856
H	2.88334	2.08594	-2.00215
H	0.23212	3.8805	-0.2662
C	0.1526	4.06669	-2.40478
H	-0.79791	3.58261	-2.48964
H	0.01228	5.12724	-2.38576
H	0.7634	3.80267	-3.24269

TS2

Symbolic Z-matrix:
Charge = 1 Multiplicity = 1

C	2.71784	3.82704	0.21872

C	2.12958	3.29271	1.34843
C	1.4481	2.06962	1.27372
C	1.42446	1.22925	0.12615
C	1.99109	1.8706	-1.0075
C	2.61422	3.12791	-0.97041
H	3.23808	4.7626	0.26176
H	2.18537	3.81927	2.27879
H	1.95015	1.35886	-1.94529
H	3.01954	3.54694	-1.86746
C	0.65004	1.5917	2.52174
H	0.89672	1.97124	3.49008
N	-0.34464	0.74485	2.39103
C	-0.99415	0.17738	3.5798
H	-1.78498	0.82587	3.89483
Rh	-1.28883	0.05794	-0.2977
C	-4.09995	-0.54059	-0.75924
C	-3.85533	1.08278	-1.17783
C	-2.95734	1.11671	-2.43356
C	-3.47134	-1.39512	-1.8649
C	-2.76059	-0.46278	-2.87023
C	1.18784	-1.6055	0.50089
C	2.33868	-0.79143	0.52448
C	1.16908	-3.10711	0.83968
H	1.94173	-3.32175	1.54685
H	0.21971	-3.36556	1.25924
H	1.33285	-3.67776	-0.05208
C	3.81088	-1.17778	0.75966
C	4.15685	-2.51522	1.00343
C	4.80698	-0.19384	0.71703
C	5.50207	-2.87089	1.17612
H	3.39485	-3.26456	1.05656
C	6.15176	-0.55015	0.8883
H	4.54102	0.82924	0.55082
C	6.50086	-1.88957	1.11028
H	5.76669	-3.89111	1.35762
H	6.91245	0.20122	0.84994
H	7.52947	-2.16239	1.23041
C	-1.67869	-0.93054	-3.86618
H	-2.12337	-1.09223	-4.82537
H	-0.92124	-0.17914	-3.94594
H	-1.23989	-1.84458	-3.51983
C	-2.94734	2.25224	-3.4725
H	-2.10488	2.13413	-4.11887
H	-3.8478	2.21582	-4.04965

H	-2.88398	3.19517	-2.97001
C	-4.89323	2.17736	-0.87424
H	-4.44467	3.14026	-0.99903
H	-5.72094	2.07942	-1.54514
H	-5.23666	2.07244	0.13379
C	-5.3206	-1.07347	0.01942
H	-5.5045	-0.44459	0.8661
H	-6.18172	-1.07319	-0.61672
H	-5.12326	-2.07091	0.3514
C	-3.07712	-2.86793	-1.64294
H	-2.42335	-2.93878	-0.79947
H	-3.95735	-3.44809	-1.46182
H	-2.5772	-3.23991	-2.51381
C	-1.57766	-1.20869	3.24577
H	-2.29745	-1.11343	2.46011
H	-0.79113	-1.86209	2.93124
H	-2.05091	-1.61315	4.11608
H	-0.27384	0.08253	4.36447

V

Symbolic Z-matrix:
Charge = 1 Multiplicity = 1

C	-1.99582	4.44318	0.27381
C	-1.27592	3.96552	-0.82571
C	-1.26859	2.59715	-1.13781
C	-1.98541	1.69126	-0.31371
C	-2.74548	2.19679	0.75389
C	-2.74012	3.5594	1.05699
H	-1.97733	5.48586	0.51432
H	-0.72685	4.65155	-1.43538
H	-3.33281	1.52653	1.34631
H	-3.3057	3.92515	1.88627
C	-0.52565	2.16948	-2.4222
H	-0.46145	2.87062	-3.22688
N	0.03212	1.02775	-2.57283
C	0.29433	0.4967	-3.92126
H	0.2881	-0.57326	-3.89239
Rh	0.87904	-0.41886	-0.19984
C	3.45295	-1.75051	0.48911
C	3.68183	-0.15706	0.76893
C	2.81648	0.23582	1.95858
C	2.36898	-2.27494	1.58908
C	1.9928	-1.09207	2.47339

C	-1.03536	-0.69822	-0.8143
C	-2.05787	0.15889	-0.52262
C	-1.36525	-1.98653	-1.59239
H	-2.37197	-2.28155	-1.37928
H	-1.25947	-1.80763	-2.64088
H	-0.69493	-2.7661	-1.29324
C	-3.4638	-0.45363	-0.3581
C	-3.65383	-1.84218	-0.40643
C	-4.56092	0.3951	-0.15976
C	-4.94285	-2.37703	-0.25548
H	-2.81836	-2.49307	-0.5572
C	-5.84783	-0.13887	-0.02049
H	-4.41555	1.45414	-0.11813
C	-6.03943	-1.5242	-0.06608
H	-5.09002	-3.4364	-0.28447
H	-6.68613	0.51328	0.12017
H	-7.02331	-1.93254	0.04491
C	2.36023	-3.71997	2.11894
H	3.1904	-3.86311	2.77865
H	1.44813	-3.90084	2.64957
H	2.43542	-4.39986	1.297
C	1.58402	-1.3023	3.9445
H	0.87501	-2.10122	4.00728
H	2.44957	-1.54721	4.52413
H	1.14296	-0.40434	4.32566
C	3.2358	1.36879	2.91191
H	2.40722	1.63873	3.53087
H	4.04796	1.03853	3.5243
H	3.54468	2.21849	2.33827
C	4.54342	-2.66987	-0.09066
H	5.29221	-2.8461	0.65269
H	4.10453	-3.59972	-0.38436
H	4.99032	-2.20085	-0.94269
C	5.01168	0.55429	0.45719
H	5.74828	0.26051	1.1748
H	5.34184	0.27988	-0.52412
H	4.86871	1.61235	0.50216
C	1.67145	0.99663	-4.39829
H	2.42689	0.659	-3.72055
H	1.8705	0.61339	-5.37599
H	1.67053	2.06706	-4.42746
H	-0.46379	0.83666	-4.59679

TS3

Symbolic Z-matrix:

Charge = 1 Multiplicity = 1

C	3.03305	1.99811	1.60759
C	1.66955	1.83438	1.33314
C	1.20319	0.56911	0.96207
C	2.10333	-0.50915	0.78923
C	3.46535	-0.34092	1.08691
C	3.92148	0.91477	1.49584
H	3.40303	2.96493	1.9309
H	0.98028	2.66383	1.44728
H	4.16265	-1.16432	0.97606
H	4.97243	1.05786	1.72183
C	-0.23336	0.22611	0.76367
H	-0.73131	-0.23724	1.62698
Rh	-0.26632	-0.03889	-1.83206
C	-1.13833	0.64049	-4.33574
C	0.02352	1.32966	-3.9768
C	1.11615	0.34939	-3.92837
C	-0.78652	-0.76533	-4.59592
C	0.60617	-0.91304	-4.44235
C	0.24794	-1.47305	-0.36784
C	1.43925	-1.70669	0.27032
C	-0.85765	-2.46084	-0.66494
H	-1.25529	-2.9203	0.24938
H	-1.72176	-1.98379	-1.16576
H	-0.5186	-3.2558	-1.33912
C	-2.45475	1.05483	0.13487
H	-2.65097	0.91359	1.1772
N	-1.00196	0.88438	-0.13604
C	2.00068	-3.11104	0.5605
C	1.79983	-3.69881	1.80976
C	2.71035	-3.79538	-0.42621
C	2.30914	-4.97036	2.07239
H	1.23888	-3.16069	2.58758
C	3.21903	-5.06774	-0.16399
H	2.86859	-3.33235	-1.41094
C	3.01868	-5.65523	1.08511
H	2.15126	-5.4321	3.05787
H	3.77818	-5.60724	-0.9423
H	3.42011	-6.65782	1.29239
C	-2.82402	2.49129	-0.27963
H	-3.88856	2.59916	-0.28258

H	-2.39727	3.18392	0.41539
H	-2.44279	2.68887	-1.2597
H	-3.01878	0.35185	-0.44184
C	0.1417	2.81753	-3.59748
H	0.13466	2.91561	-2.53201
H	1.05684	3.21306	-3.98603
H	-0.68429	3.35768	-4.01085
C	2.59116	0.67042	-3.6236
H	2.9703	1.3428	-4.36458
H	2.66499	1.12537	-2.65795
H	3.16302	-0.23385	-3.6365
C	-2.55839	1.22797	-4.43516
H	-2.83979	1.6427	-3.48979
H	-2.57552	1.99537	-5.18061
H	-3.24653	0.45401	-4.70414
C	-1.77517	-1.85289	-5.0557
H	-2.54341	-1.97048	-4.32025
H	-2.2147	-1.5644	-5.98762
H	-1.25431	-2.77944	-5.17866
C	1.42866	-2.19821	-4.65078
H	2.41663	-1.94132	-4.97144
H	1.48226	-2.74063	-3.73002
H	0.95855	-2.80564	-5.39572

Int3

Symbolic Z-matrix:
Charge = 1 Multiplicity = 1

C	0.48112	1.50244	3.70341
C	1.54939	1.35597	2.79287
C	1.546	0.23652	1.96664
C	0.49079	-0.64625	1.95132
C	-0.55388	-0.56123	2.86562
C	-0.55477	0.53177	3.75755
H	0.45317	2.34749	4.35912
H	2.33879	2.07675	2.74515
H	-1.33328	-1.29402	2.88636
H	-1.34174	0.63242	4.47549
C	2.62263	-0.23028	0.96959
H	3.04129	0.57173	0.39824
Rh	2.80428	-3.12291	3.32654
C	4.15079	-3.62857	5.997
C	2.68746	-4.24117	5.95746
C	2.71976	-5.46676	4.9205

C	5.02685	-4.29216	4.68431
C	4.22014	-5.59924	4.32193
C	1.85284	-1.2559	0.10687
C	0.68152	-1.63115	0.78783
C	2.29144	-1.77421	-1.27539
H	1.89032	-1.13976	-2.03786
H	3.35988	-1.77166	-1.3348
H	1.92891	-2.77131	-1.41392
C	4.38033	0.05625	2.57915
N	3.7131	-0.90447	1.68884
H	5.17485	-0.43409	3.10178
C	1.78991	-4.17751	7.20724
H	0.79267	-4.46342	6.94513
H	2.16826	-4.8456	7.95247
H	1.78515	-3.17928	7.59245
C	4.45975	-2.23367	6.57204
H	3.83435	-1.506	6.09836
H	4.27298	-2.23281	7.62559
H	5.48661	-1.99302	6.39167
C	6.55831	-4.19585	4.55445
H	6.86512	-3.18063	4.6962
H	7.01872	-4.8145	5.29616
H	6.85514	-4.52552	3.58073
C	4.51646	-6.43445	3.06236
H	4.48535	-5.80224	2.1997
H	5.48795	-6.87492	3.14693
H	3.78202	-7.20653	2.96542
C	1.84378	-6.72407	5.07367
H	1.86352	-7.28562	4.1631
H	2.22179	-7.32693	5.87275
H	0.8374	-6.43322	5.29162
H	3.67287	0.4398	3.28436
C	4.95397	1.21643	1.74461
H	5.43997	1.91555	2.39255
H	5.66113	0.83278	1.03918
H	4.15936	1.70704	1.22226
C	-0.25514	-2.79569	0.41666
C	-0.1268	-4.03196	1.06394
C	-1.23605	-2.61897	-0.56844
C	-0.97996	-5.09132	0.72664
H	0.62251	-4.16701	1.81576
C	-2.08901	-3.67836	-0.90593
H	-1.3337	-1.67511	-1.06287
C	-1.96105	-4.91453	-0.25831

H	-0.88226 -6.03515 1.22112
H	-2.83802 -3.54338 -1.658
H	-2.61242 -5.7234 -0.5159

3.6.4 Characterization of newly synthesized compounds

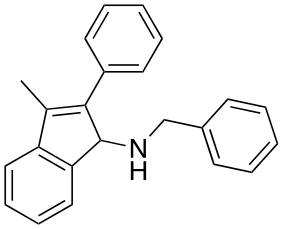

N-benzyl-3-methyl-2-phenyl-1*H*-inden-1-amine, (**4a**)

Using the general procedure described above, compound (**4a**) was obtained from benzaldehyde (0.1 mmol, 11 μL), benzylamine (0.12 mmol, 13.1 μL) and prop-1-yn-1-ylbenzene (0.12 mmol, 15 μL) as a light yellow solid (31.0 mg) in 99 % yield.

^{1}H NMR ($CDCl_3$, 500 MHz): δ = 7.68 (m, 1H), 7.48 (m, 4H), 7.44 – 7.34 (m, 3H), 7.32 (m, 1H), 7.24 – 7.15 (m, 3H), 7.10 – 7.03 (m, 2H), 5.10 – 4.88 (q, J = 1.9 Hz, 1H), 3.37 (d, J = 12.6, Hz, 1H), 3.29 (dd, J = 12.6, Hz, 1H), 2.32 (d, J = 1.9 Hz, 3H).

^{13}C NMR ($CDCl_3$, 126 MHz): δ = 145.7, 143.9, 143.7, 140.5, 135.7, 135.5, 128.9, 128.6, 128.2, 128.1, 127.8, 126.9, 126.7, 125.5, 123.3, 119.2, 65.7, 47.4, 11.7.

HRMS (ESI) m/z: $[M + H]^+$ calculated for $C_{23}H_{22}N$ 312.1752, found 312.1743.

Rf (Hexane/Et_2O 4:1): 0.4.

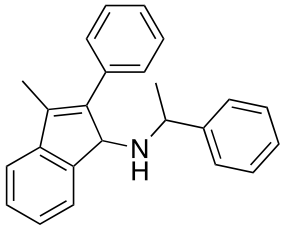

3-methyl-2-phenyl-*N*-(1-phenylethyl)-1*H*-inden-1-amine, (**4b**)

Using the general procedure described above, compound (**4b**) was obtained from benzaldehyde (0.1 mmol, 11.0 μL), 1-phenylethan-1-amine (0.12 mmol, 15.5 μL) and prop-1-yn-1-ylbenzene (0.12 mmol, 15.0 μL) as a light yellow solid (21.5 mg) in 66 % yield.

^{1}H NMR ($CDCl_3$, 500 MHz): δ = 7.62 – 7.58 (m, 1H), 7.50 – 7.46 (m, 2H), 7.40 – 7.31 (m, 9H), 7.23 – 7.19 (m, 1H), 4.64 (d, J = 2.0 Hz, 1H), 4.21 (q, J = 6.6 Hz, 1H), 2.26 (d, J = 2.0 Hz, 3H), 1.26 (d, J = 6.6 Hz, 3H).

^{13}C NMR ($CDCl_3$, 126 MHz): δ = 145.63, 145.60, 145.3, 143.9, 135.5, 134.8, 129.3, 128.33, 128.30, 127.5, 127.2, 127.0, 126.9, 125.2, 123.7, 119.3, 63.2, 55.8, 24.9, 11.6.

HRMS (ESI) m/z: $[M + H]^+$ calculated for $C_{24}H_{24}N$ 326.1909, found 326.1904.

Rf (Hexane/Et_2O 4:1): 0.6.

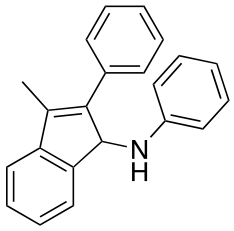

3-methyl-*N*,2-diphenyl-1*H*-inden-1-amine, (**4c**)

Using the general procedure described above, compound (**4c**) was obtained from benzaldehyde (0.1 mmol, 11.0 μL), aniline (0.12 mmol, 11.0 μL) and prop-1-yn-1-ylbenzene (0.12 mmol, 15.0 μL) as a yellow solid (10.4 mg) in 35 % yield.

^{1}H NMR ($CDCl_3$, 500 MHz): δ = 7.55 – 7.51 (m, 1H), 7.46 – 7.35 (m, 6H), 7.32 – 7.27 (m, 1H), 7.22 – 7.09 (m, 3H), 6.74 – 6.70 (m, 1H), 6.68 – 6.66 (m, 2H), 5.54 (q, *J* = 2.2 Hz, 1H), 2.32 (d, *J* = 2.2 Hz, 3H).

^{13}C NMR ($CDCl_3$, 126 MHz): δ = 147.7, 145.1, 144.8, 142.2, 135.7, 135.1, 129.19, 129.10, 128.3, 127.9, 126.9, 125.9, 122.9, 119.4, 117.6, 113.7, 62.1, 11.9.

HRMS (ESI) m/z: $[M + H]^+$ calculated for $C_{22}H_{20}N$ 298.1596, found 398.1590.

Rf (Hexane/Et_2O 4:1): 0.4.

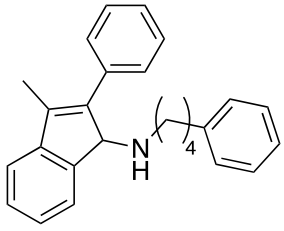

3-methyl-2-phenyl-*N*-(4-phenylbutyl)-1*H*-inden-1-amine, (**4d**)

Using the general procedure described above, compound (**4d**) was obtained from benzaldehyde (0.1 mmol, 11.0 μL), 4-phenylbutan-1-amine (0.12 mmol, 18.9 μL) and prop-1-yn-1-ylbenzene (0.12 mmol, 15 μL) as a light yellow solid (35.2 mg) in 99 % yield.

^{1}H NMR ($CDCl_3$, 500 MHz): δ = 7.57 -7.55 (m, 1H), 7.48 – 7.40 (m, 4H), 7.38 – 7.29 (m, 3H), 7.28 – 7.26 (m, 1H), 7.25 -7.20 (m, 2H), 7.16 – 7.12 (m, 1H), 7.04 – 7.01 (m, 2H), 4.87 (q, *J* = 1.9 Hz, 1H), 3.50 (d, *J* = 7.0 Hz, 1H), 3.47 (d, *J* = 7.0 Hz, 1H), 2.40 (dd, *J* = 8.7, 6.7 Hz, 2H), 2.27 – 2.22 (m, 3H), 2.11 (ddd, *J* = 11.2, 7.6, 6.3 Hz, 1H).

^{13}C NMR ($CDCl_3$, 126 MHz): δ = 145.6, 144.2, 143.9, 142.4, 135.8, 135.2, 128.8, 128.5, 128.3, 128.1, 127.6, 126.8, 125.5, 125.4, 123.2, 119.1, 65.9, 42.8, 35.4, 29.8, 28.7, 11.6.

HRMS (ESI) m/z: $[M + H]^+$ calculated for $C_{26}H_{27}N$ 353,2143, found 353.2140.

Rf (Hexane/Et_2O 4:1): 0.5.

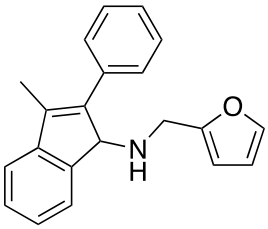

N-(furan-2-ylmethyl)-3-methyl-2-phenyl-1*H*-inden-1-amine, (**4e**)

Using the general procedure described above, compound (**4e**) was obtained from benzaldehyde (0.1 mmol, 11.0 μL), furan-2-ylmethanamine (0.12 mmol, 10.7 μL) and prop-1-yn-1-ylbenzene (0.12 mmol, 15.0 μL) as a light yellow solid (16.6 mg) in 55 % yield.

^{1}H NMR ($CDCl_3$, 500 MHz): δ = 7.66 – 7.63 (m, 1H), 7.51 – 7.47 (m, 2H), 7.46 – 7.41 (m, 2H), 7.40 – 7.38 (m, 1H), 7.37 – 7.34 (m, 2H), 7.32 – 7.26 (m, 2H), 6.23 (dd, *J* = 3.2, 1.8 Hz, 1H), 5.96 (d, *J* = 3.2 Hz, 1H), 4.96 (t, *J* = 2.0 Hz, 1H), 3.45 (d, *J* = 14.1 Hz, 1H), 3.36 (d, *J* = 14.1 Hz, 1H), 2.29 (d, *J* = 2.0 Hz, 3H).

^{13}C NMR ($CDCl_3$, 126 MHz): δ = 153.8, 145.6, 143.5, 143.1, 141.6, 135.8, 135.5, 128.8, 128.6, 127.9, 127.0, 125.6, 123.4, 119.2, 110.0, 106.7, 65.1, 40.5, 11.6.

HRMS (ESI) m/z: $[M + H]^+$ calculated for $C_{21}H_{20}NO$ 302.1545, found 302.1534.

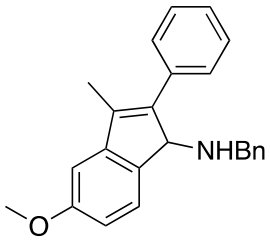

N-benzyl-5-methoxy-3-methyl-2-phenyl-1*H*-inden-1-amine, (**4f**)

Using the general procedure described above, compound (**4f**) was obtained from 4-methoxybenzaldehyde (0.1 mmol, 12.1 μL), benzylamine (0.12 mmol, 13.1 μL) and prop-1-yn-1-ylbenzene (0.12 mmol, 15 μL) as a light yellow solid (20.5 mg) in 60 % yield.

^{1}H NMR ($CDCl_3$, 500 MHz): δ = 7.55 – 7.53 (m, 1H), 7.51 – 7.43 (m, 4H), 7.38 – 7.32 (m, 1H), 7.23 – 7.13 (m, 3H), 7.08 – 7.00 (m, 2H), 6.94 – 6.92 (m, 1H), 6.85 – 6.83 (m, 1H), 4.94 (q, J = 1.8 Hz, 1H), 3.91 (s, 3H), 3.34 (d, J = 12.7 Hz, 1H), 3.28 (d, J = 12.7 Hz, 1H), 2.28 (d, J = 1.8 Hz, 3H).

^{13}C NMR ($CDCl_3$, 126 MHz): δ = 160.1, 147.3, 145.2, 140.7, 136.0, 135.7, 135.1, 128.8, 128.5, 128.2, 128.1, 126.9, 126.6, 123.8, 110.5, 105.5, 65.1, 55.5, 47.3, 11.6.

HRMS (ESI) m/z: $[M + H]^+$ calculated for $C_{24}H_{24}NO$ 342.1858, found 342.1850.

Rf (Hexane/Et_2O 4:1): 0.3.

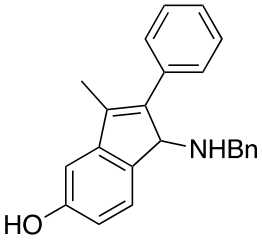

1-(benzylamino)-3-methyl-2-phenyl-1*H*-inden-5-ol, (**4g**)

Using the general procedure described above, compound (**4g**) was obtained from 4-hydroxybenzaldehyde (0.1 mmol, 12.2 mg), benzylamine (0.12 mmol, 11.8 μL) and prop-1-yn-1-ylbenzene (0.12 mmol, 15.0 μL) as a light yellow solid (13.1 mg) in 40 % yield.

^{1}H NMR ($CDCl_3$, 500 MHz): δ = 7.58 – 7.55 (m, 1H), 7.50 – 7.46 (m, 2H), 7.44 – 7.39 (m, 2H), 7.38 – 7.34 (m, 1H), 7.22 – 7.16 (m, 3H), 7.05 – 6.99 (m, 2H), 6.84 – 7.81 (m, 1H), 6.73 – 6.70 (m, 1H), 4.99 (d, J = 2.1 Hz, 1H), 3.38 (d, J = 2.9 Hz, 2H), 2.23 (d, J = 1.8 Hz, 3H).

^{13}C NMR ($CDCl_3$, 126 MHz): δ = 156.6, 147.5, 143.8, 139.1, 136.0, 135.1, 134.1, 128.8, 128.7, 128.5, 128.3, 127.2, 127.1, 124.4, 112.6, 107.2, 64.4, 47.3, 11.6.

HRMS (ESI) m/z**:** $[M + H]^+$ calculated for $C_{23}H_{21}NO$ 328.1695, found 328.1692.

Rf (Hexane/Et_2O 4:1): 0.3.

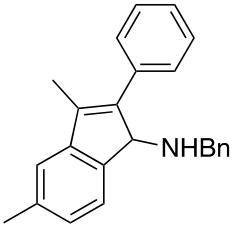

N-benzyl-3,5-dimethyl-2-phenyl-1*H*-inden-1-amine, (**4h**)

Using the general procedure described above, compound (**4h**) was obtained from 4-methylbenzaldehyde (0.1 mmol, 11.8 μL), benzylamine (0.12 mmol, 11.8 μL) and prop-1-yn-1-ylbenzene (0.12 mmol, 15.0 μL) as a light yellow solid (27.7 mg) in 85 % yield.

^{1}H NMR ($CDCl_3$, 500 MHz): δ = 7.59 – 7.56 (m, 1H), 7.52 – 7.44 (m, 4H), 7.39 – 7.34 (m, 1H), 7.24 – 7.16 (m, 4H), 7.15 – 7.12 (m, 1H), 7.08 – 7.04 (m, 2H), 4.98 (d, *J* = 2.0 Hz, 1H), 3.35 (d, *J* = 12.6 Hz, 1H), 3.30 (d, *J* = 12.6 Hz, 1H), 2.49 (s, 3H), 2.30 (d, *J* = 2.0 Hz, 3H).

^{13}C NMR ($CDCl_3$, 126 MHz): δ = 145.9, 143.8, 140.9, 140.5, 137.5, 135.7, 135.5, 128.9, 128.6, 128.2, 128.1, 126.9, 126.7, 126.2, 123.1, 120.0, 65.4, 47.3, 21.7, 11.7.

HRMS (ESI) m/z: $[M + H]^+$ calculated for $C_{24}H_{24}N$ 326.1909, found 326.1903.

Rf (Hexane/Et_2O 4:1): 0.5.

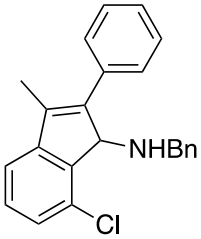

N-benzyl-7-chloro-3-methyl-2-phenyl-1*H*-inden-1-amine, (**4i**)

Using the general procedure described above, compound (**4i**) was obtained from 2-chlorobenzaldehyde (0.1 mmol, 11.2 μL), benzylamine (0.12 mmol, 11.8 μL) and prop-1-yn-1-ylbenzene (0.12 mmol, 15.0 μL) as a light yellow solid (19.4 mg) in 56 % yield.

^{1}H NMR ($CDCl_3$, 500 MHz): δ = 7.56 – 7.52 (m, 2H), 7.52 – 7.46 (m, 2H), 7.41 – 7.33 (m, 2H), 7.30 – 7.26 (m, 1H), 7.24 – 7.20 (m, 1H), 7.19 – 7.13 (m, 3H), 7.00 – 6.95 (m, 2H), 5.19 (q, *J* = 2.0 Hz, 1H), 3.20 (m, 2H), 2.29 (d, *J* = 2.0 Hz, 2H).

^{13}C NMR ($CDCl_3$, 126 MHz): δ = 173.1, 148.2, 143.7, 139.8, 135.2, 134.9, 130.0, 129.6, 129.2, 128.4, 128.3, 128.0, 127.2, 126.7, 126.1, 117.7, 66.2, 46.7, 11.8.

HRMS (ESI) m/z: $[M + H]^+$ calculated for $C_{23}H_{21}ClN$ 346.1363, found 346.1357.

Rf (Hexane/Et_2O 4:1): 0.4.

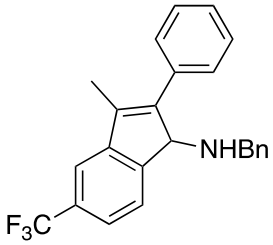

N-benzyl-3-methyl-2-phenyl-5-(trifluoromethyl)-1*H*-inden-1-amine, (**4j**)

Using the general procedure described above, compound (**4j**) was obtained from 4-(trifluoromethyl)benzaldehyde (0.1 mmol, 11.5 μL), benzylamine (0.12 mmol, 13.1 μL) and prop-1-yn-1-ylbenzene (0.12 mmol, 15.0 μL) as a light yellow solid (31.8 mg) in 84 % yield.

^{1}H NMR ($CDCl_3$, 500 MHz): δ = 7.80 – 7.74 (m, 1H), 7.61 – 7.52 (m, 2H), 7.55 – 7.46 (m, 2H), 7.49 – 7.41 (m, 2H), 7.44 – 7.36 (m, 1H), 7.25 – 7.14 (m, 3H), 7.08 – 7.00 (m, 2H), 5.04 (s, 1H), 3.35 (d, J = 12.5 Hz, 1H), 3.23 (d, J = 12.5 Hz, 1H), 2.33 (d, J = 2.0 Hz, 3H).

^{13}C NMR ($CDCl_3$, 126 MHz): δ = 147.4, 146.3, 145.4, 139.8, 134.9, 134.8, 130.4 (q, J_{C-F}= 31.7 Hz), 128.9, 128.7, 128.2, 127.4, 126.9, 125.6, 123.58, 123.52 (q, J_{C-F}= 274 Hz), 122.6 (q, J_{C-F}= 4.0 Hz), 115.96 (q, J_{C-F}= 3.8 Hz), 65.6, 47.4, 11.6.

^{19}F NMR ($CDCl_3$, 471 MHz): δ = -61.9.

HRMS (ESI) m/z: $[M + H]^+$ calculated for $C_{24}H_{21}F_3N$ 380.1621, found 380.1626.

Rf (Hexane/Et_2O 4:1): 0.5.

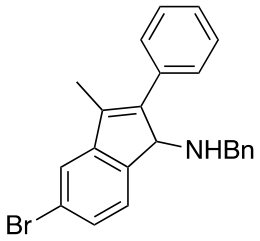

N-benzyl-5-bromo-3-methyl-2-phenyl-1*H*-inden-1-amine, (**4k**)

Using the general procedure described above, compound (**4k**) was obtained from 4-bromobenzaldehyde (0.1 mmol, 18.5 mg), benzylamine (0.12 mmol, 13.1 μL) and prop-1-yn-1-ylbenzene (0.12 mmol, 15.0 μL) as a light yellow solid (32.8 mg) in 84 % yield.

^{1}H NMR ($CDCl_3$, 500 MHz): δ = 7.55 – 7.54 (m, 1H), 7.53 – 7.47 (m, 3H), 7.46 – 7.43 (m, 3H), 7.42 – 7.37 (m, 1H), 7.24 – 7.18 (m, 3H), 7.06 – 7.02 (m, 2H), 4.96 (d, J = 2.0 Hz, 1H), 3.33 (d, J = 12.7 Hz, 1H), 3.25 (d, J = 12.6 Hz, 1H), 2.28 (d, J = 2.0 Hz, 3H).

^{13}C NMR ($CDCl_3$, 126 MHz): δ = 147.8, 145.3, 142.5, 140.1, 135.1, 134.6, 128.9, 128.7, 128.27, 128.24, 128.23, 127.3, 126.9, 124.8, 122.5, 121.9, 65.3, 47.3, 11.6.

HRMS (ESI) m/z: $[M + H]^+$ calculated for $C_{23}H_{21}NBr$ 390.0851, found 390.0858.

Rf (Hexane/Et_2O 4:1): 0.4.

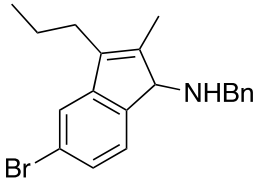

N-benzyl-5-bromo-2-methyl-3-propyl-1*H*-inden-1-amine, (**4l**)

Using the general procedure described above, compound (**4l**) was obtained from 4-bromobenzaldehyde (0.1 mmol, 18.5 mg), benzylamine (0.12 mmol, 13.1 μL) and 2-hexyne (0.12 mmol, 13.5 μL) as a light yellow solid (19.4 mg) in 24 % yield.

^{1}H NMR ($CDCl_3$, 500 MHz): δ = 7.44 – 7.35 (m, 1H), 7.35 – 7.33 (m, 1H), 7.35 – 7.26 (m, 5H), 7.25 – 7.22 (m, 1H), 4.26 (s, 1H), 3.46 – 3.30 (m, 2H), 2.48 (t, J = 7.4 Hz, 2H), 2.05 (s, 3H), 1.62 (q, J = 7.4 Hz, 2H), 0.99 (t, J = 7.4 Hz, 3H).

^{13}C NMR ($CDCl_3$, 126 MHz): δ = 147.6, 142.8, 142.1, 138.3, 137.6, 128.9, 128.7, 128.4, 128.36, 128.35, 128.32, 127.0, 126.9, 124.2, 121.7, 121.6, 66.4, 47.3, 27.1, 21.5, 14.1, 11.9.

HRMS (ESI) m/z: $[M + H]^+$ calculated for $C_{20}H_{23}NBr$ 356.1008, found 356.1015.

Rf (Hexane/Et_2O 4:1): 0.4.

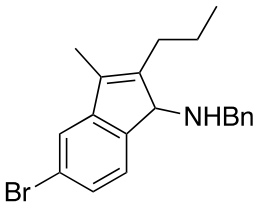

N-benzyl-5-bromo-3-methyl-2-propyl-1*H*-inden-1-amine, (**4l'**)

Using the general procedure described above, compound (**4l'**) was obtained from 4-bromobenzaldehyde (0.1 mmol, 18.5 mg), benzylamine (0.12 mmol, 13.1 μL) and 2-hexyne (0.12 mmol, 13.5 μL) as a light yellow solid (19.4 mg) in 44 % yield.

^{1}H NMR ($CDCl_3$, 500 MHz): δ = 7.41 – 7,39 (m, 1H), 7.38 – 7.31 (m, 2H), 7.32 – 7.30 (m, 4H), 7.26 – 7.22 (m, 1H), 4.38 (s, 1H), 3.50 – 3.34 (m, 2H), 2.50 – 2.38 (m, 2H), 2.03 (d, J = 1.9 Hz, 3H), 1.69 – 1.62 (m, 1H), 1.54 – 1.47 (m, 1H), 0.98 (t, J = 7.3 Hz, 3H).

^{13}C NMR ($CDCl_3$, 126 MHz): δ = 148.2, 142.9, 142.5, 140.4, 139.9, 128.4, 128.35, 128.32, 128.2, 127.9, 127.3, 127.15, 127.10, 124.2, 124.1, 121.6, 64.2, 47.6, 27.9, 22.9, 14.1, 10.3.

HRMS (ESI) m/z: $[M + H]^+$ calculated for $C_{20}H_{23}NBr$ 356.1008, found 356.1014.

Rf (Hexane/Et_2O 4:1): 0.5.

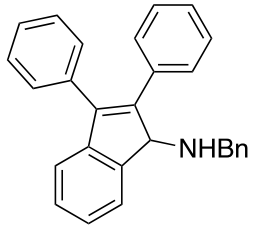

N-benzyl-2,3-diphenyl-1*H*-inden-1-amine, (**4m**)

Using the general procedure described above, compound (**4m**) was obtained from benzaldehyde (0.1 mmol, 11.0 μL), benzylamine (0.12 mmol, 13.1 μL) and 1,2-diphenylethyne (0.12 mmol, 17.9 mg) as a light yellow solid (14.9 mg) in 40 % yield.

^{1}H NMR ($CDCl_3$, 500 MHz): δ = 7.78 – 7.74 (m, 1H), 7.45 – 7.37 (m, 5H), 7.37 – 7.33 (m, 2H), 7.33 – 7.24 (m, 6H), 7.24 – 7.16 (m, 3H), 7.09 – 7.04 (m, 2H), 5.15 (s, 1H), 3.42 (m, 2H).

^{13}C NMR ($CDCl_3$, 126 MHz): δ = 144.8, 144.6, 144.1, 140.3, 140.2, 135.00, 134.9, 129.4, 129.2, 128.6, 128.39, 128.33, 128.2, 127.8, 127.5, 127.1, 126.8, 125.7, 123.8, 120.5, 65.8, 47.5.

HRMS (ESI) m/z: $[M + H]^+$ calculated for $C_{28}H_{24}N$ 374.1909, found 374.1900.

Rf (Hexane/Et_2O 4:1): 0.4.

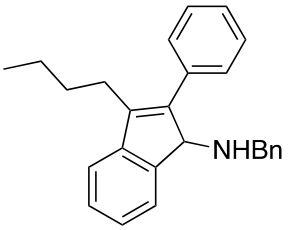

N-benzyl-3-butyl-2-phenyl-1*H*-inden-1-amine, (**4n**)

Using the general procedure described above, compound (**4n**) was obtained from benzaldehyde (0.1 mmol, 11.0 μL), benzylamine (0.12 mmol, 11.8 μL) and hex-1-yn-1-ylbenzene (0.12 mmol, 21.0 μL) as a light yellow solid (23.0 mg) in 82 % yield.

^{1}H NMR ($CDCl_3$, 500 MHz): δ = 7.73 – 7.68 (m, 1H), 7.53 – 7.48 (m, 2H), 7.46 – 7.35 (m, 5H), 7.34 – 7.28 (m, 1H), 7.24 – 7.15 (m, 3H), 7.09 – 7.04 (m, 2H), 4.99 (br, 1H), 3.38 (d, *J* = 12.7 Hz, 1H), 3.30 (d, *J* = 12.7 Hz, 1H), 2.73 (t, *J* = 7.8 Hz, 2H), 1.82 – 1.71 (m, 1H), 1.71 – 1.61 (m, 1H), 1.52 – 1.40 (m, 2H), 0.96 (t, *J* = 7.4 Hz, 3H).

^{13}C NMR ($CDCl_3$, 126 MHz): δ = 144.9, 144.1, 143.5, 140.4, 140.3, 135.9, 128.8, 128.6, 128.3, 128.3, 128.1, 127.7, 127.0, 126.8, 125.4, 123.6, 119.6, 65.9, 47.29, 31.29, 25.90, 23.08, 13.95.

HRMS (ESI) m/z: $[M + H]^+$ calculated for $C_{26}H_{28}N$ 354.2222, found 354.2216.

Rf (Hexane/Et_2O 4:1): 0.5

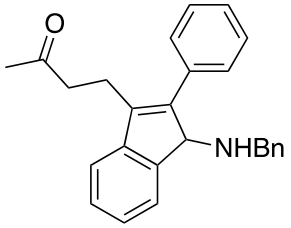

4-(1-(benzylamino)-2-phenyl-1*H*-inden-3-yl)butan-2-one, (**4o**)

Using the general procedure described above, compound (**4o**) was obtained from benzaldehyde (0.1 mmol, 11 μL), benzylamine (0.12 mmol, 13.1 μL) and 7-phenylhept-6-yn-3-one (0.12 mmol, 22.3 μL) as a light yellow solid (26.7 mg) in 70 % yield.

^{1}H NMR ($CDCl_3$, 500 MHz): δ = 7.74 – 7.69 (m, 1H), 7.52 – 7.44 (m, 2H), 7.43 – 7.36 (m, 4H), 7.37 – 7.33 (m, 1H), 7.34 – 7.30 (m, 1H), 7.26 – 7.14 (m, 3H), 7.08 – 7.02 (m, 2H), 4.98 (s, 1H), 3.37 (d, *J* = 12.7 Hz, 1H), 3.30 (d, *J* = 12.7 Hz, 1H), 3.11 – 2.93 (m, 2H), 2.81 – 2.70 (m, 2H), 2.44 (q, *J* = 7.3 Hz, 2H), 1.08 (t, *J* = 7.3 Hz, 3H).

^{13}C NMR ($CDCl_3$, 126 MHz): δ = 210.4, 144.5, 144.1, 143.9, 140.0, 138.6, 135.3, 128.8, 128.7, 128.3, 128.2, 127.9, 127.3, 126.9, 125.7, 123.8, 119.3, 66.0, 47.3, 41.1, 35.9, 20.1, 7.8.

HRMS (ESI) m/z: $[M + Na]^+$ calculated for $C_{27}H_{27}NONa$ 404.1985, found 404.2003.

Rf (Hexane/Et_2O 4:1): 0.3.

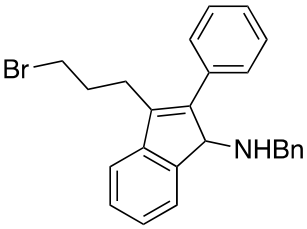

N-benzyl-3-(3-bromopropyl)-2-phenyl-1*H*-inden-1-amine1, (**4p**)

Using the general procedure described above, compound (**4p**) was obtained from benzaldehyde (0.1 mmol, 11 μL), benzylamine (0.12 mmol, 13.1 μL) and (5-bromopent-1-yn-1-yl)benzene (0.12 mmol, 20.4 μL) as a light white solid (25.1 mg) in 60 % yield.

^{1}H NMR ($CDCl_3$, 500 MHz): δ = 7.75 – 7.71 (m, 1H), 7.51 – 7.47 (m, 2H), 7.45 – 7.35 (m, 6H), 7.34 – 7.30 (m, 1H), 7.26 – 7.14 (m, 3H), 7.09 – 7.01 (m, 2H), 5.00 (s, 1H), 3.52 – 3.40

(m, 2H), 3.37 (d, *J* = 12.7 Hz, 1H), 3.31 (d, *J* = 12.7 Hz, 1H), 2.95 – 2.83 (m, 2H), 2.32 – 2.13 (m, 2H).

^{13}C NMR ($CDCl_3$, 126 MHz): δ = 144.6, 144.3, 143.7, 139.8, 138.5, 135.3, 128.82, 128.80, 128.3, 128.2, 128.0, 127.4, 126.9, 125.7, 123.8, 119.5, 65.9, 47.3, 33.5, 31.9, 24.7.

HRMS (ESI) m/z: $[M + H]^+$ calculated for $C_{25}H_{25}BrN$ 418.1165, found 418.1163.

Rf (Hexane/Et_2O 4:1): 0.3.

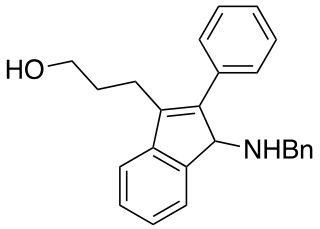

3-(1-(benzylamino)-2-phenyl-1*H*-inden-3-yl)propan-1-ol, (**4q**)

Using the general procedure described above, compound (**4q**) was obtained from benzaldehyde (0.1 mmol, 11 μL), benzylamine (0.12 mmol, 13.1 μL) and 5-phenylpent-4-yn-1-ol (0.12 mmol, 18.5 μL) as a light yellow solid (30.2 mg) in 85 % yield.

^{1}H NMR ($CDCl_3$, 500 MHz): δ = 7.74 – 7.69 (m, 1H), 7.51 – 7.46 (m, 2H), 7.46 – 7.40 (m, 3H), 7.40 – 7.35 (m, 2H), 7.32 – 7.29 (m, 1H), 7.24 – 7.15 (m, 3H), 7.08 – 7.02 (m, 2H), 4.99 (s, 1H), 3.75 – 3.63 (m, 2H), 3.37 (d, *J* = 12.7 Hz, 1H), 3.31 (d, *J* = 12.7 Hz, 1H), 2.90 – 2.73 (m, 2H), 1.99 – 1.88 (m, 2H).

^{13}C NMR ($CDCl_3$, 126 MHz): δ = 144.5, 144.1, 143.8, 140.0, 139.5, 135.6, 128.8, 128.7, 128.3, 128.2, 127.9, 127.3, 126.9, 125.6, 123.7, 119.6, 65.9, 62.4, 47.3, 31.7, 22.1.

HRMS (ESI) m/z: $[M + H]^+$ calculated for $C_{25}H_{26}NO$ 356.2009, found 356.2007.

Rf (Hexane/Et_2O 4:1): 0.1.

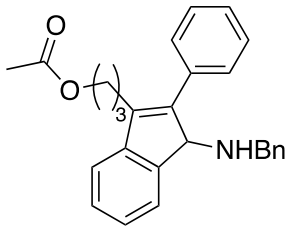

3-(1-(benzylamino)-2-phenyl-1*H*-inden-3-yl)propyl acetate, (**4r**)

Using the general procedure described above, compound (**4r**) was obtained from benzaldehyde (0.1 mmol, 11 μL), benzylamine (0.12 mmol, 13.1 μL) and 5-phenylpent-4-yn-1-yl acetate (0.12 mmol, 23.1 μL) as a light yellow solid (32.6 mg) in 82 % yield.

^{1}H NMR ($CDCl_3$, 500 MHz): δ = 7.73 – 7.69 (m, 1H), 7.53 – 7.47 (m, 2H), 7.46 – 7.37 (m, 6H), 7.35 – 7.32 (m, 1H), 7.25 – 7.17 (m, 3H), 7.10 – 7.05 (m, 2H), 5.00 (s, 1H), 4.17 – 4.05 (m, 2H), 3.39 (d, *J* = 12.6 Hz, 1H), 3.31 (d, *J* = 12.6 Hz, 1H), 2.93 – 2.77 (m, 2H), 2.13 – 2.01 (m, 2H), 2.00 (s, 3H).

^{13}C NMR ($CDCl_3$, 126 MHz): δ = 171.1, 144.9, 144.3, 144.2, 140.3, 138.6, 135.6, 128.8, 128.7, 128.29, 128.22, 127.8, 127.2, 126.8, 125.6, 123.7, 119.4, 66.1, 63.9, 47.4, 27.7, 22.3, 20.8.

HRMS (ESI) m/z: $[M + Na]^+$ calculated for $C_{27}H_{27}NO_2Na$ 420.1934, found 420.1942.

Rf (Hexane/Et_2O 4:1): 0.4.

3.7 References

[1] Davies, H. M.; Morton, D., *J. Org. Chem.,* **2016,** *81*, 343-50.
[2] Yamaguchi, J.; Yamaguchi, A. D.; Itami, K., *Angew. Chem. Int. Ed.,* **2012,** *51*, 8960-9009.
[3] McMurray, L.; O'Hara, F.; Gaunt, M. J., *Chem. Soc. Rev.,* **2011,** *40*, 1885-1898.
[4] Bruckl, T.; Baxter, R. D.; Ishihara, Y.; Baran, P. S., *Acc. Chem. Res.,* **2012,** *45*, 826-839.
[5] Zhu, R. Y.; Farmer, M. E.; Chen, Y. Q.; Yu, J. Q., *Angew. Chem. Int. Ed.,* **2016,** *55*, 10578-99.
[6] Sun, H.; Guimond, N.; Huang, Y., *Org. Biomol. Chem.,* **2016,** *14*, 8389-97.
[7] Mo, F.; Dong, G., *Science,* **2014,** *345*, 68-72.
[8] Rousseau, G.; Breit, B., *Angew. Chem. Int. Ed.,* **2011,** *50*, 2450.
[9] Yang, K.; Li, Q.; Liu, Y.; Li, G.; Ge, H., *J. Am. Chem. Soc.,* **2016,** *138*, 12775-12778.

[10] Liu, X. H.; Park, H.; Hu, J. H.; Hu, Y.; Zhang, Q. L.; Wang, B. L.; Sun, B.; Yeung, K. S.; Zhang, F. L.; Yu, J. Q., *J. Am. Chem. Soc.,* **2017,** *139*, 888-896.
[11] Franzén, R., *Can. J. Chem.,* **2000,** *78*, 957-962.
[12] Brahmachari, G., *Chem. Rec.,* **2016,** *16*, 98-123.
[13] Miyaura, N.; Suzuki, A., *Chem. Rev.,* **1995,** *95*, 2457-2483.
[14] Yin, L.; Liebscher, J., *Chem. Rev.,* **2007,** *107*, 133-73.
[15] Bhunia, A.; Yetra, S. R.; Biju, A. T., *Chem. Soc. Rev.,* **2012,** *41*, 3140-52.
[16] Barluenga, J.; Tomas-Gamasa, M.; Aznar, F.; Valdes, C., *Nat. Chem.,* **2009,** *1*, 494-499.
[17] Perez, M.; Fananas-Mastral, M.; Bos, P. H.; Rudolph, A.; Harutyunyan, S. R.; Feringa, B. L., *Nat. Chem.,* **2011,** *3*, 377-81.
[18] Muller, T. J., *Beilstein J. Org. Chem.,* **2011,** *7*, 960-1.
[19] Hulme, C., Applications of Multicomponent Reactions in Drug Discovery – Lead Generation to Process Development. In *Multicomponent Reactions*, Wiley-VCH Verlag GmbH & Co. KGaA: 2005; p 311.
[20] Ramon, D. J.; Yus, M., *Angew. Chem. Int. Ed.,* **2005,** *44*, 1602-34.
[21] Volla, C. M.; Atodiresei, I.; Rueping, M., *Chem. Rev.,* **2014,** *114*, 2390-431.
[22] Domling, A.; Wang, W.; Wang, K., *Chem. Rev.,* **2012,** *112*, 3083-135.
[23] Brauch, S.; van Berkel, S. S.; Westermann, B., *Chem. Soc. Rev.,* **2013,** *42*, 4948-62.
[24] Bienayme, H.; Hulme, C.; Oddon, G.; Schmitt, P., *Chemistry,* **2000,** *6*, 3321-9.
[25] Ruijter, E.; Scheffelaar, R.; Orru, R. V., *Angew. Chem. Int. Ed.,* **2011,** *50*, 6234-46.
[26] Huang, Y.; Yazbak, A.; Dömling, A., Multicomponent Reactions. In *Green Techniques for Organic Synthesis and Medicinal Chemistry*, John Wiley & Sons, Ltd: 2012; p 497.
[27] Estevez, V.; Villacampa, M.; Menendez, J. C., *Chem. Soc. Rev.,* **2010,** *39*, 4402-21.
[28] Cioc, R. C.; Ruijter, E.; Orru, R. V. A., *Green Chem.,* **2014,** *16*, 2958-2975.
[29] Toure, B. B.; Hall, D. G., *Chem. Rev.,* **2009,** *109*, 4439-86.
[30] Rajanarendar, E.; Venkateshwarlu, P.; Krishna, S. R.; Reddy, K. G.; Thirupathaiah, K., *Green and Sustainable Chemistry,* **2015,** *05*, 107-114.
[31] Anastas, P.; Eghbali, N., *Chem. Soc. Rev.,* **2010,** *39*, 301-312.
[32] Feng, M. H.; Jiang, X. F., *Synthesis,* **2017,** *49*, 4414-4433.
[33] Balme, G.; Bouyssi, D.; Monteiro, N., Metal-Catalyzed Multicomponent Reactions. In *Multicomponent Reactions*, Wiley-VCH Verlag GmbH & Co. KGaA: 2005; p 224.
[34] Wan, J. P.; Gan, L.; Liu, Y., *Org. Biomol. Chem.,* **2017,** *15*, 9031-9043.
[35] Jahier-Diallo, C.; Morin, M. S. T.; Queval, P.; Rouen, M.; Artur, I.; Querard, P.; Toupet, L.; Crévisy, C.; Baslé, O.; Mauduit, M., *Chem. Eur. J.,* **2015,** *21*, 993-997.
[36] Wang, D.-H.; Engle, K. M.; Shi, B.-F.; Yu, J.-Q., *Science,* **2010,** *327*, 315.
[37] Cai, G.; Fu, Y.; Li, Y.; Wan, X.; Shi, Z., *J. Am. Chem. Soc.,* **2007,** *129*, 7666-7673.
[38] Zhang, T.; Wu, L.; Li, X., *Org. Lett.,* **2013,** *15*, 6294-6297.
[39] Wang, C.; Chen, H.; Wang, Z.; Chen, J.; Huang, Y., *Angew. Chem. Int. Ed.,* **2012,** *51*, 7242-7245.
[40] Wang, N.-J.; Mei, S.-T.; Shuai, L.; Yuan, Y.; Wei, Y., *Org. Lett.,* **2014,** *16*, 3040-3043.
[41] Xu, W.; Yoshikai, N., *Angew. Chem. Int. Ed.,* **2016,** *55*, 12731-12735.
[42] Zhou, B.; Ma, P.; Chen, H.; Wang, C., *Chem. Commun.,* **2014,** *50*, 14558-14561.

[43] Jun, C.-H.; Hong, J.-B.; Kim, Y.-H.; Chung, K.-Y., *Angew. Chem. Int. Ed.,* **2000,** *39*, 3440-3442.
[44] Thalji, R. K.; Ahrendt, K. A.; Bergman, R. G.; Ellman, J. A., *J. Org. Chem.,* **2005,** *70*, 6775-6781.
[45] Liu, W.; Zell, D.; John, M.; Ackermann, L., *Angew. Chem. Int. Ed.,* **2015,** *54*, 4092-4096.
[46] Ding, S.; Shi, Z.; Jiao, N., *Org. Lett.,* **2010,** *12*, 1540-1543.
[47] Yamakawa, T.; Yoshikai, N., *Org. Lett.,* **2013,** *15*, 196-199.
[48] Fukutani, T.; Umeda, N.; Hirano, K.; Satoh, T.; Miura, M., *Chem. Commun.,* **2009**, 5141-5143.
[49] Sun, Z.-M.; Chen, S.-P.; Zhao, P., *Chem. Eur. J.,* **2010,** *16*, 2619-2627.
[50] He, R.; Huang, Z.-T.; Zheng, Q.-Y.; Wang, C., *Angew. Chem. Int. Ed.,* **2014,** *53*, 4950-4953.
[51] Zhang, J.; Ugrinov, A.; Zhao, P., *Angew. Chem. Int. Ed.,* **2013,** *52*, 6681-6684.
[52] Zhang, D.; Yum, E. K.; Liu, Z.; Larock, R. C., *Org. Lett.,* **2005,** *7*, 4963-6.
[53] Zhang, D.; Liu, Z.; Yum, E. K.; Larock, R. C., *J. Org. Chem.,* **2007,** *72*, 251-62.
[54] Jin, X. Q.; Yang, X. X.; Yang, Y. H.; Wang, C. Y., *Org. Chem. Front.,* **2016,** *3*, 268-272.
[55] Hung, C. H.; Gandeepan, P.; Cheng, C. H., *ChemCatChem,* **2014,** *6*, 2692-2697.
[56] Tran, D. N.; Cramer, N., *Angew. Chem. Int. Ed.,* **2011,** *50*, 11098-11102.
[57] Yamakawa, T.; Yoshikai, N., *Tetrahedron,* **2013,** *69*, 4459-4465.
[58] Zhou, B.; Chen, H.; Wang, C., *J. Am. Chem. Soc.,* **2013,** *135*, 1264-1267.
[59] Trost, B. M., *Acc. Chem. Res.,* **2002,** *35*, 695-705.
[60] Trost, B. M., *Angew. Chem. Int. Ed.,* **1995,** *34*, 259-281.
[61] Trost, B. M., *Science,* **1991,** *254*, 1471-1477.
[62] Wender, P. A.; Verma, V. A.; Paxton, T. J.; Pillow, T. H., *Acc. Chem. Res.,* **2008,** *41*, 40-9.
[63] Grondal, C.; Jeanty, M.; Enders, D., *Nat. Chem.,* **2010,** *2*, 167-78.
[64] Majetich, G.; Shimkus, J. M., *J. Nat. Prod.,* **2010,** *73*, 284-98.
[65] Lee, B. H.; Choi, Y. L.; Shin, S.; Heo, J. N., *J. Org. Chem.,* **2011,** *76*, 6611-8.
[66] Schneider, M. R.; Ball, H., *J. Med. Chem.,* **1986,** *29*, 75-9.
[67] Froimowitz, M.; Wu, K. M.; Moussa, A.; Haidar, R. M.; Jurayj, J.; George, C.; Gardner, E. L., *J. Med. Chem.,* **2000,** *43*, 4981-4992.
[68] Di Stefano, A.; Sozio, P.; Cacciatore, I.; Cocco, A.; Giorgioni, G.; Costa, B.; Montali, M.; Lucacchini, A.; Martini, C.; Spoto, G.; Di Pietrantonio, F.; Di Matteo, E.; Pinnen, F., *J. Med. Chem.,* **2005,** *48*, 2646-54.
[69] Liu, C. C.; Korivi, R. P.; Cheng, C. H., *Chemistry,* **2008,** *14*, 9503-6.
[70] Tsukamoto, H.; Ueno, T.; Kondo, Y., *Org. Lett.,* **2007,** *9*, 3033-6.
[71] Yu, X. F.; Lu, X. Y., *Adv. Synth. Catal.,* **2011,** *353*, 2805-2813.
[72] Li, C. J., *Acc. Chem. Res.,* **2010,** *43*, 581-90.
[73] Li, C.-J.; Wei, C.; Li, Z., *Synlett,* **2004,** *2004*, 1472-1483.
[74] Querard, P.; Girard, S. A.; Uhlig, N.; Li, C. J., *Chem. Sci.,* **2015,** *6*, 7332-7335.
[75] Li, L.; Brennessel, W. W.; Jones, W. D., *Organometallics,* **2009,** *28*, 3492-3500.
[76] Rayabarapu, D. K.; Cheng, C. H., *Chem. Commun.,* **2002,** *9*, 942-3.
[77] Chang, K. J.; Rayabarapu, D. K.; Cheng, C. H., *J. Org. Chem.,* **2004,** *69*, 4781-7.

[78] Liu, C. R.; Yang, F. L.; Jin, Y. Z.; Ma, X. T.; Cheng, D. J.; Li, N.; Tian, S. K., *Org. Lett.,* **2010,** *12*, 3832-5.
[79] Sun, Z. M.; Chen, S. P.; Zhao, P., *Chemistry,* **2010,** *16*, 2619-27.
[80] Patureau, F. W.; Besset, T.; Kuhl, N.; Glorius, F., *J. Am. Chem. Soc.,* **2011,** *133*, 2154-6.
[81] Zhang, J.; Ugrinov, A.; Zhao, P., *Angew. Chem. Int. Ed.,* **2013,** *52*, 6681-4.
[82] Manan, R. S.; Zhao, P., *Nat. Commun.,* **2016,** *7*, 11506.
[83] Hung, C.-H.; Gandeepan, P.; Cheng, C.-H., *ChemCatChem,* **2014,** *6*, 2692-2697.
[84] Ackermann, L., *Chem. Rev.,* **2011,** *111*, 1315-1345.
[85] Ackermann, L., *Acc. Chem. Res.,* **2014,** *47*, 281-295.
[86] Qi, X.; Li, Y.; Bai, R.; Lan, Y., *Acc. Chem. Res.,* **2017,** *50*, 2799-2808.
[87] Doxsee, K. M.; Juliette, J. J. J., *Polyhedron,* **2000,** *19*, 879-890.
[88] Li, Y.; Shan, C.; Yang, Y.-F.; Shi, F.; Qi, X.; Houk, K. N.; Lan, Y., *J. Phys. Chem. A,* **2017,** *121*, 4496-4504.
[89] Dateer, R. B.; Chang, S., *J. Am. Chem. Soc.,* **2015,** *137*, 4908-4911.
[90] Guimond, N.; Fagnou, K., *J. Am. Chem. Soc.,* **2009,** *131*, 12050-12051.
[91] Li, Y.; Osuna, S.; Garcia-Borràs, M.; Qi, X.; Liu, S.; Houk, K. N.; Lan, Y., *Chem. Eur. J.,* **2016,** *22*, 12819-12824.
[92] Huestis, M. P.; Chan, L.; Stuart, D. R.; Fagnou, K., *Angew. Chem. Int. Ed.,* **2011,** *50*, 1338-41.
[93] Tran, D. N.; Cramer, N., *Angew. Chem. Int. Ed.,* **2011,** *50*, 11098-102.

Chapter 4 – Copper–Catalyzed Asymmetric sp^3 C–H Arylation of Tetrahydroisoquinoline Mediated by Visible Light Photoredox Catalyst

4.1 Background

With the development of new C-H bond functionalization strategies, chemists intend to use these new tools to synthesize, modify and discover new useful compounds. To cite one example amongst others, the 1,2,3,4-tetrahydroisoquinoline framework (THIQ) is a commonplace and important structural element found in numerous natural products. Many of these natural products exhibit valuable biological properties and are used as antidepressants, antihypertensive agents, antidiuretics and other drugs.[1-2] The synthesis of THIQs and their corresponding modification and functionalization is of tremendous interest because of their flexible biological potential. A great number of chiral natural alkaloids owe their chirality to the presence of a chiral center at the C-1 carbon of the tetrahydroisoquinoline moiety (Scheme 88). Thus, there has been many synthetic attempts to access enantiomerically pure C-1 carbon center.

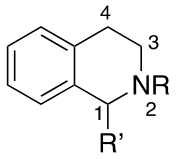

Scheme 88. 1,2,3,4-tetrahydroisoquinoline framework

For the past 30 years, the THIQ family has been studied for their biological activities. It started in 1974, Kluepfel and co-workers isolated naphthyridinomycin from a bacteria named Streptomyces lusitanus AYB-1026 as an unstable ruby red crystalline solid.[3] To date, around 55 natural products containing the THIQ moiety have been isolated. Among the traditional synthesis of isoquinolines derivatives, the asymmetric synthesis is based generally on two strategies: 1) modification of classical named reactions (the Bischer-

Napieralski reaction, the Pictet-Spengler reaction and the Pomeranz-Fritsch reaction)[4-5] and 2) the formation of new carbon-carbon bond at the C-1 position.

The Bischer-Napieralski reaction allows the access of 3,4-dihydroisoquinolines from the cyclization of β-ethylamines (Scheme 89).[6] During the 80's, Fodor and Nagubandi showed that the reaction of β-ethylamines with $POCl_3$ lead to the formation of the corresponding nitrilium salt, a key intermediate of the reaction.[7] Later, numerous asymmetric modifications of the BN reaction were investigated. In presence of a chiral catalyst, the reduction or hydrogenation of 3,4-dihydroisoquinoline was the major pathway to synthesize chiral isoquinoline alkaloids. For instance, Hajipour and Hantehzadeh developed a chiral reducing agent, generated from sodium borohydride and protected amino acids, to perform an asymmetric reduction of prochiral cyclic imines, such as isoquinolines.[8]

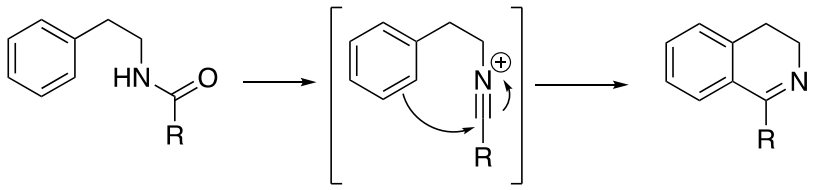

Scheme 89. The classical Bischer-Napieralski reaction

The well-known Pictet-Spengler reaction, discovered in 1911, is the condensation reaction of an aldehyde or ketone with an amine that undergoes ring closure ultimately (Scheme 90).[9] This named reaction is a particularly popular cyclization method and is still widely use in the total synthesis of alkaloids and biologically active analogs of tetrahydroisoquinoline and tetrahydro-β-carboline.[10] In the Pictet–Spengler asymmetric version, the chirality transfer occurs from the chiral auxiliary introduced to the amine or the aldehyde. As an example, Comins and co-workers investigated the influence of a chiral auxiliary appended to the amine nitrogen.[11]

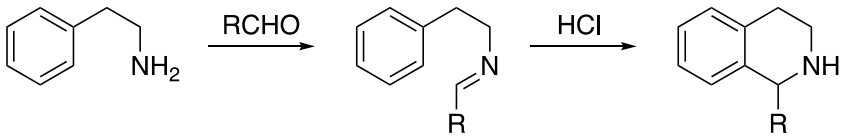

Scheme 90. The Pictet–Spengler tetrahydroisoquinoline synthesis

Historically, the last and well-known reaction developed to access isoquinoline ring is the so-called Pomeranz-Fritsch reaction. The original Pomeranz-Fritsch reaction involves an acid catalyzed cyclization of benzalamino acetals to yield a full aromatic isoquinoline compound (Scheme 91).[12-13] Kaufman developed an asymmetric modification of the Pomeranz-Fritsch reaction to synthesize (S)-(-)-salsolidine, from chiral benzyl alcohols.[14-15] Under acidic conditions followed by regioselective reduction, the synthesis of (S)-(-)-salsolidine was achieved in a satisfactory yield, with enantioselectivity up to 95%.

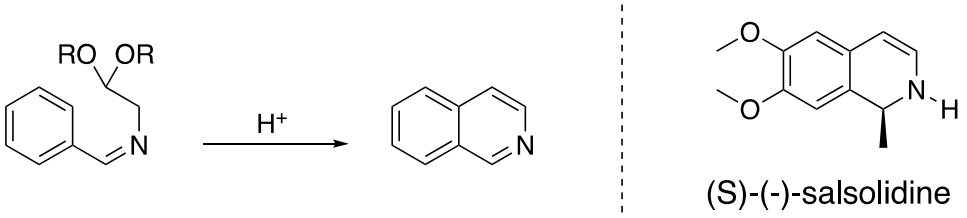

Scheme 91. The original Pomeranz-Fritsch isoquinoline synthesis / example of natural product

More recently, novel catalytic asymmetric strategies were discovered for the synthesis of C1-chiral 1,2,3,4-tetrahydroisoquinolines. First, the nucleophilic addition to isoquinoline via the formation of a C1-Cα connection represents a straightforward approach for the synthesis of C1-chiral THIQs. Jacobsen and co-workers reported in 2005 the intermolecular addition of preformed silyl ketene acetal to *in-situ* generated N-acylisoquinolines catalyzed by a chiral thiourea derivative (Scheme 92).[16] Inspired by the activation of iminium ions, numerous chiral nucleophilic additions were described for the synthesis of THIQs.[17]

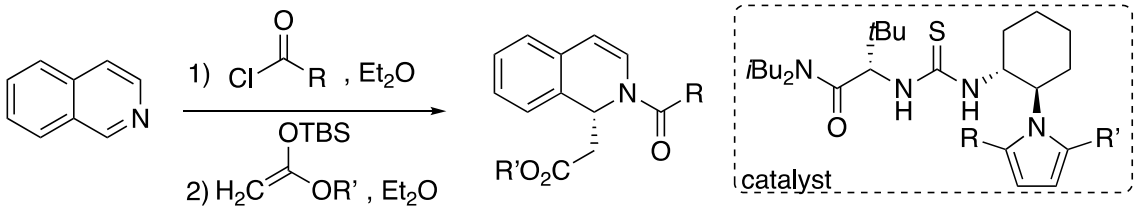

Scheme 92. Thiourea catalyzed asymmetric addition of silyl ketene acetal to isoquinoline

Second, the discovery of facile oxidation of N-aryl THIQ with various oxidants opened up new routes for the formation of C1-substituted THIQs. Discovered by Li in early 2000's, this oxidative asymmetric cross-dehydrogenative coupling (CDC) strategy is highly efficient.[29-31] As mentioned earlier, the functionalization of sp^3 C–H bonds is a unique and powerful transformation that converts C–H bonds into other functional groups and represents an area of invaluable and economical chemistry.[32-35] While more difficult to cleave than other types of C-H bonds, sp^3 C–H bonds are not completely inert. Towards a greener purpose without use of DGs, the direct oxidative sp^3 C-H functionalization methodology was developed, allowing the cross-coupling of large variety of substrates without DG (Scheme 93).[36]

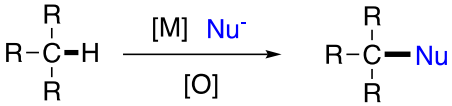

Scheme 93. Direct oxidative sp^3 C-H functionalization

This methodology was applied to the modification of THIQs, producing chiral and non-chiral C1-substituted isoquinolines. After the oxidation of N-aryl THIQs followed by enantioselective addition of an external nucleophile, a variety of C1-chiral THIQs can be synthesized with high efficiency. Li and co-workers discovered in 2004 that copper/pyridine bisoxazolidine complex appeared to be an excellent complex catalyst to successfully achieve chiral alkynylation of N-aryl THIQs, at C1-position. They observed that

aryl substituted alkynes delivered good to moderate ee, while heteroaromatic-, sylil- or alkyl-substituted products were obtained with moderate to low ee (Scheme 94).[37]

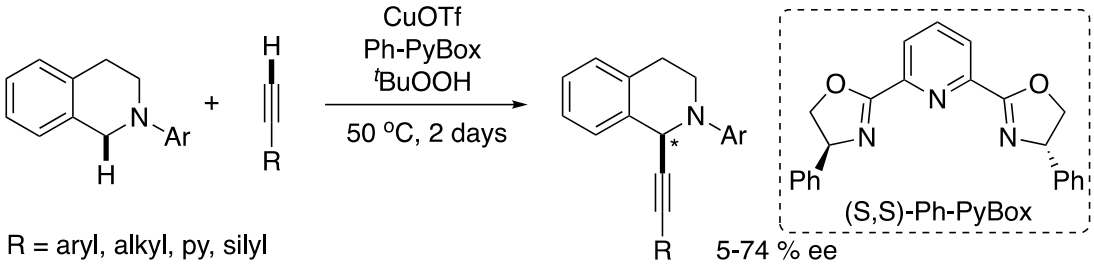

Scheme 94. Asymmetric copper catalyzed alkynylation of N-aryl THIQs.

Later on, Li's group found that CuOTf/QUINAP combination showed comparable selectivities regarding similar alkynylation reaction with TBHP as an oxidant.[38] In 2008, Li and co-workers developed a copper catalyzed arylation reaction of THIQs under oxidative conditions, using boronic acids derivatives. An asymmetric version of this reaction was preliminarily undertaken using Ph-PyBox chiral ligand and copper(I) triflate, affording the chiral arylated product in moderate enantiomeric excess (Scheme 95).[39]

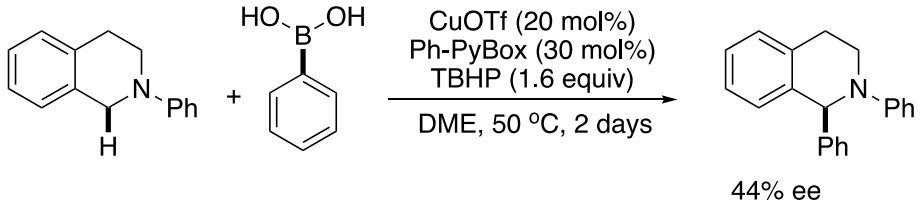

Scheme 95. Asymmetric copper catalyzed arylation of N-aryl THIQs

The requirement of 50 °C or higher temperature possibly impeded the development of a highly enantioselective process. Therefore, the development of a new process to functionalize sp^3 C–H bonds under mild conditions and lower temperature is of interest in order to achieve high ee efficiently.[40]

Regarding the aspect of building up molecular complexity, introduced earlier in Chapter 1, these methods disclose various advantages. Nevertheless, the overall molecular complexity built up after the named reaction is mediocre.

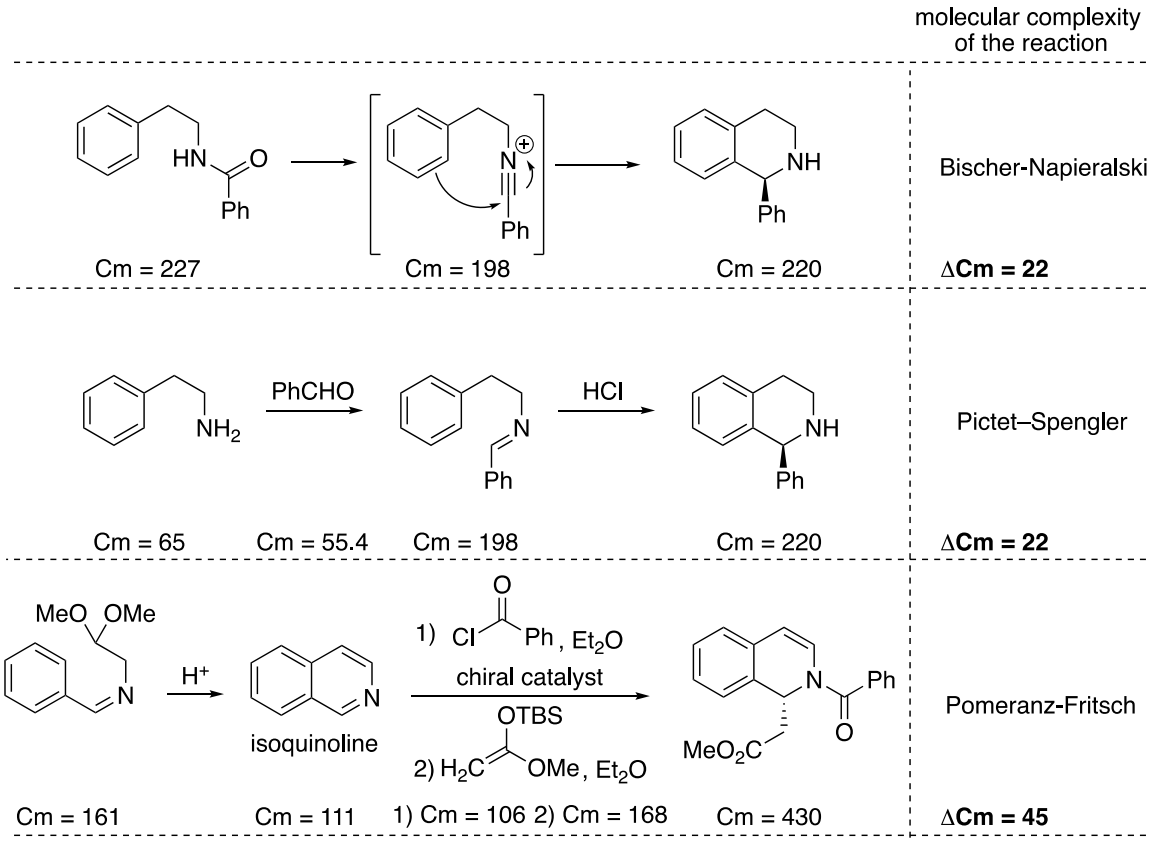

Scheme 96. Comparison of molecular complexity gain from classical THIQ asymmetric arylation/ alkylation reactions

The asymmetric Bischer-Napieralski reaction possesses a low ΔCm of 22 mainly because the starting N-phenethylbenzamide needs to be pre-synthesized and has a high molecular complexity Cm of 227. In Scheme 96, we reported the molecular complexity of each compounds necessitated for Bischer-Napieralski, Pictet-Spingler and Pomeranz-Fritsch reactions with the overall gain of complexity. Respectively, those three reactions have a mediocre gain of ΔCm of 22 , 22 and 45.

From these observations, the development of a new asymmetric arylation of THIQs with efficient gain of molecular complexity is of huge interest.

4.2 Research objectives & plan

During the last decade, numerous examples of sp^3 C–H bond arylation procedures have been developed.[41-49] As mentioned above, in 2008, our group developed the first direct sp^3 C–H arylation of THIQ with aryl boronic acids using a copper catalyst (Scheme 95).[39] Oxygen gas and *tert*-butyl hydroperoxide (TBHP) were used as external oxidants which gave moderate to good isolated yields (up to 75%). In addition, we demonstrated the enantioselective arylation of THIQ using phenylboronic acid with 44% enantiomeric excess, but very poor yield of the optically active products. Lowering the reaction temperature, in order to increase the corresponding ee, resulted in inhibition of the reaction.

The emerging and expanding field of visible-light-mediated photoredox catalysis presents unique opportunities for the conception of new synthetic routes.[50-58] Upon exposure to visible light, photoredox catalysts can function as both reductant and oxidant, thereby providing extremely important tools for potential transition metal-catalyzed enantioselective reactions of sp^3 C–H bonds, which could be carried out at low temperature and under mild reaction conditions.[59-60] We envisioned that combining photoredox catalysis with our developed oxidative cross–coupling method will allow us to design a visible light mediated photoredox asymmetric arylation of tetrahydroisoquinolines.

Recently, Li and co-workers have merged photoredox catalysis with the traditional copper catalytic system used in CDC reaction, achieving a highly enantioselective transformation. This alkynylation of N-aryl THIQs was achieved using copper catalyzed cross-dehydrogenative-coupling of C-H bonds with the assistance of an iridium photocatlyst and visible light at low temperature (Scheme 97).[59] The mechanism of this reaction was proposed as shown in Scheme 97, based on the well-established photocatalytic mechanism.[61-63]

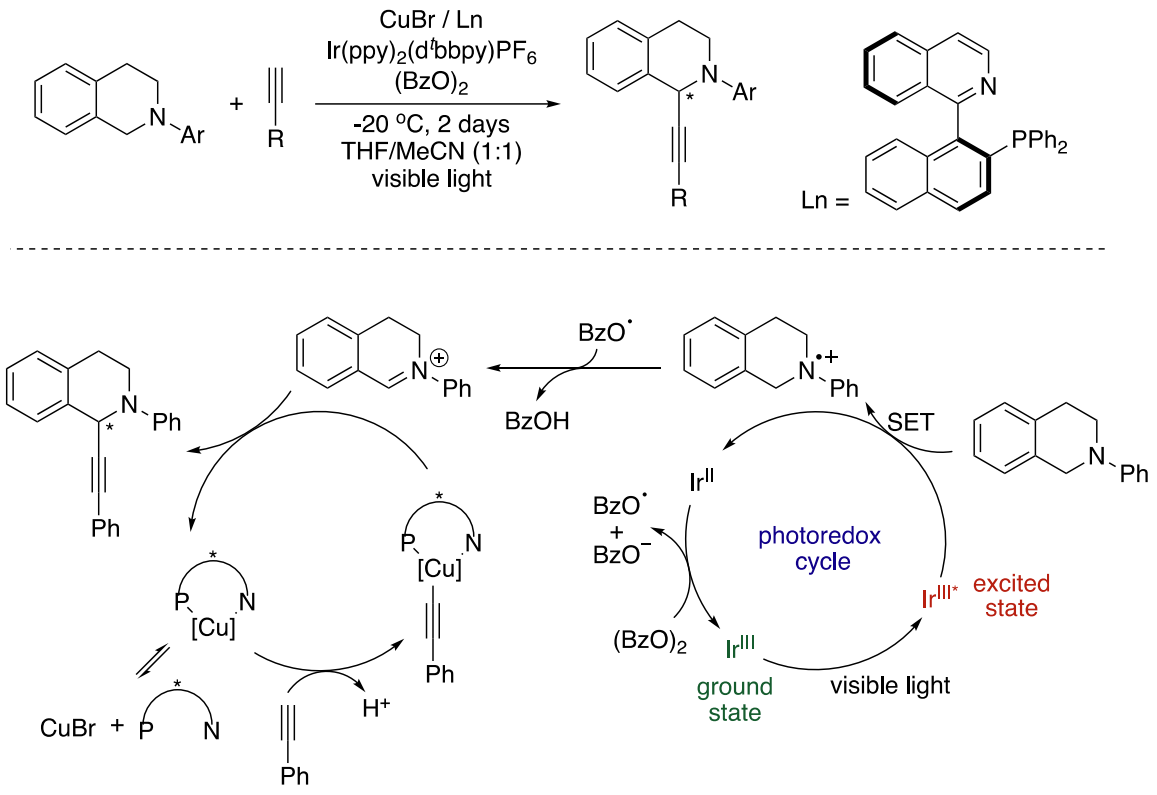

Scheme 97. Merging copper and photoredox catalysis for the asymmetric CDC alkynylation of N-aryl THIQs

It was proposed that under irradiation of visible light, the iridium photoredox complex is excited to its excited state Ir(III)*. In this state, the iridium complex possesses strong oxidation potential and oxidizes the nitrogen atom from N-aryl THIQ via a single electron process, yielding the reduced form of Ir(II) photoredox catalyst.[64] The oxidation of the nitrogen produces the corresponding nitrogen cationic radical that undergoes loss of H^+ and further oxidation to give the iminium intermediate. The copper acetylide chiral complex undergoes asymmetric nucleophilic addition to the iminium and produces the corresponding enantio-enriched alkynylated N-aryl THIQ.

More recently, Liu and co-workers have demonstrated the arylation of THIQs with arylboronic esters using an asymmetric organocatalysis methodology.[45, 48] Chiral tartaric acid derivatives, 2,3-dichloro-5,6-dicyano-1,4-benzoquinone (DDQ) and low temperature (-20 °C) were found to be the optimal conditions to obtain the desired arylated product

with acceptable yield and good enantioselectivity. However, this methodology has shown limitations in terms of substrate scope: only phenylboronic esters with electron-donating substituents yielded the corresponding products (Scheme 98).

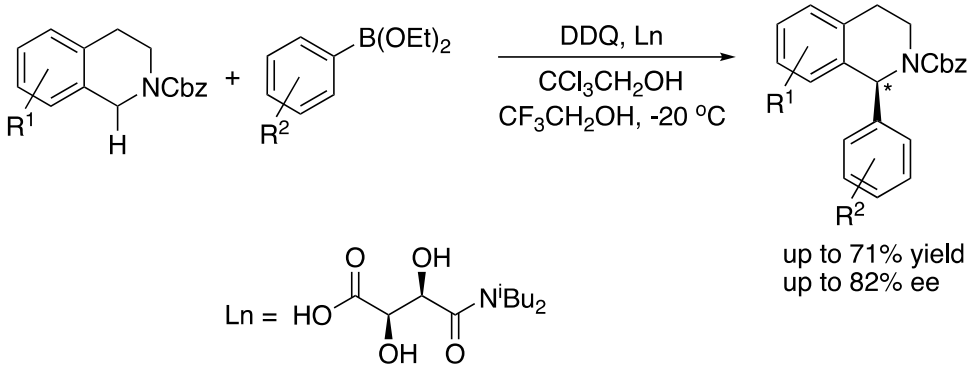

Scheme 98. Organocatalytic asymmetric C—H arylation of N-acyl THIQs

With the emerging field of photoredox catalysis and the developed catalytic tools on arylation of N-substituted THIQs, we envision that a cross–coupling arylation of aryl boronic acids and THIQs mediated by visible light is of huge interest. Moreover, the reported enantiomeric excess has shown limitations and thus, the asymmetric arylation transformation is attractive.

4.3 Results and discussion

We established that the oxidation of N-arylated THIQ with a photoredox catalyst would lead to an iminium intermediate, which would undergo asymmetric arylation catalyzed by a transition metal catalyst (Scheme 99).

Scheme 99. Conceptual reaction for the asymmetric arylation of N-arylated THIQs

However, the proposed reaction remains challenging since a very specific combination of transition metal catalyst with chiral ligand must be found to carry on the asymmetric arylation of THIQ. Also, as mentioned earlier, only mediocre enantiomeric excess were reported for similar arylation reaction.[45, 59, 65]

4.3.1 Development of reaction conditions

During the optimization of our previous oxidative arylation of N-arylated THIQs, we discovered that the choice of oxidants was crucial for the reaction to occur. At first, we reasoned that this reaction could occur under our previous and similar reaction conditions: use copper as a catalyst, a photoredox catalyst with a light transparent solvent and an external oxidant. To achieve our goal in performing an enantioselective arylation of THIQ, we reasoned that we could use our previous similar system at low temperature with the help of a light-mediated photoredox catalyst.

To begin our study, we evaluated the reaction of N-phenyl THIQ (**1**) and phenyl boronic acid (**2**) catalyzed by copper by screening different oxidants such as TBHP in water or in nonane. We were pleased to discover that the corresponding product (**3**) was obtained in 14% and 19% yield, respectively (Table 10, entries 1 & 2). The relatively small difference in yield might be due to the presence of water, inhibiting the catalytic activity of copper. Other oxidants, such as TBP, $(BzO)_2$, DDQ, dicumyl peroxide and *ter*-butyl peracetate were evaluated under this reaction conditions producing no desired product or only trace amount (entries 3-7). In entry 8, the amount of TBHP was increased from 1.6 equivalents to 2 equivalents, resulting in a slight increase of yield. However, higher loading of TBHP decreased the yield from 29% to 21% (entry 9). We found that compound (**1**) was oxidized to 2-phenyl-3,4-dihydroisoquinolin-1(2H)-one extremely quickly with higher amount of TBHP to impede the reaction. Different copper salts were evaluated, showing that copper(I) bromide CuBr was less active (entry 10) than copper(II) bromide, which provided the highest yield for the arylation of THIQ (entry 8). Other copper salts such as $Cu(OTf)_2$ and $Cu(OAc)_2$ showed a decrease in the effectiveness of the reaction (entries 12 and 13). A significant increase of yield was observed when the stoichiometry of the system was changed to a slight excess of phenyl boronic acid (**2**). When more than

1.6 equivalents of (**2a**) were involved in the reaction, a drastic acceleration of the reaction was observed, leading up to 85% yield (entries 14 and 15). Polar solvents such as DCE gave the best yield, compared to fewer polar solvents such as toluene and THF (entries 18 & 19). On the other hand, running the reaction with highly polar solvents such as MeCN and MeOH, was not beneficial for the formation of the desired product (**3**) (entries 16 & 17). To better understand the mechanism of the reaction, a few control experiments were conducted. In the absence of photoredox catalyst and/or transition metal copper(II) salt (entries 20 & 21), very poor yields were observed. Moreover, in the absence of TBHP, no yield was obtained (entries 22 & 23), showing that the oxidation via TBHP is crucial for the reaction to occur. Different iridium and ruthenium photoredox catalysts were evaluated and $Ir[(ppy)_2(dtbbpy)]PF_6$ ($E_{1/2\ Ox}$ = 1.21 V) was found to be the most efficient. The photoredox catalyst with higher oxidation potential such as $Ir(dF(CF_3)ppy)_2(dtbbpy)PF_6$ or $Ru(bpy)_3(PF_6)_2$ (respectively $E_{1/2\ Ox}$ = 1.51 V and $E_{1/2\ Ox}$ = 1.29 V) have resulted in a lower conversion to the corresponding product (**3**).

Table 10. Optimization of reaction conditions

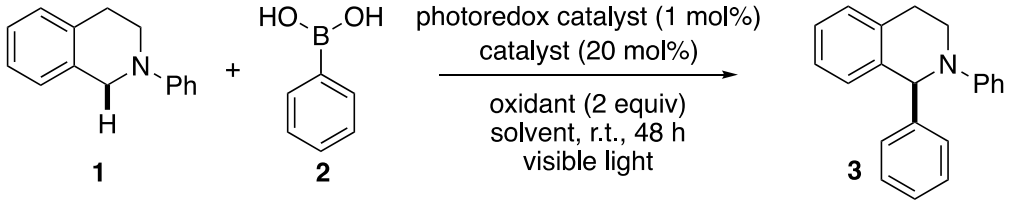

Entry	Catalyst	Photoredox catalyst	Solvent	Oxidant	2 (equiv)	3 (%)[b]
1 [a]	$CuBr_2$	$Ir(ppy)_2(dtbbpy)PF_6$	DCE	T-Hydro	1.6	14
2 [a]	$CuBr_2$	$Ir(ppy)_2(dtbbpy)PF_6$	DCE	TBHP	1.6	19
3 [a]	$CuBr_2$	$Ir(ppy)_2(dtbbpy)PF_6$	DCE	TBP	1.6	0
4 [a]	$CuBr_2$	$Ir(ppy)_2(dtbbpy)PF_6$	DCE	$(BzO)_2$	1.6	0
5 [a]	$CuBr_2$	$Ir(ppy)_2(dtbbpy)PF_6$	DCE	DDQ	1.6	0
6 [a]	$CuBr_2$	$Ir(ppy)_2(dtbbpy)PF_6$	DCE	Dicumyl peroxide	1.6	0
7 [a]	$CuBr_2$	$Ir(ppy)_2(dtbbpy)PF_6$	DCE	^{t}Bu-peracetate	1.6	trace
8	$CuBr_2$	$Ir(ppy)_2(dtbbpy)PF_6$	DCE	TBHP	1.6	29
9[b]	$CuBr_2$	$Ir(ppy)_2(dtbbpy)PF_6$	DCE	TBHP	1.6	21

10	CuBr	$Ir(ppy)_2(dtbbpy)PF_6$	DCE	TBHP	1.6	19
11	CuBr	$Ir(ppy)_2(dtbbpy)PF_6$	DCE	TBHP	1.6	19
12	$Cu(OTf)_2$	$Ir(ppy)_2(dtbbpy)PF_6$	DCE	TBHP	1.6	2
13	$Cu(OAc)_2$	$Ir(ppy)_2(dtbbpy)PF_6$	DCE	TBHP	1.6	14
14	$CuBr_2$	$Ir(ppy)_2(dtbbpy)PF_6$	DCE	TBHP	2	72
15	$CuBr_2$	$Ir(ppy)_2(dtbbpy)PF_6$	DCE	TBHP	3	**85**
16	$CuBr_2$	$Ir(ppy)_2(dtbbpy)PF_6$	MeOH	TBHP	3	13
17	$CuBr_2$	$Ir(ppy)_2(dtbbpy)PF_6$	MeCN	TBHP	3	11
18	$CuBr_2$	$Ir(ppy)_2(dtbbpy)PF_6$	THF	TBHP	3	15
19	$CuBr_2$	$Ir(ppy)_2(dtbbpy)PF_6$	toluene	TBHP	3	23
20	$CuBr_2$	-	DCE	TBHP	3	12
21	-	$Ir(ppy)_2(dtbbpy)PF_6$	DCE	TBHP	3	0
22	$CuBr_2$	-	DCE	-	3	0
23	$CuBr_2$	$Ir(ppy)_2(dtbbpy)PF_6$	DCE	-	3	0
24	$CuBr_2$	$Ir(dF(CF_3)ppy)_2(dtbbpy)PF_6$	DCE	TBHP	3	29
25	$CuBr_2$	$Ru(bpy)_3(PF_6)_2$	DCE	TBHP	3	72

Reaction conditions: [a] oxidant (0.16 mmol). [b] oxidant (0.20 mmol). All reported yields were determined by ^{1}H NMR spectroscopy using dibromomethane as an internal standard.

4.3.2 Substrate scope

With the optimised reaction conditions in hand, the scope of the reaction was investigated (Scheme 100). As mentioned above, the reaction of N–phenyl–tetrahydroisoquinoline (**1**) combined with phenylboronic acid (**2**) produced the corresponding arylated product (**3a**), in 85% yield. N–phenyl substituted THIQs bearing electron-donating groups (EDG), such a –OMe and –Me, were tolerated in our reaction system. We surprisingly observed that strong electron-donating substituents such as –OMe gave lower yields (**3b**, **3c** and **3d**). We attributed this effect to the lower oxidation potentials of the tertiary amine, favouring side reactions such as the formation of 2-phenyl-3,4-dihydroisoquinolin-1(2H)-one. It was notable that weaker EDG substituents on the aryl moiety (–Me) produced the corresponding product (**3e**) in higher yields (78%). Electron-withdrawing groups (EWG) such as –Br were tolerated and yielded the desired product in 80% yield (**3f**). Aromatic boronic acids bearing both electron-

withdrawing and electron-donating substituents were evaluated under our reaction conditions and all resulted in good yields. While aromatic boronic acids substituted with EWG (–acyl, –F or $–CF_3$) produced compounds (**3g**), (**3h**), (**3i**) and (**3j**) in mediocre yield, aromatic boronic acids substituted with EDG resulted in the formation of the corresponding arylated products with higher yields (**3k**, **3l**, **3m**, **3n**). It is noteworthy that an example of a sp^3 C–H alkylation using non–aromatic cyclohexylboronic acid also afforded the alkylated product (**3o**), albeit in 35% yield.

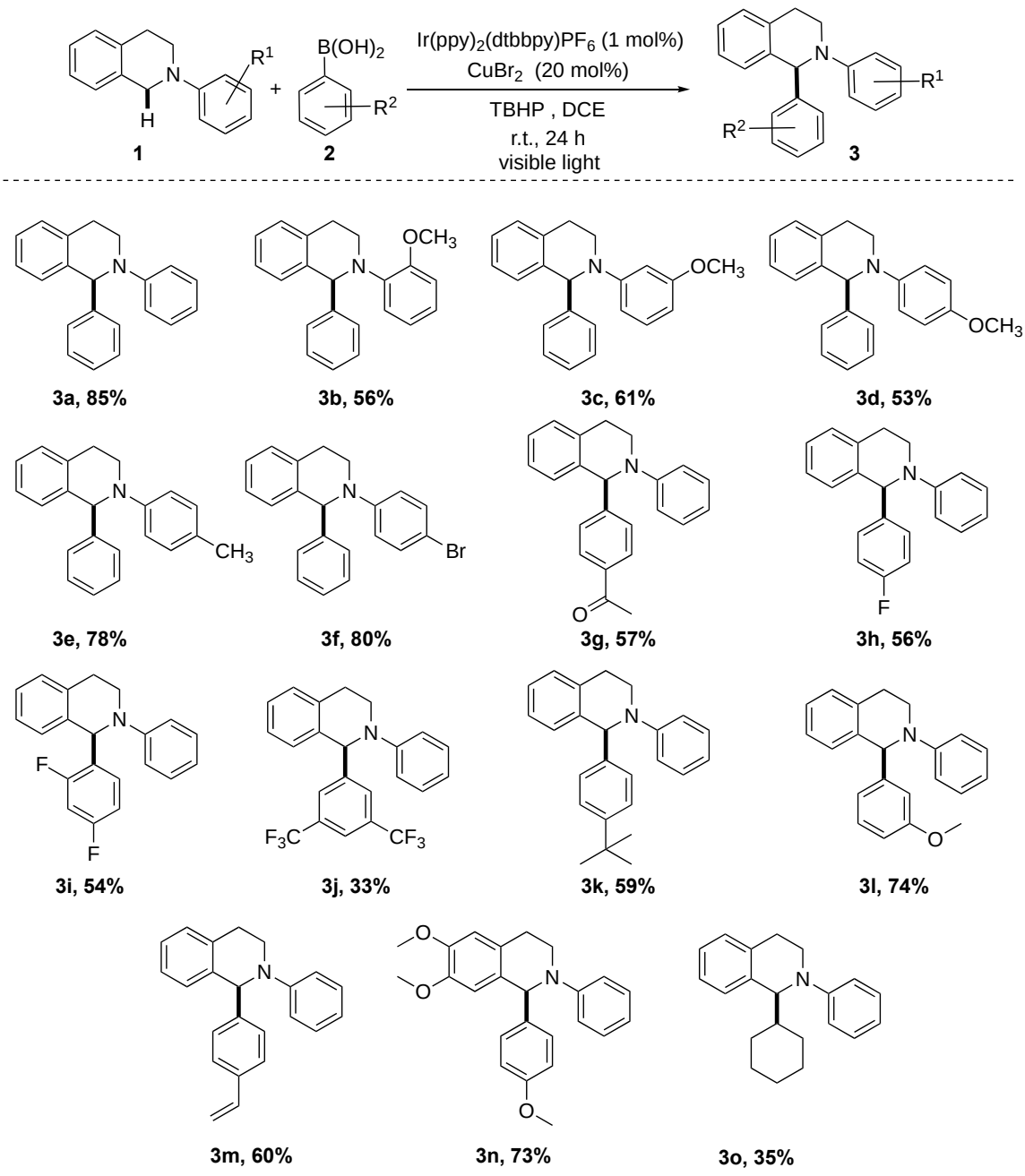

Reaction conditions: N-aryl THIQs (0.10 mmol), arylboronic acid (0.30 mmol), TBHP (0.2 mmol), $Ir(ppy)_2(dtbbpy)PF_6$ (0.001 mmol), $CuBr_2$ (0.02 mmol), DCE (0.5 mL), under argon atmosphere.

Scheme 100. Substrate scope

4.3.3 Enantioselective arylation reaction

In our continuing effort to achieve our goal, asymmetric arylation reaction, we explored the ability of various chiral ligands. Our primary study, based on our previous work on the asymmetric alkynylation of N-aryl THIQs, was to observe the potential influence of chiral phosphine-based ligand. Li's asymmetric alkynylation was performed in presence of copper(I) bromide catalyst with QUINAP ligand (Scheme 94). Preceding our investigation of chiral ligands, we found that lowering the temperature of the reaction from room temperature to 4°C was beneficial to the enantiomeric excess. It is important to note that the enantiomeric ratios observed in all following experiments were higher when copper(I) bromide was used as a catalyst, compared to copper(II) bromide. Differences of Lewis acid properties and differences of solubility between Cu(I) and Cu(II), are possible reasons why lower enantiomeric ratios were obtained. Thus, we optimized the reaction conditions to the use of copper(I) bromide in 10 mol% associated with a chiral ligand (12 mol%). However, the yield of the desired optically active product (**3a**) dropped by about half (43% yield), when 10 mol% of CuBr was used.

Investigating the activity of QUINAP ligand (Scheme 101, **L'1**) under our reaction conditions, we observed a racemic mixture of enantiomers via LCMS. Modifying the ligand from a P-N based to a P-P based chiral ligand was generally not beneficial for the reaction to occur enantioselectively. However, a few P-P based ligands shown in Scheme 101 yielded the corresponding arylated product with a range of enantiomeric ratios between 60:40 for **L'6**, **L'10** and 68:32 for **L'9**. Despite our attempt to solve the enantioselectivity issue unsuccessfully using P-P based ligands, we also evaluated a chiral N-heterocyclic carbene (NHC) ligand **L'7**. However, under our reaction conditions the complex Cu-**L'7** catalyzed the reaction towards a racemic mixture of both enantiomers.

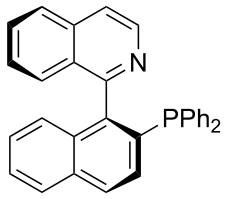

L'1 *rac*

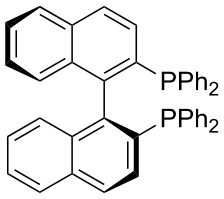

L'2 *rac*

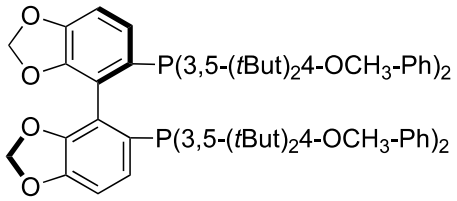

L'3 *rac*

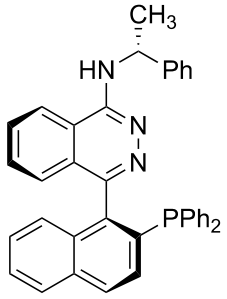

L'4 *rac*

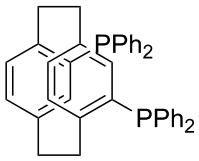

L'5 *rac*

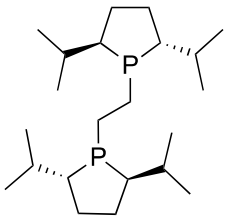

L'6 *er 60:40*

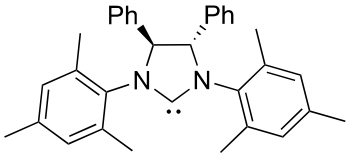

L'7 *rac*

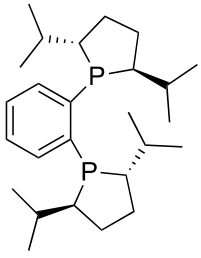

L'8 *rac*

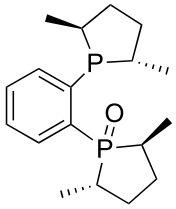

L'9 *er 68:32*

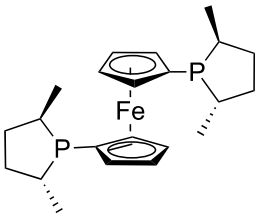

L'10 *er 60:40*

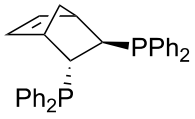

L'11 *rac*

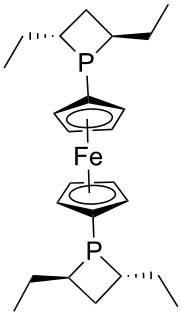

L'12 *rac*

The enantiomeric ratios were determined using a Chiralcel OD-H column and 96:4 hexane/isopropanol as an eluent.

Scheme 101. Screening of carbon- and phosphine-based ligand

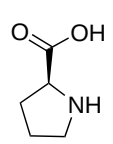

L1
rac

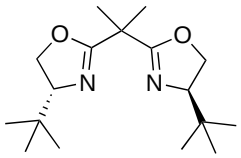

L2
rac

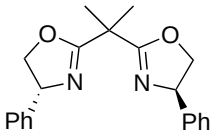

L3
er 54:46

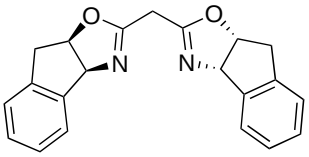

L4
er 56:44

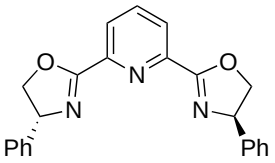

L5
er 82:18

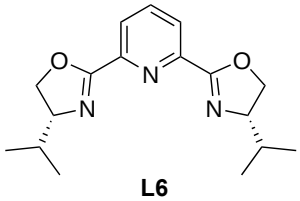

L6
er 53:47

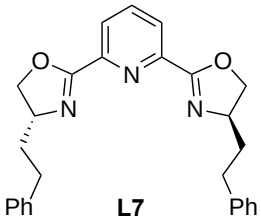

L7
er 54:46

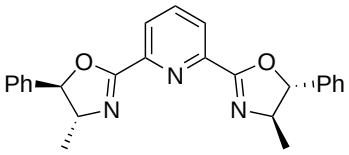

L8
er 58:42

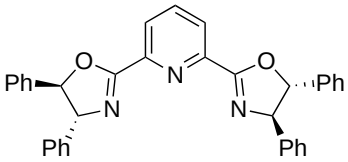

L9
er 69:31

The enantiomeric ratios were determined using a Chiralcel OD-H column and 96:4 hexane/isopropanol as an eluent.

Scheme 102. Screening of nitrogen-based ligand

Based on previously reported literature, the asymmetric arylation of THIQs was performed using O- and N-based chiral ligands (Scheme 95 & Scheme 98). In order to enhance our results regarding enantiomeric ratios, we investigated the influence of O- and N-based ligands (Scheme 102). Ligands possessing N and O linkages, such as (L)-proline **L1,** resulted in the formation of the arylated compound in a racemic mixture. Box-type ligands have demonstrated a good performance in this reaction,[39] affording mediocre enantioselectivities. In presence of Box type ligands, we observed the formation of a major enantiomer for ligands **L3** and **L4**. Unfortunately, the enantiomeric ratios of 54:46 and 56:44 for **L3** and **L4,** respectively, were not satisfying. Moreover, the use of Box ligand **L2** resulted in a racemic mixture. From these results, we observed that the phenyl group adjacent to the nitrogen atom, absent in **L2** and present in **L3** and **L4**, was extremely

important to induce enantioselectivity. We also modified the bridge linking both oxazoline moieties to evaluate its influence. Enlarging the angle between the two nitrogen atoms by removing the methyl groups (**L4**) present on the carbon bridge in **L3**, did not affect the selectivity. However, by increasing the bridge between oxazolines by adding a pyridine coordinating group (**L5**) drastically increased the enantiomeric ratio from 56:44 to 82:18. It is remarkable that the adjacent phenyl group is extremely important since its removal in ligand **L6** or its distancing by two carbon atoms in **L7**, drastically decreased the enantiomeric ratio. Modifying the position of this very important phenyl group and replacing it with a methyl group in **L8** did not result in higher enantiomeric ratio. Adding phenyl groups adjacent to phenyl groups present in **L5**, decreased the er obtained (**L9**).

Continuing our effort to develop a general method for the asymmetric arylation of N-aryl THIQs, we evaluated the effectiveness of ligand **L5** regarding different functional group. We were pleased to see that our model reaction yielded compound (**3a**) with good enantiomeric ratio (Table 11, entry 1). In presence of **L5**'s, opposite enantiomer (*S*,*S*)-PhPyBox, the reaction afforded good er when 2–methoxy-N–phenyl tetrahydroisoquinoline was used. The corresponding enantiomer was obtained with similar enantioselectivity (84:16, entry 2). The arylation of N–aryl substituted THIQs was obtained with high er when EDG such as -OMe was present (entries 2–5). Substituted by EWG such as –Br, a good enantiomeric ratio of 19:81 was observed (entry 6). Good to moderate enantiomeric ratios were obtained respectively, when fluoro–substituted aryl boronic acids and vinyl–substituted aryl boronic acids were subjected to the reaction system (entries 7 and 8).

Table 11. Enantioselective arylation of substituted N-aryl THIQs

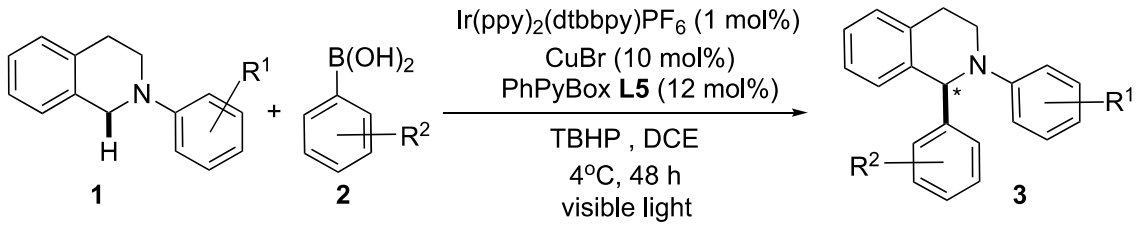

entry	product	R^1	R^2	Yield (%)	**er** (%)[b]
1	**3a**	H	H	43	19:81
2[b]	**3b**	2-OMe	H	35	84:16
3	**3c**	3-OMe	H	39	10:90
4	**3d**	4-OMe	H	34	15:85
5	**3e**	4-Me	H	42	24:76
6	**3f**	4-Br	H	43	19:81
7	**3i**	H	4-vinyl	27	37:63
8	**3m**	H	2,4-difluoro	31	19:81

Reaction conditions: [a] THIQs (0.10 mmol), arylboronic acid (0.30 mmol), TBHP (0.2 mmol), $Ir(ppy)_2(dtbbpy)PF_6$ (0.001 mmol), CuBr (0.01 mmol), (*R*,*R*)-2,6-bis(4-phenyl-2-oxazolinyl)pyridine (0.012 mmol), DCE (0.5 mL), under argon atmosphere. [b] (*S*,*S*)-2,6-bis(4-phenyl-2-oxazolinyl)pyridine was used instead All reported yields are isolated. All reported enantiomeric ratios were determined using a Chiralcel OD–H column and 96:4 hexane/isopropanol as an eluent.

4.3.4 Mechanistic considerations

A tentative reaction mechanism has been proposed in Scheme 103 to rationalize this arylation reaction. Upon visible light irradiation, $[Ir(ppy)_2(dtbbpy)]PF_6$ **I** converts to its excited state **II**, Ir(III)*.[63, 66-69] In the presence of the N-phenyl THIQ **IV**, Ir(III)* undergoes a single electron transfer (SET) and oxidizes the nitrogen atom in compound **IV**, to give a radical cation **V** which rearranges to the iminium salt form **VI**. Under these oxidative reaction conditions, CuBr is oxidized to a Cu(II) species and form a chiral Cu–PhPyBox complex.[70] Then, this complex coordinates to the iminium cation **VI,** followed by a nucleophilic addition of the aryl boronic acid to produce the desired enantioenriched

arylated product **VII**. To close the catalytic cycle, Ir(III)* is reduced to Ir(II) **III** via a SET step and regenerates to Ir(III) by oxidation with TBHP.

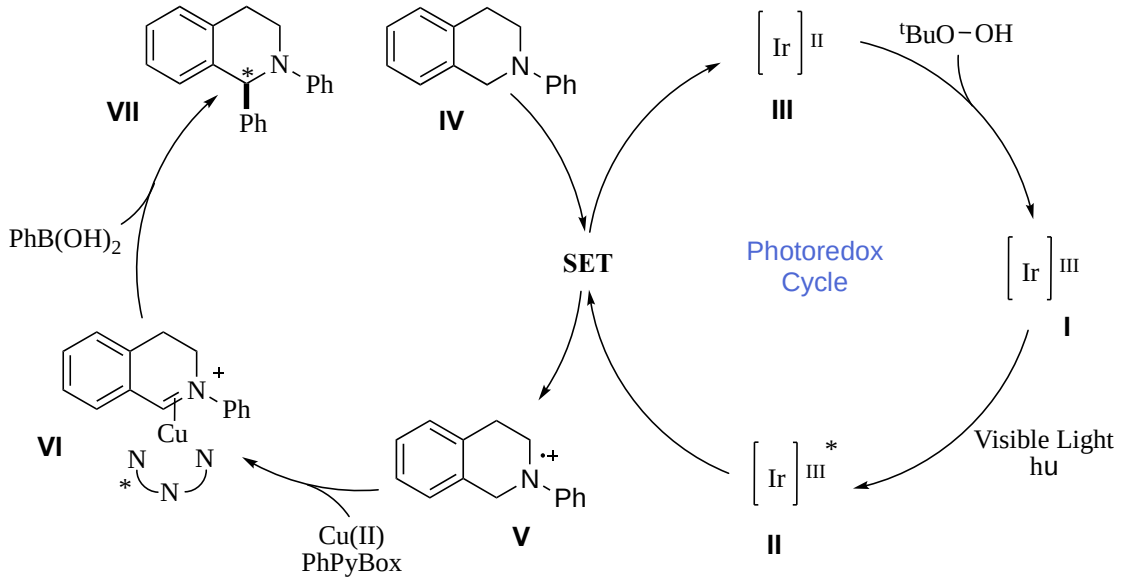

Scheme 103. Proposed mechanism

4.4 Conclusion and outlook

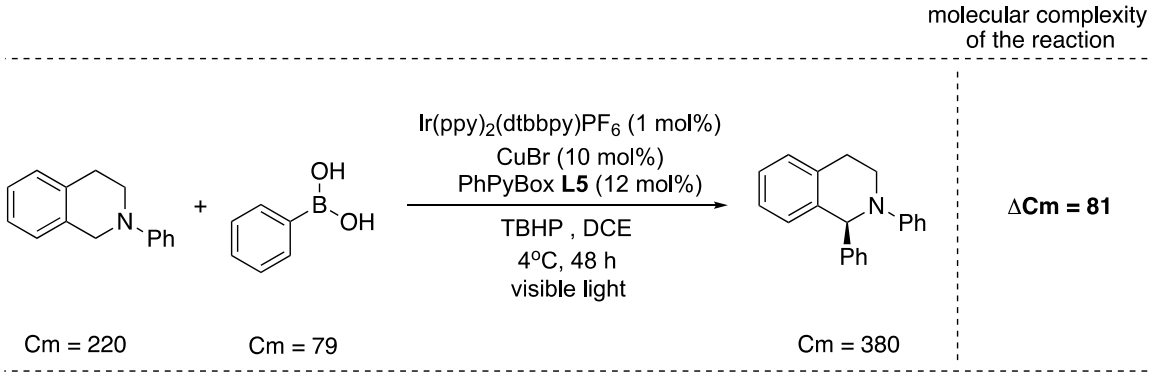

Scheme 104. Calculated molecular complexity for our model reaction

In conclusion, we successfully developed a highly efficient light-mediated coupling method for the direct asymmetric arylation of N-arylated tetrahydroisoquinolines with arylboronic acids. The use of Ir(ppy)$_2$(d*t*bbpy)PF$_6$ as photoredox catalyst provided a novel

and facile approach to build important arylated compounds in very high yields under very mild conditions. The combination of copper salts and PhPyBox as chiral ligand have demonstrated its efficiency producing good enantioselectivity and tolerated a fairly diverse substrate scope. Moreover, this method shows a very satisfying gain of molecular complexity with a value of ΔC_m= 81, with the simplest substrates (Scheme 104).

We envisioned that this visible light-mediated asymmetric arylation reaction could be extended to other sp^3 C–H bonds. The development of new pyBox ligand for the exclusive selectivity is, as well, a very important aspect of the future of this project.

4.5 Contribution

The reaction and conditions for the arylation of N-aryl THIQs were developed by me (Pierre Querard) and Dr. Inna Perepichka, with supervision by Prof. Dr. Chao-Jun Li. All reactions, isolations, and characterizations (with the exception of high-resolution mass spectrometry) were performed by us. High-resolution mass spectrometry was performed by Dr. Nadim Saadeh at the McGill University Department of Chemistry Mass Spectrometry Laboratory. The manuscript upon which this chapter is based was prepared by me and Dr. Inna Perepichka, with revision by Prof. Dr. Chao-Jun Li.

4.6 Experimental section

4.6.1 General information

Reaction setup: All reactions were carried out in flamed-dried V-shaped microwave reaction vials, covered by aluminum seals with PTFE-faced silicone septa, under an atmosphere of argon. The reaction vials were placed at 10 cm of distance from the compact fluorescent lamp (CFL) HELICAL 26W, 120VAC, 60Hz, 5000K, 1610 lumens.

Purifications: All work-up and purification procedures were carried out with reagent-grade solvents. Analytical thin-layer chromatography (TLC) was performed using E. Merck silica gel 60 F254 pre-coated plates (0.25 mm). Flash column chromatography was performed with E. Merck silica gel P60 (40–63 μm particle size, 230–400 mesh) (SiO2). Visualization was accomplished with UV light and/or iodine (I_2) or potassium permanganate (KMnO4) solution. Retention factor (Rf) values reported were measured

using a 6 × 2 cm TLC plate in a developing chamber containing the solvent system (10 mL) described. Automated flash column chromatography was performed on Biotage Isolera™ Spektra Systems with ACI™.

Solvents: Tetrahydrofuran (THF), methanol and toluene were taken directly from the Pure Solvent MD-7 purification system (Innovative Technology). Solvents for reaction, filtration, transfers, chromatography, and recrystallization were dichloromethane (CH_2Cl_2) (ACS grade, amylene stabilized), ether (Et_2O) (Fisher, BHT stabilized ACS grade), dichloroethane (ACS grade), acetonitrile (ACS grade), acetone (ACS grade), ethyl acetate (EtOAc) (Fisher, ACS grade).

NMR spectroscopy: Nuclear magnetic resonance (^1H, ^{13}C $\{^1H\}$ and ^{31}P $\{^1H\}$ NMR) spectra were recorded on a Bruker AV500 equipped with a 60-position SampleXpress sample changer (^1H, 500 MHz; ^{13}C, 125 MHz; ^{31}P, 202 MHz), a Varian MERCURY plus-500 spectrometer (^1H, 500 MHz; ^{13}C, 125 MHz) or Bruker AV400 spectrometer (^1H, 400 MHz; ^{13}C, 100 MHz). Chemical shifts for both ^1H NMR and ^{13}C NMR spectra were expressed in parts per million (ppm) units downfield from TMS, with the solvent residue peak as the chemical shift standard ($CDCl_3$: δ 7.28 ppm in ^1H NMR; δ 77.0 ppm in ^{13}C NMR; DMSO-d6: δ 2.50 ppm in ^1H NMR; δ 39.5 ppm in ^{13}C NMR). Data were reported as following: chemical shift, multiplicity (s = singlet, d = doublet, dd = doublet of doublets, t = triplet, td = triplet of doublets, q = quartet, quin = quintet, sep = septet, m = multiplet, br = broad singlet), coupling constants J (Hz), and integration.

Mass spectrometry: Mass spectrometry (MS) was performed by the McGill Chemistry Department Mass Spectrometry Facility. High Resolution Mass spectra were recorded using electrospray ionization (ESI+) and/or atmospheric pressure chemical ionization APCI (+/-), performed either on "Exactive Plus Orbitrap" a ThermoScientific high resolution accurate mass (HR/AM) FT mass spectrometer, or a Bruker Daltonics Maxis Impact quadrupole-time of flight (QTOF) mass spectrometer.

4.6.2 General procedure

2-Phenyl tetrahydroisoquinolines (**1**)[71-75] and $[Ir(ppy)_2(dtbbpy)]PF_6$ photoredox catalyst[76-77] were synthesized according to the published procedures and spectroscopic data were consistent with those previously reported for these compounds.

4.6.2.1 General procedure for the synthesis of 2-phenyl tetrahydroisoquinoline

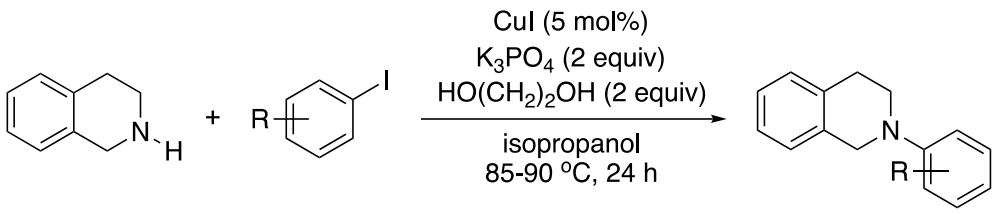

Scheme 105. Synthesis of 2-phenyl tetrahydroisoquinoline

Copper(I) iodide (200 mg, 1.0 mmol) and potassium phosphate (4.25 g, 20.0 mmol) were placed into a 50 mL three-neck flask. The flask was evacuated and back-filled with argon. 2-Propanol (10.0 mL), ethylene glycol (1.11 mL), 1,2,3,4-tetrahydroisoquinoline (2.0 mL, 15 mmol) and iodobenzene (1.12 mL, 10.0 mmol) were added successively by syringe at room temperature. The reaction mixture was heated at 90 °C for 24 h and then allowed to cool to room temperature. Diethyl ether (20 mL) and water (20 mL) were then added to the reaction mixture. The organic layer was extracted with diethyl ether (2 × 20 mL). The combined organic phases were washed with brine and dried over sodium sulfate. The solvent was removed and the residue was purified by column chromatography on silica gel using hexane/ethyl acetate (20:1) as an eluent.

4.6.2.2 Characterization of starting materials

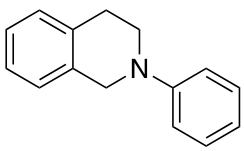

2-Phenyl-1,2,3,4-tetrahydroisoquinoline, (**1a**)

^{1}H NMR (400 MHz, $CDCl_3$): δ 7.32-7.26 (m, 2 H), 7.21-7.15 (m, 4 H), 7.00 (d, J = 8.0 Hz, 2 H), 6.84 (t, J =8.0 Hz, 1 H), 4.42 (s, 2 H), 3.58 (t, J = 6 Hz, 2 H), 3.00 (t, J= 5.6 Hz, 2H).

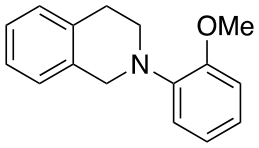

2-(2-Methoxyphenyl)-1,2,3,4-tetrahydroisoquinoline, (**1b**)

^{1}H NMR (300 MHz, $CDCl_3$): δ 7.18-7.11 (m, 4 H), 7.03-7.0 (m, 2 H), 6.94-6.89 (m, 2 H), 4.31 (s, H), 3.89 (s, 3 H), 3.43 (t, J =6.0 Hz, 2 H), 2.99 (t, J = 6.0 Hz, 2H).

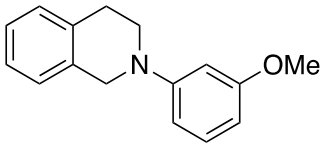

2-(3-Methoxyphenyl)-1,2,3,4-tetrahydroisoquinoline, (**1c**)

^{1}H NMR (400 MHz, $CDCl_3$): δ 7.25–7.15 (m, 4 H), 6.62–6.59 (m, 1 H), 6.53–6.52 (m, 1H), 6.41-6.39 (m, 1 H), 4.42 (s, 2 H), 3.81 (s, 3 H), 3.56 (t, J =6.4 Hz, 2 H), 2.99 (t, J = 5.6 Hz, 2H).

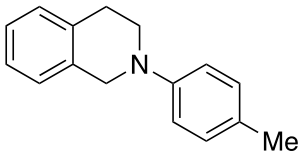

2-(4-Methylphenyl)-1,2,3,4-tetrahydroisoquinoline, (**1e**)

^{1}H NMR (500MHz, $CDCl_3$): δ 7.18-7.11 (m, 4 H), 7.00 (d, J = 5 Hz, 2 H), 6.93 (d, J = 5 Hz, 2 H), 4.37 (s, 2 H), 3.52 (t, J = 5 Hz, 2 H), 2.99 (t, J = 5.5 Hz, 2 H), 2.29 (s, 1H).

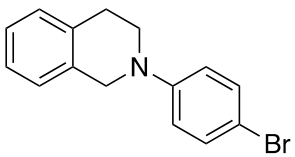

2-(4-Bromophenyl)-1,2,3,4-tetrahydroisoquinoline, (**1f**)

^{1}H NMR (300 MHz,$CDCl_3$): δ 7.37-7.34 (d, *J* = 9.0 Hz, 2 H), 7.20-7.15 (m, 4 H), 6.84 (d, *J* = 9.0 Hz, 2 H), 4.38 (s, 2 H), 3.54 (t, *J* = 6.9 Hz, 2 H), 3.00 (t, *J* = 6.0 Hz, 2H).

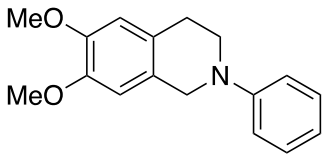

6,7-Dimethoxy-2-phenyl-1,2,3,4-tetrahydroisoquinoline, (**1n**)

^{1}H NMR (300 MHz, $CDCl_3$): δ 7.33-7.25 (m, 2 H), 7.02-6.95 (m, 2 H), 6.87-6.78 (m, 1 H), 6.66, 6.65 (s, 2H), 4.34 (s, 2H), 3.88 (s, 3 H), 3.87 (s, 3H), 3.55 (t, *J* =5.8 Hz, 2 H), 2.90 (t, *J* = 5.8 Hz, 2H).

4.6.2.3 General procedure for the arylation of 2-phenyl tetrahydroisoquinoline

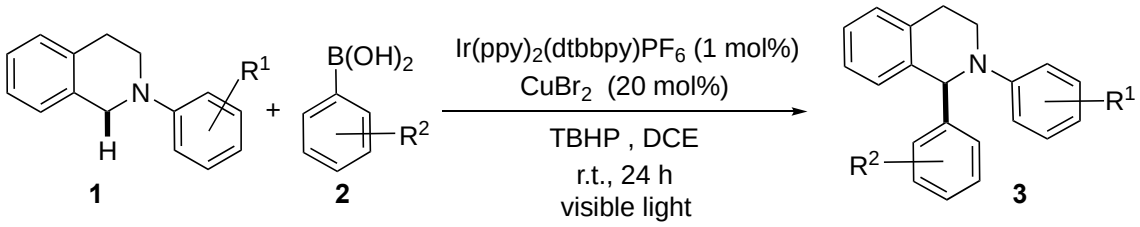

Scheme 106. Arylation of THIQs

A V-shaped 10 mL Biotage reaction vial was charged with $[Ir(ppy)_2(dtbbpy)]PF_6$ (1 mol %), $CuBr_2$ (20 mol %), N-aryl-tetrahydroisoquinoline (0.1 mmol), and the corresponding phenylboronic acid (0.3 mmol), evacuated and refilled with argon three times. DCE (0.5 mL) was added, followed by subsequent slow addition of TBHP (0.2 mmol). The reaction vessel was sealed, placed under white light bulbs irradiation with vigorous stirring (approx. 1000 rpm) and hold for 24 h. The mixture was diluted with ethyl acetate (2 mL), washed with water (2 mL), filtered through a pad of silica, and rinsed with additional ethyl

acetate. The combined organic phase was concentrated and purified by column chromatography or preparative thin-layer chromatography on silica gel to yield the corresponding arylated compound **3**. Dibromomethane was used as internal standard for ^{1}H NMR analysis.

4.6.2.4 General procedure for the asymmetric arylation of 2-phenyl tetrahydroisoquinoline

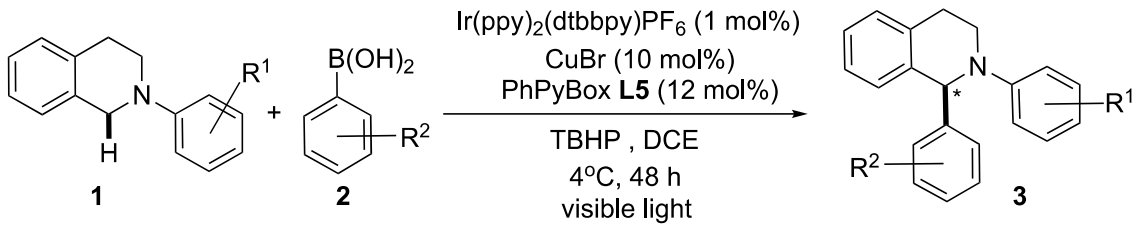

Scheme 107. Asymmetric arylation of THIQs

A V-shaped 10 mL Biotage reaction vial was charged with CuBr (10 mol %) and PhPybox (12 mol %), evacuated and refilled with argon three times, and then 0.1 mL of DCE was added. The reaction was stirred for 30 min. N-phenyltetrahydroisoquinoline (0.1 mmol), $[Ir(ppy)_2(dtbbpy)]PF_6$ (1 mol %) and the corresponding phenylboronic acid (0.3 mmol) were added, and the atmosphere was evacuated and refilled with argon three times. DCE (0.4 mL) was added followed by subsequent slow addition of TBHP (0.2 mmol). The reaction vessel was sealed, placed under white light bulbs irradiation with vigorous stirring (approx. 1000 rpm) and held for 48 h in a cold room (4 °C). The mixture was diluted with ethyl acetate (2 mL), washed with water (2 mL), filtered through a pad of silica, and rinsed with additional ethyl acetate. The combined organic phase was concentrated and purified by column chromatography or preparative thin-layer chromatography on silica gel to yield the corresponding arylated compound **3**. Dibromomethane was used as internal standard for ^{1}H NMR analysis.

4.6.2.5 Synthesis of $[Ir(ppy)_2(dtbbpy)]PF_6$

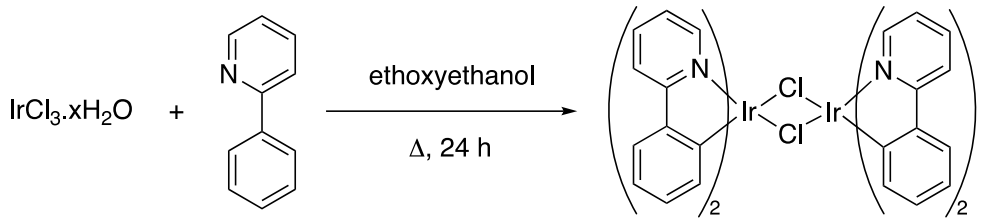

Scheme 108. Synthesis of $[Ir(ppy)_2Cl]_2$

Iridium trichloride hydrate (0.389 g, 1.31 mmol) was combined with 2- phenylpyridine (0.76 g, 4.9 mmol), dissolved in a mixture of 2-ethoxyethanol (30 mL) and water (10 mL), and refluxed for 24 h. The solution was cooled to room temperature, and the yellow precipitate was collected on a glass filter frit. The precipitate was washed with ethanol (60 mL) and acetone (60 mL) and then dissolved in dichloromethane (75 mL) and filtered. Toluene (25 mL) and hexanes (10 mL) were added to the filtrate, which was then reduced in volume by evaporation to 50 mL, and cooled to give crystals of $[Ir(ppy)_2Cl]_2$ in 75% yield (0.44 g).

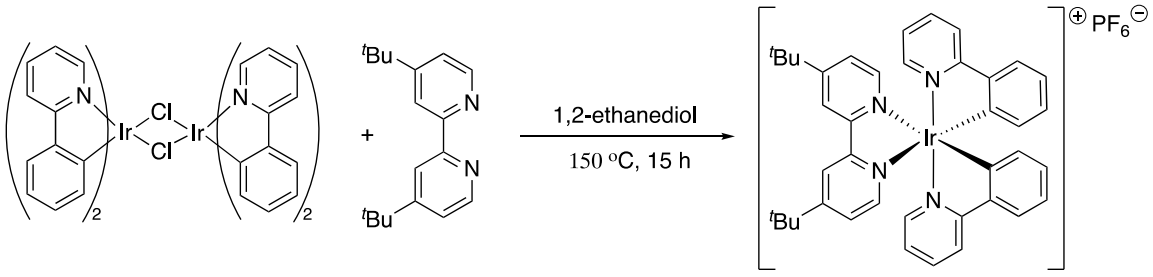

Scheme 109. Synthesis of $[Ir(ppy)_2(dtbbpy)]PF_6$

A stirred suspension of 4,4′-di-*tert*-butyl-2,2′-dipyridyl (0.44 g, 0.88 mmol) and tetrakis(2-phenylpyridine-C,N)(μ-dichloro)-diiridium, **A** (0.428g, 0.400 mmol) in 20 mL of 1,2-ethanediol under nitrogen was heated to 150 °C for 15 h. All the solids dissolved to yield a clear, yellow solution. After cooling the mixture to room temperature, 200 mL of

water was added. The excess of bipyridine ligand was removed through three extractions with diethyl ether (3×50 mL), and the aqueous layer was subsequently heated to 70 °C. NH_4PF_6 (2 g) in 20 mL of water was added, and the PF_6 salt of the iridium complex immediately precipitated. After cooling the suspension to 5 °C, the yellow solid was separated through filtration, dried, and recrystallized through acetonitrile/ether. Yield: 0.50 g (66%).

4.6.2.6 Characterisation of $[Ir(ppy)_2(dtbbpy)]PF_6$

^{1}H NMR (acetone-d_6, 400 MHz): δ 8.88 (d, *J* =2.0 Hz, dtb-bpy-H3, 2H), 8.24 (ppy-H6, pyridine, 2H, d, *J* = 8), 7.99-7.93 (m, dtb-bpy-H6, 2H, ppy-H5, pyridine, 2H), 7.90 (ppy-H3, phenyl, 2H, dd, *J* = 7.2, 0.8 Hz), 7.79 (ppy-H6, phenyl, 2H, d, *J* = 6 Hz), 7.71 (dtb-bpy-H5, 2H, dd, *J* = 6.0, 2.0 Hz), 7.14 (ppy-H4, pyridine, 2H, dt, *J* = 7.2, 1.6 Hz), 7.04 (ppy-H4, phenyl, 2H, dt, *J*= 7.6, 0.8 Hz), 6.91 (ppy-H5, phenyl, 2H, dt, *J* = 6.8, 1.2 Hz), 6.34 (ppy-H3, pyridine, 2H, d, *J* = 8), 1.42 (18H, s).

HRMS (ESI) *m/z* calculated for $C_{40}H_{40}N_4Ir^+$ ($[M - PF_6]^+$) 769.2876, found 769.2866.

4.6.3 Characterization of newly synthesized compounds

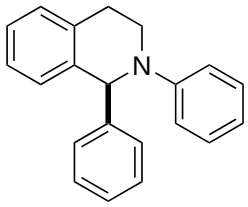

1,2-Diphenyl-1,2,3,4-tetrahydroisoquinoline (**3a**)

Using the general procedure described in the manuscript, compound (**3a**) was obtained from 2-phenyl-1,2,3,4-tetrahydroisoquinoline (0.1 mmol, 21.0 mg) and phenylboronic acid (0.3 mmol, 36.5 mg) as a white solid (21.4 mg) in 85 % yield.

Rf (hexane/EtOAc 3:0.5): 0.8.

^{1}H NMR ($CDCl_3$, 500 MHz): δ = 7.38 – 7.10 (m, 11H), 6.85 (m, 2H), 6.75 (m, 1H), 5.83 (s, 1H), 3.73 (dt, J = 11.1, 5.2 Hz, 1H), 3.52 (ddd, J = 11.1, 8.6, 5.2 Hz, 1H), 3.21 – 2.42 (m, 2H).

^{13}C NMR ($CDCl_3$, 126 MHz): δ = 149.5, 143.0, 137.8, 135.7, 129.1, 128.2, 128.0, 127.7, 127.2, 127.0, 126.7, 126.1, 117.4, 113.8, 62.7, 43.8, 28.0.

HRMS (ESI) m/z: $[M + H]^+$ calculated for $C_{21}H_{20}N$ 286.15903, found 286.15840.

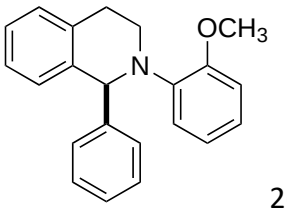

2(2-Methoxyphenyl)-1-phenyl-1,2,3,4-tetrahydroisoquinoline (**3b**)

Using the general procedure described in the manuscript, compound (**3b**) was obtained from 2-(2-methoxyphenyl)-1,2,3,4-tetrahydroisoquinoline (0.1 mmol, 23.9 mg) and phenylboronic acid (0.3 mmol, 36.5 mg) as a white solid (17.6 mg) in 56 % yield.

Rf (hexane/EtOAc 3:0.5): 0.7.

^{1}H NMR ($CDCl_3$, 500 MHz): δ = 7.20 (m, 2H), 7.16 – 7.08 (m, 4H), 6.96 (m, 2H), 6.87 (m, 3H), 6.73 (m, 1H), 6.58 (m, 1H), 5.91 (s, 1H), 3.91 (s, 3H), 3.41 (ddd, J = 12.2, 10.3, 4.5 Hz, 1H), 3.31 (ddd, J = 12.2, 6.2, 3.0 Hz, 1H), 3.14 (ddd, J = 16.4, 10.3, 6.2 Hz, 1H), 2.96 (dt, J = 16.4, 3.0 Hz, 1H).

^{13}C NMR ($CDCl_3$, 126 MHz): δ = 153.0, 142.0, 140.0, 137.2, 135.0, 129.3, 128.8, 128.7, 127.3, 126.7, 126.2, 125.5, 122.9, 121.9, 120.8, 111.5, 62.7, 55.6, 43.0, 28.7.

HRMS (ESI) m/z: $[M + H]^+$ calculated for $C_{22}H_{22}NO$ 316.16959, found 316.16980.

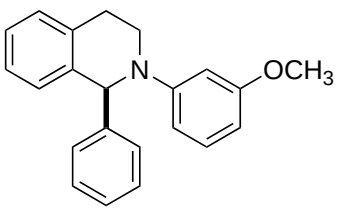

2-(3-Methoxyphenyl)-1-phenyl-1,2,3,4-tetrahydroisoquinoline (**3c**)

Using the general procedure in the manuscript, compound (**3c**) was obtained from 2-(3-methoxyphenyl)-1,2,3,4-tetrahydroisoquinoline (0.1 mmol, 23.9 mg) and phenylboronic acid (0.3 mmol, 36.5 mg) as a white solid (19.2 mg) in 61 % yield.

Rf (hexane/EtOAc 3:0.5): 0.7.

^{1}H NMR ($CDCl_3$, 500 MHz): δ = 7.37 – 6.99 (m, 10H), 6.60 – 6.14 (m, 3H), 5.83 (s, 1H), 3.76 (s, 3H), 3.75 – 3.67 (m, 1H), 3.51 (m, 1H), 2.93 (m, 2H).

^{13}C NMR ($CDCl_3$, 126 MHz): δ = 160.6, 150.8, 143.0, 137.8, 135.7, 129.8, 128.2, 128.0, 127.7, 127.1, 127.0, 126.7, 126.1, 106.7, 102.0, 100.2, 62.7, 55.1, 43.9, 28.0.

HRMS (ESI) m/z: $[M + H]^+$ calculated for $C_{22}H_{22}NO$ 316.16959, found 316.16950.

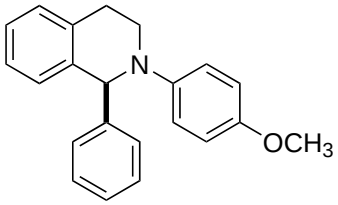

2-(4-Methoxyphenyl)-1-phenyl-1,2,3,4-tetrahydroisoquinoline (**3d**)

Using the general procedure described above, compound (**3d**) was obtained from 2-(4-methoxyphenyl)-1,2,3,4-tetrahydroisoquinoline (0.1 mmol, 23.9 mg) and phenylboronic acid (0.3 mmol, 36.5 mg) as a white solid (16.7 mg) in 53 % yield.

Rf (hexane/EtOAc 3:0.5): 0.7

^{1}H NMR ($CDCl_3$, 500 MHz): δ = 7.28 – 7.15 (m, 9H), 6.89 – 6.79 (m, 4H), 5.69 (s, 1H), 3.77 (s, 3H), 3.61 (ddd, J = 12.0, 6.7, 5.2 Hz, 1H), 3.44 (ddd, J = 12.0, 7.2, 5.2 Hz, 1H), 3.04 – 2.92 (m, 2H).

^{13}C NMR ($CDCl_3$, 126 MHz): δ = 152.8, 144.4, 143.2, 137.6, 135.5, 128.3, 128.1, 128.09, 128.02, 126.8, 126.7, 125.9, 117.7, 114.4, 64.3, 55.6, 44.5, 28.1.

HRMS (ESI) m/z: $[M + H]^+$ calculated for $C_{22}H_{22}NO$ 316.16959, found 316.16847.

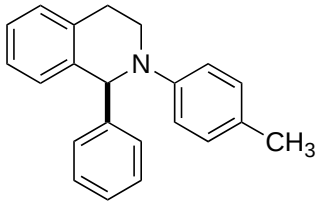

1-Phenyl-2-(p-tolyl)-1,2,3,4-tetrahydroisoquinoline (**3e**)

Using the general procedure described in the manuscript, compound (**3e**) was obtained from 2-(p-tolyl)-1,2,3,4-tetrahydroisoquinoline (0.1 mmol, 22.3 mg) and phenylboronic acid (0.3 mmol, 36.5 mg) as a white solid (23.3 mg) in 78 % yield.

Rf (hexane/EtOAc 3:0.5): 0.75.

^{1}H NMR ($CDCl_3$, 500 MHz): δ = 7.31 – 7.12 (m, 9H), 7.04 (m, 2H), 6.79 (m, 2H), 5.79 (s, 1H), 3.68 (dt, J = 11.4, 5.6 Hz, 1H), 3.49 (ddd, J = 11.4, 8.2, 5.6 Hz, 1H), 3.19 – 2.68 (m, 2H), 2.26 (s, 3H).

^{13}C NMR ($CDCl_3$, 126 MHz): δ = 147.5, 143.3, 137.8, 135.7, 129.6, 128.7, 128.17, 128.13, 127.9, 127.5, 126.9, 126.7, 126.0, 114.5, 63.1, 43.9, 27.9, 20.3.

HRMS (ESI) m/z: $[M + H]^+$ calculated for $C_{22}H_{24}NO$ 300.17468, found 300.17507.

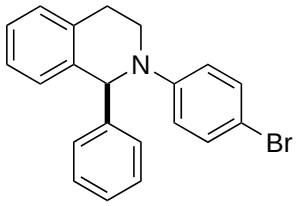

2-(4-Bromophenyl)-1-phenyl-1,2,3,4-tetrahydroisoquinoline (**3f**)

Using the general procedure described above, compound (**3f**) was obtained from 2-(4-bromophenyl)-1,2,3,4-tetrahydroisoquinoline (0.1 mmol, 28.8 mg) and phenylboronic acid (0.3 mmol, 36.5 mg) as a white solid (29.1 mg) in 80 % yield.

Rf (hexane/EtOAc 3:0.5): 0.85.

^{1}H NMR ($CDCl_3$, 500 MHz): δ = 7.35 – 7.09 (m, 11H), 6.71 (m, 2H), 5.76 (s, 1H), 3.71 (dt, J = 11.2, 5.3 Hz, 1H), 3.47 (dt, J = 11.2, 7.2 Hz, 1H), 2.94 (m, 2H).

^{13}C NMR ($CDCl_3$, 126 MHz): δ = 148.3, 142.4, 137.5, 135.4, 131.8, 128.3, 128.0, 127.7, 127.2, 127.1, 126.9, 126.3, 115.4, 109.4, 62.8, 44.1, 27.9.

HRMS (ESI) m/z: $[M + H]^+$ calculated for $C_{21}H_{19}NBr$ 364.06954, found 364.06927.

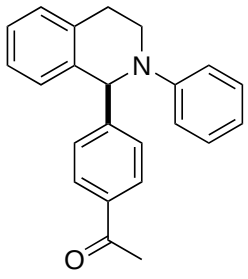

1-(4-(2-Phenyl-1,2,3,4-tetrahydroisoquinolin-1-yl)phenyl)ethanone (**3g**)

Using the general procedure described above, compound (**3g**) was obtained from 2-phenyl-1,2,3,4-tetrahydroisoquinoline (0.1 mmol, 21.0 mg) and (4-acetylphenyl)boronic acid (0.3 mmol, 49.2 mg) as a white solid (18.6 mg) in 57 % yield.

Rf (hexane/EtOAc 3:0.5): 0.45

^{1}H NMR ($CDCl_3$, 500 MHz): δ = 7.91 – 7.83 (m, 2H), 7.43 – 7.37 (m, 2H), 7.35 – 7.17 (m, 6H), 6.95 – 6.76 (m, 3H), 5.87 (s, 1H), 3.78 (dt, *J* = 10.9, 5.2 Hz, 1H), 3.61 – 3.50 (m, 1H), 3.01 (q, *J* = 7.5, 5.2 Hz, 1H), 2.57 (s, 2H).

^{13}C NMR ($CDCl_3$, 126 MHz): δ = 197.7, 148.5, 137.0, 135.9, 135.6, 129.2, 128.4, 128.2, 127.7, 127.5, 127.4, 126.4, 124.4, 118.0, 114.0, 63.0, 44.2, 28.1, 26.6.

HRMS (ESI) m/z: $[M + H]^+$ calculated for $C_{23}H_{22}NO$ 328.1701, found 328.1697.

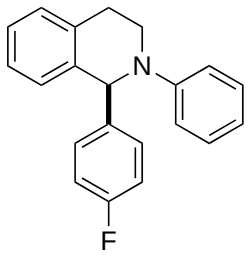

1-(4-Fluorophenyl)-2-phenyl-1,2,3,4-tetrahydroisoquinoline (**3h**)

Using the general procedure described above, compound (**3h**) was obtained from 2-phenyl-1,2,3,4-tetrahydroisoquinoline (0.1 mmol, 21.0 mg) and (4-fluorophenyl)boronic acid (0.3 mmol, 42.0 mg) as a white solid (17.0 mg) in 56 % yield.

Rf (hexane/EtOAc 3:0.5): 0.55.

^{1}H NMR ($CDCl_3$, 500 MHz): δ = 7.27 – 7.15 (m, 8H), 6.95 – 6.89 (m, 2H), 6.87 – 6.83 (m, 2H), 6.79 – 6.70 (m, 1H), 5.80 (s, 1H), 3.68 (dt, J = 11.4, 5.2 Hz, 1H), 3.50 (ddd, J = 11.4, 8.7, 5.2 Hz, 1H), 2.97 (dt, J = 15.6, 5.2 Hz, 1H), 2.88 (ddd, J = 15.6, 8.7, 5.3 Hz, H).

^{13}C NMR ($CDCl_3$, 126 MHz): δ = 162.7, 160.7, 149.4, 138.75, 138.73, 137.5, 135.6, 129.1, 128.9, 128.8, 128.2, 127.7, 127.1, 126.1, 117.8, 115.0, 114.8, 114.2, 104.9, 62.2, 43.6, 27.9.

^{19}F NMR ($CDCl_3$, 470 MHz): δ = -104.5.

HRMS (ESI) m/z: $[M + H]^+$ calculated for $C_{21}H_{19}NF$ 304.1496, found 304.1496.

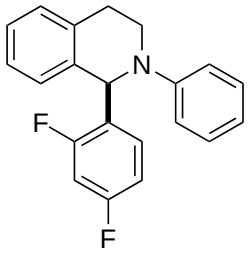

1-(2,4-Difluorophenyl)-2-phenyl-1,2,3,4-tetrahydroisoquinoline (**3i**)

Using the general procedure described above, compound (**3i**) was obtained from 2-phenyl-1,2,3,4-tetrahydroisoquinoline (0.1 mmol, 21.0 mg) and (2,4-difluorophenyl)boronic acid (0.3 mmol, 47.3 mg) as a white solid (17.3 mg) in 54 % yield.

Rf (hexane/EtOAc 3:0.5): 0.5.

^{1}H NMR ($CDCl_3$, 500 MHz): δ = 7.29 – 7.17 (m, 6H), 7.17 – 7.12 (m, 1H), 6.94 – 6.88 (m, 2H), 6.84 – 6.77 (m, 2H), 6.77 – 6.71 (m, 1H), 6.11 (s, 1H), 3.78 (dt, J = 11.7, 6.0 Hz, 1H), 3.59 (dt, J = 11.7, 6.0 Hz, 1H), 3.07 (t, J = 6.0 Hz, 2H).

^{13}C NMR ($CDCl_3$, 126 MHz): δ = 163.0, 162.9, 161.4, 161.3, 161.0, 160.9, 149.1, 136.4, 135.4, 130.2, 130.19, 130.16, 130.11, 129.1, 128.2, 127.96, 127.93, 127.29, 127.26, 127.18, 127.15, 127.0, 126.4, 118.5, 115.1, 111.04, 111.01, 110.87, 110.84, 104.1, 103.9, 103.7, 57.0, 44.0, 28.0.

^{19}F NMR ($CDCl_3$, 470 MHz): δ = -111.5, -111.9.

HRMS (ESI) m/z: $[M + H]^+$ calculated for $C_{21}H_{18}NF_2$ 322.1402, found 322.1394.

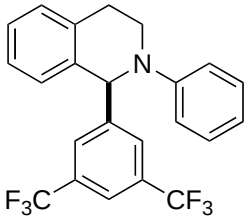

1-(3,5-Bis(trifluoromethyl)phenyl)-2-phenyl-1,2,3,4-tetrahydroisoquinoline (**3j**)

Using the general procedure described above, compound (**3j**) was obtained from 2-phenyl-1,2,3,4-tetrahydroisoquinoline (0.1 mmol, 21.0 mg) and (3,5-bis(trifluoromethyl)phenyl)boronic acid (0.3 mmol, 77.3 mg) as a white solid (13.9 mg) in 33 % yield.

Rf (hexane/EtOAc 3:0.5): 0.35.

^{1}H NMR ($CDCl_3$, 500 MHz): δ = 7.72 (s, 1H), 7.69 (s, 2H), 7.29 – 7.20 (m, 6H), 7.02 – 6.72 (m, 3H), 5.85 (s, 1H), 3.65 (ddd, J = 11.5, 6.2, 5.0 Hz, 1H), 3.51 (ddd, J = 11.5, 8.5, 4.8 Hz, 1H), 3.01 (ddd, J = 15.8, 6.2, 4.8 Hz, 1H), 2.86 (ddd, J = 15.7, 8.5, 5.0 Hz, 1H).

^{13}C NMR ($CDCl_3$, 126 MHz): δ = 149.1, 146.3, 135.7, 135.6, 131.8, 131.6, 131.3, 131.0, 129.3, 128.6, 127.79, 127.70, 127.4, 126.6, 124.3, 122.1, 121.1, 119.0, 114.9, 104.9, 63.0, 44.0, 27.8.

^{19}F NMR ($CDCl_3$, 470 MHz): δ = -62.7.

HRMS (ESI) m/z: $[M + H]^+$ calculated for $C_{23}H_{18}NF_6$ 422.1338, found 422.1332.

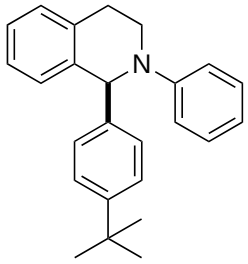

1-(4-(tert-Butyl)phenyl)-2-phenyl-1,2,3,4-tetrahydroisoquinoline (**3k**)

Using the general procedure described above, compound (**3k**) was obtained from 2-phenyl-1,2,3,4-tetrahydroisoquinoline (0.1 mmol, 21.0 mg) and (4-(tert-butyl)phenyl)boronic acid (0.3 mmol, 53.4 mg) as a white solid (20.1 mg) in 59 % yield.

Rf (hexane/EtOAc 3:0.5): 0.9.

^{1}H NMR ($CDCl_3$, 500 MHz): δ = 7.37 – 7.06 (m, 10H), 6.87 (m, 2H), 6.79 – 6.66 (m, 1H), 5.83 (s, 1H), 3.74 – 3.71 (m, 1H), 3.59 – 3.45 (m, 1H), 3.01 – 2.81 (m, 2H), 1.27 (s, 9H).

^{13}C NMR ($CDCl_3$, 126 MHz): δ = 149.5, 139.9, 138.0, 135.7, 131.7, 129.1, 128.0, 127.8, 126.9, 126.8, 126.6, 126.0, 125.2, 125.1, 117.1, 115.0, 113.5, 62.3, 43.6, 34.3, 31.3, 27.8.

HRMS (ESI) m/z: $[M + H]^+$ calculated for $C_{25}H_{28}N$ 342.2216, found 342.2211.

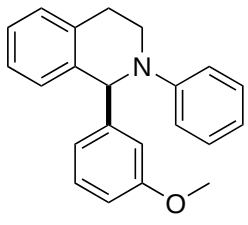

1-(3-Methoxyphenyl)-2-phenyl-1,2,3,4-tetrahydroisoquinoline (**3l**)

Using the general procedure described above, compound (**3l**) was obtained from 2-phenyl-1,2,3,4-tetrahydroisoquinoline (0.1 mmol, 21.0 mg) and (3-methoxyphenyl)boronic acid (0.3 mmol, 45.6 mg) as a white solid (23.3 mg) in 74 % yield.

Rf (hexane/EtOAc 3:0.5): 0.55.

^{1}H NMR ($CDCl_3$, 500 MHz): δ = 7.36 – 7.31 (m, 1H), 7.30 – 7.18 (m, 6H), 6.94 – 6.85 (m, 4H), 6.83 – 6.74 (m, 2H), 5.84 (s, 1H), 3.91 – 3.75 (m, 4H), 3.59 – 3.51 (m, 1H), 2.99 (m, 2H).

^{13}C NMR ($CDCl_3$, 126 MHz): δ = 159.5, 149.5, 145.0, 137.7, 135.7, 129.2, 129.1, 128.1, 127.8, 127.1, 126.2, 119.7, 117.5, 113.9, 113.5, 111.6, 62.9, 55.1, 43.8, 28.0.

HRMS (ESI) m/z: $[M + H]^+$ calculated for $C_{22}H_{22}NO$ 316.1701, found 316.1696.

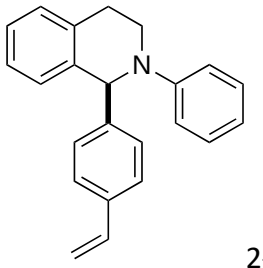

2-Phenyl-1-(4-vinylphenyl)-1,2,3,4-tetrahydroisoquinoline (**3m**)

Using the general procedure described above, compound (**3m**) was obtained from 2-phenyl-1,2,3,4-tetrahydroisoquinoline (0.1 mmol, 21.0 mg) and (4-vinylphenyl) boronic acid (0.3 mmol, 44.4 mg) as a white solid (18.7 mg) in 60 % yield.

Rf (hexane/EtOAc 3:0.5): 0.9.

^{1}H NMR ($CDCl_3$, 500 MHz): δ = 7.34 – 7.30 (m, 3H), 7.29 – 7.27 (m, 1H), 7.27 – 7.23 (m, 5H), 7.22 – 7.18 (m, 1H), 6.91 – 6.86 (m, 1H), 6.82 – 6.76 (m, 1H), 6.69 (dd, *J* = 17.6, 10.9 Hz, 1H), 5.85 (s, 1H), 5.71 (dd, *J* = 17.6, 0.9 Hz, 1H), 5.22 (dd, *J* = 10.9, 0.9 Hz, 1H), 3.76 (dt, *J* = 11.0, 5.1 Hz, 0H), 3.54 (ddd, *J* = 11.0, 8.7, 5.1 Hz, 1H), 3.03 – 2.92 (m, 1H).

^{13}C NMR ($CDCl_3$, 126 MHz): δ = 149.5, 142.8, 137.7, 136.4, 136.2, 135.7, 129.1, 128.1, 127.7, 127.4, 127.0, 126.2, 126.1, 117.5, 113.9, 113.6, 62.6, 43.8, 28.1.

HRMS (ESI) m/z: $[M + H]^+$ calculated for $C_{23}H_{22}N$ 312.1752, found 312.1752.

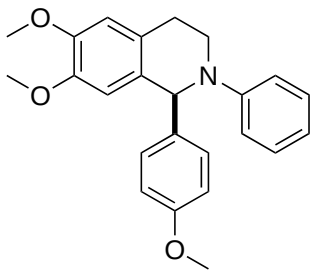

6,7-Dimethoxy-1-(3-methoxyphenyl)-2-phenyl-1,2,3,4-tetrahydroisoquinoline (**3n**)

Using the general procedure described above, compound (**3n**) was obtained from 6,7-dimethoxy-2-phenyl-1,2,3,4- tetrahydroisoquinoline (0.1 mmol, 26.9 mg) and (4-methoxyphenyl)boronic acid (0.3 mmol, 45.6 mg) as a white solid (27.4 mg) in 73 % yield.

Rf (hexane/EtOAc 3:0.5): 0.2.

^{1}H NMR ($CDCl_3$, 500 MHz): δ = 7.29 – 7.22 (m, 2H), 7.17 – 7.08 (m, 2H), 6.95 – 6.92 (m, 2H), 6.86 – 6.77 (m, 3H), 6.74 – 6.71 (m, 1H), 6.70 – 6.68 (m, 1H), 5.76 (s, 1H), 3.89 (s, 3H), 3.86 (s, 3H), 3.78 (s, 3H), 3.65 – 3.48 (m, 2H), 3.01 – 2.88 (m, 1H), 2.80 – 2.77 (m, 1H).

^{13}C NMR ($CDCl_3$, 126 MHz): δ = 158.5, 149.8, 147.8, 147.2, 135.4, 129.1, 128.8, 127.6, 117.9, 115.0, 114.7, 113.4, 111.2, 111.0, 61.9, 56.0, 55.9, 55.2, 42.91, 27.0.

HRMS (ESI) m/z: $[M + H]^+$ calculated for $C_{24}H_{25}NO_3$ 376.1907, found 376.1914.

4.6.4 HPLC chromatogram for the racemic- and chiral synthesized compounds

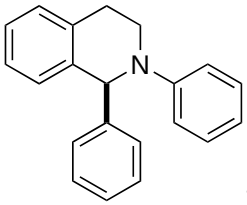

1,2-Diphenyl-1,2,3,4-tetrahydroisoquinoline (**3a**)

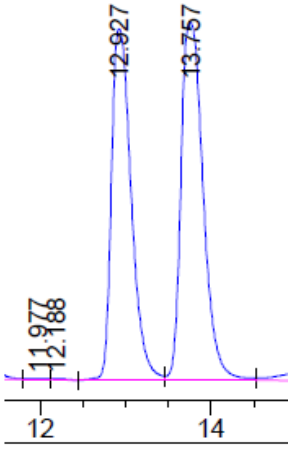

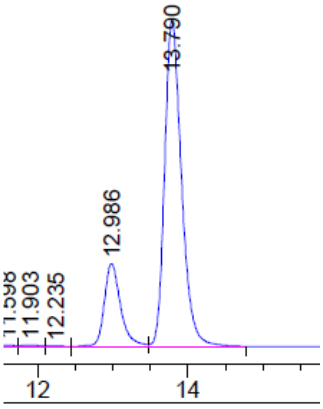

Peak	Retention time (min)	Area (%)
Major isomer	12.986	19.2879
Minor isomer	13.790	78.4008

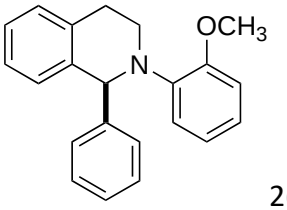

2(2-Methoxyphenyl)-1-phenyl-1,2,3,4-tetrahydroisoquinoline (**3b**)

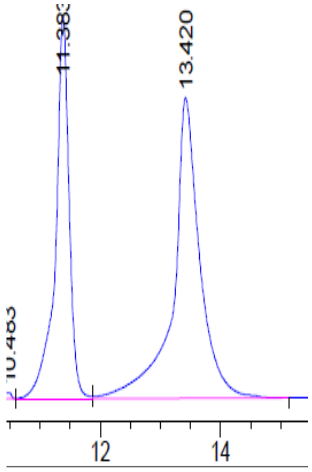

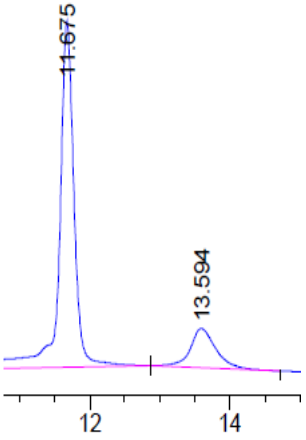

Peak	Retention time (min)	Area (%)
Major isomer	11.675	60.1237
Minor isomer	13.594	11.9011

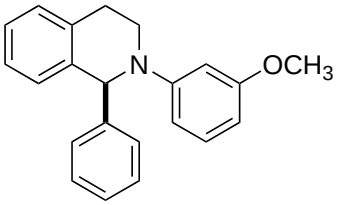

2-(3-Methoxyphenyl)-1-phenyl-1,2,3,4-tetrahydroisoquinoline (**3c**)

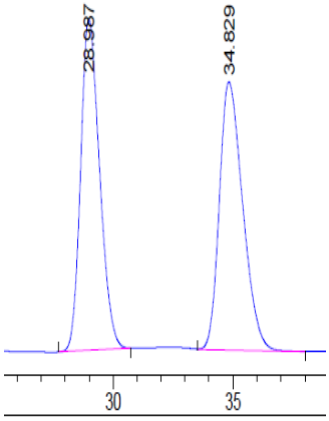

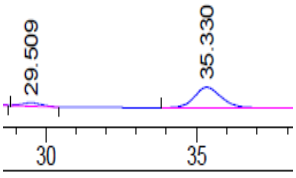

Peak	Retention time (min)	Area (%)
Major isomer	29.509	1.8996
Minor isomer	35.330	16.4503

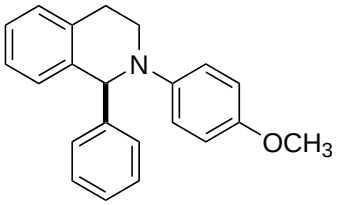

2-(4-Methoxyphenyl)-1-phenyl-1,2,3,4-tetrahydroisoquinoline (**3d**)

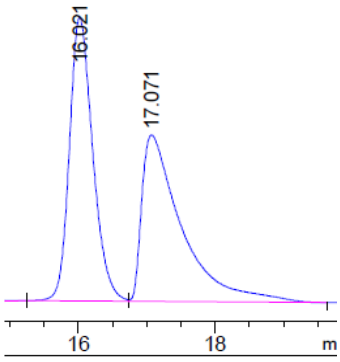

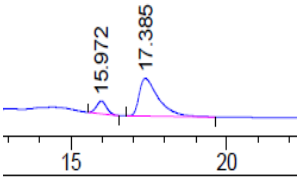

Peak	Retention time (min)	Area (%)
Major isomer	15.972	3.1868
Minor isomer	17.385	18.4472

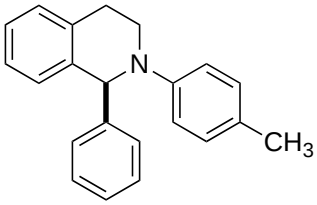

1-Phenyl-2-(p-tolyl)-1,2,3,4-tetrahydroisoquinoline (**3e**)

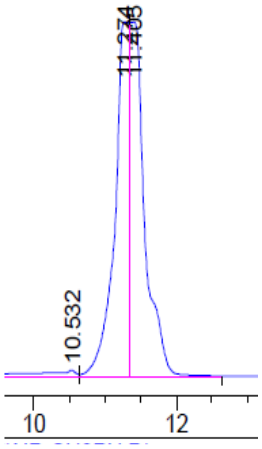

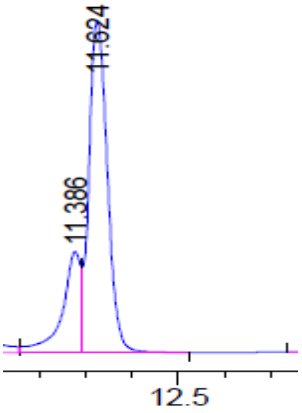

Peak	Retention time (min)	Area (%)
Major isomer	11.386	20.9969
Minor isomer	11.624	68.4203

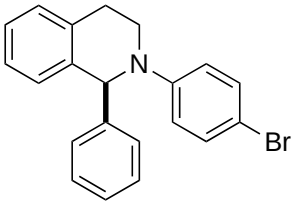

2-(4-Bromophenyl)-1-phenyl-1,2,3,4-tetrahydroisoquinoline (**3f**)

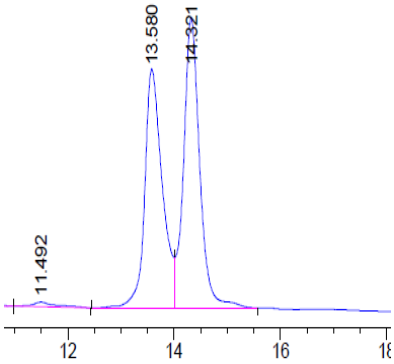

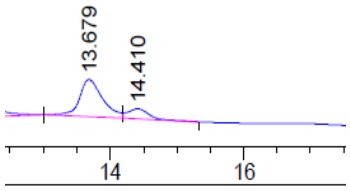

Peak	Retention time (min)	Area (%)
Major isomer	13.679	6.0486
Minor isomer	14.410	1.4782

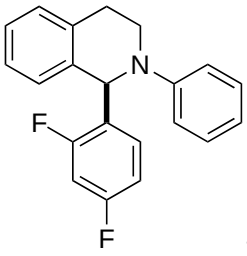

1-(2,4-Difluorophenyl)-2-phenyl-1,2,3,4-tetrahydroisoquinoline (**3i**)

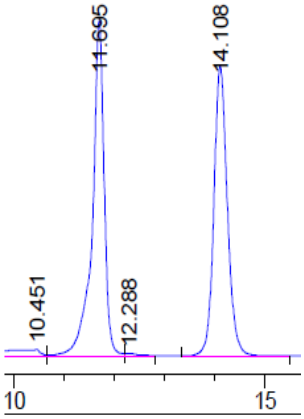

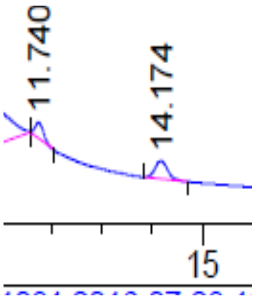

Peak	Retention time (min)	Area (%)
Major isomer	11.740	1.88420
Minor isomer	14.174	3.0673

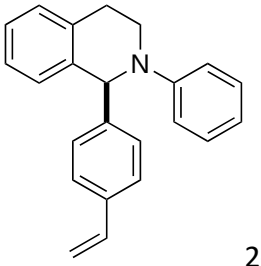

2-Phenyl-1-(4-vinylphenyl)-1,2,3,4-tetrahydroisoquinoline (**3m**)

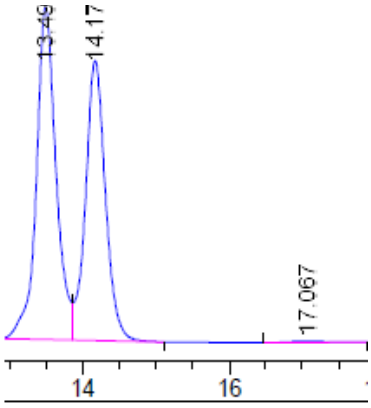

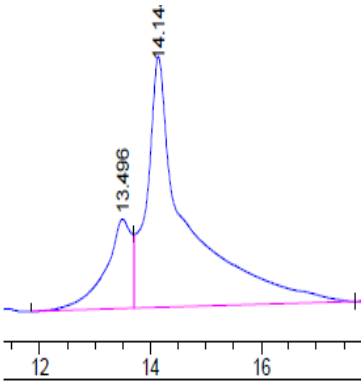

Peak	Retention time (min)	Area (%)
Major isomer	13.496	10.2151
Minor isomer	14.144	43.9473

4.7 References

[1] Singh, I. P.; Shah, P., *Expert Opin. Ther. Pat.,* **2017,** *27*, 17-36.

[2] Miyazaki, M.; Ando, N.; Sugai, K.; Seito, Y.; Fukuoka, H.; Kanemitsu, T.; Nagata, K.; Odanaka, Y.; Nakamura, K. T.; Itoh, T., *J. Org. Chem.,* **2011,** *76*, 534-542.

[3] Le, V. H.; Inai, M.; Williams, R. M.; Kan, T., *Nat. Prod. Rep.,* **2015,** *32*, 328-347.

[4] Santangelo Freel, R. M.; Ogden, K. K.; Strong, K. L.; Khatri, A.; Chepiga, K. M.; Jensen, H. S.; Traynelis, S. F.; Liotta, D. C., *J. Med. Chem.,* **2013,** *56*, 5351-5381.

[5] Dzierszinski, F.; Coppin, A.; Mortuaire, M.; Dewailly, E.; Slomianny, C.; Ameisen, J.-C.; DeBels, F.; Tomavo, S., *Antimicrob. Agents Chemother.,* **2002,** *46*, 3197-3207.

[6] Forró, E.; Megyesi, R.; Paál, T. A.; Fülöp, F., *Tetrahedron: Asymmetry,* **2016,** *27*, 1213-1216.

[7] Renaud, J.; Bischoff, S. F.; Buhl, T.; Floersheim, P.; Fournier, B.; Geiser, M.; Halleux, C.; Kallen, J.; Keller, H.; Ramage, P., *J. Med. Chem.,* **2005,** *48*, 364-379.

[8] Ludwig, M.; Hoesl, C. E.; Höfner, G.; Wanner, K. T., *Eur. J. Med. Chem.,* **2006,** *41*, 1003-1010.
[9] Gao, M.; Wang, M.; Miller, K. D.; Sledge, G. W.; Zheng, Q.-H., *Eur. J. Med. Chem.,* **2008,** *43*, 2211-2219.
[10] Gessier, F.; Kallen, J.; Jacoby, E.; Chène, P.; Stachyra-Valat, T.; Ruetz, S.; Jeay, S.; Holzer, P.; Masuya, K.; Furet, P., *Bioorg. Med. Chem. Lett.,* **2015,** *25*, 3621-3625.
[11] Holzer, P.; Masuya, K.; Furet, P.; Kallen, J.; Valat-Stachyra, T.; Ferretti, S.; Berghausen, J.; Bouisset-Leonard, M.; Buschmann, N.; Pissot-Soldermann, C.; Rynn, C.; Ruetz, S.; Stutz, S.; Chène, P.; Jeay, S.; Gessier, F., *J. Med. Chem.,* **2015,** *58*, 6348-6358.
[12] Scott, J. S.; Bailey, A.; Davies, R. D. M.; Degorce, S. L.; MacFaul, P. A.; Gingell, H.; Moss, T.; Norman, R. A.; Pink, J. H.; Rabow, A. A.; Roberts, B.; Smith, P. D., *ACS Med. Chem. Lett.,* **2016,** *7*, 94-99.
[13] Scott, J. D.; Williams, R. M., *Chem. Rev.,* **2002,** *102*, 1669-1730.
[14] Sygusch, J.; Brisse, F.; Hanessian, S.; Kluepfel, D., *Tetrahedron Lett.,* **1974,** *15*, 4021-4023.
[15] Chrzanowska, M.; Rozwadowska, M. D., *Chem. Rev.,* **2004,** *104*, 3341-3370.
[16] Chrzanowska, M.; Grajewska, A.; Rozwadowska, M. D., *Chem. Rev.,* **2016,** *116*, 12369-12465.
[17] Bischler, A.; Napieralski, B., *Ber.,* **1893,** *26*, 1903-1908.
[18] Fodor, G.; Nagubandi, S., *Tetrahedron,* **1980,** *36*, 1279-1300.
[19] Hajipour, A. R.; Hantehzadeh, M., *J. Org. Chem.,* **1999,** *64*, 8475-8478.
[20] Pictet, A.; Spengler, T., *Ber.,* **1911,** *44*, 2030-2036.
[21] Pulka, K., *Curr. Opin. Drug. Discov. Devel.,* **2010,** *13*, 669-684.
[22] Comins, D. L.; Thakker, P. M.; Baevsky, M. F.; Badawi, M. M., *Tetrahedron,* **1997,** *53*, 16327-16340.
[23] Pomeranz, C., *Monath. Chem. Verw. Teile Anderer Wiss.,* **1893,** *14*, 116-119.
[24] Fritsch, P., *Ber.,* **1893,** *26*, 419-422.
[25] Ponzo, V. U.; Kaufman, T. S., *Tetrahedron Lett.,* **1995,** *36*, 9105-9108.
[26] Kaufman, T. S., *Tetrahedron Lett.,* **1996,** *37*, 5329-5332.
[27] Taylor Mark, S.; Tokunaga, N.; Jacobsen Eric, N., *Angew. Chem. Int. Ed.,* **2005,** *44*, 6700-6704.
[28] Liu, W.; Liu, S.; Jin, R.; Guo, H.; Zhao, J., *Org. Chem. Front.,* **2015,** *2*, 288-299.
[29] Girard, S. A.; Knauber, T.; Li, C.-J., CHAPTER 1 The Evolution of the Concept of Cross-Dehydrogenative-Coupling Reactions. In *From C-H to C-C Bonds: Cross-Dehydrogenative-Coupling*, The Royal Society of Chemistry: **2015**; pp 1-32.
[30] Li, C.-J., *Acc. Chem. Res.,* **2009,** *42*, 335-344.
[31] Girard, S. A.; Knauber, T.; Li, C.-J., *Angew. Chem. Int. Ed.,* **2014,** *53*, 74-100.
[32] Pitts, C. R.; Bloom, S.; Woltornist, R.; Auvenshine, D. J.; Ryzhkov, L. R.; Siegler, M. A.; Lectka, T., *J. Am. Chem. Soc.,* **2014,** *136*, 9780-9791.
[33] Hartwig, J. F.; Larsen, M. A., *ACS Cent. Sci.,* **2016,** *2*, 281-292.
[34] Labinger, J. A.; Bercaw, J. E., *Nature,* **2002,** *417*, 507.
[35] He, J.; Li, S.; Deng, Y.; Fu, H.; Laforteza, B. N.; Spangler, J. E.; Homs, A.; Yu, J.-Q., *Science,* **2014,** *343*, 1216-1220.

[36] Kuhl, N.; Hopkinson Matthew, N.; Wencel-Delord, J.; Glorius, F., *Angew. Chem. Int. Ed.,* **2012,** *51*, 10236-10254.
[37] Li, Z.; Li, C. J., *Org. Lett.,* **2004,** *6*, 4997-9.
[38] Li, Z.; MacLeod, P. D.; Li, C.-J., *Tetrahedron: Asymmetry,* **2006,** *17*, 590-597.
[39] Baslé, O.; Li, C.-J., *Org. Lett.,* **2008,** *10*, 3661-3663.
[40] Li, C.-J., From C-H to C-C Bonds : Cross-Dehydrogenative-Coupling. RSC Green Chemistry: **2015**.
[41] Barham, J. P.; John, M. P.; Murphy, J. A., *Beilstein J. Org. Chem.,* **2014,** *10*, 2981-2988.
[42] Cuthbertson, J. D.; MacMillan, D. W. C., *Nature,* **2015,** *519*, 74-77.
[43] Muramatsu, W.; Nakano, K.; Li, C.-J., *Org. Biomol. Chem.,* **2014,** *12*, 2189-2192.
[44] Dhineshkumar, J.; Lamani, M.; Alagiri, K.; Prabhu, K. R., *Org. Lett.,* **2013,** *15*, 1092-1095.
[45] Liu, X.; Sun, S.; Meng, Z.; Lou, H.; Liu, L., *Org. Lett.,* **2015,** *17*, 2396-2399.
[46] Li, Z.; Bohle, D. S.; Li, C.-J., *Proc. Natl. Acad. Sci. U. S. A.,* **2006,** *103*, 8928-8933.
[47] Yan, C.; Li, L.; Liu, Y.; Wang, Q., *Org. Lett.,* **2016,** *18*, 4686-4689.
[48] Liu, X.; Meng, Z.; Li, C.; Lou, H.; Liu, L., *Angew. Chem. Int. Ed.,* **2015,** *54*, 6012-6015.
[49] Bergonzini, G.; Schindler, C. S.; Wallentin, C.-J.; Jacobsen, E. N.; Stephenson, C. R. J., *Chem. Sci.,* **2014,** *5*, 112-116.
[50] Prier, C. K.; Rankic, D. A.; MacMillan, D. W. C., *Chem. Rev.,* **2013,** *113*, 5322-5363.
[51] Cismesia, M. A.; Yoon, T. P., *Chem. Sci.,* **2015,** *6*, 5426-5434.
[52] Nicewicz, D. A.; MacMillan, D. W. C., *Science,* **2008,** *322*, 77-80.
[53] Nagib, D. A.; Scott, M. E.; MacMillan, D. W. C., *J. Am. Chem. Soc.,* **2009,** *131*, 10875-10877.
[54] Narayanam, J. M. R.; Stephenson, C. R. J., *Chem. Soc. Rev.,* **2011,** *40*, 102-113.
[55] Kalyani, D.; McMurtrey, K. B.; Neufeldt, S. R.; Sanford, M. S., *J. Am. Chem. Soc.,* **2011,** *133*, 18566-18569.
[56] Ischay, M. A.; Anzovino, M. E.; Du, J.; Yoon, T. P., *J. Am. Chem. Soc.,* **2008,** *130*, 12886-12887.
[57] Yoon, T. P.; Ischay, M. A.; Du, J., *Nat. Chem.,* **2010,** *2*, 527-532.
[58] Du, J.; Skubi, K. L.; Schultz, D. M.; Yoon, T. P., *Science,* **2014,** *344*, 392-396.
[59] Perepichka, I.; Kundu, S.; Hearne, Z.; Li, C.-J., *Org. Biomol. Chem.,* **2015,** *13*, 447-451.
[60] Buschmann, H.; Scharf, H.-D.; Hoffmann, N.; Esser, P., *Angew. Chem. Int. Ed.,* **1991,** *30*, 477-515.
[61] Nicewicz, D. A.; MacMillan, D. W. C., *Science,* **2008,** *322*, 77.
[62] Yoon, T. P.; Ischay, M. A.; Du, J., *Nat. Chem.,* **2010,** *2*, 527.
[63] Du, J.; Skubi, K. L.; Schultz, D. M.; Yoon, T. P., *Science,* **2014,** *344*, 392.
[64] Teegardin, K.; Day, J. I.; Chan, J.; Weaver, J., *Org. Process Res. Dev.,* **2016,** *20*, 1156-1163.
[65] Basle, O.; Li, C. J., *Green Chem.,* **2007,** *9*, 1047-1050.
[66] Condie, A. G.; González-Gómez, J. C.; Stephenson, C. R. J., *J. Am. Chem. Soc.,* **2010,** *132*, 1464-1465.

[67] Rueping, M.; Koenigs, R. M.; Poscharny, K.; Fabry, D. C.; Leonori, D.; Vila, C., *Chem. Eur. J.,* **2012,** *18*, 5170-5174.
[68] Boess, E.; Schmitz, C.; Klussmann, M., *J. Am. Chem. Soc.,* **2012,** *134*, 5317-5325.
[69] Lowry, M. S.; Goldsmith, J. I.; Slinker, J. D.; Rohl, R.; Pascal, R. A.; Malliaras, G. G.; Bernhard, S., *Chem. Mat.,* **2005,** *17*, 5712-5719.
[70] Panera, M.; Díez, J.; Merino, I.; Rubio, E.; Gamasa, M. P., *Inorg. Chem.,* **2009,** *48*, 11147-11160.
[71] Rueping, M.; Koenigs René, M.; Poscharny, K.; Fabry David, C.; Leonori, D.; Vila, C., *Chem. Eur. J.,* **2012,** *18*, 5170-5174.
[72] Zhang, J.; Wei, C.; Li, C.-J., *Tetrahedron Lett.,* **2002,** *43*, 5731-5733.
[73] Kwong, F. Y.; Klapars, A.; Buchwald, S. L., *Org. Lett.,* **2002,** *4*, 581-584.
[74] Nauth Alexander, M.; Otto, N.; Opatz, T., *Adv. Synth. Catal.,* **2015,** *357*, 3424-3428.
[75] Zeng, T.; Song, G.; Moores, A.; Li, C.-J., *Synlett,* **2010**, 2002-2008.
[76] Slinker, J. D.; Gorodetsky, A. A.; Lowry, M. S.; Wang, J.; Parker, S.; Rohl, R.; Bernhard, S.; Malliaras, G. G., *J. Am. Chem. Soc.,* **2004,** *126*, 2763-2767.
[77] Sprouse, S.; King, K. A.; Spellane, P. J.; Watts, R. J., *J. Am. Chem. Soc.,* **1984,** *106*, 6647-6653

Chapter 5 – Conclusions and Contributions to Knowledge

Over the years, the Li group has explored innovative chemical reactivity to develop sustainable molecular transformations. Typical examples include Grignard type reactions in water, alkyne-aldehyde-amine coupling (A^3-coupling) and cross-dehydrogenative-coupling (CDC) reactions. Aligned with this major theme, the development of mild and selective methods for the functionalization of simple C–H bonds is an important challenge in organic chemistry (Chapter 1). In this dissertation we have explored Au-, Rh- and Ir/Cu-catalyzed C–H functionalization as a means to achieve this goal. Specifically, we have designed syntheses that promote C–H activation, site-selective functionalization and molecular complexity formation.

The first step towards the functionalization of C-H bonds, was the successful development of a highly efficient gold(I)-catalyzed one-pot coupling of amides, aldehydes and alkynes for the synthesis of oxazoles. This transformation made use of a single catalyst to accomplish the A^3 coupling via sp C-H activation and the cyclization reaction, to produce oxazole derivatives. The multicomponent strategy proved to be atom economical and a convenient alternative to construct important heterocyclic compounds, since water was the only side product. The new method found to rapidly construct tri-substituted oxazoles possesses conceivable implications for polymer synthesis, chemical biology, and natural product synthesis.

With the above-mentioned methodology, one-pot sp^2 C-H functionalization and coupling of amides, aldehydes and terminal alkynes was developed. Indene-amines were successfully produced by a rhodium-catalyzed sp^2 C-H functionalization reaction. Under very mild reaction conditions, the in-situ formed imines were found to be an effective and traceless directing group for the rhodium-catalyzed annulation reaction. The reaction showed excellent regioselectivity and featured a great atom-economy. This process occurred at room-temperature, and water was the only stoichiometric side-product. Furthermore, the synthetic viability and efficiency of this process towards a large range of functional groups was presented, opening up new possibilities for late-stage

functionalization of value-added compounds. Thanks to computational investigations, the mechanism of the rhodium-catalyzed C-H activation was elucidated. Additionally, DFT calculations revealed that the regioselectivity was essentially governed by electronic effects.

Lastly, we successfully developed a highly efficient light-mediated coupling method for the direct asymmetric functionalization of sp^3 C–H bonds. The use of $Ir(ppy)_2(dtbbpy)PF_6$ as photoredox catalyst and copper catalyst, provided a novel and facile approach for the arylation of N-arylated tetrahydroisoquinolines with arylboronic acids. The combination of copper salts and PhPyBox as chiral ligand have demonstrated its efficiency producing good enantioselectivity and tolerated a fairly diverse substrate scope. We envisioned that this visible light-mediated asymmetric arylation reaction could be extended to other types of C-H bonds.

The reactions described in this thesis characterize our efforts to develop C-H bond functionalization reactions for the chemistry community. Our goal was to make chemistry easier, more applicable and greener by using simple molecules with ubiquitous C-H bonds, exploiting the different reactivity of their hybridization (*sp*, sp^2 and sp^3), and developing syntheses involving C-H bond activation that produce complexity and high-valued targets. We believe that our work has brought us closer to that goal. In today's evolution of modern chemistry, the synthesis of new and interesting products is extremely important. As for our work, the majority of synthesized products described in this thesis have never been previously reported. Therefore, the panel of molecules that we synthesized may find applications in biological chemistry, medicinal chemistry, and materials design. We strongly believe that we contributed positively to help the evolution of modern chemistry.

Chapter 6 – Future Work

With the enormous endeavour of developing C-H bond functionalization reactions, this C-H bond functionalization field has become a key concept that cannot be ignored in the design of synthetic molecules. Our effort to make annulation reactions as described in Chapter 2 and 3, oriented our curiosity to this area.

As presented in Chapter 2, Indene-amines were successfully produced by a rhodium-catalyzed sp^2 C-H functionalization reaction. By using imines as a directing group, the annulation reaction was found to be extremely effective. Also, the alkynes were efficiently added into the Rh-C bond under mild conditions to produce indenes derivatives. However, under these reaction conditions, the addition of alkenes into the Rh-C bond were not achieved efficiently and thus, would need further improvements.[1-5] The multicomponent reaction with alkenes would generate indane derivatives. Based on the proposed mechanism, *i.e.* C-H bond activation, addition of alkyne followed by annulation reaction, a modification of reaction conditions can be envisioned to favor alkene addition (Scheme 110).

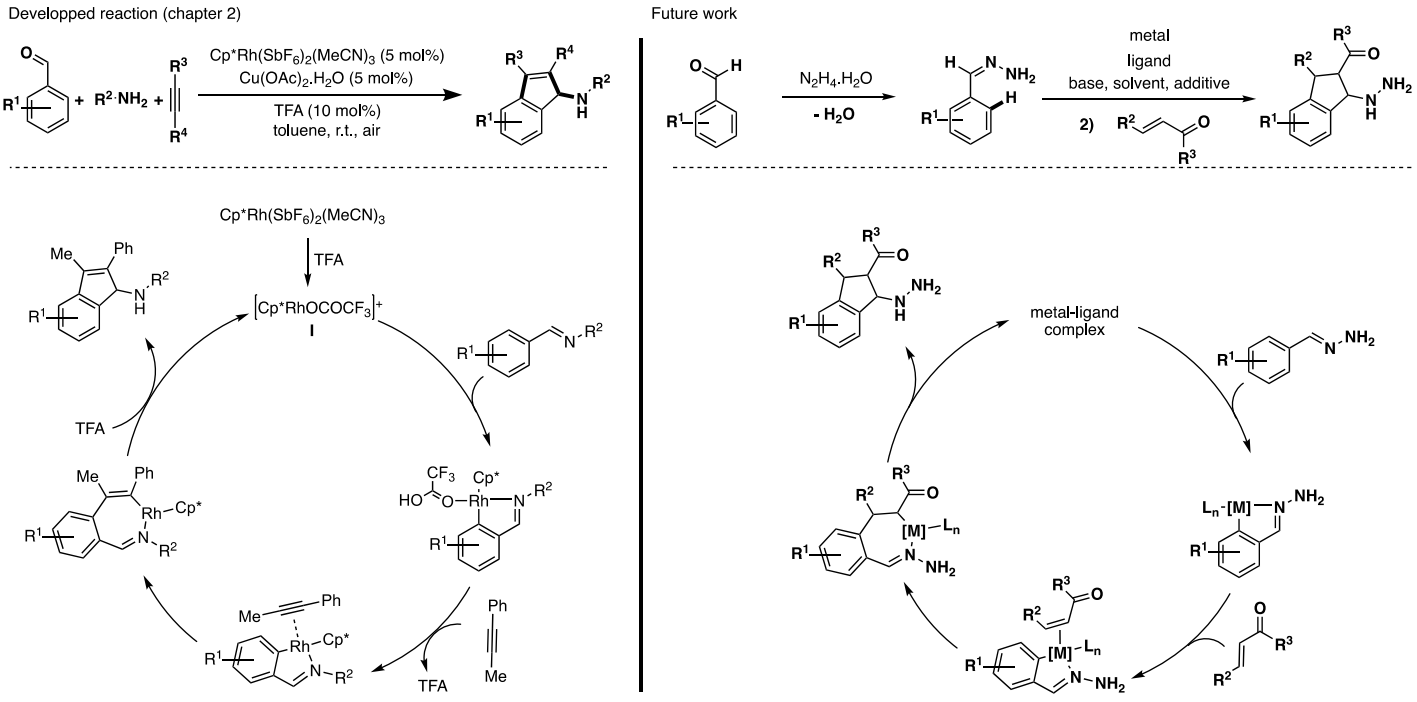

Scheme 110. Developed reaction in chapter 2 and future work

The modification of the directing group from an imine to the corresponding hydrazone is also of interest.[6] Recently, our laboratory discovered a catalytic, ruthenium-based, and efficient methodology for additions of aldehydes to carbonyl compounds (Scheme 111, a).[7-8] After the development of alkene addition into *sp*^{2} C-H bond, the hydrazone directing group can be used in a subsequent addition reaction. With this concept, we expected that many aryl aldehydes can be transformed into 1,2,3,4-tetrahydronaphthalene derivatives (Scheme 111, b).

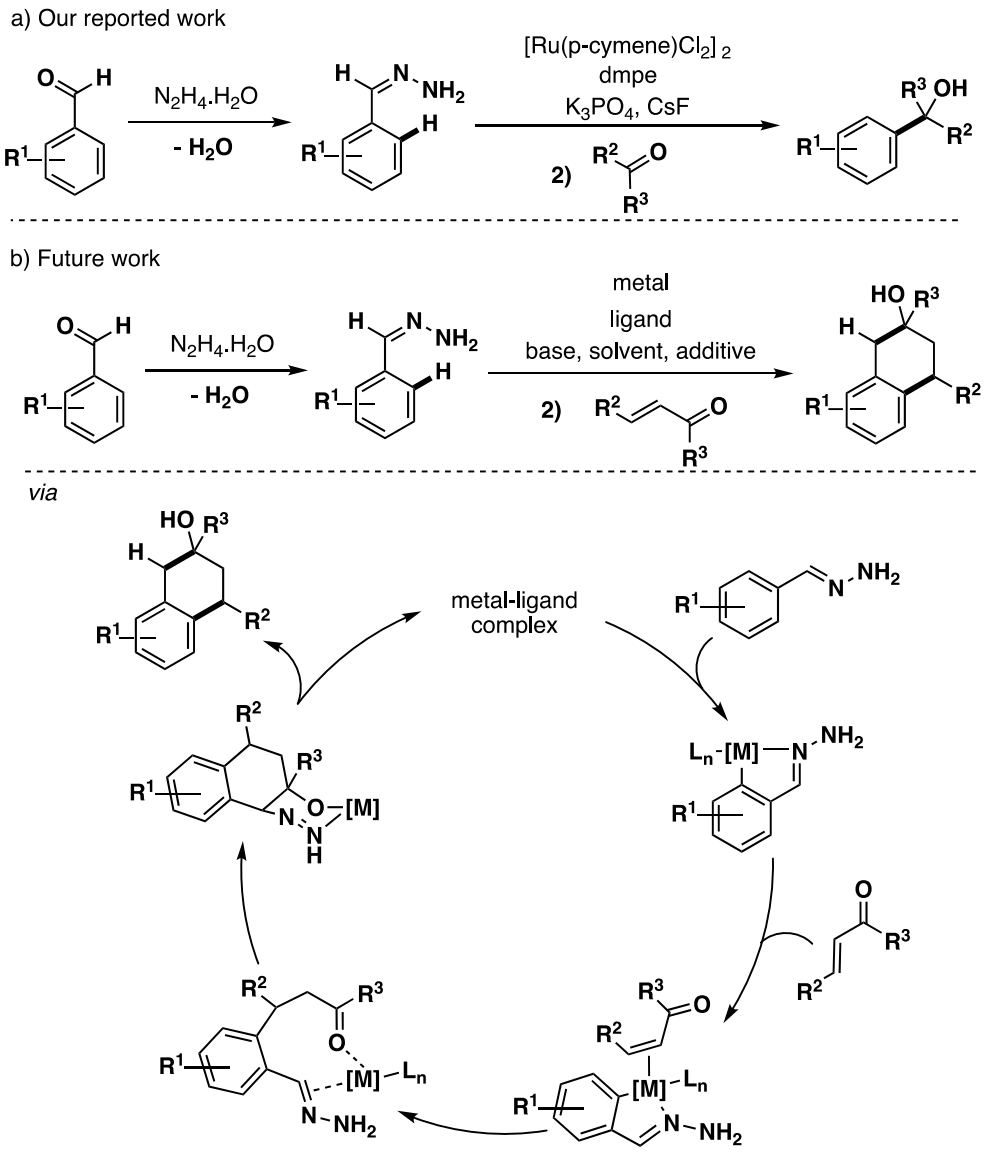

Scheme 111. Future work: C-H activation and umpolung of carbonyl group

6.1 References

[1] Wang, D.-H.; Engle, K. M.; Shi, B.-F.; Yu, J.-Q., *Science,* **2010,** *327*, 315-319.

[2] Ackermann, L., *Chem. Rev.,* **2011,** *111*, 1315-1345.

[3] Mo, F.; Dong, G., *Science,* **2014,** *345*, 68-72.

[4] Gao, Y.; Gao, Y.; Wu, W.; Jiang, H.; Yang, X.; Liu, W.; Li, C.-J., *Chem. Eur. J.,* **2017,** *23*, 793-797.

[5] Piou, T.; Romanov-Michailidis, F.; Romanova-Michaelides, M.; Jackson, K. E.; Semakul, N.; Taggart, T. D.; Newell, B. S.; Rithner, C. D.; Paton, R. S.; Rovis, T., *J. Am. Chem. Soc.,* **2017,** *139*, 1296-1310.

[6] Zheng, L.; Hua, R., *Chem. Eur. J.,* **2014,** *20*, 2352-2356.

[7] Wang, H.; Dai, X.-J.; Li, C.-J., *Nat. Chem.,* **2017,** *9*, 374-378.

[8] Dai, X. J.; Wang, H.; Li, C. J., *Angew. Chem. Int. Ed.,* **2017,** *56*, 6302-6306.

Supporting information

Spectra for compounds in Chapter 2

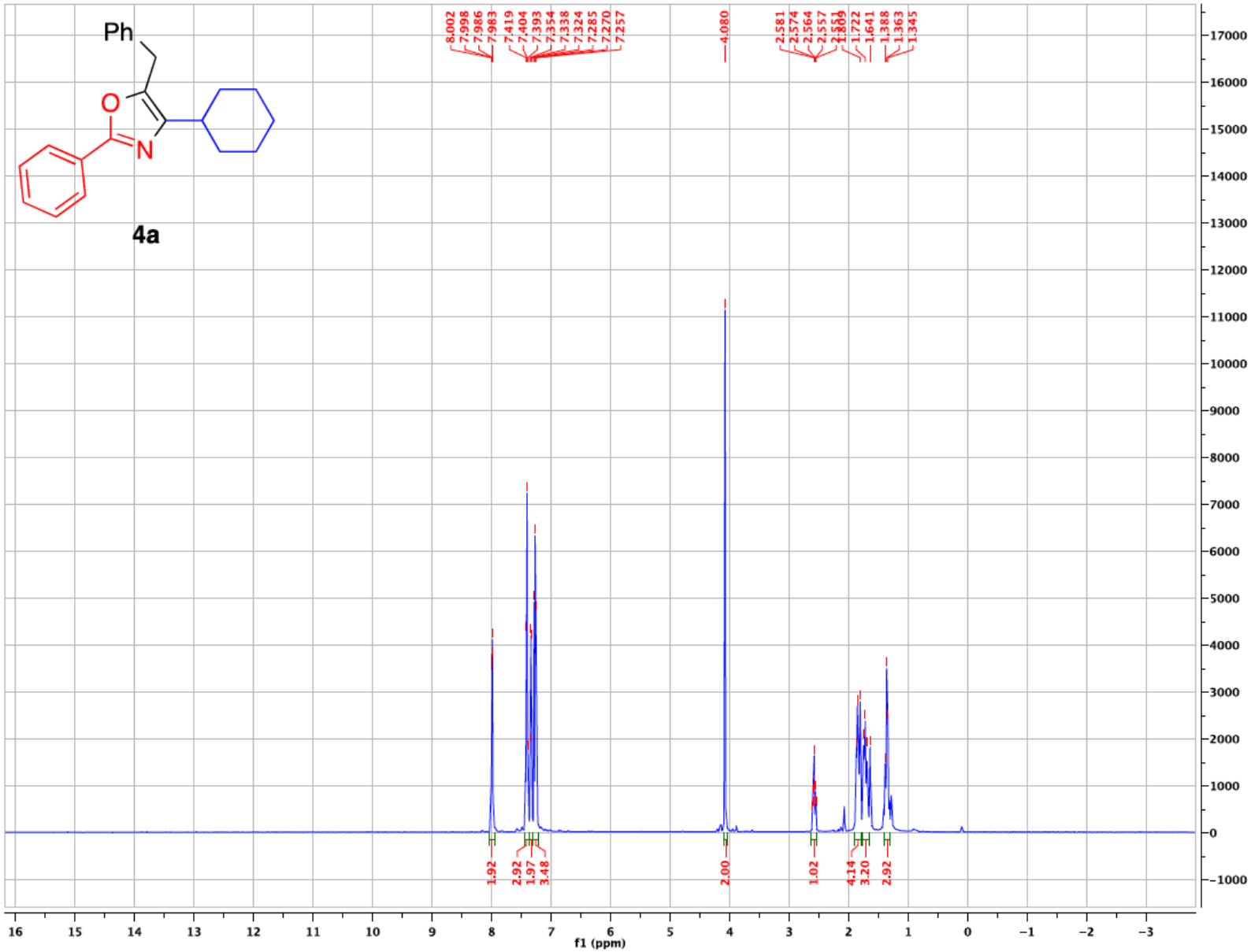
Ph
O
N
4a
8.002
7.998
7.986
7.983
7.419
7.404
7.393
7.354
7.338
7.324
7.285
7.270
7.257
4.080
2.581
2.574
2.564
2.557
2.551
1.809
1.722
1.641
1.388
1.363
1.345
1.92
2.92
1.97
3.48
2.00
1.02
4.14
3.20
2.92
f1 (ppm)

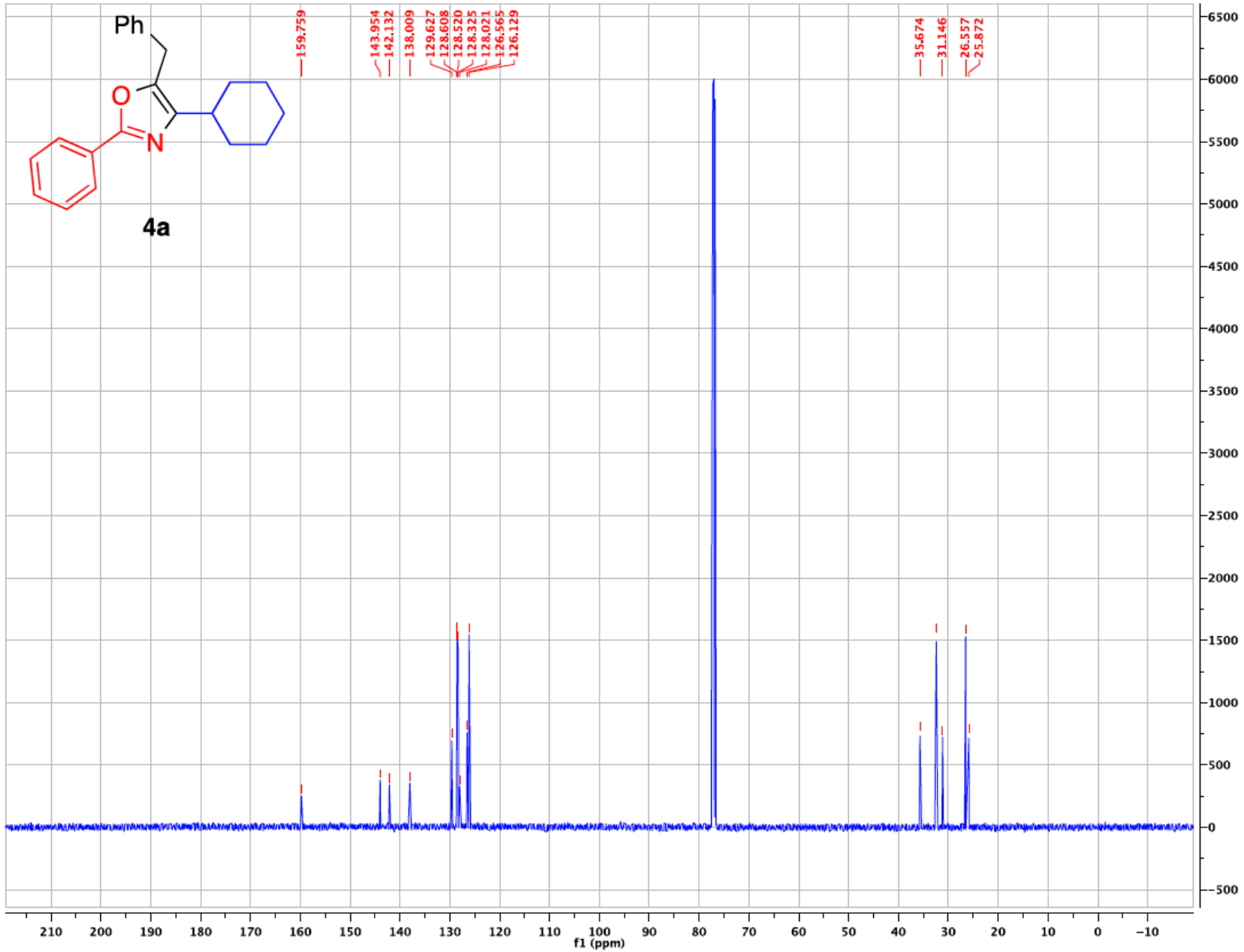
Ph
O
N
4a
159.759
143.954
142.132
138.009
129.627
128.608
128.520
128.325
128.021
126.565
126.129
35.674
31.146
26.557
25.872
f1 (ppm)

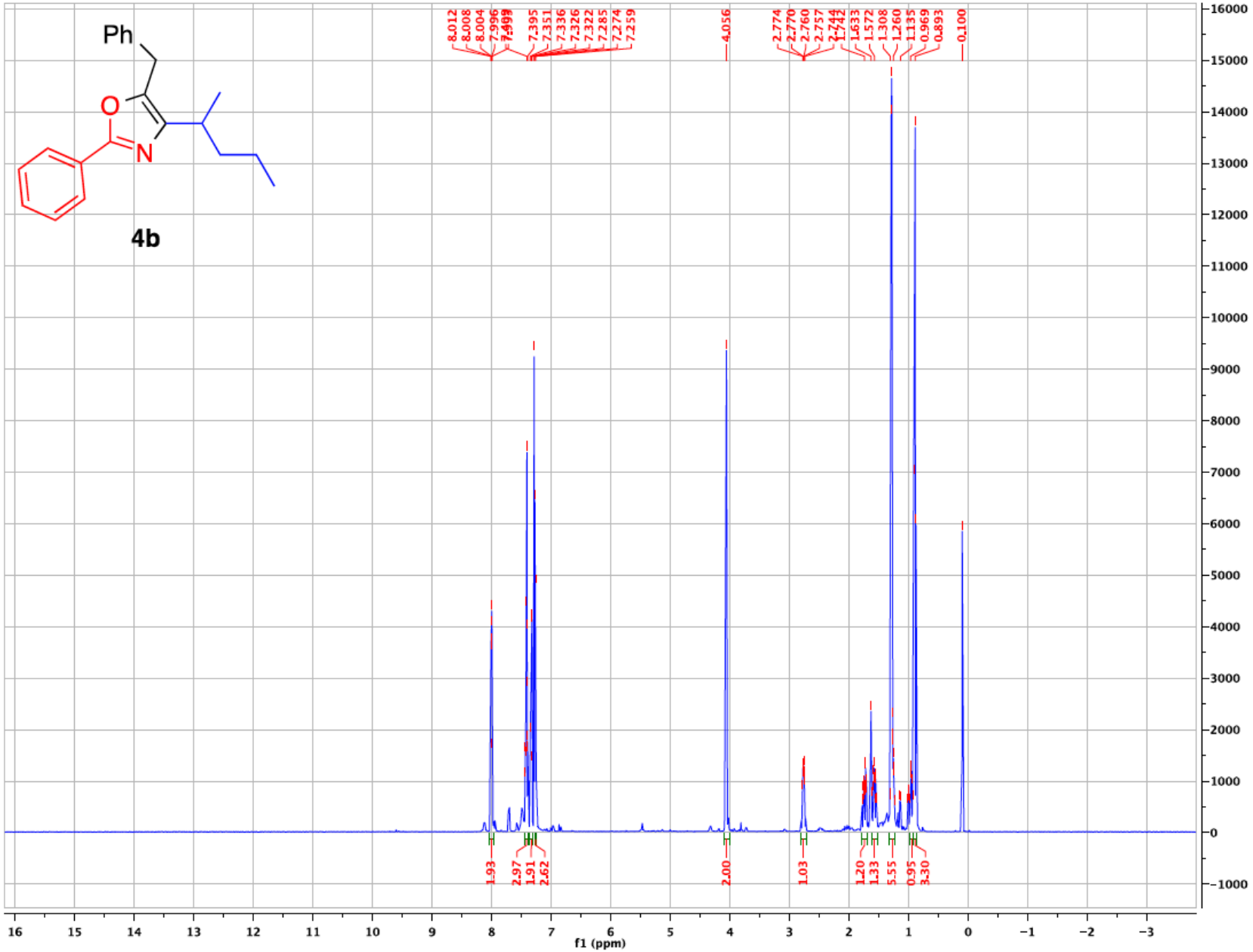
Ph
O
N
4b
8.012
8.008
8.004
7.996
7.395
7.351
7.336
7.326
7.322
7.285
7.274
7.259
4.056
2.774
2.770
2.760
2.757
1.633
1.572
1.308
1.260
1.135
0.969
0.893
0.100
1.93
2.97
1.91
2.62
2.00
1.03
1.20
1.33
5.55
0.95
3.30
f1 (ppm)

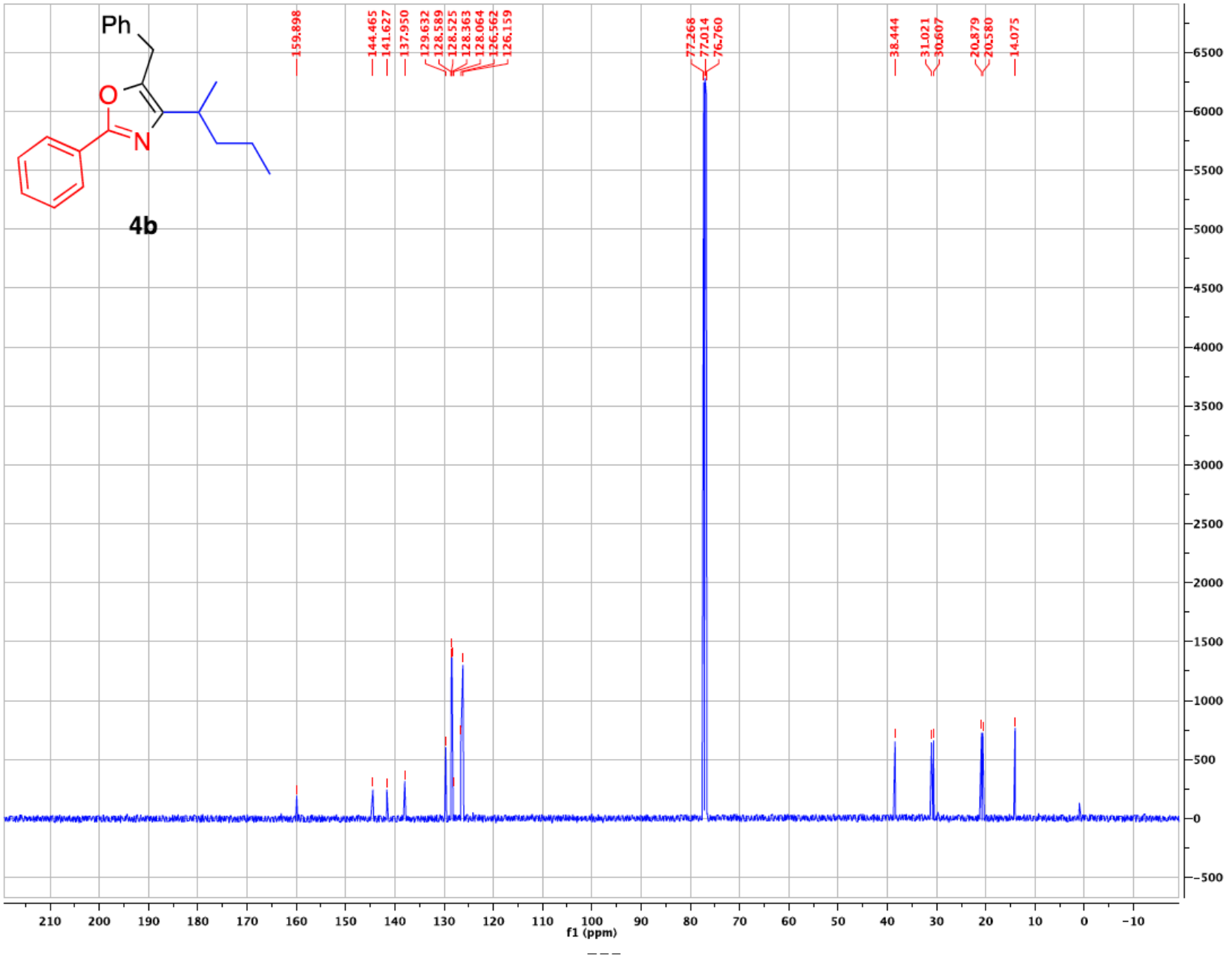
Ph
O
N
4b
159.898
144.465
141.627
137.950
129.632
128.589
128.525
128.363
128.064
126.562
126.159
77.268
77.014
76.760
38.444
31.021
30.607
20.879
20.580
14.075
f1 (ppm)

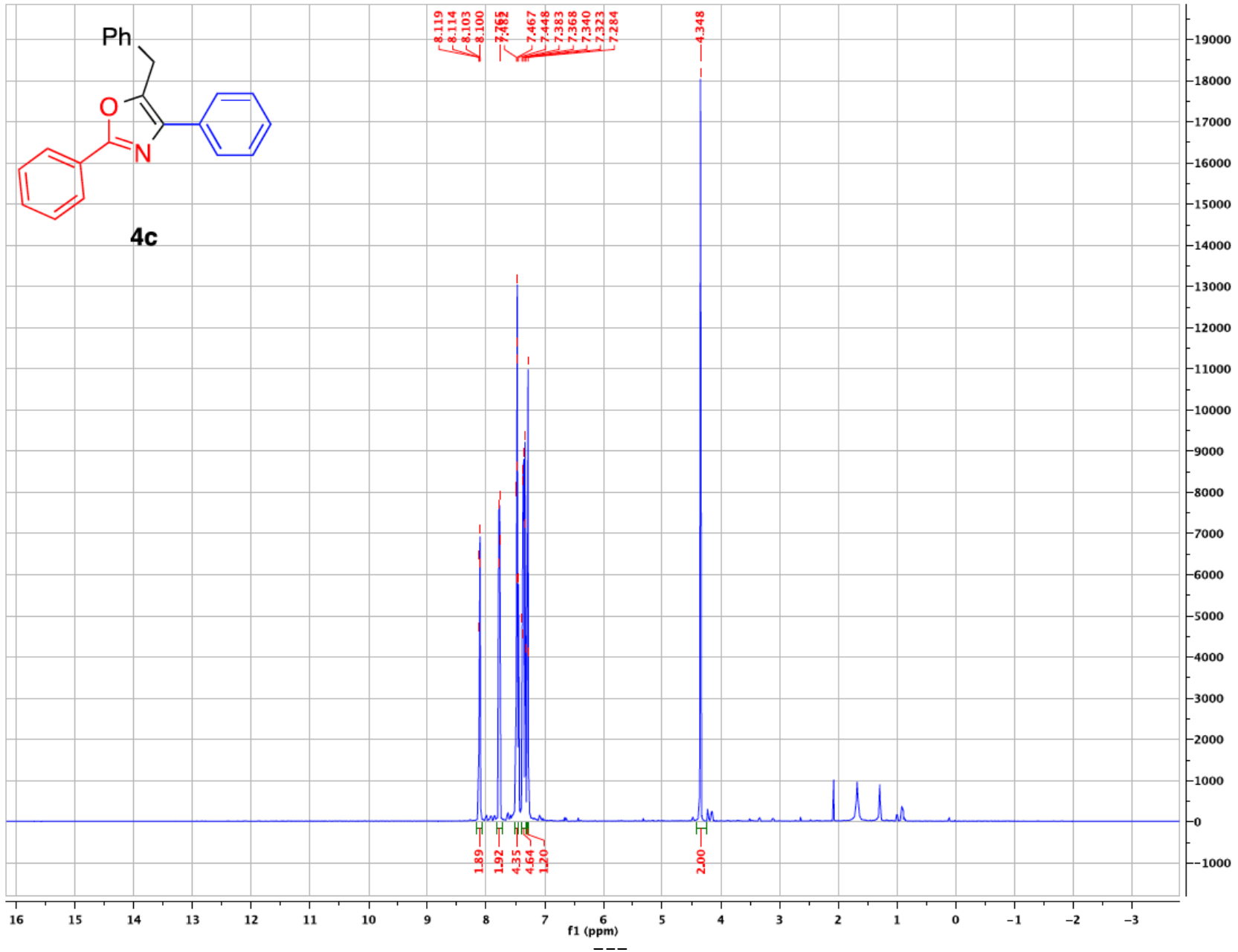
Ph
O
N
4c
8.119
8.114
8.103
8.100
7.482
7.467
7.448
7.383
7.368
7.340
7.323
7.284
4.348
1.89
1.92
4.35
4.64
1.20
2.00
f1 (ppm)

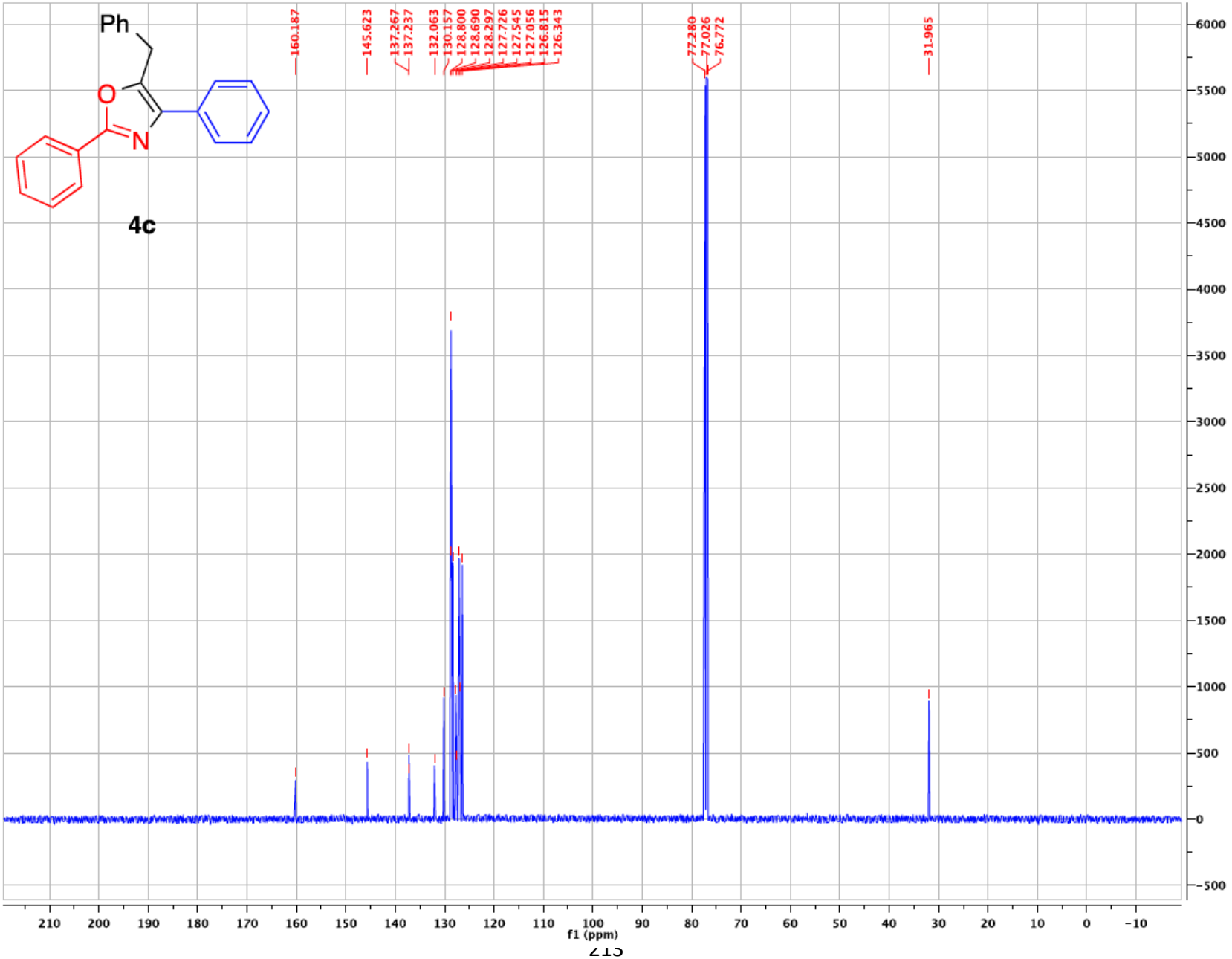
Ph
O
N
4c
160.187
145.623
137.267
137.237
132.063
130.157
128.800
128.690
128.297
127.726
127.545
127.056
126.815
126.343
77.280
77.026
76.772
31.965
f1 (ppm)

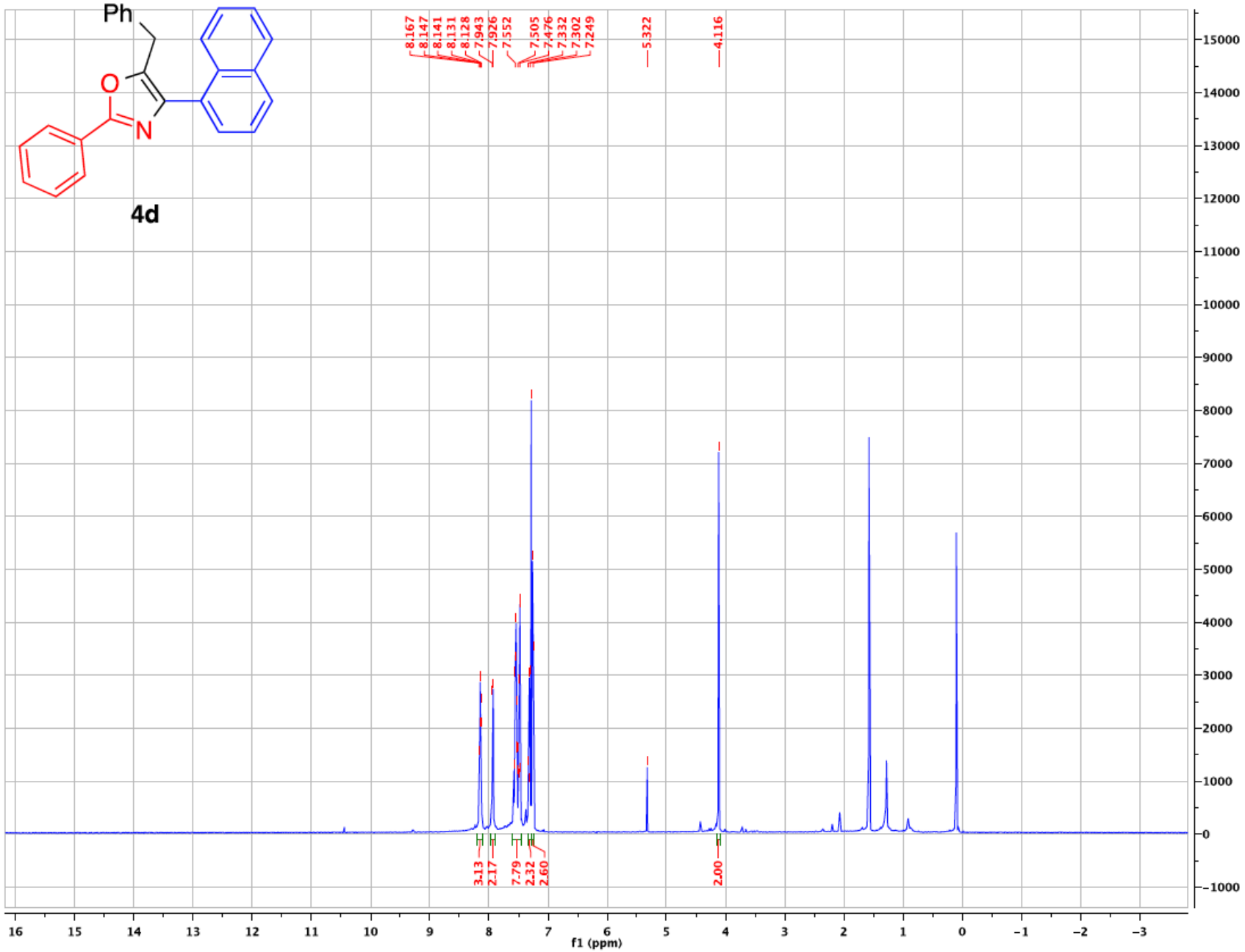
Ph
O
N
4d
8.167
8.147
8.141
8.131
8.128
7.943
7.926
7.552
7.505
7.476
7.332
7.302
7.249
5.322
4.116
3.13
2.17
7.79
2.32
2.60
2.00
f1 (ppm)

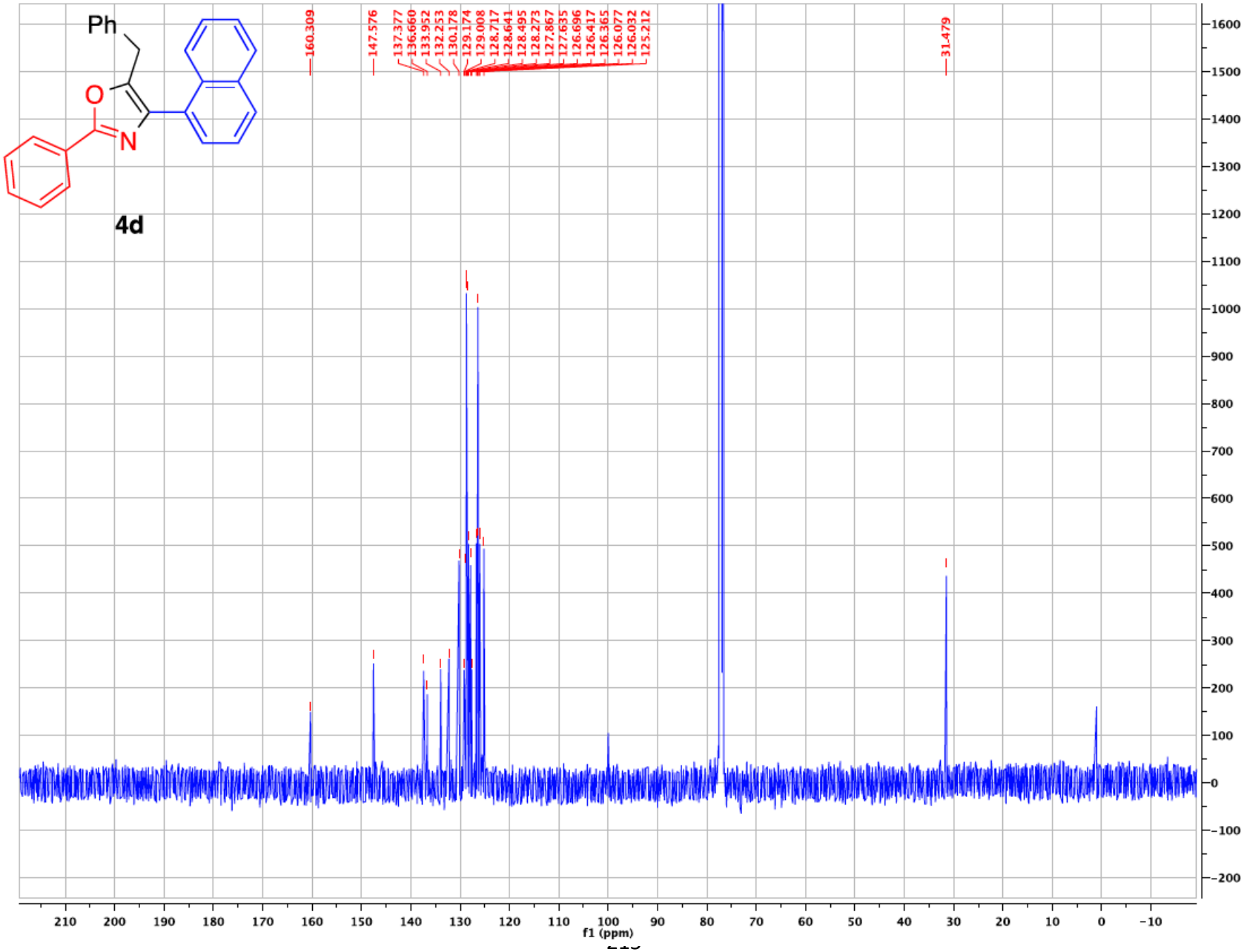
Ph
O
N
4d
160.309
147.576
137.377
136.660
133.952
132.253
130.178
129.174
129.008
128.717
128.641
128.495
128.273
127.867
127.635
126.696
126.417
126.365
126.077
126.032
125.212
31.479
f1 (ppm)

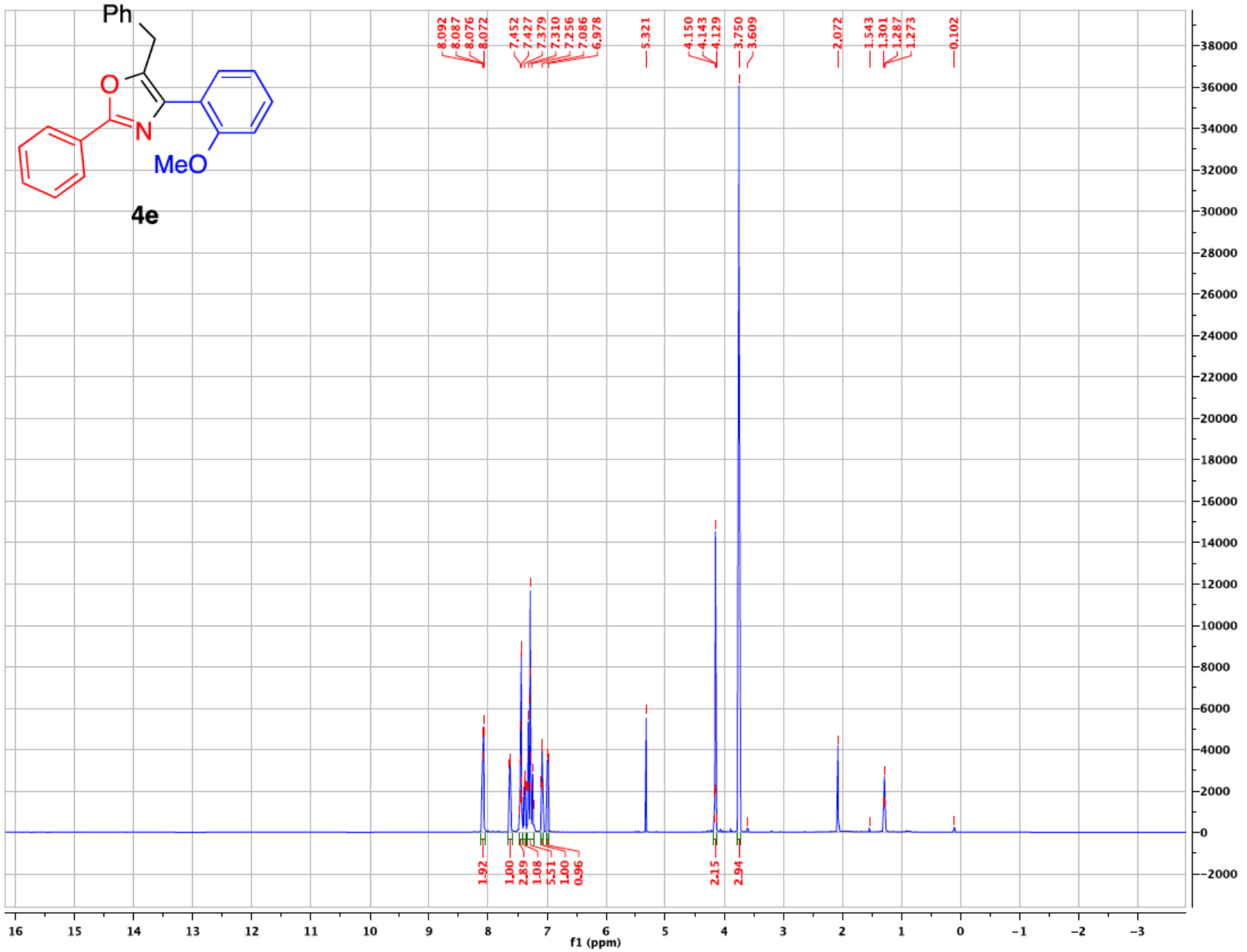
Ph
O
N
MeO
4e
8.092
8.087
8.076
8.072
7.452
7.427
7.379
7.310
7.256
7.086
6.978
5.321
4.150
4.143
4.129
3.750
3.609
2.072
1.543
1.301
1.287
1.273
0.102
1.92
1.00
2.89
1.08
5.51
1.00
0.96
2.15
2.94
f1 (ppm)

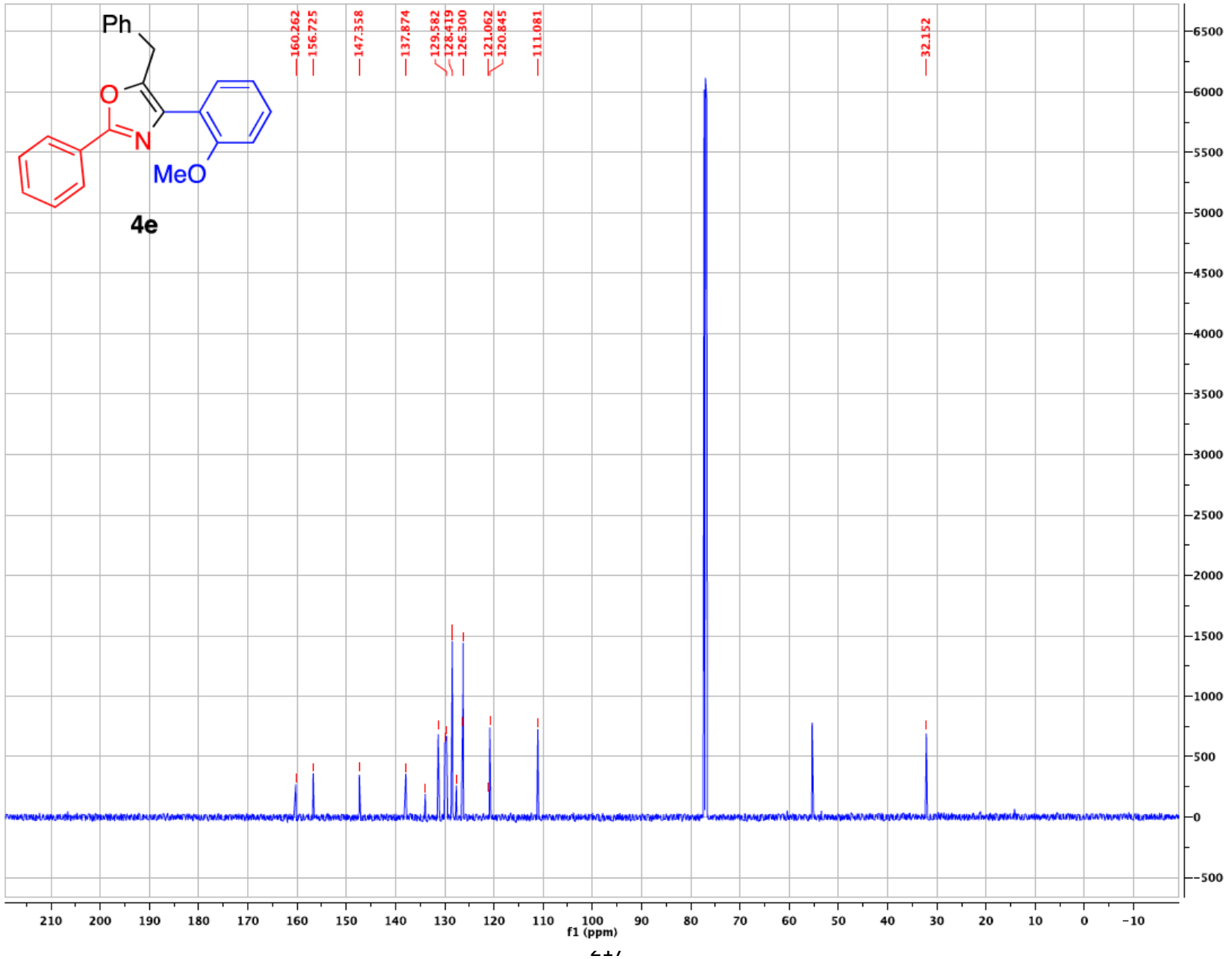
Ph
O
N
MeO
4e
160.262
156.725
147.358
137.874
129.582
128.419
126.300
121.062
120.845
111.081
32.152
f1 (ppm)

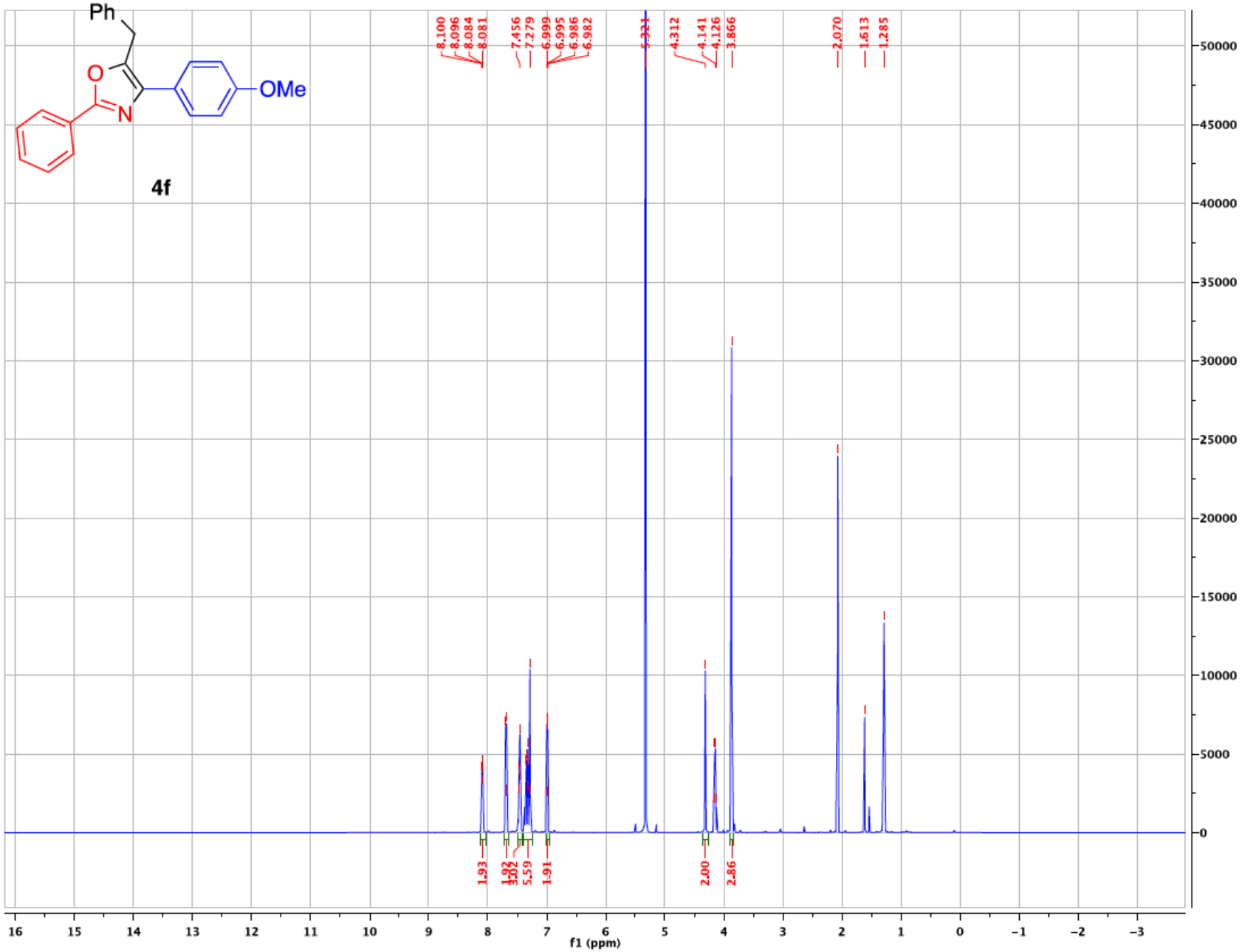
Ph
O
N
OMe
4f
8.100
8.096
8.084
8.081
7.456
7.279
6.999
6.995
6.986
6.982
5.321
4.312
4.141
4.126
3.866
2.070
1.613
1.285
1.93
1.82
3.02
5.59
1.91
2.00
2.86
f1 (ppm)

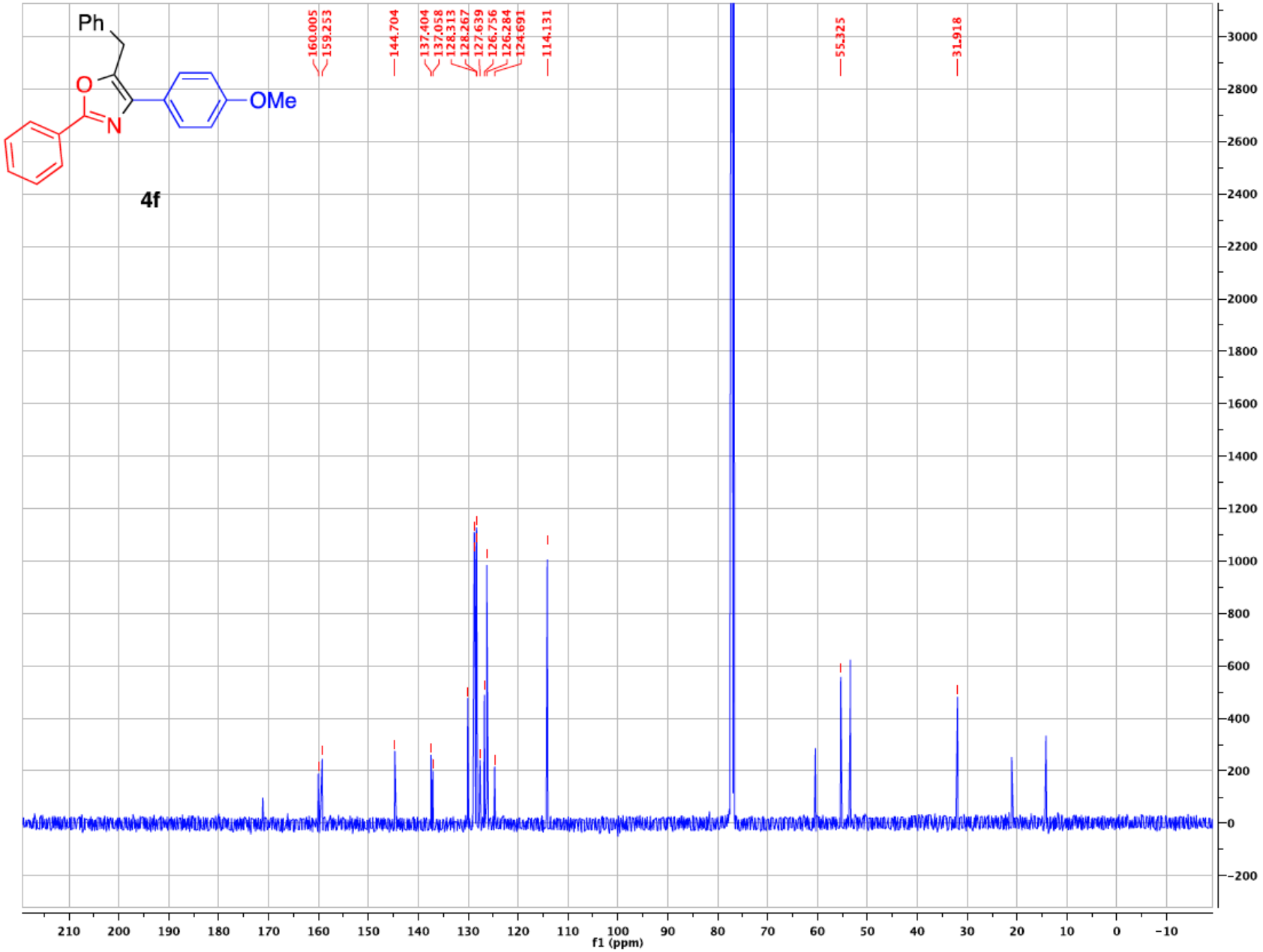
Ph
O
N
OMe
4f
160.005
159.253
144.704
137.404
137.058
128.313
128.267
127.639
126.756
126.284
124.691
114.131
55.325
31.918
f1 (ppm)

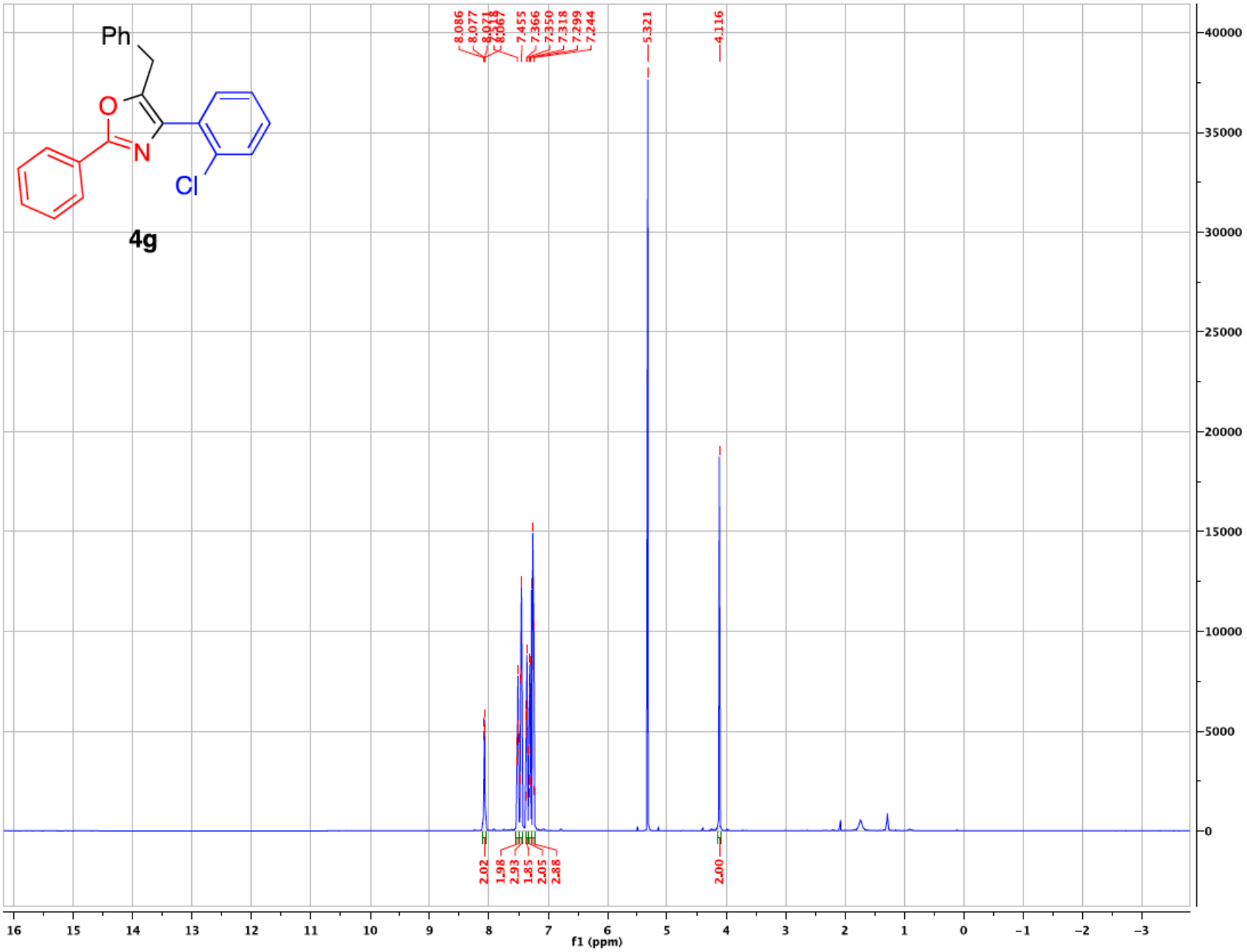
Ph
O
N
Cl
4g
8.086
8.077
8.071
8.067
7.455
7.366
7.350
7.318
7.299
7.244
5.321
4.116
2.02
1.98
2.93
1.85
2.05
2.88
2.00
f1 (ppm)

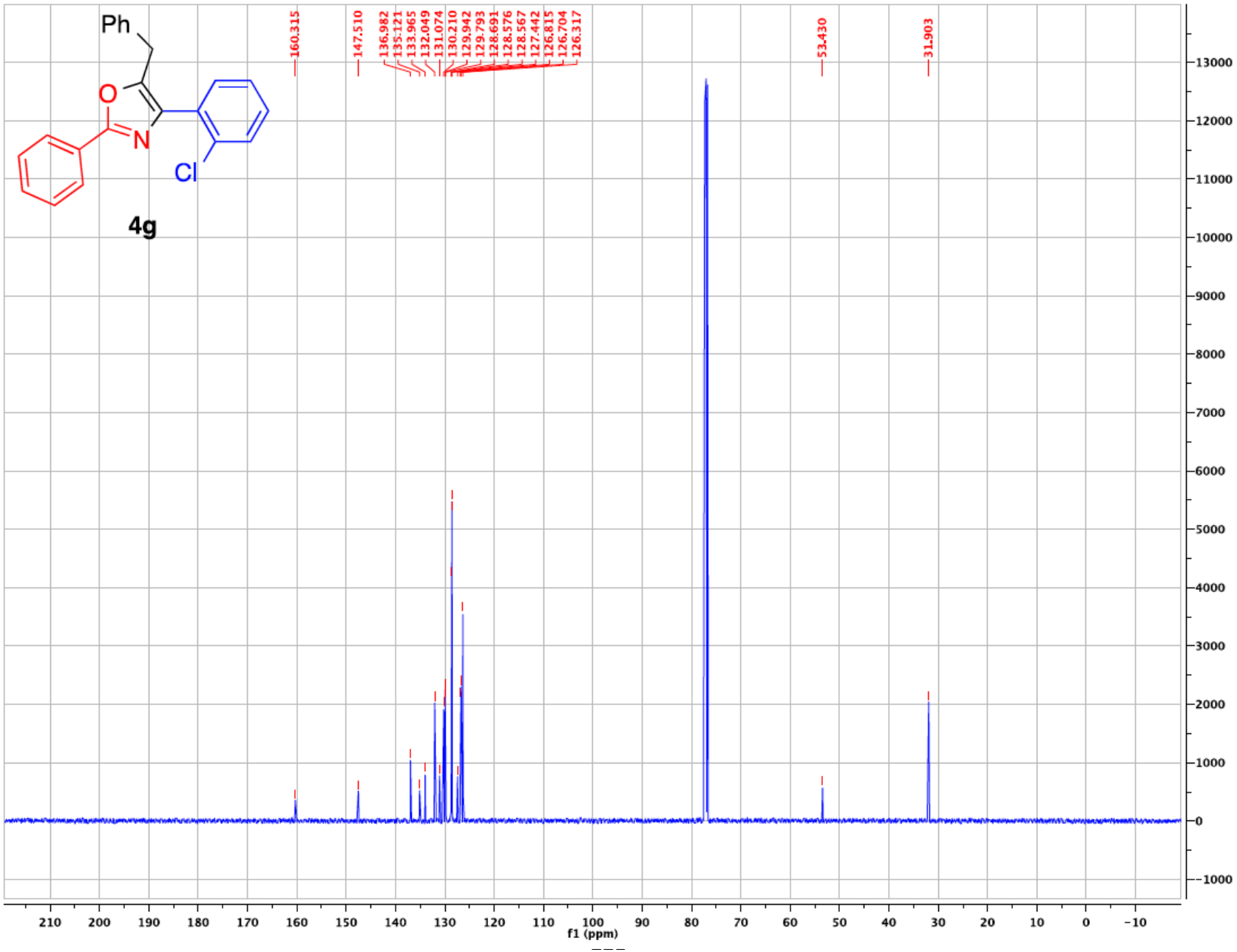
Ph
O
N
Cl
4g
160.315
147.510
136.982
135.121
133.965
132.049
131.074
130.210
129.942
129.793
128.691
128.576
128.567
127.442
126.815
126.704
126.317
53.430
31.903
13000
12000
11000
10000
9000
8000
7000
6000
5000
4000
3000
2000
1000
0
-1000
210
200
190
180
170
160
150
140
130
120
110
100
90
80
70
60
50
40
30
20
10
0
-10
f1 (ppm)

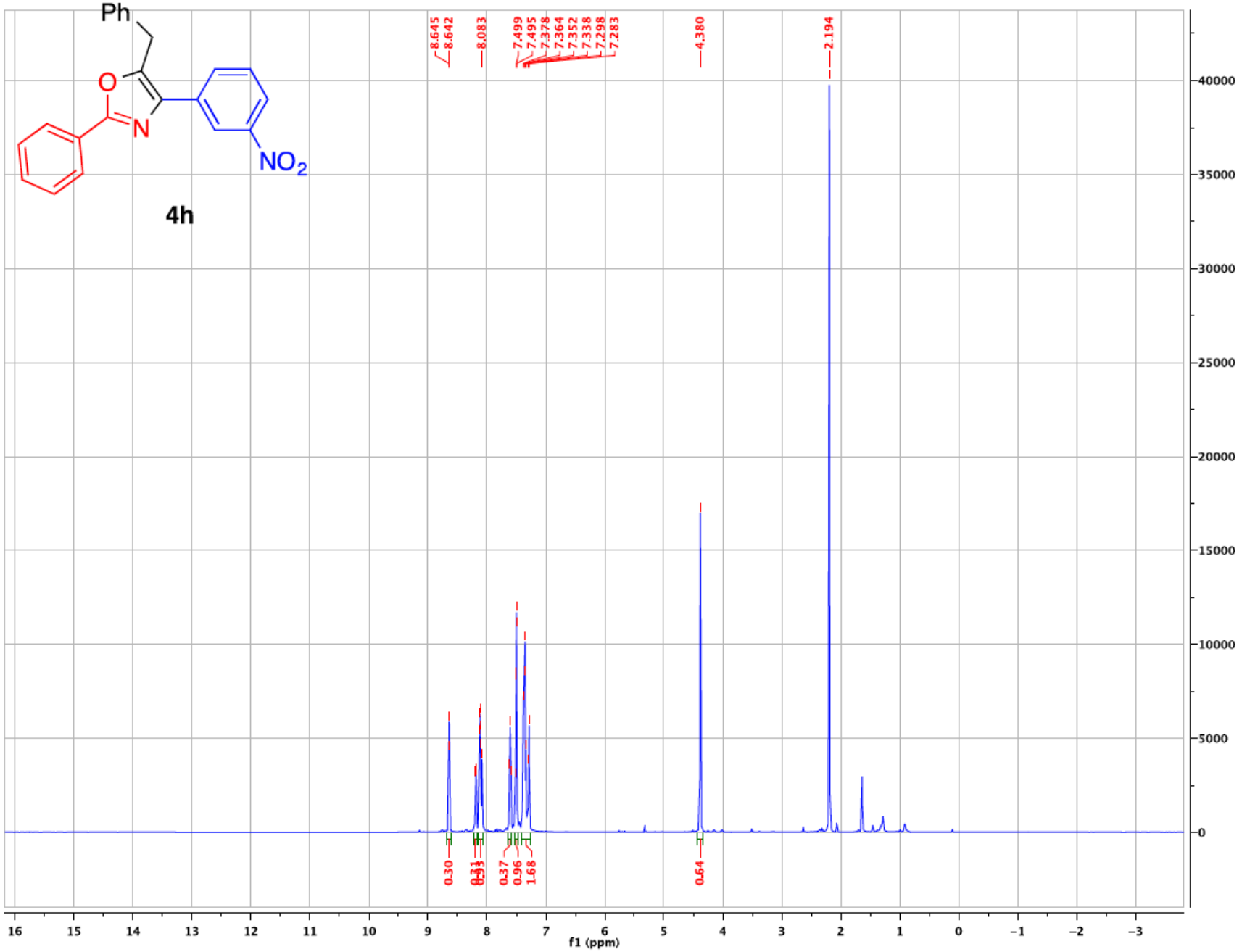
Ph
O
N
NO2
4h
8.645
8.642
8.083
7.499
7.495
7.378
7.364
7.352
7.338
7.298
7.283
4.380
2.194
0.30
0.37
0.96
1.68
0.64
f1 (ppm)

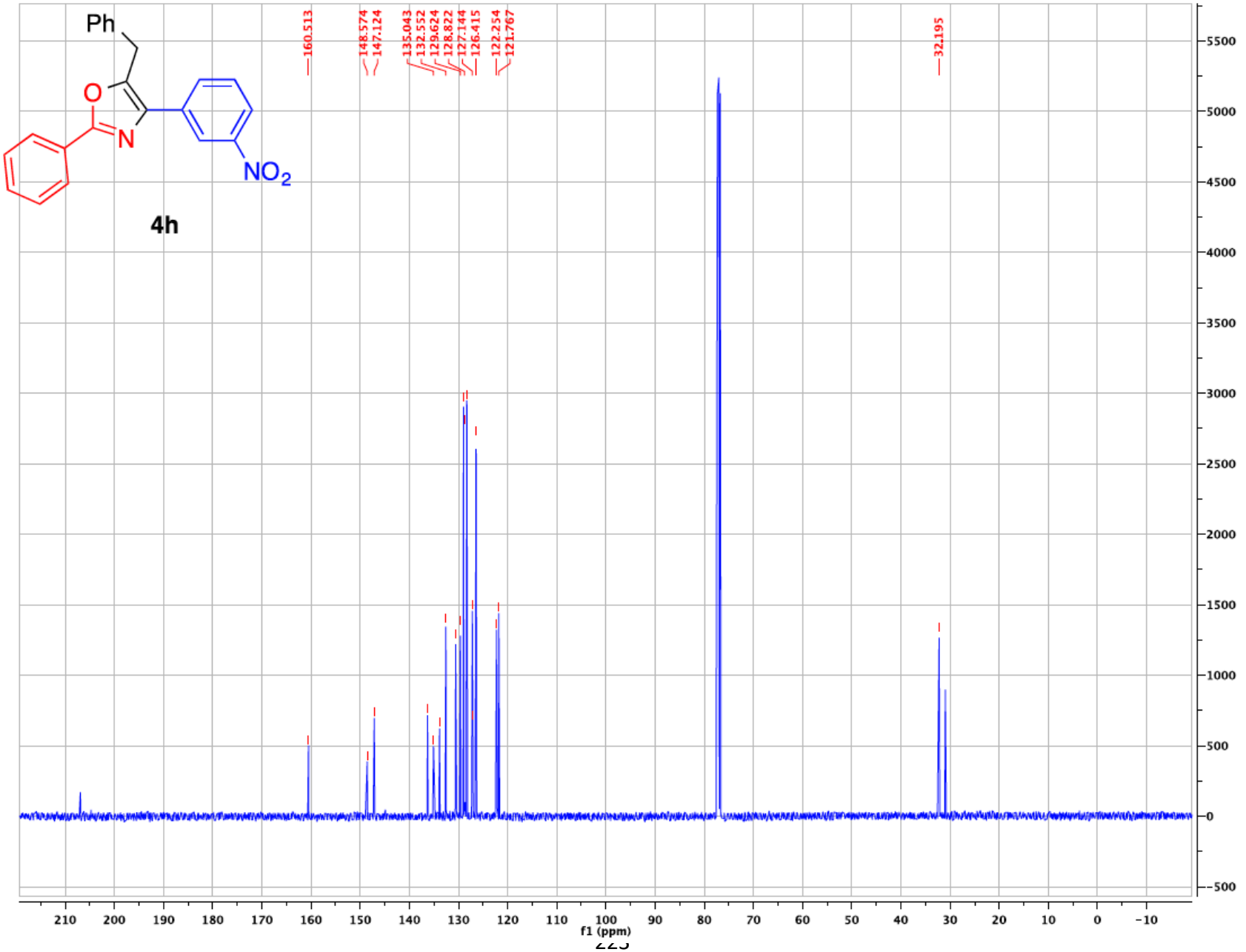
Ph
O
N
NO2
4h
160.513
148.574
147.124
135.043
132.552
129.624
128.822
127.144
126.415
122.254
121.767
32.195
f1 (ppm)

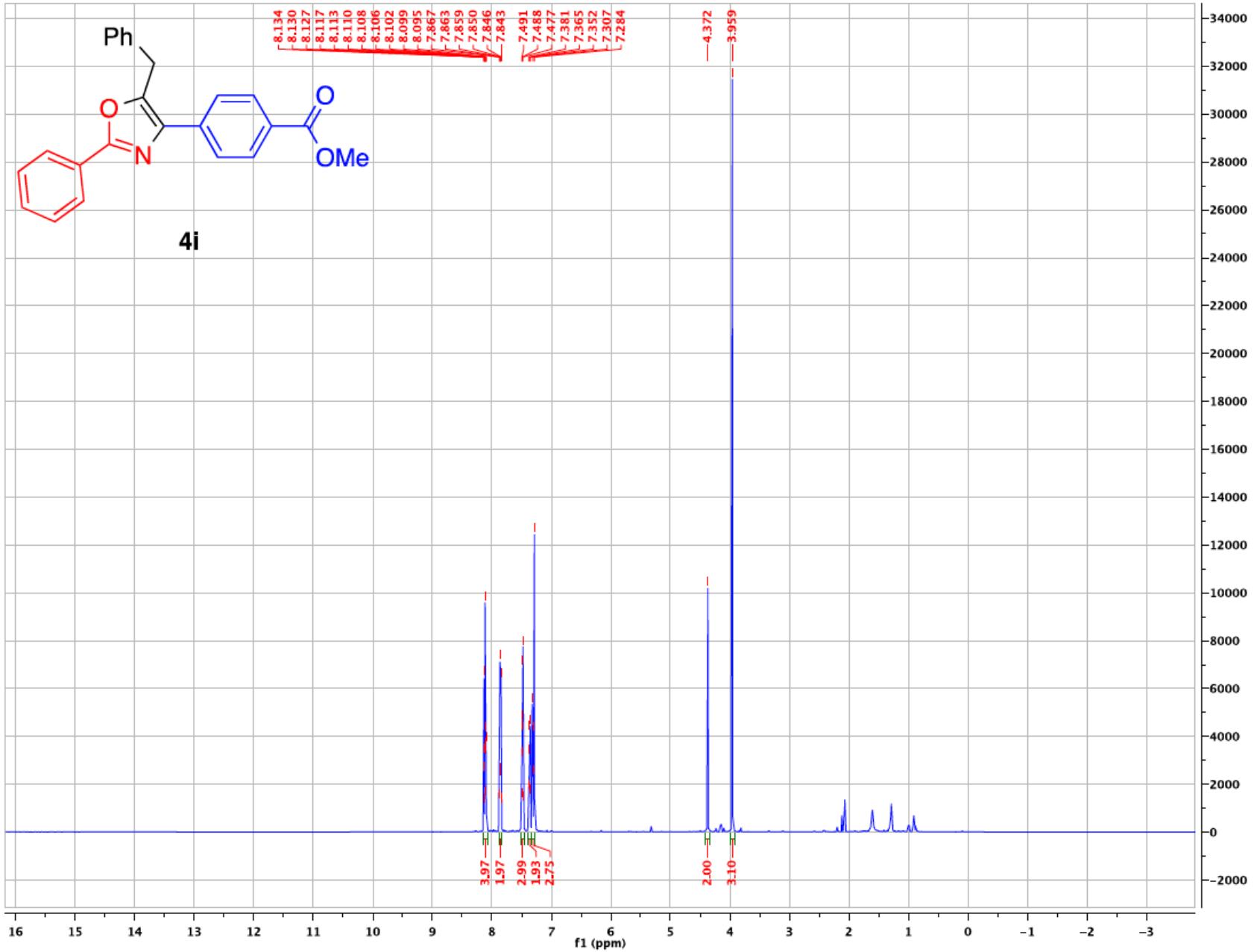
Ph
O
N
O
OMe
4i
8.134
8.130
8.127
8.117
8.113
8.110
8.108
8.106
8.102
8.099
8.095
7.867
7.863
7.859
7.850
7.846
7.843
7.491
7.488
7.477
7.381
7.365
7.352
7.307
7.284
4.372
3.959
3.97
1.97
2.99
1.93
2.73
2.00
3.10
f1 (ppm)

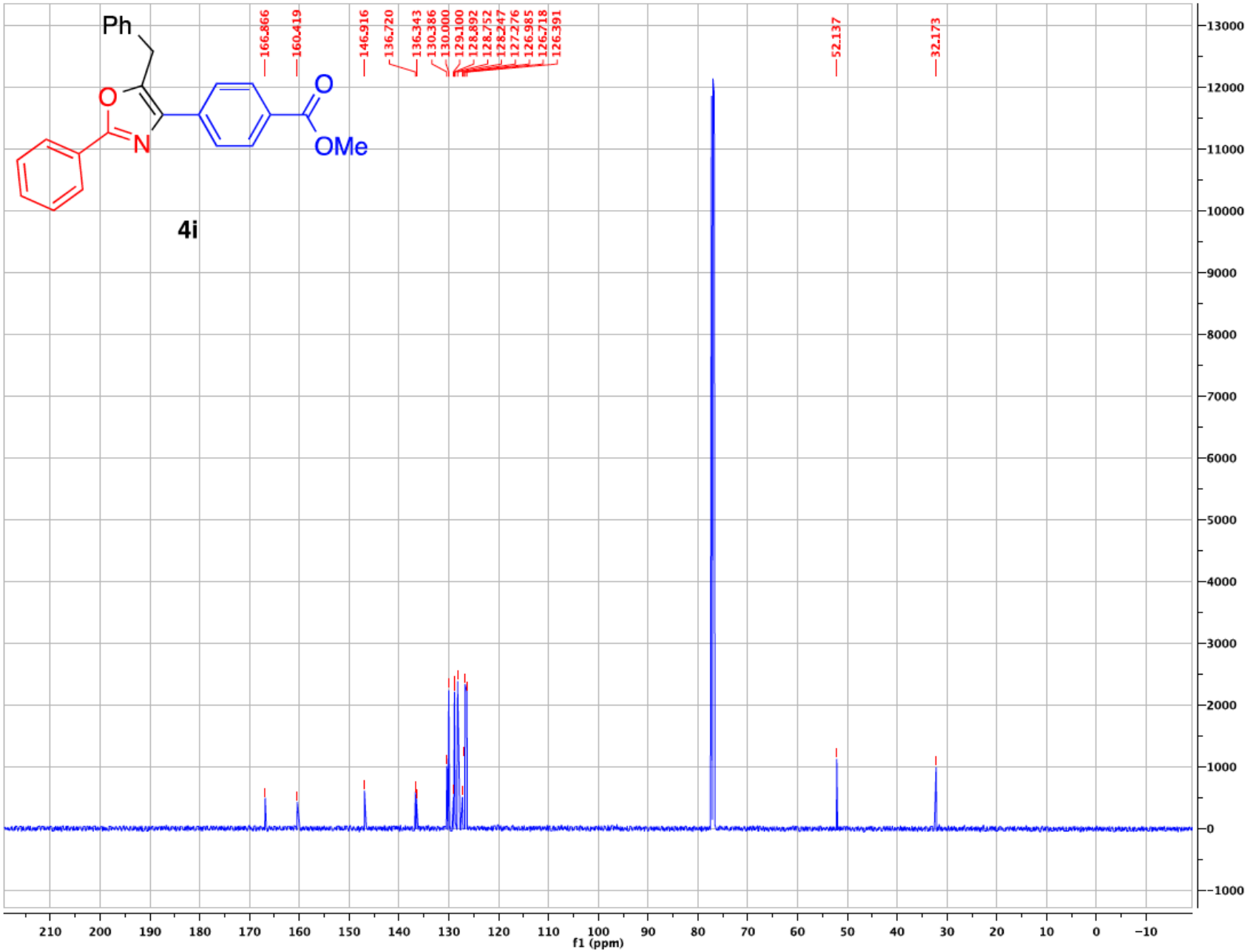
Ph
O
N
O
OMe
4i
166.866
160.419
146.916
136.720
136.343
130.386
130.000
129.100
128.892
128.752
128.247
127.276
126.985
126.718
126.391
52.137
32.173
13000
12000
11000
10000
9000
8000
7000
6000
5000
4000
3000
2000
1000
0
−1000
210
200
190
180
170
160
150
140
130
120
110
100
90
80
70
60
50
40
30
20
10
0
−10
f1 (ppm)

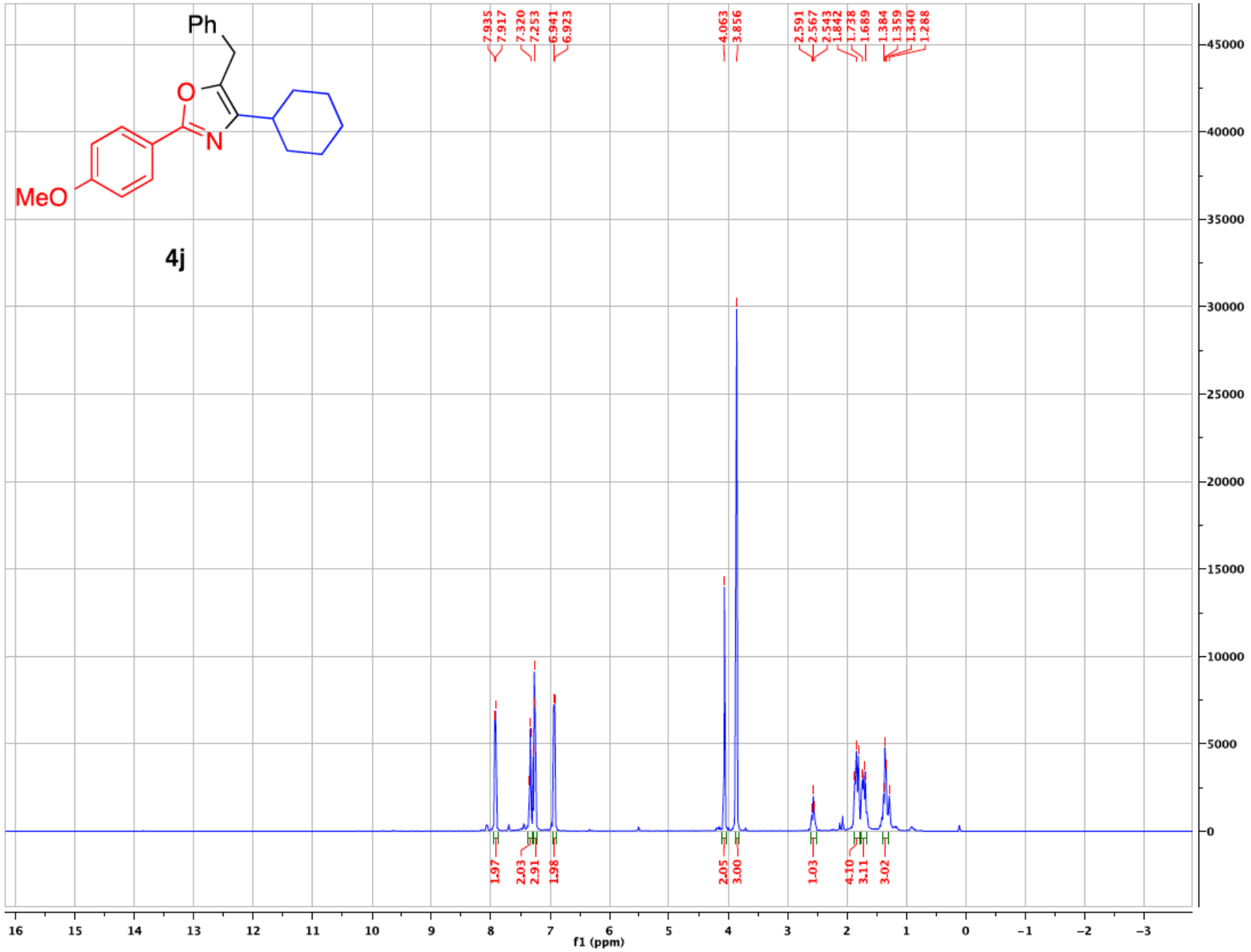
Ph
O
N
MeO
4j
7.935
7.917
7.320
7.253
6.941
6.923
4.063
3.856
2.591
2.567
2.543
1.842
1.738
1.689
1.384
1.359
1.340
1.288
1.97
2.03
2.91
1.98
2.05
3.00
1.03
4.10
3.11
3.02
f1 (ppm)

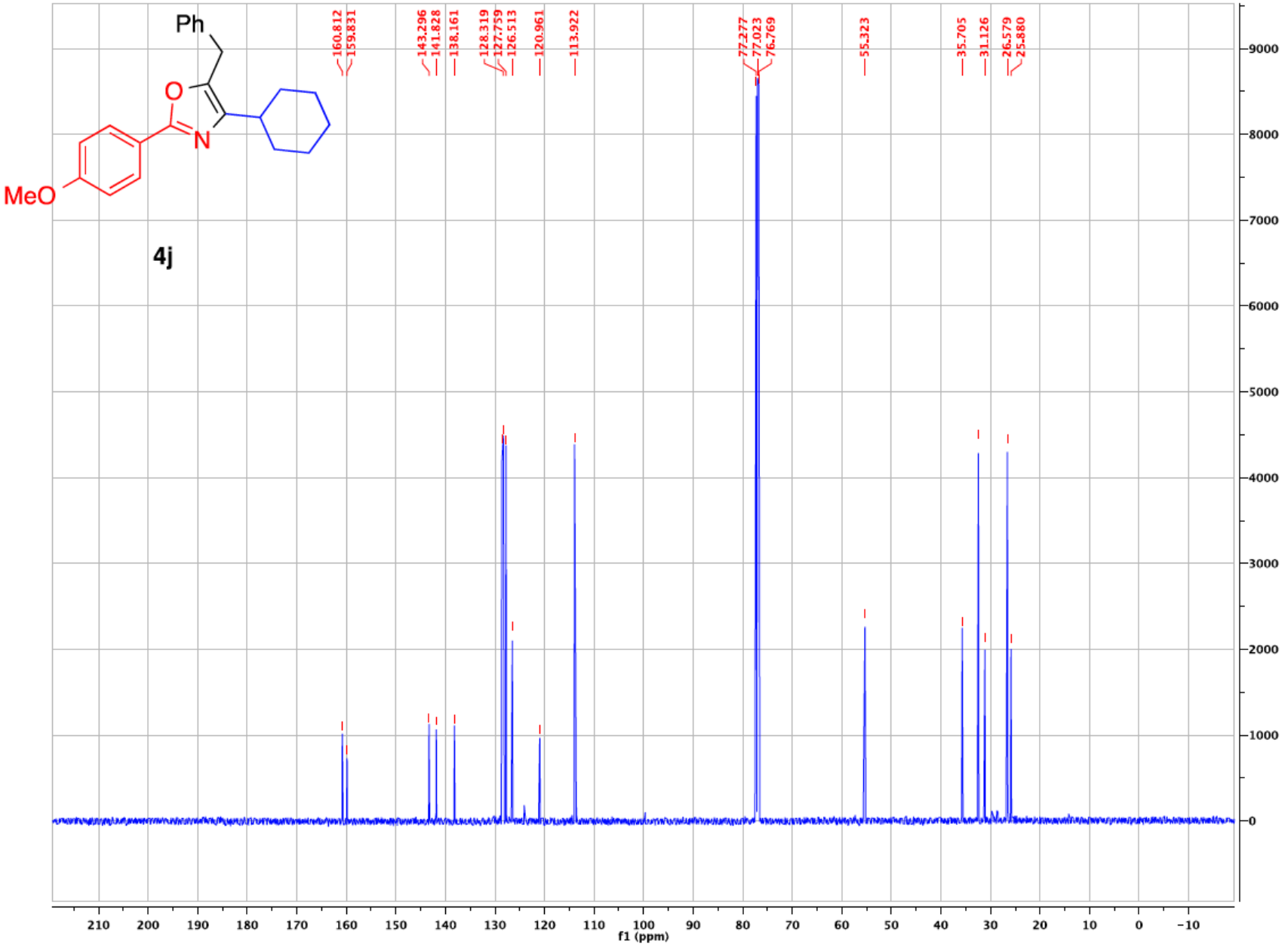
Ph
O
N
MeO
4j
160.812
159.831
143.296
141.828
138.161
128.319
127.759
126.513
120.961
113.922
77.277
77.023
76.769
55.323
35.705
31.126
26.579
25.880
9000
8000
7000
6000
5000
4000
3000
2000
1000
0
210
200
190
180
170
160
150
140
130
120
110
100
90
80
70
60
50
40
30
20
10
0
-10
f1 (ppm)

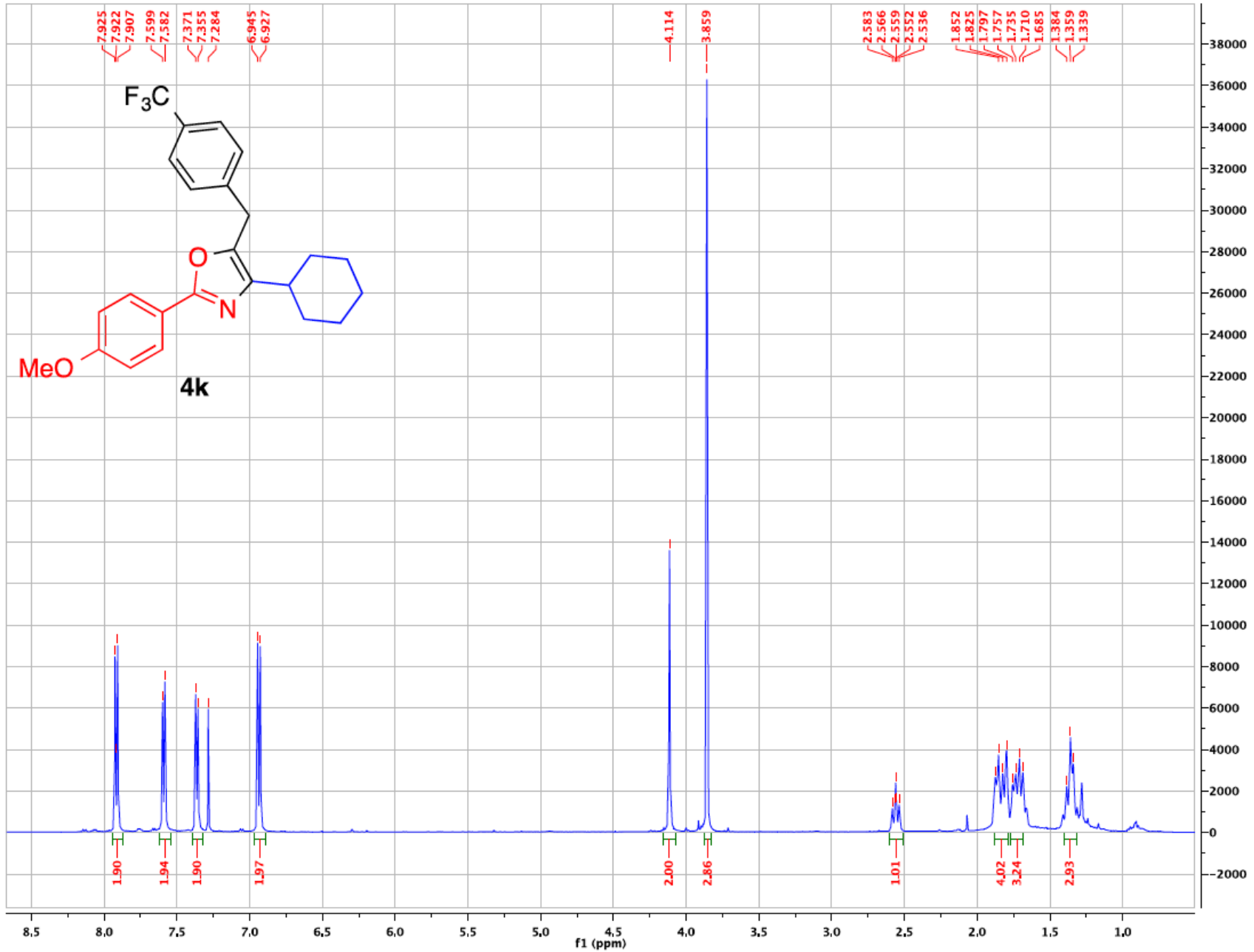
7.925
7.922
7.907
7.599
7.582
7.371
7.355
7.284
6.945
6.927
4.114
3.859
2.583
2.566
2.559
2.552
2.536
1.852
1.825
1.797
1.757
1.735
1.710
1.685
1.384
1.359
1.339
F3C
O
N
MeO
4k
1.90
1.94
1.90
1.97
2.00
2.86
1.01
4.02
3.24
2.93
f1 (ppm)

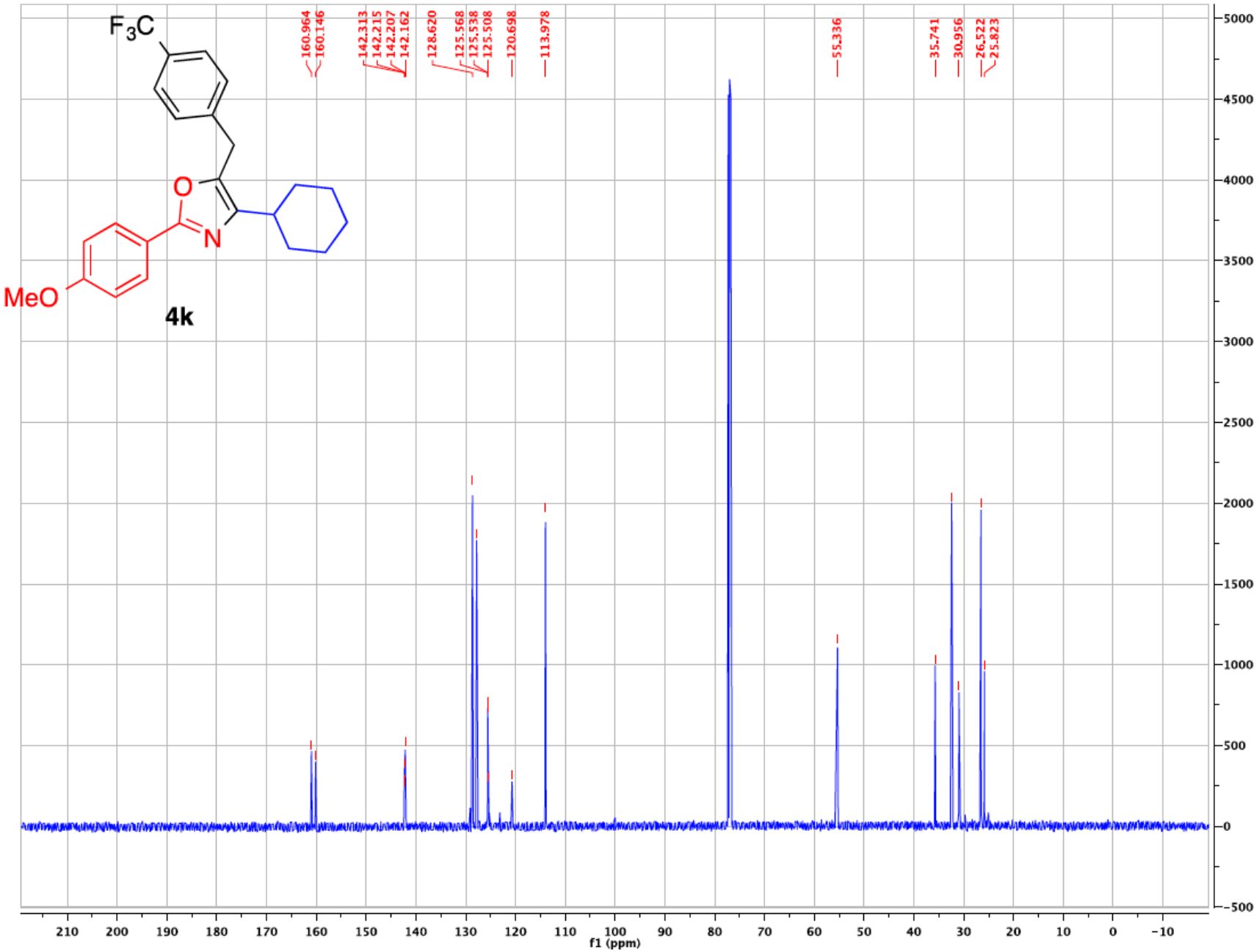
F3C
O
N
MeO
4k
160.964
160.146
142.313
142.215
142.207
142.162
128.620
125.568
125.538
125.508
120.698
113.978
55.336
35.741
30.956
26.522
25.823
5000
4500
4000
3500
3000
2500
2000
1500
1000
500
0
-500
210
200
190
180
170
160
150
140
130
120
110
100
90
80
70
60
50
40
30
20
10
0
-10
f1 (ppm)

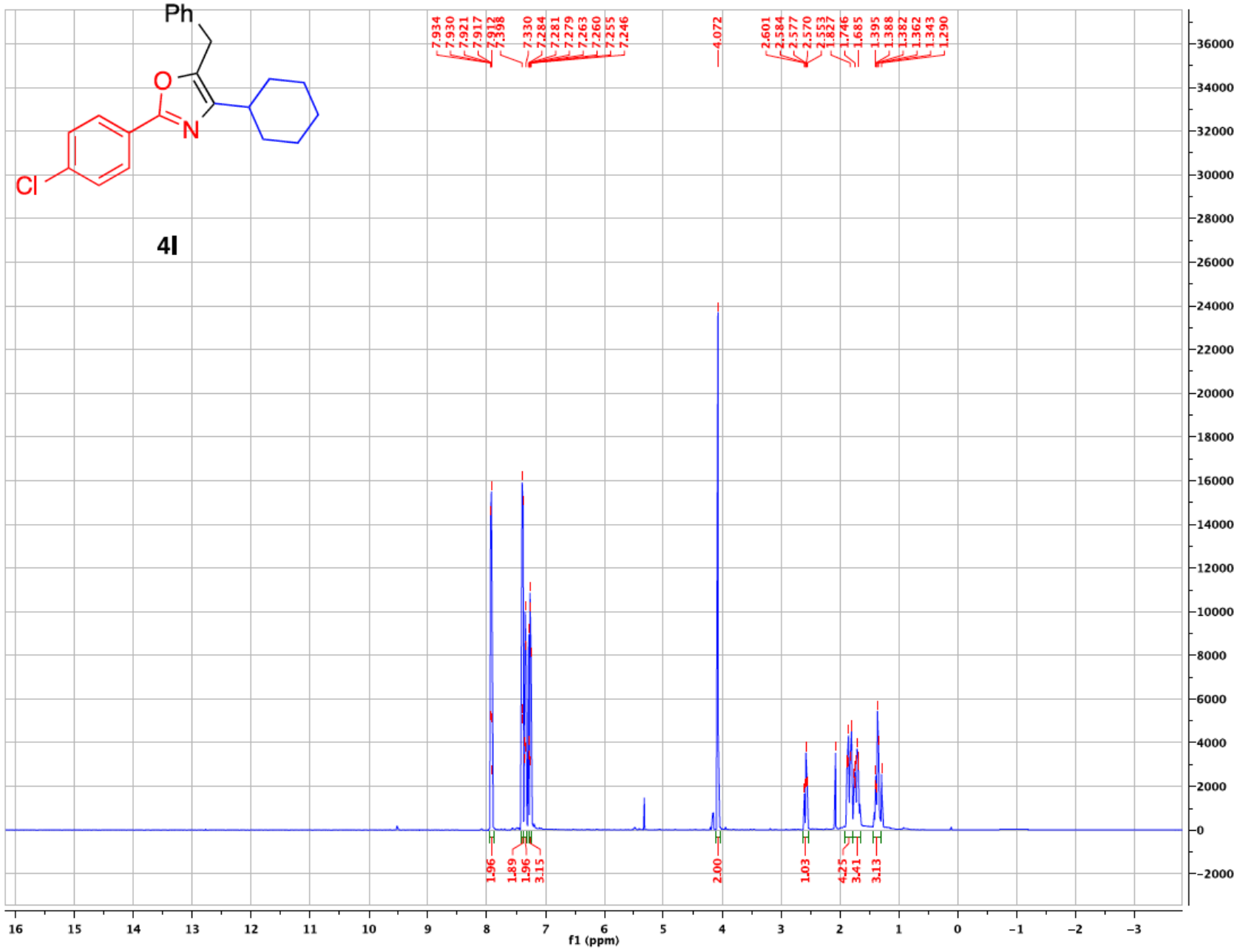
Ph
O
N
Cl
4l
7.934
7.930
7.921
7.917
7.913
7.398
7.330
7.284
7.281
7.279
7.263
7.260
7.255
7.246
4.072
2.601
2.584
2.577
2.570
2.553
1.827
1.746
1.685
1.395
1.388
1.382
1.362
1.343
1.290
1.96
1.89
1.96
3.15
2.00
1.03
4.25
3.41
3.13
f1 (ppm)

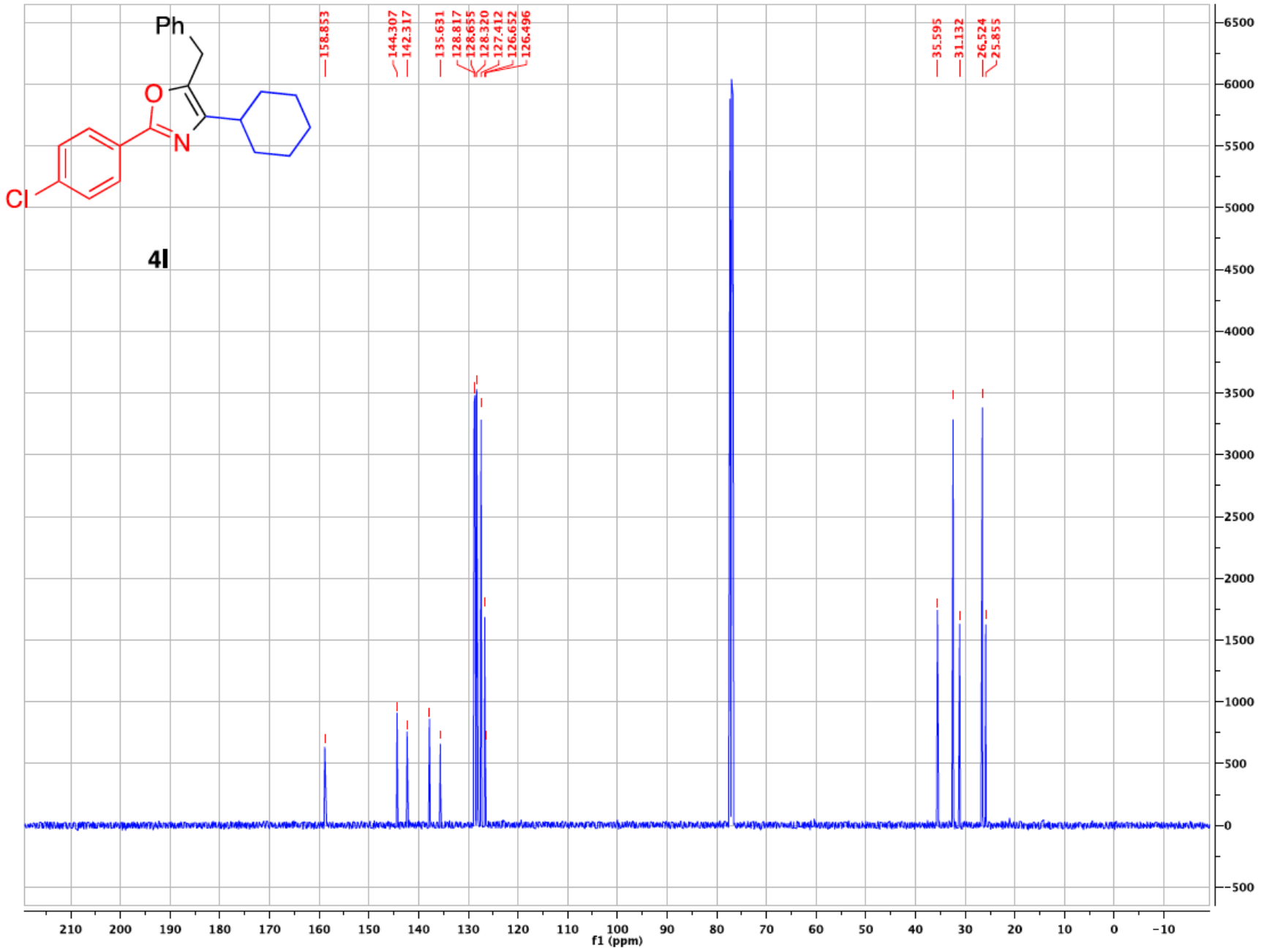
Ph
O
N
Cl
4l
158.853
144.307
142.317
135.631
128.817
128.655
128.320
127.412
126.652
126.496
35.595
31.132
26.524
25.855
f1 (ppm)

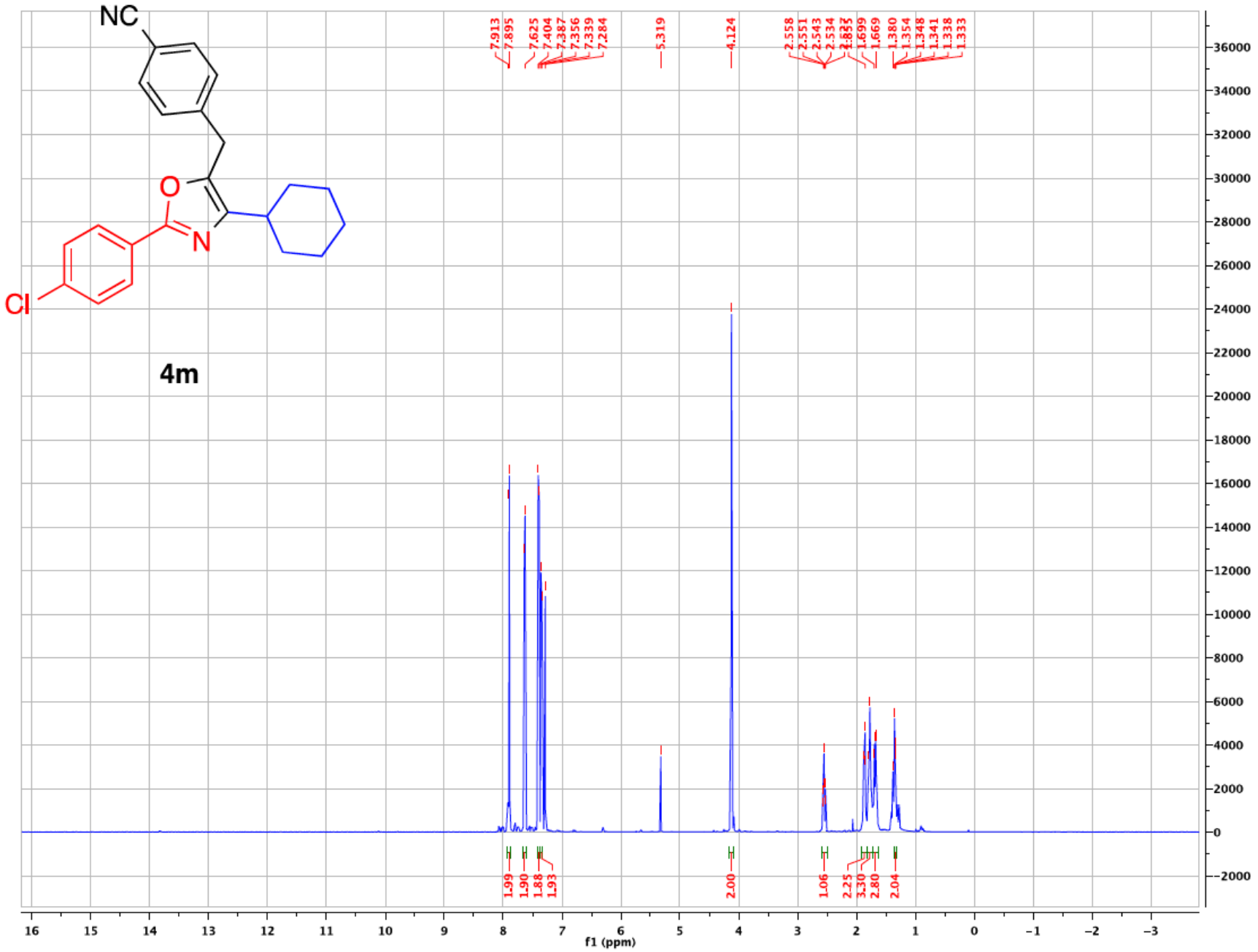
NC
O
N
Cl
4m
7.913
7.895
7.625
7.404
7.387
7.356
7.339
7.284
5.319
4.124
2.558
2.551
2.543
2.534
1.699
1.669
1.380
1.354
1.348
1.341
1.338
1.333
1.99
1.90
1.88
1.93
2.00
1.06
2.25
3.30
2.80
2.04
f1 (ppm)

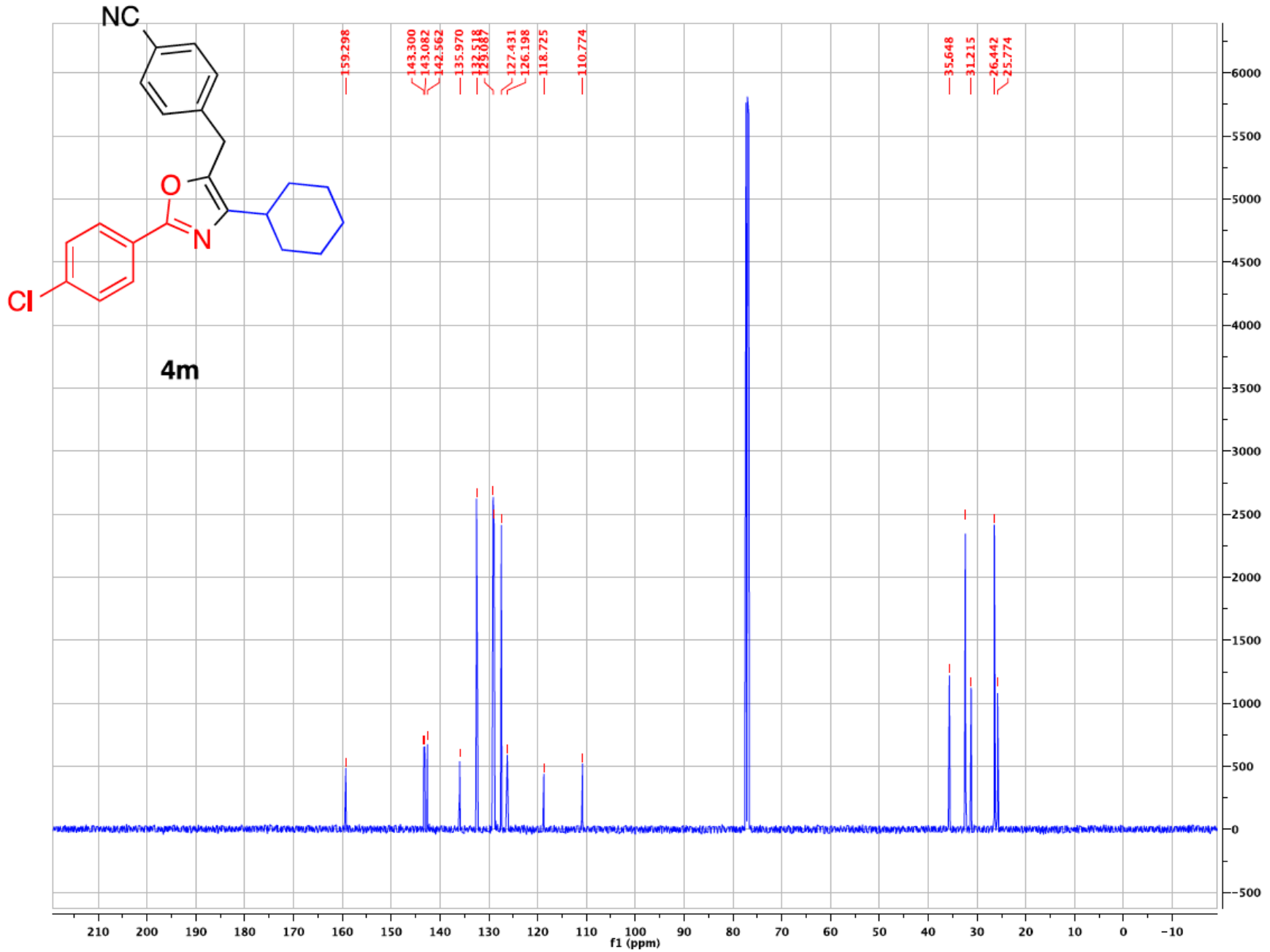
NC
O
N
Cl
4m
159.298
143.300
143.082
142.562
135.970
132.518
129.087
127.431
126.198
118.725
110.774
35.648
31.215
26.442
25.774
f1 (ppm)

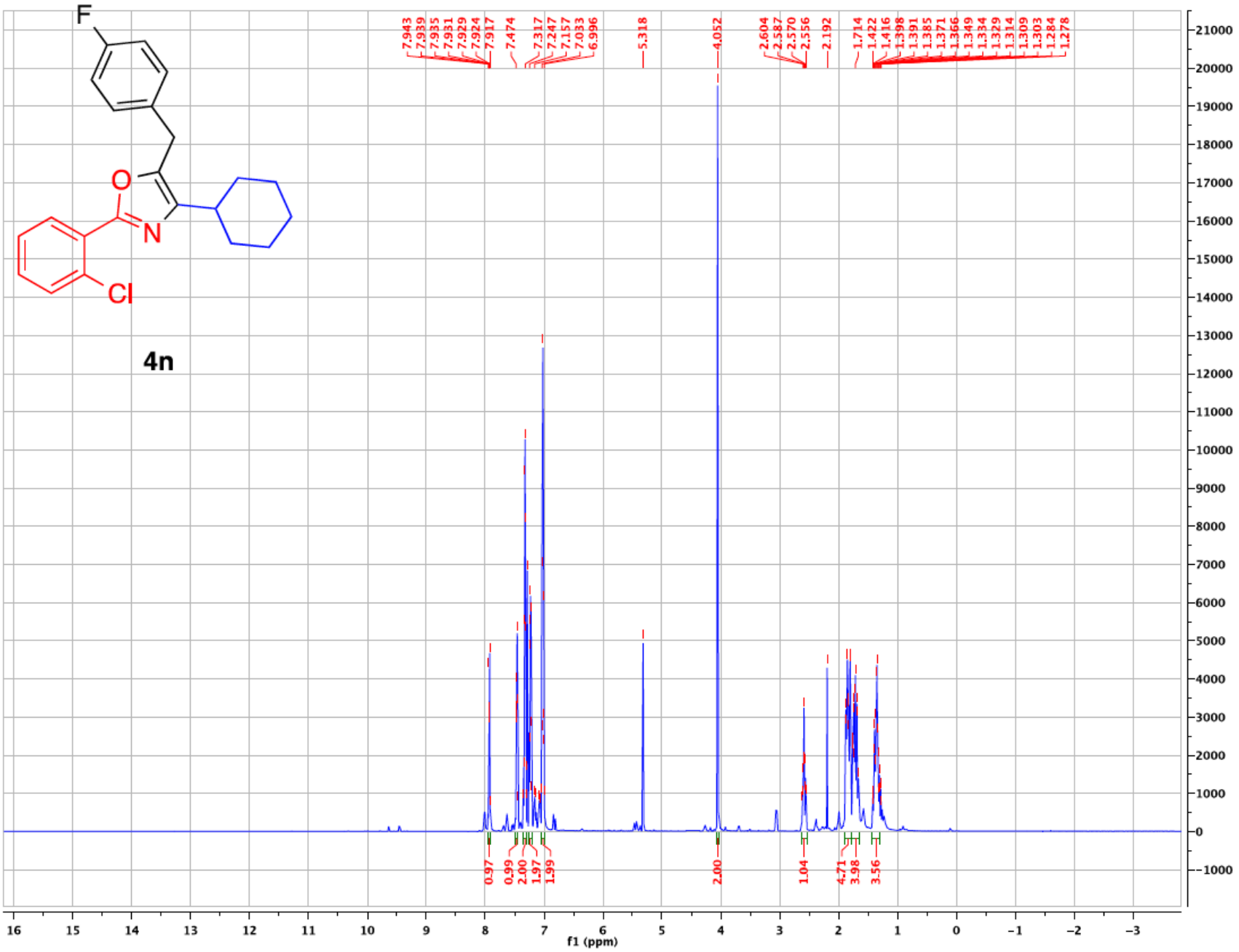
F
O
N
Cl
4n
7.943
7.939
7.935
7.931
7.929
7.924
7.917
7.474
7.317
7.247
7.157
7.033
6.996
5.318
4.052
2.604
2.587
2.570
2.556
2.192
1.714
1.422
1.416
1.398
1.391
1.385
1.371
1.366
1.349
1.334
1.329
1.314
1.309
1.303
1.284
1.278
0.97
0.99
2.00
1.97
1.99
2.00
1.04
4.71
3.98
3.56
f1 (ppm)

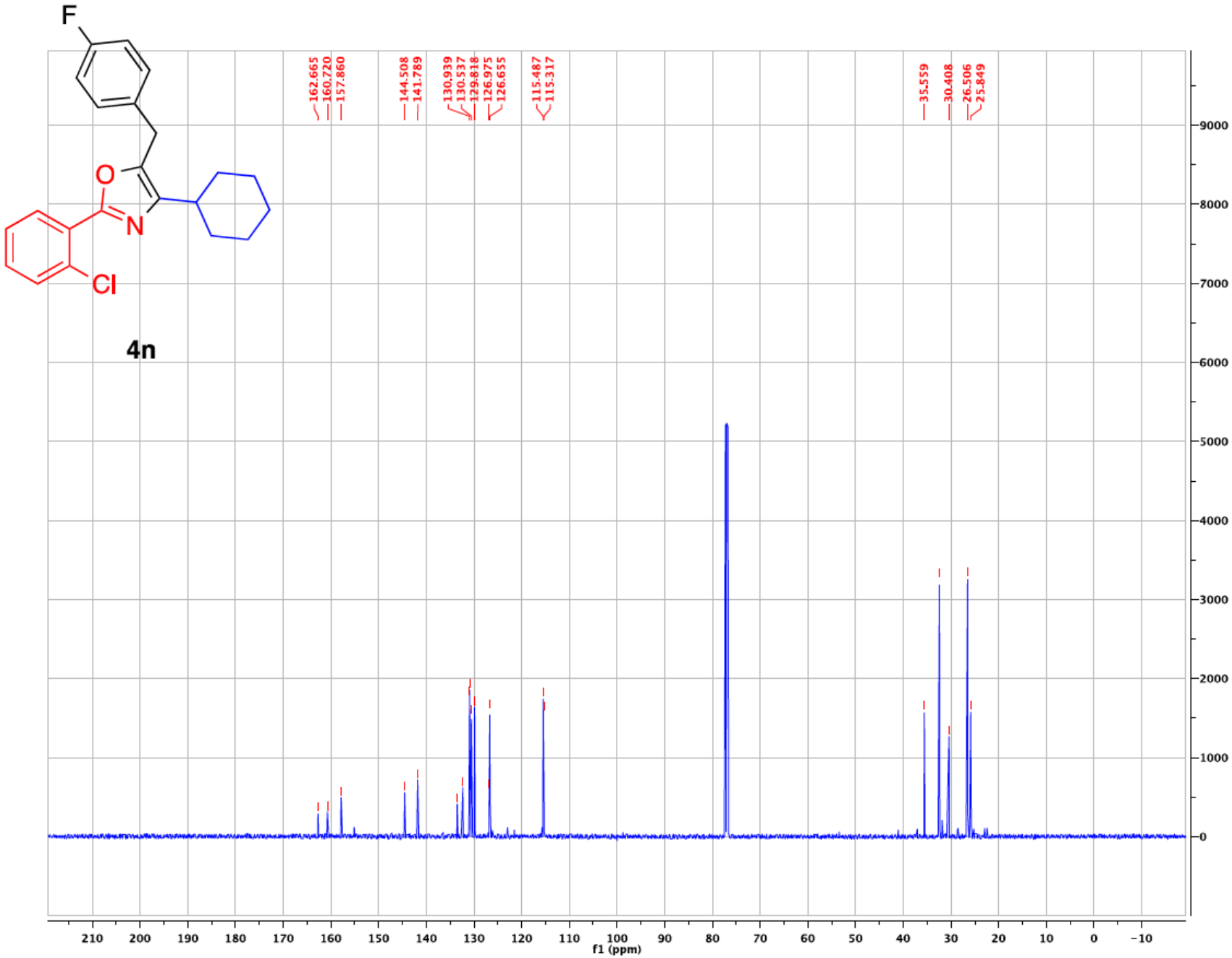
F
O
N
Cl
4n
162.665
160.720
157.860
144.508
141.789
130.939
130.537
129.818
126.975
126.655
115.487
115.317
35.559
30.408
26.506
25.849
9000
8000
7000
6000
5000
4000
3000
2000
1000
0
210
200
190
180
170
160
150
140
130
120
110
100
90
80
70
60
50
40
30
20
10
0
-10
f1 (ppm)

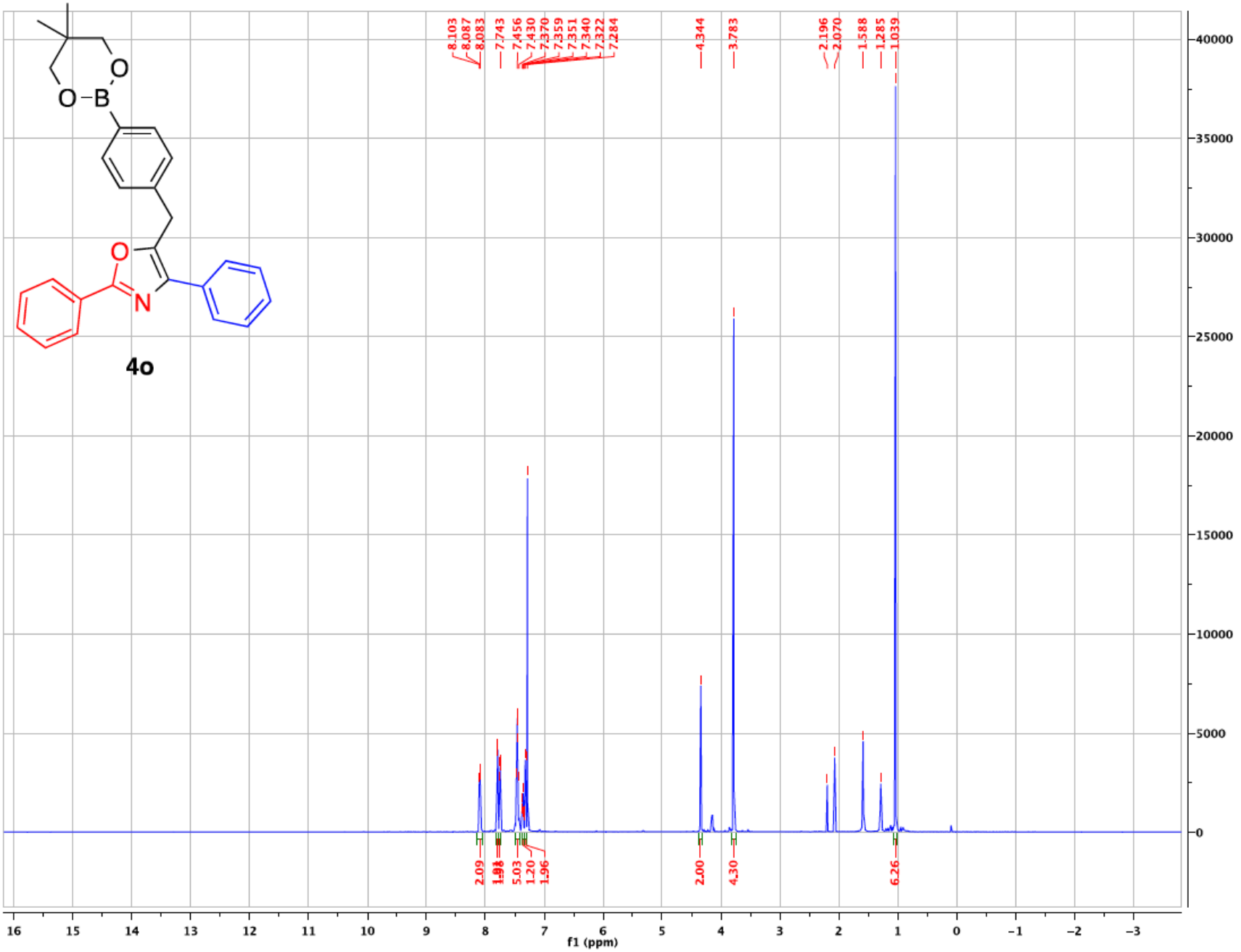
8.103
8.087
8.083
7.743
7.456
7.430
7.370
7.359
7.351
7.340
7.322
7.284
4.344
3.783
2.196
2.070
1.588
1.285
1.039
2.09
5.03
1.20
1.96
2.00
4.30
6.26
f1 (ppm)
4o

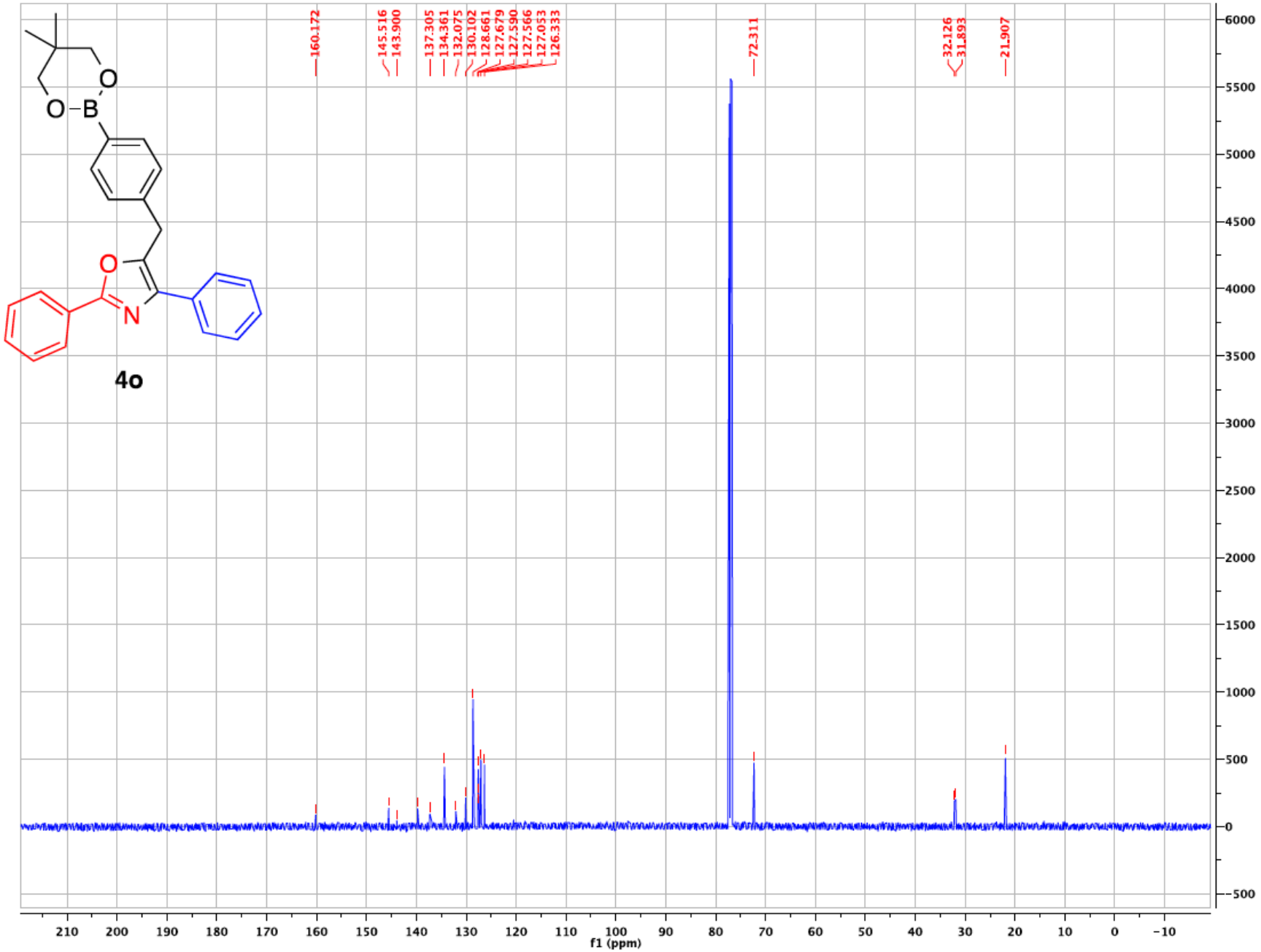
160.172
145.516
143.900
137.305
134.361
132.075
130.102
128.661
127.679
127.590
127.566
127.053
126.333
72.311
32.126
31.893
21.907
O
O
B
O
N
4o
6000
5500
5000
4500
4000
3500
3000
2500
2000
1500
1000
500
0
-500
210
200
190
180
170
160
150
140
130
120
110
100
90
80
70
60
50
40
30
20
10
0
-10
f1 (ppm)

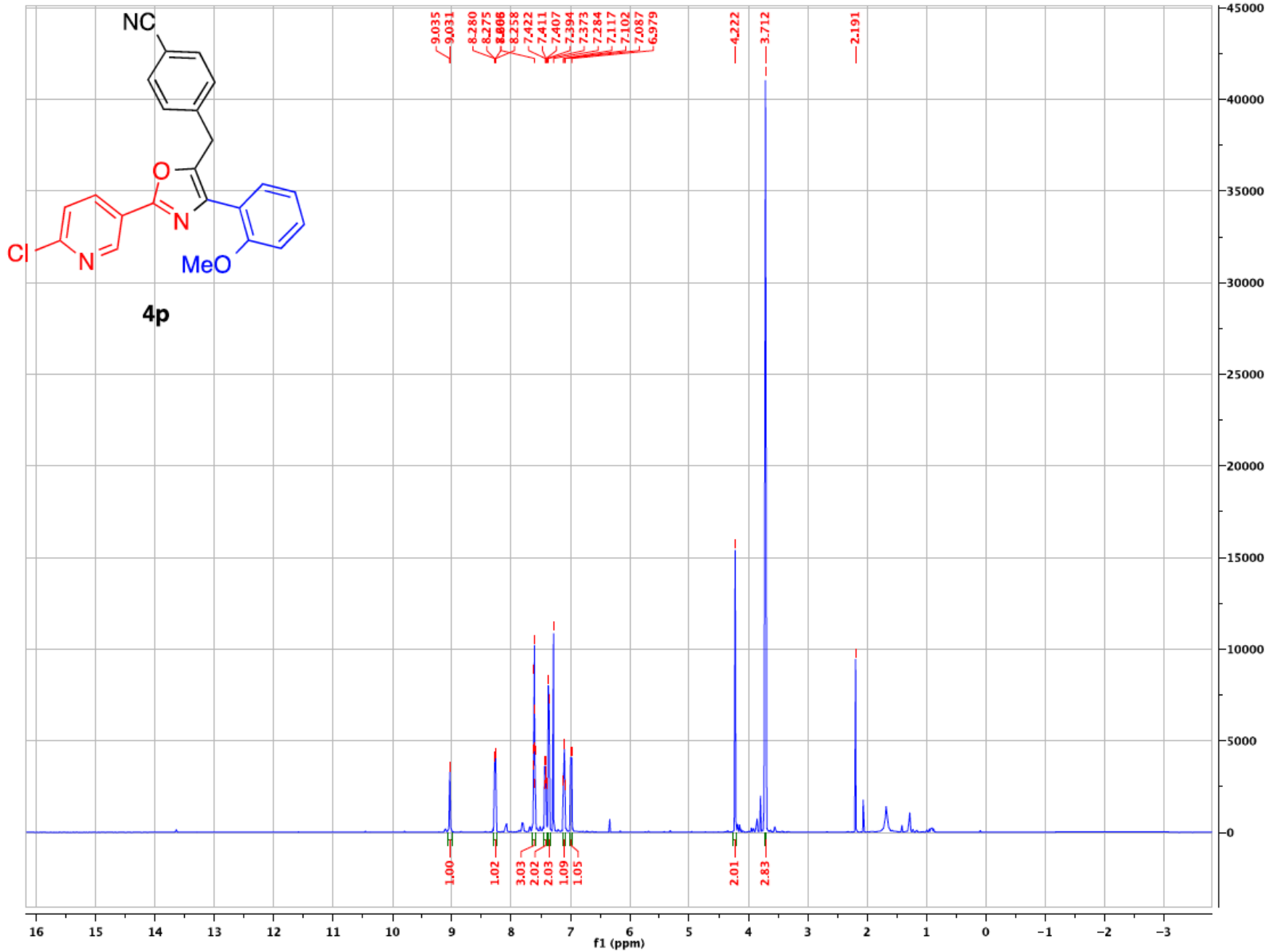
NC
O
N
Cl
N
MeO
4p
9.035
9.031
8.280
8.275
8.258
7.422
7.411
7.407
7.394
7.373
7.284
7.117
7.102
7.087
6.979
4.222
3.712
2.191
1.00
1.02
3.03
2.02
2.03
1.09
1.05
2.01
2.83
f1 (ppm)

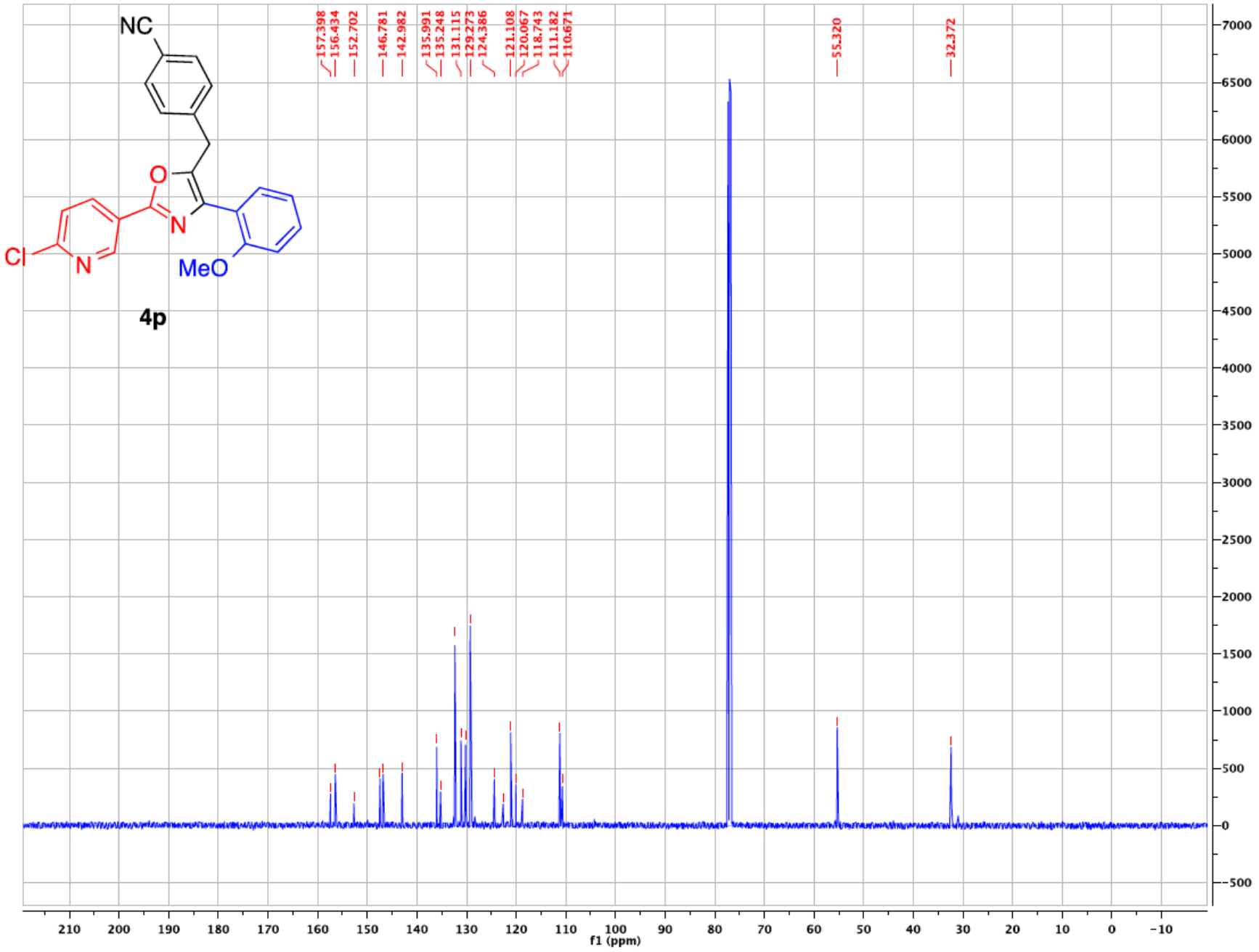
NC
O
N
Cl
N
MeO
4p
157.398
156.434
152.702
146.781
142.982
135.991
135.248
131.115
129.273
124.386
121.108
120.067
118.743
111.182
110.671
55.320
32.372
f1 (ppm)

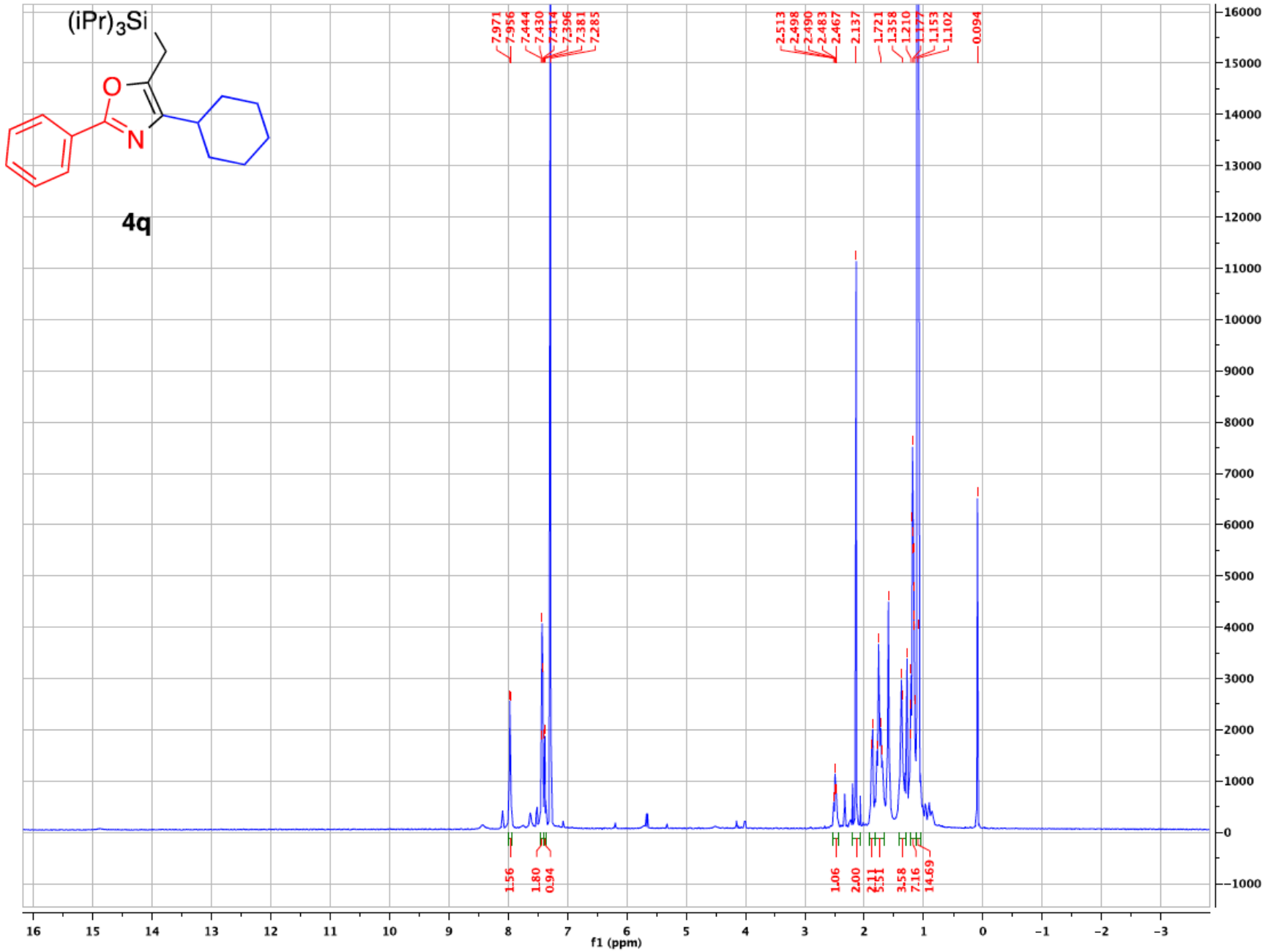
(iPr)3Si
O
N
4q
7.971
7.956
7.444
7.430
7.414
7.396
7.381
7.285
2.513
2.498
2.490
2.483
2.467
2.137
1.721
1.358
1.210
1.177
1.153
1.102
0.094
1.56
1.80
0.94
1.06
2.00
2.11
5.51
3.58
7.16
14.69
f1 (ppm)

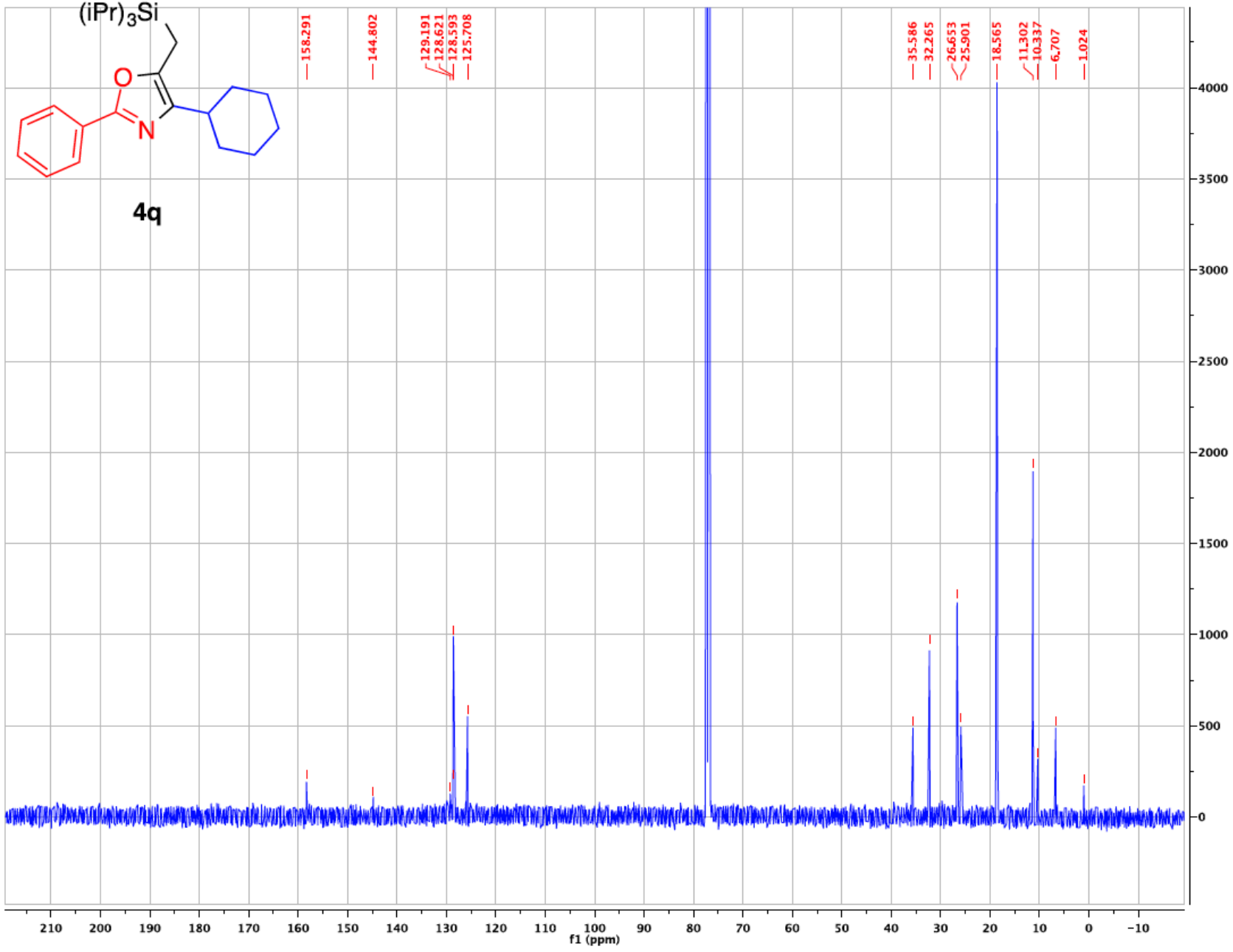
(iPr)3Si
O
N
4q
158.291
144.802
129.191
128.621
128.593
125.708
35.586
32.265
26.653
25.901
18.565
11.302
10.337
6.707
1.024
f1 (ppm)

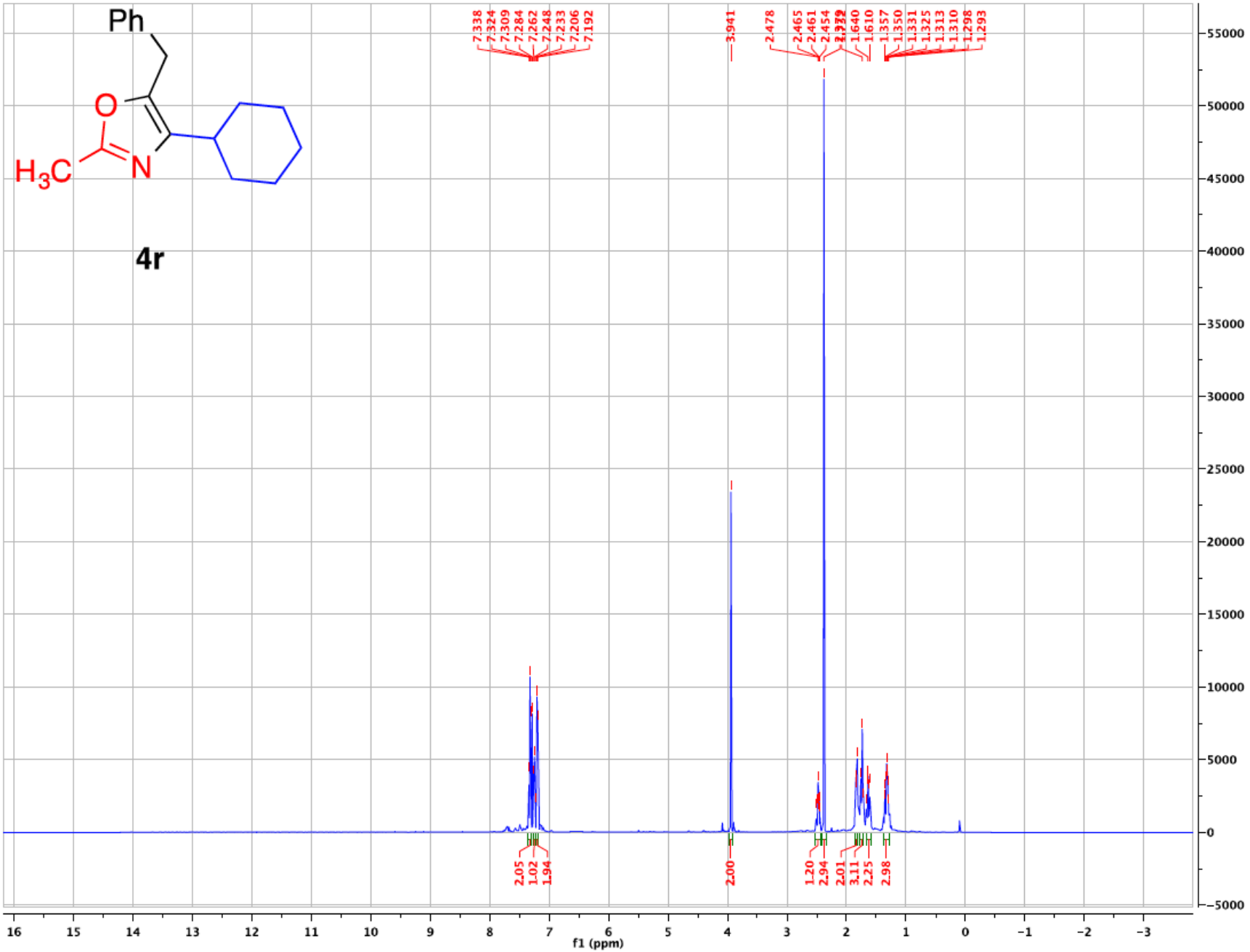
Ph
O
H_3C
N
4r
7.338
7.324
7.309
7.284
7.262
7.248
7.233
7.206
7.192
3.941
2.478
2.465
2.461
2.454
1.640
1.610
1.357
1.350
1.331
1.325
1.313
1.310
1.298
1.293
2.05
1.02
1.94
2.00
1.20
2.94
2.01
3.11
2.25
2.98
f1 (ppm)

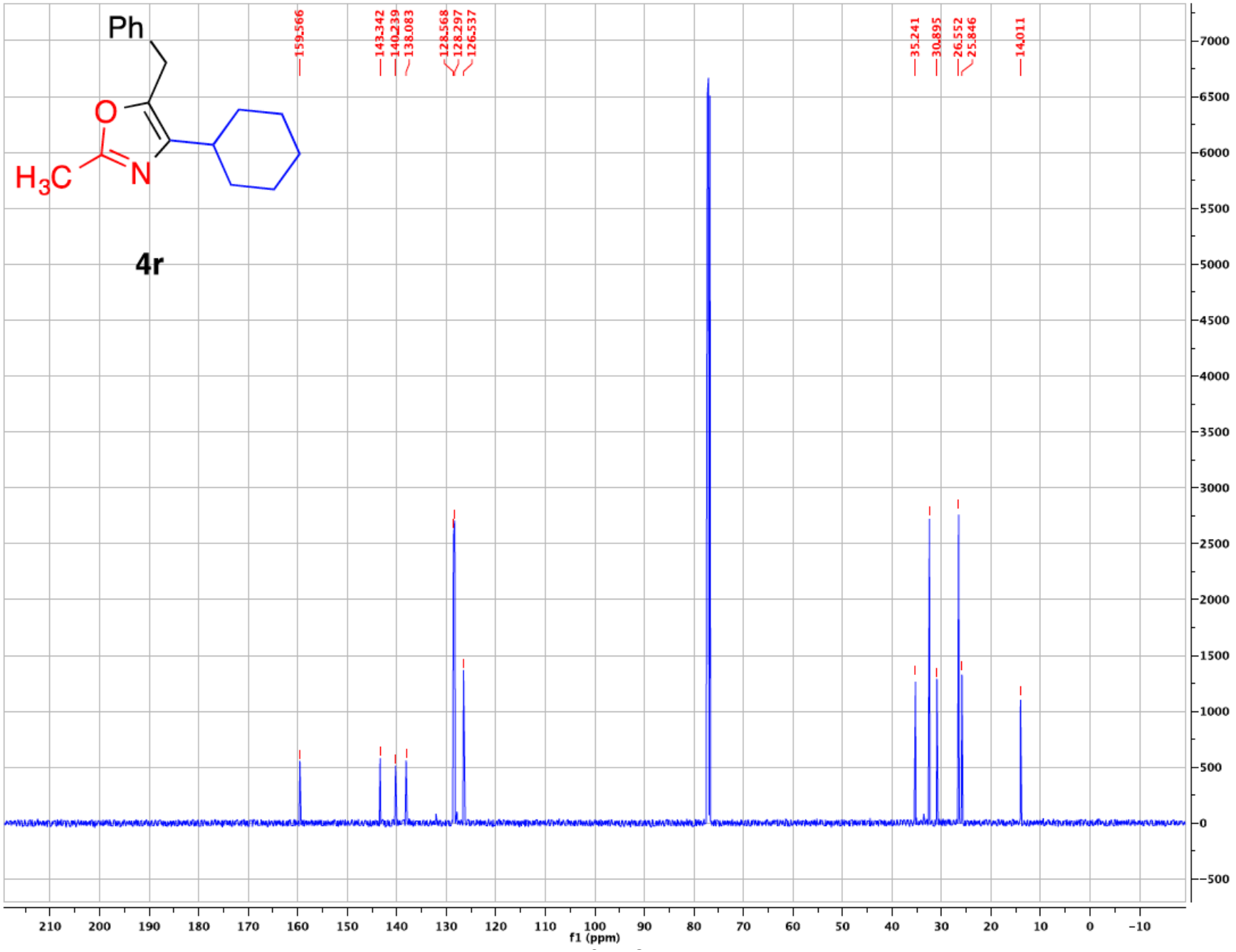
Ph
O
H_3C
N
4r
159.566
143.342
140.239
138.083
128.568
128.297
126.537
35.241
30.895
26.552
25.846
14.011
f1 (ppm)

Spectra for compounds in Chapter 3

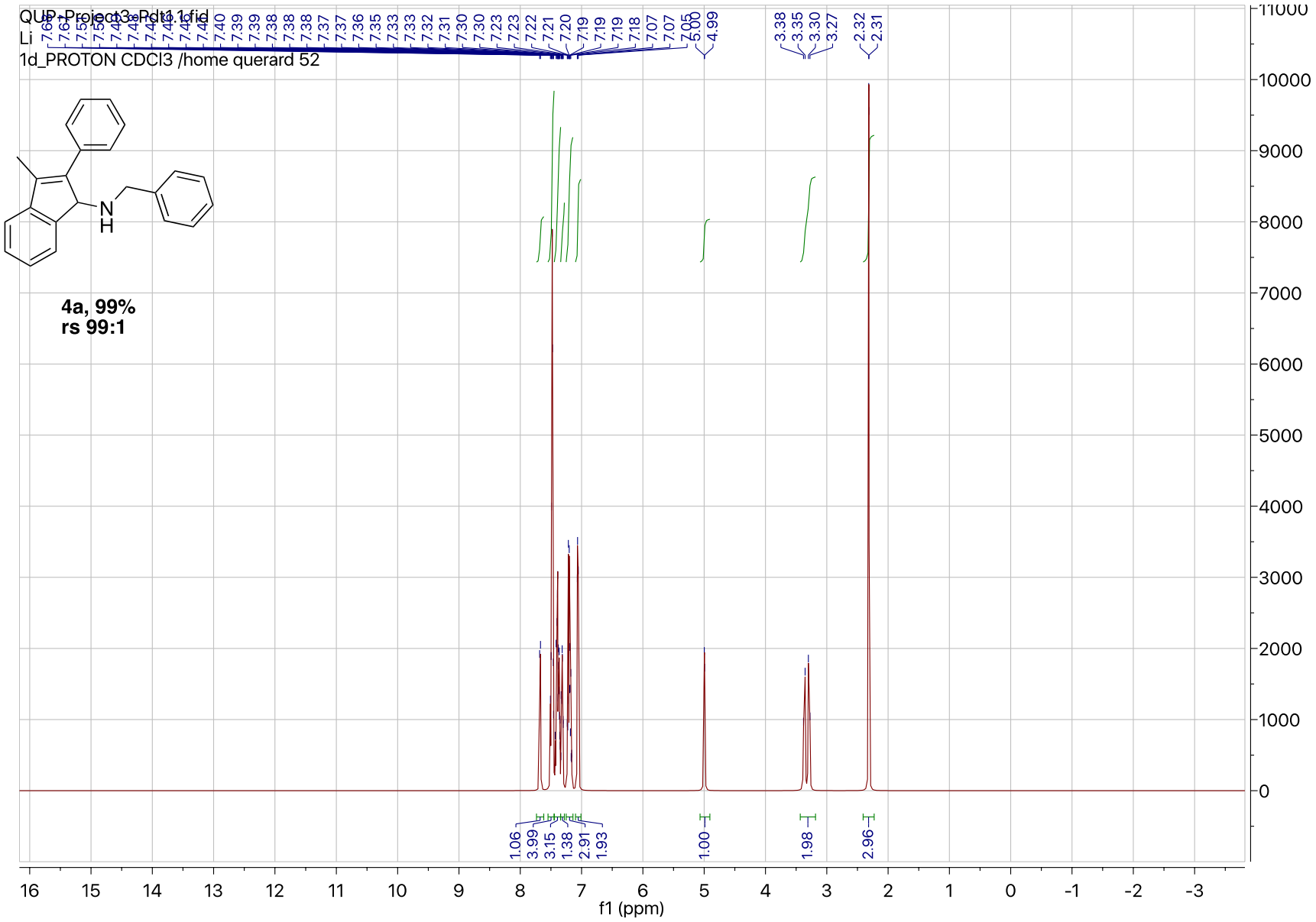
QUB-Project3-Rd11.1.fid
Li
1d_PROTON CDCl3 /home querard 52
4a, 99%
rs 99:1
f1 (ppm)

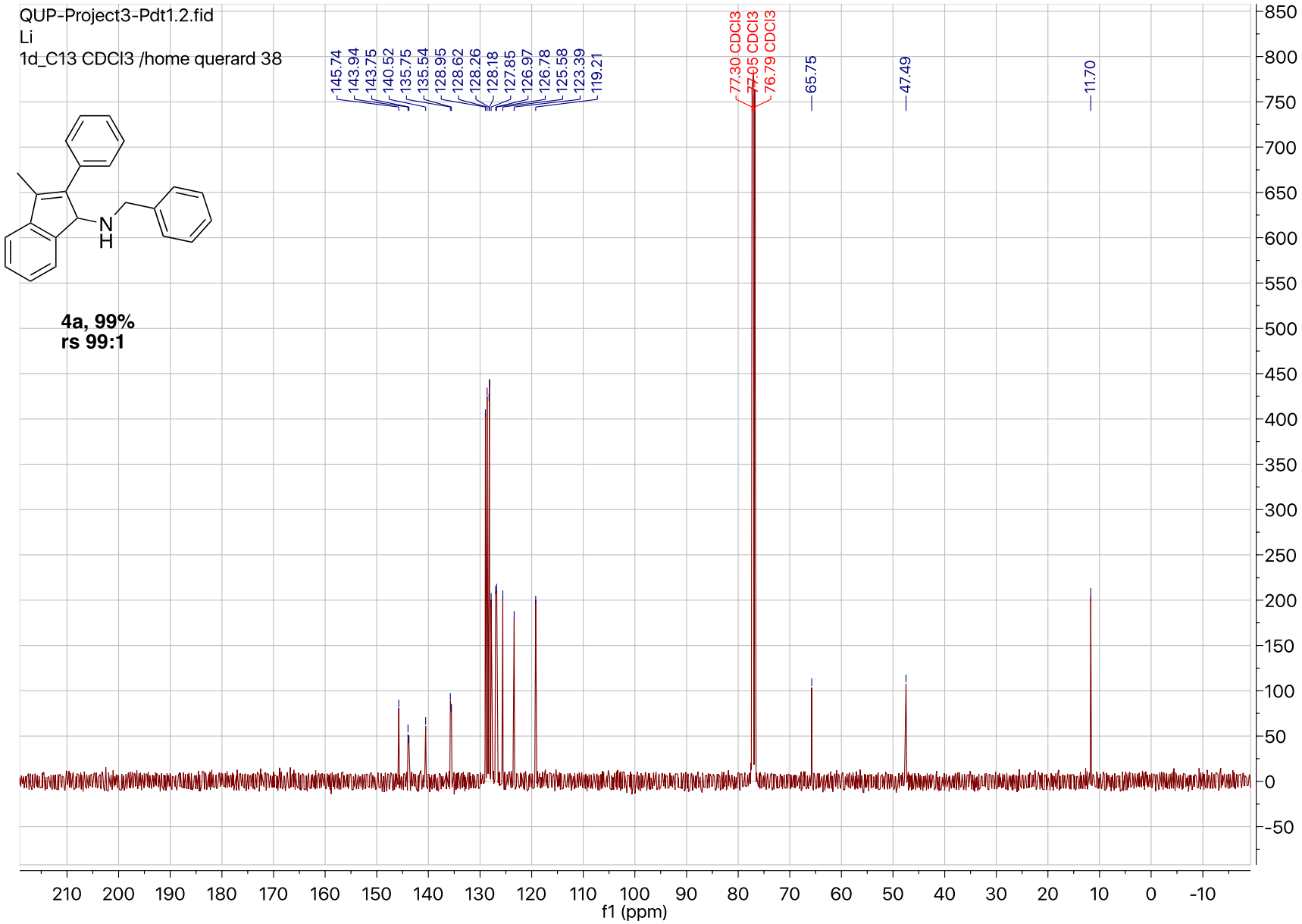
QUP-Project3-Pdt1.2.fid
Li
1d_C13 CDCl3 /home querard 38
145.74
143.94
143.75
140.52
135.75
135.54
128.95
128.62
128.26
128.18
127.85
126.97
126.78
125.58
123.39
119.21
77.30 CDCl3
77.05 CDCl3
76.79 CDCl3
65.75
47.49
11.70
N
H
4a, 99%
rs 99:1
f1 (ppm)

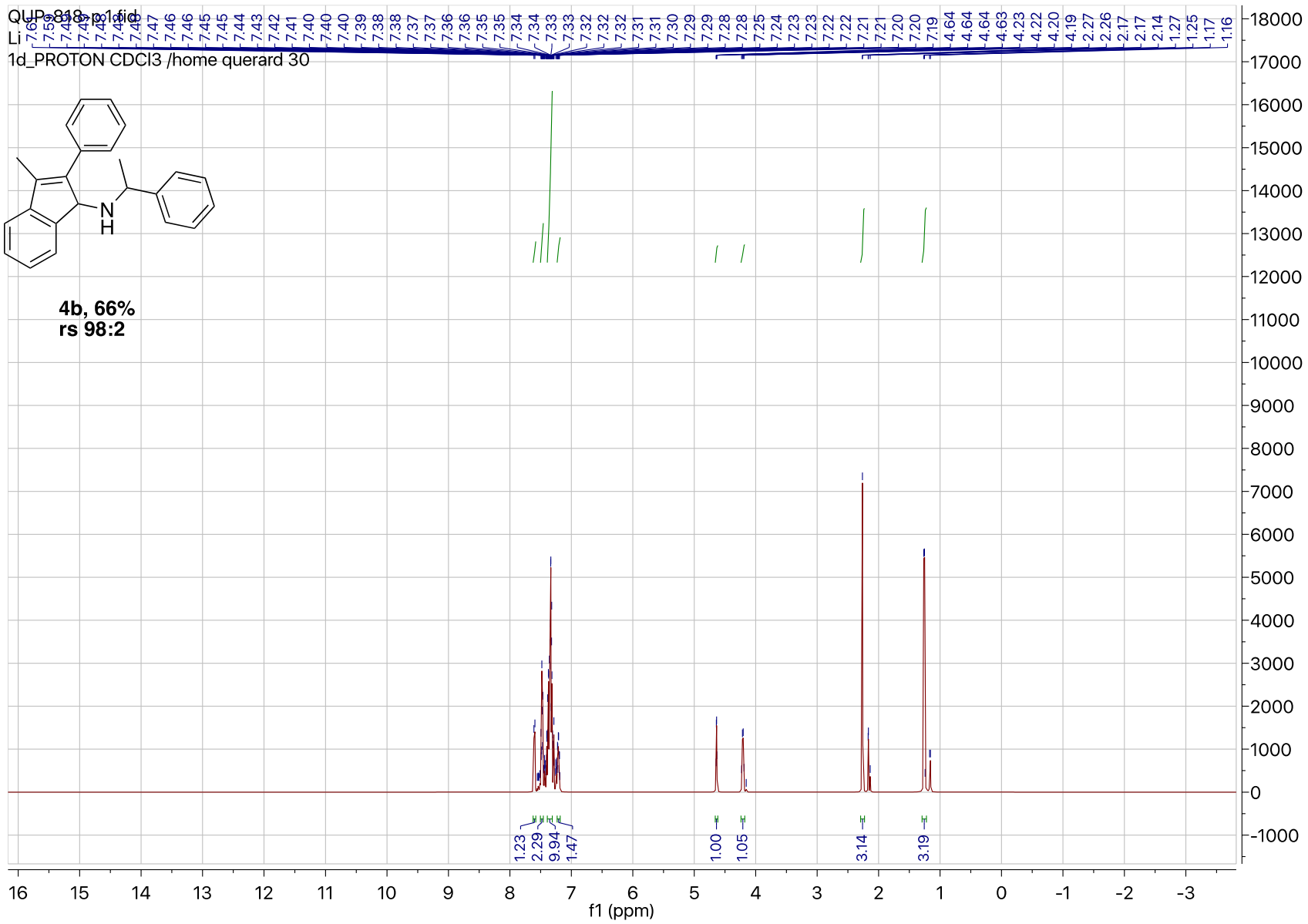
QUP-818-p1.fid
1d_PROTON CDCl3 /home querard 30
4b, 66%
rs 98:2
1.23
2.29
9.94
1.47
1.00
1.05
3.14
3.19
f1 (ppm)

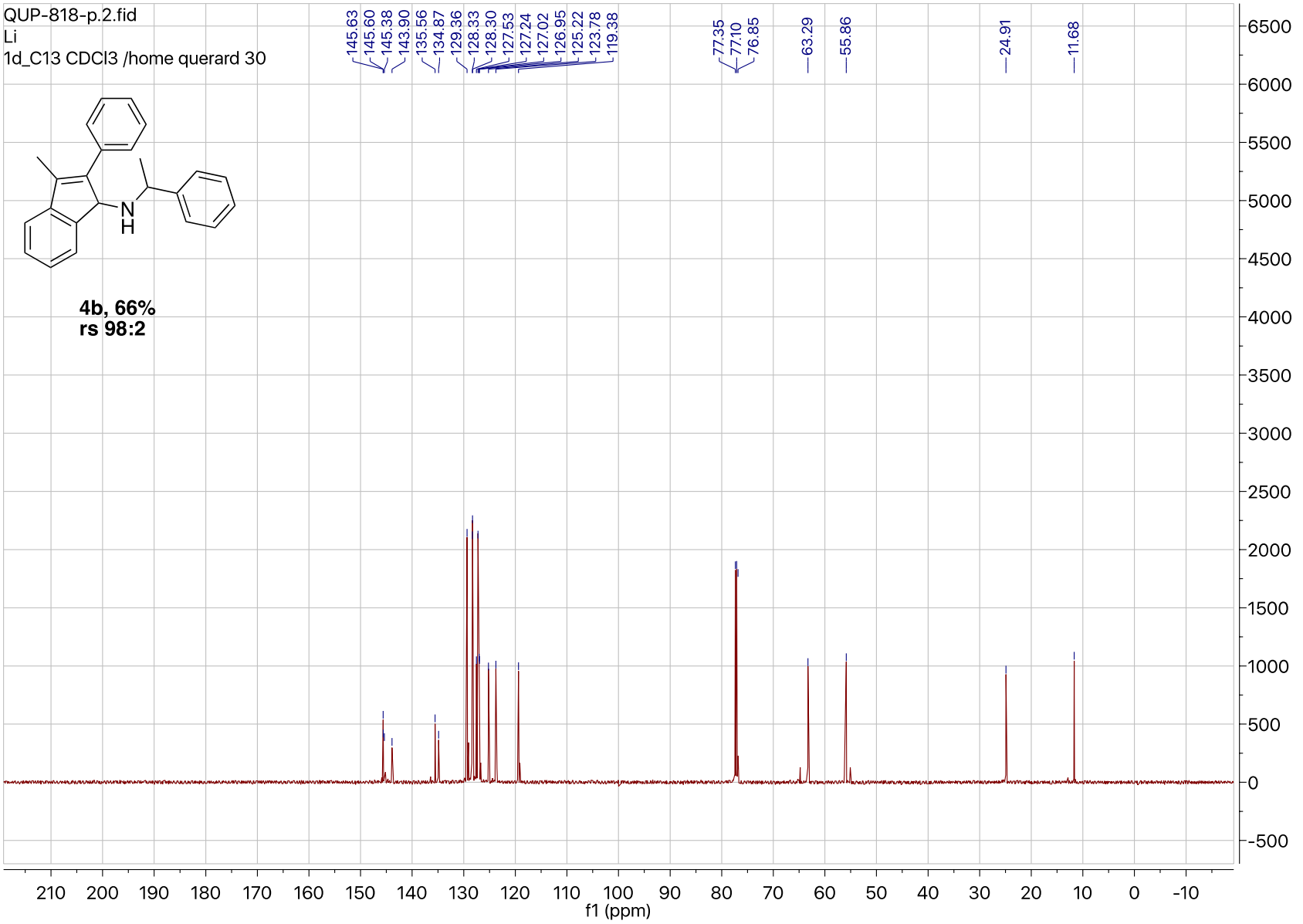
QUP-818-p.2.fid
Li
1d_C13 CDCl3 /home querard 30
145.63
145.60
145.38
143.90
135.56
134.87
129.36
128.33
128.30
127.53
127.24
127.02
126.95
125.22
123.78
119.38
77.35
77.10
76.85
63.29
55.86
24.91
11.68
N
H
4b, 66%
rs 98:2
f1 (ppm)

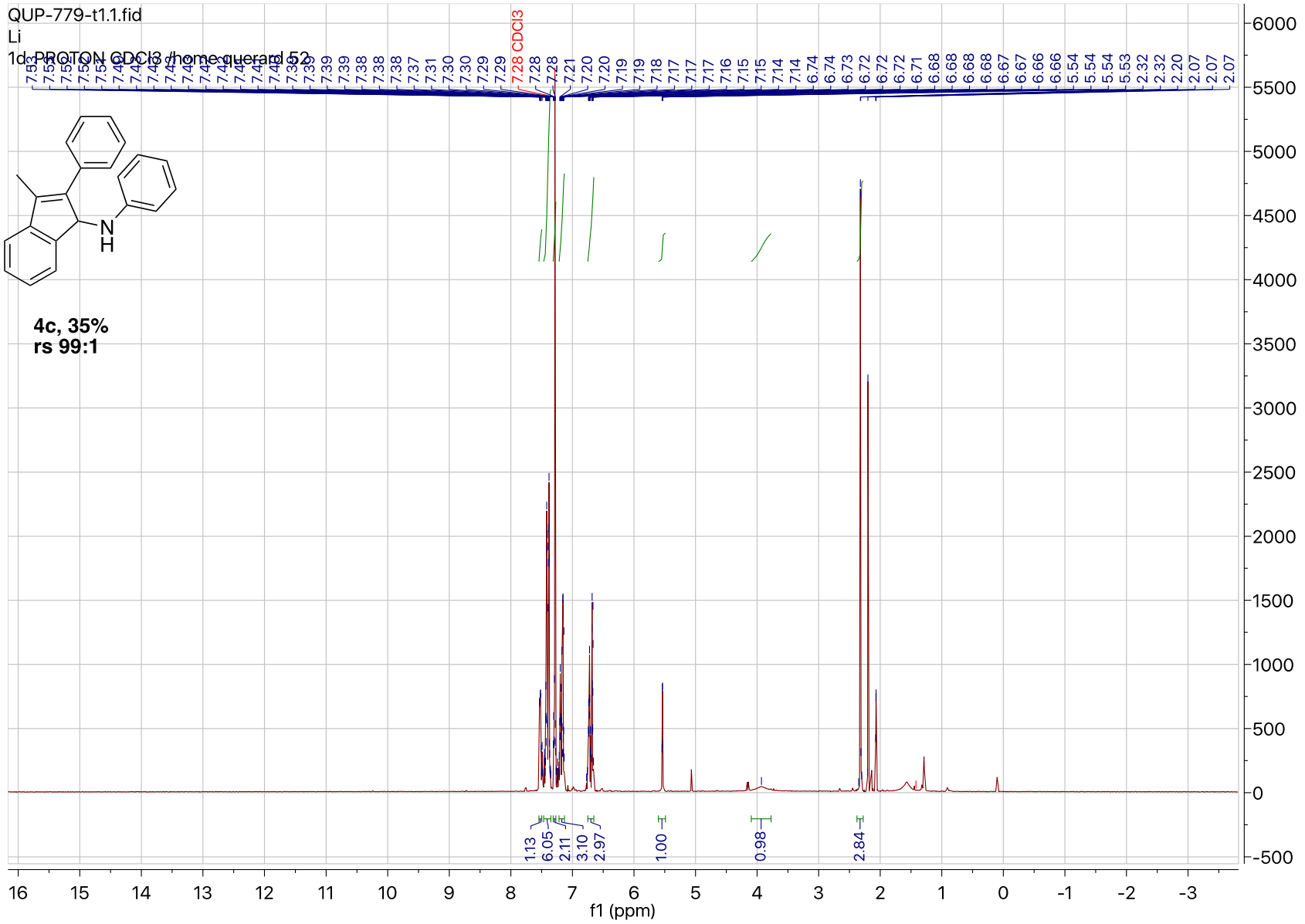
QUP-779-t1.1.fid
Li
1d_PROTON CDCl3 /home/querard 52
4c, 35%
rs 99:1
7.28 CDCl3
1.13
6.05
2.11
3.10
2.97
1.00
0.98
2.84
f1 (ppm)

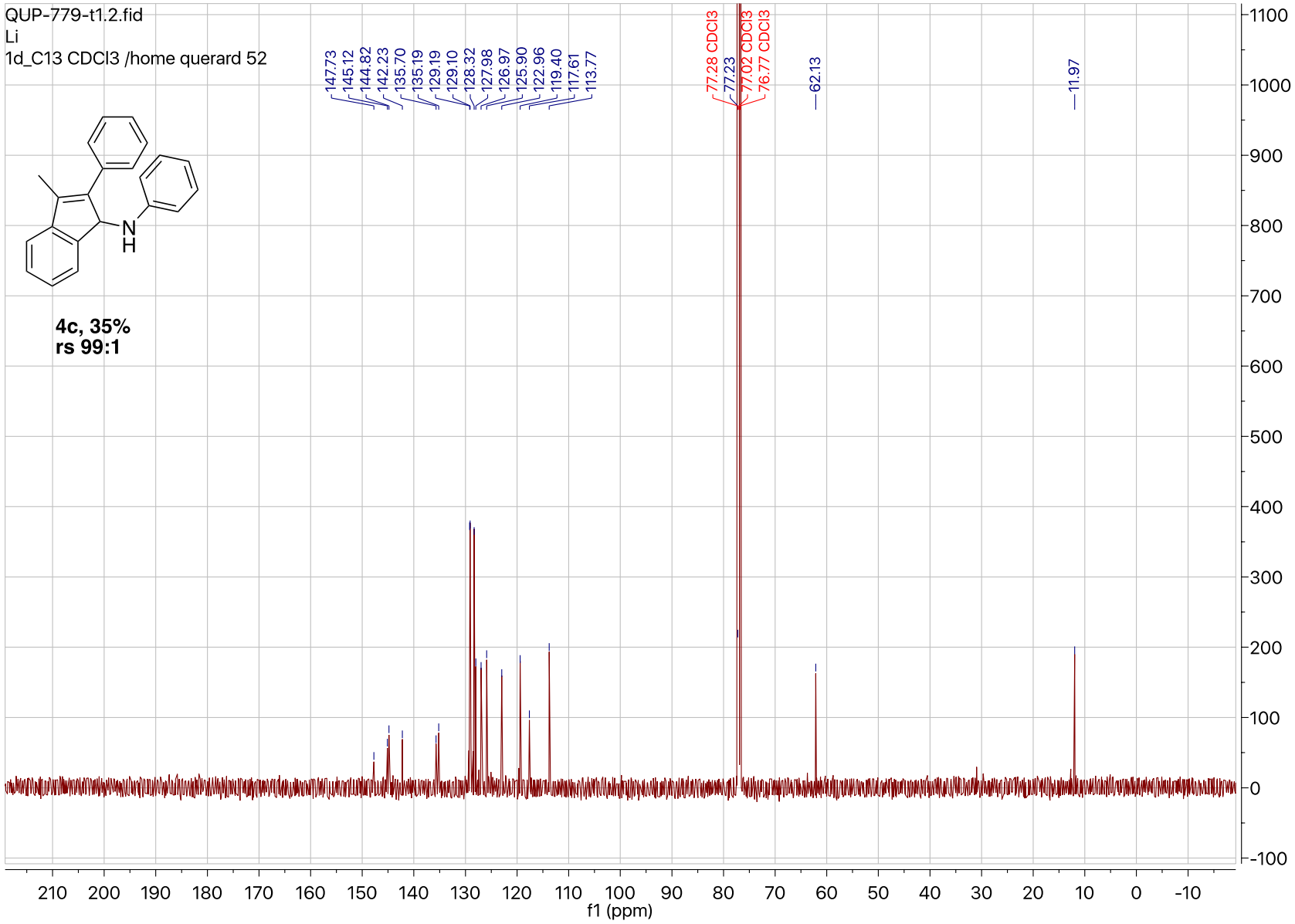
QUP-779-t1.2.fid
Li
1d_C13 CDCl3 /home querard 52
147.73
145.12
144.82
142.23
135.70
135.19
129.19
129.10
128.32
127.98
126.97
125.90
122.96
119.40
117.61
113.77
77.28 CDCl3
77.23
77.02 CDCl3
76.77 CDCl3
62.13
11.97
N
H
4c, 35%
rs 99:1
f1 (ppm)

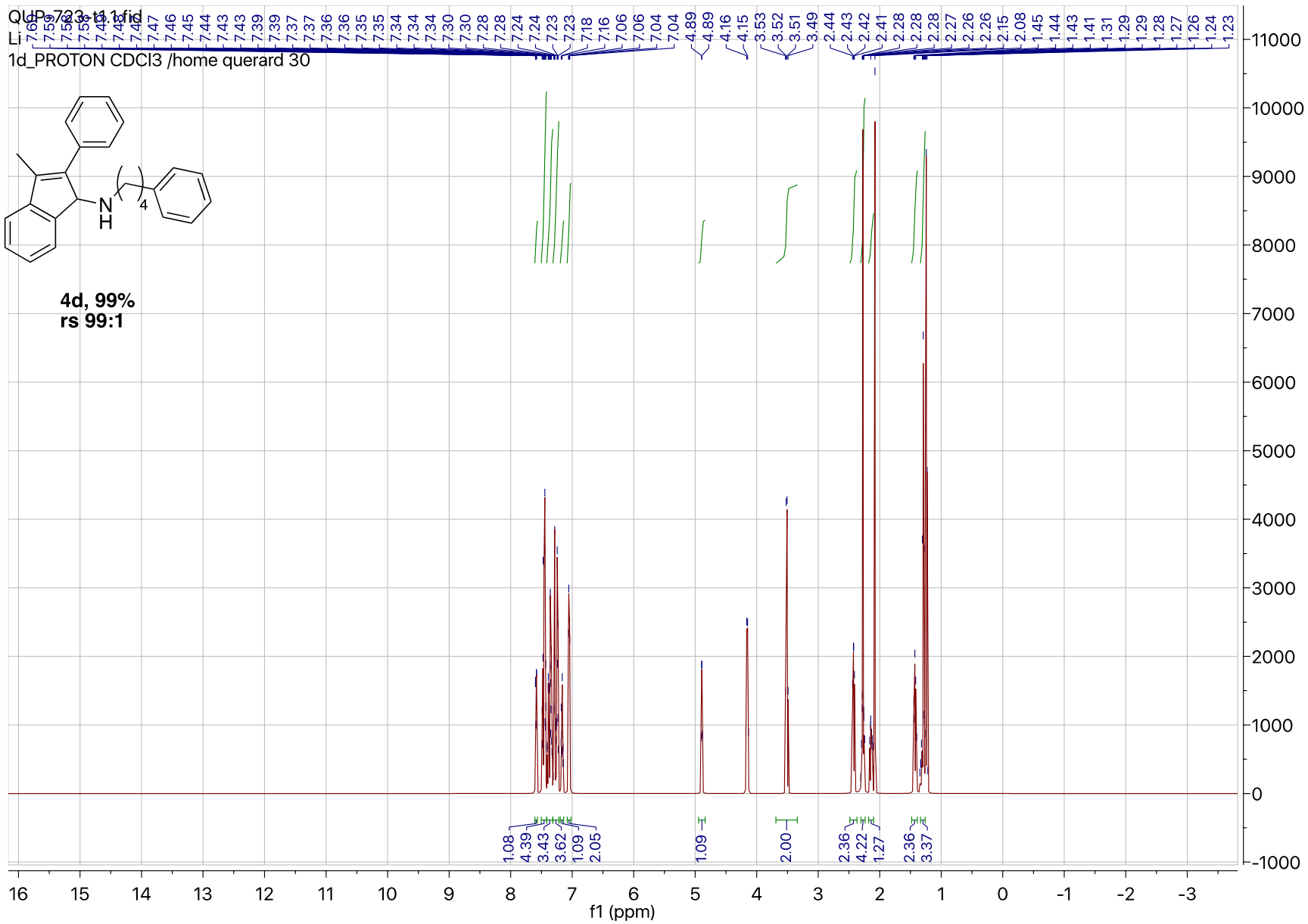
QUP-723-t11.fid
1d_PROTON CDCl3 /home querard 30
4d, 99%
rs 99:1
f1 (ppm)

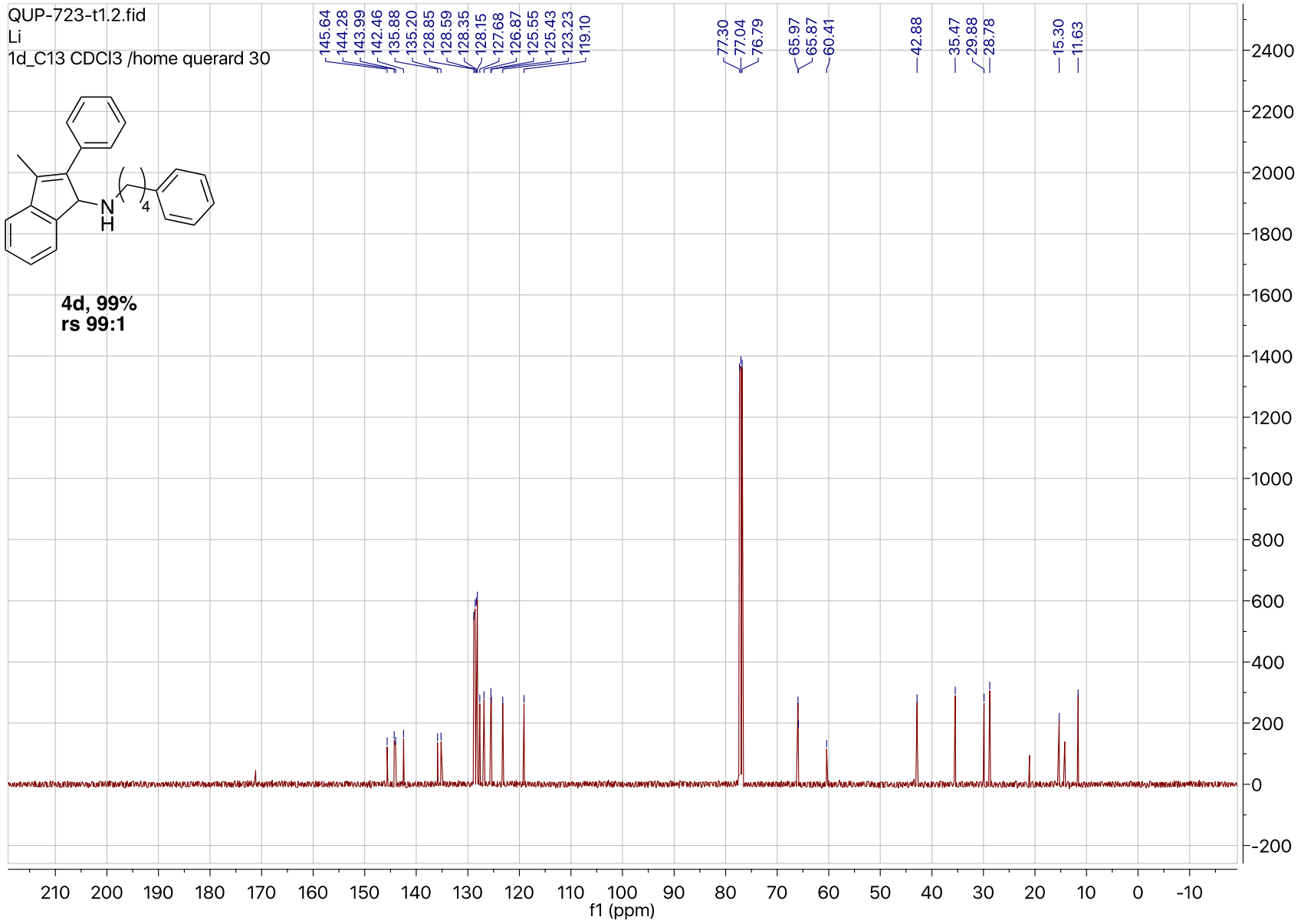
QUP-723-t1.2.fid
Li
1d_C13 CDCl3 /home querard 30
145.64
144.28
143.99
142.46
135.88
135.20
128.85
128.59
128.35
128.15
127.68
126.87
125.55
125.43
123.23
119.10
77.30
77.04
76.79
65.97
65.87
60.41
42.88
35.47
29.88
28.78
15.30
11.63
N
H
4
4d, 99%
rs 99:1
f1 (ppm)

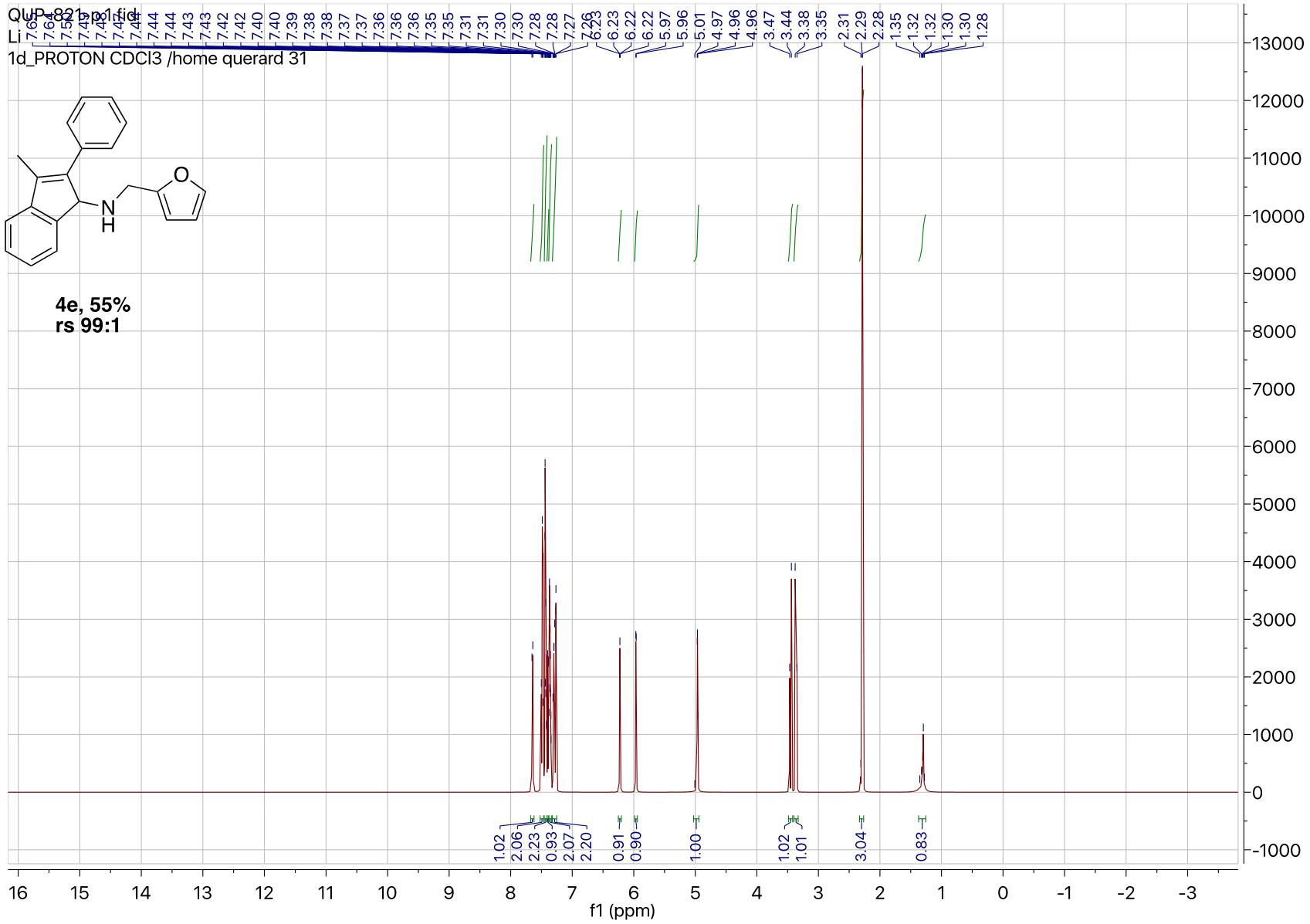
QUP-821-p1.fid
1d_PROTON CDCl3 /home querard 31
4e, 55%
rs 99:1
f1 (ppm)

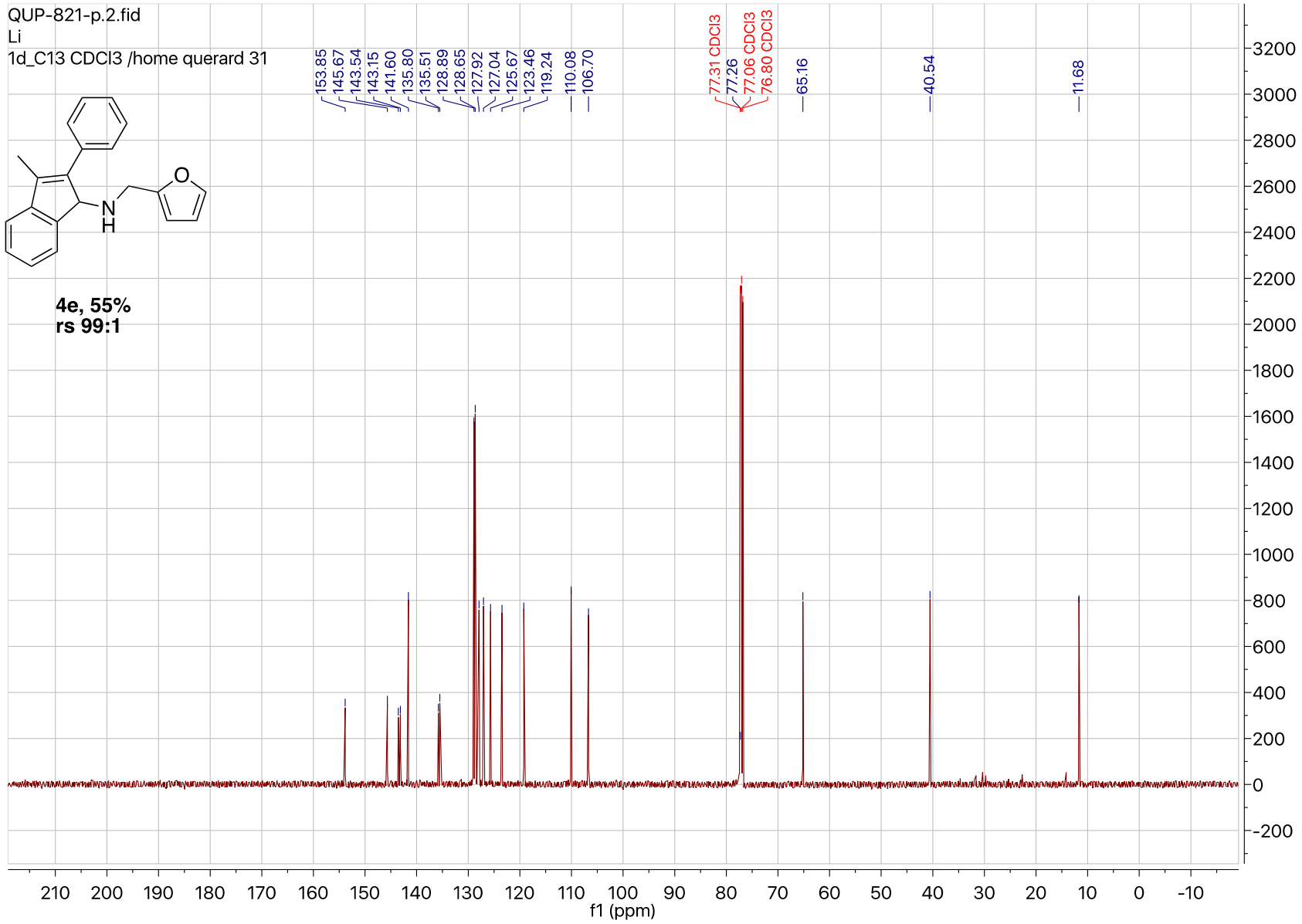
QUP-821-p.2.fid
Li
1d_C13 CDCl3 /home querard 31
153.85
145.67
143.54
143.15
141.60
135.80
135.51
128.89
128.65
127.92
127.04
125.67
123.46
119.24
110.08
106.70
77.31 CDCl3
77.26
77.06 CDCl3
76.80 CDCl3
65.16
40.54
11.68
O
N
H
4e, 55%
rs 99:1
f1 (ppm)

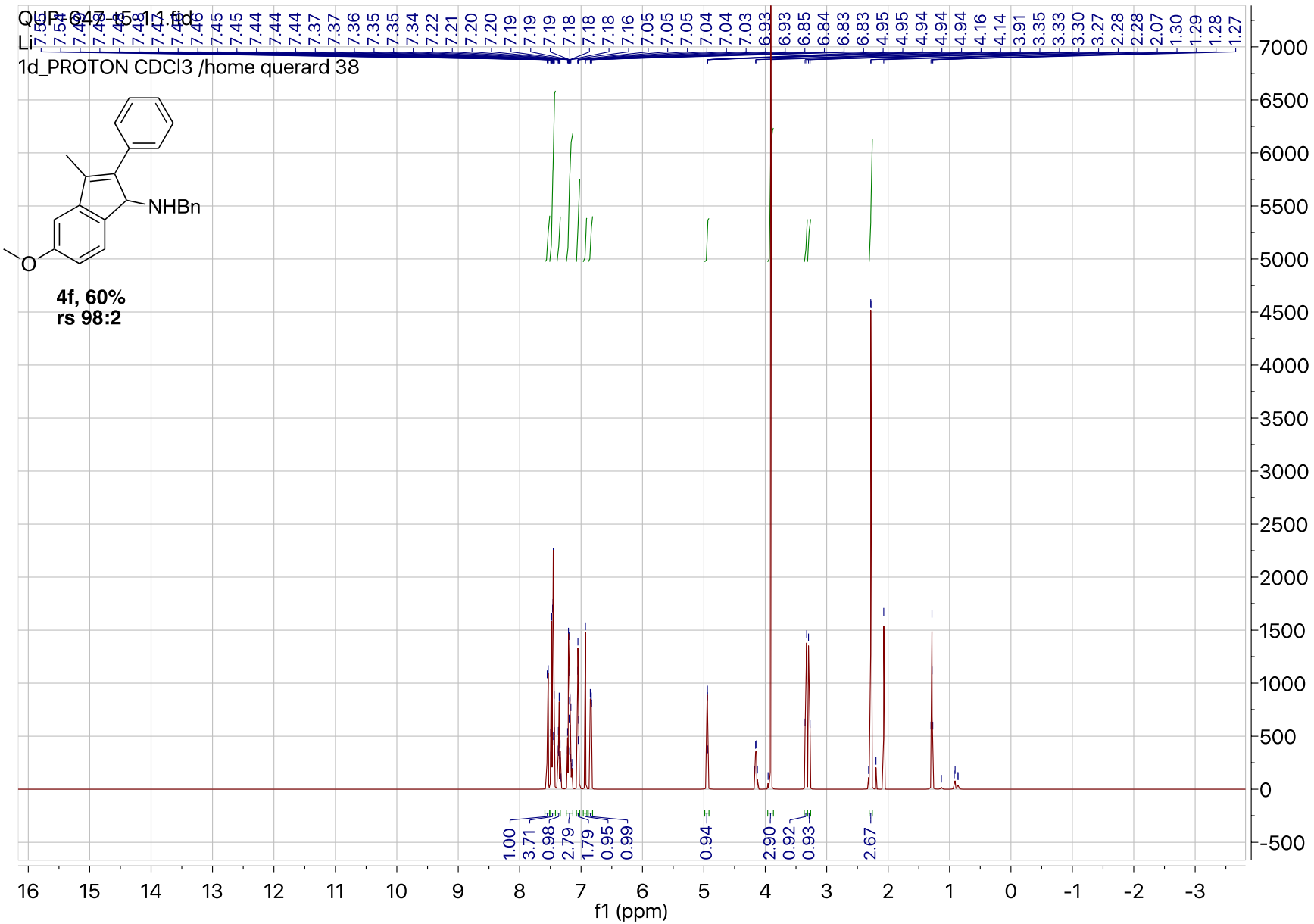
QUP-647-45-1-1.fid
1d_PROTON CDCl3 /home querard 38
NHBn
O
4f, 60%
rs 98:2
1.00
3.71
0.98
2.79
1.79
0.95
0.99
0.94
2.90
0.92
0.93
2.67
f1 (ppm)

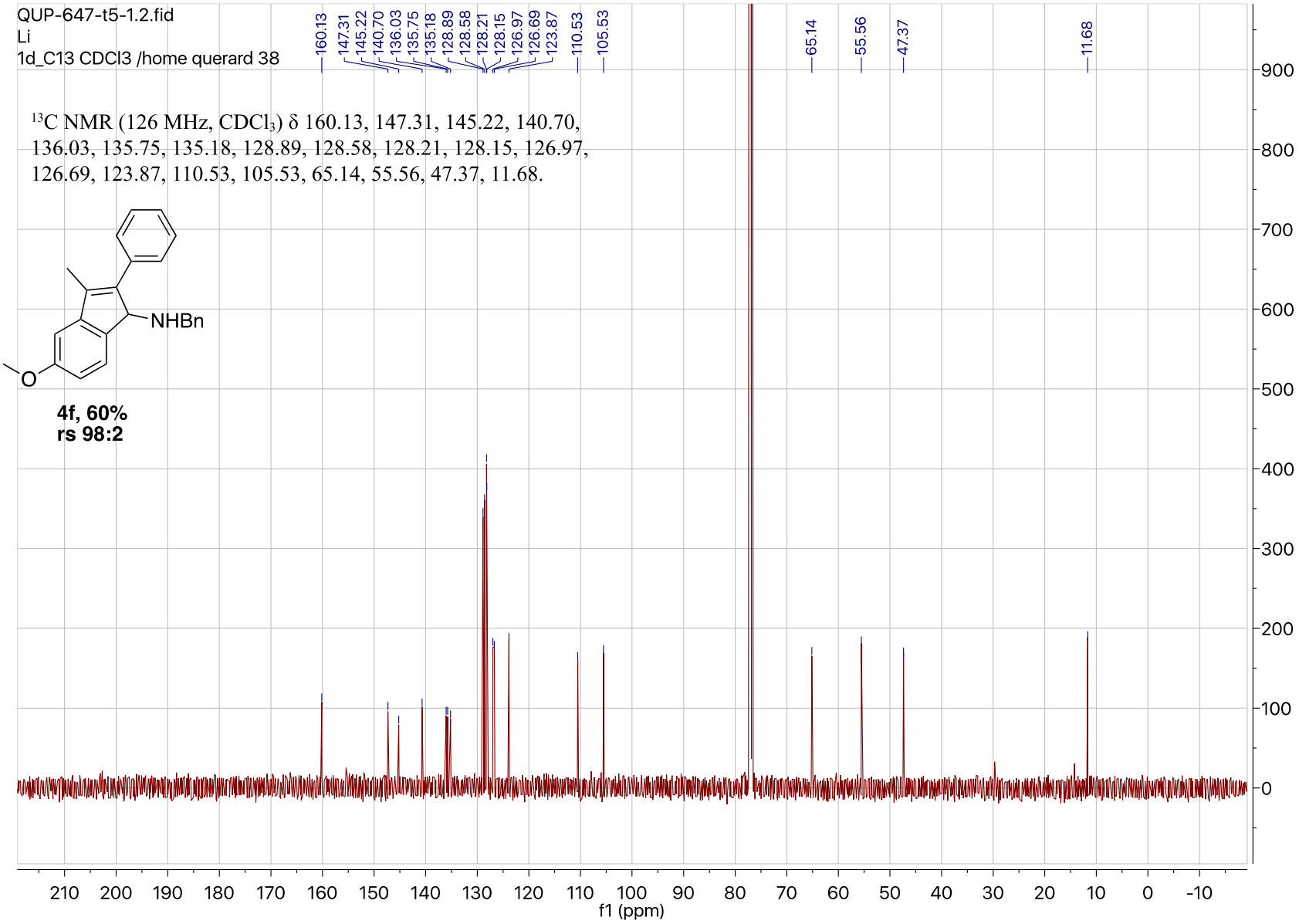
QUP-647-t5-1.2.fid
Li
1d_C13 CDCl3 /home querard 38
160.13
147.31
145.22
140.70
136.03
135.75
135.18
128.89
128.58
128.21
128.15
126.97
126.69
123.87
110.53
105.53
65.14
55.56
47.37
11.68
13C NMR (126 MHz, CDCl3) δ 160.13, 147.31, 145.22, 140.70, 136.03, 135.75, 135.18, 128.89, 128.58, 128.21, 128.15, 126.97, 126.69, 123.87, 110.53, 105.53, 65.14, 55.56, 47.37, 11.68.
NHBn
O
4f, 60%
rs 98:2
f1 (ppm)

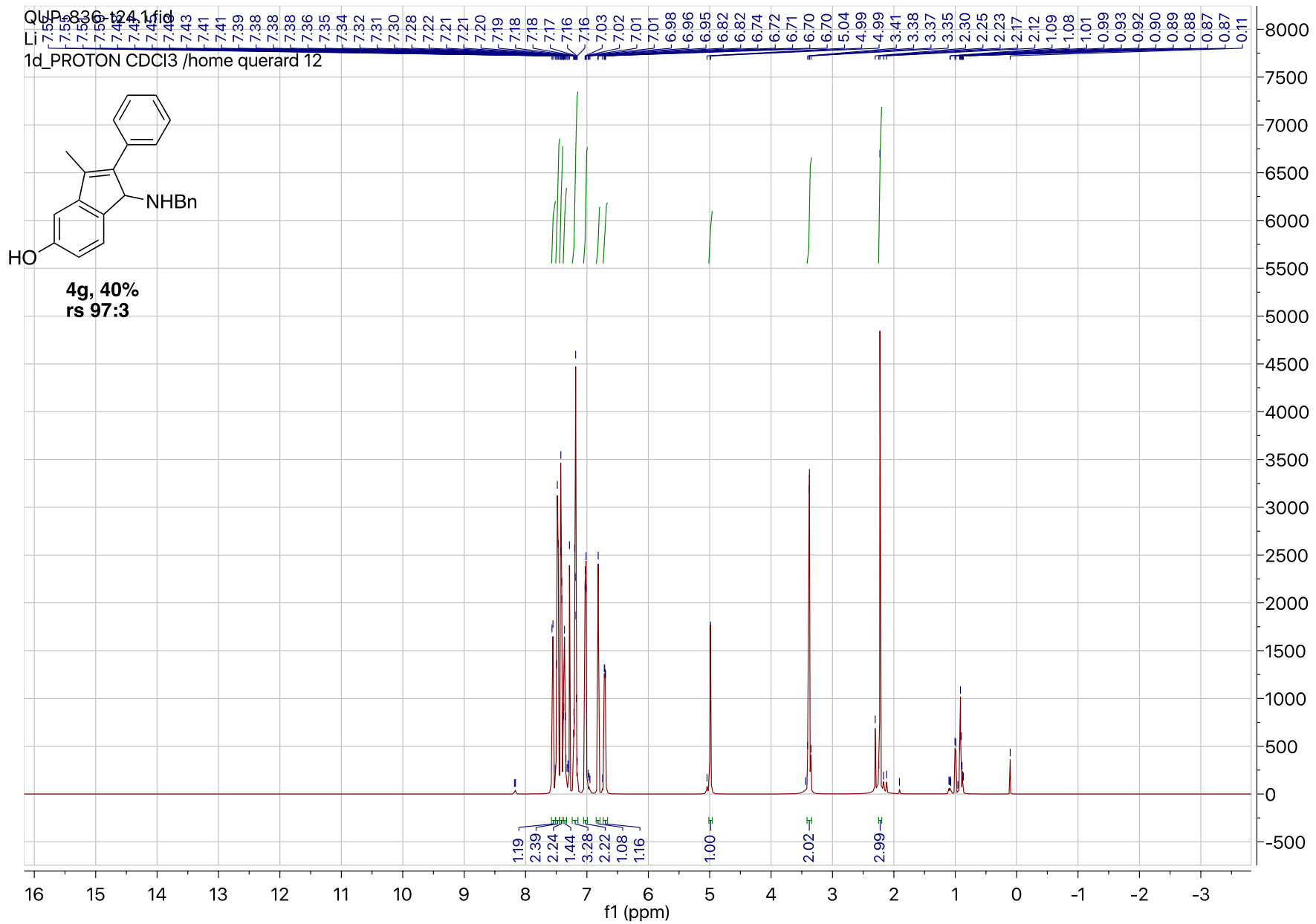
QUP-836-t24.1.fid
Li
1d_PROTON CDCl3 /home querard 12
NHBn
HO
4g, 40%
rs 97:3
f1 (ppm)

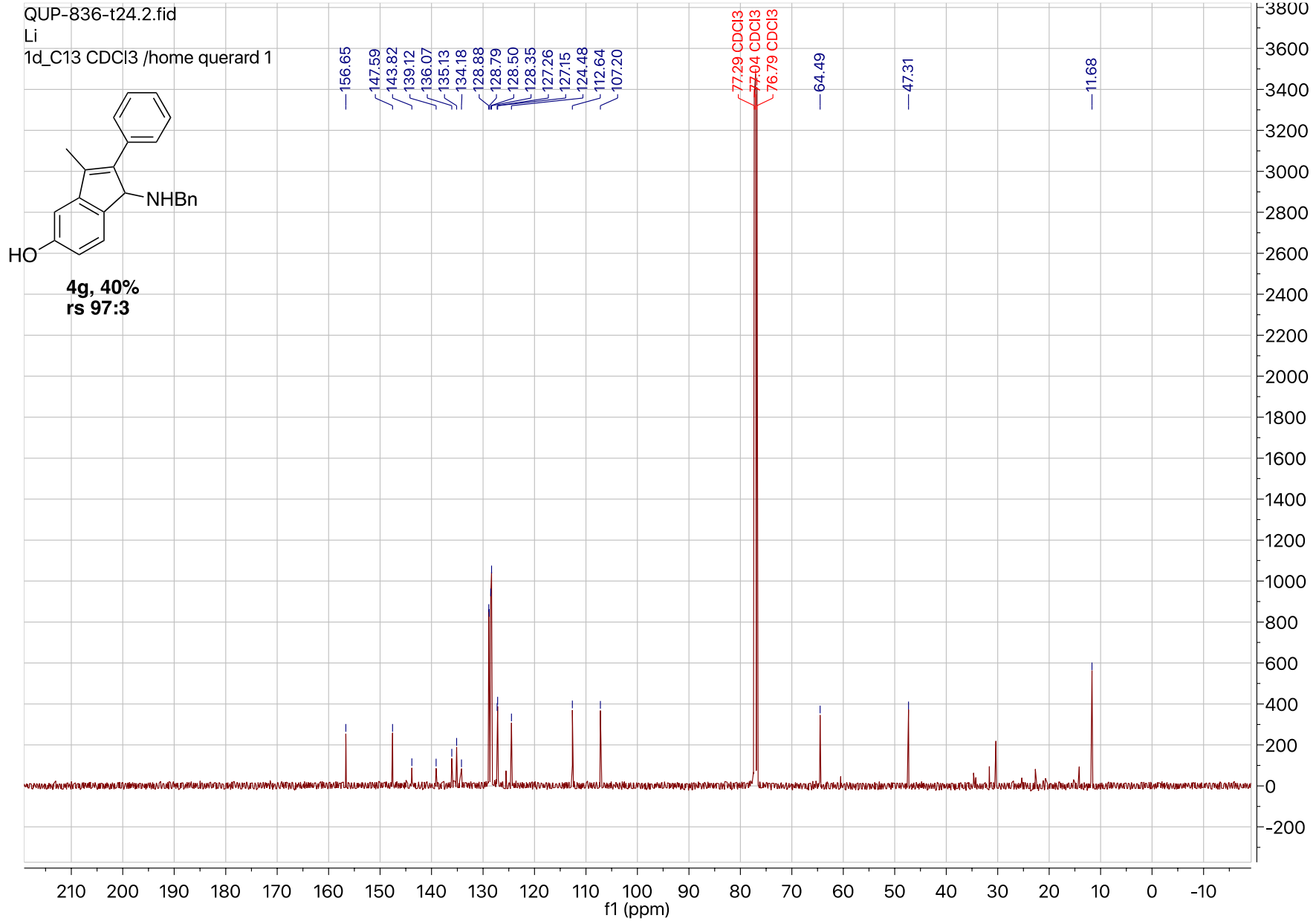
QUP-836-t24.2.fid
Li
1d_C13 CDCl3 /home querard 1
NHBn
HO
4g, 40%
rs 97:3
156.65
147.59
143.82
139.12
136.07
135.13
134.18
128.88
128.79
128.50
128.35
127.26
127.15
124.48
112.64
107.20
77.29 CDCl3
77.04 CDCl3
76.79 CDCl3
64.49
47.31
11.68
f1 (ppm)

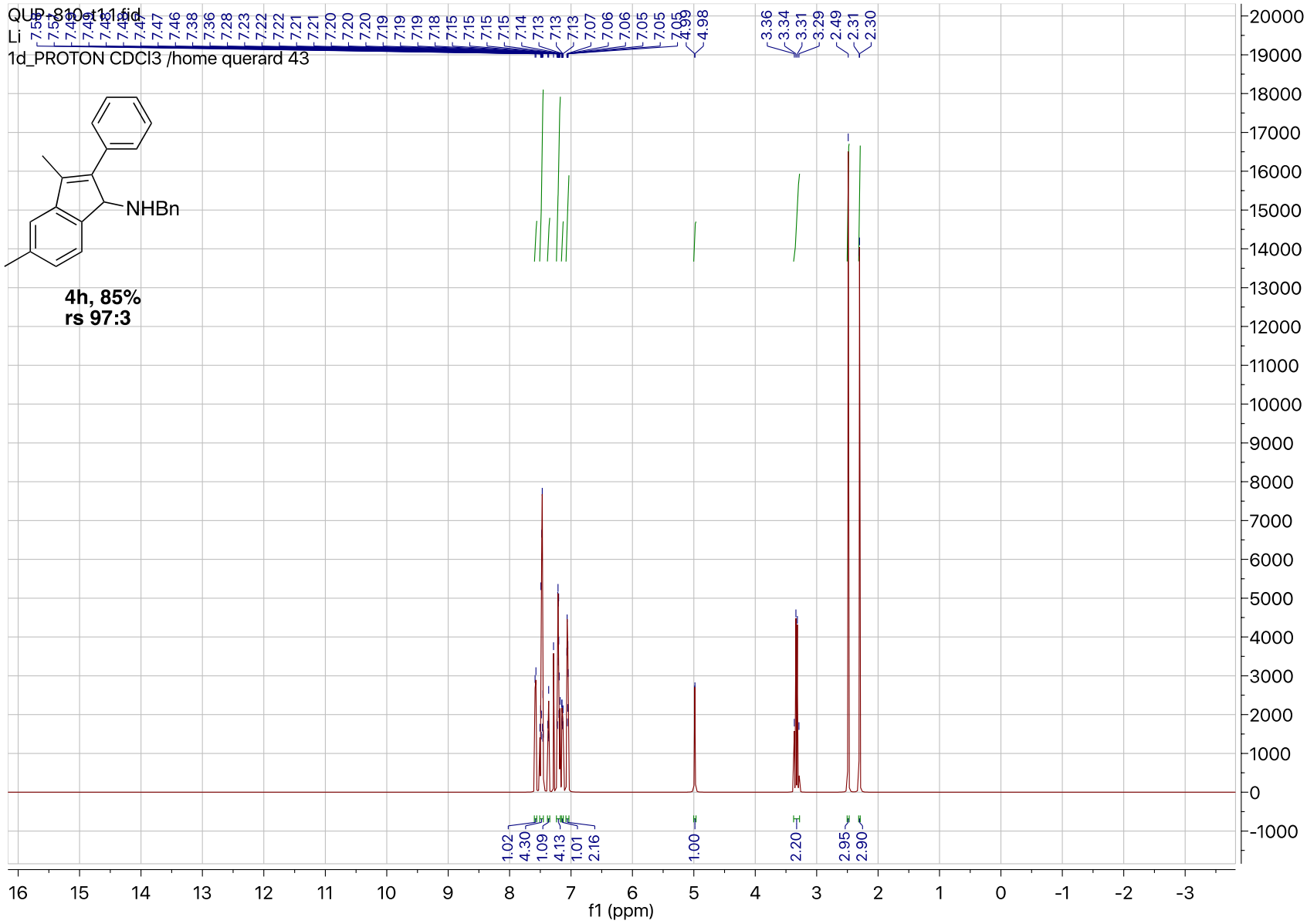
QUP-810-t11.fid
Li
1d_PROTON CDCl3 /home querard 43
NHBn
4h, 85%
rs 97:3
f1 (ppm)

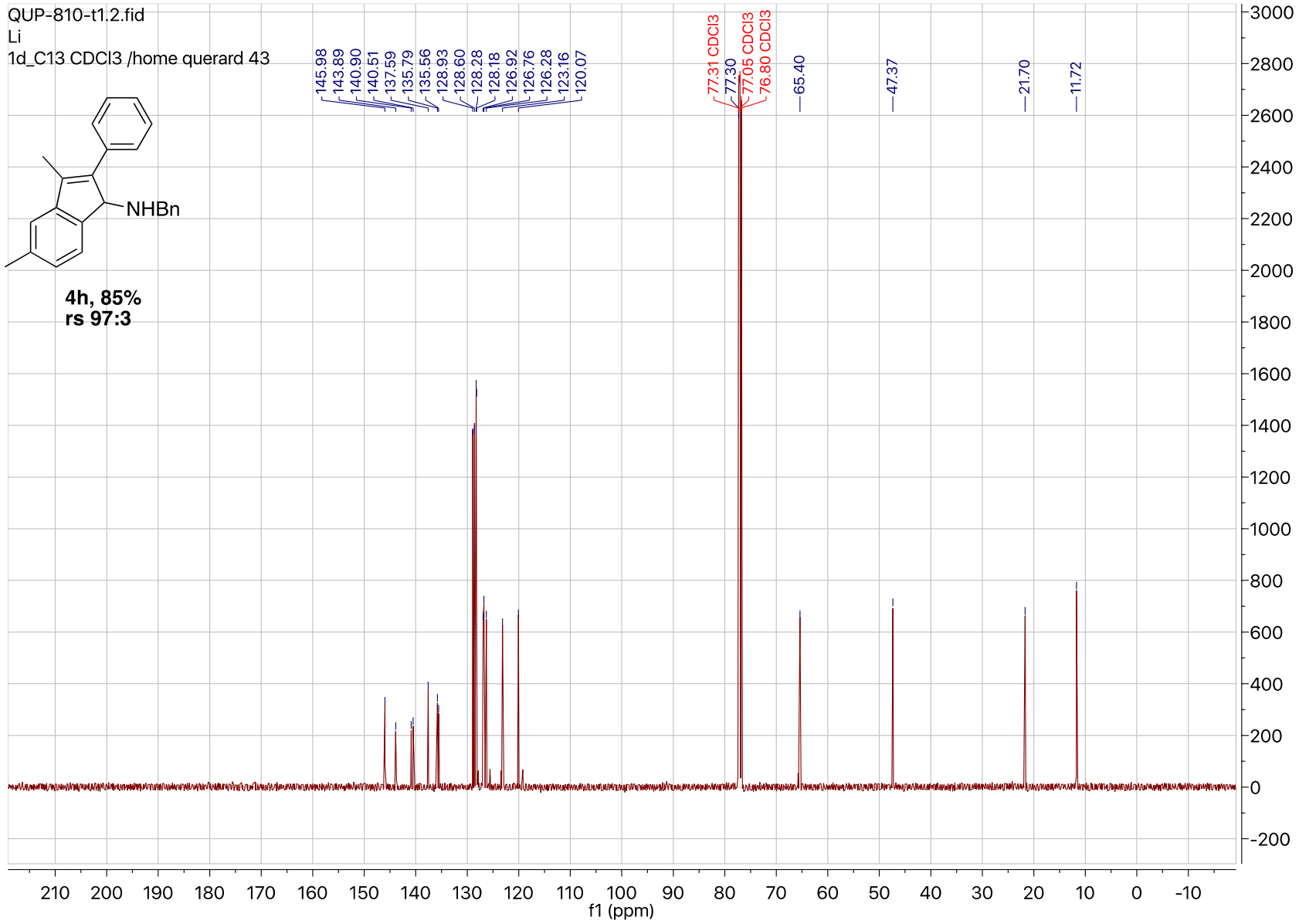
QUP-810-t1.2.fid
Li
1d_C13 CDCl3 /home querard 43
NHBn
4h, 85%
rs 97:3
145.98
143.89
140.90
140.51
137.59
135.79
135.56
128.93
128.60
128.28
128.18
126.92
126.76
126.28
123.16
120.07
77.31 CDCl3
77.30
77.05 CDCl3
76.80 CDCl3
65.40
47.37
21.70
11.72
f1 (ppm)

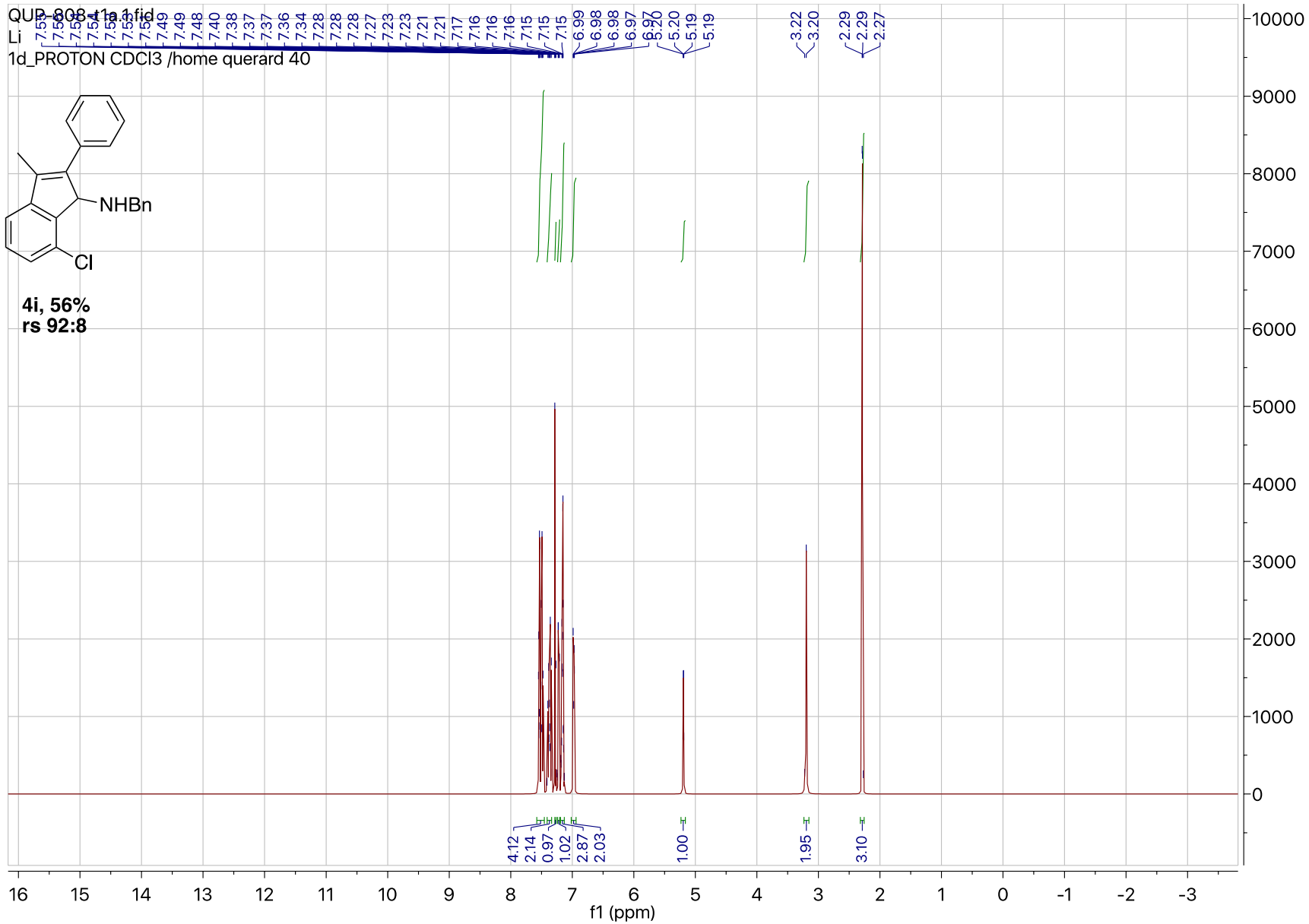
QUB-808-t1a.1.fid
Li
1d_PROTON CDCl3 /home querard 40
NHBn
Cl
4i, 56%
rs 92:8
f1 (ppm)

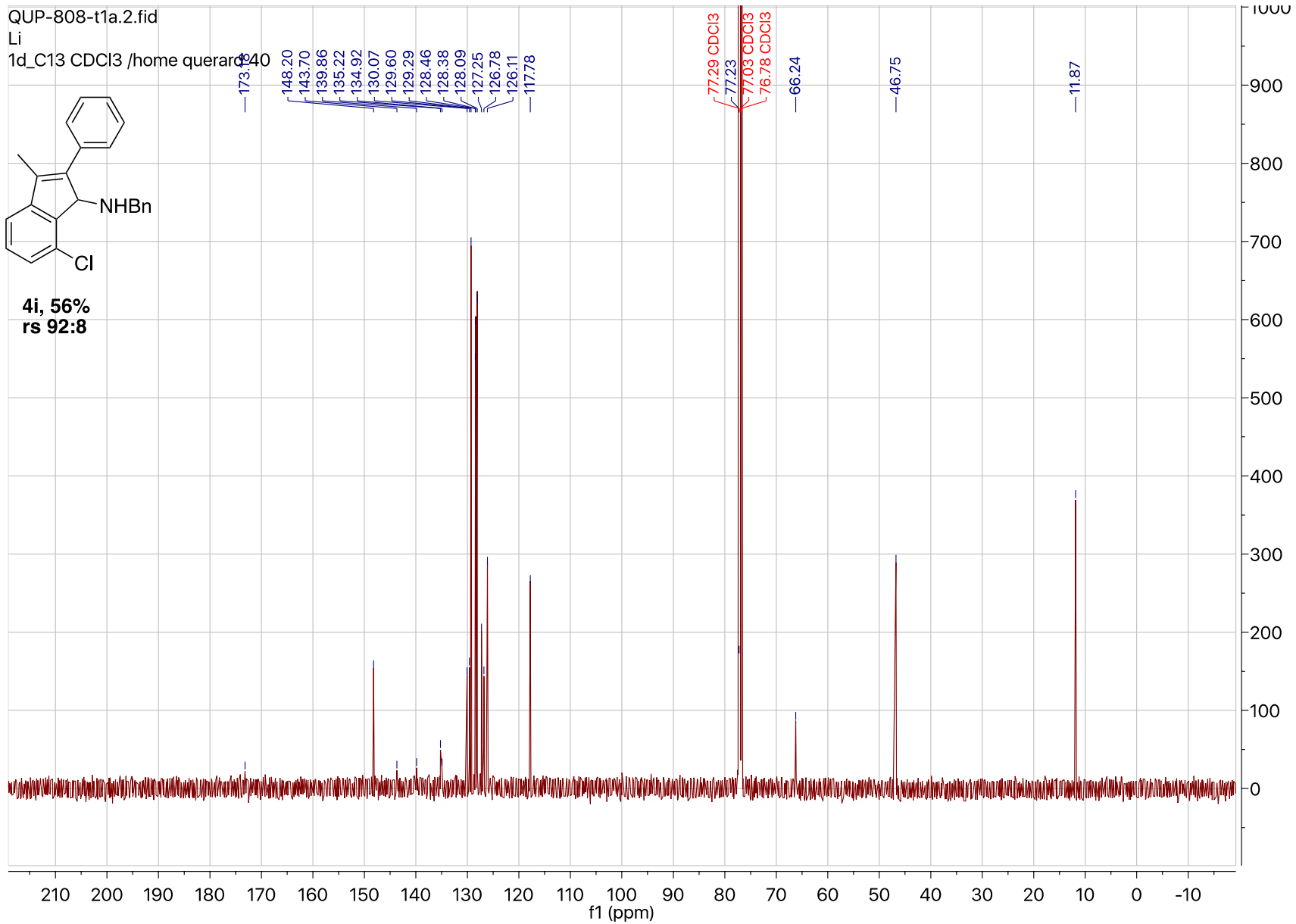
QUP-808-t1a.2.fid
Li
1d_C13 CDCl3 /home querard 40
NHBn
Cl
4i, 56%
rs 92:8
173.1
148.20
143.70
139.86
135.22
134.92
130.07
129.60
129.29
128.46
128.38
128.09
127.25
126.78
126.11
117.78
77.29 CDCl3
77.23
77.03 CDCl3
76.78 CDCl3
66.24
46.75
11.87
f1 (ppm)

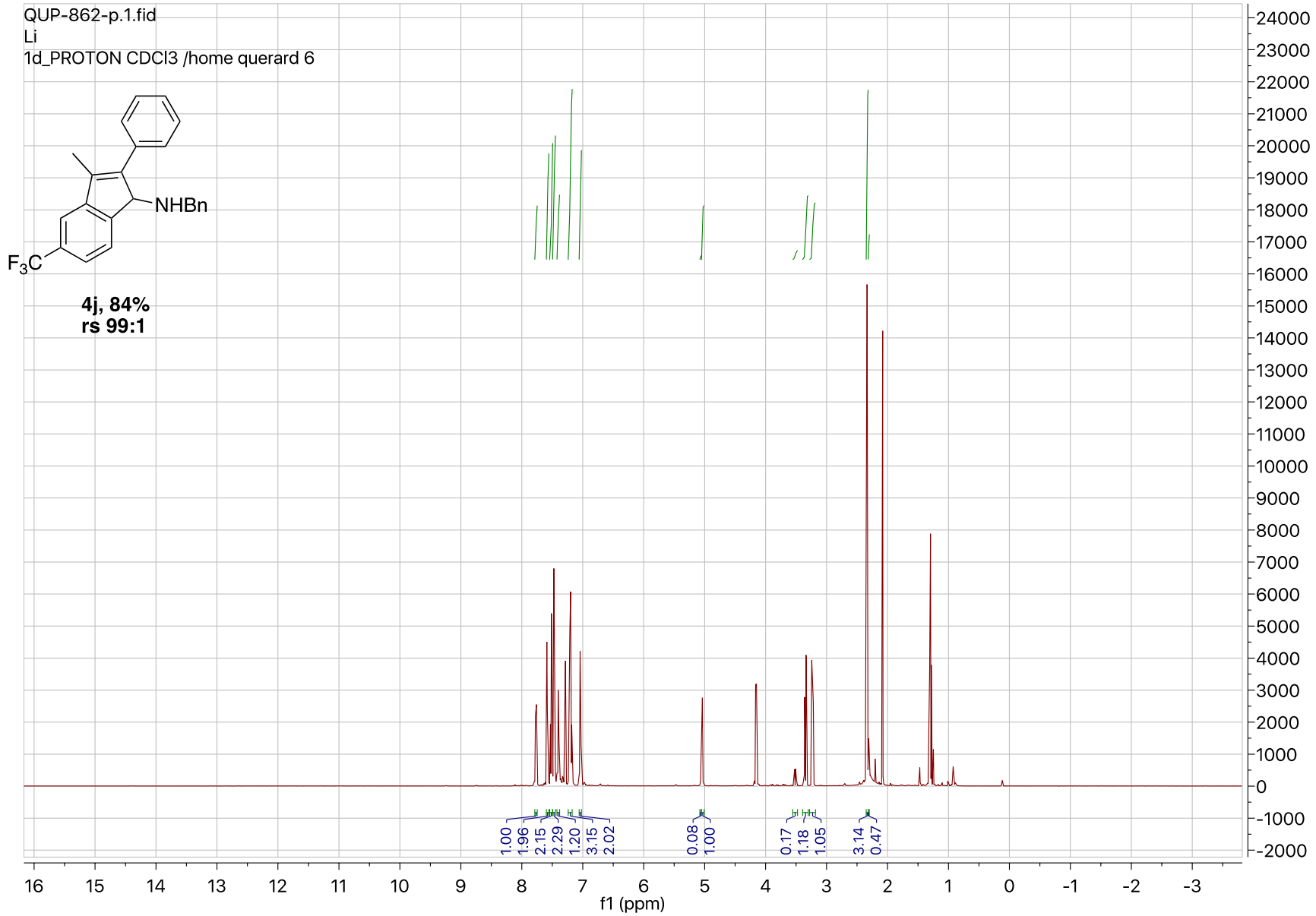
QUP-862-p.1.fid
Li
1d_PROTON CDCl3 /home querard 6
NHBn
F3C
4j, 84%
rs 99:1
1.00
1.96
2.15
2.29
1.20
3.15
2.02
0.08
1.00
0.17
1.18
1.05
3.14
0.47
f1 (ppm)

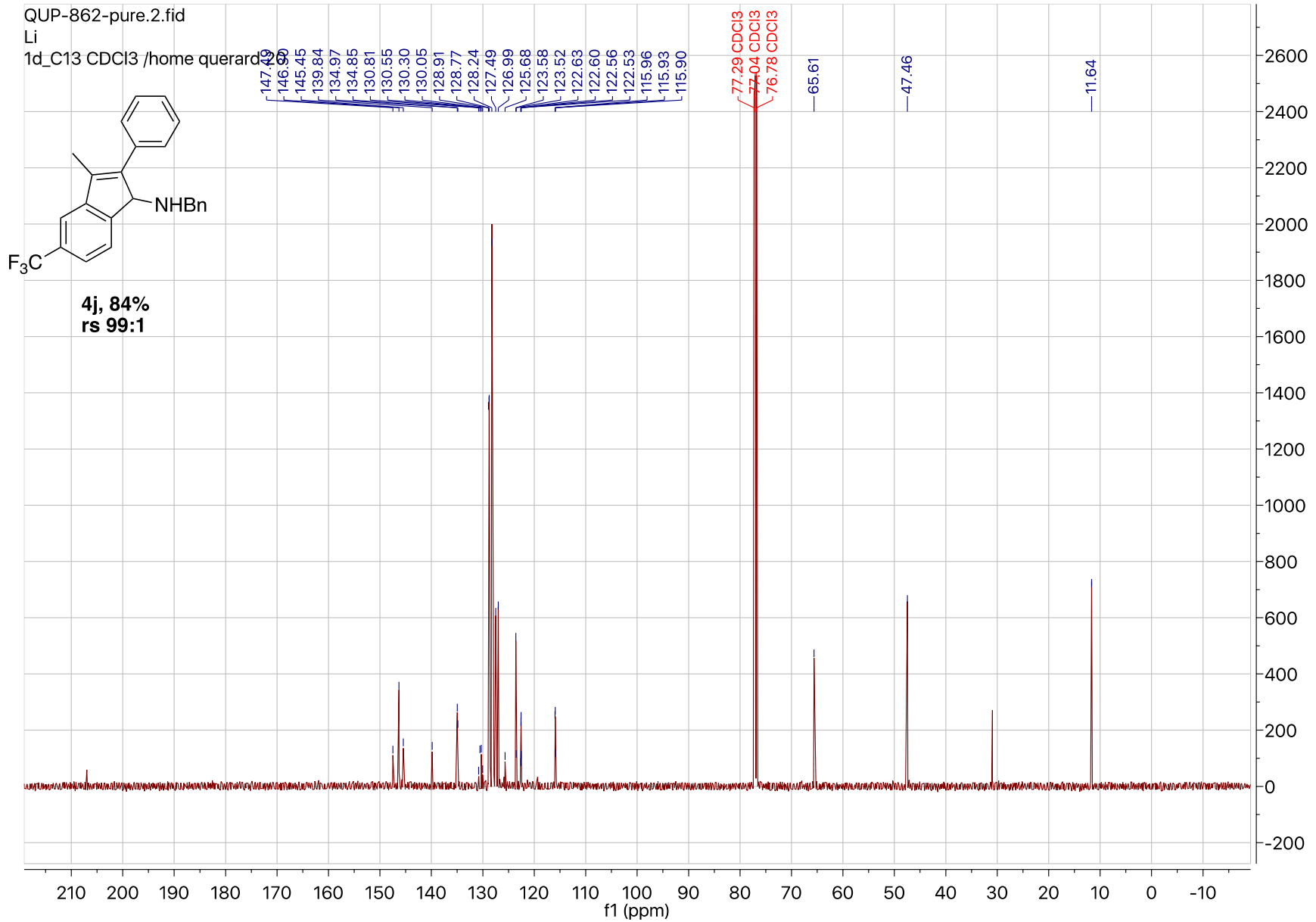
QUP-862-pure.2.fid
Li
1d_C13 CDCl3 /home querard 2
147.43
146.60
145.45
139.84
134.97
134.85
130.81
130.55
130.30
130.05
128.91
128.77
128.24
127.49
126.99
125.68
123.58
123.52
122.63
122.60
122.56
122.53
115.96
115.93
115.90
77.29 CDCl3
77.04 CDCl3
76.78 CDCl3
65.61
47.46
11.64
NHBn
F3C
4j, 84%
rs 99:1
f1 (ppm)

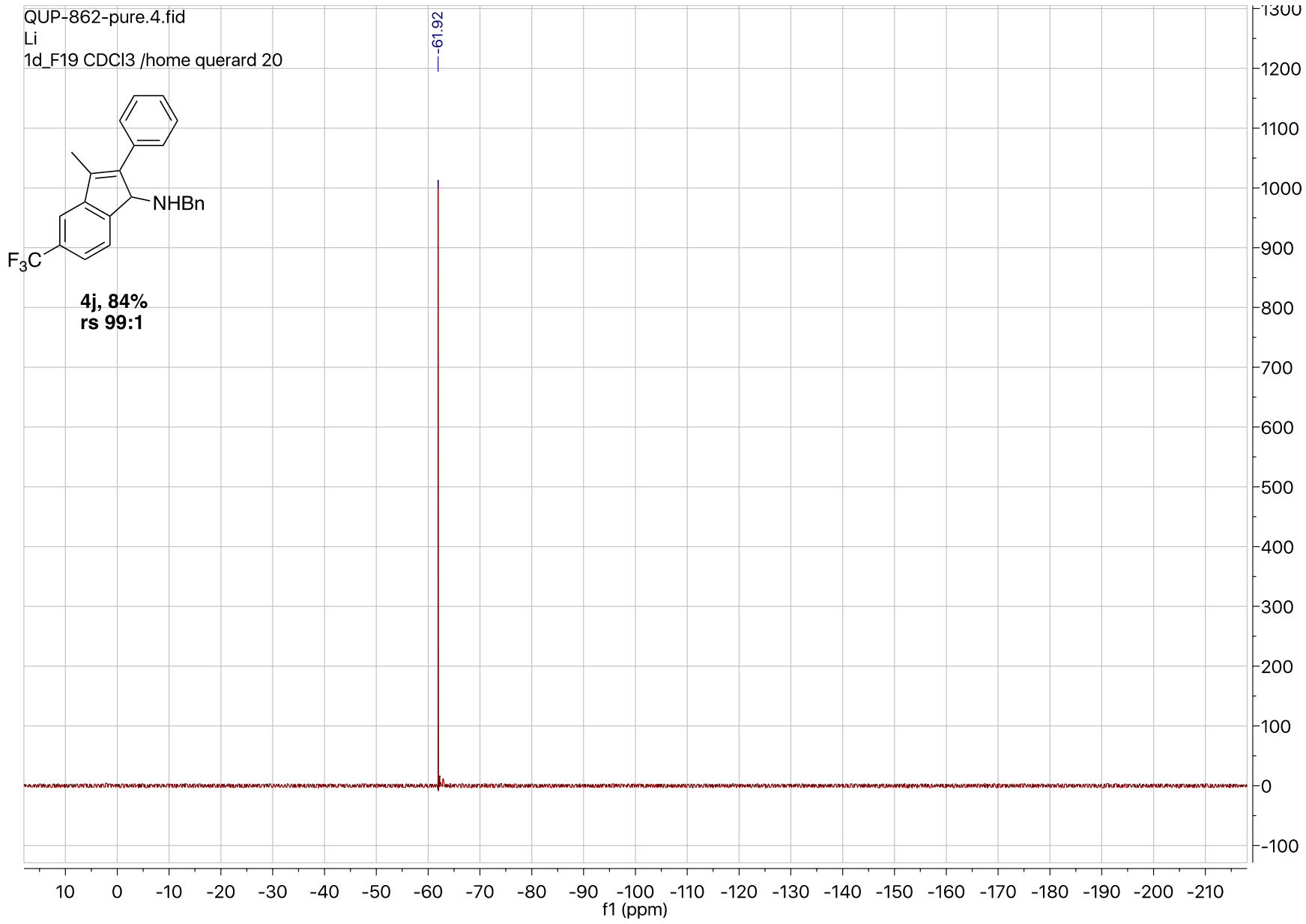
QUP-862-pure.4.fid
Li
1d_F19 CDCl3 /home querard 20
-61.92
NHBn
F3C
4j, 84%
rs 99:1
f1 (ppm)

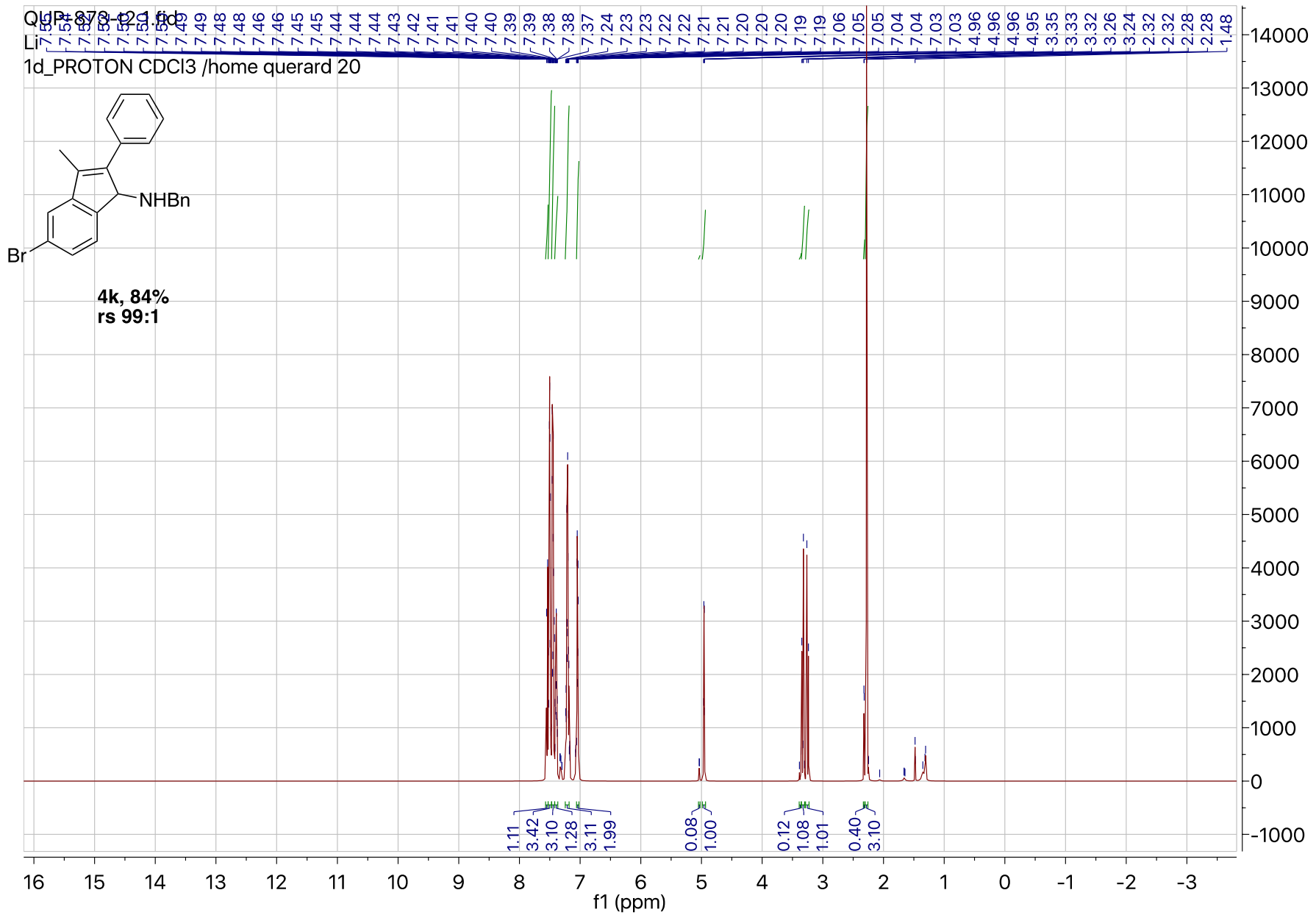
QuP-873-c2-1.fid
1d_PROTON CDCl3 /home querard 20
NHBn
Br
4k, 84%
rs 99:1
f1 (ppm)

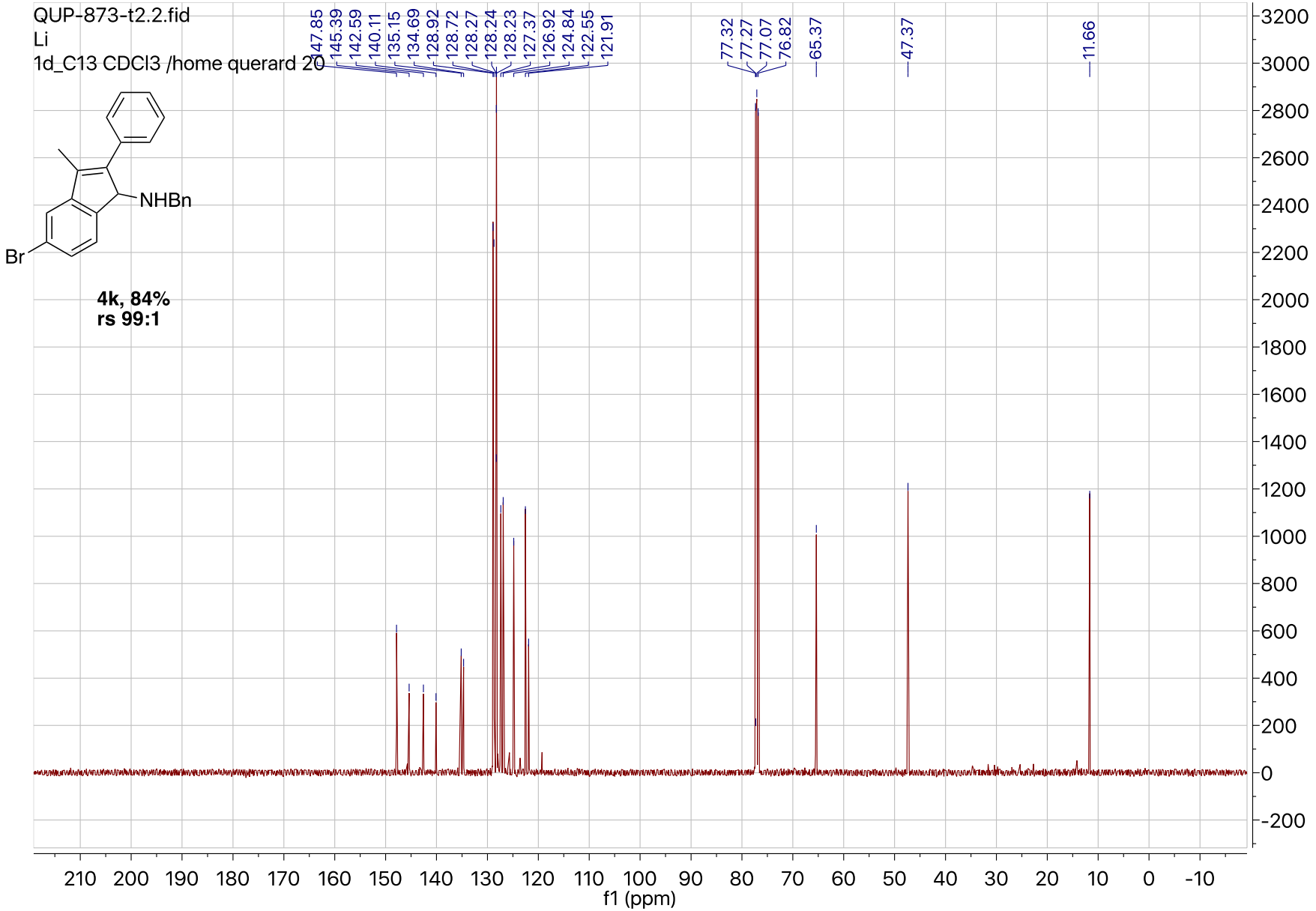
QUP-873-t2.2.fid
Li
1d_C13 CDCl3 /home querard 20
147.85
145.39
142.59
140.11
135.15
134.69
128.92
128.72
128.27
128.24
128.23
127.37
126.92
124.84
122.55
121.91
77.32
77.27
77.07
76.82
65.37
47.37
11.66
NHBn
Br
4k, 84%
rs 99:1
f1 (ppm)

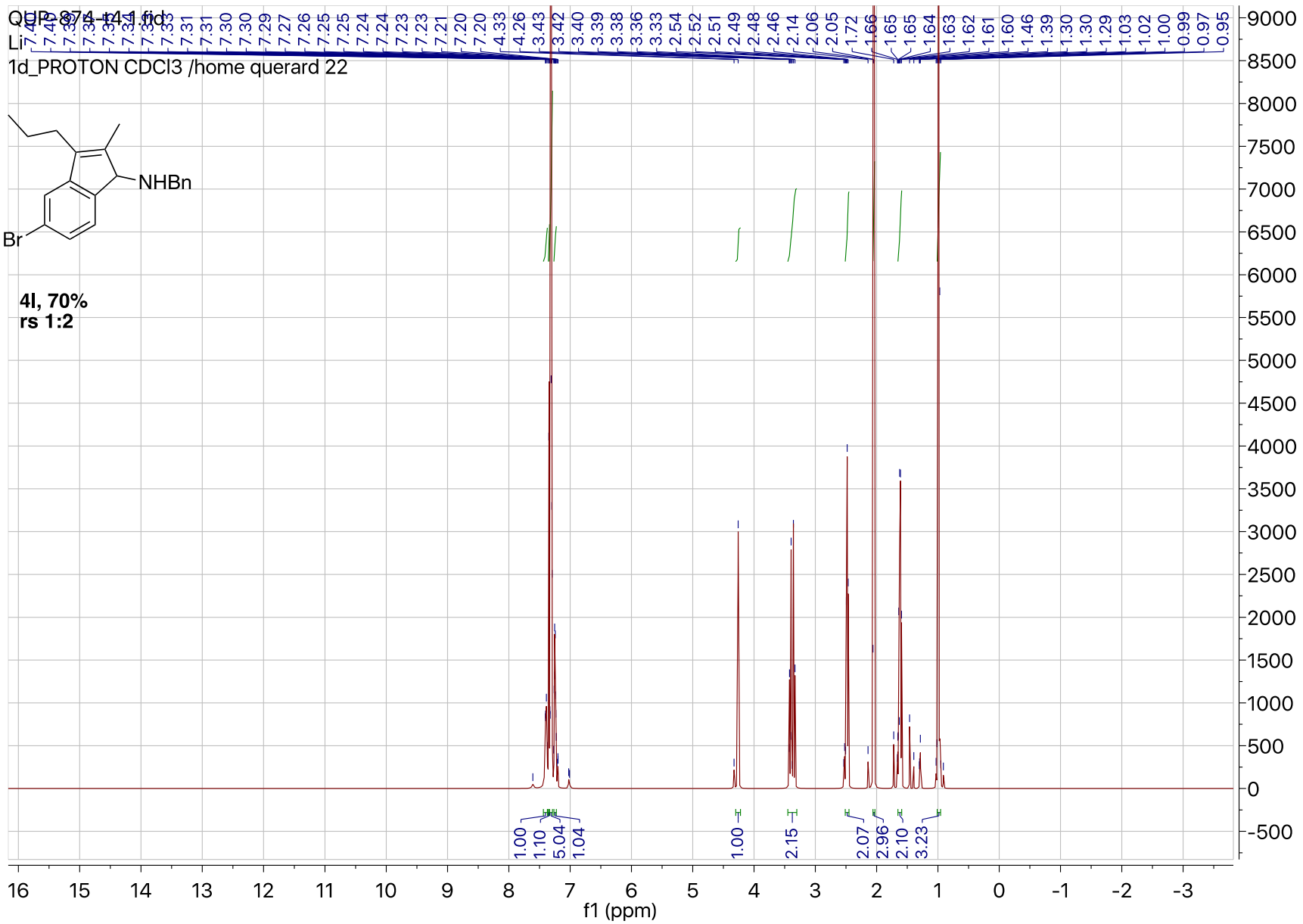
QUP-874-r4-1.fid
Li
1d_PROTON CDCl3 /home querard 22
NHBn
Br
4l, 70%
rs 1:2
f1 (ppm)

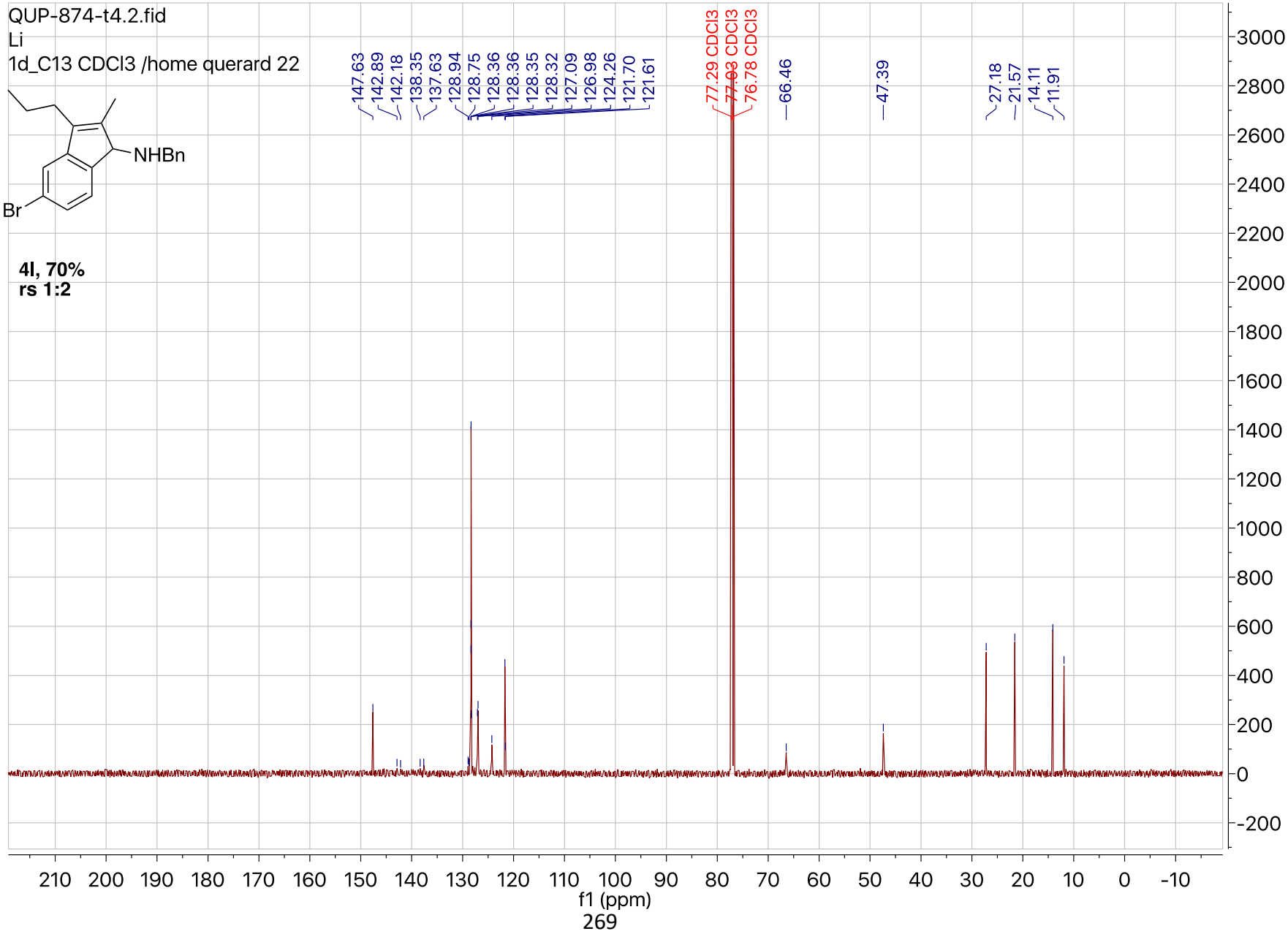
QUP-874-t4.2.fid
Li
1d_C13 CDCl3 /home querard 22
NHBn
Br
4l, 70%
rs 1:2
147.63
142.89
142.18
138.35
137.63
128.94
128.75
128.36
128.36
128.35
128.32
127.09
126.98
124.26
121.70
121.61
77.29 CDCl3
77.03 CDCl3
76.78 CDCl3
66.46
47.39
27.18
21.57
14.11
11.91
f1 (ppm)

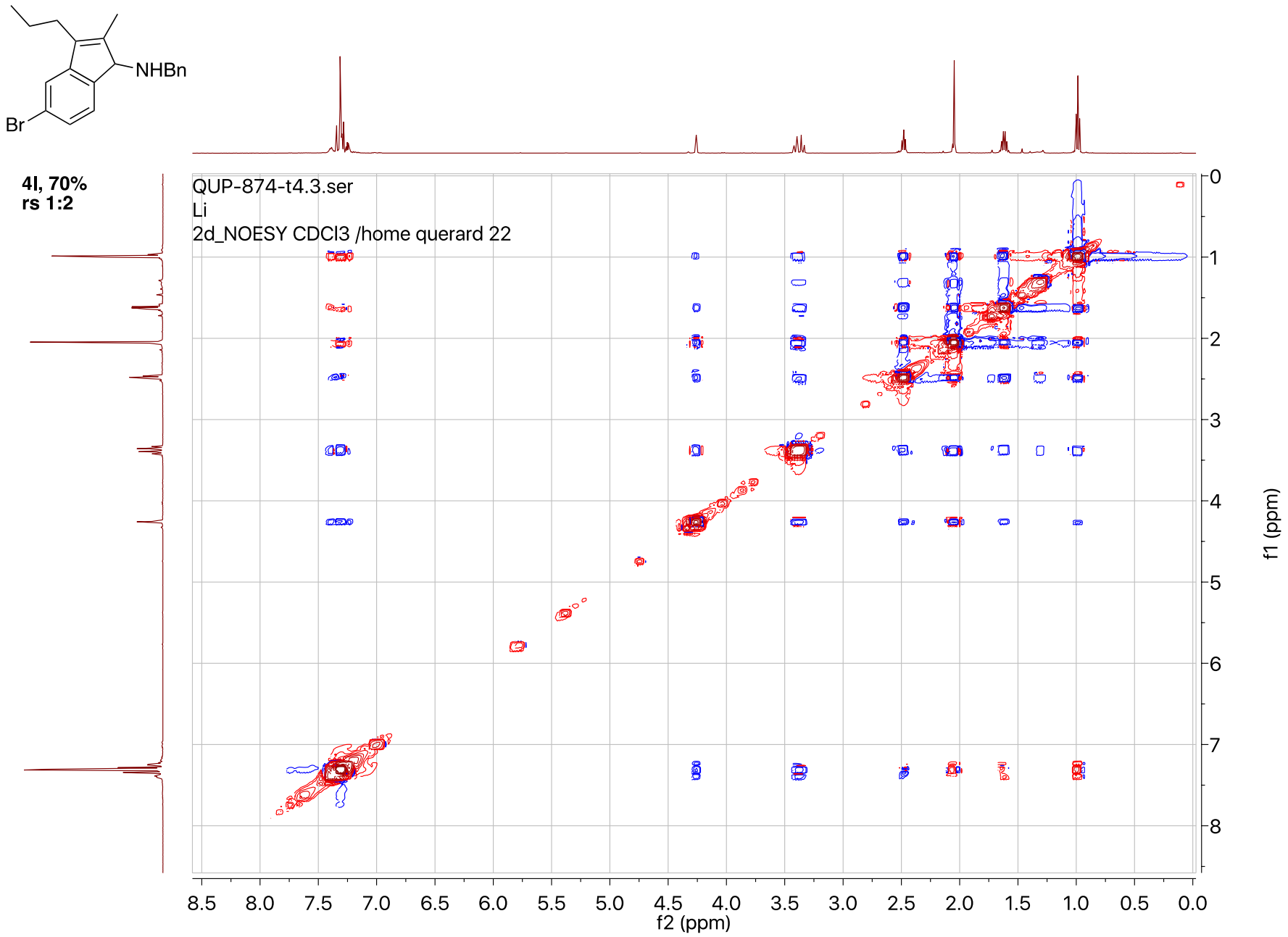
NHBn
Br
4l, 70%
rs 1:2
QUP-874-t4.3.ser
Li
2d_NOESY CDCl3 /home querard 22
8.5 8.0 7.5 7.0 6.5 6.0 5.5 5.0 4.5 4.0 3.5 3.0 2.5 2.0 1.5 1.0 0.5 0.0
f2 (ppm)
0 1 2 3 4 5 6 7 8
f1 (ppm)

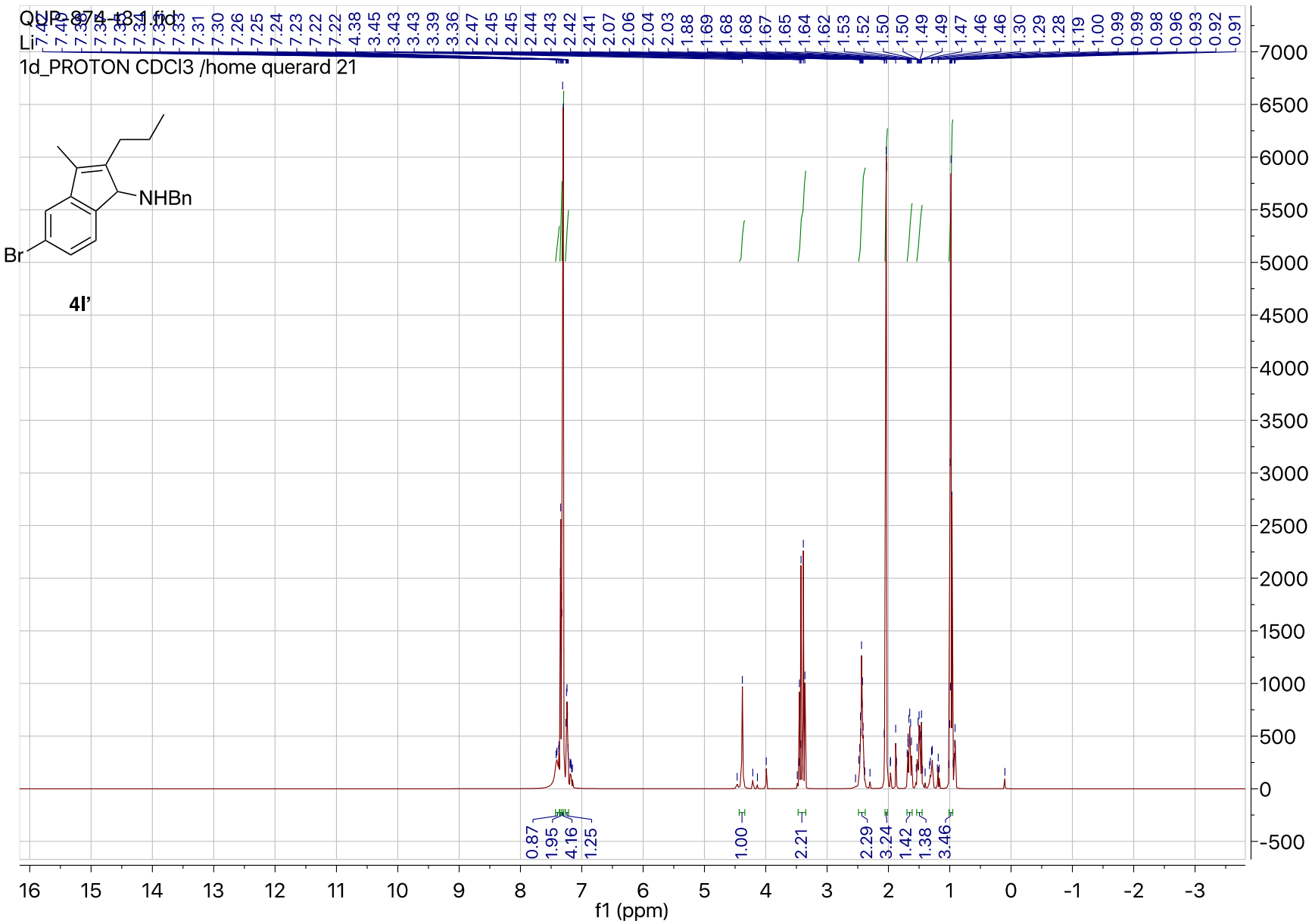
QUP-874-t3-1.fid
1d_PROTON CDCl3 /home querard 21
NHBn
Br
4l'
f1 (ppm)

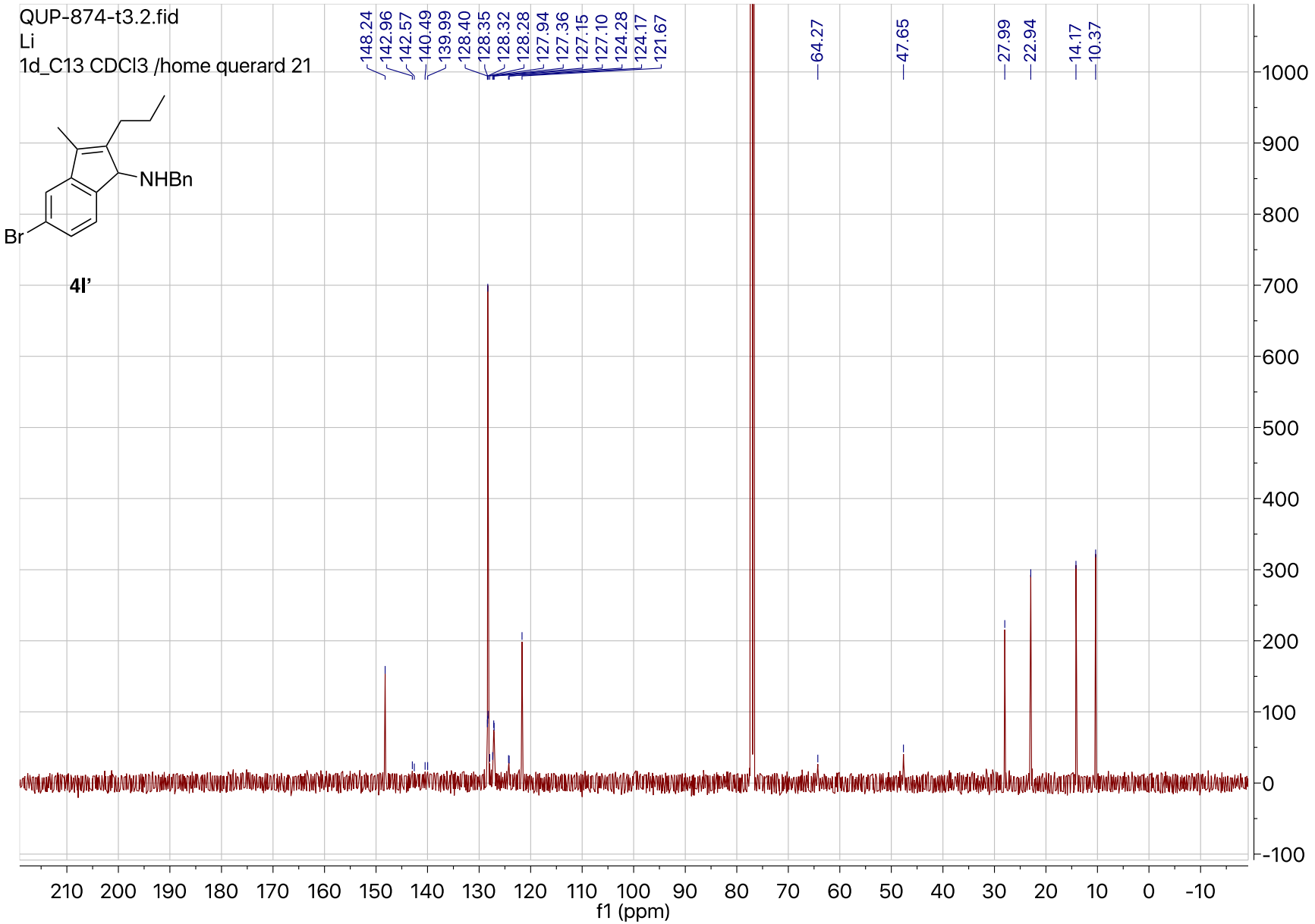
QUP-874-t3.2.fid
Li
1d_C13 CDCl3 /home querard 21
148.24
142.96
142.57
140.49
139.99
128.40
128.35
128.32
128.28
127.94
127.36
127.15
127.10
124.28
124.17
121.67
64.27
47.65
27.99
22.94
14.17
10.37
NHBn
Br
4l'
f1 (ppm)

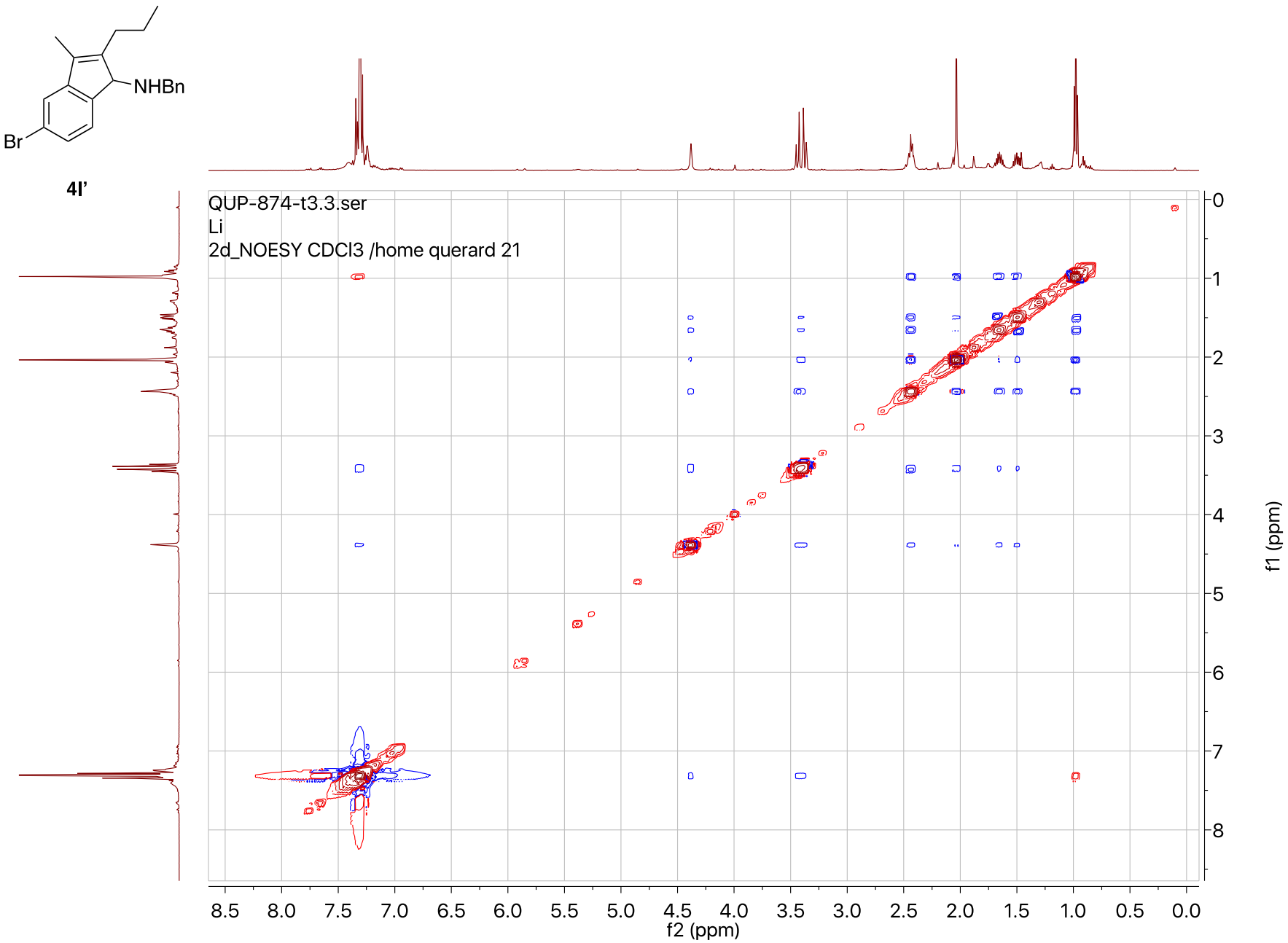
NHBn
Br
4l'
QUP-874-t3.3.ser
Li
2d_NOESY CDCl3 /home querard 21
8.5 8.0 7.5 7.0 6.5 6.0 5.5 5.0 4.5 4.0 3.5 3.0 2.5 2.0 1.5 1.0 0.5 0.0
f2 (ppm)
0 1 2 3 4 5 6 7 8
f1 (ppm)

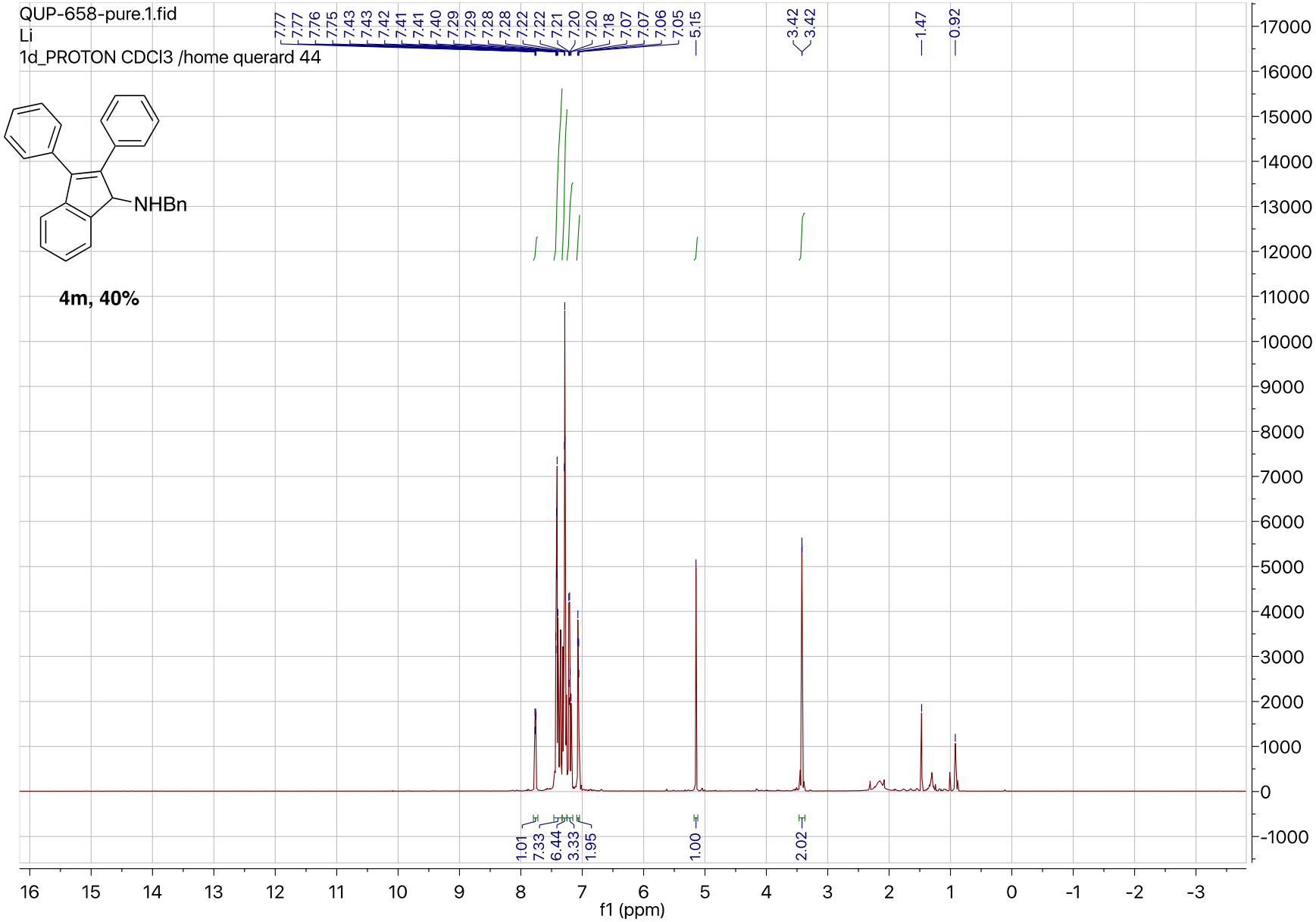
QUP-658-pure.1.fid
Li
1d_PROTON CDCl3 /home querard 44
NHBn
4m, 40%
7.77
7.77
7.76
7.75
7.43
7.43
7.42
7.41
7.41
7.40
7.29
7.29
7.28
7.28
7.22
7.22
7.21
7.20
7.20
7.18
7.07
7.07
7.06
7.05
5.15
3.42
3.42
1.47
0.92
1.01
7.33
6.44
3.33
1.95
1.00
2.02
f1 (ppm)

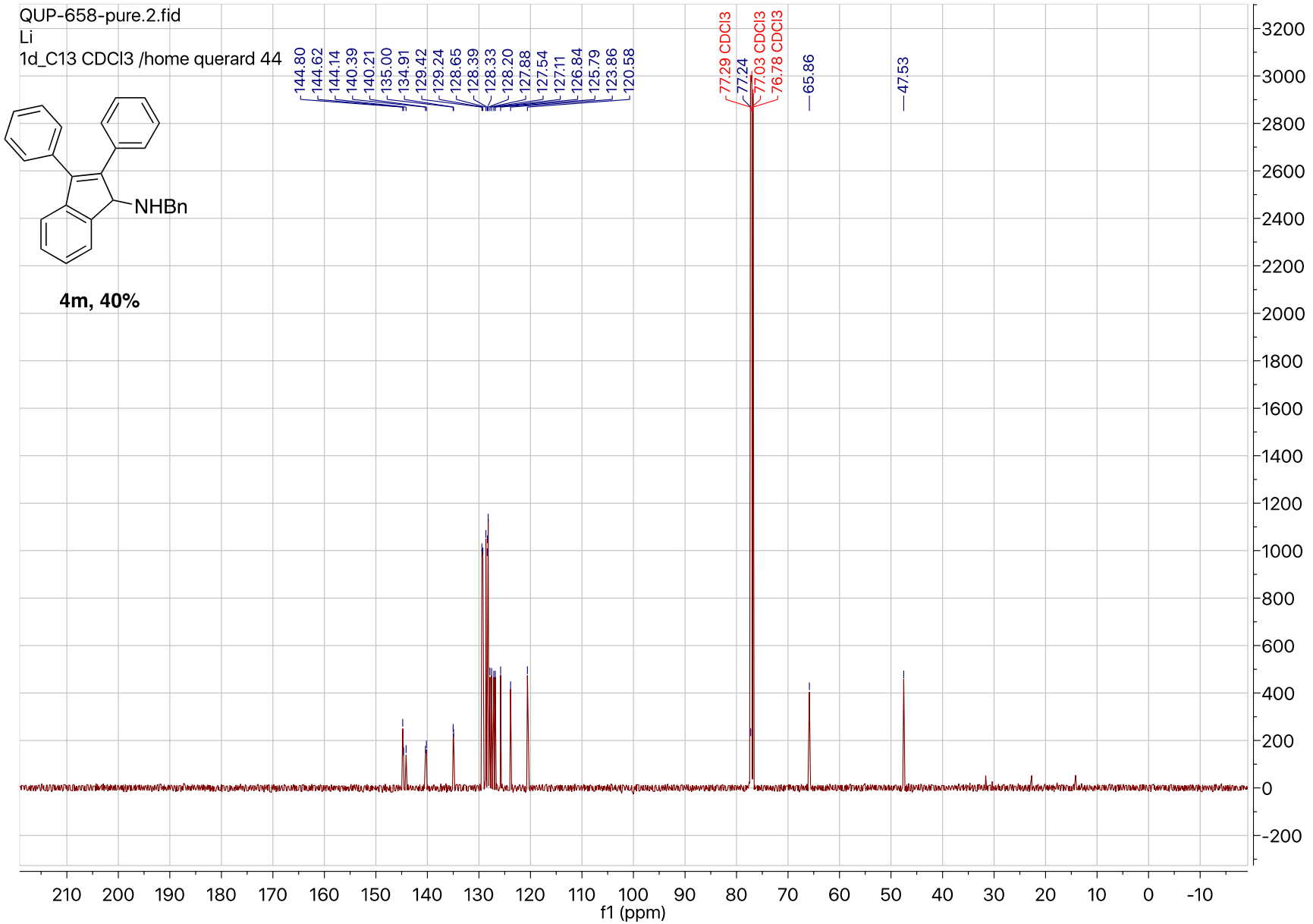
QUP-658-pure.2.fid
Li
1d_C13 CDCl3 /home querard 44
NHBn
4m, 40%
144.80
144.62
144.14
140.39
140.21
135.00
134.91
129.42
129.24
128.65
128.39
128.33
128.20
127.88
127.54
127.11
126.84
125.79
123.86
120.58
77.29 CDCl3
77.24
77.03 CDCl3
76.78 CDCl3
65.86
47.53
f1 (ppm)

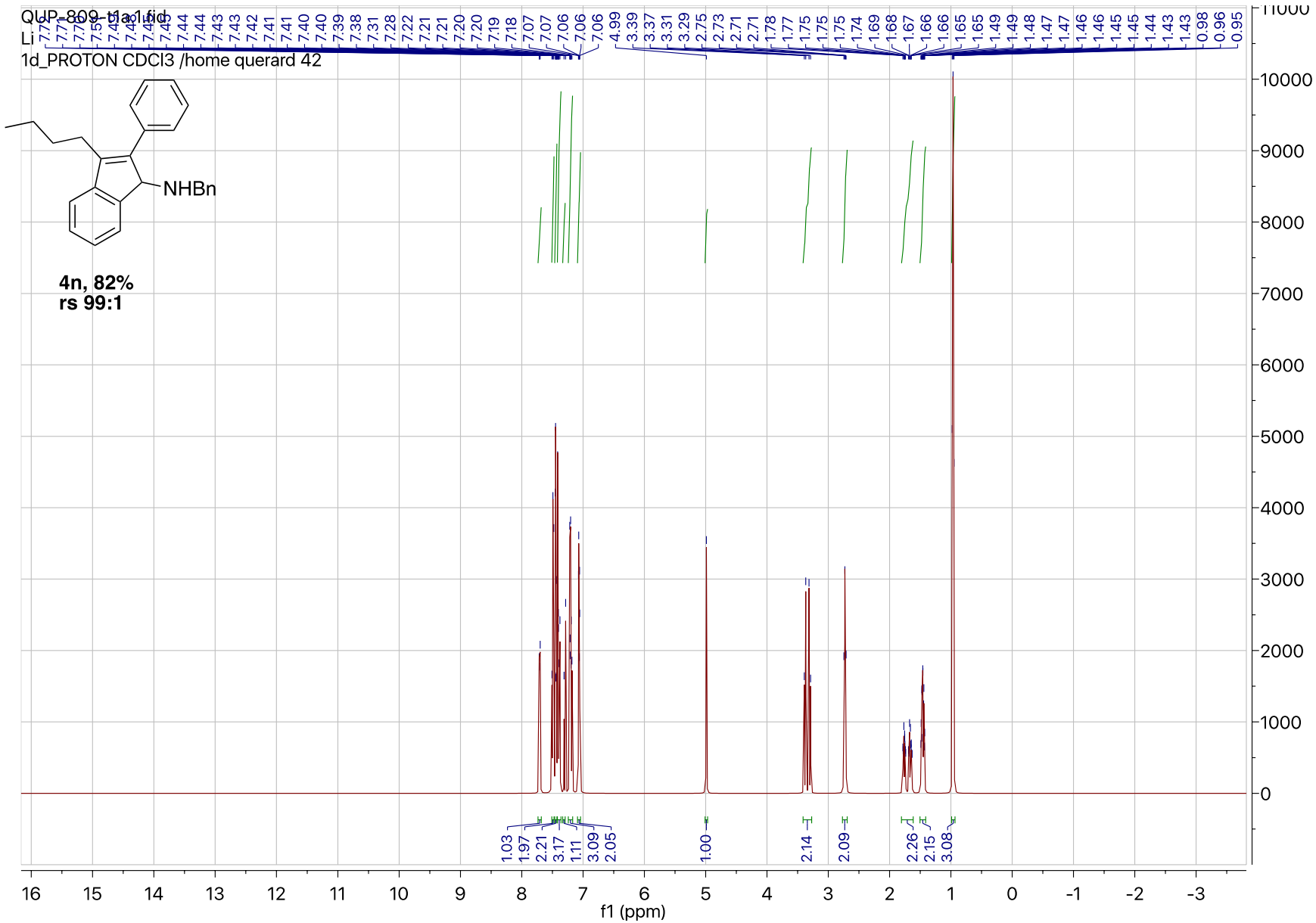
QUP-809-1a-1.fid
Li
1d_PROTON CDCl3 /home querard 42
NHBn
4n, 82%
rs 99:1
f1 (ppm)

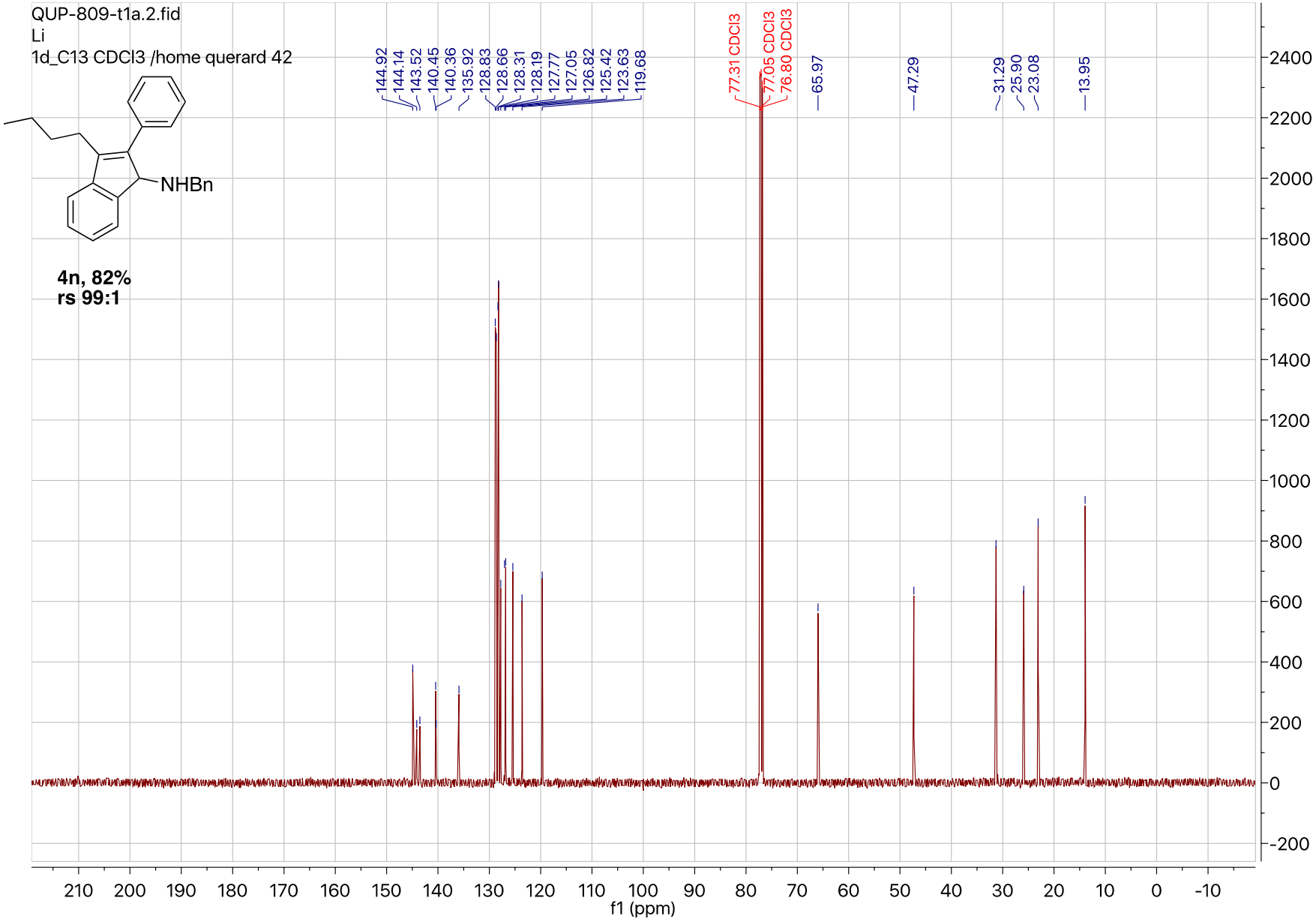
QUP-809-t1a.2.fid
Li
1d_C13 CDCl3 /home querard 42
NHBn
4n, 82%
rs 99:1
144.92
144.14
143.52
140.45
140.36
135.92
128.83
128.66
128.31
128.19
127.77
127.05
126.82
125.42
123.63
119.68
77.31 CDCl3
77.05 CDCl3
76.80 CDCl3
65.97
47.29
31.29
25.90
23.08
13.95
f1 (ppm)

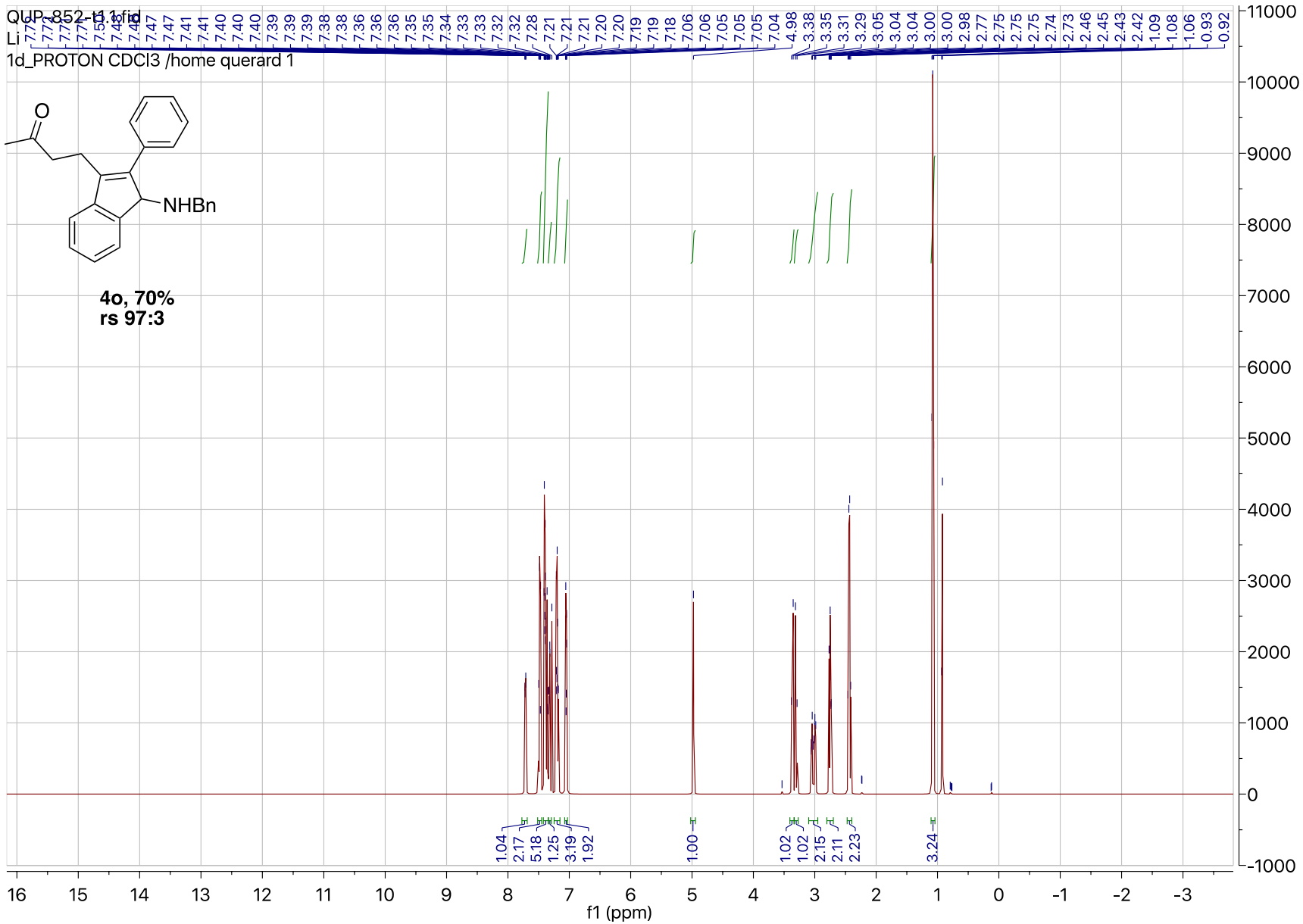
QUP-852-h1.fid
1d_PROTON CDCl3 /home querard 1
O
NHBn
4o, 70%
rs 97:3
f1 (ppm)

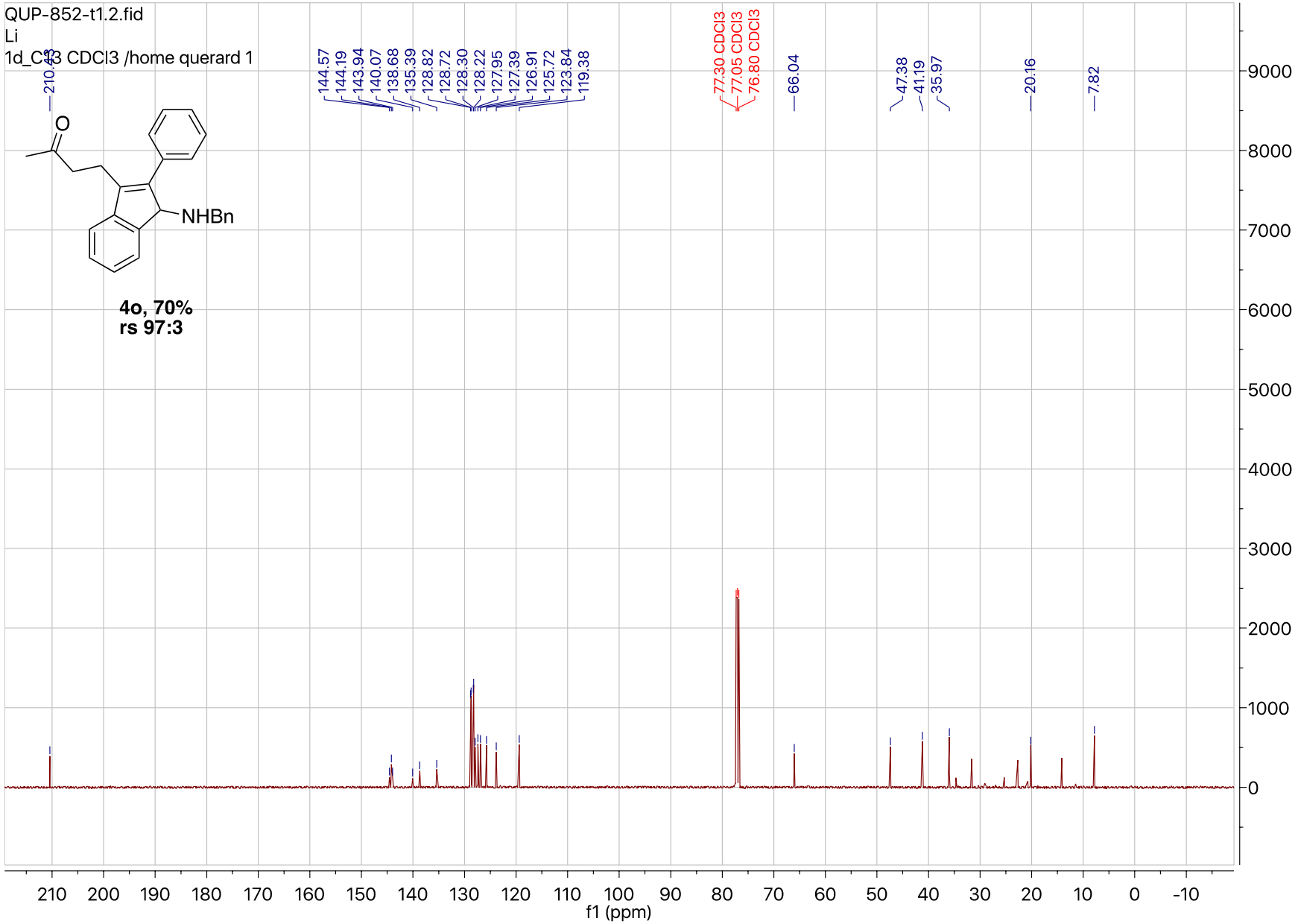
QUP-852-t1.2.fid
Li
1d_C13 CDCl3 /home querard 1
210.43
144.57
144.19
143.94
140.07
138.68
135.39
128.82
128.72
128.30
128.22
127.95
127.39
126.91
125.72
123.84
119.38
77.30 CDCl3
77.05 CDCl3
76.80 CDCl3
66.04
47.38
41.19
35.97
20.16
7.82
O
NHBn
4o, 70%
rs 97:3
f1 (ppm)

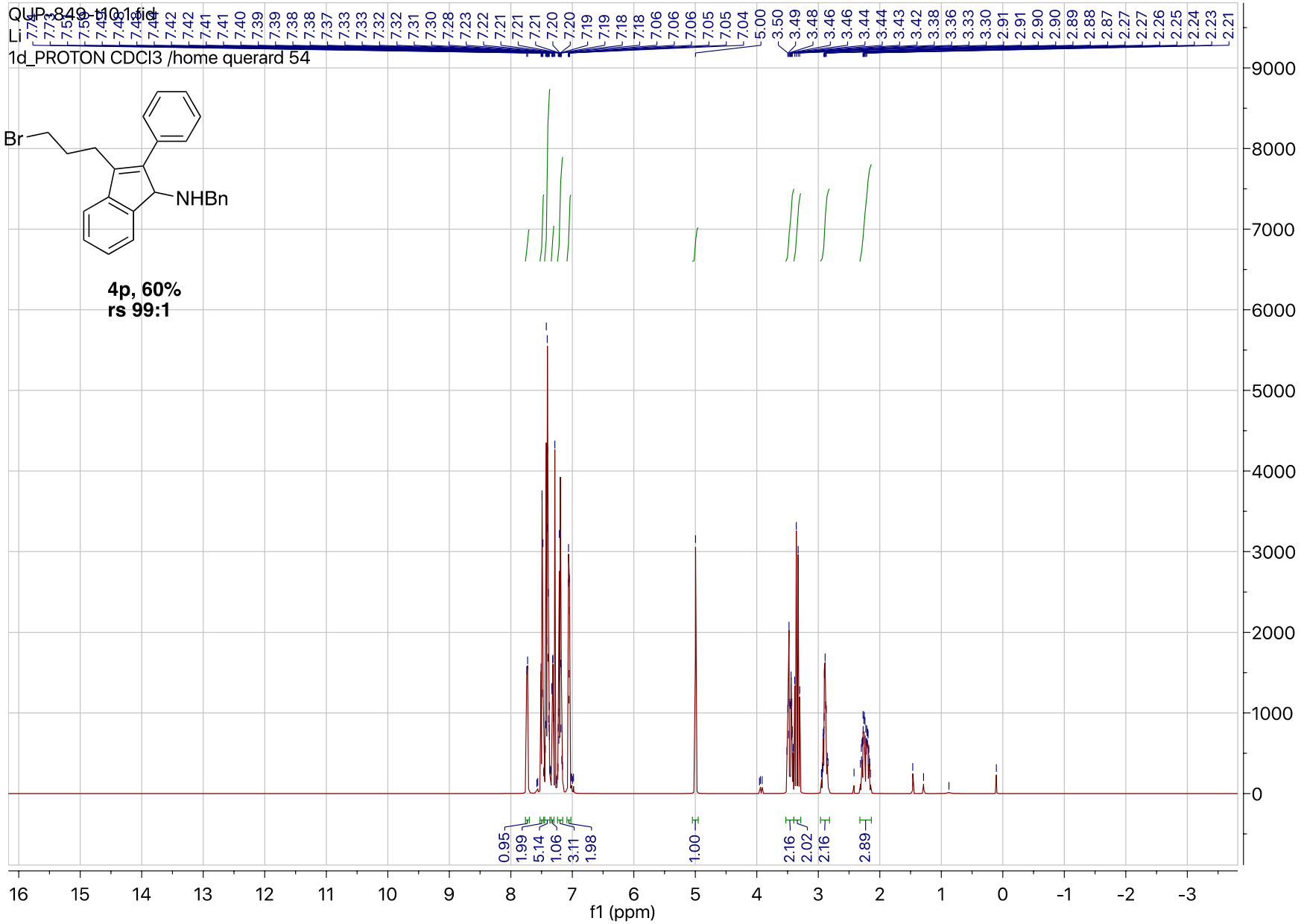
QUP-849-t101.fid
Li
1d_PROTON CDCl3 /home querard 54
Br
NHBn
4p, 60%
rs 99:1
f1 (ppm)

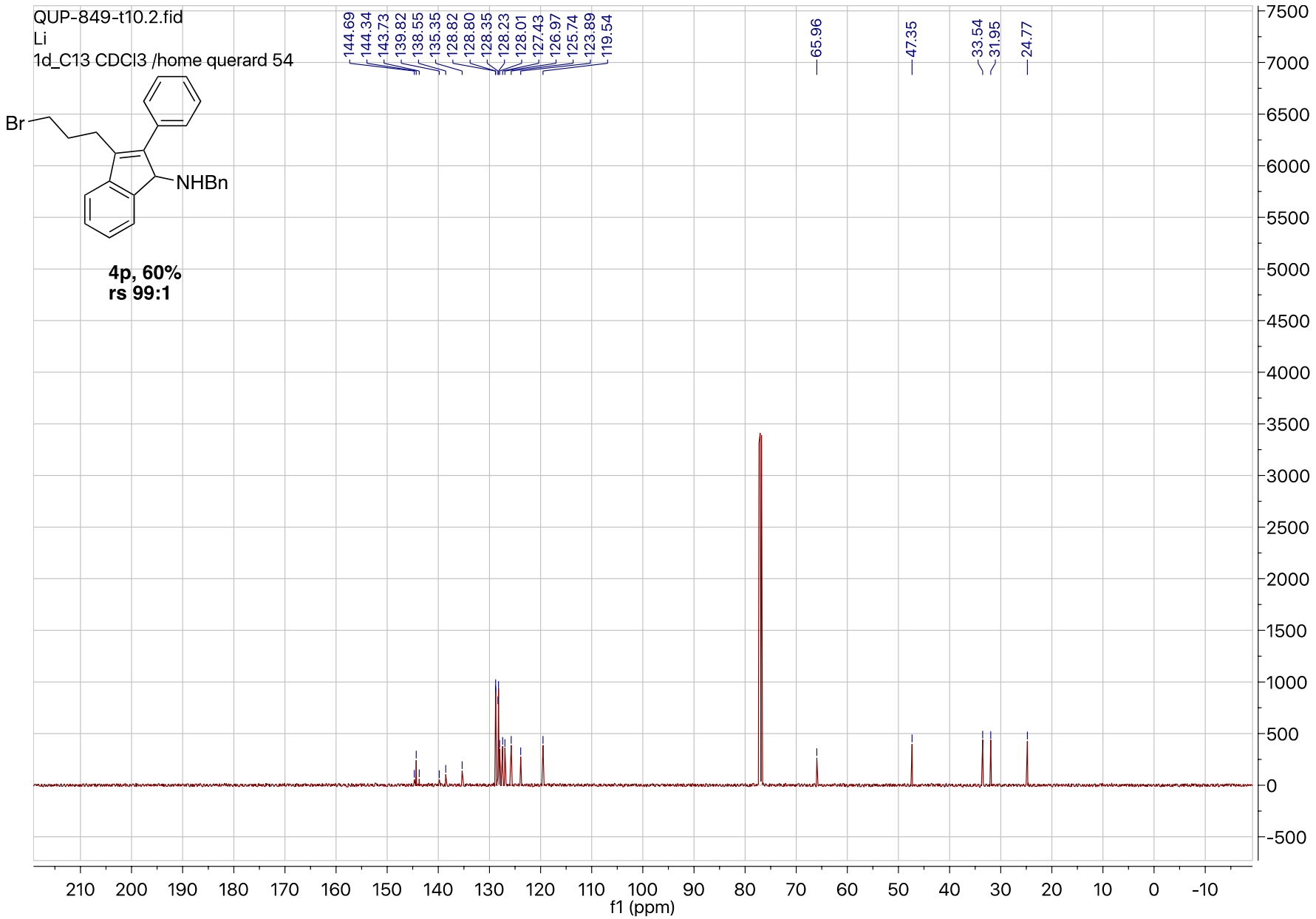
QUP-849-t10.2.fid
Li
1d_C13 CDCl3 /home querard 54
144.69
144.34
143.73
139.82
138.55
135.35
128.82
128.80
128.35
128.23
128.01
127.43
126.97
125.74
123.89
119.54
65.96
47.35
33.54
31.95
24.77
Br
NHBn
4p, 60%
rs 99:1
f1 (ppm)

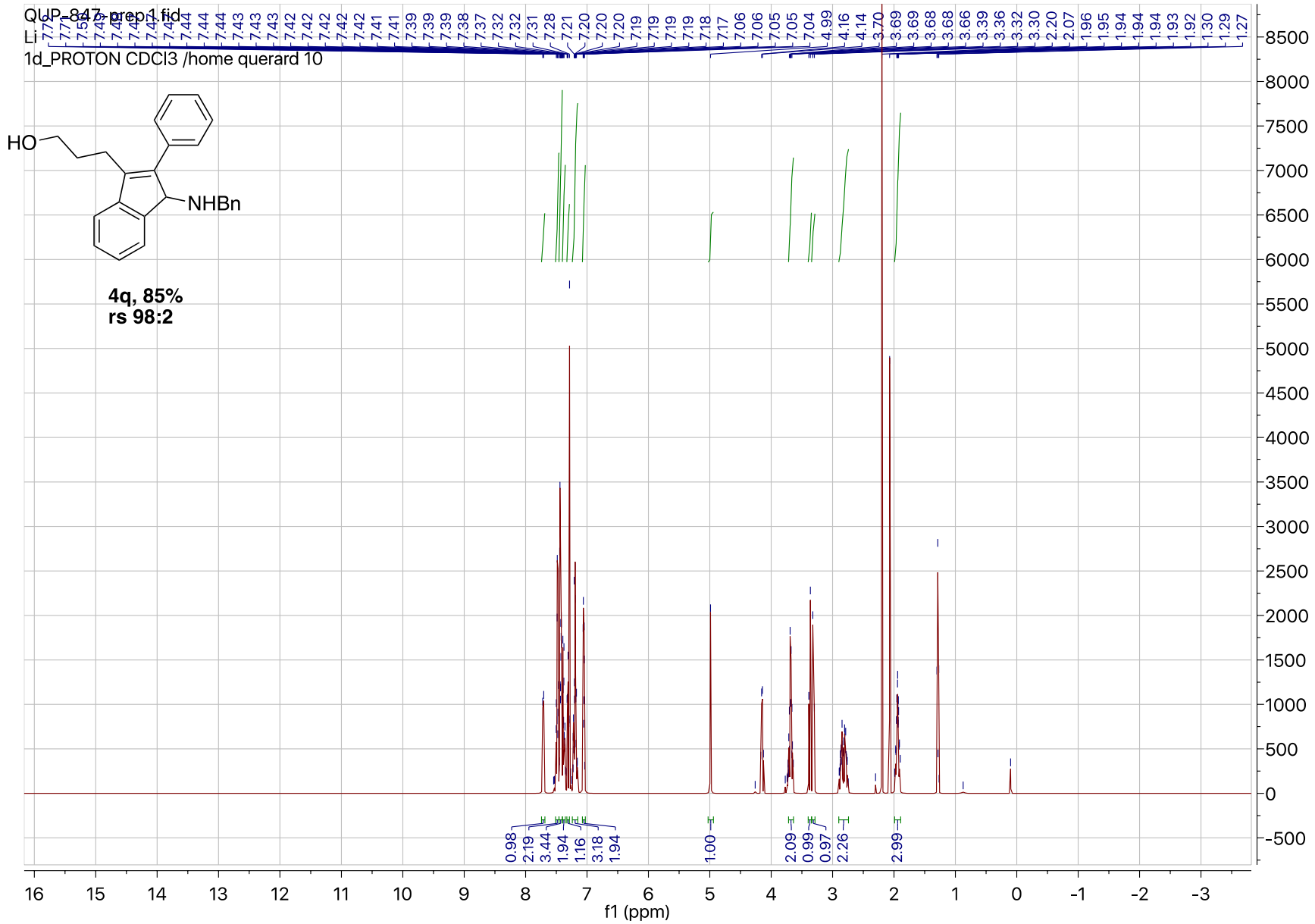
QUP-847-prep 1.fid
1d_PROTON CDCl3 /home querard 10
HO
NHBn
4q, 85%
rs 98:2
f1 (ppm)

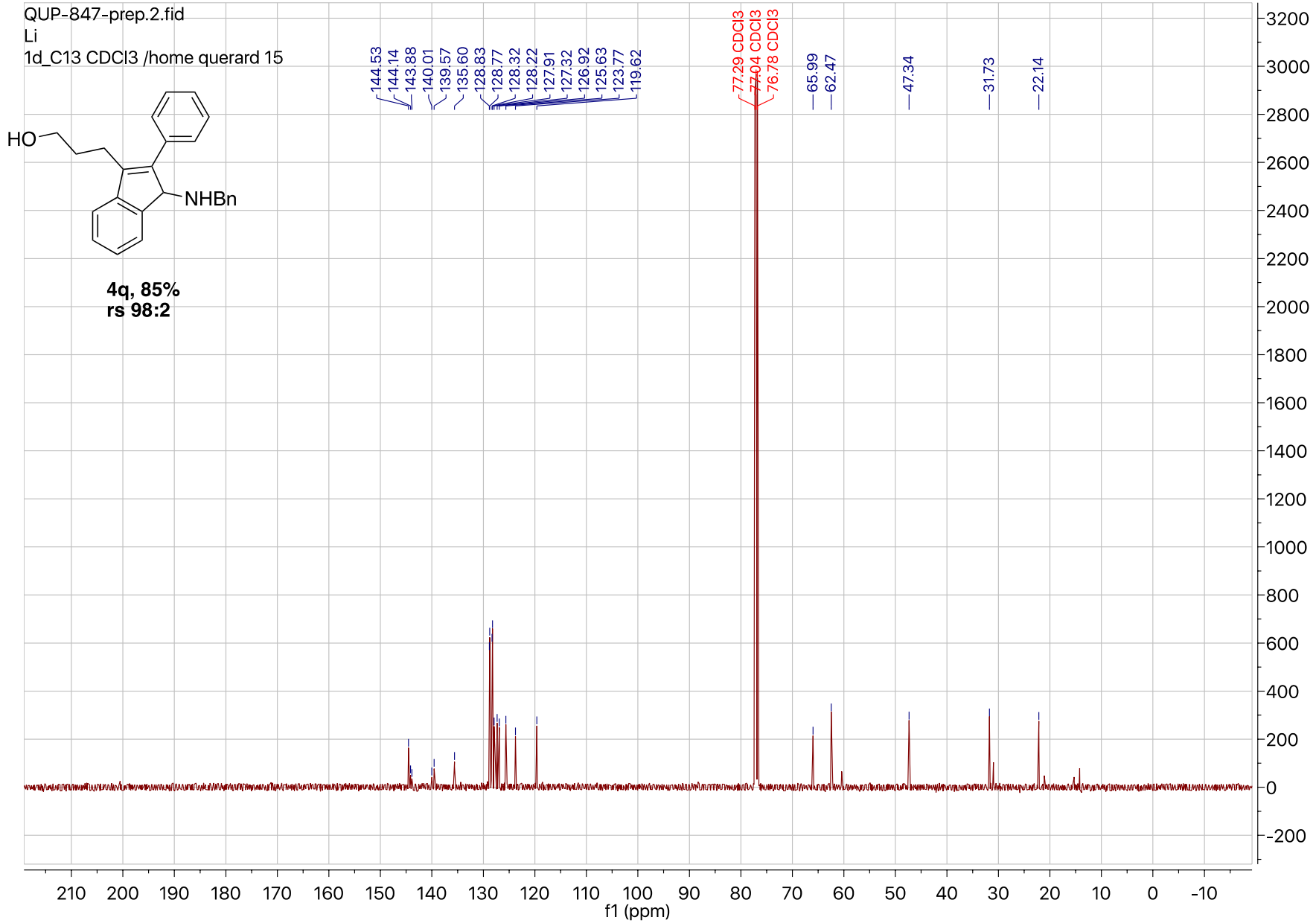
QUP-847-prep.2.fid
Li
1d_C13 CDCl3 /home querard 15
HO
NHBn
4q, 85%
rs 98:2
144.53
144.14
143.88
140.01
139.57
135.60
128.83
128.77
128.32
128.22
127.91
127.32
126.92
125.63
123.77
119.62
77.29 CDCl3
77.04 CDCl3
76.78 CDCl3
65.99
62.47
47.34
31.73
22.14
f1 (ppm)

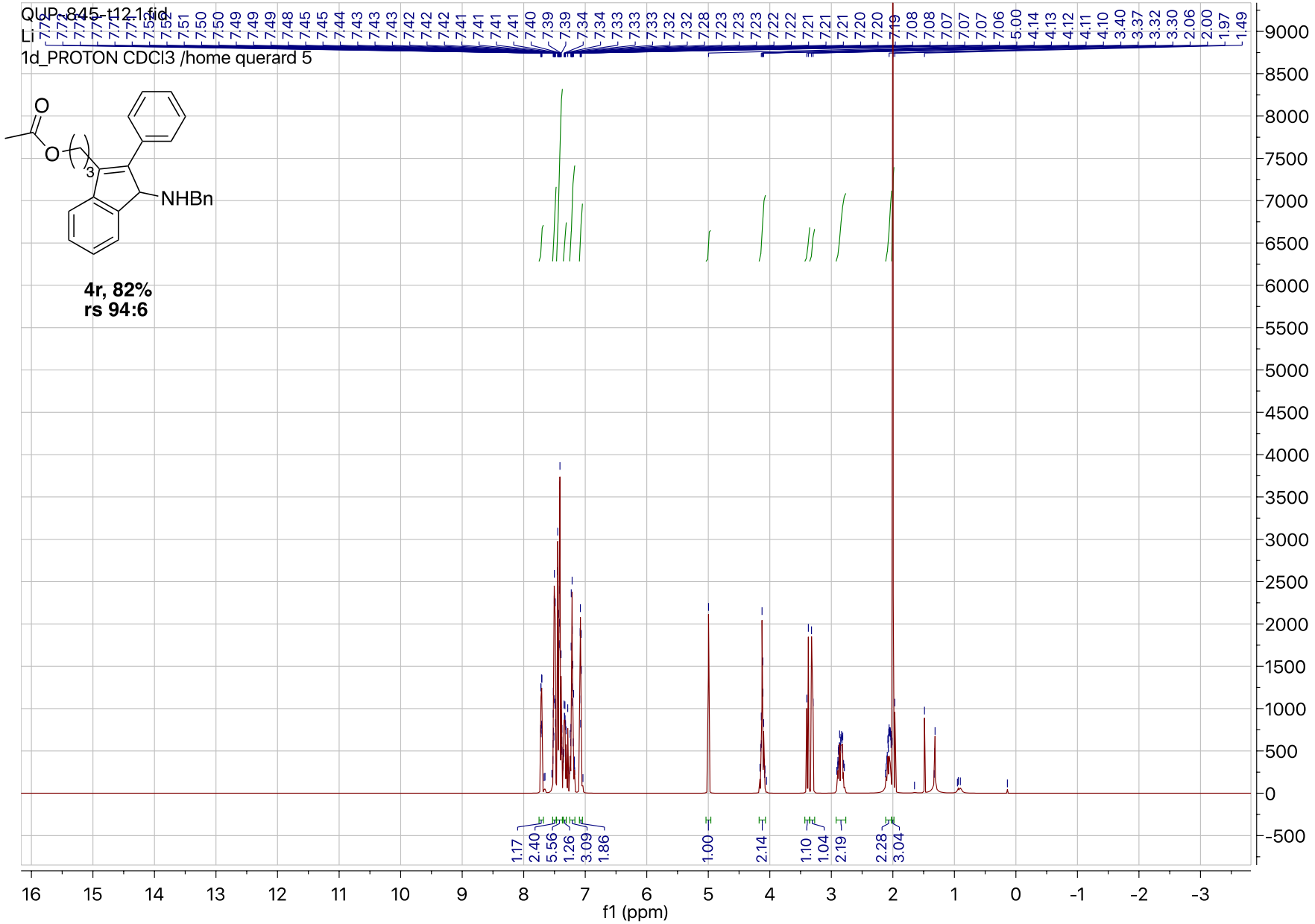
QUP-845-t12.1.fid
Li
1d_PROTON CDCl3 /home querard 5
O
O
3
NHBn
4r, 82%
rs 94:6
f1 (ppm)

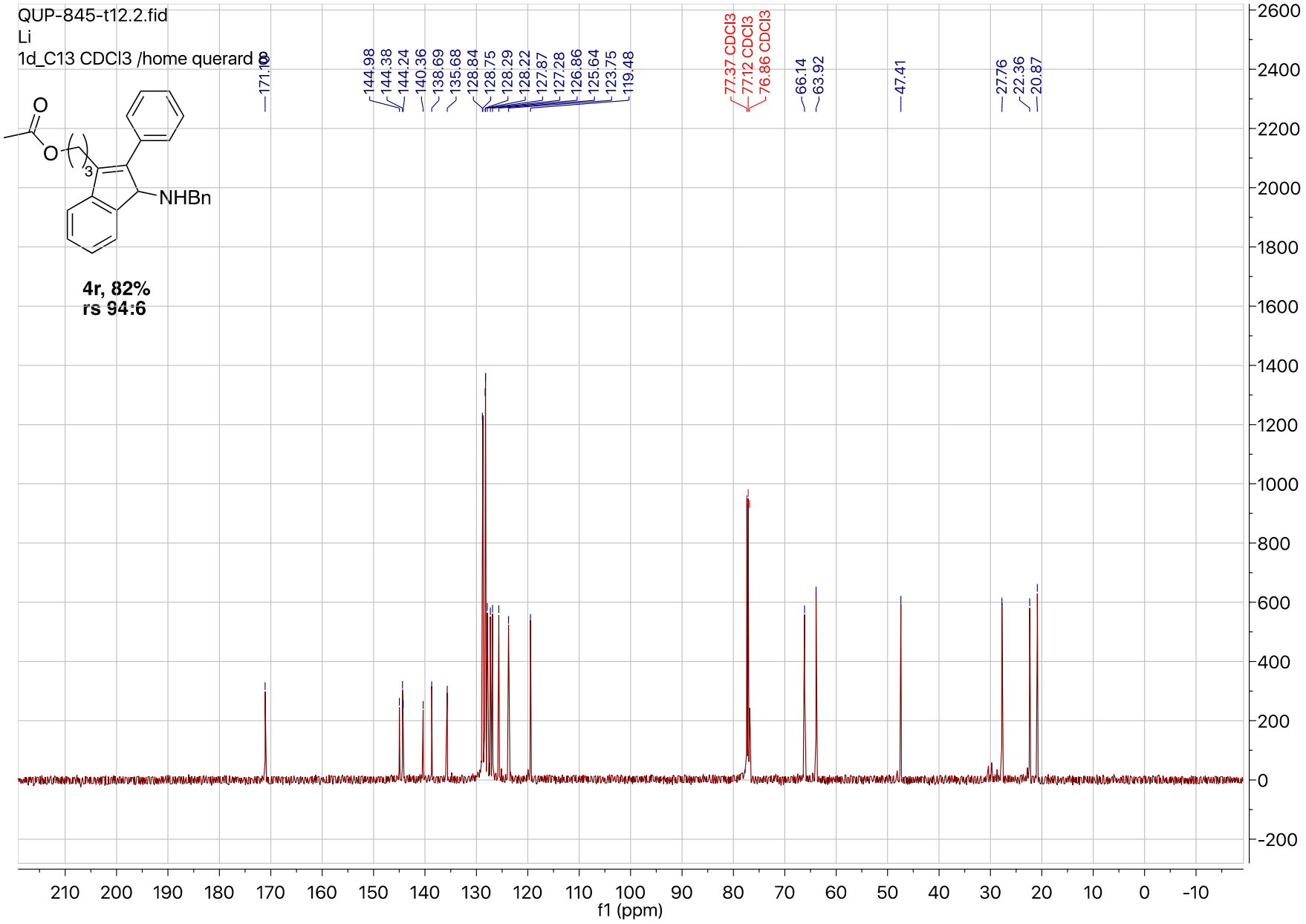
QUP-845-t12.2.fid
Li
1d_C13 CDCl3 /home querard 8
O
O
3
NHBn
4r, 82%
rs 94:6
171.10
144.98
144.38
144.24
140.36
138.69
135.68
128.84
128.75
128.29
128.22
127.87
127.28
126.86
125.64
123.75
119.48
77.37 CDCl3
77.12 CDCl3
76.86 CDCl3
66.14
63.92
47.41
27.76
22.36
20.87
f1 (ppm)

Spectra for compounds in Chapter 4

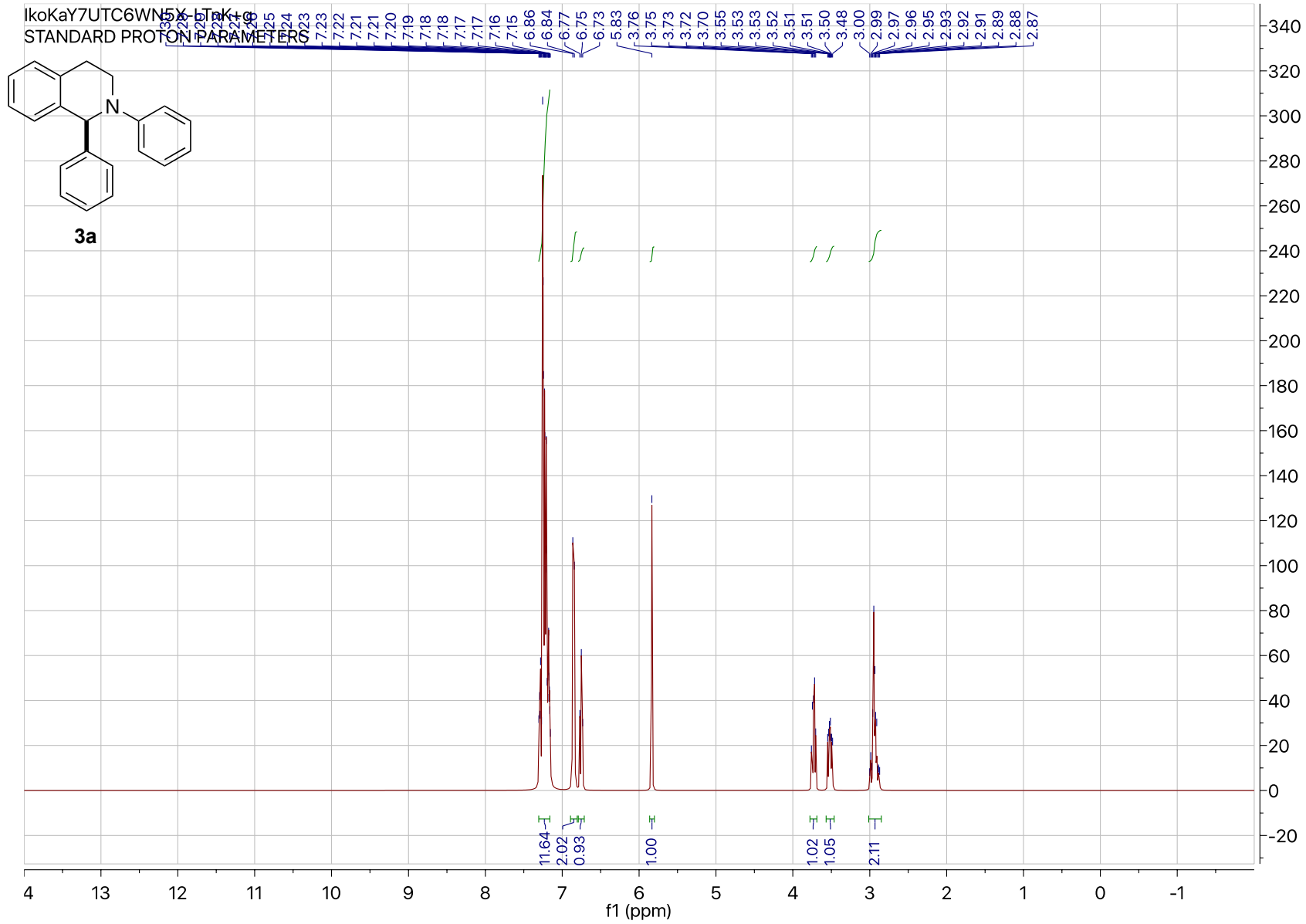
IkoKaY7UTC6WN5X-LTnK+g
STANDARD PROTON PARAMETERS
3a
f1 (ppm)

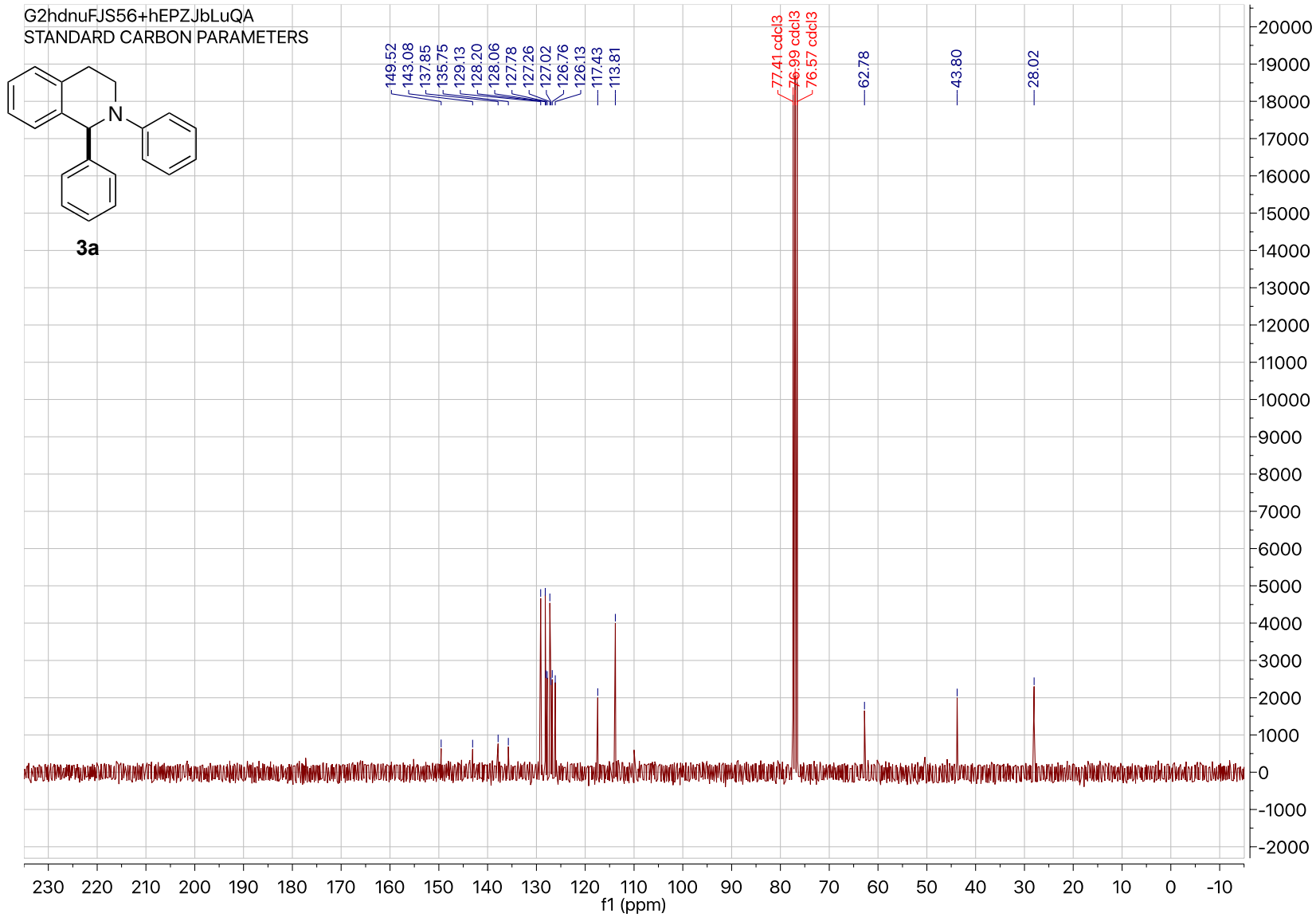
G2hdnuFJS56+hEPZJbLuQA
STANDARD CARBON PARAMETERS
3a
149.52
143.08
137.85
135.75
129.13
128.20
128.06
127.78
127.26
127.02
126.76
126.13
117.43
113.81
77.41 cdcl3
76.99 cdcl3
76.57 cdcl3
62.78
43.80
28.02
f1 (ppm)

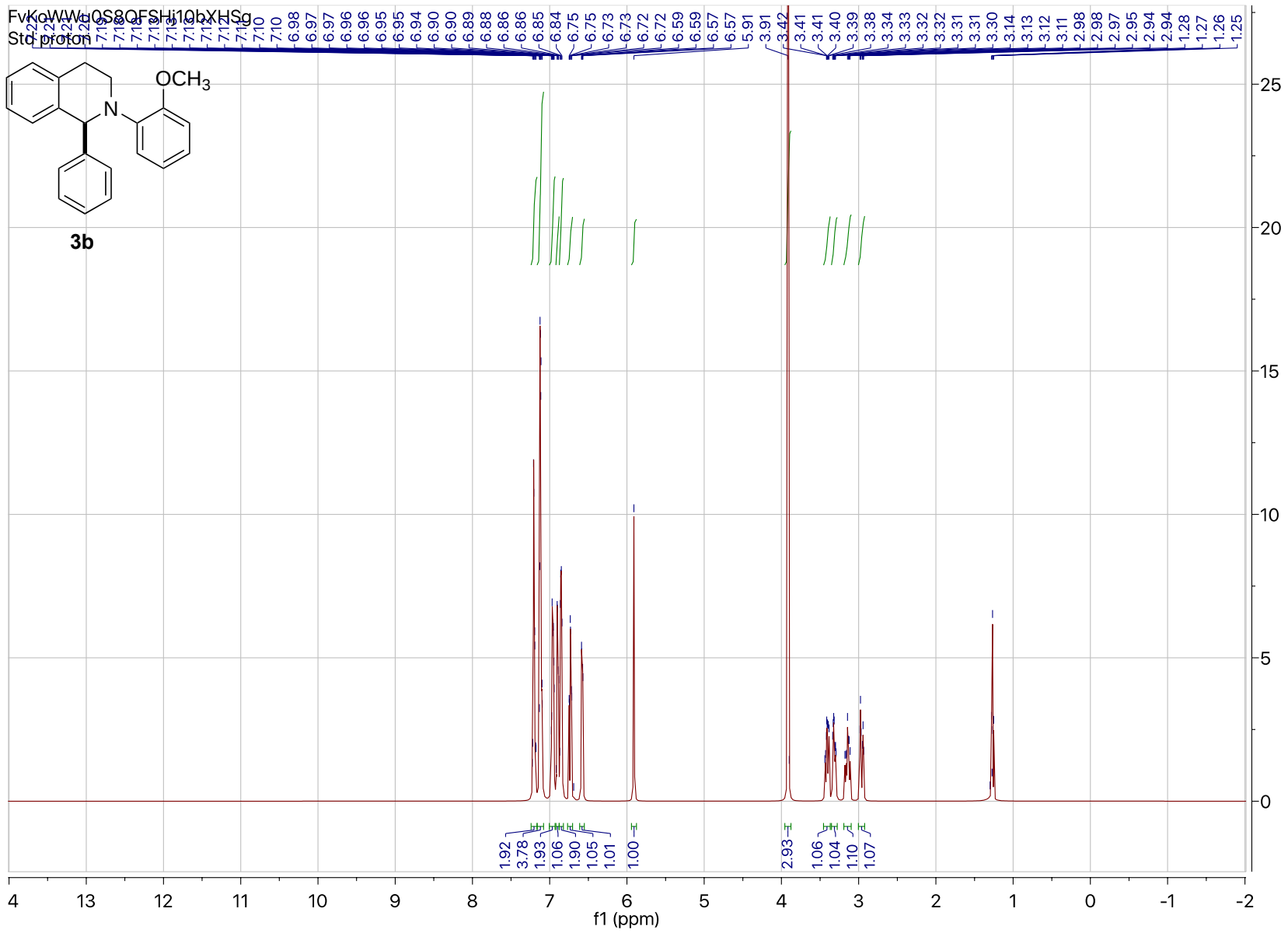
Std proton
OCH3
N
3b
f1 (ppm)

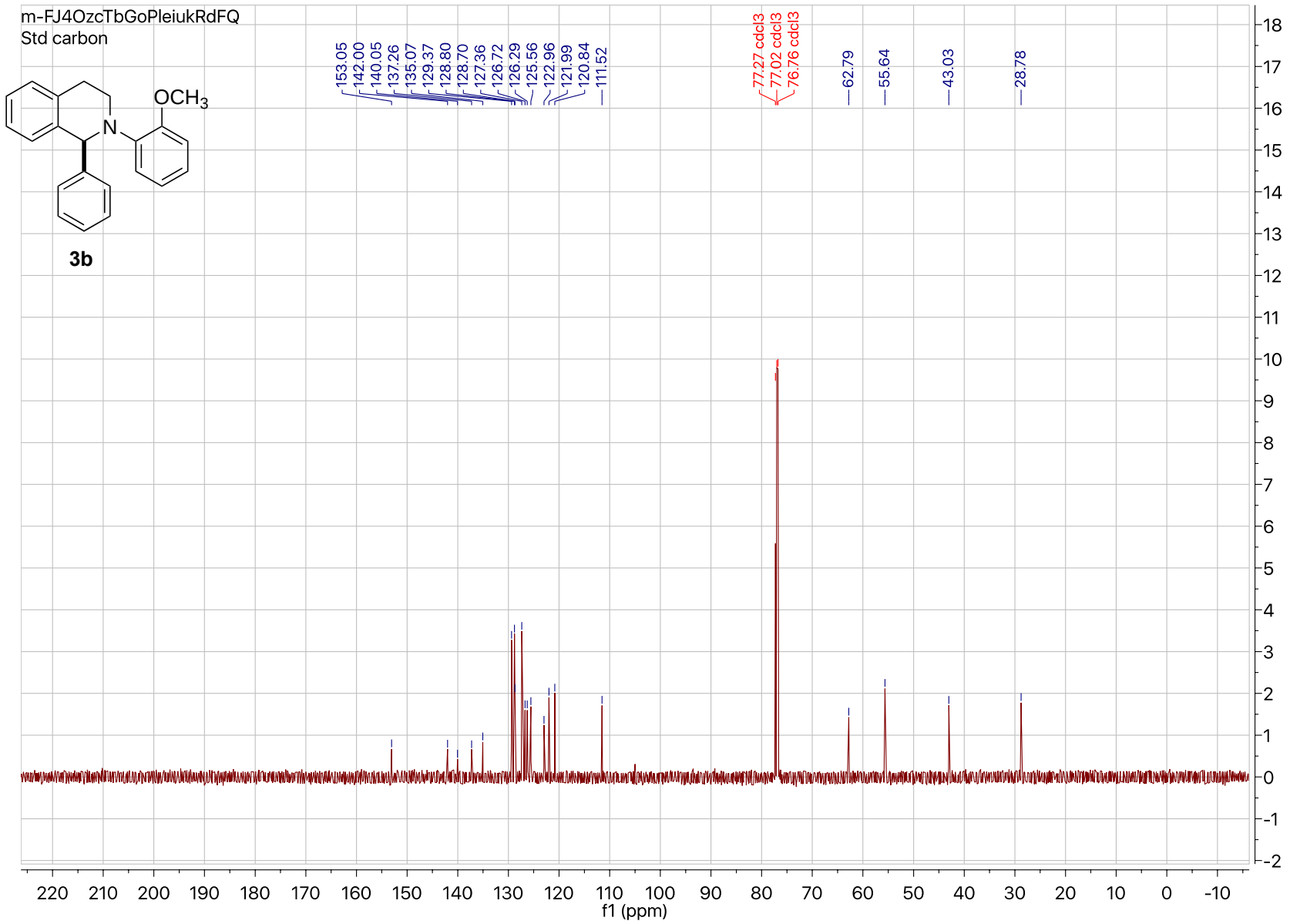
m-FJ4OzcTbGoPleiukRdFQ
Std carbon
OCH3
N
3b
153.05
142.00
140.05
137.26
135.07
129.37
128.80
128.70
127.36
126.72
126.29
125.56
122.96
121.99
120.84
111.52
77.27 cdcl3
77.02 cdcl3
76.76 cdcl3
62.79
55.64
43.03
28.78
f1 (ppm)

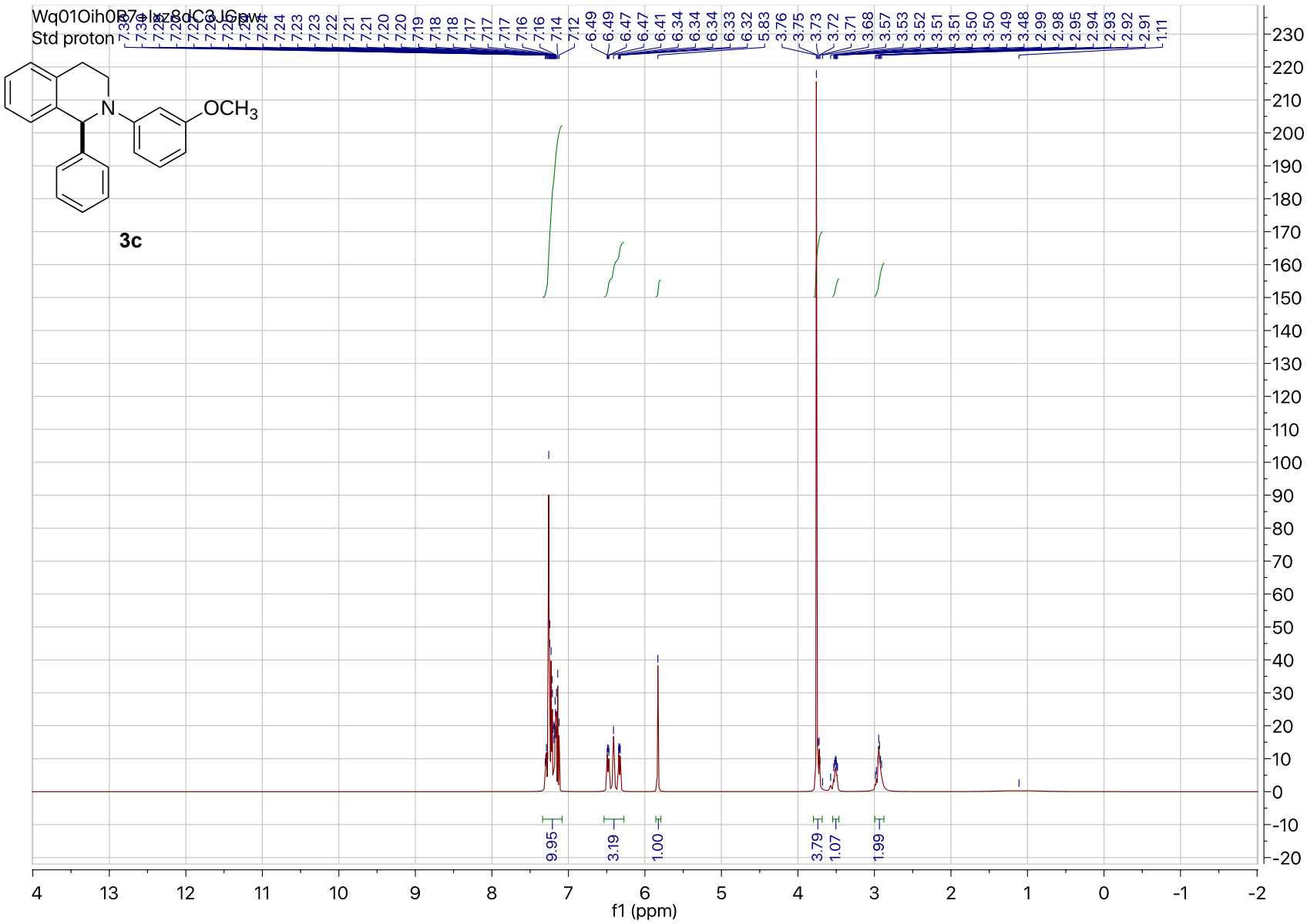
Std proton
N
OCH3
3c
9.95
3.19
1.00
3.79
1.07
1.99
f1 (ppm)

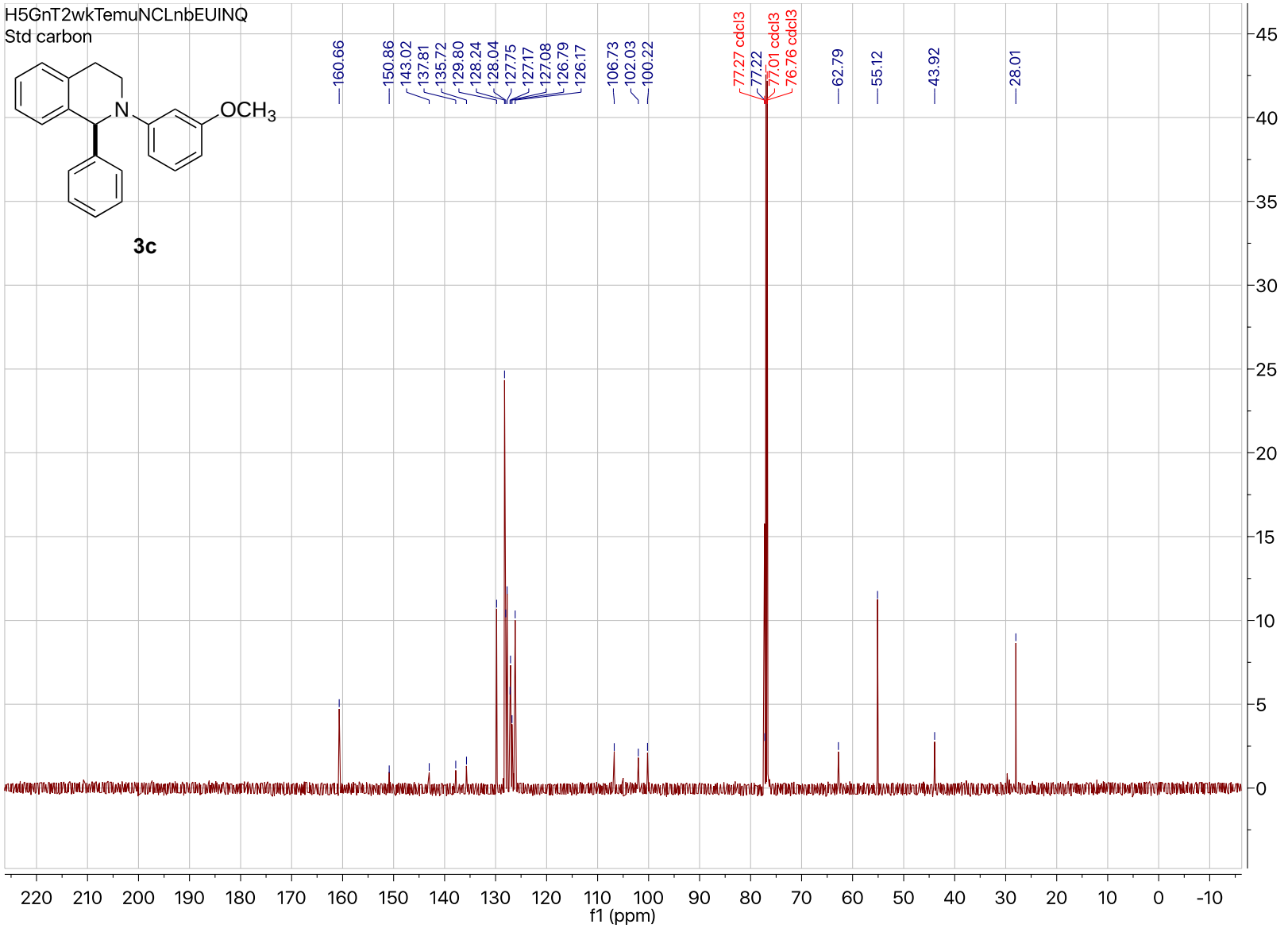
H5GnT2wkTemuNCLnbEUINQ
Std carbon
N
OCH3
3c
160.66
150.86
143.02
137.81
135.72
129.80
128.24
128.04
127.75
127.17
127.08
126.79
126.17
106.73
102.03
100.22
77.27 cdcl3
77.22
77.01 cdcl3
76.76 cdcl3
62.79
55.12
43.92
28.01
f1 (ppm)

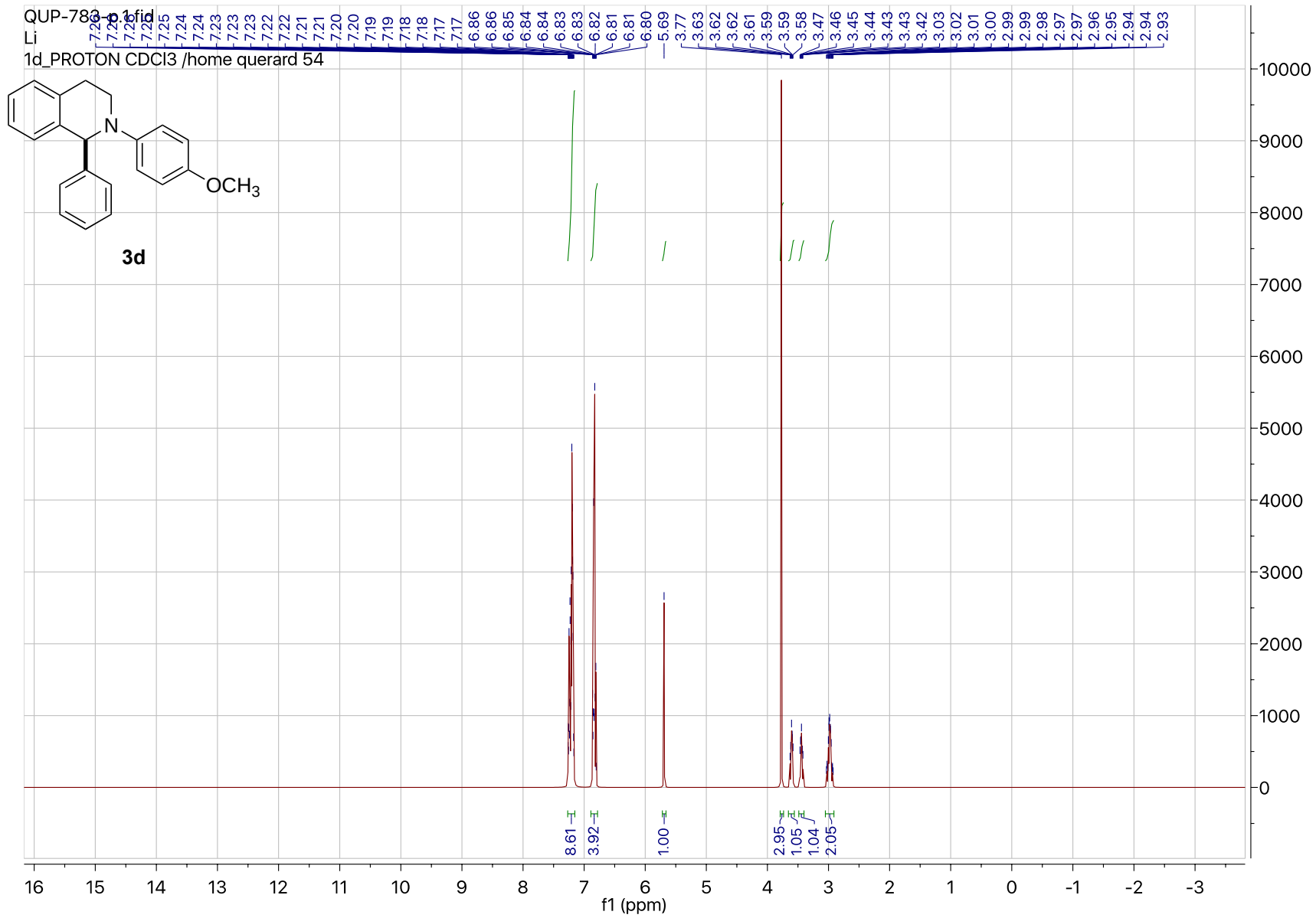
QUP-783-p.1.fid
Li
1d_PROTON CDCl3 /home querard 54
N
OCH3
3d
8.61
3.92
1.00
2.95
1.05
1.04
2.05
f1 (ppm)

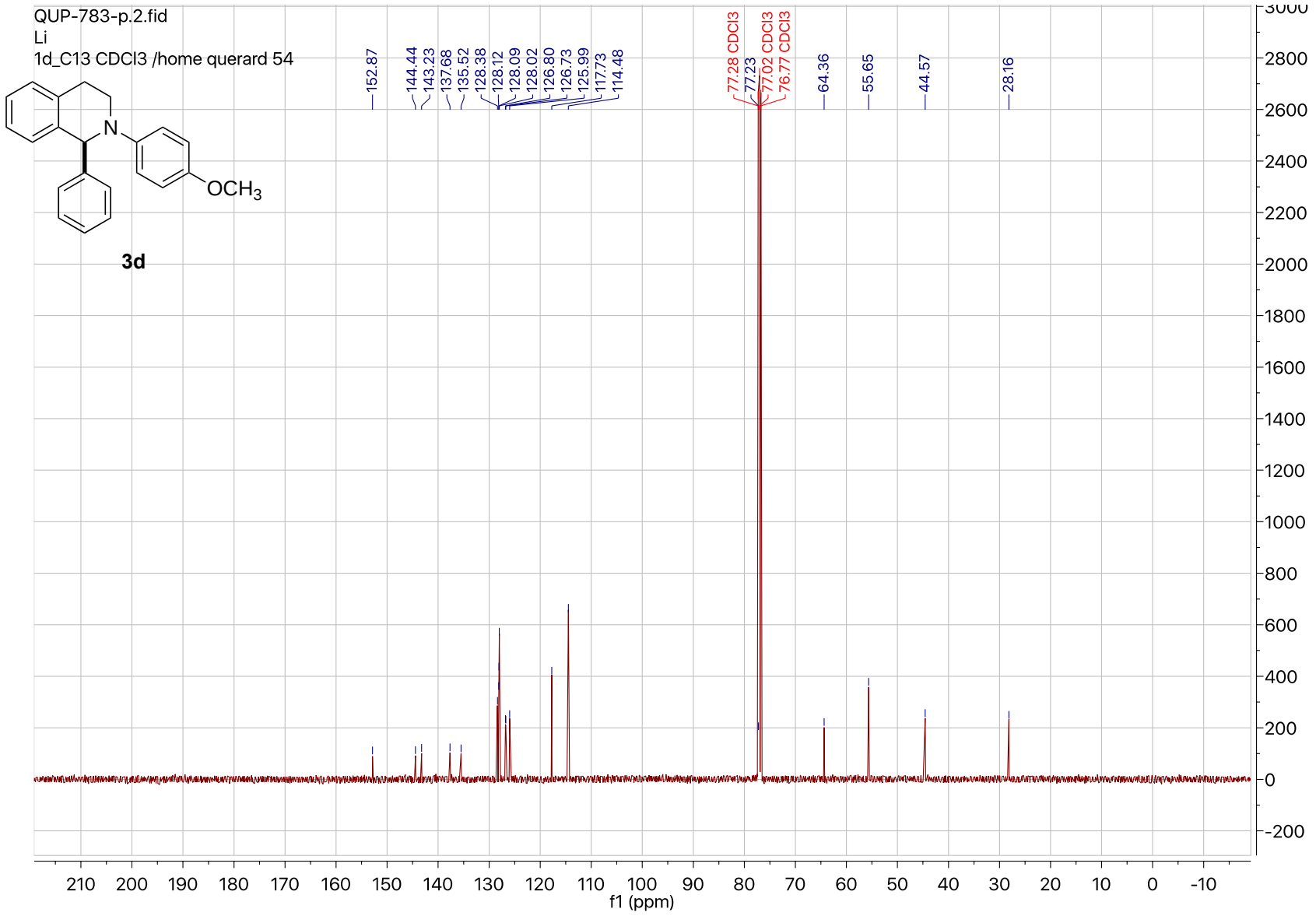
QUP-783-p.2.fid
Li
1d_C13 CDCl3 /home querard 54
N
OCH3
3d
152.87
144.44
143.23
137.68
135.52
128.38
128.12
128.09
128.02
126.80
126.73
125.99
117.73
114.48
77.28 CDCl3
77.23
77.02 CDCl3
76.77 CDCl3
64.36
55.65
44.57
28.16
f1 (ppm)

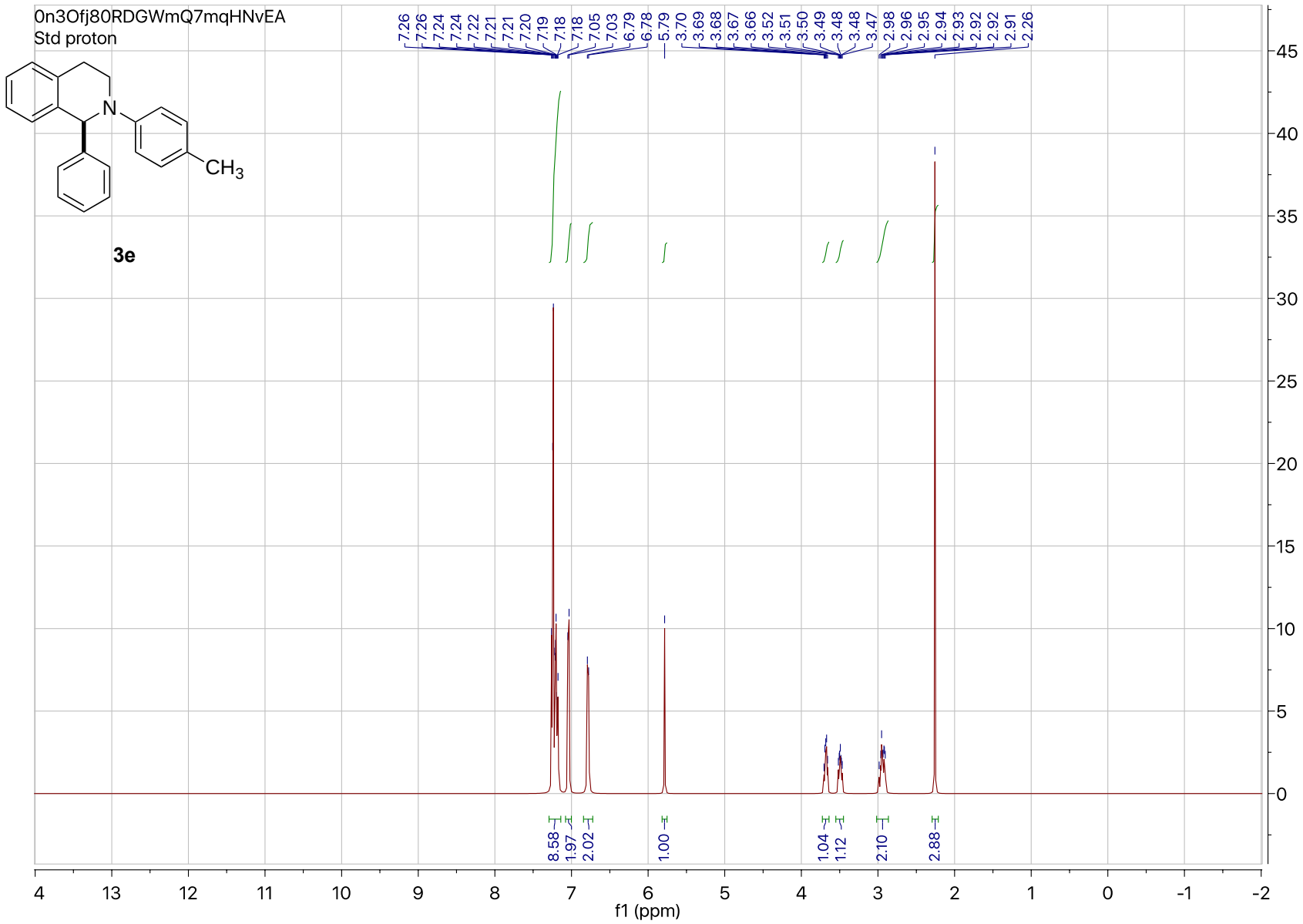
0n3Ofj80RDGWmQ7mqHNvEA
Std proton
N
CH3
3e
7.26
7.26
7.24
7.24
7.22
7.21
7.21
7.20
7.19
7.18
7.18
7.05
7.03
6.79
6.78
5.79
3.70
3.69
3.68
3.67
3.66
3.52
3.51
3.50
3.49
3.48
3.48
3.47
2.98
2.96
2.95
2.94
2.93
2.92
2.92
2.91
2.26
8.58
1.97
2.02
1.00
1.04
1.12
2.10
2.88
f1 (ppm)

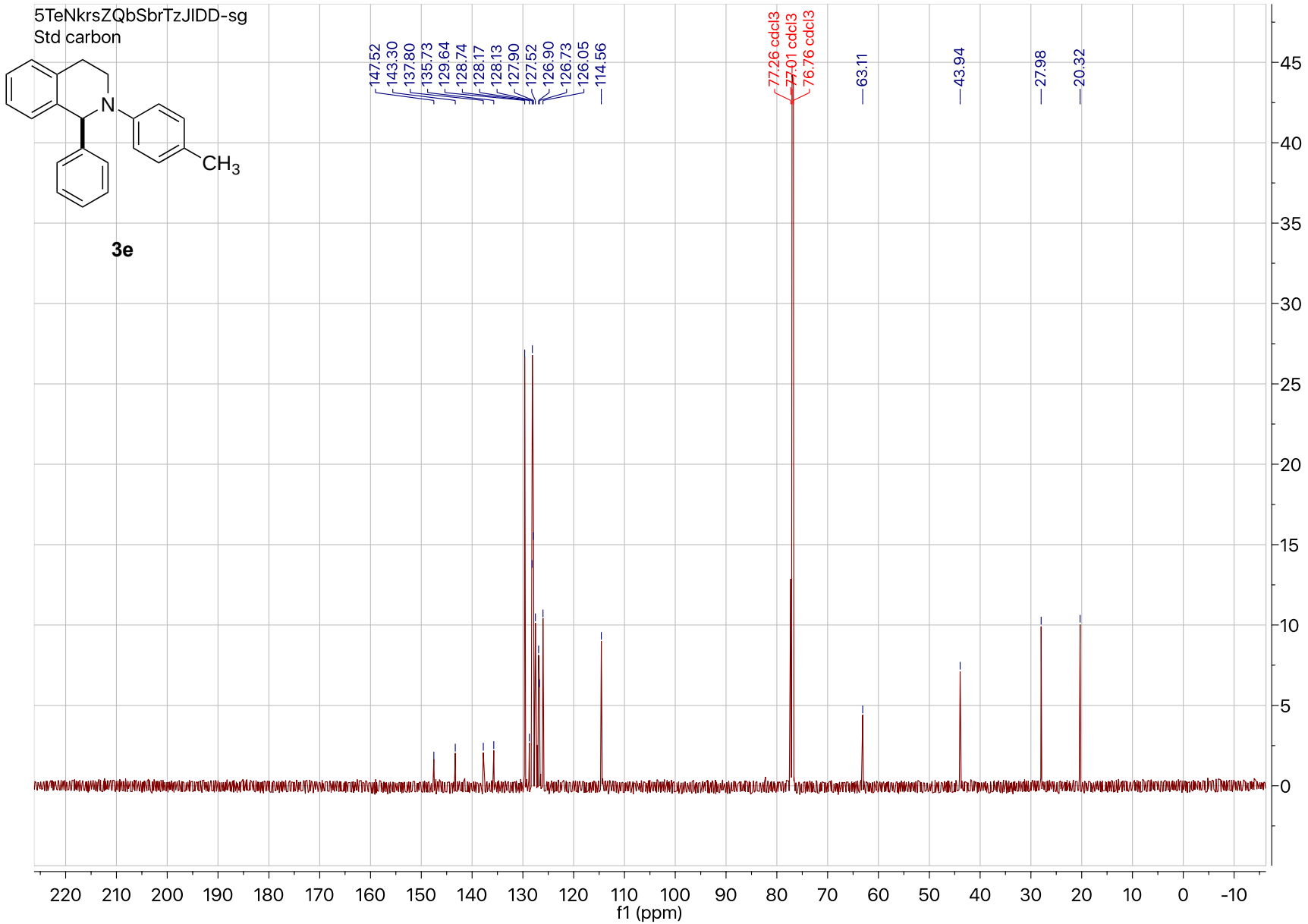
5TeNkrsZQbSbrTzJIDD-sg
Std carbon
N
CH3
3e
147.52
143.30
137.80
135.73
129.64
128.74
128.17
128.13
127.90
127.52
126.90
126.73
126.05
114.56
77.26 cdcl3
77.01 cdcl3
76.76 cdcl3
63.11
43.94
27.98
20.32
f1 (ppm)

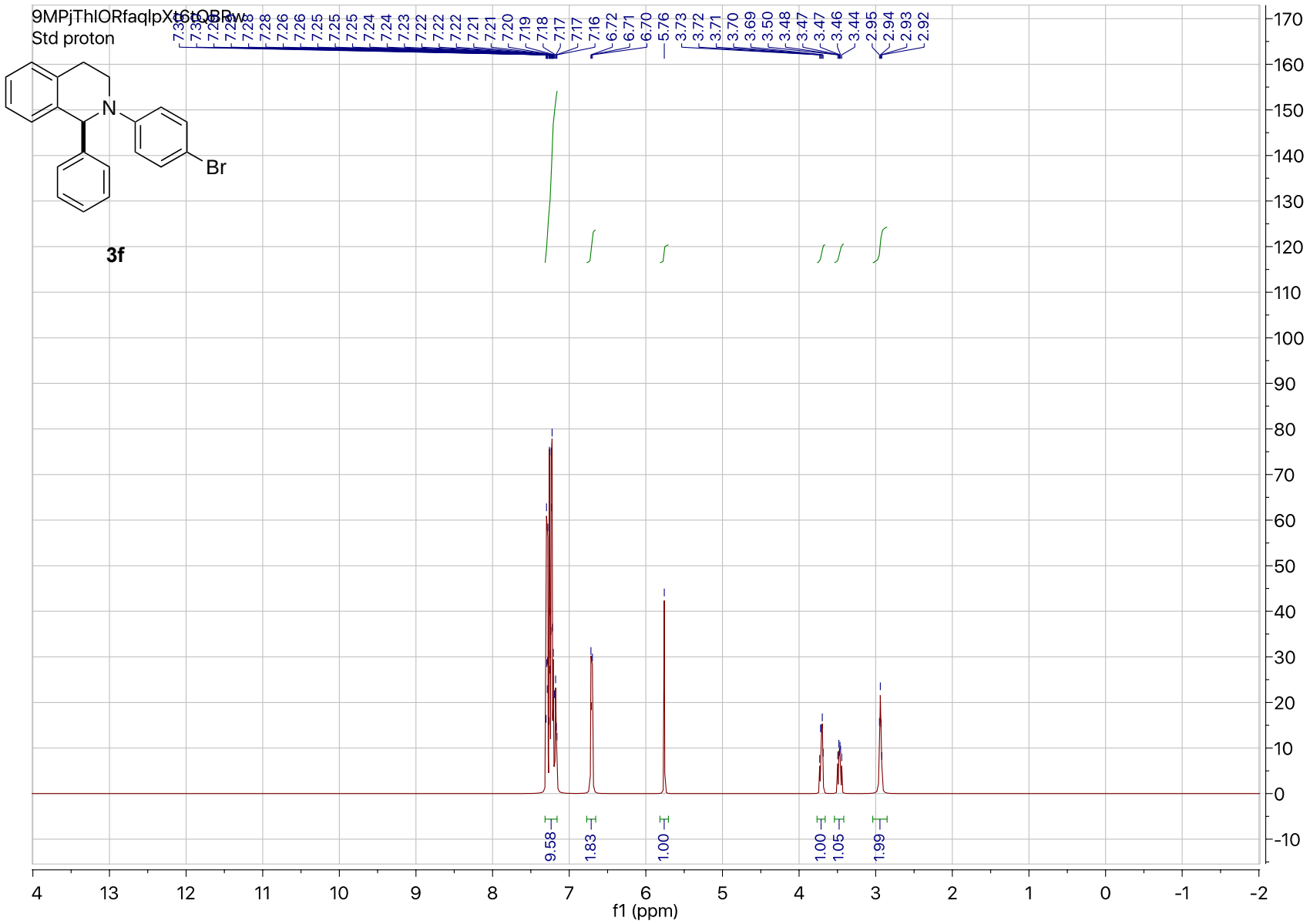
9MPjThIORfaqlpXt6tQBRw
Std proton
N
Br
3f
f1 (ppm)

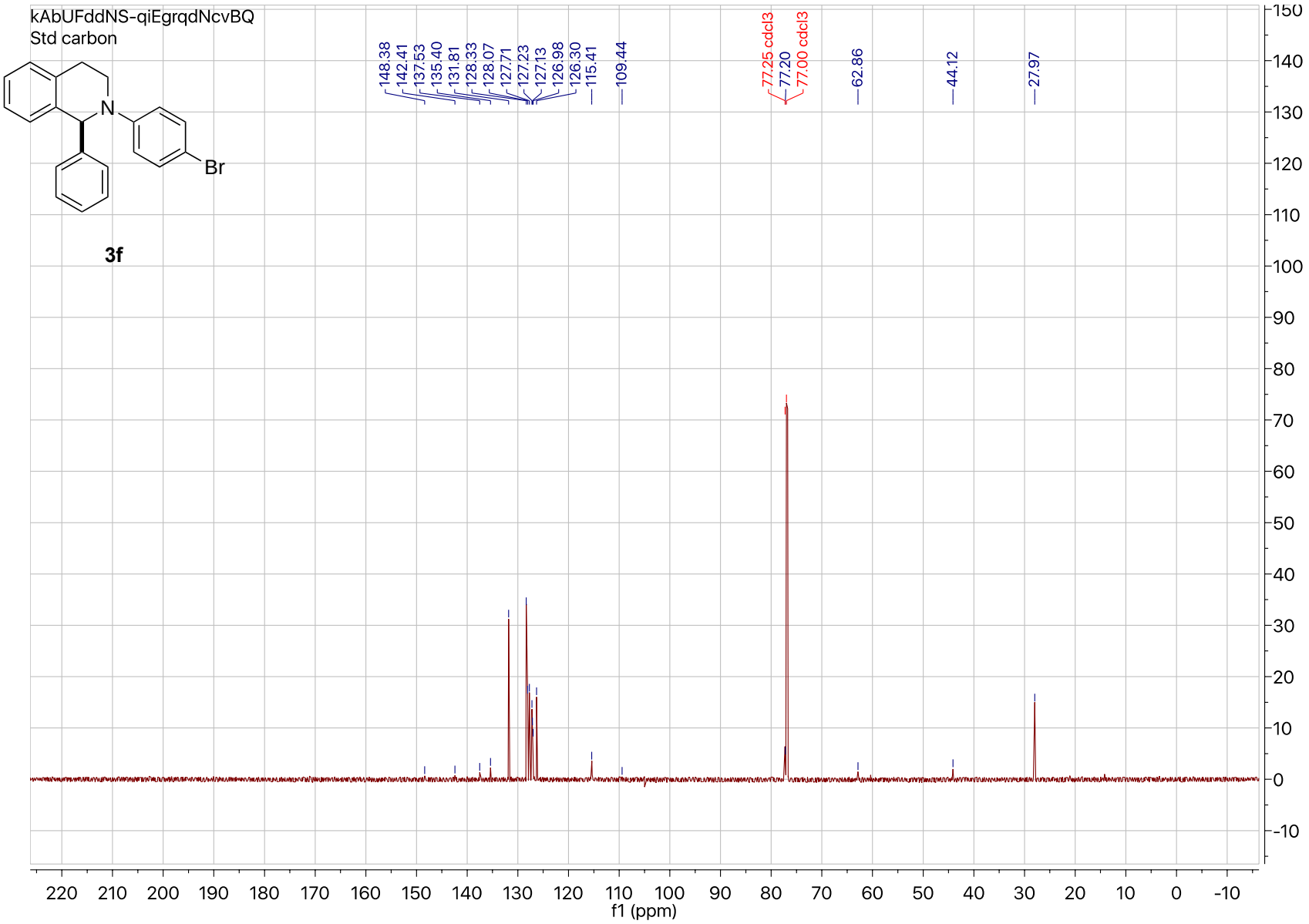
kAbUFddNS-qiEgrqdNcvBQ
Std carbon
N
Br
3f
148.38
142.41
137.53
135.40
131.81
128.33
128.07
127.71
127.23
127.13
126.98
126.30
115.41
109.44
77.25 cdcl3
77.20
77.00 cdcl3
62.86
44.12
27.97
f1 (ppm)

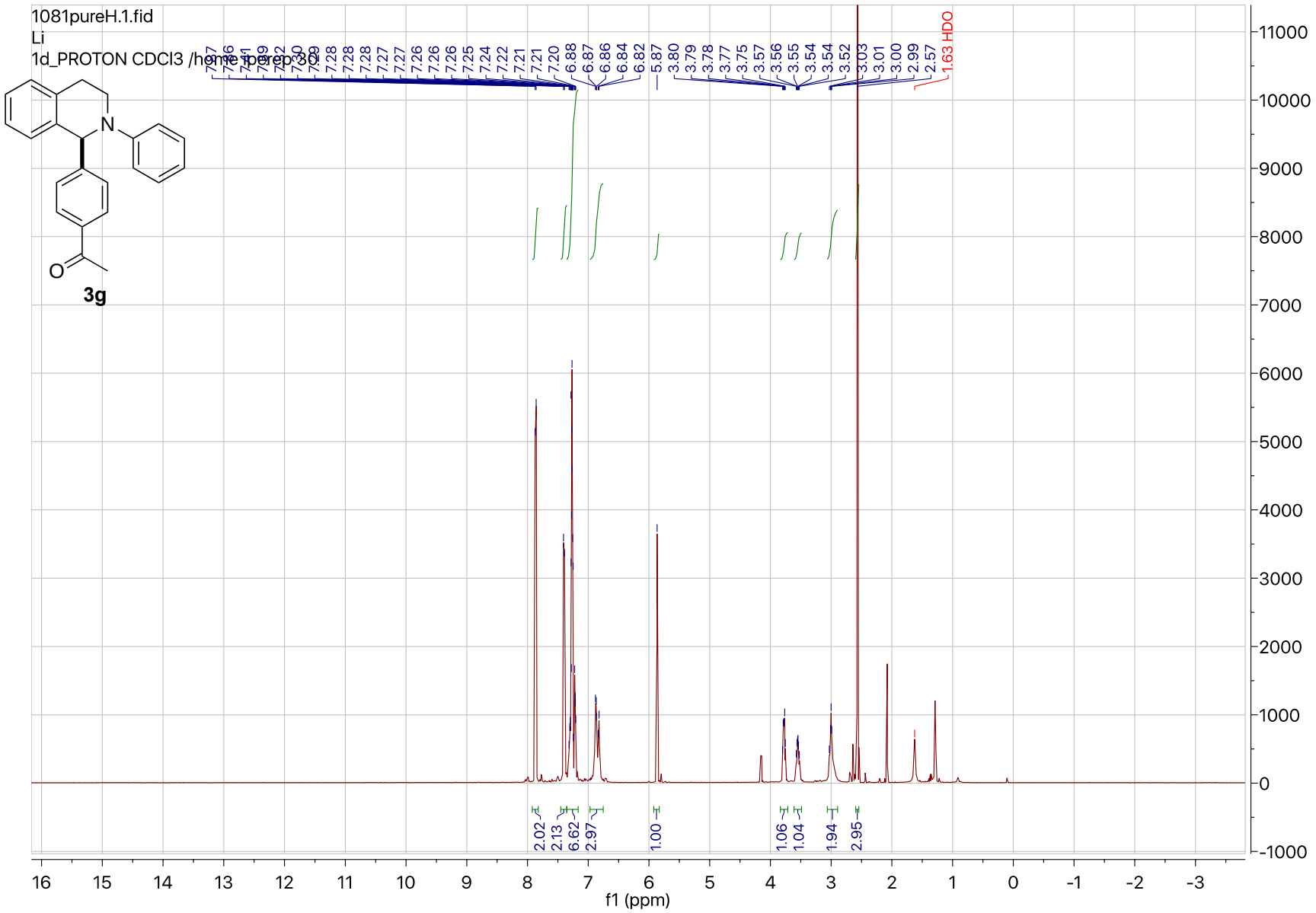
1081pureH.1.fid
Li
1d_PROTON CDCl3 /home/iperep/30
3g
7.77 7.76 7.41 7.39 7.22 7.20 7.09 7.28 7.28 7.27 7.27 7.26 7.26 7.25 7.24 7.22 7.21 7.21 7.20 6.88 6.87 6.86 6.84 6.82 5.87 3.80 3.79 3.78 3.77 3.75 3.57 3.56 3.55 3.54 3.54 3.52 3.03 3.01 3.00 2.99 2.57 1.63 HDO
2.02 2.13 6.62 2.97 1.00 1.06 1.04 1.94 2.95
f1 (ppm)

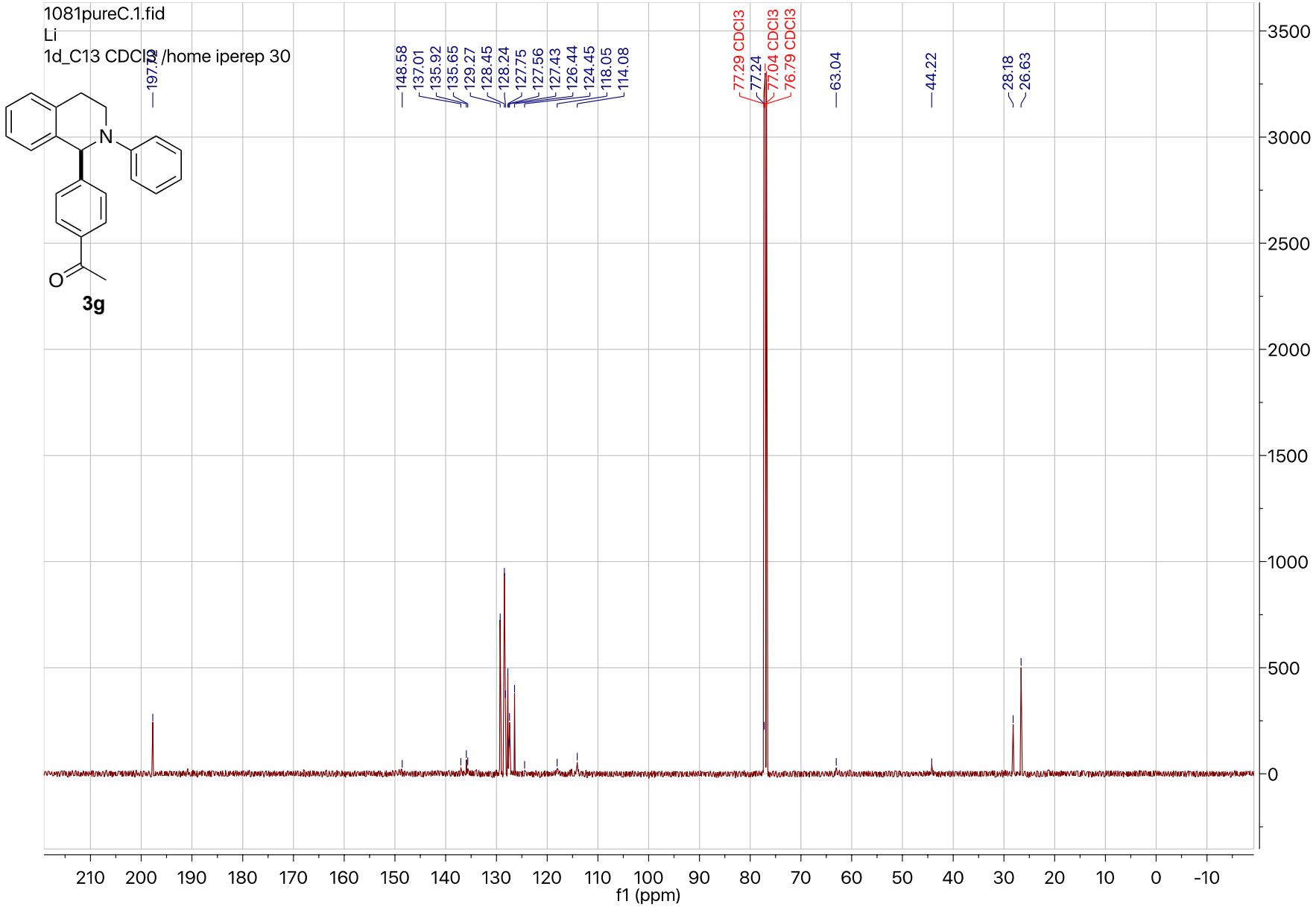
1081pureC.1.fid
Li
1d_C13 CDCl3 /home iperep 30
197.73
148.58
137.01
135.92
135.65
129.27
128.45
128.24
127.75
127.56
127.43
126.44
124.45
118.05
114.08
77.29 CDCl3
77.24
77.04 CDCl3
76.79 CDCl3
63.04
44.22
28.18
26.63
N
O
3g
f1 (ppm)

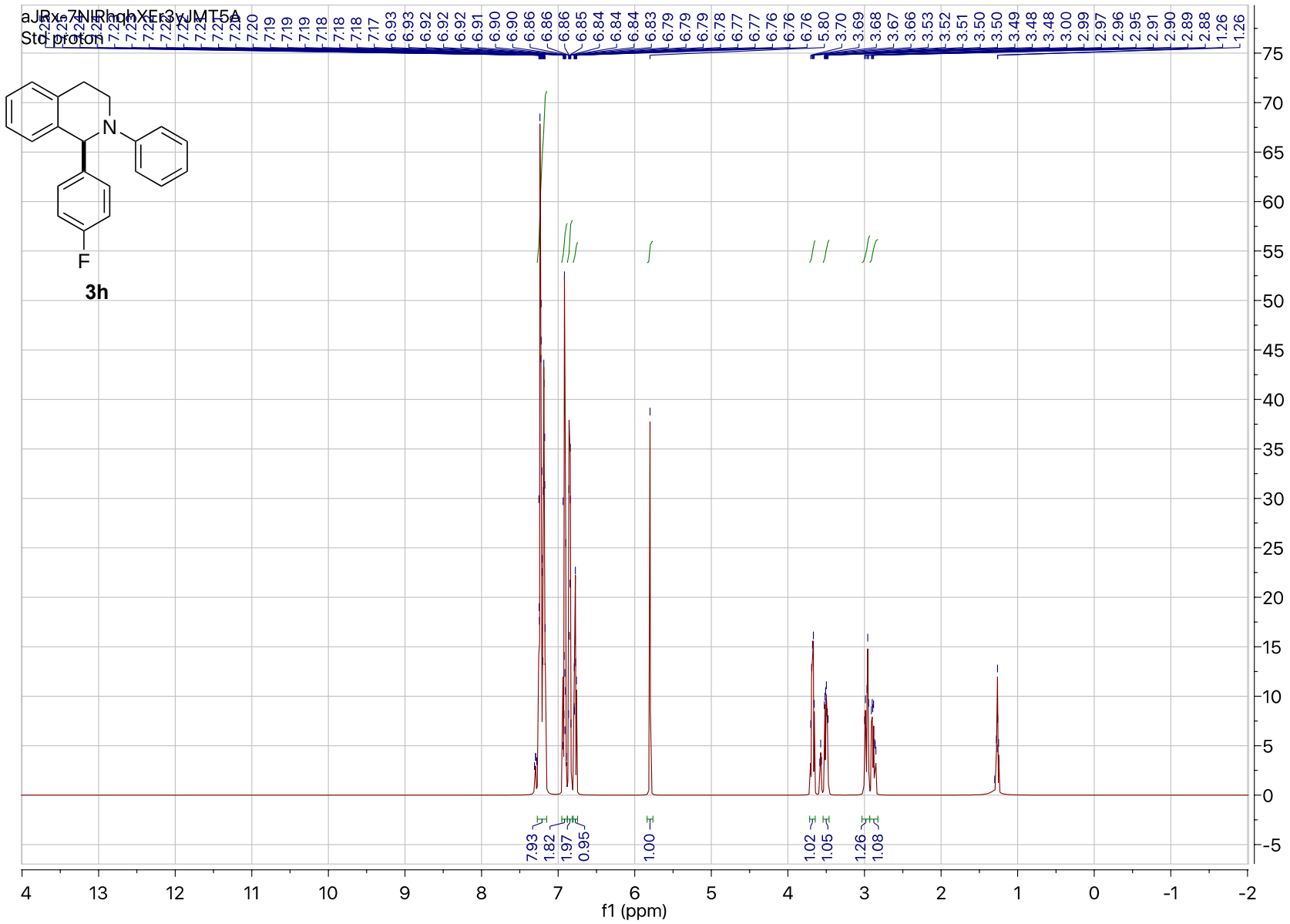
aJRx-7NIRhqhXEr3yJM-5a
Std proton
N
F
3h
7.93
1.82
1.97
0.95
1.00
1.02
1.05
1.26
1.08
f1 (ppm)

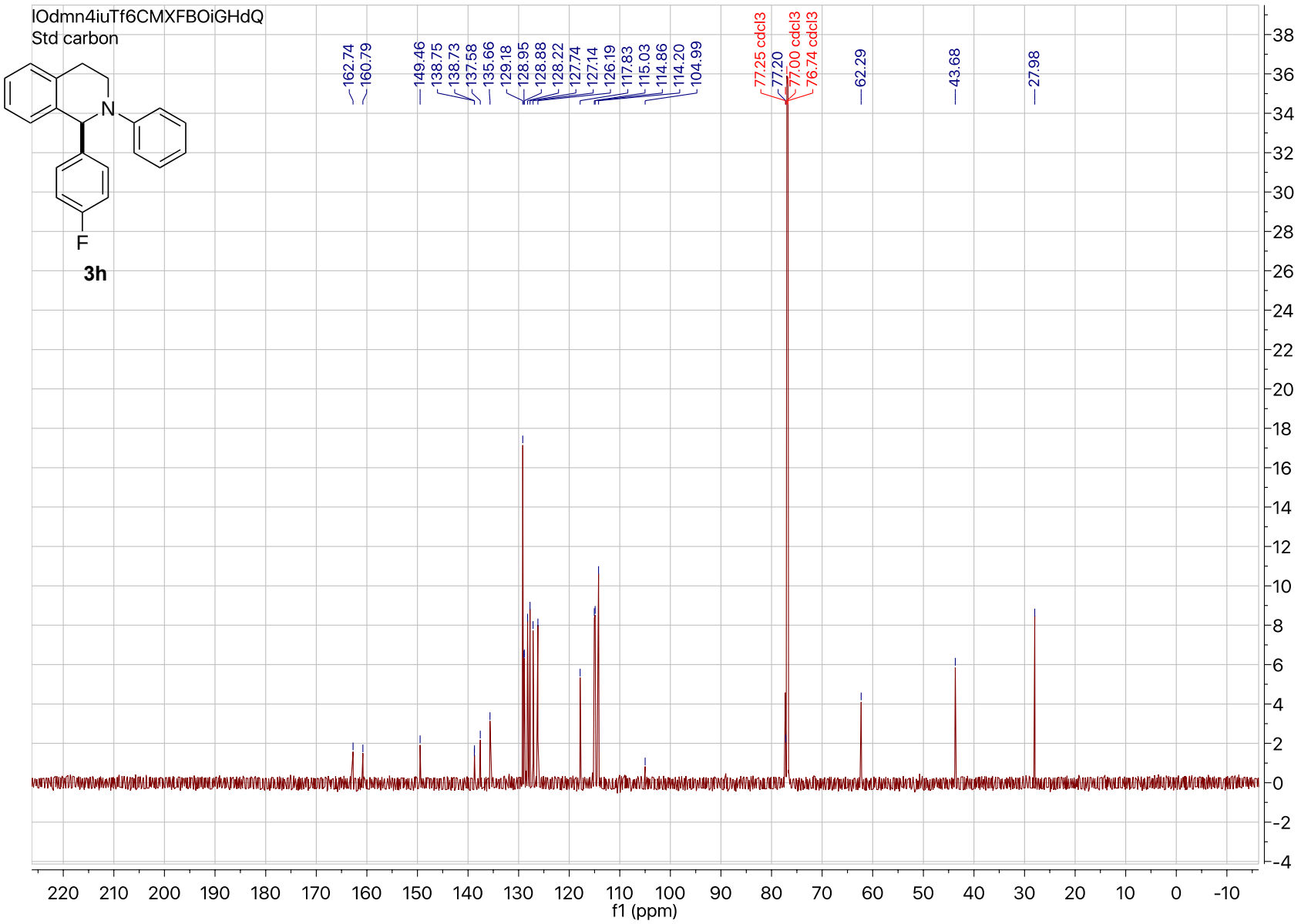
lOdmn4iuTf6CMXFBOiGHdQ
Std carbon
N
F
3h
162.74
160.79
149.46
138.75
138.73
137.58
135.66
129.18
128.95
128.88
128.22
127.74
127.14
126.19
117.83
115.03
114.86
114.20
104.99
77.25 cdcl3
77.20
77.00 cdcl3
76.74 cdcl3
62.29
43.68
27.98
f1 (ppm)

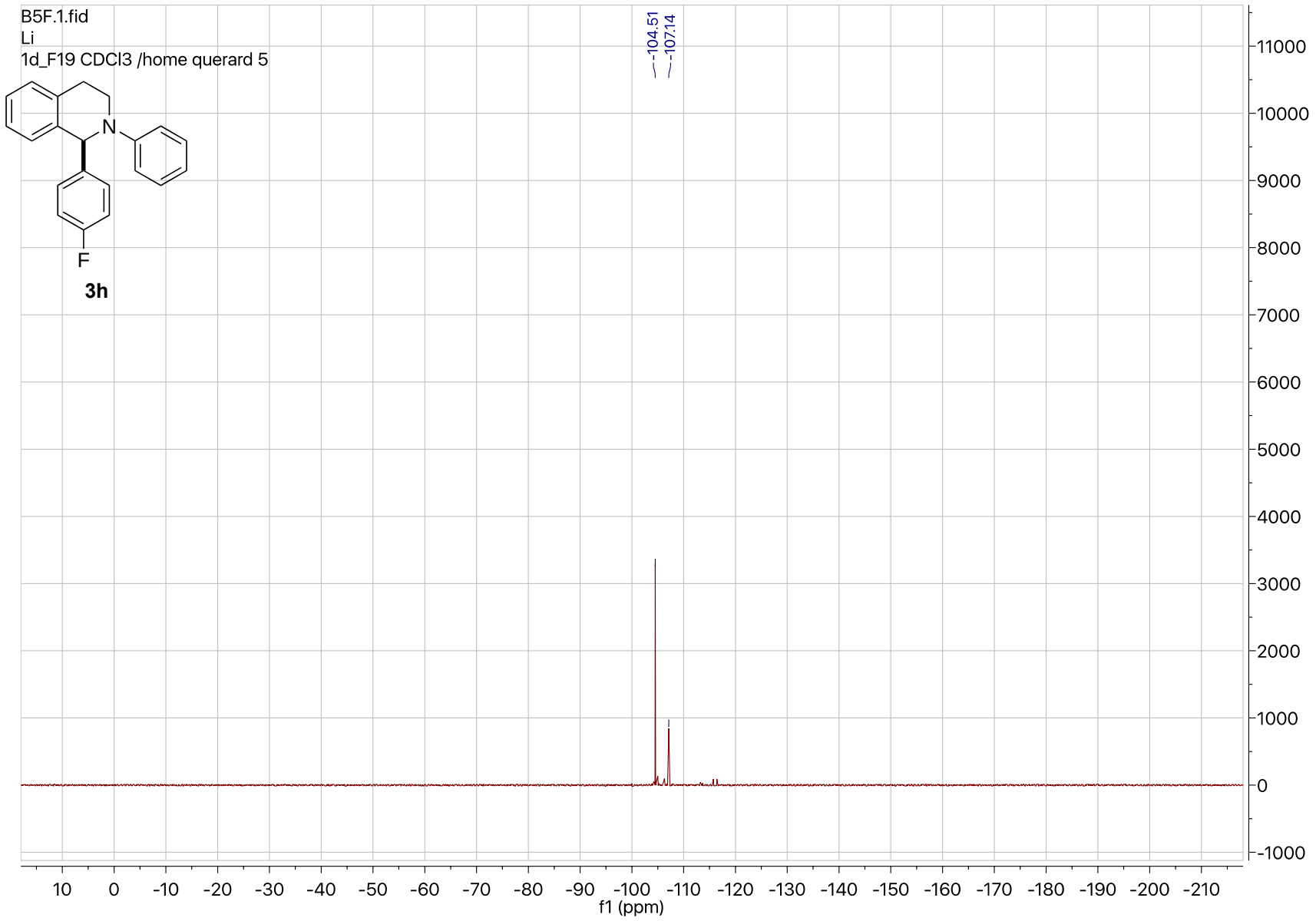
B5F.1.fid
Li
1d_F19 CDCl3 /home querard 5
-104.51
-107.14
N
F
3h
11000
10000
9000
8000
7000
6000
5000
4000
3000
2000
1000
0
-1000
10 0 -10 -20 -30 -40 -50 -60 -70 -80 -90 -100 -110 -120 -130 -140 -150 -160 -170 -180 -190 -200 -210
f1 (ppm)

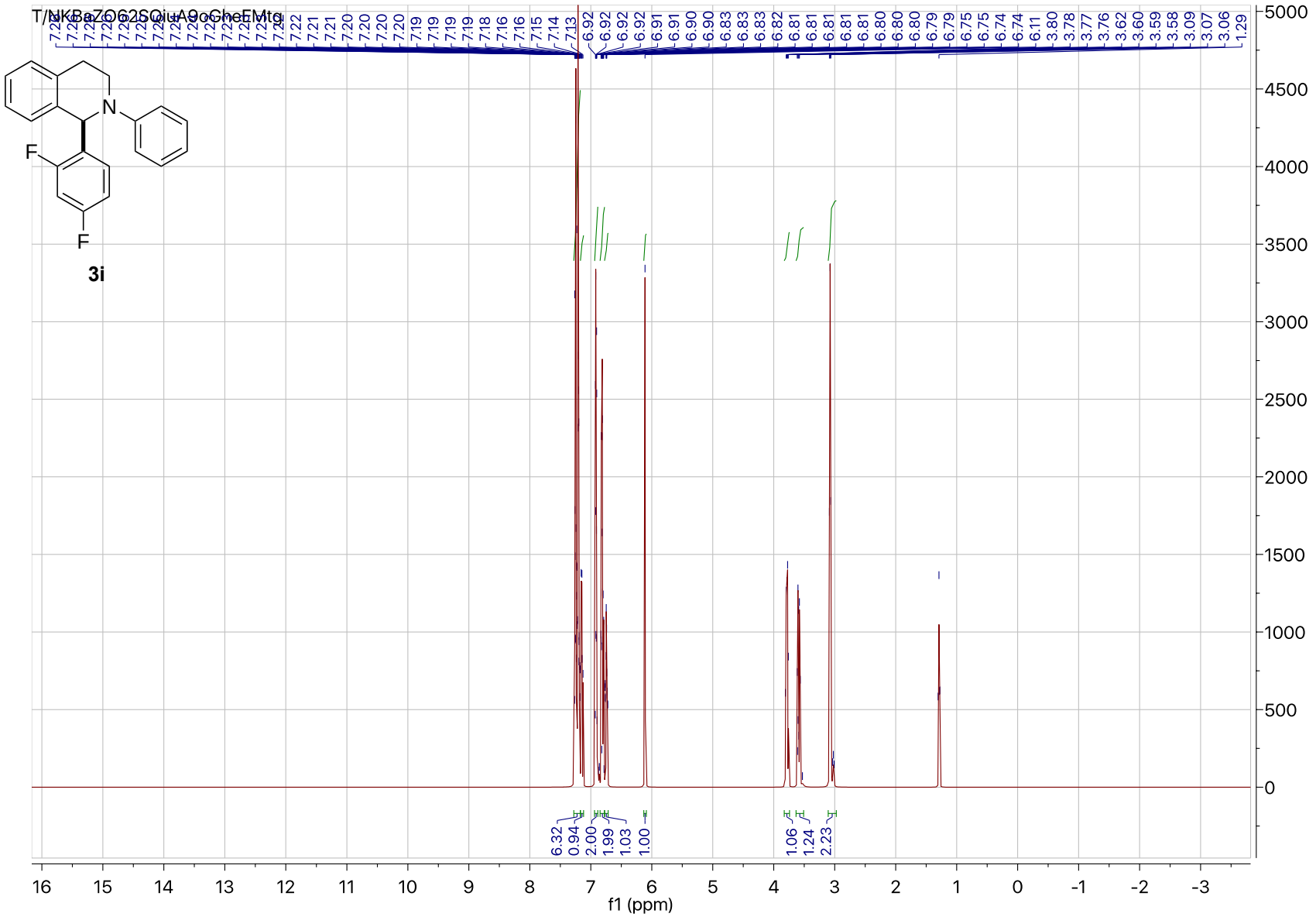
T/NKBaZO62SQiuA9oChcEMtg
N
F
F
3i
6.32
0.94
2.00
1.99
1.03
1.00
1.06
1.24
2.23
f1 (ppm)

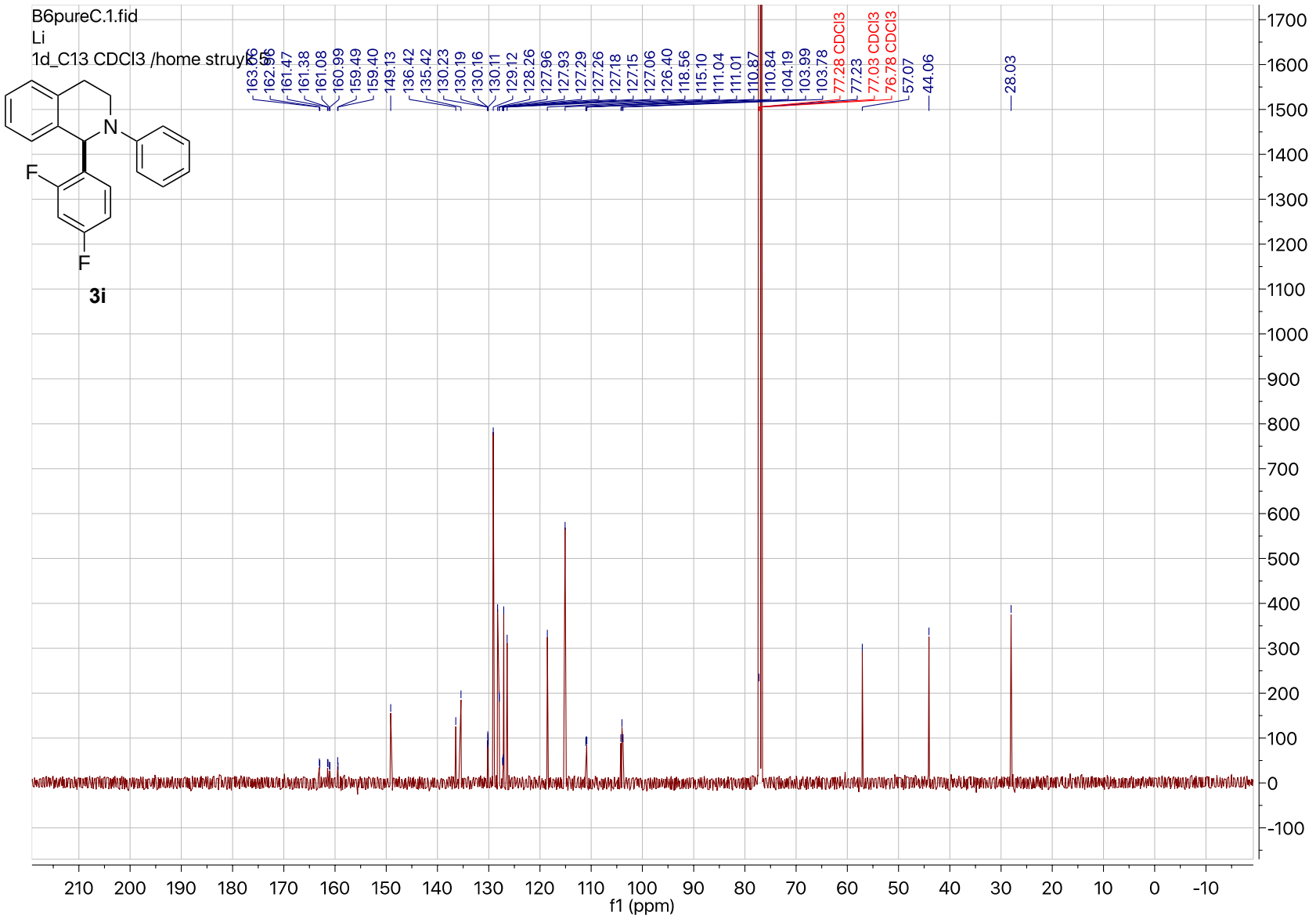
B6pureC.1.fid
Li
1d_C13 CDCl3 /home struyk
163.66
162.96
161.47
161.38
161.08
160.99
159.49
159.40
149.13
136.42
135.42
130.23
130.19
130.16
130.11
129.12
128.26
127.96
127.93
127.29
127.26
127.18
127.15
127.06
126.40
118.56
115.10
111.04
111.01
110.87
110.84
104.19
103.99
103.78
77.28 CDCl3
77.23
77.03 CDCl3
76.78 CDCl3
57.07
44.06
28.03
N
F
F
3i
f1 (ppm)

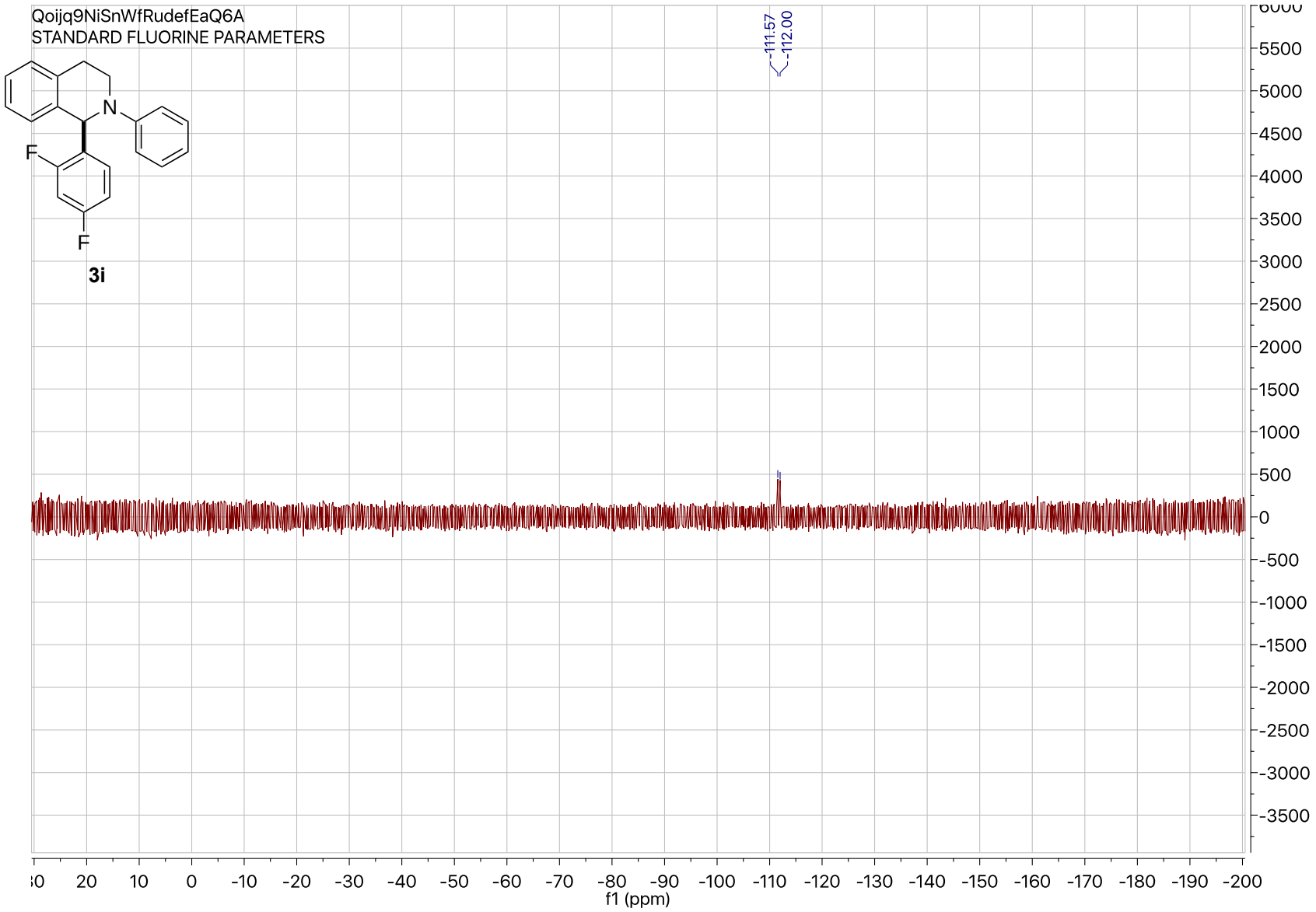
Qoijq9NiSnWfRudefEaQ6A
STANDARD FLUORINE PARAMETERS
F
N
F
3i
-111.57
-112.00
6000
5500
5000
4500
4000
3500
3000
2500
2000
1500
1000
500
0
-500
-1000
-1500
-2000
-2500
-3000
-3500
30 20 10 0 -10 -20 -30 -40 -50 -60 -70 -80 -90 -100 -110 -120 -130 -140 -150 -160 -170 -180 -190 -200
f1 (ppm)

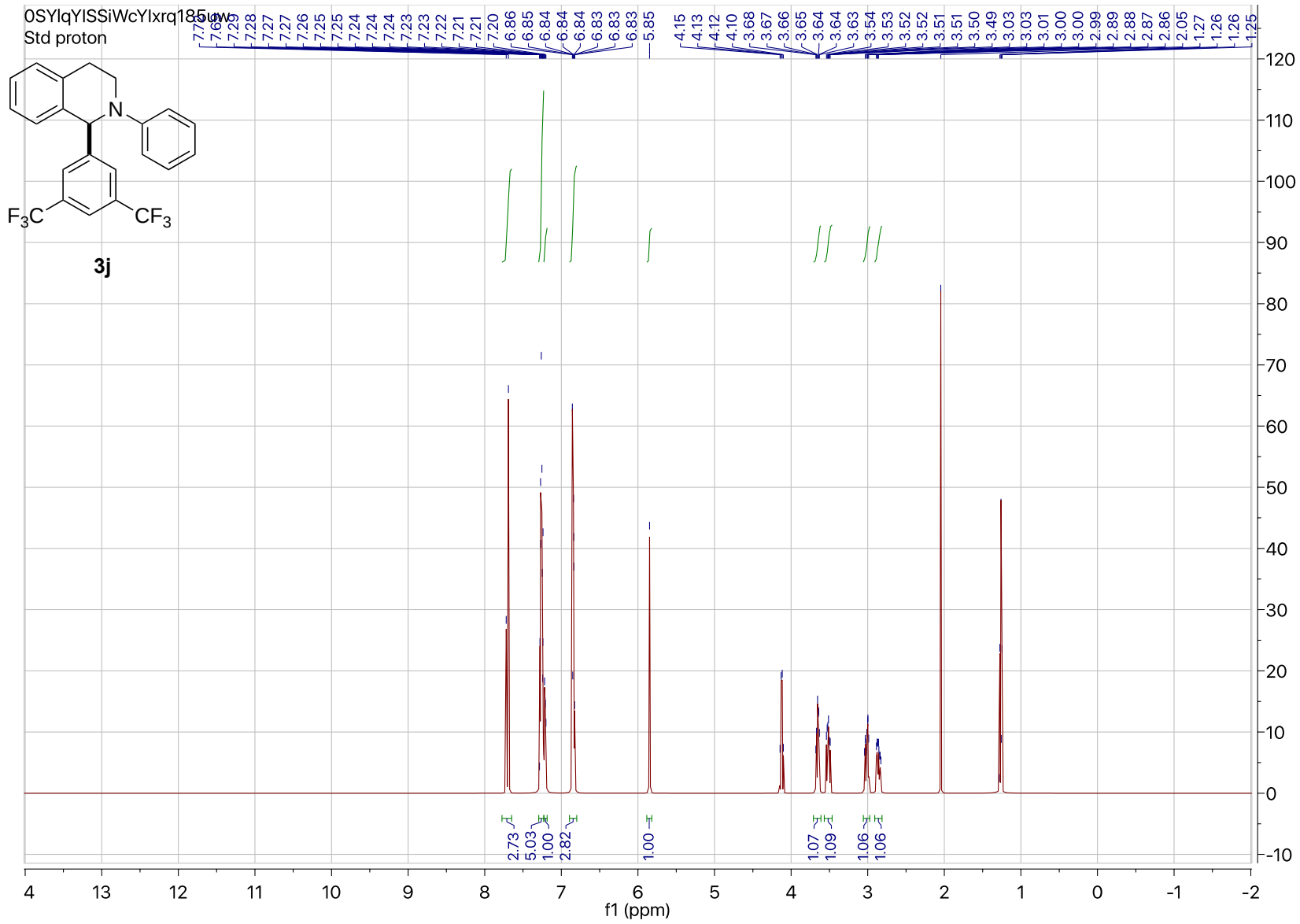
0SYlqYlSSiWcYlxrq185uw
Std proton
N
F3C
CF3
3j
f1 (ppm)

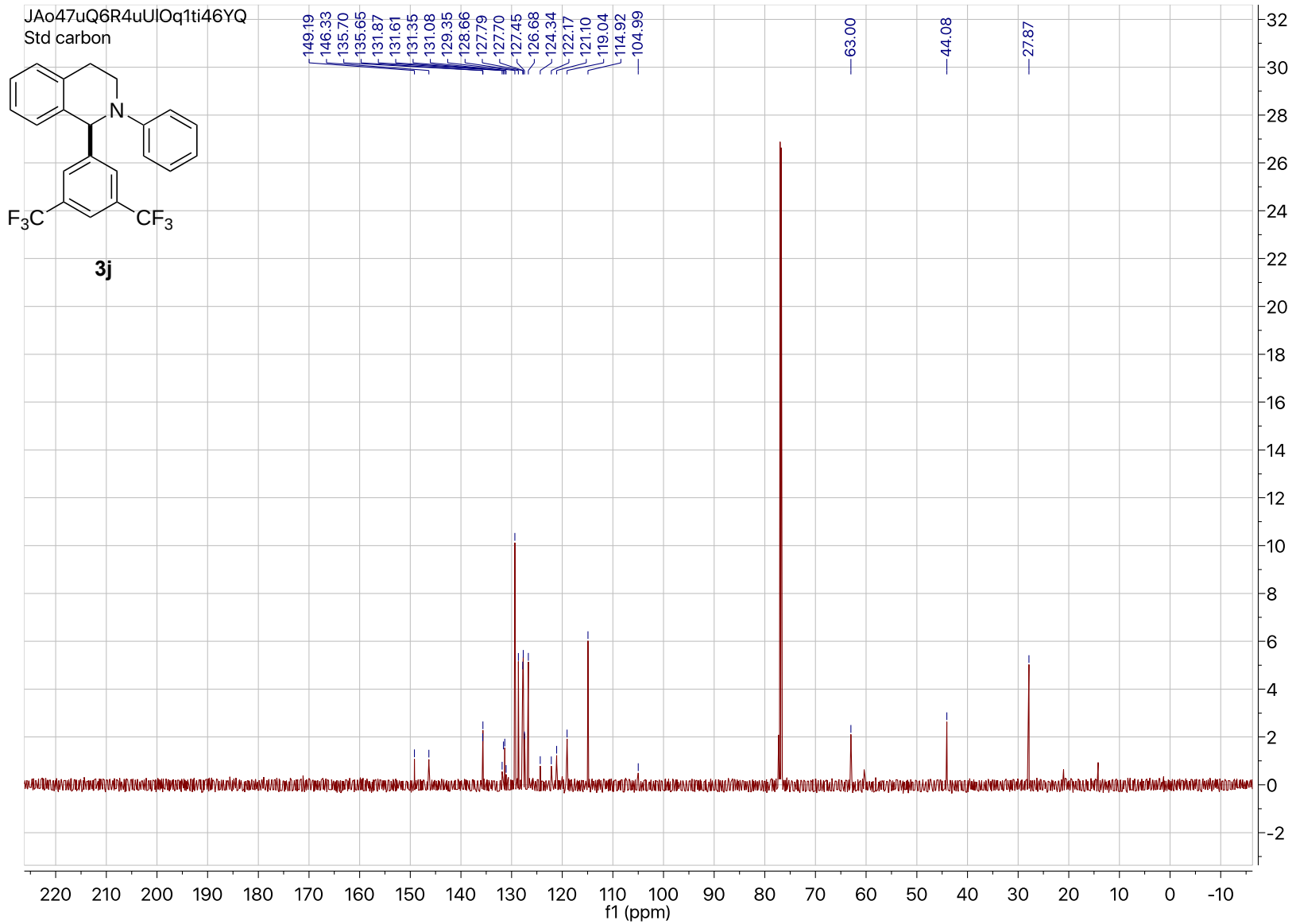
JAo47uQ6R4uUlOq1ti46YQ
Std carbon
149.19
146.33
135.70
135.65
131.87
131.61
131.35
131.08
129.35
128.66
127.79
127.70
127.45
126.68
124.34
122.17
121.10
119.04
114.92
104.99
63.00
44.08
27.87
N
F3C
CF3
3j
f1 (ppm)

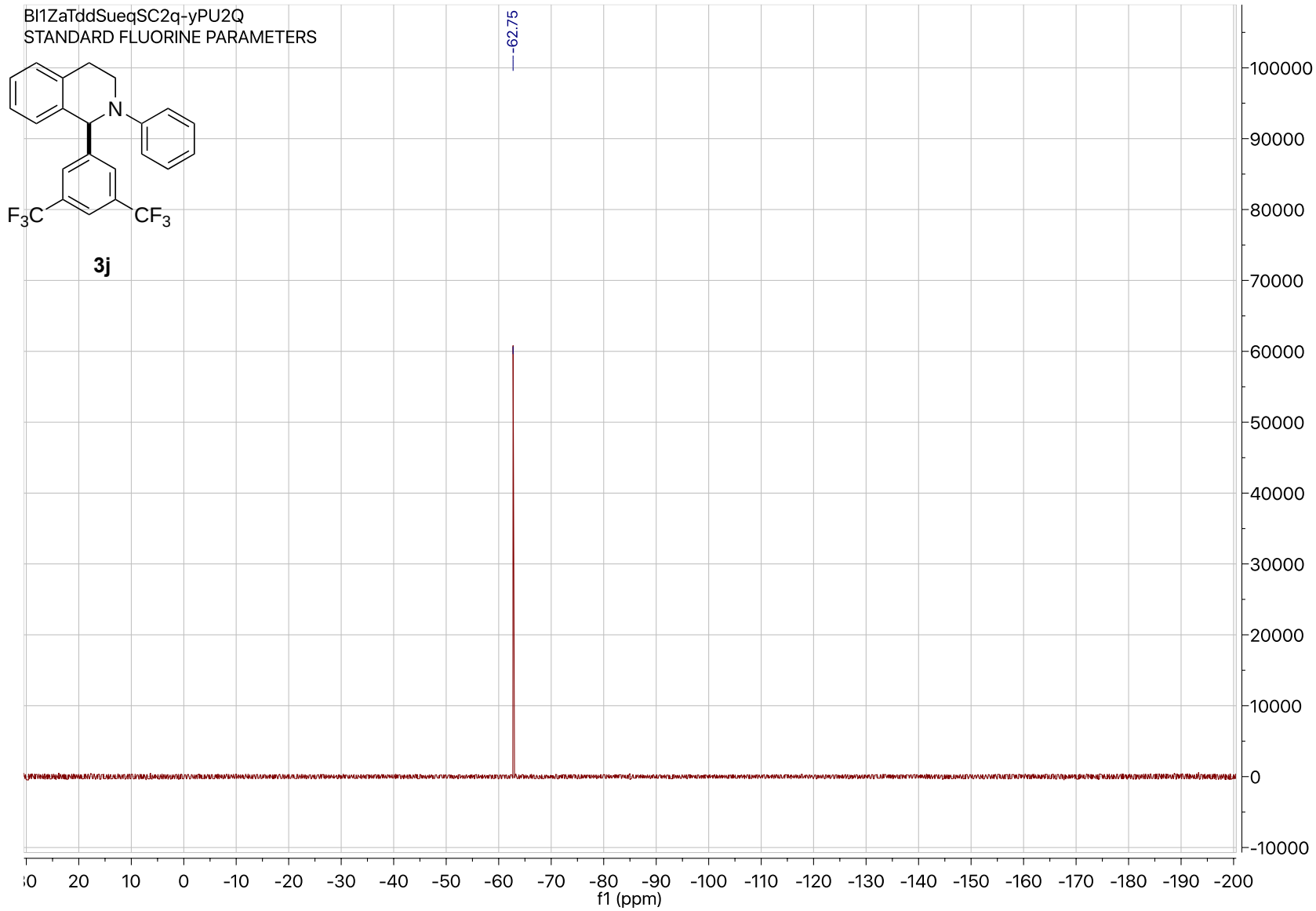
BI1ZaTddSueqSC2q-yPU2Q
STANDARD FLUORINE PARAMETERS
-62.75
N
F3C
CF3
3j
100000
90000
80000
70000
60000
50000
40000
30000
20000
10000
0
-10000
20 10 0 -10 -20 -30 -40 -50 -60 -70 -80 -90 -100 -110 -120 -130 -140 -150 -160 -170 -180 -190 -200
f1 (ppm)

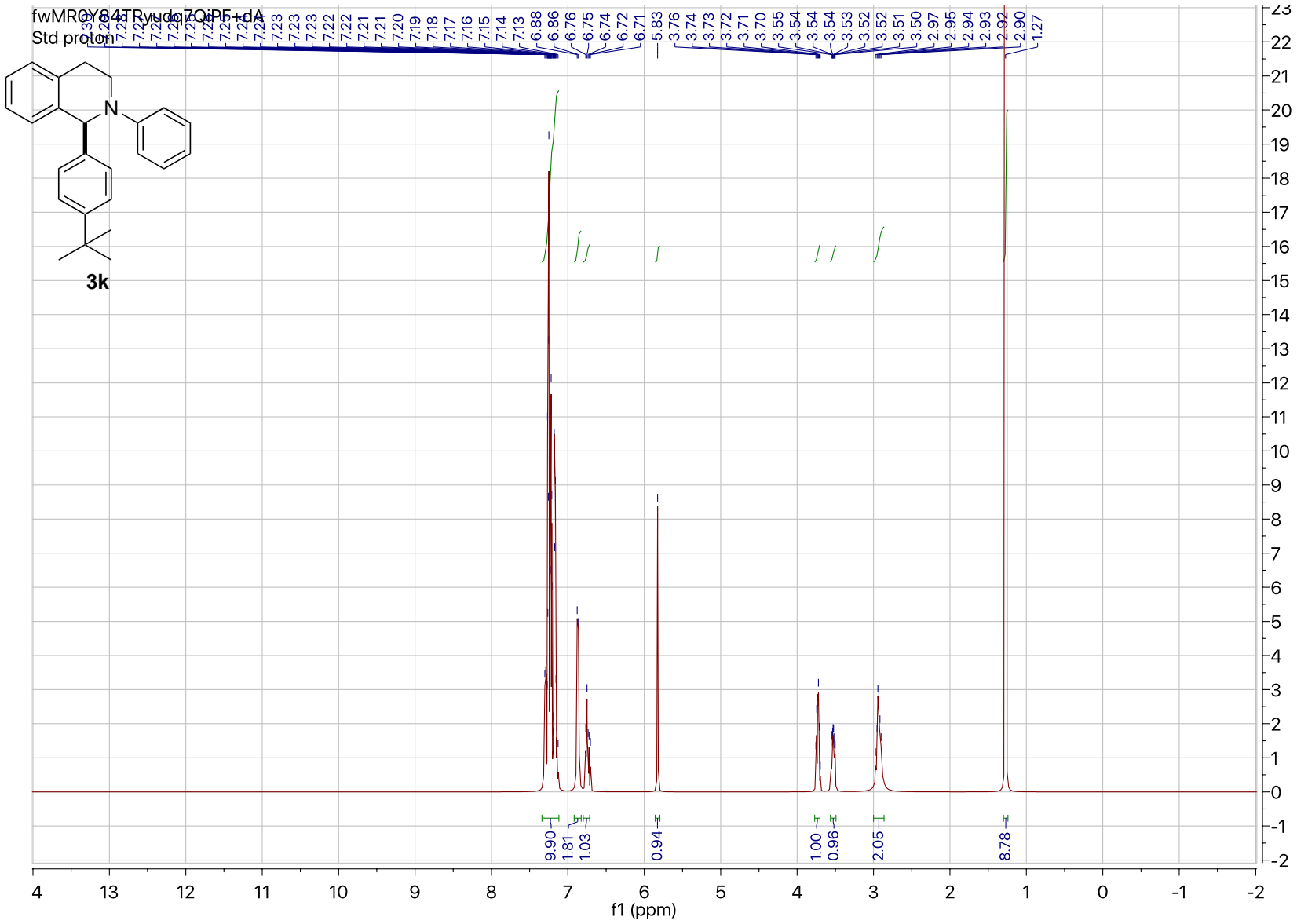
fwMR0Y84TRyudq7QiPF+dA
Std proton
N
3k
f1 (ppm)

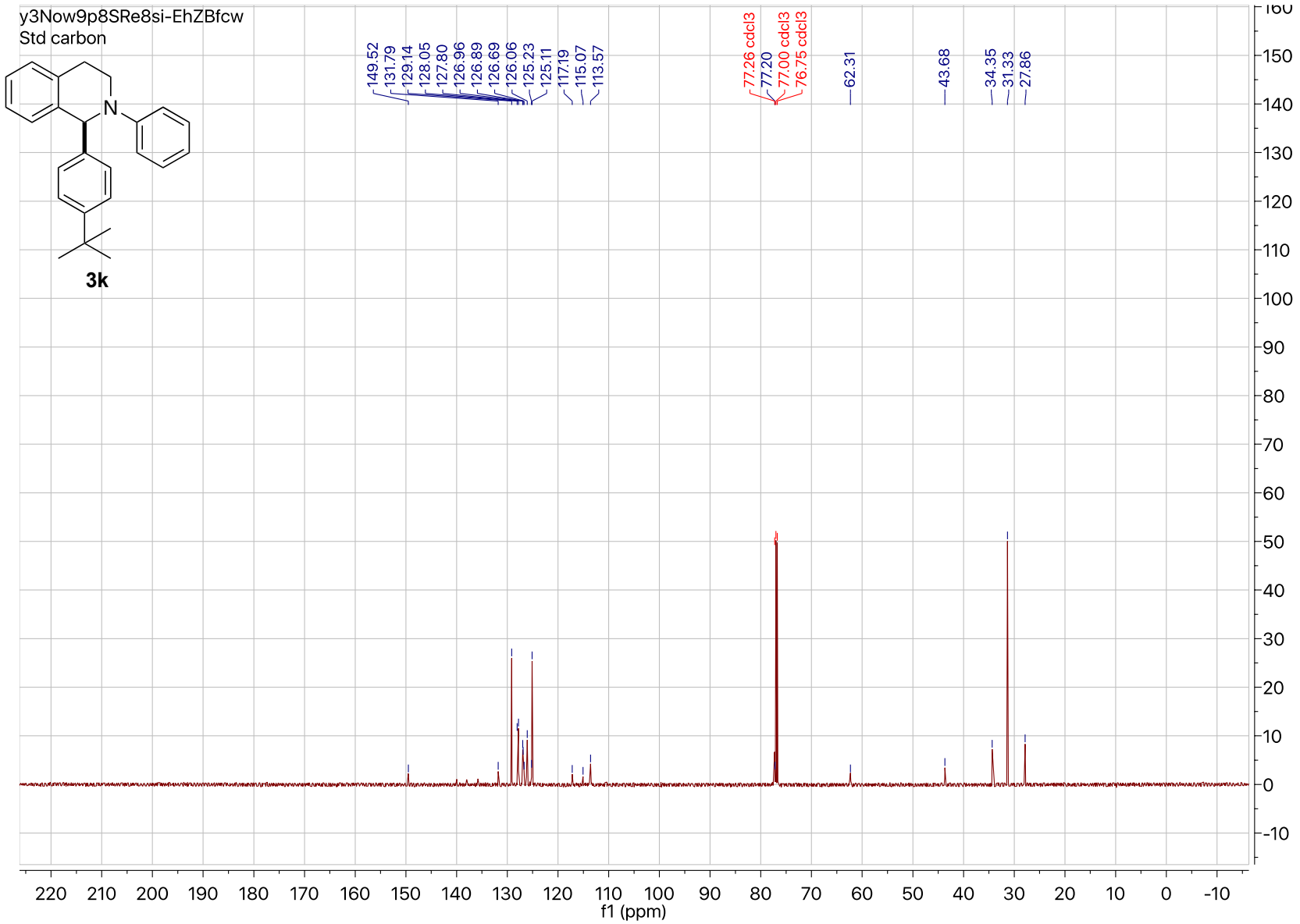
y3Now9p8SRe8si-EhZBfcw
Std carbon
3k
149.52
131.79
129.14
128.05
127.80
126.96
126.89
126.69
126.06
125.23
125.11
117.19
115.07
113.57
77.26 cdcl3
77.20
77.00 cdcl3
76.75 cdcl3
62.31
43.68
34.35
31.33
27.86
f1 (ppm)

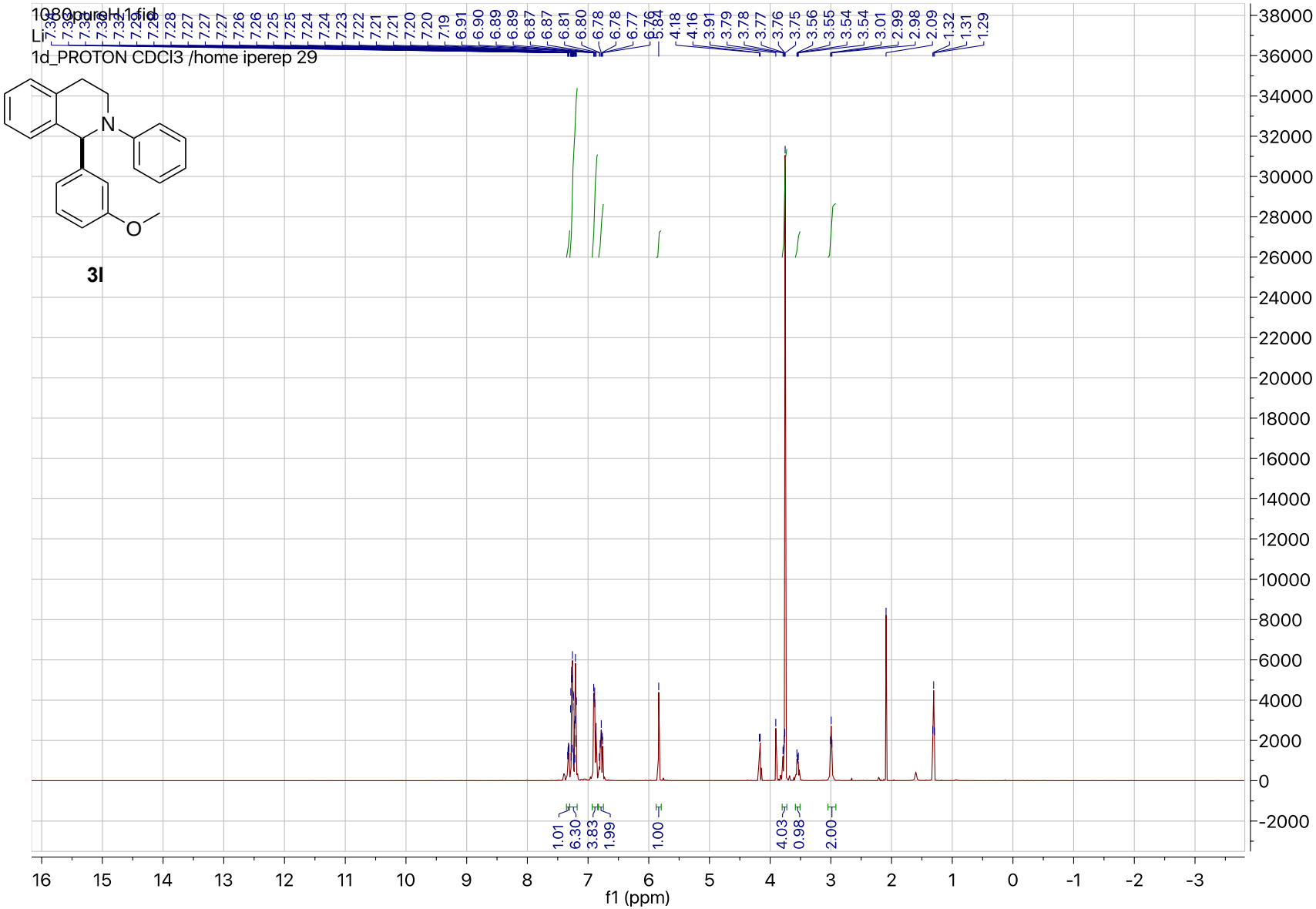
1089pureH1.fid
1d_PROTON CDCl3 /home iperep 29
3l
f1 (ppm)

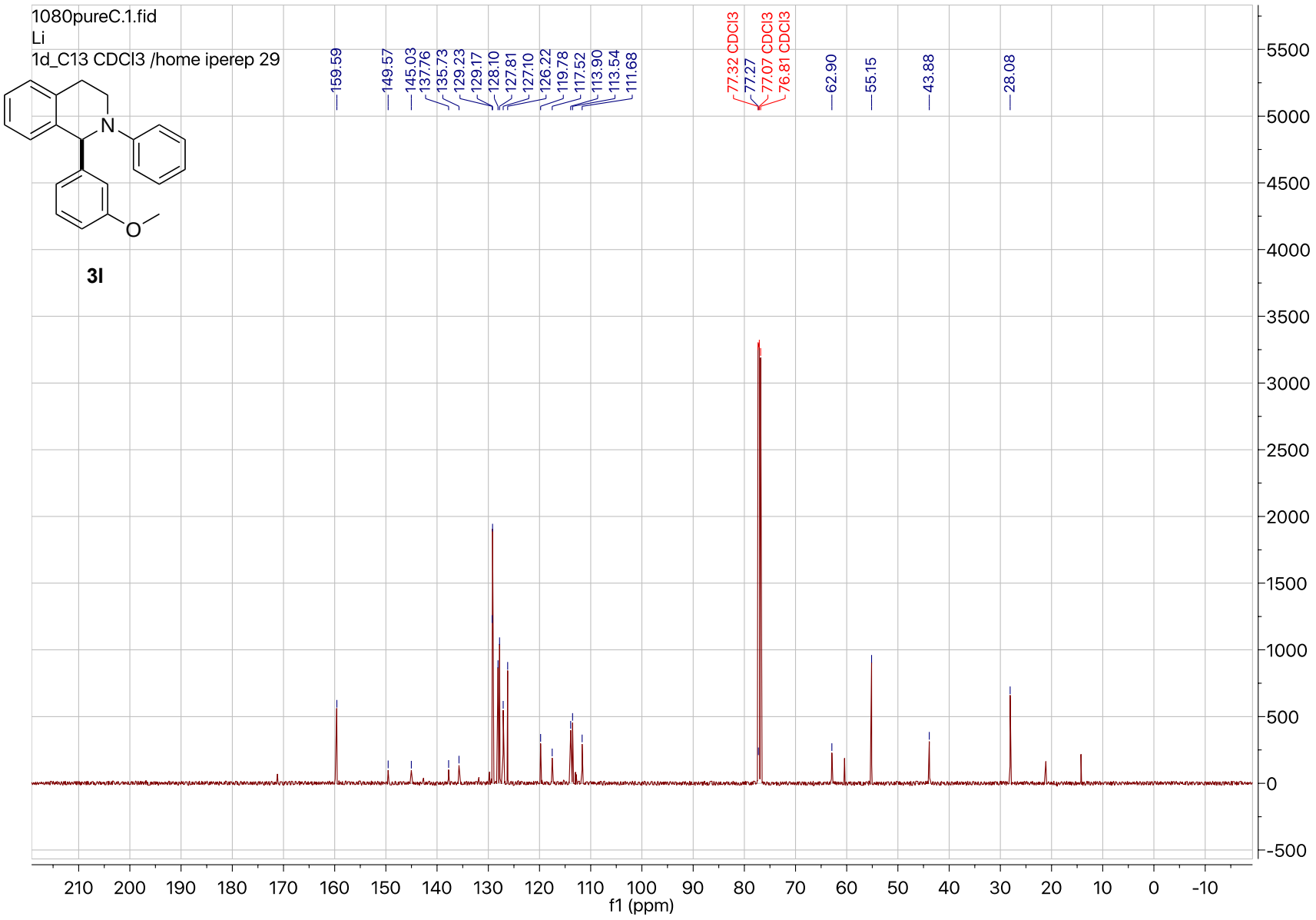
1080pureC.1.fid
Li
1d_C13 CDCl3 /home iperep 29
159.59
149.57
145.03
137.76
135.73
129.23
129.17
128.10
127.81
127.10
126.22
119.78
117.52
113.90
113.54
111.68
77.32 CDCl3
77.27
77.07 CDCl3
76.81 CDCl3
62.90
55.15
43.88
28.08
N
O
3l
f1 (ppm)

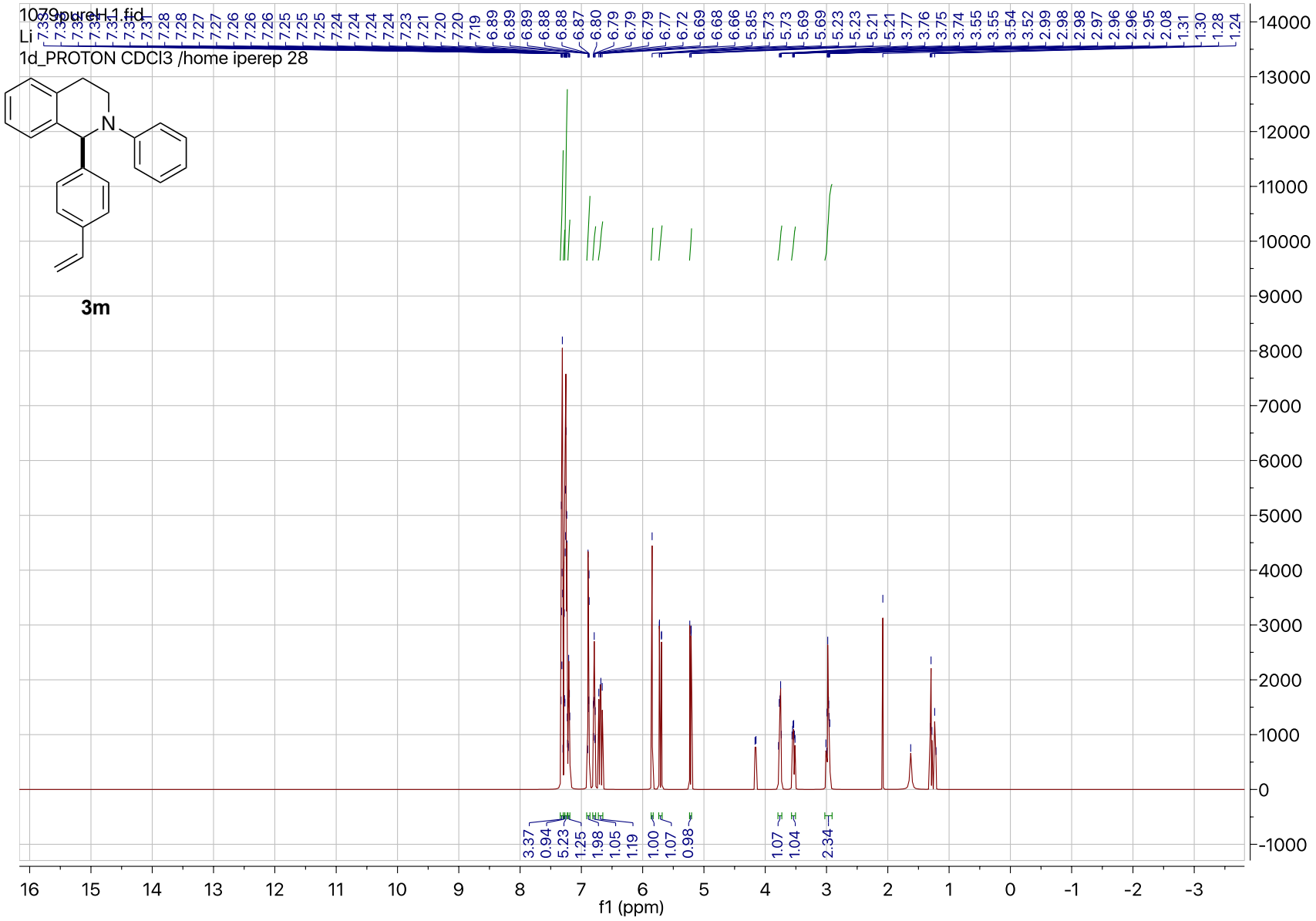
1079pureH1.fid
1d_PROTON CDCl3 /home iperep 28
N
3m
f1 (ppm)

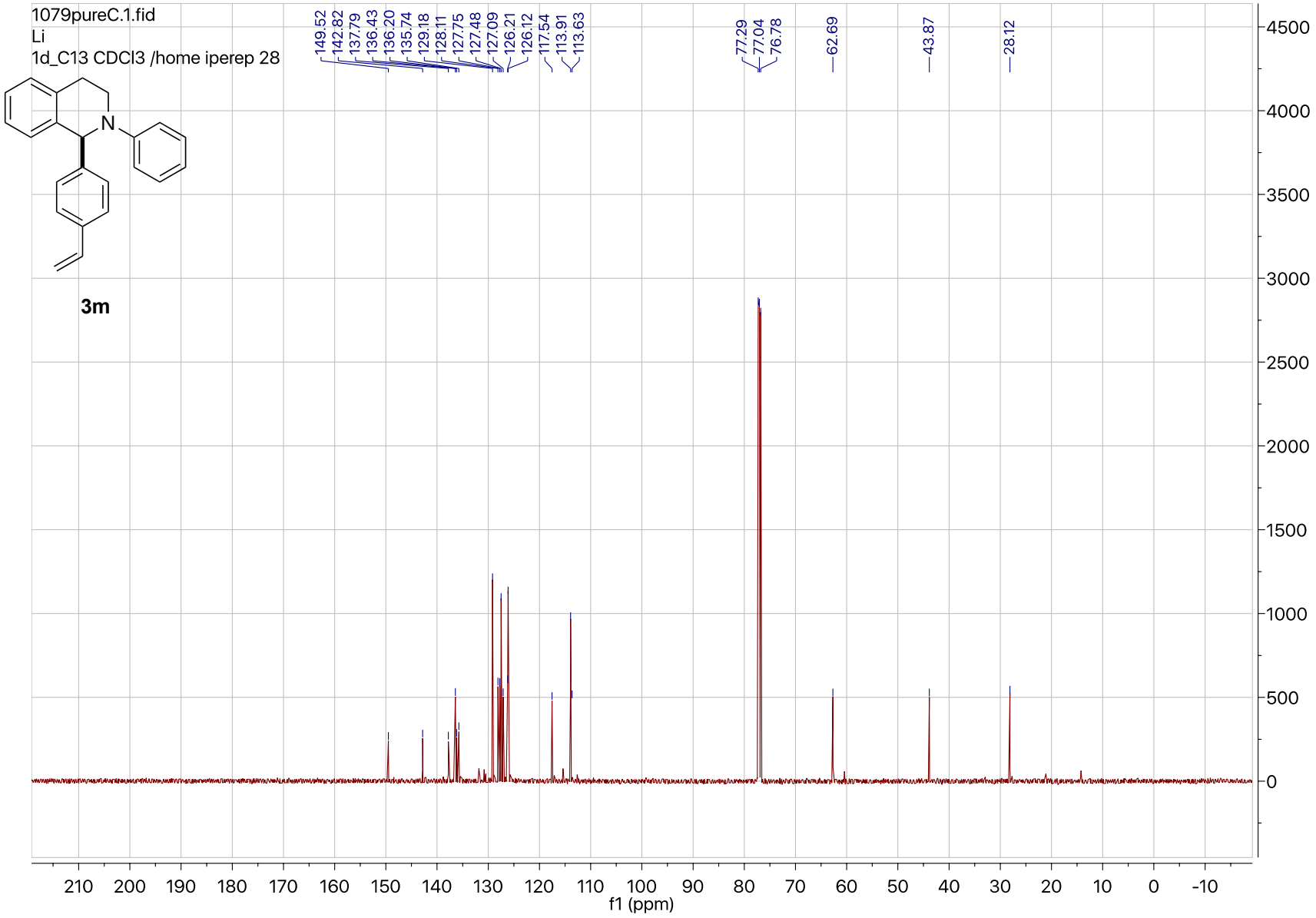
1079pureC.1.fid
Li
1d_C13 CDCl3 /home iperep 28
3m
149.52
142.82
137.79
136.43
136.20
135.74
129.18
128.11
127.75
127.48
127.09
126.21
126.12
117.54
113.91
113.63
77.29
77.04
76.78
62.69
43.87
28.12
f1 (ppm)

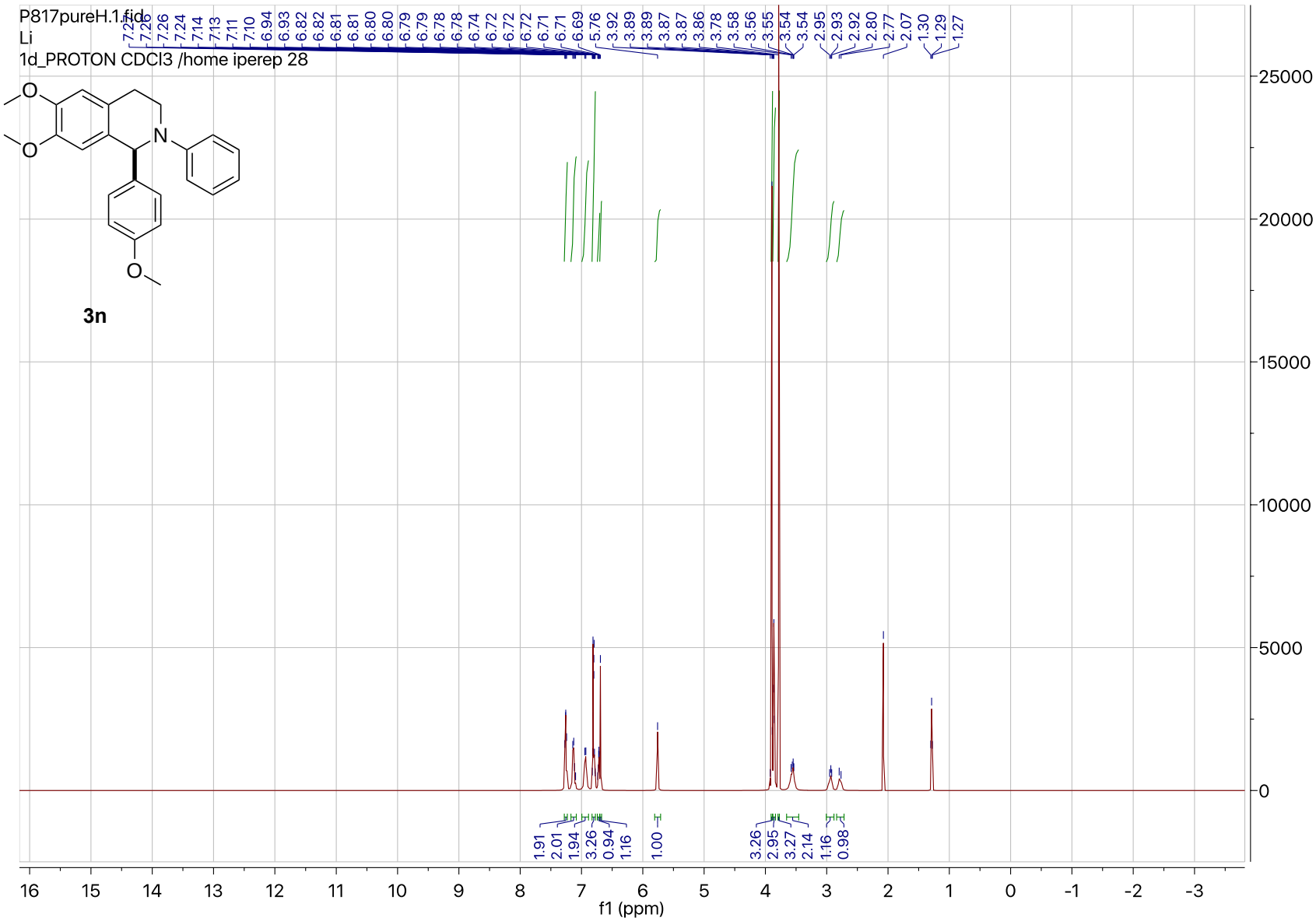
P817pureH.1.fid
Li
1d_PROTON CDCl3 /home iperep 28
3n
f1 (ppm)

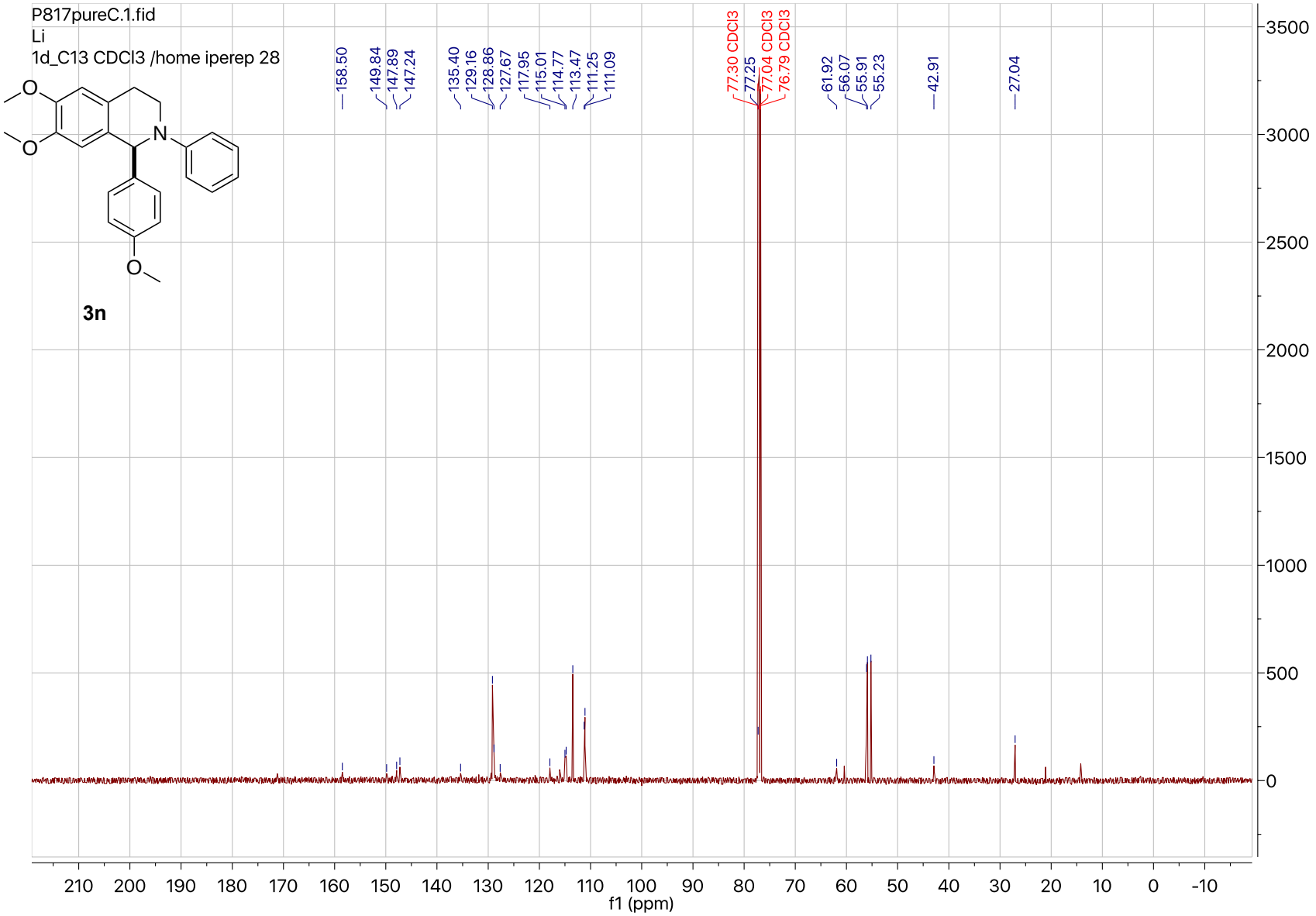
P817pureC.1.fid
Li
1d_C13 CDCl3 /home iperep 28
3n
158.50
149.84
147.89
147.24
135.40
129.16
128.86
127.67
117.95
115.01
114.77
113.47
111.25
111.09
77.30 CDCl3
77.25
77.04 CDCl3
76.79 CDCl3
61.92
56.07
55.91
55.23
42.91
27.04
f1 (ppm)